Synthesis and Crystal Design of Rubrene Derivatives for Use in Organic Electronics

A DISSERTATION

SUBMITTED TO THE FACULTY OF

THE UNIVERSITY OF MINNESOTA

BY

Kathryn Ada McGarry

IN PARTIAL FULFILLMENT OF THE REQUIREMENTS

FOR THE DEGREE OF

DOCTOR OF PHILOSOPHY

Advisor: Christopher J. Douglas

September, 2013

Acknowledgements

Thanks to Sean Murray and Kyle Kalstabakken for analyzing my samples by mass spectrometry. Thanks to Victor G. Young, Jr. for guidance, assistance and many, many helpful discussions in deciphering my single-crystal X-ray diffraction data. Thanks to Wei Xie for insight into materials device fabrication and all of your hard work to make functioning devices of the various rubrenes I synthesized. Thanks to Wade Luhman and Tyler Mullenbach for your efforts to examine rubrenes in organic photovoltaic devices. Thanks to Prof. Dan Frisbie and Prof. Russ Holmes for collaborating on these projects with Chris and I.

Thanks to everyone in the Douglas group who gave me advice, worked and laughed with me during these last five years. It has been a pleasure working and learning alongside every one of you. Thanks to Billy Ogden and Dylan Walsh for making me smile during the rare occasion you weren't driving me crazy. Special thanks to Ashley Dreis, Giang Hoang, and Jodi Ogilvie for your incredible patience, support, and friendship even through the times when I wasn't sane. I wouldn't have gotten through without you.

Most importantly, thanks to Chris. Thank you for your guidance through the ups and downs of my projects, your support of my extracurricular activities, and for being a leader who strives for excellence while also understanding that life is more than just work. I'm glad to have been one of the first few in your group and I'm excited to see where the research will take you and your future group members.

Dedication

To my loving family.

Thanks for giving me strength, showing me the value of hard work, and keeping me laughing even when times get hard. I'm so glad you are the people sharing this journey with me.

Abstract

My research probes the structure-property relationship of organic semiconductors in order to gain insight into effectively tuning materials. Rubrene is one of the best organic semiconductors to date due to the π-stacking that occurs when rubrene is crystallized in the orthorhombic setting. We sought to explore the effect of limited and extensive substitution on rubrene on its solid state and resulting electrical properties. We anticipated that selectively substituting rubrene would allow us to manipulate the solid-state structure to maintain the π-stacking while changing the packing in other ways. Calculations have indicated that the surrounding layers of the rubrene crystal structure polarize charge moving through the crystal, acting as a trap. We propose that if the layers could be pushed further apart, the charge carrier mobility could be increased. Alternatively, fully substituting the rubrene structure with deuterium or fluorine may significantly influence the electrical properties while minimally changing the solid-state packing. My projects focus on exploring the effects of these substitutions on the solid-state structure of rubrene derivatives through the synthesis and crystallization of these compounds so that they might be studied in electrical devices.

Table of Contents

LIST OF SCHEMES

LIST OF TABLES

LIST OF FIGURES

LIST OF ABBREVIATIONS

Ac_2O	Acetic Anhydride
AcOH	Acetic Acid
CI	Chemical Ionization
CNT	Carbon Nanotubes
DIEA	Diisopropylethylamine (Hünig's Base)
DIPA	Diisopropylamine
DMF	Dimethyl Formamide
DSC	Differential Scanning Calorimetry
EI	Electron Ionization
ESI	Electrospray Ionization
Et_2O	Diethyl Ether
EtMgBr	Ethyl Magnesium Bromide
EtOAc	Ethyl Acetate
HOMO	Highest Occupied Molecular Orbital
HRMS	High Resolution Mass Spectrometry
IR	Infrared
LRMS	Low Resolution Mass Spectrometry
LUMO	Lowest Unoccupied Molecular Orbital
MeOH	Methanol
Mes	Mesitylene
Ms_2O	Methane Sulfonic Anhydride

MsCl	Methanesulfonyl Chloride
*n*BuLi	*n*-Butyl Lithium
NMR	Nuclear Magnetic Resonance
OFET	Organic Field-Effect Transistor
OLED	Organic Light-Emitting Diode
OPV	Organic Photovoltaic
ORTEP	Oak Ridge Thermal Ellipsoid Plot
PCC	Pyridinium Chlorochromate
PDMS	Polydimethylsiloxane
PEPPSI-IPR	Pyridine-Enhanced Precatalyst Preparation Stabilization and Initiation-Isopropyl
PMMA	Polymethyl Methacrylate
Pyr	Pyridine
TEA	Triethylamine
THF	Tetrahydrofuran
TLC	Thin-Layer Chromatography
TMSA	(Trimethylailyl)acetylene
Tol	Toluene
VT	Variable Temperature

1 INTRODUCTION

One of the most intriguing organic compounds from a materials perspective is rubrene (**1.1**, 5,6,11,12-tetraphenylnaphthacene, Figure 1.1). Known since the 1920s, rubrene is a red solid with a core of four fused benzene rings (tetracene, **1.2**) flanked by four side phenyl groups that are twisted out of the plane of the tetracene backbone. Rubrene has exhibited a variety of interesting properties, such as electrochemiluminesence,[1–4] photooxidation,[5–7] fluorescence,[8,9] and chemiluminesence[10–12] which has prompted its study for use in organic light emitting diodes (OLED),[13–15] organic photovoltaics (OPV),[16,17] and notably organic field-effect transistors (OFET).[18,19] OFET devices determine the charge carrier mobility of organic semiconductors, which is a key aspect in material performance for applications. Since OFET research began in the 1980s, organic semiconductors have since been applied to commercial devices in which silicon semiconductors are unsuited to perform, including radio frequency identification tags, electronic papers and flexible displays.[20] Research on improving the performance of organic semiconductors has focused on understanding and enhancing the mobility in organic materials in order to create superior devices. The best organic semiconductors to date are highly conjugated and rich in π-electrons.[21] In single-crystal architectures of OFET, rubrene has provided the highest hole charge carrier mobilities for an organic semiconductor to date.[22] This exceptional mobility has been found to depend on the extent of structural organization[23] and has led researchers to try to mimic aspects of the rubrene structure to create improved materials. The research to be described in this dissertation sought to manipulate and enhance the rubrene core so as to expand our fundamental understanding of organic semiconductors. In this introduction, an

overview of the synthesis, molecular and solid-state properties, as well as a brief summary on OFET device performance of rubrene will be discussed.

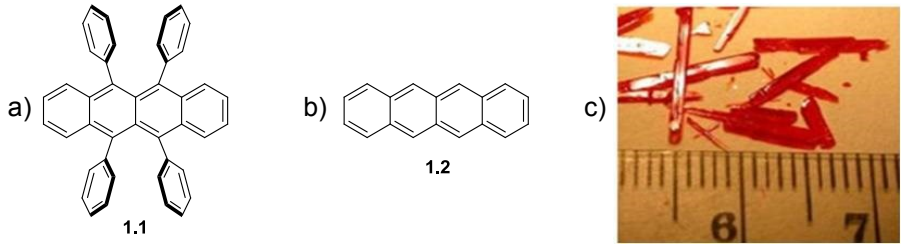

Figure 1.1. Molecular structure of **a**) rubrene (**1.1**) and **b**) tetracene (**1.2**). **c**) Image of rubrene crystals.[24]

1.1 HISTORY OF RUBRENE SYNTHESIS

Structure-property relationship studies on rubrene derivatives would provide more insight into what aspects, aside from the conjugation in rubrene, impact the device properties. A number of syntheses have led to the preparation of rubrene over the years, yet few allow for control of substituent placement in rubrene congeners. The following summarizes the various routes to rubrene published through the years.

Rubrene was first synthesized in 1926 by Moureu et al., by heating 3-chloro-1,3,3-triphenylpropyne (**1.3**) in the absence of solvent,[18] which is considered the classical route to rubrene. At the time, the mechanism of this reaction was believed to begin with the transformation of propargyl chloride **1.3** into 1,3,3-triphenyl-chloroallene (**1.4**), from which the reaction could proceed via [4+2] cycloaddition, electrocylcization, and loss of two HCl (Scheme 1.1a). In 1963, Landor and Landor employed thionyl chloride to effect the transformation to rubrene from propargyl alcohol **1.5** through chloroallene **1.4**.[25] A diagnostic allene peak in the IR was markedly absent from the isolated compound, leading the authors to suggest intermediate **1.6**. Heating **1.6** proceeded with loss of HCl to provide **1.1**. They proposed the dimerization occurred

via an acid-catalyzed mechanism (Scheme 1.1b), which can account for the formation of intermediate **1.6**.

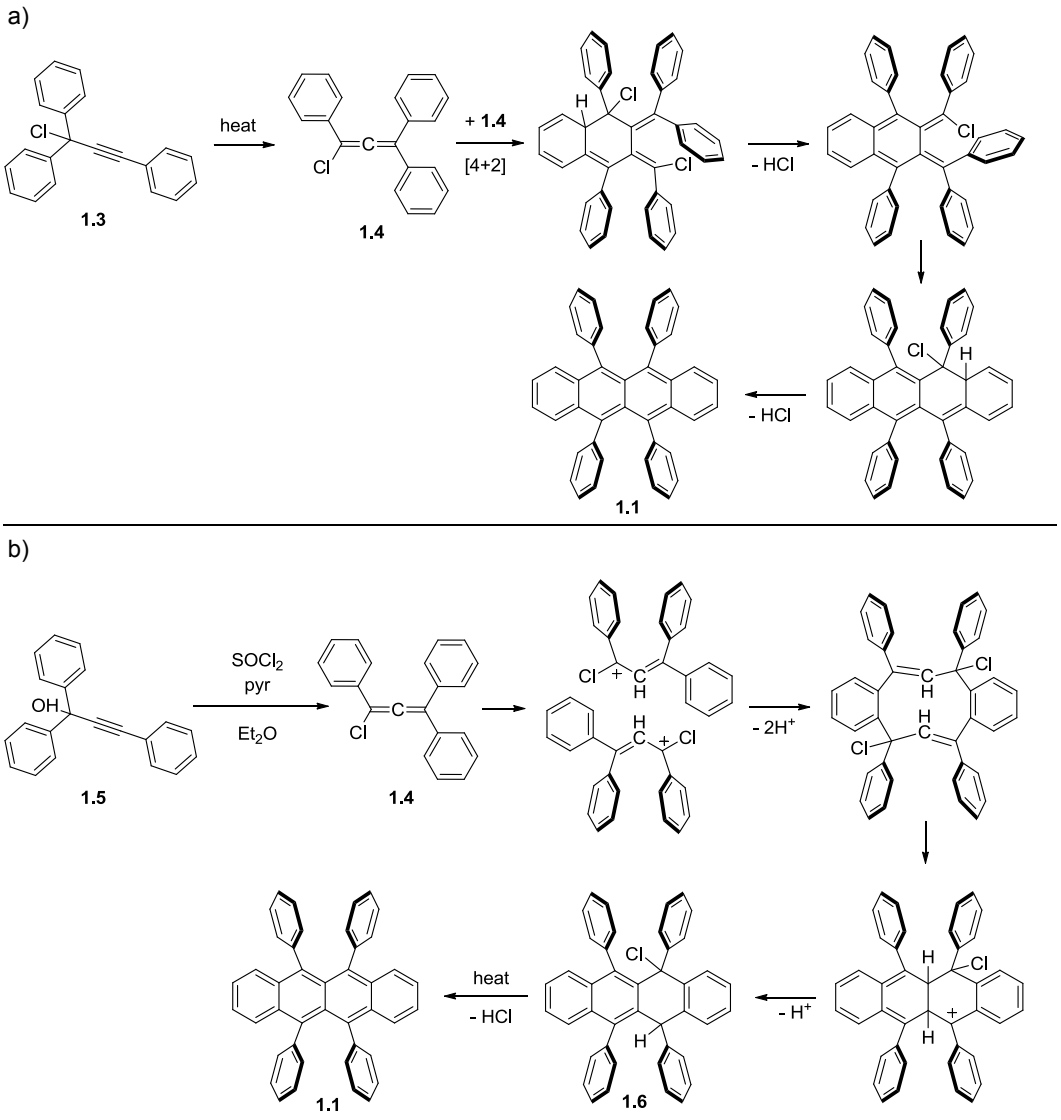

Scheme 1.1. a) Rubrene (**1.1**) formation from propargyl chloride **1.2** via pericyclic mechanism. **b**) Rubrene formation via acid-catalyzed mechanism from propargyl alcohol **1.5**.

In 1977, Rigaudy and Capdevielle proposed instead that after formation of allene **1.4**, radical dimerization occurs to form bis-allyl diradical **1.7**, followed by recombination and loss of

two HCl to form rubrene (Scheme 1.2a).[26] Rigaudy and Capdevielle also identified cyclobutene **1.8** could form via this route by radical combination followed by loss of Cl_2 (Scheme 1.2b), but they did not isolate this compound. Later studies into the dimerization of allenes have provided support for the radical mechanism.[27,28]

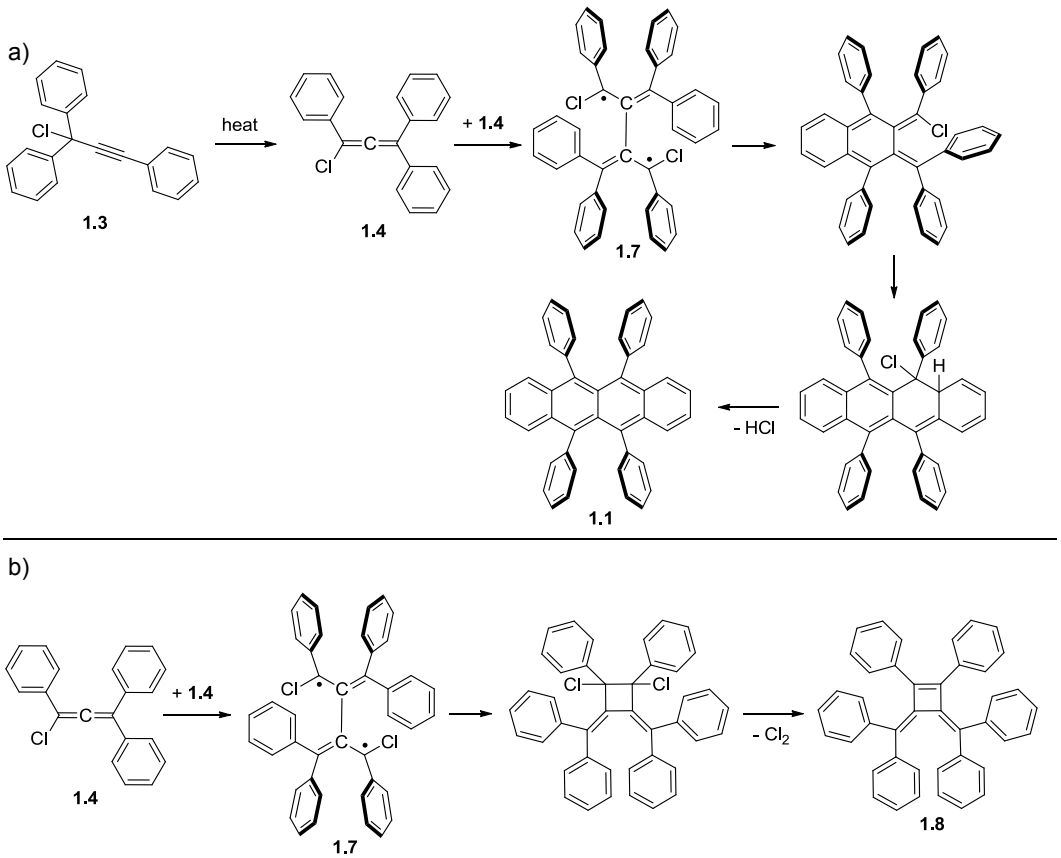

Scheme 1.2. a) Rubrene formation from propargyl chloride **1.3** via radical mechanism. **b**) Cyclobutene **1.8** formation via radical mechanism from chloroallene **1.4**.

In the work of Moureu, propargyl chloride **1.3** was presumably made from (*E*)-(2-bromovinyl)benzene through the same route as Wittig and Waldi (Scheme 1.3).[29] Elimination of hydrogen bromide provided phenyl acetylene, which was then deprotonated with sodium and added to benzophenone to give the propargyl alcohol **1.5**. Compound **1.5** was then transformed

into **1.3** using phosphorous trichloride followed by heating to form **1.1**. Although this first sequence has only a few steps, the yield for the last reaction was low (23%) and required a troublesome purification procedure using various solvents. The inefficiency of this route motivated other scientists to develop alternative routes to rubrene as well as an easier purification method.

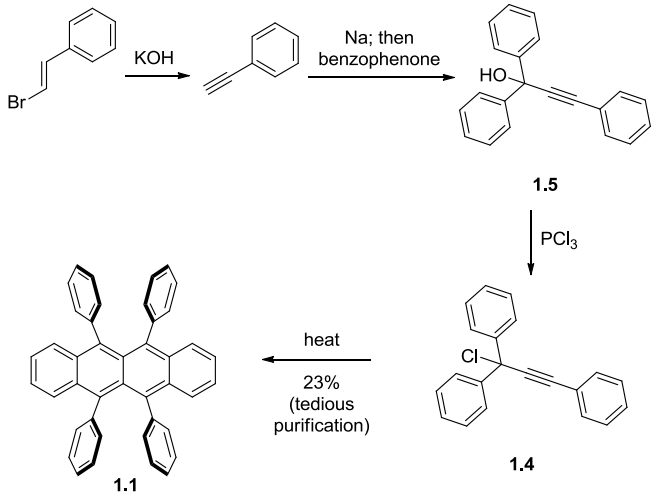

Scheme 1.3. Synthetic route to rubrene (**1.1**) employed by Wittig and Waldi.

Using a different method to **1.1**, Allen and Gilman proposed the preparation of rubrene from tetracene-5,12-dione **1.9** (Scheme 1.4), highlighting the 1,4-addition of a Grignard reagent into a quinone.[30] Quinone **1.9** was made from a Friedel-Crafts acylation between isobenzofuran-1,3-dione and 1,2,3,4-tetrahydronaphthalene, followed by oxidation to the fully conjugated **1.9** using bromine in glacial acetic acid.[31] From **1.9**, addition of phenyl magnesium bromide and alcoholic potash workup provided 6,11-diphenyltetracene-5,12-dione, which was then treated with phenyl lithium to afford the diol **1.10**. Reduction of the diol using iron in acetic acid gave **1.1**. Purification of rubrene was achieved by sublimation, an improvement over the previous

synthetic route. However, the yields for the key reactions were low (< 35% for both the Grignard and phenyl lithium additions; no yield was reported for the reduction), indicating, unfortunately, that this route was not any more efficient than the previous route.

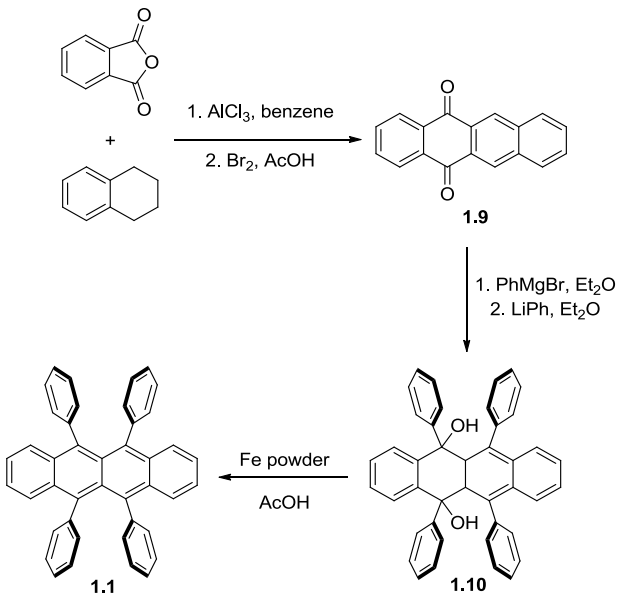

Scheme 1.4. Synthetic route to rubrene (**1.1**) employed by Allen and Gilman.

Working towards a more efficient route to both rubrene and its derivatives, Dodge et al. published two complementary syntheses from 1,3-diarylisobenzofurans in 1990 (Scheme 1.5).[32] The synthesis of these precursors began from treating 3-phenylphtahlide (**1.11**) with phenyl lithium followed by acetic anhydride providing 1,3-diphenylisobenzofuran **1.12**. Route A then combines the prepared isobenzofuran with 1,4-naphthoquinone **1.13** via a Diels-Alder reaction, then dehydration and oxidation to form the naphthacenequinone **1.14**. Nucleophilic addition into the quinone using two equivalents of an aryllithium afforded the diol **1.15,** similar to the previous synthesis discussed. Treatment of **1.15** with HI in refluxing diethyl ether yielded derivatives of **1.1**. Alternatively, Route B began by coupling **1.12** with (Z)-1,2-dibromoethene to obtain the

dibromonaphthalene **1.16**, which was then transformed into a benzyne intermediate for participation in a Diels-Alder reaction with **1.11**, affording the oxo-bridged tetracene **1.17**. Removal of the oxo-bridge proved difficult, but optimized conditions were found which used aluminum tribromide and cesium iodide to give rubrene in 70-88% yields which was purified by column chromatography followed by recrystallization. These routes were a vast improvement over the previous ones because of the ability to form derivatives easily, achievement of higher yields (ranging from 45-99% depending on the substituents), and ease of rubrene purification.

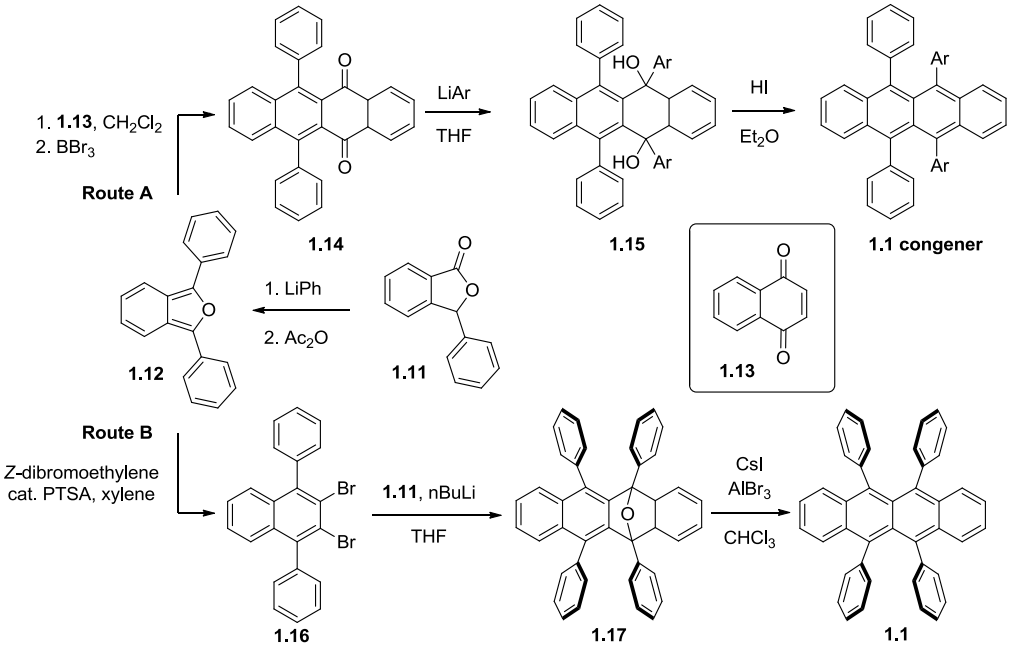

Scheme 1.5. Synthesis of rubrene (**1.1**) via Route A or Route B employed by Dodge et al.

In an effort to provide a simple and efficient route with a high purity product that could be used on large scale, Begley et al. filed a patent that proposed reacting a propargyl alcohol with methane sulfonyl chloride in the presence of triethyl amine (TEA) to form a chloride intermediate, followed by heating to form rubrene (Scheme 1.6).[33] Using similar reactions to the

first synthesis of rubrene, this route combined the formation of **1.3** and the electrocyclic dimerization into one step, thereby shortening the synthesis. However, after acidic workup and removal of solvent in vacuo, purification was simplified by treating the residue with a 1:1 solution of ether and methanol. Rubrene was precipitated out of the solution and collected in > 99% purity. Due to its similarity to the route published by Moureu, this last step likely gave very low yields, although no mention of yields was found.

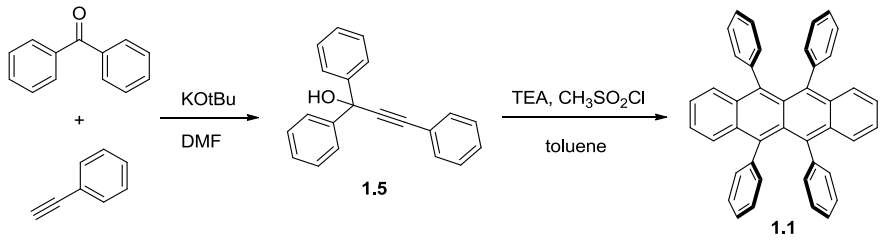

Scheme 1.6. Modification by Begley et al to the classical route to rubrene (**1.1**).

In 2011, Braga et al. discussed the synthetic details and mechanism of the classical route to rubrene.[34] They provided two slightly modified processes beginning from propargyl alcohol **1.5** to obtain rubrene: one in which the chloroallene was formed in situ followed by heating (Scheme 1.7a), another in which the chloroallene **1.4** was isolated and then heated (Scheme 1.7b). Both routes provided **1.1** in acceptable yield (40-60%).

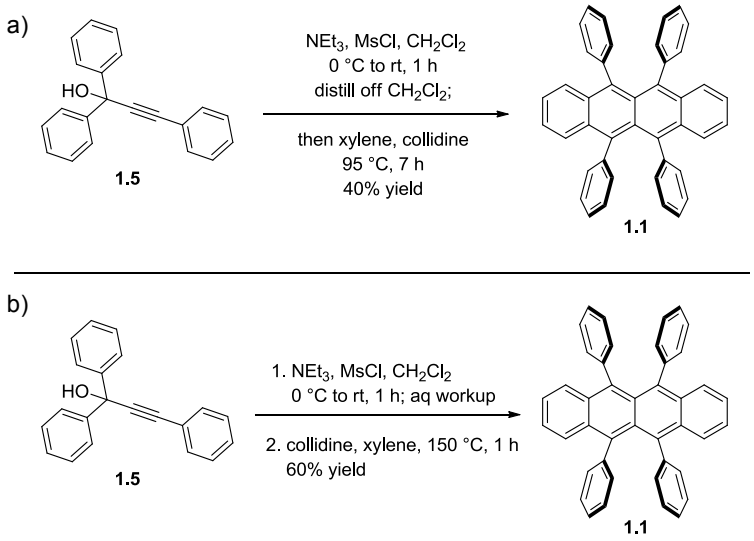

Scheme 1.7. a) One pot method and **b**) two step method to form rubrene (**1.1**) employed by Braga et al.

The variety of synthetic routes to rubrene illuminates the challenges in forming highly conjugated molecules efficiently and of high purity. Although all of the routes could give derivatives depending on the starting materials, only the routes by Allen and Gilman and Dodge et al provide rubrene derivatives with controlled placement of the substituents on the flanking phenyl rings, although the former suffers from low yields and the latter requires the introduction of one of the side phenyls early on in the synthesis, potentially limiting what substituents might be used. Efficient routes to rubrene and its derivatives are necessary for their study in electronic devices, in which the unique characteristics of rubrene influence the device performance. A new route to rubrene will be present in Chapter 3.

1.2 MOLECULAR AND SOLID-STATE PROPERTIES OF RUBRENE

At its core, rubrene (**1.1**) is made of tetracene (**1.2**) and four side phenyls. Examining the molecular structure computationally, the Brédas group found that in the neutral molecules the

shapes and energies of the highest occupied and lowest unoccupied molecular orbitals (HOMO and LUMO) are very similar between rubrene (**1.1**) and tetracene (**1.2**, Figure 1.2).[35] This similarity indicates that the molecular orbitals of the side phenyls have little mixing with the orbitals of the backbone, likely due to the side phenyls being orthogonal to the core. The HOMO and LUMO levels were calculated to be –4.69 eV and –2.09 eV respectively for rubrene and –4.87 and –2.09 eV respectively for tetracene. Experimentally, the ionization energy was measured at 4.9 eV,[36,37] which agrees well with the calculated HOMO level. The HOMO and LUMO levels of both rubrene **1.1** and tetracene **1.2** make these molecules susceptible to reaction with singlet oxygen, thereby forming an endoperoxide structure (**1.17** and **1.18**, Figure 1.2d,h respectively).[38] Endoperoxide formation is a major problem to be avoided during the fabrication of single-crystal OFET. Although the electronics of rubrene **1.1** and tetracene **1.2** are similar by calculation, their performance as semiconductors, specifically as single-crystal semiconductors, is quite different, indicating intermolecular interactions in the solid state play a role in their semiconducting properties.

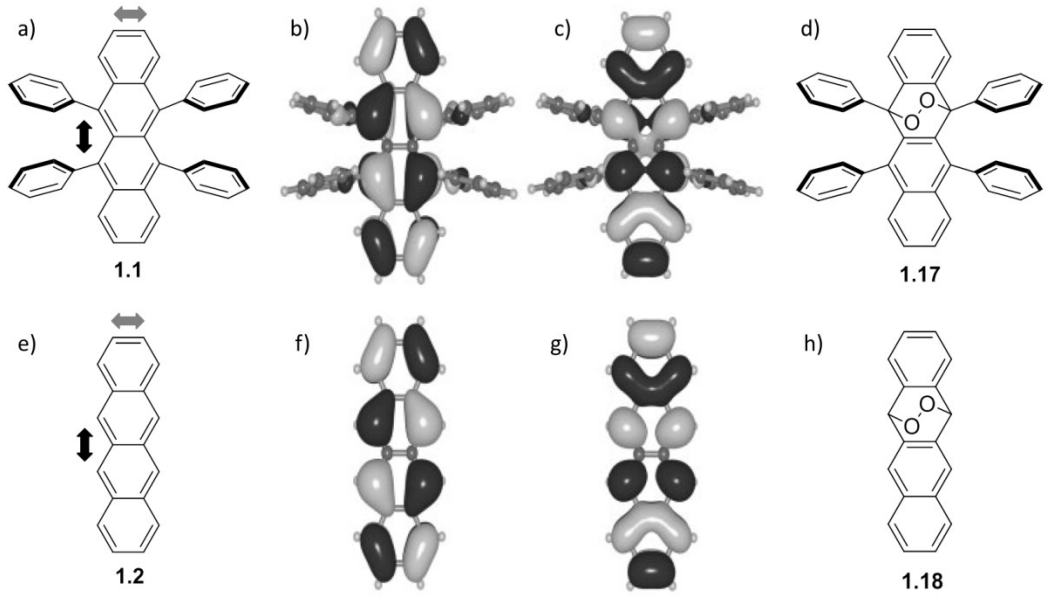

Figure 1.2. Comparison of rubrene (**1.1**, top) and tetracene (**1.2**, bottom). Molecular structures **a**) rubrene (**1.1**), **d**) rubrene endoperoxide (**1.17**) **e**) tetracene (**1.2**), **h**) tetracene endoperoxide (**1.18**). Black and grey arrows indicate molecular long and short axes respectively. Frontier orbital diagram of rubrene **b**) HOMO, **c**) LUMO and tetracene **f**) HOMO, **g**) LUMO (adapted images[35]).

The solid-state structure of rubrene has been found to adopt a variety of motifs; these related crystal settings are referred to as polymorphs. The unit cell constants for these polymorphs found in the Cambridge Crystallographic Database (Table 1.1) differ notably between the systems (triclinic, monoclinic, orthorhombic), but the polymorphs in the orthorhombic setting are quite similar, indicating similarity in their packing motifs.[39–45]

Table 1.1. Polymorphic crystal settings of rubrene **1.1.**

Crystal system	**Triclinic**	**Triclinic**	**Monoclinic**	**Monoclinic**
Space group	P-1[a]	P-1	$P2_1/c$	$P2_1/a$
Unit cell dimensions	a = 9.15 Å	a = 7.0196(14) Å	a = 8.7397(17) Å	a = 15.5 Å
	b = 11.60 Å	b = 8.5432(17) Å	b = 10.125(2) Å	b = 10.1 Å
	c = 7.16 Å	c = 11.948(2) Å	c = 15.635(3) Å	c = 8.8 Å
	α = 103.53°	α = 93.04(3)°	α = 90°	α = 90°
	β = 112.97°	β = 105.58(3)°	β = 90.98(3)°	β = 90.55°
	γ = 90.98°	γ = 96.28(3)°	γ = 90°	γ = 90°
Volume	675.279 $Å^3$	683.504 $Å^3$	1383.33 $Å^3$	1377.577 $Å^3$
Temperature	283-303 K	173 K	173 K	283-303 K
Crystal system	**Orthorhombic**	**Orthorhombic**	**Orthorhombic**	**Orthorhombic**
Space group	Aba2	Bbam	Bbcm	Cmca
Unit cell dimensions	a = 14.44 Å	a = 7.184(1) Å	a = 7.175(2) Å	a = 26.860(10) Å
	b = 7.18Å	b = 14.433(3) Å	b = 14.435(4) Å	b = 7.193(3) Å
	c = 26.97 Å	c = 26.897(7) Å	c = 26.812(7) Å	c = 14.433(5) Å
	$\alpha = \beta = \gamma$ = 90°	$\alpha = \beta = \gamma$ = 90°	$\alpha = \beta = \gamma$ = 90°	$\alpha = \beta = \gamma$ = 90°
Volume	2796.23 $Å^3$	2788.86 $Å^3$	2776.95 $Å^3$	2788.51 $Å^3$
Temperature	283-303 K	283-303 K	293 K	293 K

[a]Proposed space group based on reported data.

In the orthorhombic system, rubrene adopts a conformation that enhances charge carrier mobility. Although all of the orthorhombic space groups exhibit similar features, this discussion will focus on rubrene in the Cmca crystal structure. In this setting, rubrene has a planar tetracene core with the side phenyls twisted about ~85° away from the plane of the backbone (Figure 1.3b,d).[35] The side phenyls also distort away from the plane of the backbone by tilting ~15°, with one phenyl above and one phenyl below the plane of the core on either side of the tetracene backbone (Figure 1.3c). This orientation allows rubrene to adopt a herringbone packing motif within the solid-state. Within this motif, rubrene molecules align to minimize steric and electronic interactions.

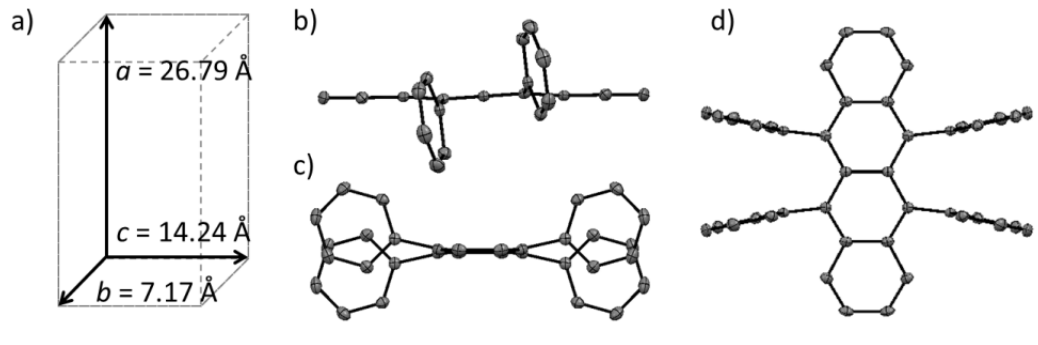

Figure 1.3. a) Unit cell parameters of rubrene Cmca crystal structure. Crystal structure of rubrene viewed down **b**) molecular short axis and **c**) molecular long axis. **d**) Crystal structure of rubrene showing the orthogonal relationship between the tetracene core and the side phenyls. Hydrogen atoms omitted for clarity.

In many herringbone packed acenes, displacement along both the molecular long and short axes occurs, respectively known as pitch and roll displacement, and edge-to-face interactions usually dominate.[46] Interestingly, examining the *b-c* plane of the rubrene crystal structure (Figure 1.4a) reveals that rubrene is dominated by face-to-face interactions between the tetracene cores, arising from the absence of roll displacement (Figure 1.4b). This orientation maximizes the overlap of the backbone π-orbitals at a distance of 3.68 Å. Alternatively, rubrene exhibits a pitch displacement of 6.17 Å (Figure 1.4c). Examining the *a-c* plane of the crystal structure (Figure 1.4d) shows the π-stacking layers to be 13.41 Å apart, arising from the accommodation of the side phenyls. These different aspects of the solid-state structure influence the electronic properties, and thereby performance, of the rubrene single crystal.

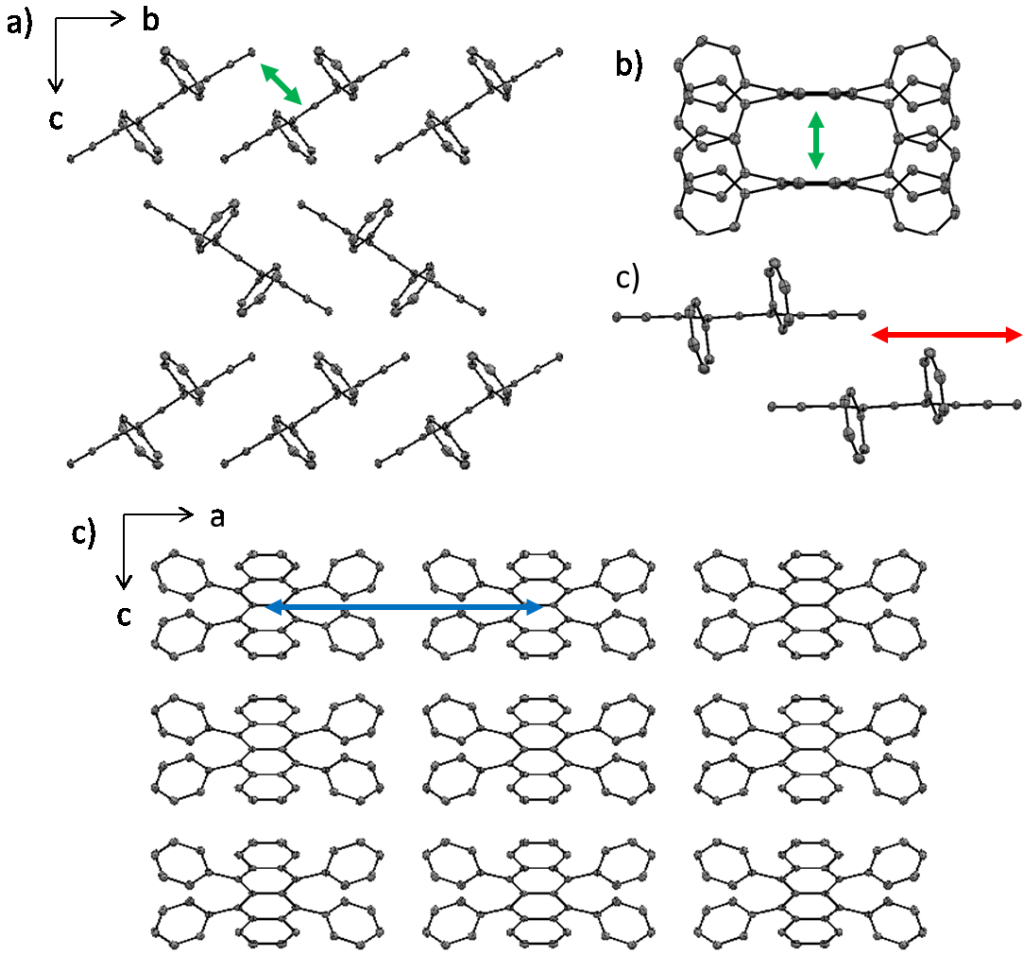

Figure 1.4. a) Rubrene crystal structure in the b-c plane. **b**) View of rubrene π-stacks down molecular long axis. **c**) View of rubrene π-stacks down molecular short axis. **d**) Rubrene crystal structure in the *a-c* plane. Green arrows indicate π-stacking distance of 3.68 Å, red arrow indicates pitch displacement distance of 6.17 Å, and blue arrow indicates interlayer distance of 13.41 Å. Distances for –100 °C X-ray Diffraction data.[41] Hydrogen atoms omitted for clarity.

From the solid-state packing structure, calculations can be performed to predict the electrical properties of a material. One of the most indicative calculations for charge transport is the intermolecular electronic coupling (transfer integral). This coupling represents the propensity for charge to transfer between neighboring molecules; thus, molecules with larger propensities

should yield higher charge carrier mobilities. For rubrene **1.1**, the transfer integrals were found to be about 340 and 160 meV for holes and electrons, respectively, along the π-stacking axis, while the values were negligible in all other directions.[35] The orientation of the molecules in the solid-state structure of rubrene coincides with large wave function overlap in the oscillations of both the HOMO and LUMO, which gives rise to the significant electronic couplings.

When performing electrical measurements on single crystal organic semiconductors, the quality and purity of the crystal is of upmost importance. A number of techniques have been developed to form suitable crystals via solution phase, vapor phase, or melt growth.[47] The choice of method depends upon the interactions exhibited by the individual molecules. In the case of rubrene, physical vapor transport (Figure 1.5) has proven effective in forming crystals for study in OFET.[48] This technique was developed to not only form suitable crystals of the organic material, but also to crystallize the organic material away from impurities.[49] Using a tube surrounded by heating coils that are on a temperature gradient, the organic semiconductor begins at the source (vaporization region) and is gradually heated until it sublimes. The flow of the carrier gas then moves the sublimed material down the tube where the lower temperature of the heating coils allows the material to crystallize (growth region) while the impurities continue further down the tube (light impurity region). This method purifies the organic semiconductor based on the different sublimation temperatures of the impurities and the organic material – in the flow tube, the impurities and the organic semiconductor will solidify in different areas. Obtaining high quality and high purity crystals is essential for an accurate measurement of the electrical properties of the crystal, particularly when determining the intrinsic mobility of a material.

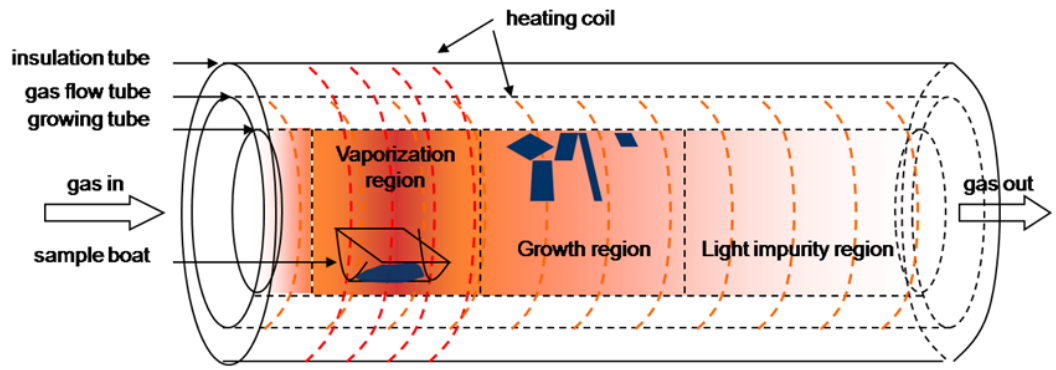

Figure 1.5. Schematic of physical vapor transport growth of a single crystal. Image courtesy of Dr. Yu Xia, Department of Chemical Engineering and Materials Science, University of Minnesota, Minneapolis, MN.

1.3 SINGLE-CRYSTAL OFET DEVICE PERFORMANCE OF RUBRENE

Although there are a variety of ways in which to fabricate OFET, the highest mobilities for rubrene have been achieved in single-crystal OFET. Such a device architecture allows for the intrinsic electronic properties of the organic material to be obtained due to the decreased imperfections and impurities in the single crystal as compared to thin-film devices.[24,50–52] The basic structure of a single-crystal OFET device consists of the following: a substrate, usually the polymer polydimethylsiloxane (PDMS); a dielectric layer, such as air or vacuum, the polymer polymethyl methacrylate (PMMA), or an ionic liquid; a source and drain electrode, often made of gold; and the single crystal material (Figure 1.6). To measure mobility in the semiconductor, a gate voltage is applied to the substrate to induce a layer of charge at the interface of the single crystal and dielectric layer. A drain voltage is then applied between the source and drain electrodes causing the built-up charge to move. By plotting the square root of the drain current from the saturation regime ($I_{D_{Sat}}$) with respect to gate voltage (V_{G}), one can obtain the charge carrier mobility (from the slope) and the threshold voltage (V_{T}, from extrapolation to the x-

intercept). This plot is described by Equation 1 in which $I_{D_{Sat}}$ is the drain current in the saturation regime, W is the channel width, L is the channel length, V_D is the drain voltage, V_G is the gate voltage, μ is the charge carrier mobility, V_T is the threshold voltage, and C_i is the capacitance (per unit area) of the insulator layer. The saturation regime occurs when V_D approaches V_G, causing the channel current to become independent of V_D.

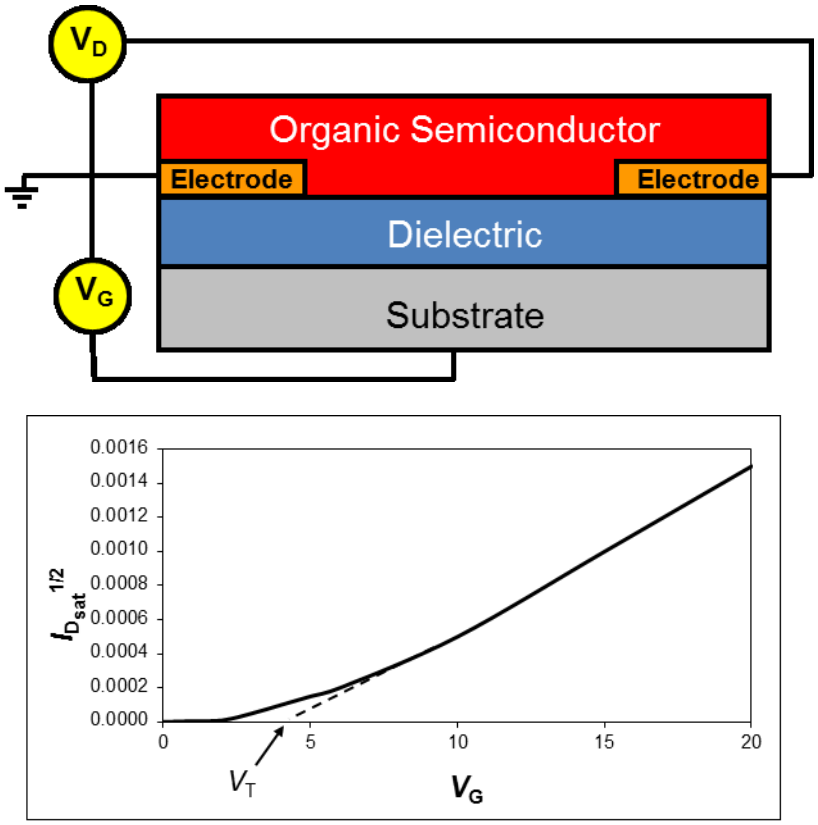

$$I_{D_{Sat}} = \frac{W}{2L} C_i \mu (V_G - V_T)^2, \qquad V_D > V_G - V_T \qquad (1)$$

Figure 1.6. Schematic of a single crystal OFET (top), example plot of the square root of $I_{D_{Sat}}$ versus V_G and Equation 1 (bottom).

One important aspect to consider when fabricating an OFET is the ability of charge to be injected into the semiconductor. This relies on the Fermi level of the electrodes and the HOMO-LUMO levels of the organic semiconductor.[53] The orientation of these levels determines the ease and preference of charge injection from the metal electrode to the semiconductor. When the HOMO is closer to the Fermi level, injection of holes is easier therefore the semiconductor is defined as p-type. Alternatively, when the LUMO is closer to the Fermi level, the semiconductor is said to be n-type because injection of electrons is easier. Some semiconductors may act as both p-type and n-type due to the position of their frontier orbitals; these are referred to as ambipolar. In the case of rubrene, the HOMO-LUMO levels are 1.1 eV and 1.57 eV apart from the Fermi level of gold respectively (in thin film), which indicates a preference for hole injection.[54] In most studies of rubrene, gold has been used as the electrode metal, likely due to beneficial alignment mentioned.

In the single crystal OFET architecture at room temperature, rubrene has consistently measured hole charge carrier mobilities on the order of 15 $cm^2V^{-1}s^{-1}$,[22,55] and as high as 20 $cm^2V^{-1}s^{-1}$ in vacuum gap devices.[56] However, the mobility changes with orientation of the crystal – higher mobility occurs along the *b*-axis (15.4 $cm^2V^{-1}s^{-1}$) as compared to the *c*-axis (4.4 $cm^2V^{-1}s^{-1}$) by at least a factor of two.[55] This anisotropy of mobility has been shown computationally to arise from a difference in the transfer integral along the two axes. This transfer integral, or the electronic coupling between neighboring molecules, describes the propensity for band-like charge transport in a given direction. Along the *b*-axis in rubrene, the transfer integral was calculated to be about 340 and 160 meV for holes and electrons respectively, while the transfer integral along the *c*- and *a*-axes were found to be negligible.[35] Although discrepancies exist between theory and practice, the computational data, while an imperfect fit, supports the experimental observations.

The amount of orbital overlap influences the magnitude of the transfer integral, thus the largest transfer integral occurs in the π-stacking direction.[57] Essentially this high amount of uniform π-orbital overlap between molecules forms a network through which the induced charge can travel.[58] The total intramolecular reorganization energy, which describes the rate of transport in the hopping regime, was found to be 159 meV, much greater than tetracene (114 meV). Both the transfer integral and reorganization energy values are quite high even though rubrene exhibits pitch displacement. To explain this, Filho et al correlated the transfer integral oscillations in the HOMO and LUMO as the pitch displacement changes. They found the pitch displacement distance (6.17 Å) corresponds to a local maxima in the oscillations. Clearly the components of the crystal structure are poised to effect high charge transport in rubrene.

When mobility measurements were collected with varied temperature in the vacuum gap architecture, rubrene single crystals revealed hole mobilities that increased to ~30 $cm^2V^{-1}s^{-1}$ as temperature decreased to ~150 K, after which mobility decreased with decreasing temperature.[22] Podzorov et al indicated that this change in mobility is accompanied by change in the anisotropy – at higher temperatures the mobility is anisotropic, but at temperatures below ~150 K the anisotropy vanishes. The disappearance of anisotropic mobility corresponds to the low temperature regime being dominated by traps. Evidence of traps comes from the increase in threshold voltage with decreasing temperature. This interesting mobility profile of rubrene suggests two different forms of charge transport with temperature dependence – in the first regime (> ~150 K), the mobility is dominated by band-like or intrinsic transport while in the second regime (< ~150K) the mobility is dominated by activated or hopping transport (Figure 1.7). In this second regime, the trap-dominated regime, charge travels mostly through traps and due to the isotropic distribution of traps the mobility loses its anisotropy. Band dispersion at

room temperature has been supported by angle-resolved ultraviolet photoelectron spectroscopy measurements,[59] as well as observations of the Hall effect in rubrene single crystal OFETs.[60]

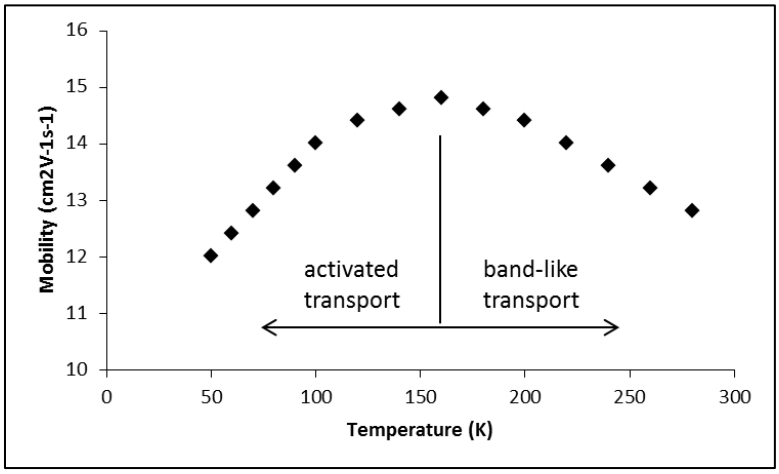

Figure 1.7. Schematic of temperature dependent band-like and activated transport regimes for rubrene charge carrier mobility.

The origin of this transition temperature (~150 K) has not yet been identified. Focused on single crystalline rubrene, an appropriate assumption would be that a phase transition occurs at this temperature in the crystal; however, there is no evidence of such a transition by X-ray Diffraction data.[41] Another proposed reason is the presence of static disorder or traps.[61] An alternative hypothesis was suggested after analysis of the rubrene single crystal by Raman spectroscopy revealed a broadening in the low-frequency peaks between 30-300 K with a significant broadening event ~150 K.[62] This broadening is supposed to be due to the disorder of the side phenyls of rubrene as they transition from one side of the tetracene core to the other. In later studies, the transition temperature in rubrene has been found to be sample dependent, signifying the origin of this point is likely due to a change in the crystal structure.[63] Although

whether the difference in samples stems from the varied presence of traps across samples or the propensity for some of the crystals to undergo a subtle physical change remains to be determined.

Studies into the charge mobility of rubrene continue to provide insight into the fundamental aspects of charge transport in organic semiconductors. However, few studies have successfully explored structure-property relationship studies on rubrene derivatives. In the work that follows, rubrene has been functionalized in a variety of ways and examined for the effect of these alterations on charge carrier mobility. Each chapter includes a discussion of the specific modifications made to the rubrene structure, the synthetic plan and execution, as well as a brief analysis of device performance as determined by project collaborators. The endeavors outlined in this dissertation demonstrate the feasibility of structure-property relationship studies of rubrene as well as the significance of these studies in the development of future organic semiconductors.

1.4 REFERENCES

(1) Hercules, D. M. *Science* **1964**, *145*, 808–809.

(2) Omer, K. M.; Bard, A. J. *J. Phys. Chem. C* **2009**, *113*, 11575–11578.

(3) Vinyard, D. J.; Su, S.; Richter, M. M. *J. Phys. Chem. A* **2008**, *112*, 8529–8533.

(4) Rodríguez-López, J.; Shen, M.; Nepomnyashchii, A. B.; Bard, A. J. *J. Am. Chem. Soc.* **2012**, *134*, 9240–9250.

(5) Kytka, M.; Gerlach, A.; Schreiber, F.; Kováč, J. *Appl. Phys. Lett.* **2007**, *90*, 131911.

(6) Fumagalli, E.; Raimondo, L.; Silvestri, L.; Moret, M.; Sassella, A.; Campione, M. *Chem. Mater.* **2011**, *23*, 3246–3253.

(7) Uttiya, S.; Raimondo, L.; Campione, M.; Miozzo, L.; Yassar, A.; Moret, M.; Fumagalli, E.; Borghesi, A.; Sassella, A. *Synth. Met.* **2012**, *161*, 2603–2606.

(8) Yee, W. A.; Kuzmin, V. A.; Kliger, D. S.; Hammond, G. S.; Twarowski, A. J. *J. Am. Chem. Soc.* **1979**, *101*, 5104–5106.

(9) Wilson, T. *J. Am. Chem. Soc.* **1969**, *91*, 2387–2388.

(10) Rauhut, M. M.; Roberts, B. G.; Semsel, A. M. *J. Am. Chem. Soc.* **1966**, *88*, 3604–3617.

(11) Adam, W.; Cueto, O.; Yany, F. *J. Am. Chem. Soc.* **1978**, *100*, 2587–2589.

(12) Larena, A.; Martinez-Urreaga, J. *Spectrosc. Lett.* **1985**, *18*, 463–472.

(13) Sakamoto, G.; Adachi, C.; Koyama, T.; Taniguchi, Y.; Merritt, C. D.; Murata, H.; Kafafi, Z. H. *Appl. Phys. Lett.* **1999**, *75*, 766–768.

(14) Zhi-lin, Z.; Xue-yin, J.; Shao-hong, X.; Nagatomo, T.; Omoto, O. *J. Phys. Appl. Phys.* **1998**, *31*, 32.

(15) Xue, Q.; Xie, G.; Chen, P.; Lu, J.; Zhang, D.; Tang, Y.; Zhao, Y.; Hou, J.; Liu, S. *Synth. Met.* **2010**, *160*, 829–831.

(16) Taima, T.; Sakai, J.; Yamanari, T.; Saito, K. *Sol. Energy Mater. Sol. Cells* **2009**, *93*, 742–745.

(17) Perez, M. D.; Borek, C.; Forrest, S. R.; Thompson, M. E. *J. Am. Chem. Soc.* **2009**, *131*, 9281–9286.

(18) Moureu, C.; Dufraisse, C.; Dean, P. M. *Comptes Rendus Hebd. Seances Acad. Sci.* **1926**, *182*, 1440–1443.

(19) Podzorov, V.; Pudalov, V. M.; Gershenson, M. E. *Appl. Phys. Lett.* **2003**, *82*, 1739–1741.

(20) Wang, C.; Dong, H.; Hu, W.; Liu, Y.; Zhu, D. *Chem. Rev.* **2011**.

(21) Newman, C. R.; Frisbie, C. D.; da Silva Filho, D. A.; Bredas, J.-L.; Ewbank, P. C.; Mann, K. R. *Chem. Mater.* **2004**, *16*, 4436–4451.

(22) Podzorov, V.; Menard, E.; Borissov, A.; Kiryukhin, V.; Rogers, J. A.; Gershenson, M. E. *Phys. Rev. Lett.* **2004**, *93*, 086602.

(23) Garnier, F. *Chem. Phys.* **1998**, *227*, 253–262.

(24) De Boer, R. W. I.; Gershenson, M. E.; Morpurgo, A. F.; Podzorov, V. *Phys Status Solidi* **2004**, *201*, 1302–1331.

(25) Landor, P. D.; Landor, S. R. *J. Chem. Soc. Resumed* **1963**, 2707–2711.

(26) Rigaudy, J.; Capdevielle, P. *Tetrahedron.* **1977**, *33*, 767–773.

(27) Gajewski, J. J.; Shih, C. N. *J. Am. Chem. Soc.* **1972**, *94*, 1675–1682.

(28) Gajewski, J. J.; Shih, C. N. *J. Am. Chem. Soc.* **1967**, *89*, 4532–4533.

(29) Wittig, G.; Waldi, D. *J. Prakt. Chem.* **1942**, *160*, 242–244.

(30) Allen, C. F. H.; Gilman, L. *J. Am. Chem. Soc.* **1936**, *58*, 937–940.

(31) Fieser, L. F. *J. Am. Chem. Soc.* **1931**, *53*, 2329–2341.

(32) Dodge, J.; Bain, J. D.; Chamberlin, A. R. *J. Org. Chem.* **1990**, *55*, 4190–4198.

(33) Begley, W. J.; Rajeswaran, M.; Andrievsky, N. Process for preparing triphenylnaphthacene compound. US 20060025642A1, February 2, 2006.

(34) Braga, D.; Jaafari, A.; Miozzo, L.; Moret, M.; Rizzato, S.; Papagni, A.; Yassar, A. *Eur. J. Org. Chem.* **2011**, 4160–4169.

(35) Filho, D. A. da S.; Kim, E.-G.; Brédas, J.-L. *Adv. Mater.* **2005**, *17*, 1072–1076.

(36) Nakayama, Y.; Uragami, Y.; Machida, S.; Koswattage, K. R.; Yoshimura, D.; Setoyama, H.; Okajima, T.; Mase, K.; Ishii, H. *Appl. Phys. Express* **2012**, *5*, 111601.

(37) Nakayama, Y.; Machida, S.; Minari, T.; Tsukagishi, K.; Noguchi, Y.; Ishii, H. *Appl. Phys. Lett.* **2008**, *93*, 173305.

(38) Schmidt, R.; Brauer, H.-D. *J. Photochem.* **1986**, *34*, 1–12.

(39) El Helou, M.; Medenbach, O.; Witte, G. *Cryst. Growth Des.* **2010**, *10*, 3496–3501.

(40) Huang, L.; Liao, Q.; Shi, Q.; Fu, H.; Ma, J.; Yao, J. *J. Mater. Chem.* **2009**, *20*, 159–166.

(41) Jurchescu, O. D.; Meetsma, A.; Palstra, T. T. M. *Acta Crystallogr. Sect. B* **2006**, *B62*, 330–334.

(42) Bulgarovskaya, I.; Vozzhennikov, V.; Aleksandrov, S.; Belsky, V. *Latv. PSR Zinātņu Akadēmijas Vēstis Fiz. Un Teh. Zinātņu Sērija* **1983**, 53–59.

(43) Henn, D. E.; Williams, W. G.; Gibbons, D. J. *J. Appl. Crystallogr.* **1971**, *4*, 256–256.

(44) Akopyan, R. L.; Kitaigordskii, A. I.; Struchkov, Y. T. *Zhurnal Strukt. Khimii* **1962**, *3*, 602–605.

(45) Taylor, W. H. *Z. Krist. Krist. Krist. Krist.* **1936**, *93*, 151.

(46) Curtis, M. D.; Cao, J.; Kampf, J. W. *J. Am. Chem. Soc.* **2004**, *126*, 4318–4328.

(47) Jiang, H.; Kloc, C. *MRS Bull.* **2013**, *38*, 28–33.

(48) Kim, K.; Kim, M. K.; Kang, H. S.; Cho, M. Y.; Joo, J.; Kim, J. H.; Kim, K. H.; Hong, C. S.; Choi, D. H. *Synth. Met.* **2007**, *157*, 481–484.

(49) Laudise, R. .; Kloc, C.; Simpkins, P. .; Siegrist, T. *J. Cryst. Growth* **1998**, *187*, 449–454.

(50) Gershenson, M. E.; Podzorov, V.; Morpurgo, A. F. *Rev. Mod. Phys.* **2006**, *78*, 973–989.

(51) Reese, C.; Bao, Z. *Mater. Today* **2007**, *10*, 20–27.

(52) Braga, D.; Horowitz, G. *Adv. Mater.* **2009**, *21*, 1473–1486.

(53) Horowitz, G. In *Organic Electronics, Materials, Manufacturing and Applications*; Wiley-VCH Verlag GmbH & Co. KGaA: Weinheim, 2006; pp. 3–32.

(54) Ding, H.; Gao, Y. *Appl. Phys.* **2009**, *95*, 89–94.

(55) Sundar, V. C.; Zaumseil, J.; Podzorov, V.; Menard, E.; Willett, R. L.; Someya, T.; Gershenson, M. E.; Rogers, J. A. *Science.* **2004**, *303*, 1644–1646.

(56) Menard, E.; Podzorov, V.; Hur, S.-H.; Gaur, A.; Gershenson, M. E.; Rogers, J. A. *Adv. Mater.* **2004**, *16*, 2097–2101.

(57) Brédas, J. L.; Calbert, J. P.; Filho, D. S.; A, D.; Cornil, J. *Proc. Natl. Acad. Sci.* **2002**, *99*, 5804–5809.

(58) Mas-Torrent, M.; Rovira, C. *Chem. Rev.* **2011**, *111*, 4833–4856.

(59) Machida, S.; Nakayama, Y.; Duhm, S.; Xin, Q.; Funakoshi, A.; Ogawa, N.; Kera, S.; Ueno, N.; Ishii, H. *Phys. Rev. Lett.* **2010**, *104*, 156401.

(60) Podzorov, V.; Menard, E.; Rogers, J. A.; Gershenson, M. E. *Phys. Rev. Lett.* **2005**, *95*, 226601.

(61) Minder, N. A.; Ono, S.; Chen, Z.; Facchetti, A.; Morpurgo, A. F. *Adv. Mater.* **2012**, *24*, 503–508.

(62) Ren, Z. Q.; McNeil, L. E.; Liu, S.; Kloc, C. *Phys. Rev. B* **2009**, *80*, 245211.

(63) Xie, W.; McGarry, K. A.; Liu, F.; Wu, Y.; Ruden, P. P.; Douglas, C. J.; Frisbie, C. D. *J. Phys. Chem. C* **2013**, *117*, 11522–11529.

2 SYNTHESIS OF RUBRENE-D_{28}

2.1 BACKGROUND

Recently, the study of organic electronics has expanded research into spintronics. Spintronics takes advantage of the charge as well as the spin of the electron, which allows for the development of devices that combine logic operations, storage and communication.[1] This field first emerged in 1988 when giant magnetoresistance was discovered, followed by the development of the spin-valve in the early 1990s.[2] Spin devices function based on the effect of magnetism on the flow of electrons.[3] Electrons of opposite spins flow identically in a normal metal, but the application of a magnet causes the electrons to experience different resistance depending on the alignment of their spin with the magnetization. In a spin valve (Figure 2.1), a non-magnetic material is placed between two ferromagnetic contacts. These contacts provide a source of spin-polarized electrons for spin injection.[4] When the contacts have opposite or antiparallel spin, device resistance is high; when the contacts have the same or parallel spin, device resistance is low.[1] An applied external magnetic field controls the antiparallel or parallel configuration between the two contacts.

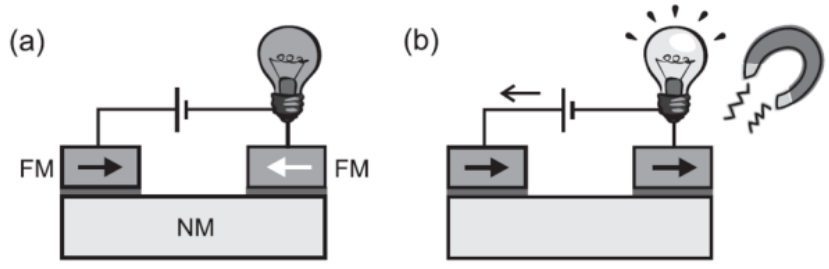

Figure 2.1. Diagram of a spin valve.[1] A non-magnetic (NM) spacer (bottom) separates two ferromagnetic (FM) contacts (magnetization denoted by arrows). One contact acts as the spin injector, the other acts as the spin detector. The light bulb indicates **a**) low conductance when the magnets have antiparallel spin and **b**) large conductance when the magnets have parallel spin. An organic spintronic would be formed when the NM spacer is an organic semiconductor.

In organic spintronics, the non-magnetic material could be an organic semiconductor. One of the features that make organics attractive for this application is the extended time that the spin polarization of carriers can be maintained.[4,5] In inorganic semiconductors, the spin relaxation time is limited while in organic semiconductors, this parameter is enhanced by the low spin-orbit coupling and hyperfine interactions.[1] Spin-orbit coupling generally increases with atomic number, thus organic materials composed of mostly carbon usually have small couplings. Hyperfine interactions originate from the interaction of the electron spin with the nuclear spins of the semiconductor, which tend to be weak in organic materials due to the high degree of π-conjugation and delocalized states. An important related parameter is the spin diffusion length of an organic material. The spin diffusion length has been measured in rubrene amorphous thin films to be 13.3 nm[6] (not yet measured in single crystals), which is moderate for a small molecule (for comparison, α-sexithiophene (Figure 2.2a) has a diffusion length of 70 nm[5]). A theoretical model has suggested that the charge carrier mobility of disordered thin films of organic semiconductors impacts the spin relaxation time, but not the spin diffusion length.[7] It has been speculated that the highly ordered nature of crystalline organic semiconductors might positively impact the spin parameters,[6] but single-crystal organic spintronics have yet to be realized.

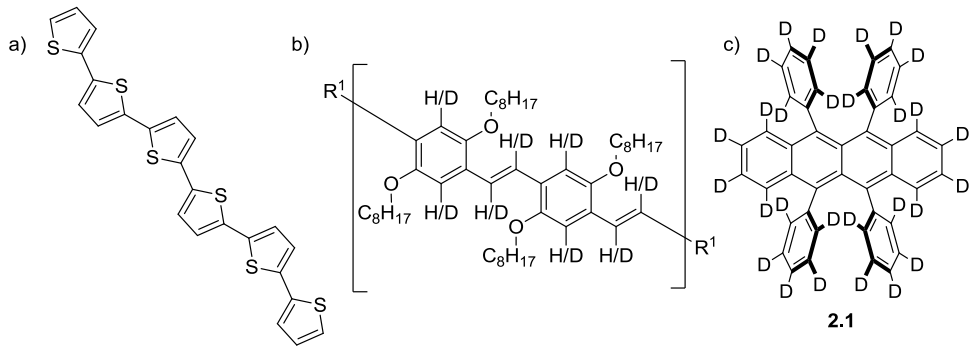

Figure 2.2. a) Molecular structure of small molecule α-sexithiophene. **b**) Molecular structure of protonated/deuterated polymer examined by Nguyen et al. **c**) Molecular structure of rubrene-d_{28} (**2.1**).

While examining the chemical versatility of an organic π-conjugated polymer (Figure 2.2b), Nguyen et al found that exchanging the protonated polymer for the deuterated version led to improved spin diffusion attributed to the weaker hyperfine interactions.[8] Based on this finding, and in anticipation of the development of single-crystal organic spintronics, we set out to synthesize rubrene-d_{28} (**2.1**, Figure 2.2c). This molecule would allow us to not only explore the effect of isotopic substitution on the charge carrier mobility of rubrene, but also delineate the effect of deuteration on spin transport in small molecule single crystals.

2.2 RESULTS AND DISCUSSION

2.2.1 Synthesis of rubrene-d_{28}

Examining Begley's synthesis for protonated rubrene,[9] we concluded that the starting materials for rubrene-d_{28} (**2.1**) via the deuterated propargyl chloride (**2.2**), benzophenone-d_{10} (**2.3**) and phenyl acetylene-d_5 (**2.4**), were too expensive to obtain commercially, but could be produced from a common precursor, bromobenzene-d_5 (**2.5**) (Scheme 2.1a). A seven-step synthesis was

therefore proposed to rubrene-d_{28}, which makes use of inexpensive and commercially available reagents, allowing us to scale up the synthesis as demanded for testing purposes (Scheme 2.1b).

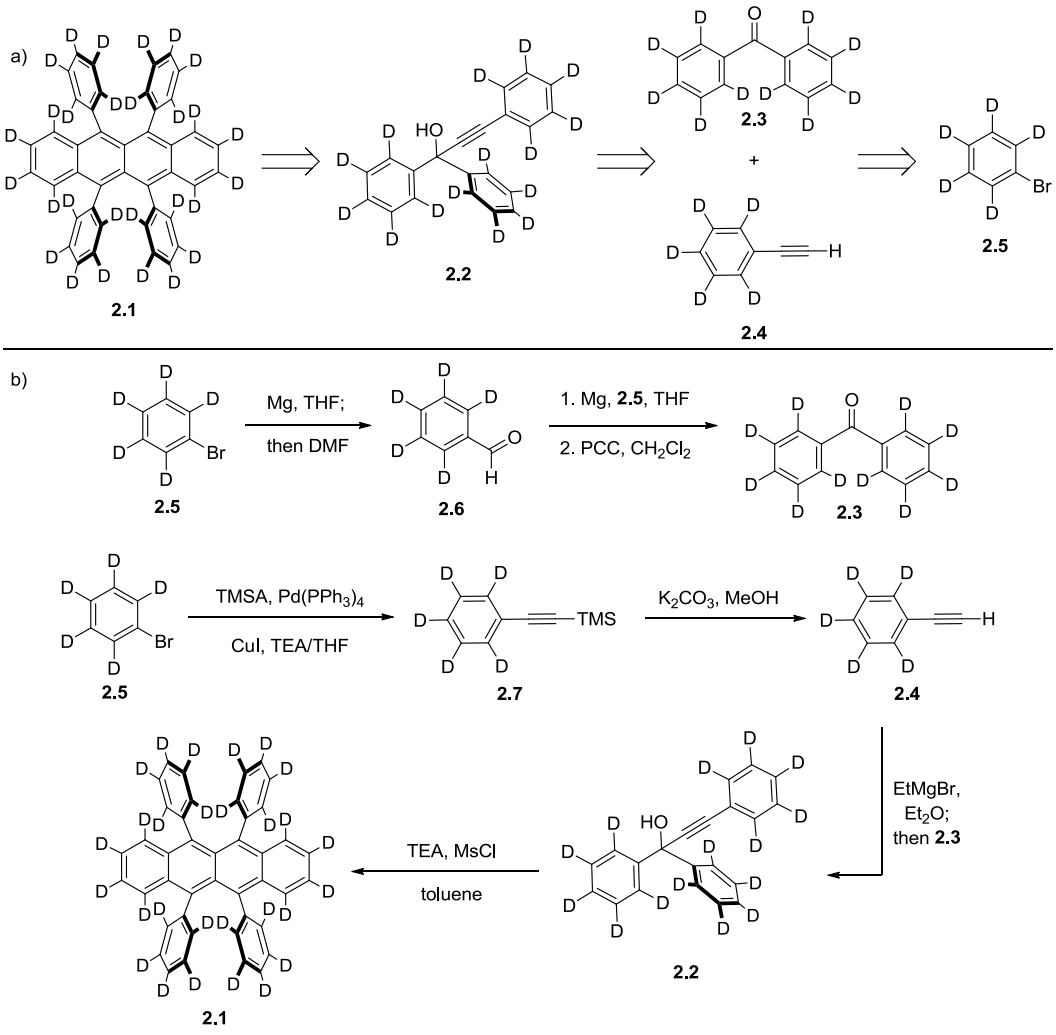

Scheme 2.1. a) Retrosynthetic analysis of rubrene-d_{28} (**2.1**). **b**) Forward synthetic sequence toward rubrene-d_{28}.

Initially, protonated compounds were used to optimize conditions. The synthesis began with commercially available bromobenzene, which was converted to benzaldehyde via the corresponding Grignard reagent. Treatment of benzaldehyde with phenyl magnesium bromide gave benzhydrol in 37% yield after two steps. Pyridinium chlorochromate (PCC) was selected

for the next reaction since it is amenable to scale up. Conversion of benzhydrol under neat conditions provided no product, but in the presence of dichloromethane and a mixture of 1:1 (m:m) PCC and Celite, benzophenone was obtained in 79% yield after column chromatography.

To obtain phenyl acetylene, a two-step sequence was envisioned beginning with a Sonogashira coupling between bromobenzene and (trimethylsilyl)acetylene (TMSA), followed by removal of the TMS group. However, the Sonogashira proved difficult and low yielding under a variety of conditions (Table 2.1). In an attempt to reproduce a literature procedure,[10] bis(triphenylphosphine)palladium(II) chloride was used as the catalyst, made in situ from palladium(II) chloride and triphenylphosphine (Entry 1). Obtaining no product, the next attempt used previously made $PdCl_2(PPh_3)_2$ which also resulted in no product, even upon adjusting the reaction time, temperature, and amount of copper(I) iodide (Entries 2 and 3). Use of $Pd(PPh_3)_4$[11] initially did not improve the results (Entries 4 and 5). However, adjusting the temperature and the time eventually did provide product, but in low yields (Entries 6–10). A maximum yield of 33% was obtained using 2% $Pd(PPh_3)_4$ and 4% CuI (Entry 10). Given such a low yield after initial optimization, a more efficient route was sought to synthesize rubrene.

Table 2.1. Conditions and results for the trials of the Sonogashira reaction between bromobenzene and (trimethylsilyl)acetyalene to form phenyl acetylene.

Entry	Catalyst	Temp (°C)	Time (h)	Pd mol %	Cu mol %	% Yield
1[a]	$PdCl_2(PPh_3)_2$[b]	35	48	2	2	0
2[a]	$PdCl_2(PPh_3)_2$	30	18	0.4	2	0
3	$PdCl_2(PPh_3)_2$	rt	22	2	4	0
4	$Pd(PPh_3)_4$	60	1	3	3	0
5	$Pd(PPh_3)_4$	30/60	24/62	3	3	0
6	$Pd(PPh_3)_4$	70	48	3	3	< 1
7	$Pd(PPh_3)_4$	30	19	50	100	16
8	$Pd(PPh_3)_4$	62	2	3	3	18
9	$Pd(PPh_3)_4$	50	4	3	3	22
10	$Pd(PPh_3)_4$	50/rt	5/18	2	4	33

Conditions: bromobenzene (1.0 equiv), (trimethylsilyl)acetylene (1.2 equiv), Pd catalyst, CuI, THF (0.63 M); [a]Reaction run in TEA (1.0 M); [b]Prepared in situ from PPh_3 and $PdCl_2$.

A new route was proposed in which the initial Grignard reactions to obtain **2.3** would still be OK, but the Sonogashira reaction of **2.4** was replaced with a Corey–Fuchs transformation of **2.6**, reducing the synthesis length by one step (Scheme 2.2).

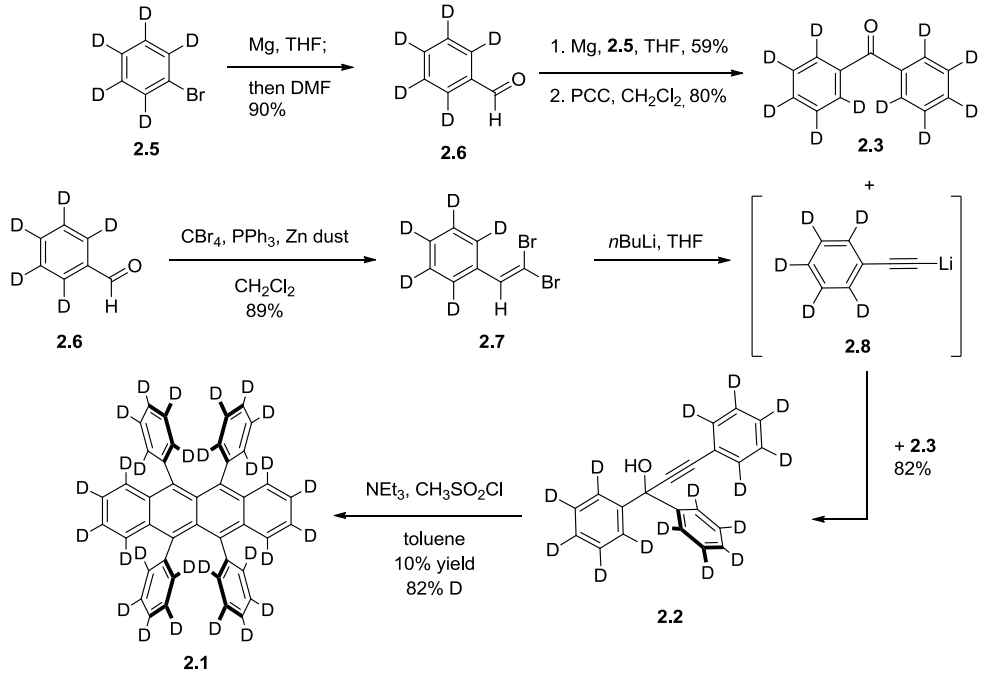

Scheme 2.2. New synthetic route to rubrene-d_{28} utilizing the Corey-Fuchs transformation.

Conditions for the Corey–Fuchs transformation were obtained from the original report.[12] Adding benzaldehyde to pre-mixed carbon tetrabromide and triphenylphosphine in the presence of zinc dust provided (2,2-dibromovinyl)benzene (**2.7**) in 71% yield after workup. This dibromo olefin underwent elimination and lithium-halogen exchange with *n*-butyl lithium (*n*BuLi) to generate lithium phenyl acetylide (**2.8**) in situ. Benzophenone was then added to the reaction to

afford 1,1,3-triphenylprop-2-yn-1-ol (**2.2**) in 76% yield. The Corey–Fuchs transformation not only improved the efficiency of the synthesis by giving higher yields, but also reduced the total number of steps, making this a more desirable route to rubrene. With the protonated propargyl alcohol having been obtained, the rubrene-forming dimerization was attempted. Following Begley's isolation procedure,[9] rubrene was obtained without difficulty, although in low yield (16% for the last step).

Having successfully prepared rubrene via the planned route, the procedure was then applied to rubrene-d_{28}. Beginning from bromobenzene-d_5 (> 99% deuterium), the reactions were performed in the same manner as the protonated synthesis and provided comparable yields in most cases. However, during the formation of the propargyl alcohol **2.2**, another compound, determined to be (*E*)-1,1,3-triphenylprop-2-en-1-ol (**2.9**, Scheme 2.3), was also obtained. This compound was identified by the diagnostic signals in the ^{1}H NMR as compared to the protonated analogue[13] – δ 6.86 (d, J = 15.9 Hz, 1H), 6.67 (d, J = 15.9 Hz, 1H), 2.49 (s, 1H, OH). These peaks confirmed that only the *E* isomer of **2.9** was formed in a 1:6 ratio to **2.2** based on the integration of the alcohol OH signal in the crude ^{1}H NMR. The formation of this byproduct made isolation of **2.2** very difficult: both column chromatography and selective precipitation proved in sufficient in separating the compounds. The mixture of alkene **2.9** and **2.2** was eventually taken on to the next reaction, successfully affording rubrene-d_{28} (**2.1**) in 10% yield after purification. To avoid this byproduct in the penultimate step, **2.7** was reacted with *n*BuLi at –78 °C for 1 h instead of 4 h. Compound **2.9** was not observed by ^{1}H NMR using this improved procedure; however, a different byproduct was seen and determined to be **2.10** from the diagnostic signals in the ^{1}H NMR as compared to the protonated analogue[14] – δ 6.39 (dt, J = 15.8, 1.3 Hz, 1H), 6.23

(dt, J = 15.8, 6.7 Hz, 1H), 2.20 (q, J = 6.8 Hz, 2H). This byproduct was a minor component (< 20%) and could be separated from **2.2** by column chromatography.

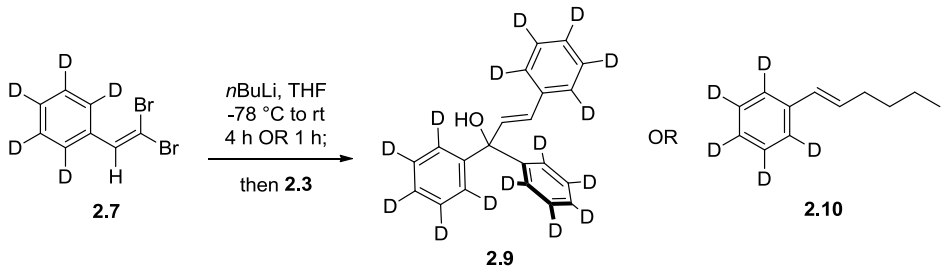

Scheme 2.3. Observed byproducts **2.9** and **2.10** in the Corey-Fuchs reaction depending on reaction time.

Percent deuterium incorporation was calculated for rubrene-d_{28} via ^{1}H NMR using an internal standard of CH_2Cl_2 and was determined to be 82%. Since the calculated deuterium incorporation for the intermediates in the synthesis were all greater than 98 percent, this value was most likely affected by the generation of HCl in the last reaction, which could exchange with deuterium in **2.1**. NMR analysis of the final product revealed certain locations on rubrene to be preferentially exchanged over others. These locations are denoted in Figure 2.3 by asterisks.

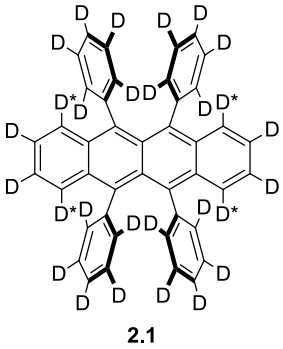

Figure 2.3. Probable locations of deuterium-proton exchange (denoted by asterisk) on **2.1** as determined by ^{1}H NMR.

A few adjustments were made to the synthesis in order to improve the deuterium incorporation of the last step (Scheme 2.4). To ensure that minimal amounts of HCl were formed

during the dimerization, the hydrogen of the alcohol in **2.2** was replaced with deuterium by washing the compound with D_2O to form **2.11**.

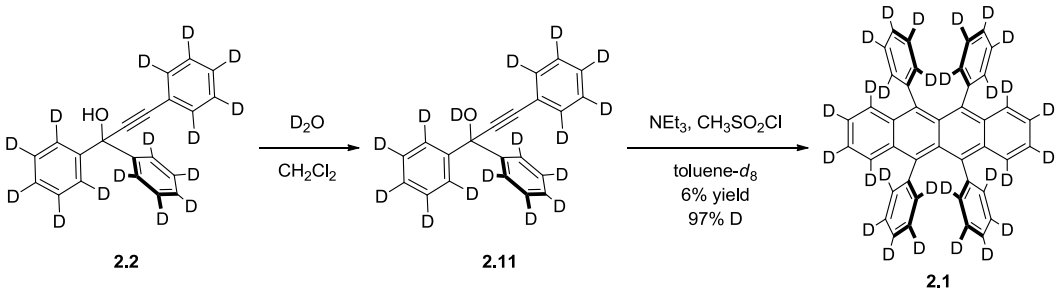

Scheme 2.4. Improvements to the final sequence in the synthesis of rubrene-d_{28} **2.1**.

Using the fully deuterated **2.11** instead of **2.2** in the next reaction produced DCl rather than HCl, allowing the high deuterium incorporation to be retained. Also as a precaution, the reaction was performed in toluene-d_8 to ensure that exchange can only take place between deuterium. The product was obtained in 6% yield and deuterium incorporation was found to be 97% by ^{1}H NMR.[15] The IR spectrum shows the expected shift of the C-D stretches in rubrene-d_{28} **2.1** at 2266 cm^{-1} as compared to the C-H stretches in rubrene **1.1** at 3077 cm^{-1} (Figure 2.4). In the fully deuterated system, we did observe a slight decrease in reaction rate based on the percent yield – after reaction for four hours followed by the same workup procedure, the protonated series provided 16% while the perdeuterated version provided 6%. However, quantitative KIE studies were not performed.

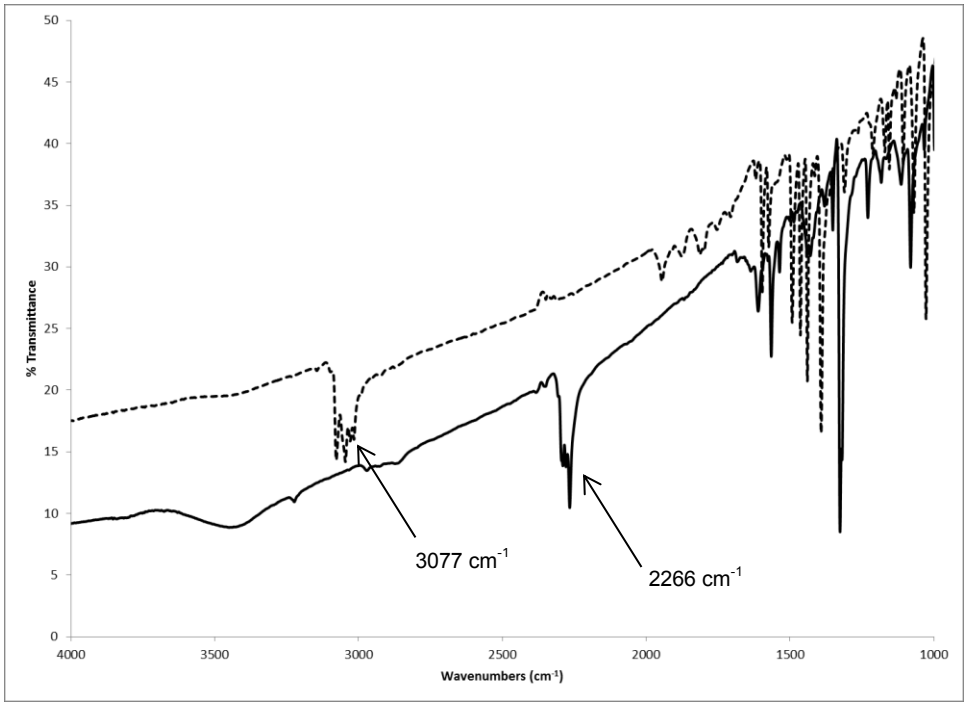

Figure 2.4. IR spectra (KBr pellet) of rubrene **1.1** (dashed line) and rubrene-d_{28} **2.1** (solid line).

2.2.2 Single-crystal OFET device performance of Rubrene-d_{28}

With rubrene-d_{28} in hand, our collaborators were now prepared to make electrical measurements on this material. Crystals were first grown using physical vapor transport (see Chapter 1.2) from the red powder that we obtained via synthesis. The crystals obtained were red/orange plates very similar in appearance to those grown from rubrene. The rubrene-d_{28} crystals were confirmed to pack in the same setting as rubrene based on out-of-plane and in-plane X-ray diffraction as discussed in the manuscript.[16] The similarity of the crystal structure implies that any differences observed in the comparison of the electrical properties of rubrene-d_{28} to rubrene could be attributed to deuteration.

In the single-crystal air-gap OFET architecture (see Figure 1.6, Chapter 1), **2.1** measured mobilities in the range 12.2 to 16.5 $cm^2V^{-1}s^{-1}$ at room temperature, which are comparable to the range for **1.1**, suggesting no isotope effect occurs on the charge carrier mobility of rubrene. However, varying the temperature led to the discovery of three different sample-dependent trends that occurred in both **2.1** and **1.1** (Figure 2.4).

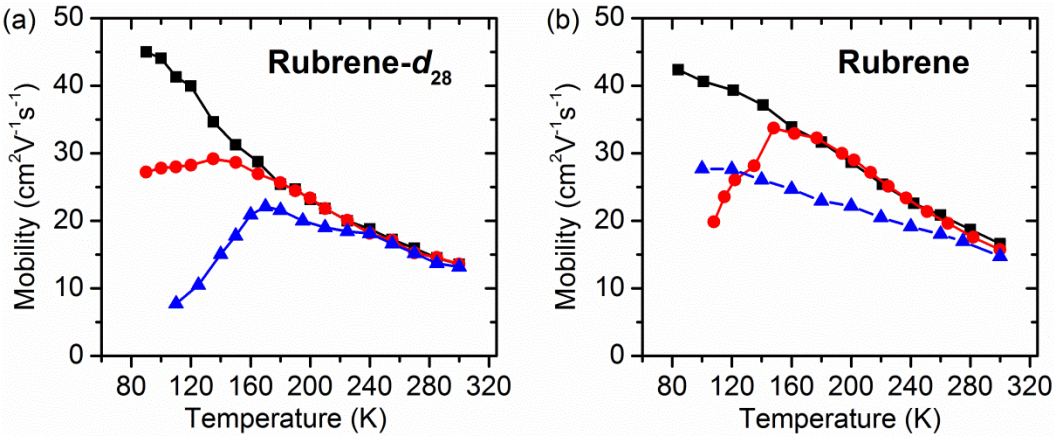

Figure 2.5. Mobility dependence with temperature for **a**) rubrene-d_{28} and **b**) rubrene. Black squares represent Sample A, red circles represent Sample B, blue triangles represent Sample C. Data and figure courtesy of Wei Xie, Department of Chemical Engineering and Materials Science, University of Minnesota, Minneapolis, MN.

Mobilities at room temperature began in the same range, then increased with decreasing temperature, as expected for band-like transport. At ~160 K, three different, reproducible, trends emerged. For Sample A, mobility continued to increase with decreasing temperature, reaching mobilities of ~45 $cm^2V^{-1}s^{-1}$ near 100 K in both **1.1** and **2.1**. In Samples B and C, mobility began to decrease with decreasing temperature after ~160 K, indicating a change from band-like to activated transport (transition temperature, see Chapter 1.3). This change is most dramatic in Sample C of rubrene-d_{28} and Sample B of rubrene. Based on the comparable charge carrier mobilities to rubrene, rubrene-d_{28} would provide great insight in spintronic studies into the effect

of perdeuteration on the spin-diffusion length and time in a small molecule organic semiconductor. The remarkable sample-dependence of the transition temperature observed in both rubrene and rubrene-d_{28} is clearly *not* a result of deuteration, but suggests that subtle differences in the crystal structure or quality can significantly affect the charge carrier mobility.

2.2.3 Crystallography studies of rubrene-d_{28}

To ensure that the rubrene (**1.1**) and rubrene-d_{28} (**2.1**) crystals were in the same setting for the entire temperature range for our comparison of mobility, parametric temperature X-ray diffraction studies were performed. Both samples were collected in an identical format, in which the crystal was cooled to 100 K, the temperature was raised for each subsequent collection, and rested for a set period of time prior to the collection at the new temperature. Both molecules were solved in the Orthorhombic, Cmca setting at all temperatures, thus any differences seen between the two data sets can be attributed to isotopic substitution, likely stemming from the difference between the carbon-hydrogen and carbon-deuterium bond lengths. Interestingly, slight but statistically significant differences were found between the cell constants of the two materials (Table 2.2, Figure 2.5a-d).

Table 2.2. Crystal cell parameters for rubrene **1.1** and **2.1** at various temperatures. Both crystallize in the Orthorhombic, Cmca space group in which all cell angles are 90°. Standard deviations are provided in parentheses.

	Rubrene (**1.1**)		Rubrene (**2.1**)	
Temp (K)	Cell constants (Å)	Volume (Å^3)	Cell constants (Å)	Volume (Å^3)
100(2)	a = 26.7842(12)	2724.60(20)	a = 26.7993(6)	2720.18(11)
	b = 7.1622(3)		b = 7.1466(2)	
	c = 14.2029(6)		c = 14.2028(3)	
150(2)	a = 26.8208(11)	2740.30(20)	a = 26.8196(3)	2736.08(11)
	b = 7.1682(3)		b = 7.1558(2)	
	c = 14.2532(6)		c = 14.2567(3)	
200(2)	a = 26.8581(7)	2758.29(13)	a = 26.8438(6)	2753.92(11)
	b = 7.1736(2)		b = 7.1638(2)	
	c = 14.3162(4)		c = 14.3207(3)	
250(2)	a = 26.8863(7)	2775.74(13)	a = 26.8672(7)	2771.93(12)
	b = 7.1808(2)		b = 7.1740(2)	
	c = 14.3772(4)		c = 14.3845(3)	

All of the cell constant lengths increase with increasing temperature in a linear fashion. The change in the *c*-axis length with temperature is quite small while still statistically significant between rubrene and rubrene-d_{28}. In contrast, the lengths of the *a*- and *b*-axes have larger, statistically significant changes with temperature and even change at different rates for rubrene and rubrene-d_{28}. Rubrene has a higher rate of change in *a*, exhibiting a larger length than rubrene-d_{28} at 250 K but a smaller length at 100 K. The length of *b* remains larger for rubrene at all temperatures, but rubrene-d_{28} exhibits a higher rate of change in this axis length. The change in volume with temperature occurs at almost the same rate for both samples, with the volume of rubrene remaining consistently larger than rubrene-d_{28}. The consistent increase with temperature of these values indicates a phase transition is unlikely for either rubrene or rubrene-d_{28}. Differential scanning calorimetry also did not suggest a phase transition in either of the crystals (Figure 2.5e-f).

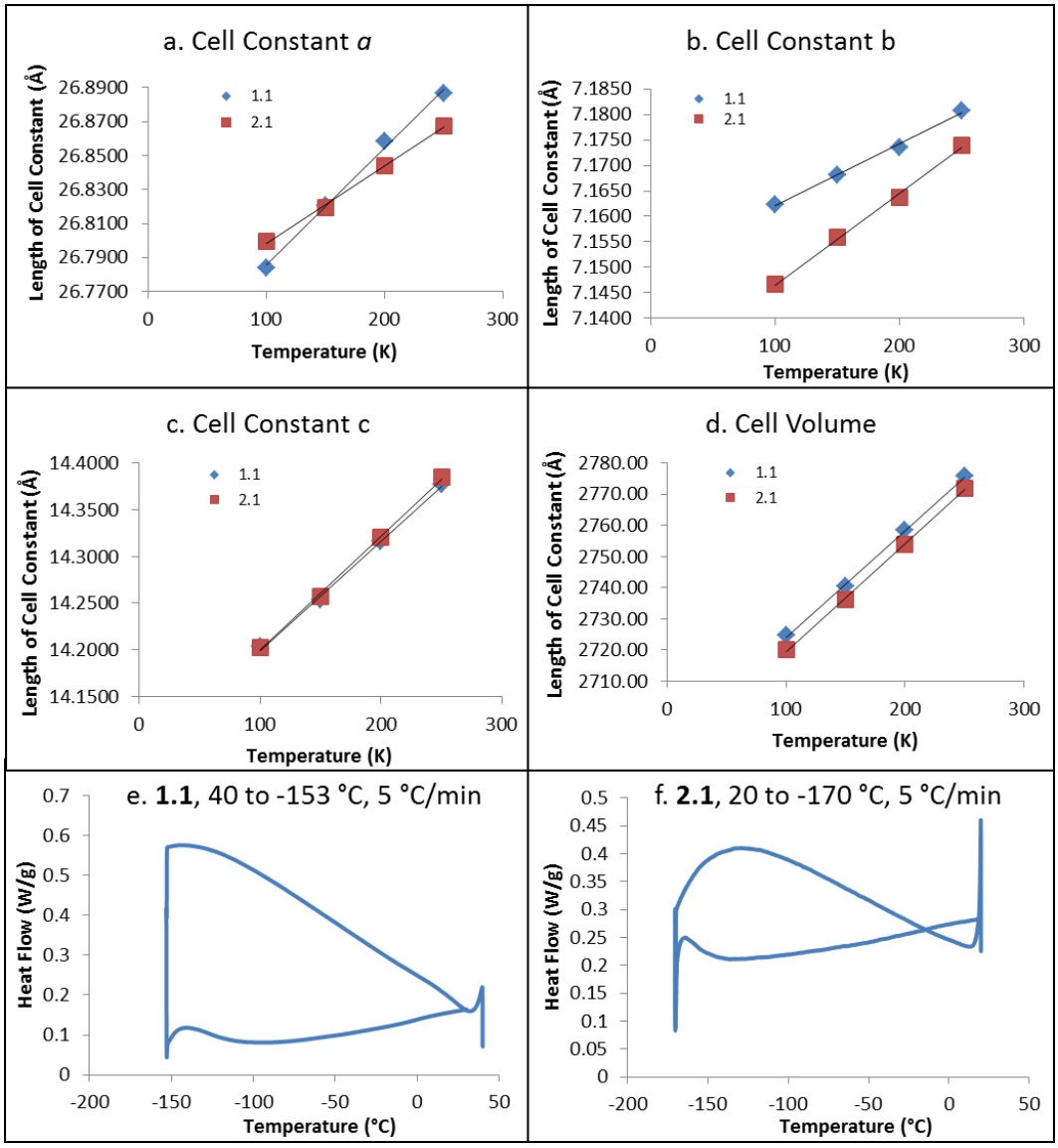

Figure 2.6. Comparison between rubrene (**1.1**) and rubrene-d_{28} (**2.1**) of cell constants **a**) *a*, **b**) *b*, **c**) *c*, and **d**) cell volume from 100–250 K. Low temperature DSC traces for **e**) rubrene and **f**) rubrene-d_{28}.

From the X-ray diffraction data collected, the thermal expansion coefficient was calculated[17] for *a*, *b*, *c*, as well as the volume for both rubrene and rubrene-d_{28} (Table 2.2). These values were found to be very similar for the volume, while rubrene-d_{28} has a larger expansion

coefficient in the *b*- and *c*-axes and rubrene has a larger coefficient in the *a*-axis. The percentage change in the cell constants indicates that the thermal expansion of both samples is anisotropic, with the largest change along the *c*-axis, which has been seen previously in rubrene.[18] The percent change in the cell volume for both **1.1** and **2.1** is very similar, suggesting there is little impact on the crystal volume with isotopic substitution.

Table 2.3. Thermal expansion coefficients and percent change for the crystals of rubrene **1.1** and **2.1** from 250-100K.

Rubrene **1.1**	*a*	*b*	*c*	*V*
Coefficient (K^{-1})	0.0000254(8)	0.0000173(6)	0.000082(2)	0.000125(3)
Percent change	0.380(5)	0.259(5)	1.212(5)	1.842(9)
Rubrene **2.1**	*a*	*b*	*c*	*V*
Coefficient (K^{-1})	0.0000169(5)	0.0000256(8)	0.000085(2)	0.000127(4)
Percent change	0.253(3)	0.382(4)	1.263(4)	1.867(6)

To determine the cause of the different rates of change in the *a*- and *b*-axes length with temperature between **1.1** and **2.1**, the common aspects of the rubrene solid state packing were examined closely and compared between the compounds. These aspects include π-stacking distance, pitch distance, pitch angle, out-of-plane torsion angle, and edge-to-face distance (Table 2.3, Figure 2.6, Figure 2.7). The π-stacking distance increases with increasing temperature linearly and almost identically for both **1.1** and **2.1**, although **2.1** has a slightly higher rate of increase leading to a larger π-stacking distance at 250 K for rubrene-d_{28}. The pitch distance decreases with increasing temperature for **1.1** in a linear manner, contrasting with rubrene-d_{28} in which the pitch distance change is statistically negligible over 200 K. This distance remains on average 0.015(±0.007) Å greater for rubrene than rubrene-d_{28} over the temperature range, suggesting an isotopic substitution effect. The pitch angle decreases with increasing temperature linearly and remains consistently larger for rubrene, which corresponds to the change in the pitch

distance. The edge-to-face distance increases linearly with increasing temperature by the same amount within error for both **1.1** and **2.1**. This distance remains on average 0.009(±0.006) Å larger for rubrene than rubrene-d_{28} over the temperature range, indicating this parameter is influenced by isotopic substitution. The out-of-plane torsion of the side phenyl from the tetracene core was found to be identical within error for the two molecules, suggesting isotopic displacement does not disrupt the side phenyl placement in the solid state.

Table 2.4. Measured and calculated distances and angles in crystal structures of rubrene **1.1** and **2.1** at various temperatures. Standard deviations are provided in parentheses.

Rubrene (**1.1**)	Temp (K)	π-Stacking Distance (Å)	Pitch Distance (Å)	Pitch Angle (°)	Edge-to-Face Distance (Å)	Out-of-Plane Torsion Angle (°)
	100	3.656(2)	6.159(3)	59.46(2)	4.161(2)	14.8(2)
	150	3.671(2)	6.157(3)	59.36(2)	4.171(2)	14.8(2)
	200	3.687(2)	6.154(3)	59.23(2)	4.181(2)	14.9(2)
	250	3.705(2)	6.151(3)	59.11(2)	4.193(2)	15.0(2)
Rubrene (**2.1**)	Temp (K)	π-Stacking Distance (Å)	Pitch Distance (Å)	Pitch Angle (°)	Edge-to-Face Distance (Å)	Out-of-Plane Torsion Angle (°)
	100	3.657(2)	6.141(3)	59.37(2)	4.151(2)	14.8(2)
	150	3.673(2)	6.141(3)	59.26(2)	4.161(2)	14.8(2)
	200	3.692(2)	6.139(3)	59.13(2)	4.172(2)	15.0(2)
	250	3.709(2)	6.138(3)	59.02(2)	4.185(2)	15.2(2)

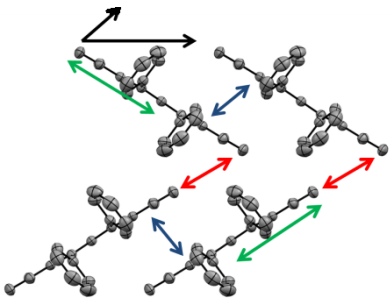

Figure 2.7. Crystal packing diagram of rubrene **1.1** showing measurements. Blue arrows indicate π-stacking distance. Green arrows indicate pitch distance. Black arrows indicate pitch angle. Red arrows indicate edge-to-face distance.

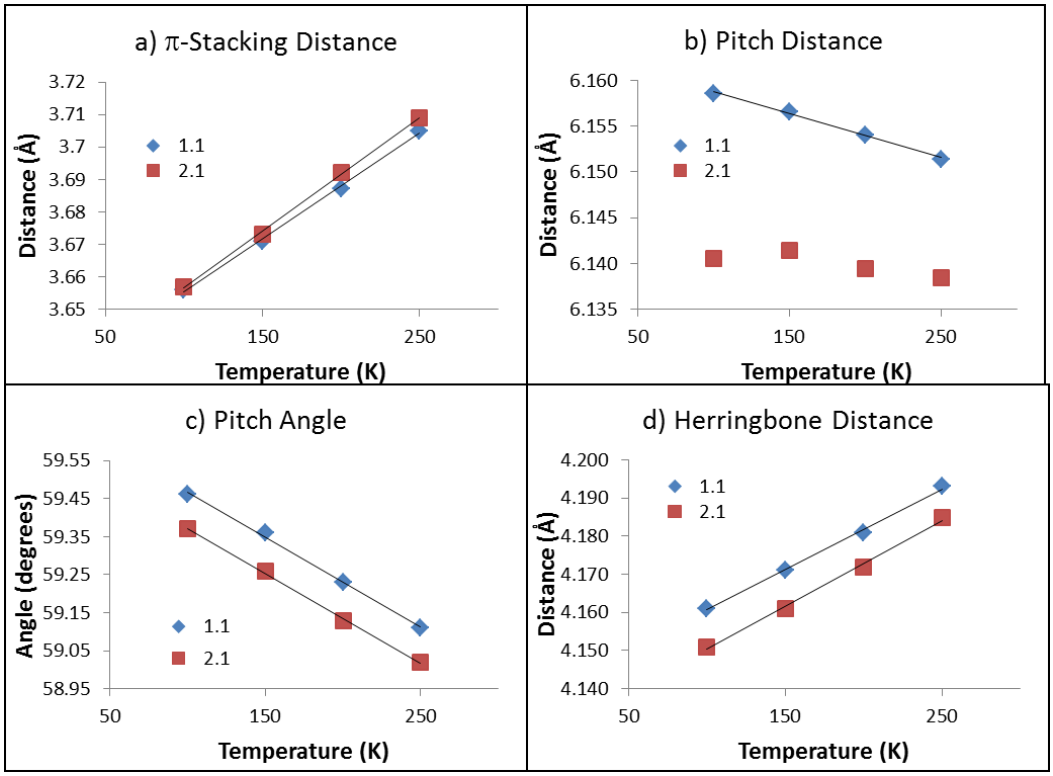

Figure 2.8. Comparison between rubrene (**1.1**) and rubrene-d_{28} (**2.1**) crystal structures of the **a**) π-stacking distance, **b**) pitch distance, **c**) pitch angle, and **d**) herringbone distance.

Both the pitch distance and the herringbone distance show significant differences with isotopic substitution in the solid-state packing of rubrene. These distances are likely influenced by the interactions of hydrogen (deuterium) with the neighboring π-cloud, which are affected by the bond length between carbon and hydrogen (deuterium). The slightly shorter carbon-deuterium bond length causes the pitch and herringbone distances to be shorter in rubrene-d_{28} as compared to the carbon-hydrogen bond length and corresponding distances in rubrene. Unfortunately, hydrogen and deuterium atoms are placed ideally in single crystal models from X-ray diffraction data, preventing us from accurately examining the effect of these lengths on the crystal structure.

2.3 CONCLUSION AND FUTURE STUDIES

Rubrene-d_{28} was successfully synthesized in six steps from commercially available bromobenzene-d_5. Rubrene-d_{28} has charge carrier mobilities remarkably similar to rubrene, indicating this material should be a good candidate for spintronic studies. Interestingly, parametric temperature X-ray diffraction studies revealed slight differences between rubrene and rubrene-d_{28}. The discrepancies observed may be explained by short contacts between C…H, H…H, or π…H, but as hydrogen/deuterium atoms are modeled ideally in X-ray diffraction, these short contacts cannot be analyzed accurately. Parametric temperature studies using neutron diffraction data would provide insight on the possible short contact differences between rubrene and rubrene-d_{28}. Neutron diffraction studies would allow for accurate determination of the C–H and C–D bond lengths at different temperatures and are currently being pursued. Another aspect to consider with the variable temperature single-crystal X-ray diffraction data is the sample size. Only one crystal of each molecule was compared, whereby we are not able to comment on whether this is a general trend or a sample specific trend. Based on the OFET data of these crystals, the solid-state structures of these molecules potentially have three sample trends. A thorough study of multiple rubrene and rubrene-d_{28} crystals examined with parametric single-crystal X-ray diffraction may shed some light on this sample dependence phenomenon.

2.4 EXPERIMENTALS

All reactions were carried out using flame-dried glassware under a nitrogen atmosphere. Tetrahydrofuran (THF) was dried by distillation from benzophenone/sodium. Dichloromethane (CH_2Cl_2) and triethylamine (TEA) were dried by distillation from CaH_2 under nitrogen. All other

chemicals were purchased from Acros Organics or Sigma-Aldrich and used as received unless otherwise noted.

Analytical thin layer chromatography (TLC) was carried out using 0.25 mm silica plates from Silicycle. Eluted plates were visualized first with UV light. Flash chromatography was performed using 230–400 mesh (particle size 0.04–0.063 mm) silica gel purchased from Silicycle. ^{1}H NMR (300 MHz), ^{13}C NMR (75 MHz), ^{2}H (46.1 MHz) spectra were obtained on Varian FT NMR or Bruker FT NMR instruments. NMR spectra were reported as δ values in ppm relative to chloroform for ^{1}H (7.26 ppm), chloroform for ^{13}C (77.00 ppm), and dichloromethane-d_2 for ^{2}H (5.30 ppm). ^{1}H and ^{13}C NMR coupling constants are reported in Hz; multiplicity was indicated as follows; s (singlet); d (doublet); t (triplet); q (quartet); quint (quintet); m (multiplet); dd (doublet of doublets); ddd (doublet of doublet of doublets); dddd (doublet of doublet of doublet of doublets); dt (doublet of triplets); td (triplet of doublets); ddt (doublet of doublet of triplets); app (apparent); br (broad).

Deuterium incorporation was calculated as follows.[19] To an NMR tube was added: rubrene-d_{28} (9.5 mg, 0.0170 mmol), trimethoxybenzene (1.1 mg, 0.0065 mmol), followed by $CDCl_3$ (0.7 mL). The ^{1}H NMR spectrum was collected (500 MHz, 48 scans). Integration of the peaks for rubrene-d_{28} (1.65, 0.804, 1.00 per hydrogen for each peak respectively) and the internal standard (47.06 per hydrogen) were calculated. The residual mmol of hydrogen was calculated for each peak (ex. 1.65 / 47.06 × 0.0065 = 0.000228 mmol H) then converted into a percentage (ex. 0.000228 / 0.0170 × 100 = 1.34%). The percent deuterium was calculated for each peak (ex. 100 – 1.34 = 98.6% deuterium) then the percentages were multiplied together to determine the overall deuterium incorporation (97.2%).

Infrared (IR) spectra were obtained as films from CH_2Cl_2. Low-resolution mass spectra (LRMS) in EI experiments were performed on a Varian Saturn 2200 GC-MS system. Low-resolution mass spectra (LRMS) in EI or CI experiments were performed on a Varian Saturn 2200 GC-MS system. High-resolution mass spectra (HRMS) in EI experiments were performed on a Finnigan MAT 95 GC-MS system or in electrospray (ESI) experiments were performed on a Bruker BioTOF II. Elemental analysis was performed by Atlantic Microlab, Inc., 6180 Atlantic Blvd, Suite M, Norcross, GA 30071.

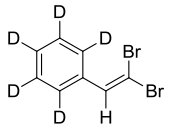

Compound **2.7**[12]: To a suspension of zinc dust (4.31 g, 66.0 mmol), triphenylphosphine (17.31 g, 66.0 mmol) in 120 mL CH_2Cl_2, was added carbon tetrabromide (21.9 g, 66.0 mmol). After 24 hours of stirring at room temperature, benzaldehyde-d_5 (3.70 g, 33.0 mmol) was added. The mixture was stirred for 2 hours, then the solvent was removed in vacuo. Residue was subjected to multiple washes with a CH_2Cl_2/pentane solution (1:4). The solution was filtered and solvent removed in vacuo gave crude product. Purification by column chromatography using 3:2 hexanes:CH_2Cl_2 provided (2,2-dibromovinyl)benzene-d_5 (**2.7**) as a light yellow oil (7.75 g, 29.3 mmol, 89%). R_f = 0.74 (3:2 hexanes:CH_2Cl_2); ^{1}H NMR (300 MHz, $CDCl_3$) δ 7.49 (s, 1 H); ^{2}H NMR (46.1 MHz, CH_2Cl_2) δ 7.46 (s, 2D), 7.25 (s, 3D); ^{13}C NMR (75 MHz, $CDCl_3$) δ 136.7 (s), 135.0 (s), 128.0 (t, $J_{C\text{-}D}$ = 24.1 Hz), 127.9 (t, $J_{C\text{-}D}$ = 24.4 Hz), 127.8 (t, $J_{C\text{-}D}$ = 24.2 Hz), 89.5 (s); LRMS (EI) *m*/*z* calcd for C_8HD_5Br $[M]^+$ 264.9150, found 265.

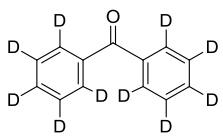

Compound **2.3**[20]: To a 250 mL round bottom flask was added: benzhydrol-d_{10} (6.08 g, 31.2 mmol) and CH_2Cl_2 (100 mL).[21] Pyridinium chlorochromate (6.73 g) followed by

celite (10 g) was then added. Reaction was stirred at room temperature for 3 h. The solvent was evaporated to provide the crude material on celite. The mixture was purified by column chromatography (5:95 EtOAc/Hex) which afforded benzophenone-d_{10} as a light gold oil (4.63 g, 24.8 mmol, 80%). R_f = 0.52 (10% ethyl acetate in hexanes); ^{2}H NMR (46.1 MHz, CH2Cl2) δ 7.69 (s, 4D), 7.45-7.35 (m, 6D); ^{13}C NMR (75 MHz, $CDCl_3$) δ 196.7 (s), 137.3 (s), 131.9 (t, $J_{C\text{-}D}$ = 23.8 Hz), 129.6 (t, $J_{C\text{-}D}$ = 24.7 Hz), 127.7 (t, $J_{C\text{-}D}$ = 24.0 Hz), 89.5 (s); IR (thin film, CH_2Cl_2) 3053, 2295, 2277, 1658, 1560 cm^{-1}; LRMS (CI, methanol) *m/z* calcd for $C_{13}D_{10}O$ $[M+H]^+$ 193.1432, found 193.

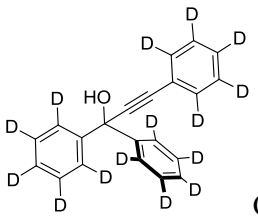

Compound **2.2**: To a solution of **2.7** (5.79 g, 22.8 mmol) in dry THF (100 mL) at −78 °C was added 2.5 M n-BuLi in hexanes (10.4 mL, 26.0 mmol). The mixture stirred for 3 hours warming to room temperature. The reaction was cooled to 0 °C, then benzophenone-d_{10} (2.50 g, 13.0 mmol) was added dropwise as a solution in THF (10 mL) and the reaction mixture was allowed to warm to room temperature. The reaction mixture was stirred for another 18 hours. The mixture was quenched by addition of 6% aq. NH_4Cl (50 mL) and the resulting mixture was extracted with diethyl ether (50 mL). The organic extracts were washed with brine (3 × 50 mL) and dried over Na_2SO_4. After filtration, removal of the solvent under reduced pressure gave the crude product. The product was purified by column chromatography using a slow gradient from hexanes to 20% ethyl acetate in hexanes providing 1,1,3-triphenylprop-2-yn-1-ol-d15 as a white solid (5.39 g, 18.7 mmol, 82%). R_f = 0.32 (1:4 EtOAc/Hex); ^{1}H NMR (300 MHz, $CDCl_3$) δ 2.87 (s, 1 H); ^{2}H NMR (46.1 MHz, CH_2Cl_2) δ 7.76

(s, 4D), 7.50 (s, 2D), 7.30 (s, 9D); ^{13}C NMR (75 MHz, $CDCl_3$) δ 144.8, 131.2 (app d, $J_{C\text{-}D}$ = 25.0 Hz), 128.0 (app t, $J_{C\text{-}D}$ = 25.4 Hz), 125.6 (t, $J_{C\text{-}D}$ = 24.0 Hz), 122.1 (s), 91.6 (s), 87.1 (s), 77.2 (s), 74.7 (s), 48.0 (s); IR (thin film, CH_2Cl_2) 3553, 3447, 3051, 1563 cm^{-1}; LRMS (EI) *m*/*z* calcd for $C_{21}HD_{15}O$ $[M\text{-}OH]^+$ 282.2110, found 282; mp 81–83 °C.

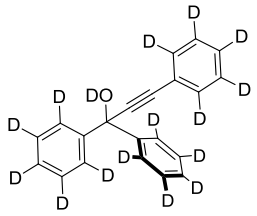

Compound **2.11**: A 100 mL round bottom flask was charged with **2.2** (5.39 g, 18.7 mmol), CH_2Cl_2 added until material dissolved (about 5 mL), then added D_2O (about 5 mL). The mixture was stirred for 30 min. The layers were separated and the organic layer was dried over Na_2SO_4, filtered, and concentrated to give 1,1,3-triphenylprop-2-yn-1-ol-d_{16} (4.86 g, 16.2 mmol, 86%) Deuterium incorporation was confirmed by ^{1}H NMR (OH peak disappearance).

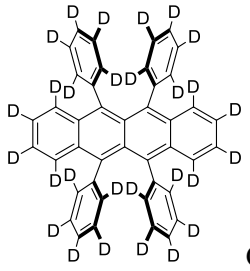

Compound **2.1**: To a solution of **2.10** (4.50 g, 15.0 mmol) in 64 mL of toluene-d_8 was added distilled NEt_3 (3.14 mL, 22.5 mmol). The mixture was cooled to 0 °C and methane sulfonyl chloride (1.74 mL, 22.5 mmol) was added dropwise. The reaction was stirred at 0 °C for 15 min, at room temperature for 30 min, then was heated at 110 °C for 6 hours. Upon cooling, the mixture was diluted with 40 mL of ethyl acetate, transferred to a separatory funnel,

and washed with 2 M HCl (3 × 40 mL). The organic layer was dried over $MgSO_4$ and the solvent was removed in vacuo. The residue was diluted with a diethyl ether/methanol solution (1:1). Filtration provided rubrene-d_{28} as a red-orange solid (0.444 g, 0.792 mmol, 5%, 97.2% deuterium). mp 322–326 °C, R_f = 0.51 (1:3 Benzene/Hex); ^{2}H NMR (46.1 MHz, CH_2Cl_2) δ 7.11 (s br, 28D); ^{13}C NMR (75 MHz, $CDCl_3$) δ 141.6 (s), 136.9 (s), 131.6 (t, $J_{C\text{-}D}$ = 24.4 Hz), 130.2 (s), 129.1 (s), 126.7 (t, $J_{C\text{-}D}$ = 22.9 Hz), 126.4-125.9 (m), 125.2 (t, $J_{C\text{-}D}$ = 23.2 Hz), 124.3 (t, $J_{C\text{-}D}$ = 21.4 Hz); IR (KBr pellet) 2266, 1610, 1565 cm^{-1}; HRMS (ESI) *m*/*z* calcd for $C_{42}D_{28}$ $[M]^+$ 560.3948, found 560.3949; Anal. calcd for $C_{42}D_{28}$: C, 89.94; D, 10.06 (seen as H, 5.30). Found: C, 89.93; H, 4.97.

2.5 REFERENCES

(1) Naber, W. J. M.; Faez, S.; Wiel, W. G. van der *J. Phys. Appl. Phys.* **2007**, *40*, R205.

(2) Awschalom, D. D.; Flatté, M. E. *Nat. Phys.* **2007**, *3*, 153–159.

(3) Sanvito, S. *Nat. Mater.* **2011**, *10*, 484–485.

(4) Ruden, P. P.; Smith, D. L. *J. Appl. Phys.* **2004**, *95*, 4898–4904.

(5) Dediu, V. A.; Hueso, L. E.; Bergenti, I.; Taliani, C. *Nat. Mater.* **2009**, *8*, 707–716.

(6) Shim, J. H.; Raman, K. V.; Park, Y. J.; Santos, T. S.; Miao, G. X.; Satpati, B.; Moodera, J. S. *Phys. Rev. Lett.* **2008**, *100*, 226603.

(7) Yu, Z.-G. *Proc. SPIE* **2011**, *8333*, 83331A.

(8) Nguyen, T. D.; Hukic-Markosian, G.; Wang, F.; Wojcik, L.; Li, X.-G.; Ehrenfreund, E.; Vardeny, Z. V. *Nat. Mater.* **2010**, *9*, 345–352.

(9) Begley, W. J.; Rajeswaran, M.; Andrievsky, N. Process for preparing triphenylnaphthacene compound. US 20060025642A1, February 2, 2006.

(10) Zhang, Y.; Wen, J. *Synthesis.* **1990**, *8*, 727–728.

(11) Lewis, F. D.; Sajimon, M. C.; Zuo, X.; Rubin, M.; Gevorgyan, V. *J. Org. Chem.* **2005**, *70*, 10447–10452.

(12) Corey, E. J.; Fuchs, P. L. *Tetrahedron Lett.* **1972**, *13*, 3769–3772.

(13) Ogata, A.; Nemoto, M.; Kobayashi, K.; Tsubouchi, A.; Takeda, T. *J. Org. Chem.* **2007**, *72*, 3816–3822.

(14) Peña-López, M.; Ayán-Varela, M.; Sarandeses, L. A.; Pérez Sestelo, J. *Chem. – Eur. J.* **2010**, *16*, 9905–9909.

(15) Greene, A. K.; Scott, L. T. *J. Org. Chem.* **2013**, *78*, 2139–2143.

(16) Xie, W.; McGarry, K. A.; Liu, F.; Wu, Y.; Ruden, P. P.; Douglas, C. J.; Frisbie, C. D. *J. Phys. Chem. C* **2013**, *117*, 11522–11529.

(17) Bhattacharya, S.; Saha, B. K. *Cryst. Growth Des.* **2012**, *12*, 4716–4719.

(18) Jurchescu, O. D.; Meetsma, A.; Palstra, T. T. M. *Acta Crystallogr. Sect. B* **2006**, *B62*, 330–334.

(19) Greene, A. K.; Scott, L. T. *J. Org. Chem.* **2012**.

(20) Zheng, C.; Hofstetter, H.; Hofstetter, O. *J. Mol. Struct.* **2008**, *875*, 173–182.

(21) Li, H.; Zhu, R.-Y.; Shi, W.-J.; He, K.-H.; Shi, Z.-J. *Org. Lett.* **2012**, *14*, 4850–4853.

3 SYNTHESIS OF PHENYL-SUBSTITUTED RUBRENES

3.1 BACKGROUND

The high charge carrier mobility exhibited by rubrene **1.1** (Figure 1.1, page 2) in single-crystal OFET makes this molecule an intriguing candidate for structure-property relationship studies. Systematically manipulating aspects of the rubrene solid-state structure using molecular changes would allow us to correlate physical changes with changes in electronic properties. Few studies have examined the effect of molecular changes on the crystal packing of rubrene,[1–3] with only one study exploring a rubrene derivative in single crystal OFET.[4] The lack of solved crystal structures for rubrene derivatives has been discussed by Bergantin and Moret in their attempt to determine a trend in the solid state packing of known crystallized rubrene derivatives, however no general trend emerged from the limited number of available samples.[5] We sought to fill this gap in knowledge by synthesizing a series of rubrene derivatives that were systematically modified and could be examined in single-crystal OFET.

A number of congeners of **1.1** have been synthesized over the years via some of the routes discussed in Chapter 1.3. To systematically manipulate the solid state structure of rubrene, the molecular structure of the derivative would need to be strategically modified. Understanding what aspects to change or keep intact is crucial in planning a series of derivatives. As previously described, the high charge carrier mobility in **1.1** has been attributed to the π-stacking in the crystal structure which exhibits a large transfer integral in the direction of the π-stacks (Figure 3.1a).[6] This leads to anisotropic mobility in the crystal with the highest mobility down the π-stacking axis.[7] When creating rubrene derivatives for the study of charge transport, it is essential to maintain the π-stacking in the crystal structure to ensure high mobilities.

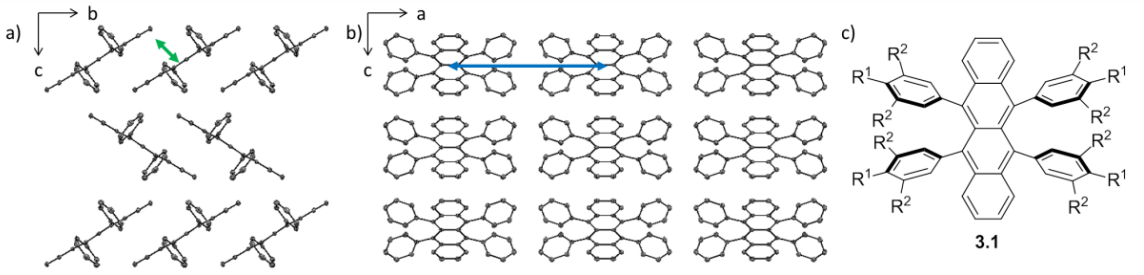

Figure 3.1. 2D image of rubrene 1.1 **a**) π-stacks and **b**) layers. Green arrow indicates π-stacking distance, blue arrow indicates interlayer distance. **c**) Generic molecular structure of proposed rubrene derivatives **3.1**.

The anisotropic character of the rubrene crystal structure also leads to another aspect worth considering. As charge travels down the π-stacks, the surrounding tetracene cores polarize toward the charge, an effect that has been suggested to suppress transport.[8] Decreasing the polarization of the cores might be achieved by increasing the interlayer spacing (Figure 3.1b), which may lead to improved charge carrier mobility. Taking these two aspects into account, the π-stacking might be maintained and the interlayer spacing might be expanded by substituent effcects. As a result, derivatives **3.1** (Figure 3.1c) were targeted.

3.2 PROPOSED SYNTHESIS

In order to synthesize compound **3.1**, we needed an accessible route to rubrene derivatives that would allow control of the substituent placement. The route by Chamberlin et al (Scheme 3.1a) would be the most applicable; however, this route has one major drawback.[9] To obtain substitution on all of the peripheral phenyls, a substituted aryl would need to be introduced early on in the synthesis of a derivative of 3-phenylphtahlide. We decided to utilize a slightly modified entry into this route (Scheme 3.1b). Instead of introducing any of the side phenyls in the formation of the tetracene core, we envisioned having the tetracene core already in place and adding the side phenyls separately. Rubrenes **3.1** would be formed via diaryltetracenediones **3.2**

using the last two steps of Chamberlin's route. Unlike the previous route though, we envisioned forming the diaryltetracenediones by a Suzuki-Miyaura coupling[10–12] with 6,11-dichlorotetracene-5,12-dione (**3.3**). This precursor could be formed in two steps from 6,11-dihydroxytetracene-5,12-dione (**3.4**), which is synthesized by the Freidel-Crafts reaction of 1,4-naphthalenediol (**3.5**) and phthaloyl chloride (**3.6**).[13–15] To realize this route, the synthesis of 6,11-dichlorotetracene-5,12-dione (**3.3**) was first optimized.

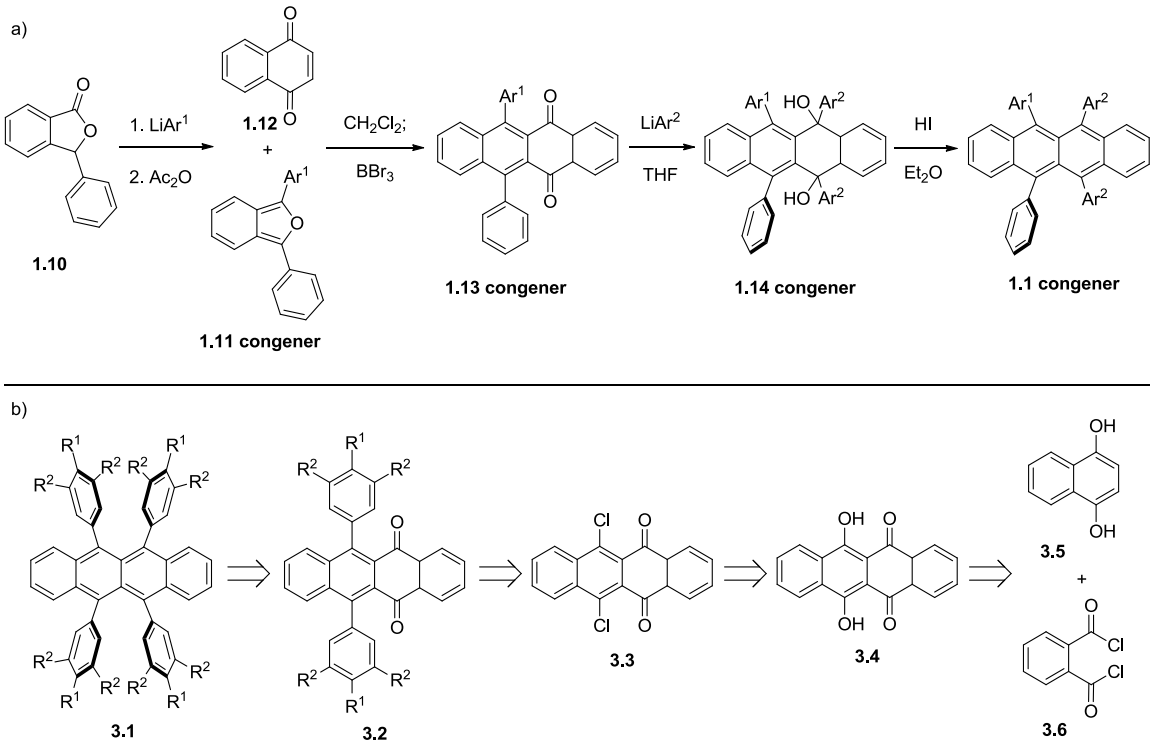

Scheme 3.1. a) Route A by Chamberlin et al to rubrene congeners; **b**) Retrosynthetic analysis to rubrenes **3.1** via dichlorotetracenedione **3.3**.

The synthesis of precursor **3.3** (Scheme 3.2) commenced with the synthesis of 6,11-dihydroxytetracene-5,12-dione (**3.4**). Although the formation of this compound is known in the literature,[16–18] these methods utilized low yielding reactions and difficult purifications. We

improved on the Freidel-Crafts reaction between 1,4-naphthalenediol (**3.5**) and phthaloyl chloride (**3.6**) by employing filtrations to purify **3.4** instead of column chromatography. Due to the expense of compound **3.5**, this starting material was made in one step via the reduction of commercially available 1,4-naphthoquinone (**1.12**), which was significantly cheaper. The desired diol **3.5** was obtained in 87-99% yield following reduction using sodium dithionite in a deoxygenated solution of water and diethyl ether.[19] The Freidel-Crafts reaction conditions were optimized to ensure consumption of the starting material, which included the formation of $AlCl_3$ slurry, portion-wise addition of the two reactants, and heating at 90 °C for 4 hours. Work up of the reaction proceeded via HCl addition and filtration followed by stirring with acetone, filtration, then stirring with aqueous potassium sodium tartrate and filtration to purify the product away from nitrobenzene and remaining aluminum-containing byproducts. Dihydroxytetracenedione **3.4** was obtained in a range of 46-97% yield as a red solid.

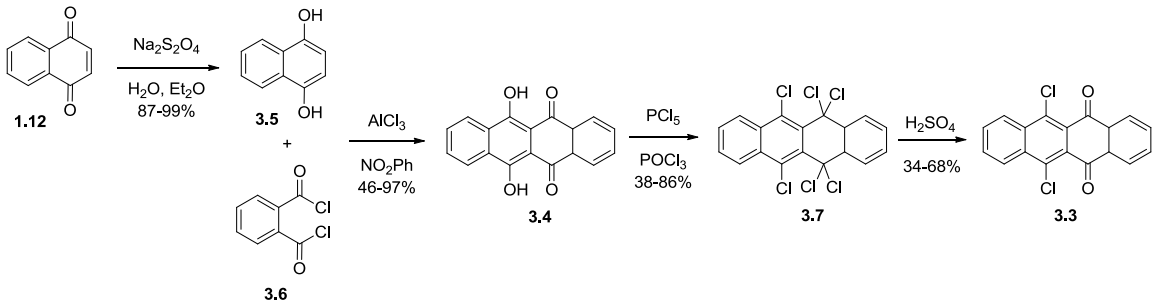

Scheme 3.2. Synthesis of dichlorotetracenedione **3.3** beginning from naphthalenediol **3.5** and phthaloyl chloride **3.6**

Having pure **3.4** in hand, our attention turned to the synthesis of the hexachloride **3.7**. Chlorination via refluxing with phosphorous pentachloride in phosphrous oxychloride furnished crude **3.7** in 38-86% yield. Removal of water from this reaction was important due to the

potential to form **3.3** from advantageous water. Treatment of crude **3.7** with concentrated sulfuric acid at room temperature for 3-4 hours provided crude **3.3** after pouring the reaction mixture into water and filtering. Pure **3.3** was obtained in 34-68% yield after recrystallization by heating in toluene, filtering the hot solution, and collecting the orange crystals that formed in the filtrate once the solution cooled. Additional crops of crystals could be obtained to increase yield. Although these reactions have a large range in yields, they can be performed on multi-gram scale (25 g), with purified final amounts of **3.3** ranging from 4.4 – 8.1 g. Precursor **3.3** is the divergent point in the synthesis of rubrene derivatives **3.1**.

With dichlorotetracenedione **3.3** prepared, a variety of rubrenes (**3.1**) could now be synthesized via a three step process (Scheme 3.3). We envisioned one set of peripheral phenyls to be introduced via a Suzuki reaction to form the diaryltetracenedione precursor (**3.2**) using a substituted aryl boronic acid **3.10**. A second set of side phenyls could be introduced via organolithium addition of a substituted aryl bromide **3.9'**, forming diol **3.8**. Oxidation of diol **3.8** using hydroiodic acid would provide the desired rubrene derivatives having structure **3.1**. Using this sequence, a variety of symmetrical and asymmetrical rubrenes could be achieved.

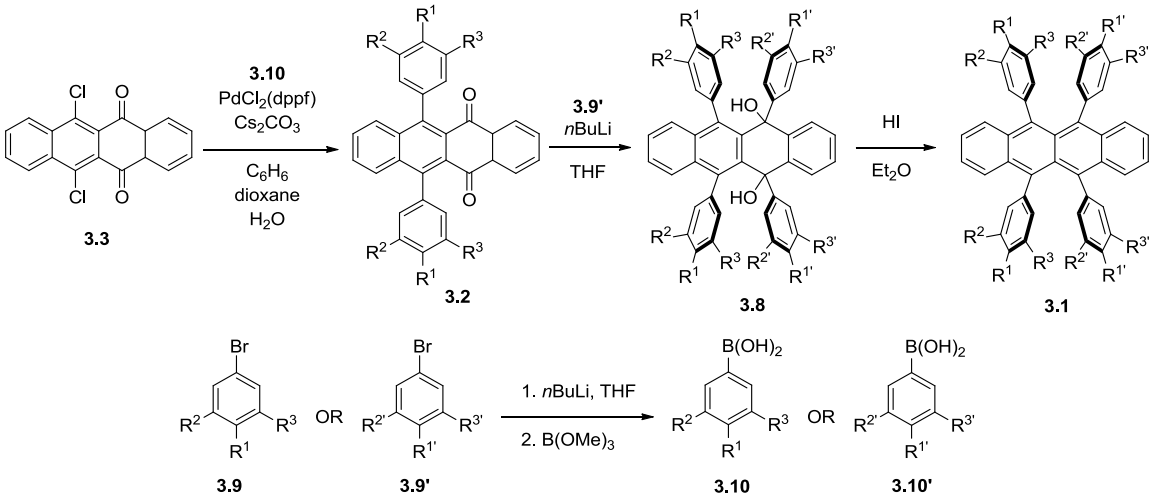

Scheme 3.3 Forward synthesis of rubrenes **3.1** from dichlorotetracenedione **3.3**.

3.3 RESULTS AND DISCUSSION

3.3.1 Synthesis of derivatives

Ten phenyl-substituted rubrene derivatives were synthesized during this work (**3.1a-j**, Figure 3.2). These structures were chosen because we predicted these molecules would pack with a planar tetracene core, allowing for the π-stacking to be maintained, while the substituents would increase the interlayer distance. However, not all of these molecules packed as we expected. The analysis of the solid-state packing and perceived interactions of each derivative informed and influenced our decision on the next target. Due to the similarity of the synthesis for each derivative, each step of the synthesis will be discussed as related to each derivative, including any optimizations and challenges encountered. The solid-state structure of each derivative and analysis that drove this project will be discussed in the following section.

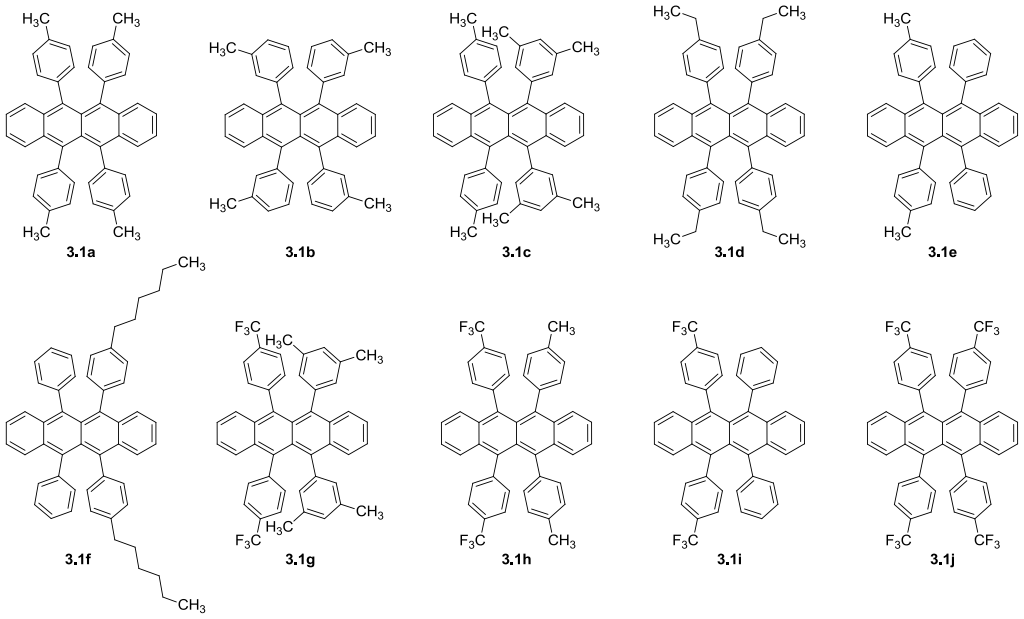

Figure 3.2. Molecular structures of the rubrenes **3.1a-j** synthesized during this work.

The synthesis for each derivative commenced with the formation of a diaryltetracenedione **3.2**. Many of the derivatives were made from the same structural precursor **3.2**, thus there are only five unique diaryltetracenediones (**3.2a-f**, Scheme 3.4). These precursors were obtained by a Suzuki coupling between the aryl boronic acid (**3.10a-f**) and dichlorotetracenedione **3.3**. Boronic acids **3.10e-f** were purchased and used as received, but all other boronic acids were synthesized from the commercially available aryl bromide, with the exception of **3.10d** in which the aryl bromide was also synthesized. Aside from the origin of the boronic acid, the synthesis of the diaryltetracenediones proceeded under the same conditions to provide the desired diaryltetracenediones (Table 3.1).

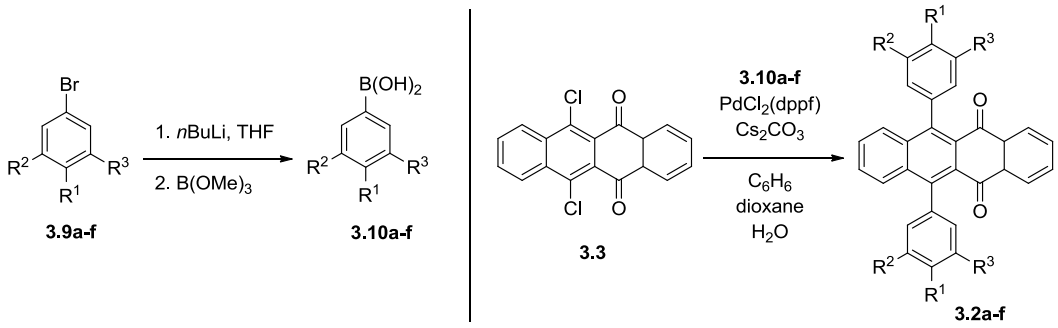

Scheme 3.4. Synthesis of aryl boronic acids **3.10a-f** and diaryltetracenediones **3.2a-f**.

Table 3.1. Synthesis of aryl boronic acids **3.11a-f** and diaryltetracenediones **3.2a-f**.

Entry	**3.10** R^1	**3.10** R^2	**3.10** R^3	**3.10a-f** Yield (%)	**3.2a-f** Yield (%)
1	CH_3	H	H	**a** 85	**a** 93
2	H	CH_3	H	**b** 74	**b** 91
3	CF_3	H	H	**c** 94	**c** 91
4	C_6H_{13}	H	H	**d** 44	**d** 26
5	CH_2CH_3	H	H	**e** –[a]	**e** 96
6	H	H	H	**f** –[a]	**f** 78

[a]Boronic acid was purchased.

The boronic acids **3.10a-d** were synthesized following a known procedure.[20] Treatment of the corresponding aryl bromide with *n*-butyl lithum at –78 °C for about 20 minutes to form the organolithium was followed by slow addition of $B(OMe)_3$ to the reaction and warming to room temperature. After alkaline aqueous workup, the desired boronic acids were obtained in good yields. The aryl bromide used to synthesize **3.10d** was synthesized in one step from the known coupling of 1,4-dibromobenzene and bromohexane.[21] The molarity of the Grignard reagent in this reaction was found to be important to achieving good conversion (titrated with menthol/1,10-phenanthroline or checked by No-D NMR[22] prior to addition). With the boronic acids **3.10a-f** obtained, the Suzuki coupling proceeded under conditions previously optimized by a Douglas

group member, Dr. Elisey Yagodkin, to provide diaryltetracenediones **3.2a-f** in high yields.[23] The yield of **3.2d** (Table 3.1, Entry 4) was low due to the presence of an unidentified impurity in the crude mixture that made purification of the diaryltetracenedione difficult. Although diphenyltetracenedione **3.2f** was synthesized in slightly diminished yield, the spectra matched literature data.[3] This compound was used to synthesize rubrenes **3.1e,i** to explore the flexibility of this synthetic route.

Having formed the desired diaryltetracenediones **3.2a-f**, the ten corresponding tetracenediols **3.8a-l** could then be synthesized via nucleophilic addition of aryl bromides **3.9'a-f** into the tetracenediones (Scheme 3.5). This reaction resulted in a mixture of unassigned diastereomers in moderate to high yields, although some derivatives (**3.8b,c**) were only isolated as one unassigned diastereomer (Table 3.2). The tetracenediols were identified by ^{1}H NMR and then taken directly into the next step. Slow addition of the organolithium reagent was found to be necessary as the increased heat generated by faster addition would impact the yield of the desired product.

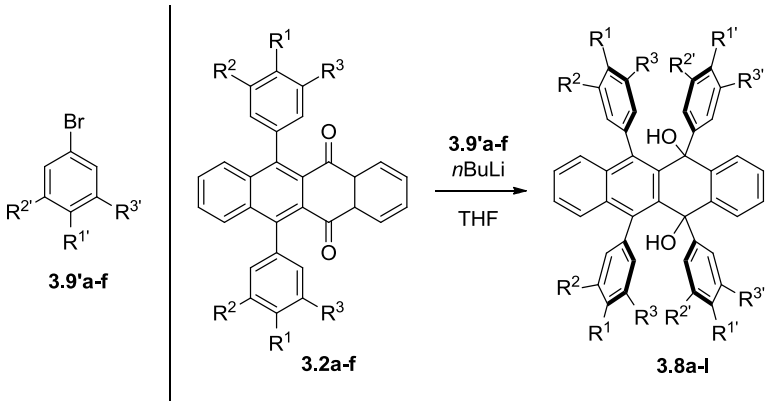

Scheme 3.5. Synthesis of tetracenediols **3.8a-l** using aryl bromide **3.9'a-f**.

Table 3.2. Synthesis of tetracenediols **3.8a-l**.

Entry	diaryl tetracenedione	aryl bromide (**3.9'**)	**3.9'** $R^{1'}$	**3.9'** $R^{2'}$	**3.9'** $R^{3'}$	**3.8a-j** Yield (%)
1	**3.2a**	**a**	CH_3	H	H	**a** 96
2	**3.2b**	**b**	H	CH_3	H	**b** 50[a]
3	**3.2a**	**c**	H	CH_3	CH_3	**c** –[a,b]
4	**3.2e**	**d**	CH_2CH_3	H	H	**d** 91
5	**3.2a**	**e**	H	H	H	**e** 95
6	**3.2d**	**e**	H	H	H	**f** 92
7	**3.2c**	**c**	H	CH_3	CH_3	**g** 84
8	**3.2c**	**a**	CH_3	H	H	**h** 91
9	**3.2c**	**e**	H	H	H	**i** 80
10	**3.2c**	**f**	CF_3	H	H	**j** 75
11	**3.2f**	**a**	CH_3	H	H	**k** 95
12	**3.2f**	**f**	CF_3	H	H	**l** 60

[a]Isolated as a single diastereomer. [b]Yield not able to be calculated due to the presence of an unidentified impurity.

During the synthesis of tetracenediol **3.8d**, the crude diol mixture was not immediately purified, leading to the formation of two byproducts. The first byproduct (**3.11**, Figure 3.3a), tentatively assigned by ^{1}H NMR, has replaced the alcohol groups with C–C bonds to the adjacent side phenyls, which creates a double indene structure. This type of structure has been identified as an impurity in batches of commercially available rubrene.[24] The second byproduct (**3.12**, Figure 3.3b) was more difficult to assign. The ^{1}H NMR spectrum has two broad singlets between 6–7ppm and shows three resolved ethyl peaks that integrate in a 2:1:1 ratio, suggesting that two ethyl groups are chemically equivalent while the other two are not. An alcohol group was detected from the IR and the disappearance of a singlet integrating to one proton in the ^{1}H NMR upon treatment with D_2O. Based on the data collected, a structure was proposed, but only after

the single crystal was solved by X-ray diffraction could the connectivity be accurately assigned to the indene-alcohol structure **3.12**.

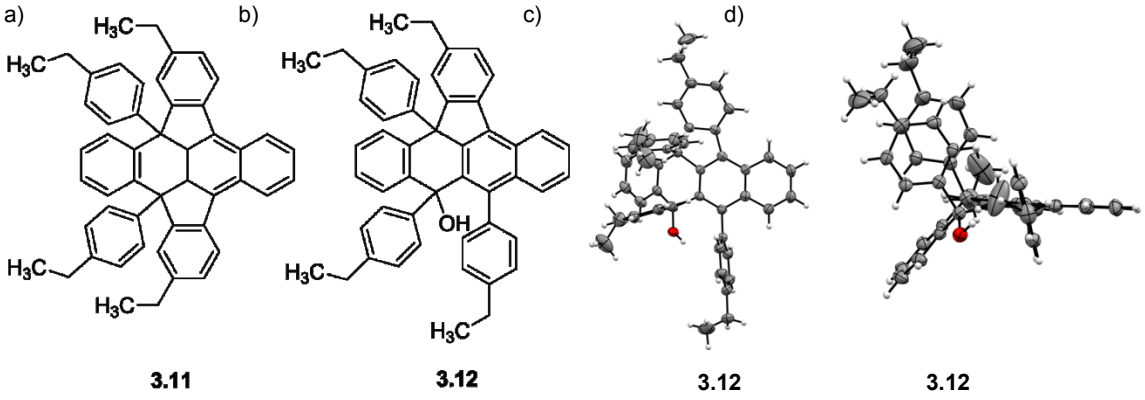

Figure 3.3. Molecular structures of byproducts **a**) **3.11**, **b**) **3.12**. ORTEP drawings of byproduct 3.12 showing **c**) full structure with one indene fused phenyl, **d**) flagpole nature of two phenyl groups. Ellipsoids shown at 50% probability. Crystal structure solved by Victoria Chemistruck, Douglas Group member, Department of Chemistry, University of Minnesota, Minneapolis, MN.

Unfortunately, these structures dominated the isolated material; none of the desired tetracenediol **3.8d** was recovered after column chromatography. These byproducts **3.11** and **3.12** likely form by electrophilic aromatic substitution in which loss of the alcohol group as a water molecule is followed by attack of the carbocation by the side phenyl. Loss of a proton to aromatize the side phenyl provides byproduct **3.12**, which can then undergo the sequence a second time to form byproduct **3.11**. The electrophilic aromatic substitution reaction was likely assisted by the electron rich nature of the side phenyl rings. During the formation of a batch of **3.8a**, the related byproduct **3.12** was believed to have formed by the diagnostic broad peaks in the ^{1}H NMR spectrum between 6-7 ppm. To avoid these byproducts in other rubrenes, *immediate purification of the diol crude products* was instituted and successfully provided the remaining tetracenediols without detection of the indene-containing byproducts.

Having obtained the pure tetracenediols **3.8a-l**, the final step could be performed to form the desired rubrene derivatives (**3.1a-j**, Scheme 3.6). Treatment of **3.8a-l** with HI (57 wt. % aqueous solution) in refluxing diethyl ether reduced the tetracenediols to rubrene **3.1a-j** in high conversion and upon purification these molecules were isolated in good yields (Table 3.3).

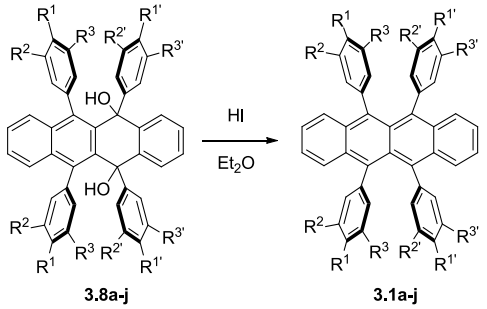

Scheme 3.6. Synthesis of rubrenes **3.1a-j**.

Table 3.3. Synthesis of rubrenes **3.1a-j**.

Entry	tetracenediol	**3.1a-j** Recrystallized Yield (%)
1	**3.8a**	**a** 54
2	**3.8b**	**b** 93[a]
3	**3.8c**	**c** 34
4	**3.8d**	**d** 45
5	**3.8e**	**e** 46
6	**3.8k**	**e** –[b]
7	**3.8f**	**f** 88[a]
8	**3.8g**	**g** 94
9	**3.8h**	**h** 65
10	**3.8i**	**i** 55
11	**3.8l**	**i** 26
12	**3.8j**	**j** 18

[a]Recrystallization unsuccessful; crude yield. [b]Material contaminated with byproduct; see discussion.

During the synthesis of a batch of **3.1a**, a white precipitate formed during the HI reaction. Isolation of the solid and characterization by ^{1}H, ^{13}C, IR, and HRMS revealed the oxo-bridged compound **3.13** (Figure 3.4) obtained in 13% yield. Presumably, this impurity formed during the reaction when the carbocation that is formed is trapped by the nearby alcohol instead of by an iodide ion (Scheme 3.7). The solubility of this compound is likely lower than the starting material and desired product, causing this compound to precipitate out of solution. To reduce the formation of this byproduct, the reaction concentration was lowered from 0.03 M to 0.015 M. This byproduct was not observed in the synthesis of the other rubrene derivatives, except during the alternative route to **3.1e** in which the reaction was performed at the original concentration and formation of byproduct **3.14** (35% yield) complicated isolation of the desired pure rubrene.

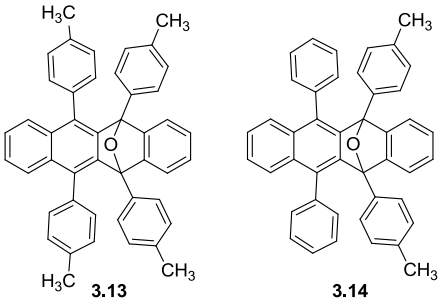

Figure 3.4. Molecular structures of oxo-bridged byproduct **3.13** and **3.14**.

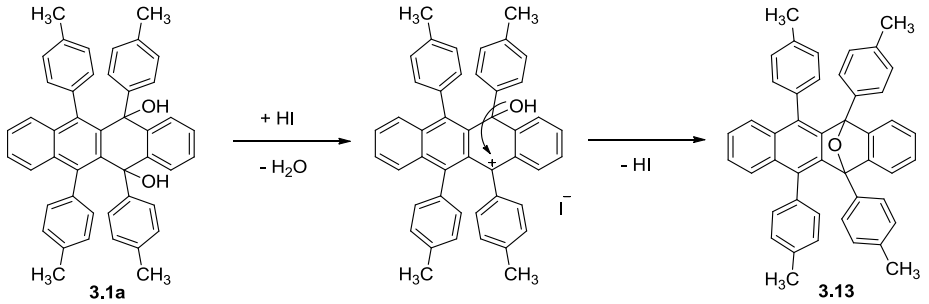

Scheme 3.7. Mechanistic hypothesis to form oxo-bridged compound **3.13**.

Purification of rubrenes **3.1a-j** was initially challenging due to the propensity of the rubrene structures to form an endoperoxide (see compound **1.17**, Figure 1.2, Chapter 1) in the presence of singlet oxygen. These molecules were found to decompose on silica gel (determined by 2D TLC analysis), likely to the endoperoxide structure. Solution phase recrystallization conditions were optimized in order to avoid column chromatography. Slow diffusion of isopropanol layered onto a dichloromethane (~3:1 v:v) solution of the crude mixture reliably provided pure crystals in good yields (Table 3.3). For **3.1i**, layered diffusion of isopropanol into ACS Grade chloroform was optimal. Rubrenes **3.1b** and **3.1f** were challenging to recrystallize using this method and a variety of other techniques were attempted. Derivative **3.1b** finally crystallized from a benzene:methanol (~1:2) layered solution at 5 °C, but crystals of **3.1f** were not able to be obtained. For the compounds that successfully formed crystals, their solid-state structures were solved by single-crystal X-ray diffraction. The packing structures guided the project as each structure was synthesized and solved immediately, which allowed for adjustments to be made to the next target based on the solid-state analysis.

3.3.2 Correlation of molecular structure to solid-state packing structure

The first derivative synthesized, **3.1a**, was chosen because we anticipated the *p*-methyl groups to provide the desired interlayer spacing while not disrupting the π-stacking between the tetracene cores. Derivative **3.1a** crystallized in the Monoclinic, C2/c setting (Table 3.4, Figure 3.5). Unfortunately, the solved structure revealed an unanticipated twist in the tetracene core. This twist was 33.9° and 42.8° for each of the unique molecules in the unit cell. We rationalized the twist in the backbone came from the steric interactions between the *p*-methyl groups. In light of this, the next targets were chosen so that the potential steric interaction would be minimized.

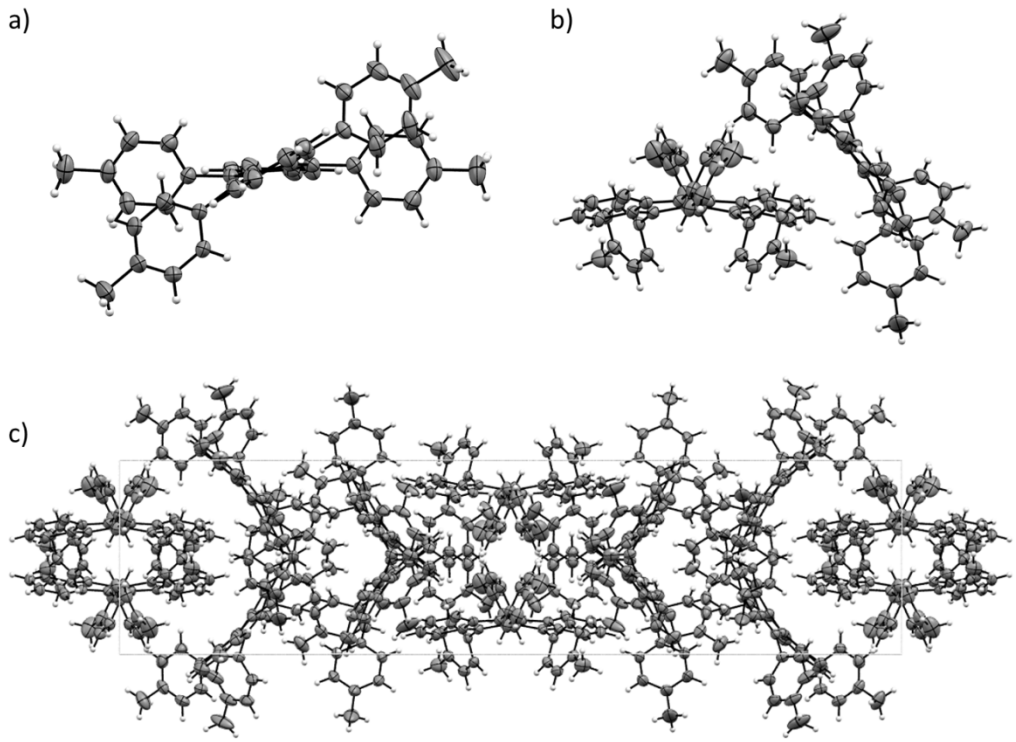

Figure 3.5. ORTEP drawings of **3.1a**: **a**) single molecule viewed down the molecular long axis (33.9° only), **b**) both unique molecules in the unit cell with twists of 42.8° and 33.9° respectively, **c**) unit cell viewed down *c*-axis.

Table 3.4. Crystal data and structure refinement for rubrenes **3.1a** and **3.1b**.

Rubrene	**3.1a**		**3.1b**	
Empirical formula	$C_{46}H_{36}$		$C_{52}H_{42}$	
Formula weight	588.75		666.86	
Temperature	173(2) K		173(2) K	
Wavelength	0.71073 Å		1.54178 Å	
Crystal system	Monoclinic		Monoclinic	
Space group	C2/c		$P2_1/n$	
Unit cell dimensions	a = 41.257(6) Å	α = 90°	a = 14.8677(4) Å	α = 90°
	b = 10.1464(14) Å	β = 96.739(4)°	b = 8.6305(2) Å	β = 94.6090(10)°
	c = 24.038(4) Å	γ = 90°	c = 28.9920(8) Å	γ = 90°
Volume	9993(3) $Å^3$		3708.10(17) $Å^3$	
Z	12		4	
Density (calculated)	1.174 Mg/m^3		1.195 Mg/m^3	
Absorption coefficient	0.066 mm-1		0.507 mm-1	
F(000)	3744		1416	
Crystal color, morphology	Red, Block		Orange, Plate	
Crystal size	0.45 x 0.30 x 0.20 mm^3		0.19 x 0.16 x 0.08 mm^3	
Theta range for data collection	0.99 to 25.11°		3.06 to 66.59°	
Index ranges	-48 £ h £ 49, -11 £ k £ 12, -28 £ l £ 28		-17 £ h £ 17, -8 £ k £ 10, -34 £ l £ 31	
Reflections collected	45776		23598	
Independent reflections	8885 [R(int) = 0.0566]		6539 [R(int) = 0.0322]	
Observed reflections	5755		5154	
Completeness to theta (θ)	99.80% (25.11°)		99.70% (66.59°)	
Absorption correction	Multi-scan		Multi-scan	
Max. and min. transmission	0.9869 and 0.9708		0.9629 and 0.9098	
Refinement method	Full-matrix least-squares on F2		Full-matrix least-squares on F2	
Data / restraints / parameters	8885 / 0 / 628		6539 / 57 / 544	
Goodness-of-fit on F2	1.017		1.039	
Final R indices [I>2sigma(I)]	R1 = 0.0475, wR2 = 0.0970		R1 = 0.0648, wR2 = 0.1745	
R indices (all data)	R1 = 0.0919, wR2 = 0.1131		R1 = 0.0820, wR2 = 0.1881	
Largest diff. peak and hole	0.187 and -0.167 $e.Å^{-3}$		1.175 and -0.431 $e.Å^{-3}$	

We anticipated rubrenes 3.1b-d would minimize the steric interactions present in the solid-state structure of **3.1a**. In derivative **3.1b**, the placement of the methyl groups in the *meta* position would allow for a conformation in which the methyl groups do not interfere with each

other, which we anticipated would be the favorable conformation. In derivative **3.1c**, we predicted that the *p*-methyl group would sit between the two *m*-methyl groups, giving rise to a planar tetracene core. We proposed that in derivative **3.1d** favorable Van der Waals interactions between the ethyl groups of neighboring rubrenes might allow for the core to planarize. These molecules were synthesized and set up to recrystallize. Initially crystals were not able to be obtained for **3.1b**, but a layered mixture of benzene and methanol (~1:2 v:v) finally proved fruitful. The solved structure was a benzene solvate, in the Monoclinic, $P2_1/n$ setting (Table 3.4, Figure 3.6a). Derivative **3.1c** crystalized in the Monoclinic, $P2_1$ setting (Table 3.5, Figure 3.6b) and **3.1d** was solved as a twinned crystal in the Triclinic, $P\bar{1}$ setting (Table 3.5, Figure 3.6c).

Table 3.5. Crystal data and structure refinement for rubrenes **3.1c** and **3.1d**.

Rubrene	**3.1c**		**3.1d**	
Empirical formula	$C_{48}H_{40}$		$C_{50}H_{44}$	
Formula weight	616.8		644.85	
Temperature	173(2) K		123(2) K	
Wavelength	0.71073 Å		0.71073 Å	
Crystal system	Monoclinic		Triclinic	
Space group	$P2_1$		P-1	
Unit cell dimensions	a = 12.7495(10) Å	α = 90°	a = 10.108(2) Å	α = 84.781(3)°
	b = 9.4141(7) Å	β = 99.576(2)°	b = 21.855(4) Å	β = 89.168(3)°
	c = 14.5027(11) Å	γ = 90°	c = 25.751(5) Å	γ = 76.821(3)°
Volume	1716.4(2) $Å^3$		5515.8(19) $Å^3$	
Z	2		6	
Density (calculated)	1.193 Mg/m^3		1.165 Mg/m^3	
Absorption coefficient	0.067 mm-1		0.066 mm-1	
F(000)	656		2064	
Crystal color, morphology	Red, Block		Orange, Block	
Crystal size	0.50 x 0.25 x 0.03 mm^3		0.50 x 0.25 x 0.25 mm^3	
Theta range for data collection	1.42 to 26.38°		0.79 to 26.37°	
Index ranges	-14 £ h £ 15, -11 £ k £ 11, -18 £ l £ 18		-12 £ h £ 12, -27 £ k £ 27, 0 £ l £ 32	
Reflections collected	16439		22399	
Independent reflections	6958 [R(int) = 0.0343]		22399 [R(int) = 0.0000]	
Observed reflections	5671		17740	
Completeness to theta (θ)	99.80% (26.38°)		98.60% (26.37°)	
Absorption correction	Multi-scan		Multi-scan	
Max. and min. transmission	0.9980 and 0.9672		0.9838 and 0.9680	
Refinement method	Full-matrix least-squares on F2		Full-matrix least-squares on F2	
Data / restraints / parameters	6958 / 1 / 439		22399 / 0 / 1364	
Goodness-of-fit on F2	1.024		1.033	
Final R indices [I>2sigma(I)]	R1 = 0.0431, wR2 = 0.0958		R1 = 0.0599, wR2 = 0.1443	
R indices (all data)	R1 = 0.0606, wR2 = 0.1051		R1 = 0.0809, wR2 = 0.1564	
Largest diff. peak and hole	0.162 and -0.166 e.$Å^{-3}$		0.896 and -0.416 e.$Å^{-3}$	

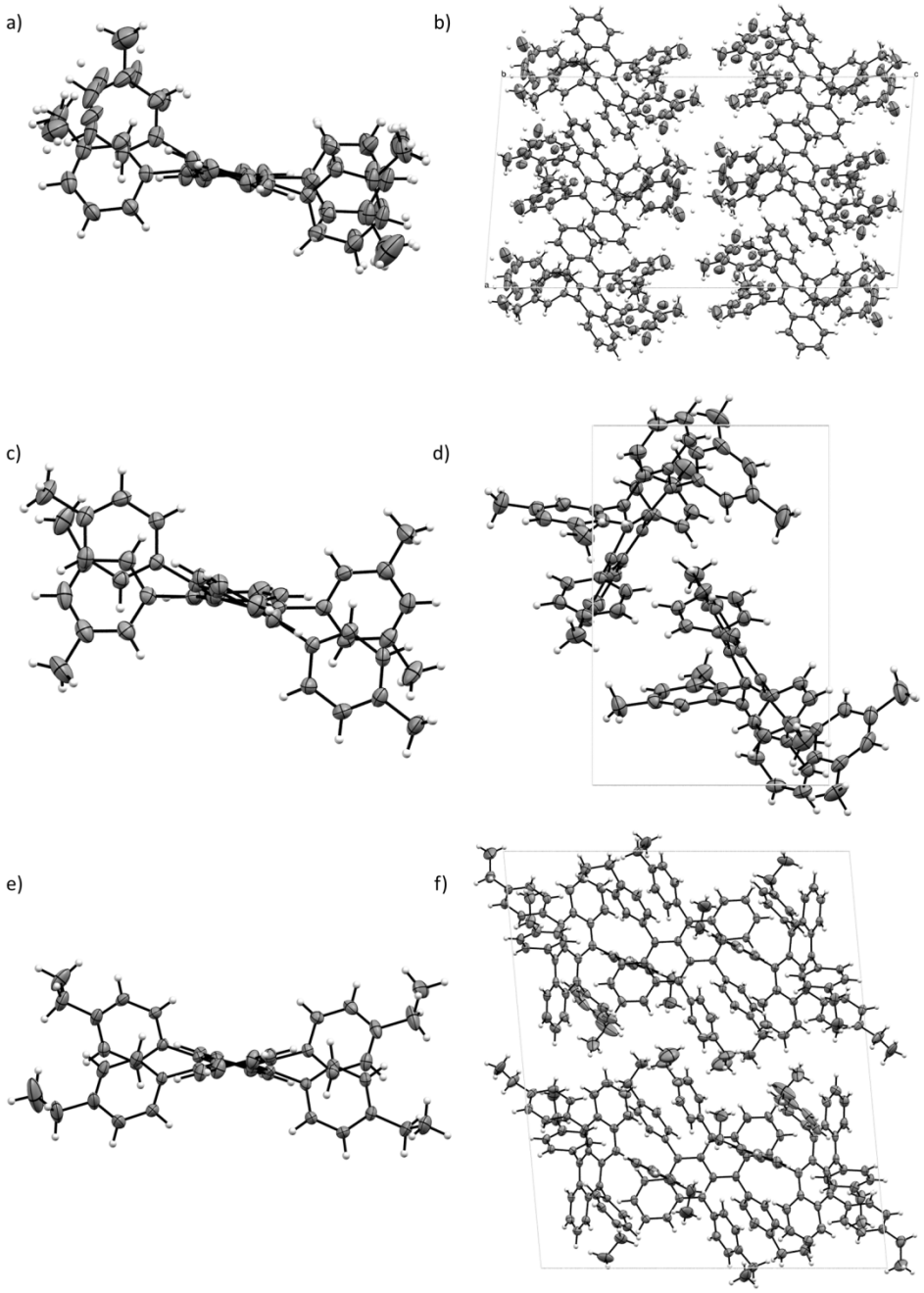

Figure 3.6. ORTEP drawings of **3.1b** (top): **a**) single molecule viewed down the molecular long axis, **b**) unit cell viewed down *b*-axis. Solvent molecules removed for clarity. ORTEP drawings of **3.1c** (middle): **c**) single molecule viewed down the molecular long axis, **d**) unit cell viewed down *a*-axis. ORTEP drawings of **3.1d** (bottom): **e**) single molecule viewed down the molecular long axis (31.2° only), **f**) unit cell viewed down *a*-axis.

Unfortunately, all three derivatives exhibited a twist in the tetracene core. Rubrene **3.1b** exhibits a twist in the tetracene core of 22.9°. There was also disorder which was modeled using constraints in one of the side phenyls as well as the solvent molecule. For **3.1c**, the twist was 30.3° and only in one direction for all molecules, thus the structure is chiral. The torsion of the core actually aligned the *p*-methyl with one of the *m*-methyl groups so that they were 4.11 Å apart. Although this distance is outside the range of the Van der Waals contact distance of 3.59 Å between carbons, the alignment is surprising. In **3.1d** there were three unique molecules in the unit cell, each with a different twist: 31.2°, 33.8°, 41.7°. This crystal likely underwent a phase transition while cooling down to the X-ray diffraction collection temperature of –150 °C, providing the twinned structure. Clearly, the crystals of these derivatives indicate that the interactions of the substituents on the side phenyls play a large role in determining the solid-state packing. The next two targets, **3.1e** and **3.1f**, were chosen to determine whether substituting only one side phenyl would alleviate the disruptive interactions in the solid-state and provide a planar tetracene core. Compound **3.1f** was not able to be crystallized, but **3.1e** crystallized in the Orthorhombic, $Pna2_1$ setting (Table 3.6, Figure 3.7).

Table 3.6. Crystal data and structure refinement for rubrenes **3.1e** and **3.1g**.

Rubrene	**3.1e**		**3.1g**	
Empirical formula	$C_{44}H_{32}$		$C_{48}H_{34}F_6$	
Formula weight	560.7		724.75	
Temperature	173(2) K		123(2) K	
Wavelength	0.71073 Å		0.71073 Å	
Crystal system	Orthorhombic		Orthorhombic	
Space group	$Pna2_1$		Pbcm	
Unit cell dimensions	a = 15.2045(8) Å	α = 90°	a = 7.5317(10) Å	α = 90°
	b = 13.9010(8) Å	β = 90°	b = 14.634(2) Å	β = 90°
	c = 14.3104(8) Å	γ = 90°	c = 32.424(4) Å	γ = 90°
Volume	3024.6(3) $Å^3$		3573.8(8) $Å^3$	
Z	4		4	
Density (calculated)	1.231 Mg/m^3		1.347 Mg/m^3	
Absorption coefficient	0.070 mm-1		0.099 mm-1	
F(000)	1184		1504	
Crystal color, morphology	Red, Block		Orange, Plate	
Crystal size	0.15 x 0.13 x 0.13 mm^3		0.50 x 0.25 x 0.03 mm^3	
Theta range for data collection	1.99 to 25.67°		2.51 to 25.03°	
Index ranges	-18 £ h £ 18, -16 £ k £ 16, -17 £ l £ 17		-8 £ h £ 8, -17 £ k £ 17, -38 £ l £ 38	
Reflections collected	27615		28413	
Independent reflections	5743 [R(int) = 0.0602]		3212 [R(int) = 0.0426]	
Observed reflections	4475		2441	
Completeness to theta (θ)	100.00% (25.67°)		100.00% (25.03°)	
Absorption correction	Multi-scan		Multi-scan	
Max. and min. transmission	0.9910 and 0.9896		0.9970 and 0.9523	
Refinement method	Full-matrix least-squares on F2		Full-matrix least-squares on F2	
Data / restraints / parameters	5743 / 1 / 397		3212 / 0 / 246	
Goodness-of-fit on F2	1.037		1.057	
Final R indices [I>2sigma(I)]	R1 = 0.0421, wR2 = 0.0861		R1 = 0.0761, wR2 = 0.2043	
R indices (all data)	R1 = 0.0635, wR2 = 0.0964		R1 = 0.0976, wR2 = 0.2221	
Largest diff. peak and hole	0.132 and -0.169 $e.Å^{-3}$		1.160 and -0.973 $e.Å^{-3}$	

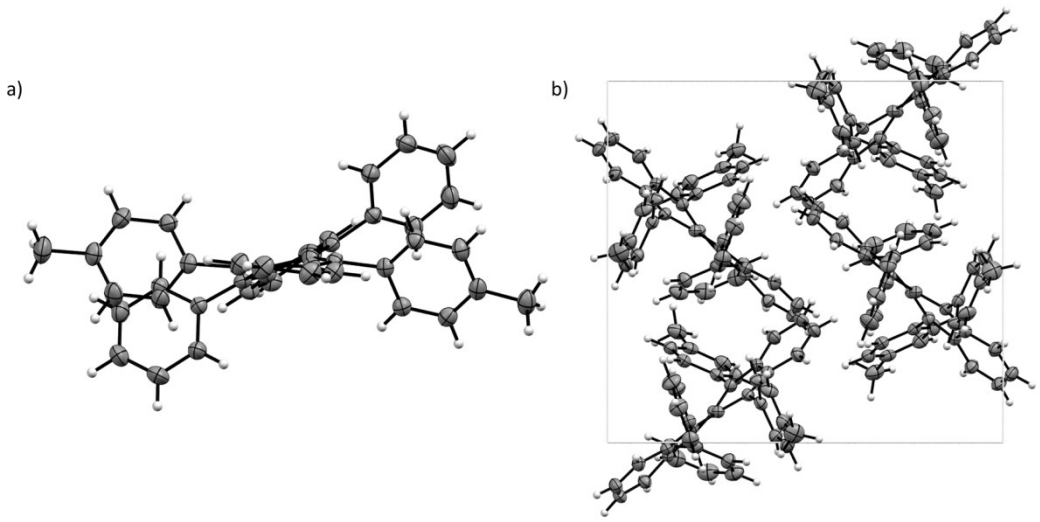

Figure 3.7. ORTEP drawing of **3.1e**: **a**) single molecule viewed down the molecular long axis, **b**) unit cell viewed down *c*-axis.

The solid-state packing of **3.1e** revealed a twisted tetracene core of 41.2°. Based on the number of structures with methyl substituents that resulted in torsion along the backbone, we recognized that steric interactions between the substituents may not be the overriding factor in the planarization of the core. The next target was chosen in an effort to control both the steric and electronic interactions. In rubrene **3.1g**, we anticipated that having a *para*-trifluoromethyl group on one of the side phenyls while the other had two *meta* methyl groups would a) minimize the steric interactions between the substituents and b) generate an electron-deficient and electron-rich attractive interaction which would planarize the tetracene core. When the crystal structure was solved, we were delighted to find that rubrene **3.1g** packed with a planar backbone in the Orthorhombic, Pbcm setting (Table 3.6, Figure 3.8a).

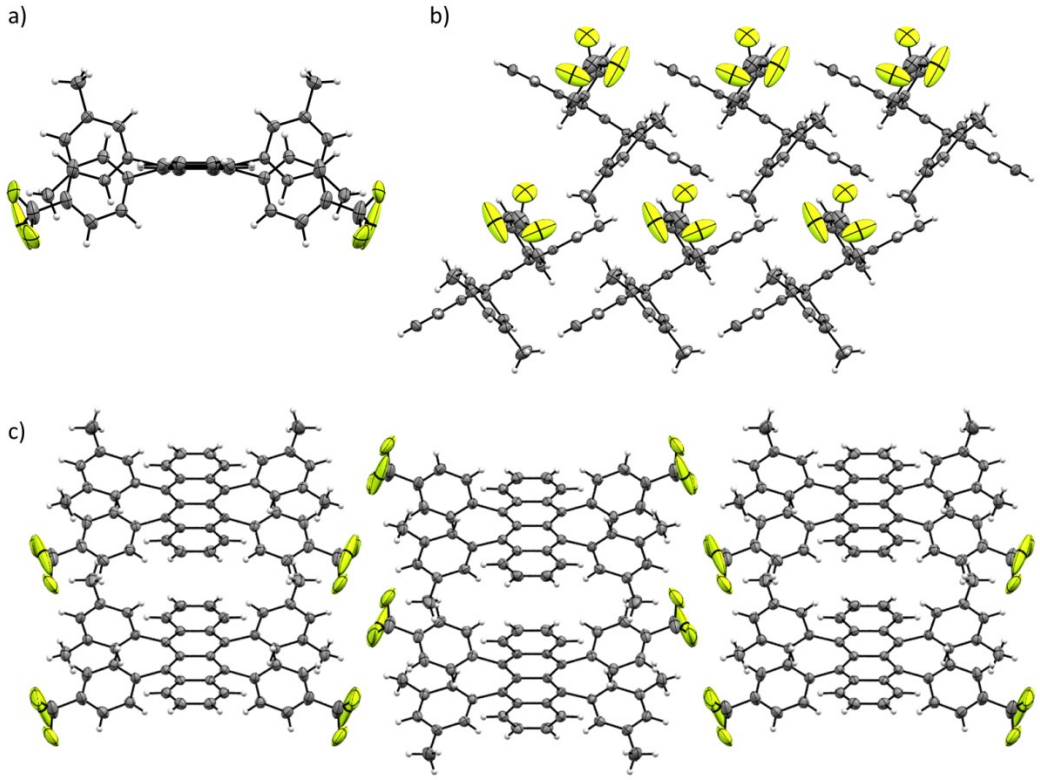

Figure 3.8. ORTEP drawing of **3.1g**: **a**) single molecule viewed down the molecular long axis, **b**) view of π-stacking tetracene cores, **c**) view of interlayer spacing.

Examining the structure of **3.1g** revealed, interestingly, that the *p*-trifluoromethyl group is aligned with one of the *m*-methyl groups, causing them to be 4.19 Å apart, quite similar to the substituent alignment seen in derivative **3.1c**. The packing structure of **3.1g** indicates that the electronic interactions between the side phenyls play a dominate role in determining the planarity of the tetracene core. As predicted, π-stacking occurs between the planar backbones and found to be 3.63 Å (Figure 3.8b), comparable to that of rubrene **1.1** (3.68 Å). When we rotate the crystal structure to examine the interlayer distance, we find the substituents successfully space the layers apart to 16.2 Å (Figure 3.8c), compared to the 13.41 Å interlayer distance of rubrene **1.1** (3.68 Å). The π-stacks and increased interlayer distance of this crystal make this structure ideally suited for

structure-property relationship studies in OFET. The effective use of the electron-deficient and electron-rich attractive interaction in **3.1g** led us to target **3.1h** and **3.1i**. The use of a *p*-methyl and *p*-trifluoromethyl in **3.1h** would reveal whether the attractive interaction between the side phenyls can override the predicted steric interactions between these two substituents, while **3.1i** would provide yet another derivative to be examined. We were pleased to find that **3.1h** crystallized in the Orthorhombic, Pbcm setting (Table 3.7, Figure 3.9a) and **3.1i** crystallized in the Orthorhombic, Pnma setting (Table 3.7, Figure 3.9d).

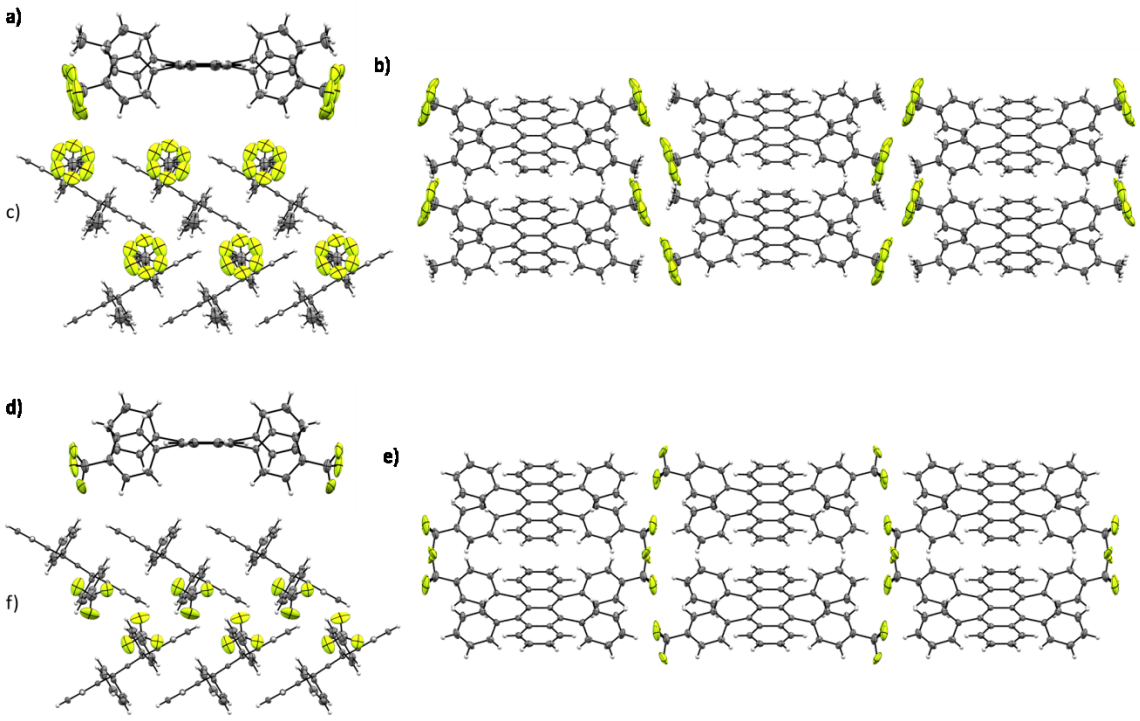

Figure 3.9. ORTEP drawing of **3.1h**: **a**) single molecule viewed down the molecular long axis, **b**) view of π-stacking tetracene cores, **c**) view of interlayer spacing. ORTEP drawing of **3.1i**: **d**) single molecule viewed down the molecular long axis, **e**) view of π-stacking tetracene cores, **f**) view of interlayer spacing.

Table 3.7. Crystal data and structure refinement for rubrenes **3.1h** and **3.1i**.

Rubrene	**3.1h**		**3.1i**	
Empirical formula	$C_{46}H_{30}F_6$		$C_{44}H_{26}F_6$	
Formula weight	696.7		668.65	
Temperature	123(2) K		123(2) K	
Wavelength	0.71073 Å		0.71073 Å	
Crystal system	Orthorhombic		Orthorhombic	
Space group	Pbcm		Pnma	
Unit cell dimensions	a = 7.1443(6) Å	α = 90°	a = 7.1162(5) Å	α = 90°
	b = 14.0510(12) Å	β = 90°	b = 31.179(2) Å	β = 90°
	c = 34.143(3) Å	γ = 90°	c = 14.2075(10) Å	γ = 90°
Volume	3427.4(5) Å^3		3152.3(4) Å^3	
Z	4		4	
Density (calculated)	1.350 Mg/m^3		1.409 Mg/m^3	
Absorption coefficient	0.100 mm-1		0.105 mm-1	
F(000)	1440		1376	
Crystal color, morphology	Red, Plate		Red, Block	
Crystal size	0.25 x 0.25 x 0.05 mm^3		0.25 x 0.20 x 0.13 mm^3	
Theta range for data collection	2.39 to 25.03°		1.58 to 27.62°	
Index ranges	-8 £ h £ 8, -16 £ k £ 16, -40 £ l £ 40		-9 ≤ h ≤ 9, -40 ≤ k ≤ 40, -18 ≤ l ≤ 18	
Reflections collected	30740		34400	
Independent reflections	3091 [R(int) = 0.0567]		3730 [R(int) = 0.0375]	
Observed reflections	2220		2420	
Completeness to theta (θ)	99.90% (25.03°)		99.70% (27.62°)	
Absorption correction	Multi-scan		Multi-scan	
Max. and min. transmission	0.9950 and 0.9754		0.9864 and 0.9741	
Refinement method	Full-matrix least-squares on F2		Full-matrix least-squares on F2	
Data / restraints / parameters	3091 / 0 / 229		3730 / 0 / 226	
Goodness-of-fit on F2	1.143		1.038	
Final R indices [I>2sigma(I)]	R1 = 0.0952, wR2 = 0.2648		R1 = 0.0459, wR2 = 0.1241	
R indices (all data)	R1 = 0.1207, wR2 = 0.2828		R1 = 0.0736, wR2 = 0.1477	
Largest diff. peak and hole	0.653 and -0.577 e.Å^{-3}		0.401 and -0.251 e.Å^{-3}	

The planar cores in both structures yield π-stacking (Figure 3.9b,e), although the distance between the cores, 3.51 Å and 3.55 Å for **3.1h** and **3.1i** respectively, is significantly shorter than the 3.68 Å seen in rubrene **1.1**. Rotating the structures shows that the interlayer distance has been

expanded in both compounds to 17.07 Å and 15.59 Å in **3.1h** and **3.1i** respectively (Figure 3.9c,f). Having successfully synthesized and crystallized three rubrene derivatives that maintain the π-stacking of the tetracene cores while increasing the interlayer distance based on the perceived electron-deficient and electron-rich attractive interaction between the side phenyls, we set out to show the necessity of the attractive interaction for a planar tetracene core by targeting **3.1j** which had *p*-trifluoromethyl groups on both side phenyls. This derivative was synthesized and found to crystallize in the Monoclinic, C2/c setting (Table 3.8, Figure 3.10).

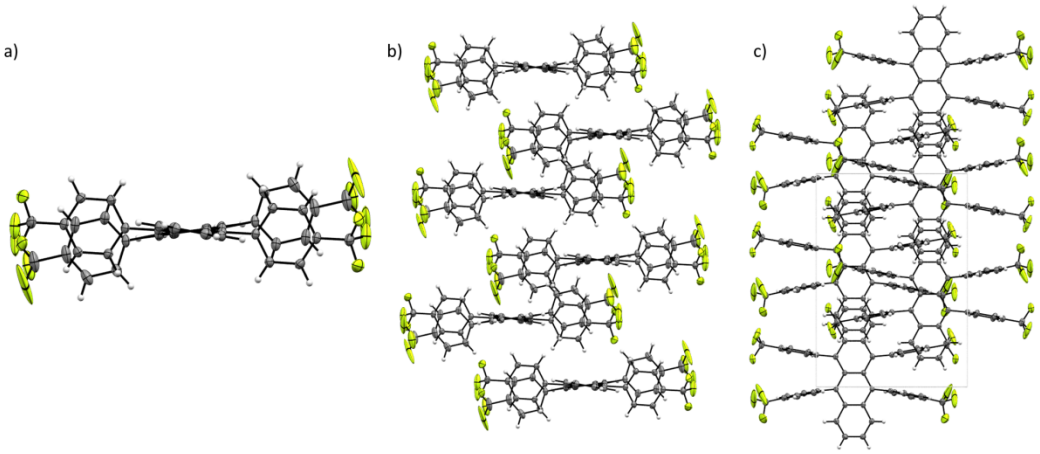

Figure 3.10. ORTEP drawing of **3.1j**: **a**) single molecule viewed down the molecular long axis, **b**) unit cell viewed down *b*-axis, **c**) unit cell viewed down *a*-axis.

Table 3.8. Crystal data and structure refinement for rubrene **3.1j**.

Rubrene	**3.1j**	
Empirical formula	$C_{46}H_{24}F_{12}$	
Formula weight	804.65	
Temperature	123(2) K	
Wavelength	0.71073 Å	
Crystal system	Monoclinic	
Space group	C2/c	
Unit cell dimensions	*a* = 18.275(2) Å	α = 90°
	b = 16.397(2) Å	β = 126.4680(10)°
	c = 14.4859(19) Å	γ = 90°
Volume	3490.7(8) Å^3	
Z	4	
Density (calculated)	1.531 Mg/m^3	
Absorption coefficient	0.133 mm^{-1}	
F(000)	1632	
Crystal color, morphology	Orange, Block	
Crystal size	0.50 x 0.25 x 0.20 mm^3	
Theta range for data collection	1.86 to 27.48°	
Index ranges	-23 £ *h* £ 23, -21 £ *k* £ 21, -18 £ *l* £ 18	
Reflections collected	19826	
Independent reflections	3989 [*R*(int) = 0.0307]	
Observed reflections	3130	
Completeness to theta (θ)	99.70% (27.48°)	
Absorption correction	Multi-scan	
Max. and min. transmission	0.9739 and 0.9364	
Refinement method	Full-matrix least-squares on F^2	
Data / restraints / parameters	3989 / 0 / 262	
Goodness-of-fit on F^2	1.084	
Final *R* indices [*I*>2sigma(*I*)]	*R*1 = 0.0713, *wR*2 = 0.1910	
R indices (all data)	*R*1 = 0.0882, *wR*2 = 0.2058	
Largest diff. peak and hole	1.083 and -0.943 e.Å^{-3}	

As anticipated, this structure has a twist in the tetracene core of 18.6°. There is significantly less torsion in **3.1j** than in the alkyl rubrene derivatives (**3.1a-e**). The organization in the solid-state structure of **3.1j** seems to be accommodating these molecules by minimizing the

intermolecular interactions of the trifluoromethyl groups. With a complete series of rubrene derivatives that contain a) electron-rich and electron rich (type A, rubrenes **3.1a-e**), b) electron-deficient and electron rich (type B, rubrenes **3.1g-i**), c) electron-deficient and electron deficient (type C, rubrenes **3.1j**) side phenyl interactions, we can analyze the effects of these interactions. Although there are likely many weak intermolecular interactions that we have not accounted for, the side phenyl interactions clearly dominate the solid-state packing structure of rubrene derivatives based on the solved crystals of **3.1a-j**. As seen in studies on substituted *peri*-diphenyl naphthalenes,[25–28] the interactions of the side phenyls in our rubrene derivatives are dominated by polar electrostatics. In derivatives with type A interactions, the increased electron density causes the side phenyls to be more strongly repelled, leading to a twist in the core. In the derivative with type C interactions, a twist in the core is also seen, although significantly reduced as compared to the twist in type A, likely due to the decreased electron density of the π-cloud. However, in derivatives of type B, the attractive Coulombic interaction leads to planarization of the core. The use of the type B interactions successfully afforded three rubrenes with π-stacks and expanded interlayer distances which were suitable for structure-property relationship studies in OFET.

The three π-stacking derivatives were further examined to clarify the similarities and differences between them and rubrene **1.1**. The most important aspects to compare were the π-stacking and interlayer distance of each derivative (Figure 3.11). The π-stacking distance is tighter than in rubrene in all three derivatives, while the interlayer distance systematically expands moving from the least substituted derivative **3.1i** (15.59 Å) to the doubly *para*-substituted derivative **3.1h** (17.07 Å). Interestingly, the tightest π-stacking distance (3.51 Å) occurs in **3.1h**, which has the largest interlayer distance. This observed narrowing of the π-stacks

is likely due to the induced dipole across the individual molecules arising from the presence of the trifluoromethyl groups.

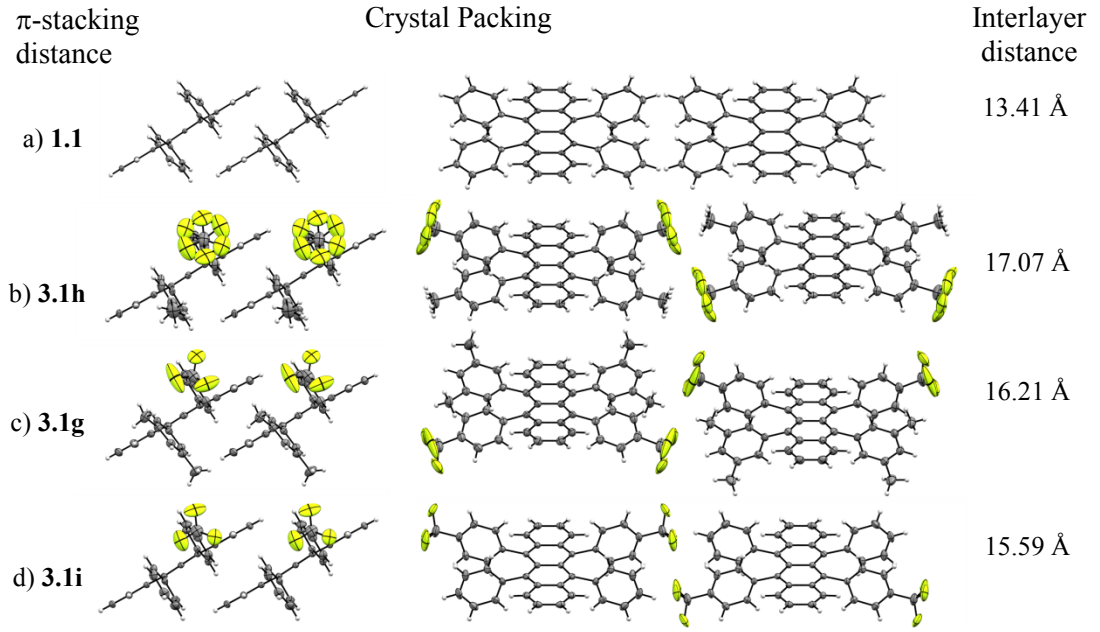

Figure 3.11. Crystal packing analysis of π-stacks (left) and interlayer distance (right) of rubrenes **a**) **1.1**, **b**) **3.1h**, **c**) **3.1g**, **d**) **3.1i**.

A few other aspects aside from the π-stacks and interlayer spacing are worth comparing in these derivatives. Due to the high degree of π-stacking in all three derivatives **3.1g,h,i**, it is unsurprising that none of the derivatives have roll displacement, which is also not seen in rubrene **1.1**. However, the different substituents influence the pitch displacement. As discussed in Chapter 1.2, rubrene exhibits a pitch displacement of 6.17 Å. Interestingly, the addition of a *p*-trifluoromethyl substituent on one set of phenyls in **3.1i** effected no change in the pitch displacement (6.17 Å), while addition of both *p*-trifluoromethyl and *p*-methyl groups on the two sets of phenyls in **3.1h** caused the pitch displacement to increase to 6.22 Å. Addition of a *p*-trifluoromethyl and two *m*-methyl groups in **3.1g** on the other hand significantly increased the

pitch displacement to 6.60 Å. The solid-state packing in this derivative accommodates the steric interactions between substituents by increasing the pitch displacement.

Due to the presence of fluorine atoms, these derivatives also exhibit interactions between hydrogen and fluorine atoms. Intermolecular short contacts (less than the sum of the Van der Waals radii) between C–H•••F were found to occur in all three derivatives (Table 3.9). These contacts likely stabilize the solid-state structure, similar to the interactions previously observed in a variety of fluorobenzenes.[29]

Table 3.9. Intermolecular short C–H•••F contacts for **3.1g-i**. To determine the short contacts, all aromatic C–H bonds were set to 1.083 Å; all sp^3 C–H bonds were set to 1.074 Å; all C–F bonds were set to 1.336 Å. Contacts below the hydrogen-fluorine Van der Waals radii summation of 2.56 Å were considered short.

Derivative	Contact (C-H…F)	Distance (Å)	Angle (°)	Symmetry Operation (Symm op1/Symm op2)
3.1g	H19…F3	2.414	143.35	x,y,z/x,1/2-y,1-z
3.1h	H23B…F3	2.549	156.03	x,y,z/1-x,1-y,1-z
	H23B…F3	2.549	156.03	x,y,1.5-z/1-x,1-y,1/2+z
	H23D…F1'	2.100	169.85	x,y,z/1-x,1/2+y,z
	H23D…F1'	2.100	169.85	x,y,1.5-z/1-x,1/2+y,1.5-z
	H23E…F3'	2.055	165.27	x,y,z/-x,1/2+y,z
	H23E…F3'	2.055	165.27	x,y,1.5-z/-x,1/2+y,1.5-z
	H19…F3	2.414	143.35	x,y,1.5-z/x,1/2-y,1/2+z
3.1i	H19A…F1	2.398	151.57	x,y,z/1/2-x,1-y,-1/2+z
	H19A…F1	2.398	151.57	x,1.5-y,z/1/2-x,1/2+y,1/2+z

Another aspect examined between the derivatives was the orientation of the π-stacks between layers. Upon close inspection, we found that only one derivative, **3.1g**, does not follow the orientation of rubrene. The π-stacking layers in rubrene **1.1** all tilt in the same direction (Figure 3.12a), which was found to be the case in derivatives **3.1h,i** (Figure 3.12c,d). However, the layers in derivative **3.1g** alternate the direction of tilt (Figure 3.12b), which may have an unknown influence on the charge carrier mobility.

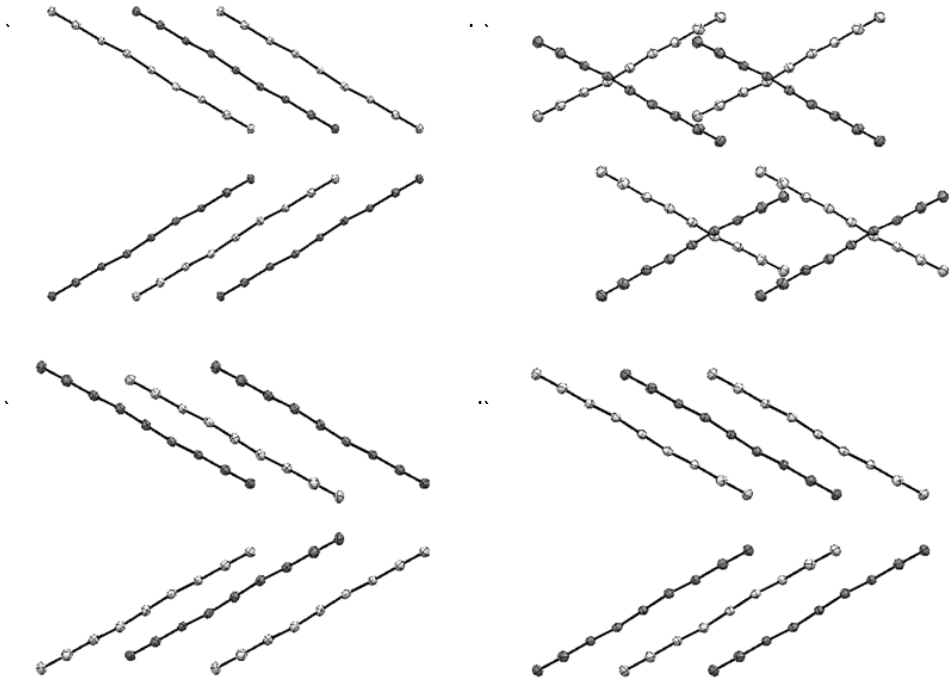

Figure 3.12. 2D representation of the tetracene core tilt in layers of rubrenes **a**) **1.1**, **b**) **3.1g**, **c**) **3.1h**, **d**) **3.1i**. Peripheral phenyls removed for clarity. Light grey tetracene cores are one layer behind in 3D space.

3.3.3 Cyclic voltammetry and computational analysis of derivatives

Having analyzed the solid-state packing, crystallized rubrenes **3.1a,c,e,g,h,i** were then compared to rubrene **1.1** using solution-phase cyclic voltammetry. The derivatives were tested in a 0.1 M tetrabutylammonium perchlorate in 1,2-dichloroethane under Ar using Au working electrode, Ag/AgCl reference electrode, and Pt counter electrode. Three runs were collected at a 100 mV/s sweep rate and averaged to obtain the potentials for each derivative. The derivatives with twisted tetracene cores (**3.1a,c,e**, Figure 3.13) were found to have oxidation potentials that were slightly smaller than rubrene **1.1** (Table 3.9, Entries 1-4) while reduction potentials were not able to be measured for any of the twisted derivatives. On the other hand, the oxidation potentials

of the π-stacking derivatives (**3.1g,h,i**, Figure 3.14) were found to be slightly larger than rubrene **1.1** (Table 3.9, Entries 5-7), which may not be surprising due to the trifluoromethyl substituents. For **3.1h** and **3.1i**, reduction potentials were measured and found to be smaller than **1.1**. The energy gap could then be calculated for **3.1h,i** and was found to be comparable to **1.1**. Our collaborators, Dr. Chad Risko and Chris Sutton, in the Brédas group of the School of Chemistry and Biochemistry at the Georgia Institute of Technology, Atlanta, GA performed calculations on the molecular structures of derivatives **3.1a,c,e,g,h,i**. Adiabatic ionization potentials and electron affinities were found to agree with the trends observed in the solution-phase measured redox potentials.

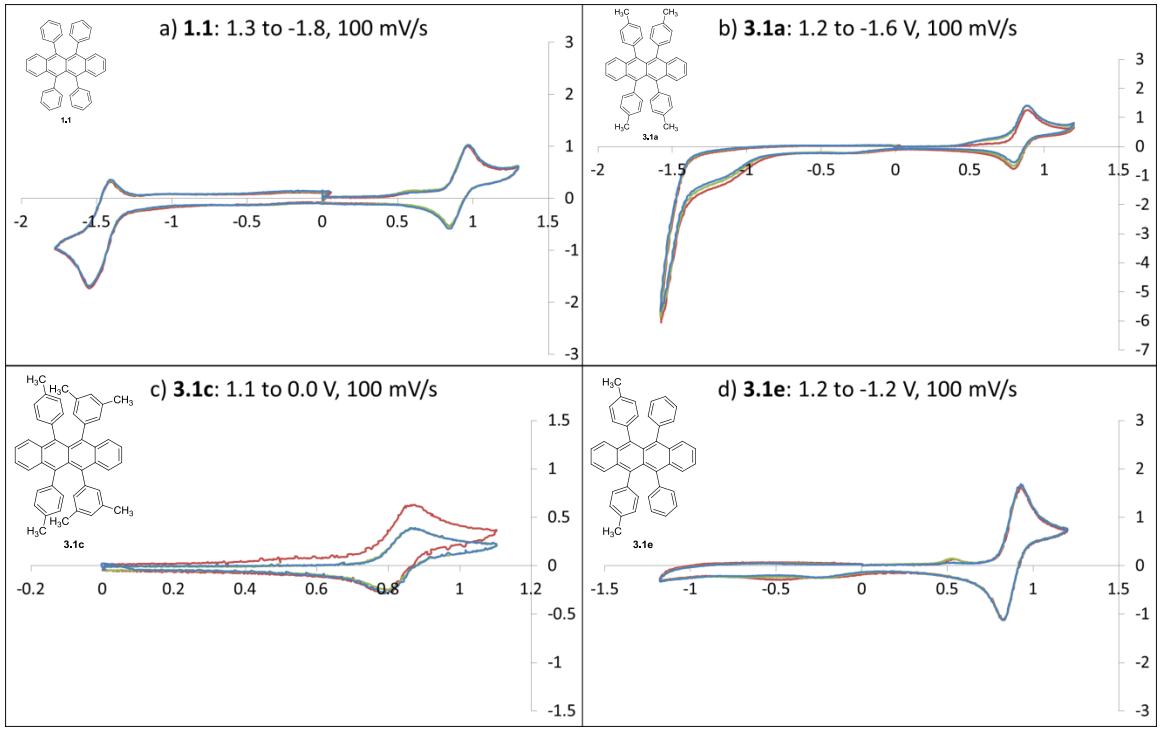

Figure 3.13. Potential traces of rubrenes **a) 1.1**, **b) 3.1a**, **c) 3.1c**, **d) 3.1e**. Reduction potentials not observed for the three derivatives.

Table 3.10. Redox potentials determined via Cyclic Voltammetry, B3LYP/6-31G(d,p)-Determined Adiabatic Ionization Potentials (AIP), and Electron Affinities (AEA).

Entry	Rubrene	$E_{1/2ox}$ (V)	$E_{1/2red}$ (V)	E_g (V)	AIP (eV)	AEA (eV)
1	**1.1**	0.36	−2.03	2.39	5.71	−1.06
2	**3.1a**	0.29	–[a]	–[b]	5.56	−1.00
3	**3.1c**	0.29	–[a]	–[b]	5.54	−0.96
4	**3.1e**	0.33	–[a]	–[b]	5.63	−1.03
5	**3.1g**	0.43	–[a]	–[b]	5.89	−1.35
6	**3.1h**	0.44	−1.89	2.33	5.93	−1.34
7	**3.1i**	0.49	−1.91	2.39	5.99	−1.41

[a]Event was not measured. [b]Could not be calculated.

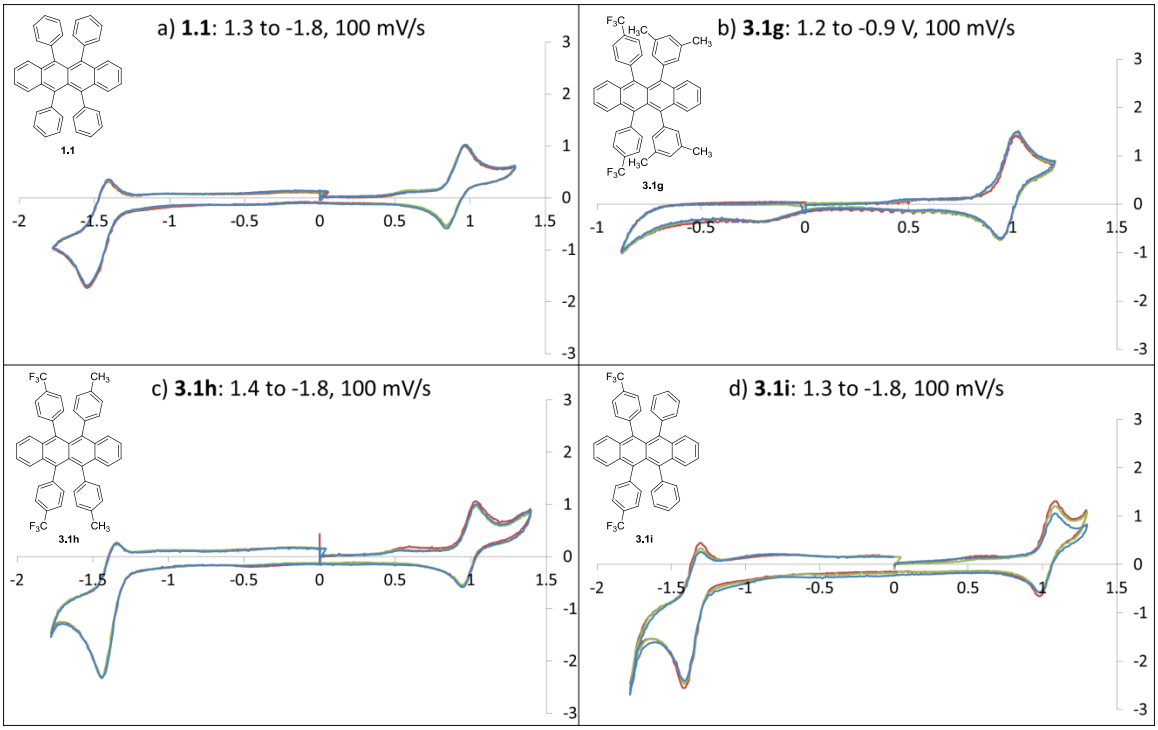

Figure 3.14. Cyclic voltammetry traces of rubrenes **a**) **1.1**, **b**) **3.1g**, **c**) **3.1h**, **d**) **3.1i**. Reduction potential not observed for derivative **3.1g.**

The similarity of the band gap and perceived minor shifts in the HOMO-LUMO levels between rubrene **1.1** and derivatives **3.1g,h,i** indicate that the chosen substituents have not greatly impacted the electronics of the material. To determine the predicted effect of the solid-state structure on the charge carrier mobility, our collaborators calculated the intermolecular electronic couplings (transfer integrals) for the π-stacking derivatives based on the solved crystal structures. The largest transfer integrals are obtained in the π-stacking direction of these molecules, due to the increased amount of π-orbital overlap. The couplings of **1.1** (100 meV for holes and 53 meV for electrons) were found to be comparable to derivative **3.1g** (95, 79 meV) for hole transport, while derivatives **3.1h** (134, 82 meV) and **3.1i** (126, 71 meV) both had larger hole and electron couplings compared to the parent compound. These couplings indicate that all three congeners should function as ambipolar materials, exhibiting both hole and electron carrier mobilities that are higher than rubrene **1.1**, providing the intrinsic mobilities can be realized.

3.3.4 Single-crystal OFET measurements of derivatives

Our collaborator, Wei Xie, in the Frisbie group of the Department of Chemical Engineering and Materials Science at the University of Minnesota, Minneapolis, MN performed single-crystal OFET measurements on our derivatives. Rubrenes **3.1h,i** were the focus of these measurements due to their similar packing motifs and systematic differences as compared to rubrene **1.1**. Crystals were first grown using physical vapor transport, then checked using various X-ray diffraction techniques to ensure the packing motif and crystal integrity matched the solution-grown crystals. A sublimed crystal of **3.1h** was checked using single-crystal X-ray diffraction to ensure the crystal was in the same setting as the solution grown crystals. Interestingly, the solved structure was found to be a polymorph (Orthorhombic, Cmca) with

almost identical unit cell constants and packing motif (Table 3.11, Figure 3.15). The intermolecular distances (π-stacks and interlayer) were found to also be almost identical with the solution grown crystals (Figure 3.15c-f). The key difference is in the orientation of the neighboring layers. In the solution grown crystals, the neighboring layers are spaced unevenly next to the π-stacks, while in the sublimation grown crystals the neighboring layers are centered next to the π-stacks (Figure 3.15g-h). This structure appears to have a high degree of symmetry in which the trifluoromethyl and the methyl group, being of similar volume, appear the same. This disorder was modeled so that both the fluorines and the methyl hydrogens are half-occupancy, which causes the molecule to appear as if it were symmetrically tetra-substituted with trifluoromethyl when it is not. The sublimation grown crystals have actually adopted the exact same packing structure as rubrene **1.1**, which makes this derivative even more appropriate for structure-property relationship studies in single-crystal OFET.

Table 3.11. Crystal data and structure refinement for rubrene **3.1h** grown by sublimation.

Rubrene	**3.1h**	
Empirical formula	$C_{46}H_{30}F_6$	
Formula weight	696.7	
Temperature	173(2) K	
Wavelength	0.71073 Å	
Crystal system	Orthorhombic	
Space group	Cmca	
Unit cell dimensions	a = 34.197(6) Å	$\alpha = 90°$
	b = 7.1577(11) Å	$\beta = 90°$
	c = 14.052(2) Å	$\gamma = 90°$
Volume	3439.5(9) Å^3	
Z	4	
Density (calculated)	1.345 Mg/m^3	
Absorption coefficient	0.100 mm^{-1}	
F(000)	1440	
Crystal color, morphology	Orange, Plate	
Crystal size	0.15 x 0.14 x 0.05 mm^3	
Theta range for data collection	2.38 to 26.37°	
Index ranges	-42 £ h £ 42, -8 £ k £ 8, -17 £ l £ 17	
Reflections collected	15175	
Independent reflections	1791 [R(int) = 0.0660]	
Observed reflections	1155	
Completeness to theta = 26.37°	99.90%	
Absorption correction	Multi-scan	
Max. and min. transmission	0.9950 and 0.9852	
Refinement method	Full-matrix least-squares on F^2	
Data / restraints / parameters	1791 / 0 / 124	
Goodness-of-fit on F^2	1.031	
Final R indices [I>2sigma(I)]	R1 = 0.0527, wR2 = 0.1331	
R indices (all data)	R1 = 0.0915, wR2 = 0.1560	
Largest diff. peak and hole	0.228 and -0.204 e.Å^{-3}	

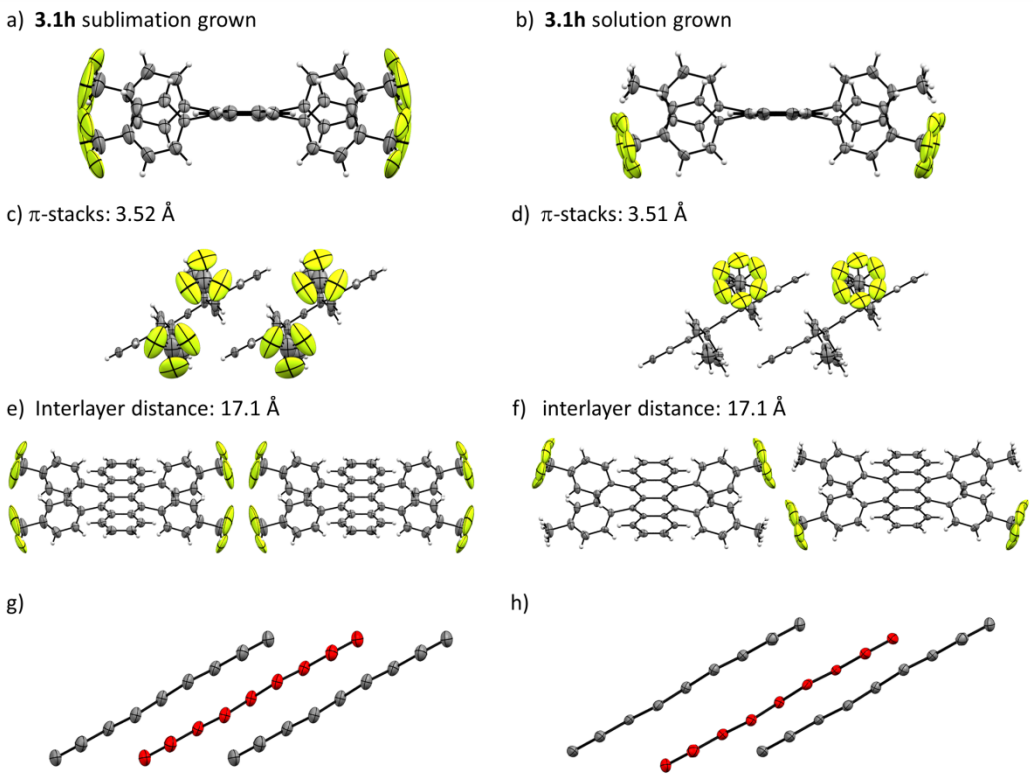

Figure 3.15. View of crystal packing aspects for **3.1h** crystals grown from sublimation (left) and solution (right). **a-b**) View down the long molecular axis of the planar tetracene core. **c-d**) View of π-stacks and π-stacking distance provided. **e-f**) View of interlayer separation and interlayer distance provided. **g-h**) View of π-stacks between tetracene cores with next layer indicated in red. Red molecules are one layer behind in 3D space. Side phenyls and hydrogens removed for clarity.

A variety of OFET architectures were attempted in order to optimize the charge carrier mobility measurements of the derivatives. Interestingly, the architecture that provides the highest mobilities in rubrene **1.1** provided very low mobilities in the derivatives. Changing the architecture to top-contact bottom-gate geometry with PMMA as the dielectric layer improved the performance of the derivatives and all three derivatives showed ambipolar mobility as predicted (Table 3.12). Average mobilities were found to be comparable to rubrene, while the maximum hole charge carrier mobility for **3.1h** exceeded that of **1.1**.[30]

Table 3.12. Summary of measured charge carrier mobilities (μ, $cm^2V^{-1}s^{-1}$) in PMMA gated, top contact architecture.

Entry	Rubrene	μ_h, avg (sdev)	μ_h, max	μ_e, avg (sdev)	μ_e, max
1	**1.1**	0.43 (0.27)	0.83	0.0038 (0.0035)	0.0077
2	**3.1g**	0.074 (0.02)	0.10	0.008 (0.005)	0.013
3	**3.1h**	0.42 (0.40)	1.54	0.091 (0.07)	0.28
4	**3.1i**	0.25 (0.19)	0.63	0.12 (0.09)	0.22

The moderate carrier mobilities and necessity of top-contact architecture suggested that these molecules are limited by low charge injection, likely stemming from the shift in the HOMO-LUMO levels. Further OFET studies have revealed how challenging charge injection is for rubrene **3.1h**. Using a bottom-contact geometry with the polymer Cytop as the dielectric layer, two different devices were fabricated. The first utilized bare gold electrodes while the second utilized gold coated with a thin layer of CNTs. The CNT coverage was controlled by varying the concentration of the CNT solution, and was categorized into low density (2-4 CNTs/μm), medium density (5-15 CNTs/μm) and high density (> 20 CNTs/μm) CNT/Au electrodes, as determined by SEM images. Mobilities and contact resistance of **3.1h** were measured in both geometries (Table 3.13). The difference between these two devices is striking. Both hole and electron mobility enhance substantially, improving with the use of CNT which has been shown to improve charge injection in organic semiconductors.[31–33] Moreover, the contact resistance decreases significantly by employing CNT coverage, a direct indicator of improved charge injection between the electrode and the organic material. These device optimization studies suggest that proper device structures and rational fabrication methods are essential to reveal the intrinsic transport properties of the rubrene **3.1h** crystal, which, as discussed previously, has been predicted to exhibit comparable or even superior electrical performance then the parent molecule, rubrene **1.1**. Further discussion can be found in the pending manuscript.[34]

Table 3.13. Summary of measured mobilities and resistivities of **3.1h** in bottom-contact devices with varied electrodes.

Electrode	μ_{hole} Avg(Max) ($cm^2V^{-1}s^{-1}$)	R_c (hole) (kΩ-cm)	$\mu_{electron}$ Avg(Max) ($cm^2V^{-1}s^{-1}$)	R_c (electron) (kΩ-cm)
Au	0.66 ± 0.44 (2.03)	2741	0.017 ± 0.023 (0.096)	498502
Au with high density CNT (> 20 CNTs/μm)	2.86 ± 1.11 (4.83)	15.7 ± 7.0	1.26 ± 0.98 (4.20)	83.9 ± 39.7

Although the initial mobilities were lower than anticipated, these values validate this synthetic route as a successful method to developing rubrene congeners with modified solid-state packing structures. However, this work only scratches the surface of structure-property relationship studies in rubrenes. Further explorations into rubrene congeners would provide great insight into the impacts of molecular and solid-state structure on the device performance of organic semiconductors.

3.4 FUTURE STUDIES

The work described in this chapter has really just begun the exploration of structure-property relationship studies of rubrenes in OFET. Future targets (Figure 3.16) for this project will examine the limits of the electron-deficient and electron-rich attractive interaction of the side phenyls by using stronger electron-withdrawing (perfluorophenyl) and electron-donating groups (methoxy). Other targets include rubrenes in which the side phenyls have been united in order to overcome the repulsion and prevent the tetracene core from twisting. The synthetic route is well suited to form and crystallize rubrene derivatives, paving the way to expanding the library of crystalline rubrene derivatives and improving our understanding of charge transport in organic semiconductors.

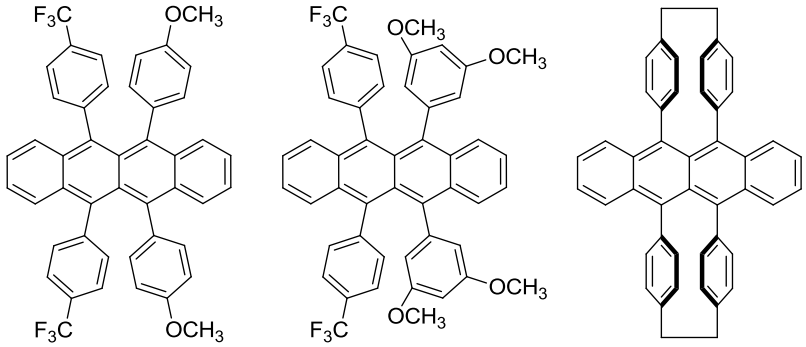

3.15 **3.16** **3.17**

Figure 3.16. Three potential future targets (**3.15**, **3.16**, **3.17)** for structure-property relationship studies.

3.5 EXPERIMENTALS

All reactions were carried out using flame-dried glassware under a nitrogen or argon atmosphere unless aqueous solutions were employed as reagents. Nitrobenzene was dried by distillation from CaH_2. Tetrahydrofuran (THF) was dried by distillation from benzophenone/sodium. Dichloromethane (CH_2Cl_2) and isopropanol were degassed by bubbling a stream of argon through the liquid in a Schlenk flask then stored and used in a N_2-filled glove box. All other chemicals were purchased from Acros Organics or Sigma-Aldrich and used as received. Analytical thin layer chromatography (TLC) was carried out using 0.25 mm silica plates from Silicycle. Eluted plates were visualized with UV light. Flash chromatography was performed using 230–400 mesh (particle size 0.04–0.063 mm) silica gel purchased from Silicycle. All other purchased reagents were used as received.

^{1}H NMR (300 and 500 MHz) and ^{13}C NMR (75 and 125 MHz) and ^{19}F (282 and 470 MHz) spectra were obtained on Varian FT NMR or Bruker FT NMR instruments. NMR spectra were reported as δ values in ppm relative to chloroform, dichloromethane, or TMS for ^{1}H (7.26, 5.32 and 0.00 ppm respectively), chloroform for ^{13}C (77.00 ppm), and hexafluorobenzene for ^{19}F (-

163.00 ppm). ^{1}H and ^{13}C NMR coupling constants are reported in Hz; multiplicity was indicated as follows; s (singlet); d (doublet); t (triplet); q (quartet); quint (quintet); m (multiplet); dd (doublet of doublets); ddd (doublet of doublet of doublets); dddd (doublet of doublet of doublet of doublets); dt (doublet of triplets); td (triplet of doublets); ddt (doublet of doublet of triplets); app (apparent); br (broad). Infrared (IR) spectra were obtained on a Thermo Scientific FT-IR as films from CH_2Cl_2 or $CDCl_3$. High-resolution mass spectra (HRMS) in EI experiments were performed on a Finnigan MAT 95 GC-MS system. Elemental analysis was performed by Atlantic Microlab, Inc., 6180 Atlantic Blvd, Suite M, Norcross, GA 30071.

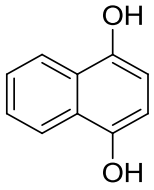

1,4-napthalenediol **3.5**: Water (600 mL) and diethyl ether (500 mL) were placed into a 2-L Erlenmeyer flask and fitted with a septum with a nitrogen inlet and outlet (attached to a mineral oil bubbler). The mixture was degassed by bubbling nitrogen through for 20 minutes at 3–5 bubbles per second. $Na_2S_2O_4$ (80 g, 0.46 mol) and 1,4-naphthoquinone (15.8 g, 0.10 mol) were added with vigorous stirring. The biphasic mixture formed a heterogeneous suspension upon vigorous stirring. The aqueous phase is removed using a 2-L separatory funnel. All separatory-funnel operations should be completed within 10 minutes; extended exposure to air leads to decreases in yield and purity. The organic phase was washed with 500 mL of water, dried over anhydrous Na_2SO_4 (20 g), filtered through cotton wool and concentrated under reduced pressure to give 1,4-naphthalenediol as a light brown solid, 14.7 g (93 % yield) that was used within 48 hours after preparation and stored in a brown-glass bottle due to its sensitivity to light and air. ^{1}H

NMR (500 MHz, $CDCl_3$) δ 8.13 (dd, J = 3.3, 6.5 Hz, 2H), 7.53 (dd, J = 3.3, 6.5 Hz, 2H), 6.67 (s, 2H).

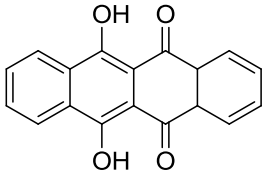

6,11-Dihydroxy-5,12-tetracenedione **3.4**: A flame-dried 500-mL 3-necked round-bottomed flask was fitted with an overhead mechanical stirrer, glass stopper and glass adapter with a line to nitrogen gas. Under a nitrogen atmosphere, $AlCl_3$ (30.0 g, 0.22 mol, 3.5 equiv.) was placed in the flask as a solid. Nitrobenzene (25 mL) was added by syringe and the mixture is stirred at 60 °C using an oil bath for 30 minutes. Additional nitrobenzene was added by syringe until a fine light yellow suspension was obtained (approximately 15 mL). 1,4-Naphthalenediol (10.0 g, 0.062 mol, 1.0 equiv., added as a solid) and phthaloyl chloride (13.0 g, 0.064 mol, 1.0 equiv., added as a liquid via syringe) were added portion-wise over 5 minutes to the reaction flask, alternating portions of each reagent. Additional nitrobenzene (approximately 10 mL) was used to wash down the starting materials that were adhering to the flask. The deep red reaction mixture was stirred for 4 hours at 90 °C using an oil bath, allowed to cool to room temperature and the septum was replaced with a dropping funnel. The dropping funnel is charged with 12 M HCl (200 mL) that was added slowly over 20 minutes (Caution, gas evolution). The black reaction mixture is transferred to a 2-L Erlenmeyer flask equipped with a magnetic stir bar and additional 12 M HCl (350 mL) was used to wash the remaining contents from the 3-necked flask into the Erlenmeyer flask. The resulting mixture is stirred vigorously with a magnetic stirring plate at room temperature for 1 hour. The slurry is filtered through a 500-mL fine porosity fritted glass filter (The filtration process is time consuming (overnight or a whole day) as

the slurry slowly goes through the fine fritted glass filter (4 – 5.5 microns). The use of a medium porosity filter (10–16 microns) gave poor mass recovery. Swirling and mixing the material on the filter with a spatula from time to time helps speed the filtration.). The resulting dark red solid (An ^{1}H NMR spectrum is provided for this compound.) was washed with acetone (200 mL) and dried overnight on the filter. The solid was transferred into a 2-L Erlenmeyer flask equipped with a magnetic stir bar using acetone (800 mL) and the resulting mixture is stirred vigorously on a magnetic stirring plate at room temperature for 14 hours. The slurry was filtered through a 500-mL fine porosity fritted glass filter and washed with acetone (200 mL), then dried overnight on the filter. The resulting solid was transferred into a 2-L Erlenmeyer flask equipped with a magnetic stir bar containing a solution of sodium potassium tartrate tetrahydrate (90 g, 0.3 mol) in H_2O (1300 mL), and the mixture is stirred vigorously with a magnetic stirrer for 2 hours at 70 °C using a hot plate, and an additional 10 hours at room temperature. The mixture is filtered through a 500-mL fine-porosity fritted glass filter, and the solid was washed sequentially with 12 M HCl (200 mL), warm (45–50°C) H_2O (1000 mL) and acetone (500 mL). The resulting solid is dried for 14 hours in a vacuum desiccator (vacuum measured to be 0.1 Torr which was then left as a static vacuum) over P_2O_5 (20 g) to give the final product as a red powder 12.0 g, 0.041 mol, 67% yield, mp 349–351 °C; ^{1}H NMR (300 MHz, $CDCl_3$) δ 15.20 (s, 2H), 8.50 (dd, J = 3.4, 6.0 Hz, 4H), 7.84 (dd, J = 3.3, 6.1 Hz, 4H); IR (thin film, CH_2Cl_2) 3102, 3056, 1624, 1579, 1510, 1464, 1417, 1264, 1045, 862, 725 cm^{-1}. Elemental analysis, calculated for $C_{18}H_{10}O_4$: C, 74.48; H, 3.47; O, 22.05; Found: C, 74.47; H, 3.36; O, 22.21. Crystals for X-ray crystallographic analysis were obtained by slow evaporation of the product in a saturated chloroform solution over about 10 days, diffraction matched the published data.[34] 6,11-dihydroxy-5,12-tetracenedione is nearly insoluble in 9 common deuterated solvents screened, making ^{13}C NMR data unobtainable.

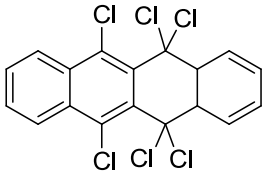

5,5,6,11,12,12-hexachloro-5,12-dihydrotetracene **3.7**: $POCl_3$ (120 mL, 210 g, 1.4 mol) was added slowly by dropping funnel to a mixture of PCl_5 (50 g, 0.35 mol) and 1.3 (10 g, 0.034 mol) in a flame-dried round bottom flask. The red reaction mixture was heated to reflux (approximately 110 °C) and maintained for 5 hours until the red color had dissipated. The reaction mixture was cooled to room temperature, filtered through a fritted glass filter, and the precipitate was washed sequentially with glacial acetic acid (50mL) and hexanes (50mL). The residue was collected and dried under vacuum to give 1.7 as a white powder (13.00 g, 0.030 mol, 89%): ^{1}H NMR (500 MHz, $CDCl_3$) δ 8.68 (dd, J = 3.3, 6.6, 2H), 8.14 (dd, J = 3.4, 6.3, 2H), 7.79 (dd, J = 3.3, 6.7, 2H), 7.55 (dd, J = 3.4, 6.3, 2H).

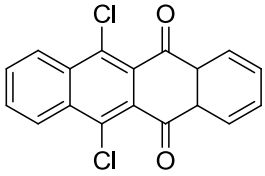

6,11-dichlorotetracene-5,12-dione **3.3**: This material was synthesized using a modified procedure.[35] Into a 2L round-bottom flask **3.7** (12.7 g, 29.1 mmol) was added. Concentrated sulfuric acid H_2SO_4 (75 mL) was slowly added and the mixture was stirred at RT for 2 h. (Caution! The addition of concentrated H_2SO_4 causes a foam to form; the large flask is needed to prevent overflow of the reaction vessel.) The reaction mixture was poured carefully into water (1000 mL). The tan precipitate was filtered and washed with water (1500mL) providing the crude product as a tan powder (9.48 g). The material was recrystallized from hot toluene during which the hot mixture was filtered through filter paper to remove a dark insoluble solid. Pure orange crystals were obtained (5.16 g, 15.8 mmol, 54%). A second crop was

obtained from concentrating the filtrate and recrystallizing from toluene, although the crystals were red (1.33 g, 4.07 mmol, 14%): ^{1}H NMR (300 MHz, $CDCl_3$) δ 8.75 (dd, J = 3.3, 6.5 Hz, 2H), 8.22 (dd, J = 3.3, 5.8 Hz, 2H), 7.86 (dd, J = 3.3, 6.6 Hz, 2H), 7.79 (dd, J = 3.3, 5.8 Hz, 2H).

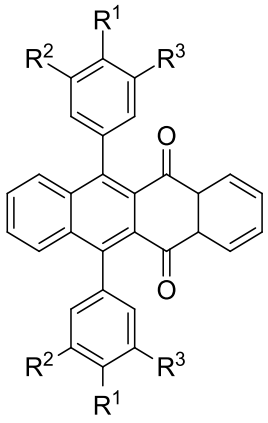

General Procedure to diaryltetracenediones **3.2a-f**: Benzene (40.8 mL), dioxane (40.8 mL), H_2O (27.2 mL) were added to a Schlenk flask. Nitrogen gas was bubbled through the solvents for 15 min. 6,11-Dichlorotetracene-5,12-dione **3.3** (2.22 g, 6.79 mmol, 1.0 equiv.), aryl boronic acid (**3.10**, 2.77 g, 20.4 mmol, 3.0 equiv.), Cs_2CO_3 (8.86 g, 27.2 mmol, 4.0 equivalents), and $PdCl_2(dppf)•CH_2Cl_2$ (0.498 g, 0.680 mmol, 0.1 equivalent) were then added. The flask was sealed and maintained at 60 °C for 16 h. The reaction mixture was allowed to cool to room temperature then transferred into a separatory funnel containing ethyl acetate and H_2O (100 mL each) with the aid of ethyl acetate and H_2O. After separating the layers, the aqueous layer was extracted ethyl acetate (3 × 100 mL). The combined organic extracts were washed with brine (1 × 100 mL), dried over Na_2SO_4, filtered through celite, and concentrated in vacuo to give a brown solid. The crude product was purified by column chromatography (gradient 4:1 hexanes:$CHCl_3$ to 1:1 hexanes: $CHCl_3$) to give **3.2** as a yellow solid.

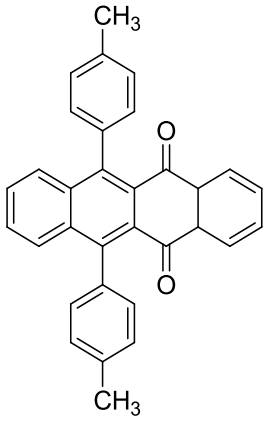

Diaryltetracenedione **3.2a**: Following the general procedure using **3.3** (2.22 g, 6.79 mmol) and **3.10a** (2.77 g, 20.4 mmol), **3.2a** was obtained as a yellow solid (2.77 g, 6.32 mmol, 93%). mp 295-296 °C; R_f = 0.27 (1:1 hexanes:CH_2Cl_2); ^{1}H NMR (300 MHz, $CDCl_3$) δ 2.55 (s, 6 H), 7.20 (d, J = 8.0 Hz, 4 H),7.40 (d, J = 7.8 Hz, 4 H), 7.49 (dd, J = 3.3, 6.6 Hz, 2 H), 7.60 (dd, J = 3.4, 6.7 Hz, 2 H), 7.66 (dd, J = 3.3, 5.9 Hz, 2 H), 8.10 (dd, J = 3.3, 5.9 Hz, 2 H); ^{13}C NMR (75 MHz, $CDCl_3$) δ 21.6, 126.9, 127.6, 128.5, 128.7, 128.8, 129.2, 133.5, 135.0, 135.8, 135.6, 137.2, 144.0, 184.4; IR (thin film, CH_2Cl_2) 3068, 2916, 1676, 1591 cm^{-1}; HRMS (EI) *m*/*z* calcd for $C_{32}H_{22}O_2$ $[M]^+$ 438.1620, found 438.1643.

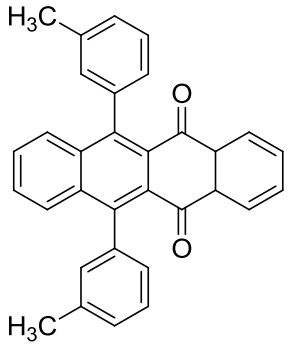

Diaryltetracenedione **3.2b**: Following the general procedure using **3.3** (1.36 g, 4.17 mmol) and **3.10b** (1.70 g, 12.5 mmol), **3.2b** was obtained as a yellow solid (1.67 g, 3.80 mmol, 91%). ^{1}H NMR (300 MHz, $CDCl_3$) δ 2.50 (s, 6H), 7.13-7.15 (m, 4H), 7.38 (d, *J* = 7.5

Hz, 2H), 7.48-7.54 (m, 4H), 7.61 (dd, J = 3.4, 6.8 Hz, 2H), 7.68 (dd, J = 3.3, 5.8 Hz, 2H), 8.12 (dd, J = 3.3, 5.8 Hz, 2H).

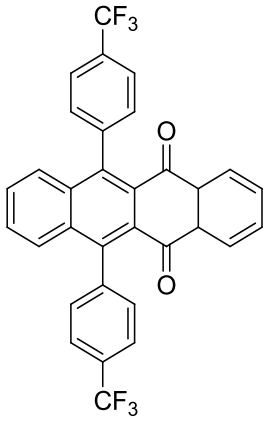

Diaryltetracenedione **3.2c**: Following the general procedure using **3.3** (1.90 g, 5.80 mmol) and **3.10c** (2.79 g, 14.7 mmol), **3.2c** was obtained as a yellow solid (2.45 g, 4.48 mmol, 91%). R_f = 0.26 (1:1 hexanes: CH_2Cl_2); Tm[1] 324.24 °C; ^{1}H NMR (500 MHz, $CDCl_3$) δ 7.44-7.47 (m, 6 H), 7.56 (dd, J = 3.3, 6.7 Hz, 2 H), 7.71 (dd, J = 3.3, 5.9 Hz, 2 H), 7.86 (d, J = 8.0 Hz, 4 H), 8.08 (dd, J = 3.4, 5.9 Hz, 2 H); ^{13}C NMR (125 MHz, $CDCl_3$) δ 124.4 (q, $J_{C\text{-}F}$ = 270.5 Hz), 125.5 (q, $J_{C\text{-}F}$ = 3.6 Hz), 127.0, 127.4, 128.5, 129.0, 129.4 (q, $J_{C\text{-}F}$ = 32.4 Hz), 129.5, 134.0, 134.6, 135.2, 142.8, 144.2, 183.8; ^{19}F NMR (470 MHz, $CDCl_3$) δ −63.46; IR (thin film, CH_2Cl_2) 3053, 2987, 1673, 1615, 1591, 1495, 1406 cm^{-1}; HRMS (EI) m/z calcd for $C_{32}H_{16}F_6O_2$ $[M]^+$ m/z 546.1054, found 546.1019.

[1] Melting point determined by TA Instruments Discovery DSC calibrated with indium; ramp 10.00 °C/min to 350.00 °C.

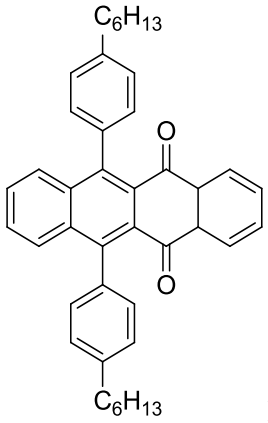

Diaryltetracenedione **3.2d**: Following the general procedure using **3.3** (0.458 g, 1.40 mmol) and **3.10d** (0.853 g, 4.14 mmol), **3.2d** was obtained as a yellow solid (0.212 g, 0.370 mmol, 26%). R_f = 0.52 (1:1 hexanes: CH_2Cl_2); ^{1}H NMR (300 MHz, $CDCl_3$) δ 0.92-0.96 (m, 6H), 1.37-1.49 (m, 12H), 1.74-1.84 (m, 4H), 2.77-2.82 (m, 4H), 7.21 (d, *J* = 8.0 Hz, 4H), 7.40 (d, *J* = 8.0 Hz, 4H), 7.49 (dd, *J* = 3.1, 6.5 Hz, 2H), 7.58 (dd, *J* = 3.4, 6.9 Hz, 2H), 7.65 (dd, *J* = 3.3, 5.9 Hz, 2H), 8.08 (dd, *J* = 3.3, 5.8 Hz, 2H).

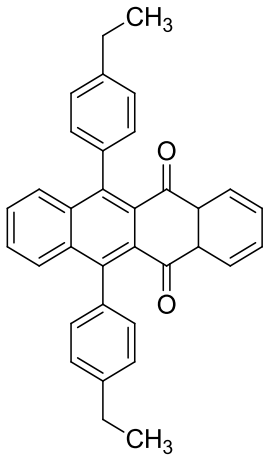

Diaryltetracenedione **3.2e**: Following the general procedure using **3.3** (2.05 g, 6.27 mmol) and **3.10e** (2.82 g, 18.8 mmol), **3.2e** was obtained as a yellow solid (2.80 g, 6.00 mmol, 96%). mp 259-260 °C, R_f = 0.30 (1:1 Hexanes:Dichloromethane), ^{1}H NMR (300 MHz, $CDCl_3$) δ 1.41 (t, *J* = 7.6 Hz, 6 H), 2.86 (q, *J* = 7.6 Hz, 4 H), 7.22 (d, *J* = 8.0 Hz, 4 H), 7.42 (d, *J*

= 8.0 Hz, 4 H), 7.49 (dd, *J* = 3.4, 6.5 Hz, 2 H), 7.60 (dd, *J* = 3.4, 6.8 Hz, 2 H), 7.66 (dd, *J* = 3.3, 5.8 Hz, 2 H), 8.09 (dd, *J* = 3.3, 5.9 Hz, 2 H) ; ^{13}C NMR (75 MHz, $CDCl_3$) δ 15.1, 28.5, 126.7, 127.5, 127.6, 128.3, 128.5, 128.7, 133.3, 134.8, 135.6, 137.2, 142.5, 143.9, 184.2; IR (thin film, CH_2Cl_2) 3076, 3053, 2966, 2920, 1678, 1374, 1338, 1260, 992, 724 cm^{-1}, HRMS (EI) *m*/*z* calcd for $C_{34}H_{26}O_2$ $[M]^+$ 466.1933, found 466.1924.

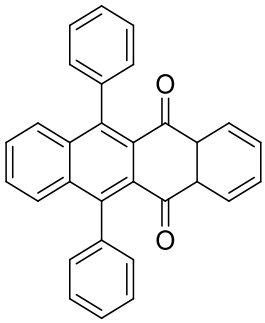

Diaryltetracenedione **3.2f**: Following the general procedure using **3.3** (4.00 g, 12.2 mmol) and **3.10f** (4.46 g, 36.6 mmol), **3.2f** was obtained as a yellow solid (3.9 g, 9.5 mmol, 78%). ^{1}H NMR (300 MHz, $CDCl_3$) δ 7.31-7.34 (m, 4H), 7.49-7.53 (m, 2H), 7.56-7.64 (m, 8H), 7.67 (dd, *J* = 3.3, 5.9 Hz, 2H), 8.09 (dd, *J* = 3.3, 5.9 Hz, 2H).

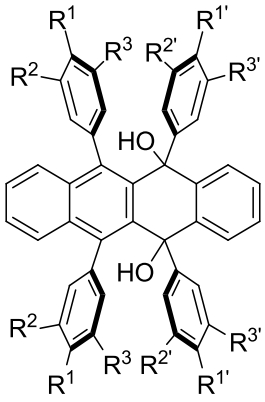

General procedure to tetracenediols **3.8a-j**: Arylbromide **3.9'** (7.01 mL, 57.0 mmol, 10.0 equiv.) and THF (95.0 mL) were added to a flame-dried 100 mL round bottom flask. The solution was cooled to –78 °C, then *n*-BuLi (2.5 M solution in hexanes, 22.0 mL, 9.8

equiv.) was added dropwise. The solution was maintained at -78 °C for 20 min. During this time, **3.2** (2.50 g, 5.70 mmol, 1 equiv.) and THF (55 mL) were added to a separate flame-dried 250 mL round bottom flask. The solution was cooled to –78 °C. The organolithium solution was then added to the tetracenedione solution dropwise via cannula. The reaction was allowed to warm to room temperature overnight. The reaction mixture was then transferred into a separatory funnel containing saturated aqueous NH_4Cl (100 mL) with the aid of diethyl ether. The aqueous layer was then extracted with diethyl ether (3 × 100 mL). The organic extracts were combined, dried over Na_2SO_4, filtered, and concentrated in vacuo to give the crude solid. Immediate purification by column chromatography (1:1 hexanes:CH_2Cl_2) gave two unassigned diastereomers **3.8** that were taken on to the next reaction based on diagnostic ^1H and ^{19}F NMR data.

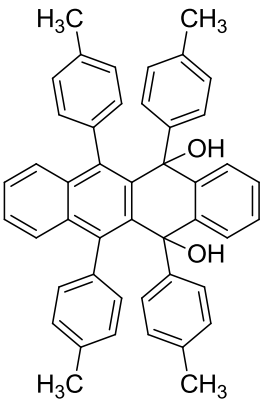

Tetracenediol **3.8a**: Following the general procedure using **3.2a** (2.50 g, 5.70 mmol) and **3.9'a** (7.01 mL, 57.0 mmol), two unassigned diastereomers were obtained as colorless solids after washing with pentane to remove non-polar impurities. Major diastereomer: (2.69 g, 4.32 mmol, 76%), R_f = 0.13 (1:1 hexanes:CH_2Cl_2); ^1H NMR (300 MHz, $CDCl_3$) δ 2.27 (s, 6H), 2.40 (s, 6H), 3.70 (s, 2H), 6.12 (d, J = 7.9 Hz, 2H), 6.70 (d, J = 8.0 Hz, 2H), 6.81 (d, J = 8.0 Hz, 4H), 6.92-7.02 (m, 8H), 7.13-7.21 (m, 8H); Minor diastereomer: (0.432 g, 0.694 mmol, 12%), R_f = 0.49 (1:1 hexanes:CH2Cl2); ^1H NMR (300 MHz, $CDCl_3$) δ 2.25 (s, 6H), 2.46 (s, 6H),

3.75 (s, 2H), 5.87 (dd, J = 1.8, 7.8 Hz, 2H), 6.79-6.99 (m, 14H), 7.15 (dd, J = 3.4, 6.6 Hz, 2H), 7.23 (dd, J = 3.4, 6.1 Hz, 2H), 7.34 (dd, J = 1.2, 7.8 Hz, 2H), 7.44 (dd, J = 1.9, 7.7 Hz, 2H).

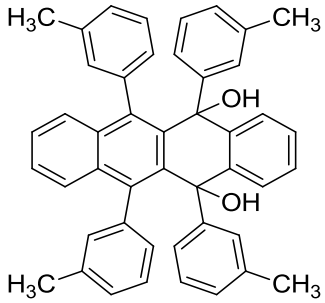

Tetracenediol **3.8b**: Following the general procedure using **3.2b** (1.21 g, 2.76 mmol) and **3.9'b** (3.40 mL, 28.0 mmol), the crude mixture was treated with toluene then filtered to obtain a single unassigned diastereomer as a colorless solid (0.8704 g, 1.40 mmol, 50%). Diagnostic ^{1}H NMR (300 MHz, $CDCl_3$) δ 2.13 (s, 12H), 4.00 (s, 2H), 5.99 (d, J = 7.8 Hz, 2H).

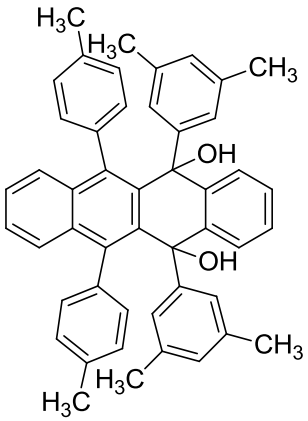

Tetracenediol **3.8c**: Following the general procedure using **3.2a** (1.80 g, 4.10 mmol) and **3.9'c** (5.57 mL, 41.0 mmol), a single diastereomer with unidentified impurity (2.18 g) was obtained after column chromatography (toluene) as a cream-colored solid with orange tint. R_f = 0.10 (1:1 hexanes:CH_2Cl_2); ^{1}H NMR (300 MHz, $CDCl_3$) δ 2.13 (s, 12H), 2.40

(s, 6H), 4.06 (bs, 2H), 5.99 (d, J = 7.9 Hz, 2H), 6.66 (app s, 8H), 6.84-6.88 (m, 2H), 7.00-7.05 (m, 8H), 7.17 (dd, J = 3.4, 6.8 Hz, 2H).

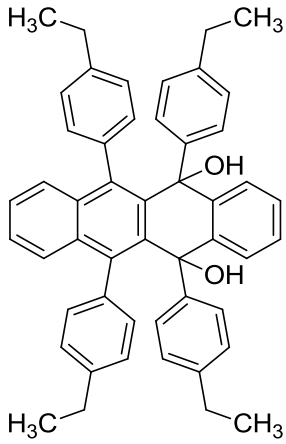

Tetracenediol **3.8d**: Following the general procedure using **3.2e** (0.100 g, 0.228 mmol) and **3.9'd** (0.320, 2.32 mmol), two unassigned diastereomers were obtained. Major diastereomer (yellow solid): (0.115 g, 0.169 mmol, 74%); R_f = 0.03 (2:1 hexanes:CH_2Cl_2); ^{1}H NMR (300 MHz, $CDCl_3$) δ 1.21 (t, *J* = 7.5 Hz, 6H), 1.32 (t, *J* = 7.5 Hz, 6H), 2.54 (q, *J* = 7.6 Hz, 4H), 2.62 (q, *J* = 7.6 Hz, 6H), 4.64 (s, 2H), 6.00 (d, *J* = 7.9 Hz, 2H), 6.58 (d, *J* = 7.9 Hz, 2H), 6.67 (dd, *J* = 3.4, 6.2 Hz, 2H), 6.77-6.84 (m, 10H), 6.88 (d, *J* = 8.3 Hz, 4H), 6.99 (dd, *J* = 3.2, 6.6 Hz, 2H), 7.11 (dd, *J* = 3.4, 6.8 Hz, 2H). Minor diastereomer (colorless solid): (0.020 g, 0.029 mmol, 13%); R_f = 0.26 (2:1 hexanes:CH_2Cl_2); ^{1}H NMR (300 MHz, $CDCl_3$) δ 1.19 (t, *J* = 7.5 Hz, 6H), 1.36 (t, *J* = 7.5 Hz, 6H), 2.54 (q, *J* = 7.5 Hz, 4H), 2.74 (q, *J* = 7.6 Hz, 4H), 3.75 (s, 2H), 5.88 (dd, *J* = 1.7, 7.9 Hz, 2H), 6.77 (dd, *J* = 1.5, 7.9 Hz, 2H), 6.85 (d, *J* = 8.3 Hz, 4H), 6.92 (d, *J* = 8.2 Hz, 4H), 6.98 (dd, *J* = 3.4, 6.3 Hz, 4H), 7.14 (dd, *J* = 3.3, 6.8 Hz, 2H), 7.22 (dd, *J* = 3.4, 6.2 Hz, 2H), 7.35 (dd, *J* = 1.5, 7.7 Hz, 2H), 7.46 (dd, *J* = 1.7, 7.7 Hz, 2H).

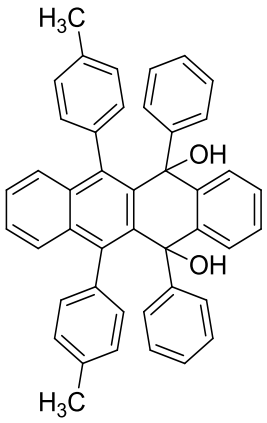

Tetracenediol **3.8e**: Following the general procedure using **3.2a** (0.172 g, 0.392 mmol) and **3.9'e** (0.410 mL, 3.90 mmol), two unassigned diastereomers were obtained as cream-colored solids. Major diastereomer: (0.172 g, 0.289 mmol, 74%); R_f = 0.05 (1:1 hexanes:CH_2Cl_2); ^{1}H NMR (500 MHz, $CDCl_3$) δ 2.41 (s, 6H), 3.61 (bs, 2H), 6.07 (d, J = 7.8 Hz, 2H), 6.69 (d, J = 7.8 Hz, 2H), 6.98-7.05 (m, 10H), 7.10-7.12 (m, 4H), 7.16 (dd, J = 3.3, 6.7 Hz, 2 H), 7.20-7.22 (m, 6H); Minor diastereomer: (0.0496 g, 0.0833 mmol, 21%); R_f = 0.37 (1:1 hexanes:CH_2Cl_2); ^{1}H NMR (500 MHz, $CDCl_3$) δ 2.46 (s, 6H), 3.81 (s, 2H), 5.83 (dd, J = 1.8, 7.8 Hz, 2H), 6.79 (d, J = 7.8 Hz, 2H), 6.96 (dd, J = 3.4, 6.7 Hz, 2H), 6.98 (dd, J = 3.3, 6.3 Hz, 2H) 7.04 (app s, 10H), 7.15 (dd, J = 3.2, 6.7 Hz, 2 H), 7.23 (dd, J = 3.5, 6.1 Hz, 2H), 7.36 (d, J = 6.6 Hz, 2H), 7.46 (dd, J = 1.8, 7.6 Hz, 2H).

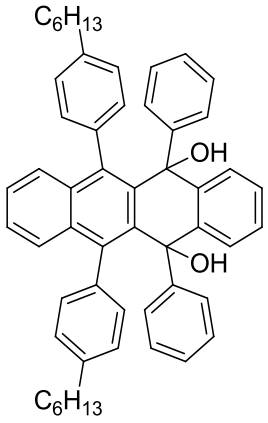

Tetracenediol **3.8f**: Following the general procedure using **3.2d** (0.211 g, 0.365 mmol) and **3.9'e** (0.370 mL, 3.52 mmol), two unassigned diastereomers were obtained. Major diastereomer (orange oil): (0.213 g, 0.304 mmol, 81%); ^{1}H NMR (300 MHz, $CDCl_3$) δ 0.97-1.01 (m, 6H), 1.38-1.51 (m, 12H), 1.67-1.71 (m, 4H), 2.55-2.61 (m, 4H), 4.54 (s, 2H), 5.99 (d, *J* = 8.0 Hz, 2H), 6.60 (d, *J* = 8.0 Hz, 2H), 6.72 (dd, *J* = 3.2, 6.0 Hz, 2H), 6.80-6.88 (m, 6H), 6.95-7.04 (m, 12H), 7.13 (dd, *J* = 3.3, 6.7 Hz, 2H). Minor diastereomer (yellow oil): (0.030 g, 0.043 mmol, 11%); ^{1}H NMR (300 MHz, $CDCl_3$) δ 1.18-1.22 (m, 6H), 1.64-1.71 (m, 12H), 1.92-2.01 (m, 4H), 2.90-2.95 (m, 4H), 3.88 (s, 2H), 5.85(dd, *J* = 1.7, 7.8 Hz, 2H), 6.78 (dd, *J* = 1.5, 7.9 Hz, 2H), 6.95-6.99 (m, 4H), 7.03-7.08 (m, 10H), 7.15 (dd, *J* = 3.3, 6.7 Hz, 2H), 7.21 (dd, *J* = 3.4, 6.2 Hz, 2H), 7.35 (dd, *J* = 1.4, 7.7 Hz, 2H), 7.47 (dd, *J* = 1.7, 7.7 Hz, 2H).

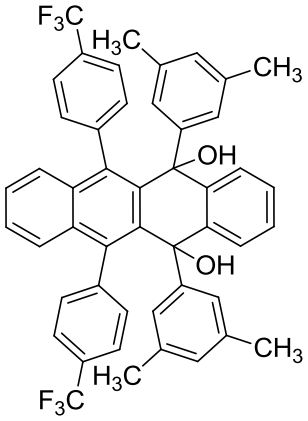

Tetracenediol **3.8g**: Following the general procedure using **3.2c** (0.200 g, 0.366 mmol) and **3.9'c** (0.500 mL, 3.70 mmol), two unassigned diastereomers were obtained. Major diastereomer (colorless amorphous solid): (0.147 g, 0.194 mmol, 52%); R_f = 0.10 (1:1 hexanes:CH_2Cl_2); ^{1}H NMR (500 MHz, $CDCl_3$) δ 2.10 (s, 12H), 2.93 (s, 2H), 6.14 (d, J = 8.0 Hz, 2H), 6.57 (s, 4H), 6.70 (s, 2H), 6.96 (dd, J = 3.4, 6.6 Hz, 2H), 7.04 (dd, J = 3.4, 6.2 Hz, 2H), 7.13-7.16 (m, 4H), 7.21 (dd, J = 3.3, 6.8 Hz, 2H), 7.72-7.77 (m, 4H); ^{19}F NMR (470 MHz, $CDCl_3$) δ −63.36; Minor diastereomer (orange amorphous solid): (0.092 g, 0.12 mmol, 33%); R_f = 0.66 (1:1 hexanes:CH_2Cl_2); 1H NMR (500 MHz, $CDCl_3$) δ 2.12 (s, 12H), 4.27 (s, 2H), 6.22 (d, J = 8.0 Hz, 2 H), 6.57 (s, 4H), 6.70 (s, 2H), 6.79-6.82 (m, 4H), 6.92 (dd, J = 3.4, 6.7 Hz, 2H), 7.07-7.10 (m, 4H), 7.20 (bs, 2H), 7.24 (dd, J = 3.2, 6.8 Hz, 2H); ^{19}F NMR (470 MHz, $CDCl_3$) δ −63.35.

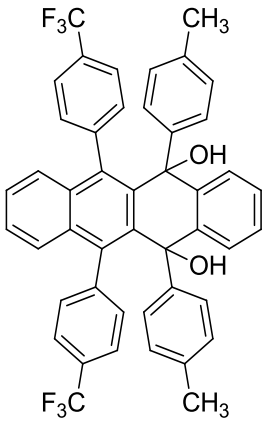

Tetracenediol **3.8h**: Following the general procedure using **3.2c** (1.20 g, 2.20 mmol) and **3.9'a** (2.70 mL, 21.9 mmol), two unassigned diastereomers were obtained. Major diastereomer (orange solid): (0.840 g, 1.15 mmol, 52%); R_f = 0.12 (1:1 hexanes:CH_2Cl_2); ^{1}H NMR (300 MHz, $CDCl_3$) δ 2.28 (s, 6H), 3.95 (s, 2H), 6.24 (d, J = 8.1 Hz, 2H), 6.82-6.84 (m, 12H), 6.93 (dd, J = 3.3, 6.6 Hz, 2H), 7.02 (app d, J = 8.2 Hz, 2H), 7.16-7.23 (m, 4H), 7.32 (app d, J = 8.5 Hz, 2H); ^{19}F NMR (470 MHz, CDCl3) δ −63.83; Minor diastereomer (colorless solid): (0.400 g, 0.55 mmol, 25%); R_f = 0.60 (1:1 hexanes:CH_2Cl_2); ^{1}H NMR (300 MHz, $CDCl_3$) δ 2.26 (s, 6H), 2.87 (s, 2H), 6.17 (d, J = 8.0 Hz, 2H), 6.80-6.87 (m, 8H), 6.95 (dd, J = 3.3, 6.6 Hz, 2H), 7.03 (dd, J = 3.4, 6.1 Hz, 2H), 7.12-7.15 (m, 4H), 7.21 (dd, J = 3.3, 6.7 Hz, 2H), 7.68-7.75 (m, 4H); ^{19}F NMR (470 MHz, $CDCl_3$) δ −63.69.

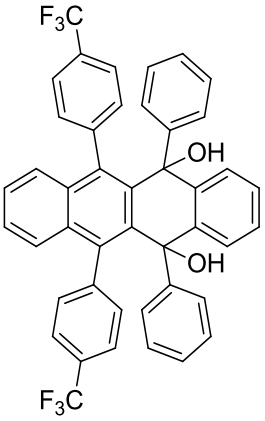

Tetracenediol **3.8i**: Following the general procedure using **3.2c** (2.76 g, 5.05 mmol) and **3.9'e** (5.31 mL, 50.5 mmol), two unassigned diastereomers were obtained. Major diastereomer (orange solid): (1.85 g, 2.63 mmol, 52%); R_f = 0.12 (1:1 hexanes:CH_2Cl_2); ^{1}H NMR (300 MHz, $CDCl_3$) δ 4.54 (s, 2H), 6.21 (d, J = 8.0 Hz, 2H), 6.73 (s, 4H), 7.06-6.91 (m, 16H), 7.26-7.16 (m, 4H); ^{19}F NMR (470 MHz, $CDCl_3$) δ −63.84; Minor diastereomer (cream-colored solid): (1.00 g, 1.42 mmol, 28%); R_f = 0.59 (1:1 hexanes:CH_2Cl_2); ^{1}H NMR (300 MHz, $CDCl_3$) δ 2.95 (s, 2H), 6.11 (d, J = 7.7 Hz, 2H), 6.93-7.05 (m, 14H), 7.11-7.14 (m, 4H), 7.21 (dd, J = 3.4, 6.8 Hz, 2H), 7.74 (app s, 4H); ^{19}F NMR (470 MHz, $CDCl_3$) δ −63.75.

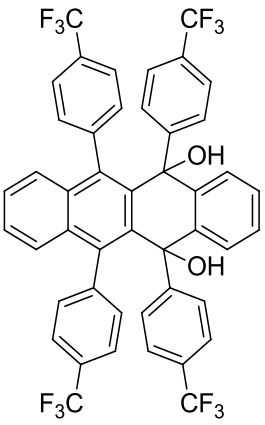

Tetracenediol **3.8j**: Following the general procedure using **3.2c** (0.123 g, 0.224 mmol) and **3.9'f** (0.300 mL, 2.13 mmol), two unassigned diastereomers were obtained. Major diastereomer (orange solid): (0.108 g, 0.129 mmol, 59%); R_f = 0.12 (1:1 hexanes:CH_2Cl_2);

^{1}H NMR (300 MHz, $CDCl_3$) δ 4.54 (s, 2H), 6.21 (d, J = 8.0 Hz, 2H), 6.73 (s, 4H), 7.06-6.91 (m, 16H), 7.26-7.16 (m, 4H); ^{19}F NMR (470 MHz, $CDCl_3$) δ -63.84; Minor diastereomer (yellow solid): (0.055 g, 0.066 mmol, 30%); R_f = 0.59 (1:1 hexanes:CH_2Cl_2); ^{1}H NMR (300 MHz, $CDCl_3$) δ 2.95 (s, 2H), 6.11 (d, J = 7.7 Hz, 2H), 6.93-7.05 (m, 14H), 7.11-7.14 (m, 4H), 7.21 (dd, J = 3.4, 6.8 Hz, 2H), 7.74 (app s, 4H); ^{19}F NMR (470 MHz, $CDCl_3$) δ −63.75.

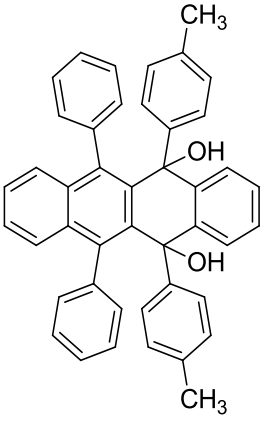

Tetracenediol **3.8k**: Following the general procedure using **3.2f** (0.686 g, 1.67 mmol) and **3.9'a** (2.10 mL, 17.1 mmol), two unassigned diastereomers were obtained as colorless solids. Major diastereomer: (0.875 g, 1.47 mmol, 88%); ^{1}H NMR (300 MHz, $CDCl_3$) δ 2.26 (s, 6H), 3.78 (s, 2H), 6.20 (d, *J* = 7.7 Hz, 2H), 6.80-6.96 (m, 14H), 7.09 (dd, *J* = 3.6, 5.7 Hz, 2H), 7.15 (dd, *J* = 3.3, 6.7 Hz, 2H), 7.21-7.25 (m, 6H) ; Minor diastereomer: (0.0707 g, 0.119 mmol, 7%); ^{1}H NMR (300 MHz, $CDCl_3$) δ 2.24 (s, 6H), 3.60 (s, 2H), 6.01 (d, *J* = 7.7 Hz, 2H), 6.84 (d, *J* = 8.1 Hz, 4H), 6.90 (d, *J* = 8.3 Hz, 4H), 6.93-7.00 (m, 6H), 7.15 (dd, *J* = 3.3, 6.7 Hz, 2H), 7.20-7.24 (m, 2H), 7.33-7.38 (m, 2H), 7.49-7.58 (m, 4H).

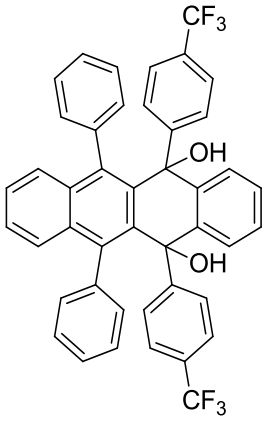

Tetracenediol **3.8l**: Following the general procedure using **3.2f** (3.89 g, 9.49 mmol) and **3.9'f** (13.3 mL, 94.9 mmol), two unassigned diastereomers were obtained. (Diagnostic ^{1}H NMRs only.) Major diastereomer (colorless solid): (2.34 g, 3.33 mmol, 35%); R_f = 0.07 (1:1 hexanes:CH_2Cl_2); ^{1}H NMR (300 MHz, $CDCl_3$) δ 4.30 (s, 2H), 6.08 (d, J = 7.8 Hz, 2H), 6.76-6.88 (m, 6H), 6.95 (dd, J = 3.3, 6.6 Hz, 2H), 7.05-7.15 (m, 8H), 7.16-7.25 (m, 4H), 7.30 (d, J = 8.3 Hz, 4H); Minor diastereomer (cream-colored solid): (1.64 g, 2.33 mmol, 25%); R_f = 0.50 (1:1 hexanes:CH_2Cl_2); ^{1}H NMR (300 MHz, $CDCl_3$) δ 3.68 (s, 2H), 5.97 (d, J = 7.8 Hz, 2H), 6.92-6.99 (m, 4H), 7.02-7.07 (m, 2H), 7.12-7.22 (m, 8H), 7.31 (d, J = 8.3 Hz, 4H), 7.38-7.41 (m, 2H), 7.53-7.61 (m, 4H).

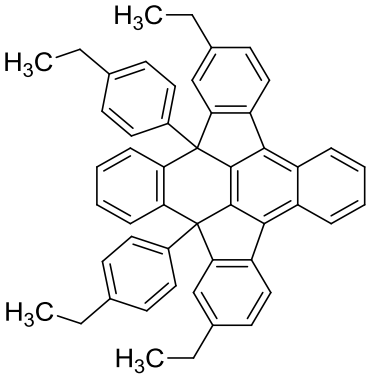

Byproduct **3.11**: While trying to form **3.8d** from **3.2e** (1.42 g, 3.04 mmol) and **3.9'd** (4.14 mL, 30.0 mmol), **3.11** was observed by NMR. Tentative assignement: ^{1}H NMR (300 MHz, $CDCl_3$) δ 1.02 (t, *J* = 7.5 Hz, 6H), 1.23-1.29 (m, 6H), 2.32 (q, *J* = 7.6 Hz, 4H), 2.70 (q, *J* = 7.6 Hz, 4H), 6.47 (d, *J* = 8.2 Hz, 4H), 6.64 (d, *J* = 7.8 Hz, 4H), 7.22-7.25 (m, 2H), 7.30 (dd, *J* = 3.4, 5.7 Hz, 2H), 7.46 (d, *J* = 1.2 Hz, 2H), 7.70 (dd, *J* = 3.3, 6.4 Hz, 2H), 8.07 (dd, *J* = 3.5, 5.7 Hz, 2H), 8.17 (d, *J* = 8.0 Hz, 2H), 8.80 (dd, *J* = 3.4, 6.4 Hz, 2H).

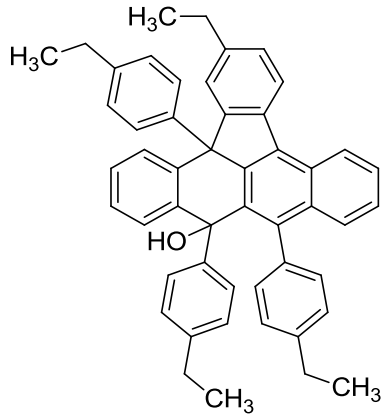

Byproduct **3.12**: While trying to form **3.8d** from **3.2e** (1.42 g, 3.04 mmol) and **3.9'd** (4.14 mL, 30.0 mmol), **3.12** was obtained as a cream-colored solid (0.250 g, 0.378 mmol, 13%); ^{1}H NMR (500 MHz, $CDCl_3$) δ 1.15 (t, *J* = 7.6 Hz, 3H), 1.22 (t, *J* = 7.6 Hz,

3H), 1.37-1.41 (m, 6H), 2.45 (q, J = 7.6 Hz, 2H), 2.49-2.55 (m, 2H), 2.61 (s, 1H), 2.76-2.84 (m, 4H), 6.26 (br s, 2H), 6.52 (br s, 2H), 6.65 (d, J = 8.1 Hz, 2H), 7.00 (d, J = 8.2 Hz, 2H), 7.19 (d, J = 7.5 Hz, 1H), 7.32 (d, J = 7.8 Hz, 1H), 7.41-7.45 (m, 3H), 7.47-7.52 (m, 3H), 7.58 (t, J = 7.4 Hz, 1H), 7.62 (d, J = 8.6 Hz, 1H), 7.76 (t, J = 7.5 Hz, 1H), 8.22 (d, J = 7.6 Hz, 1H), 8.44 (d, J = 7.9 Hz, 1H), 8.51 (d, J = 8.1 Hz, 1H), 9.03 (d, J = 8.4 Hz, 1H); ^{13}C NMR (125 MHz, $CDCl_3$) δ 15.2, 15.2, 15.7, 28.0, 28.2, 26.5, 28.9, 59.6, 78.8, 123.1, 123.6, 125.1, 126.1, 126.2, 126.2, 126.6, 126.6, 126.7, 126.8, 127.0, 127.3, 127.6, 127.6, 127.8, 128.0, 128.5, 129.3, 132.3, 133.5, 134.8, 135.0, 136.0, 136.2, 137.2, 138.5, 139.4, 140.7, 141.6, 141.7, 142.8, 143.2, 146.4, 146.7, 153.3 (not all peaks resolved); IR (thin film, CH_2Cl_2) 3574, 3022, 2962, 2925, 2853, 1507, 1473, 1454 cm^{-1}; HRMS (ESI) m/z calcd for $C_{50}H_{44}O$ $[M+Na]^+$ 683.3284, found 683.3290. DEPT; COSY; HMQC. The structure was confirmed by X-ray crystallography solved by Victoria Chemistruck, Douglas Group member, Department of Chemistry, University of Minnesota, Minneapolis, MN..

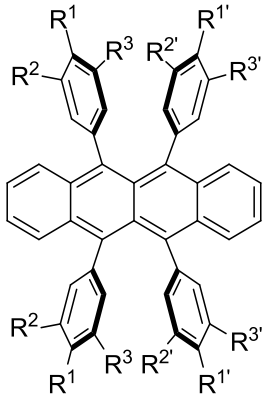

General procedure to rubrenes **3.1a-j**: Tetracenediol **3.8a** (combined major and minor diastereomers, 0.725 g, 1.16 mmol, 1.0 equiv.) and diethyl ether (45 mL) were added to a 3-neck 100 mL round bottom flask equipped with a reflux condenser, glass stopper and rubber septum. The solution was put under N_2 and heated to reflux. The remaining steps

were performed in the dark to avoid photooxidation of the product. HI (57% aqueous solution, 1.23 mL, 9.28 mmol, 8.0 equiv.) was added dropwise to the refluxing reaction mixture through the septum via syringe. Reflux was maintained for 30 min then the solution was allowed to cool to room temperature. The reaction mixture was transferred into a separatory funnel containing saturated aqueous $Na_2S_2O_5$ (40 mL). Additional portions of diethyl ether and saturated aqueous sodium meta-bisulfite were used to enable quantitative transfer. The layers were separated and the aqueous layer was extracted with diethyl ether (2 × 40 mL). The organic layers were combined, dried over Na_2SO_4, filtered, and concentrated in vacuo to give a red solid residue (0.743 g). The crude product was dissolved in a minimum amount of CH_2Cl_2 then isopropanol was layered on top of the solution (1:4 CH_2Cl_2:isopropanol), the flask was sealed with a rubber septum, placed under static nitrogen, and left standing at room temp until crystals had formed. Collection of the crystals by vacuum filtration provided **3.1a** (0.299 g, 0.507 mmol, 44%). Note: the extraction and purification were done with as little exposure to light and air as possible due to the tendency of rubrene and derivatives to react with oxygen, which is increased when in solution. In later experiments, recrystallization of the crude product was performed in a N_2-filled glove box using deoxygenated solvents.

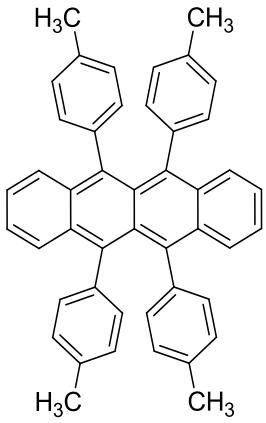

Rubrene **3.1a**. Following the general procedure using **3.8a** (0.725 g, 1.16 mmol), **3.1a** was obtained as red crystals (0.299 g, 0.507 mmol, 44%); mp 335-336 °C; ^{1}H NMR (500 MHz, $CDCl_3$) δ 2.37 (s, 12H), 6.72 (d, J = 7.9 Hz, 8H), 6.84 (d, J = 7.8 Hz, 8H), 7.09 (dd, J = 3.2, 7.1 Hz, 4H), 7.42 (dd, J = 3.3, 7.1 Hz, 4H); ^{13}C NMR (125 MHz, $CDCl_3$) δ 21.3, 124.6, 126.7, 127.6, 129.7, 130.3, 132.0, 135.0, 137.0, 139.0; IR (thin film, CH_2Cl_2) 3045, 3023, 2917, 2863, 1512 cm^{-1}; HRMS (EI) *m/z* calcd for $C_{46}H_{36}$ $[M]^+$ 588.2817, found 588.2778. Anal. Calcd for $C_{46}H_{36}$: C, 93.84; H, 6.16. Found: C, 93.62; H, 6.18. The structure was confirmed by X-ray crystallography.

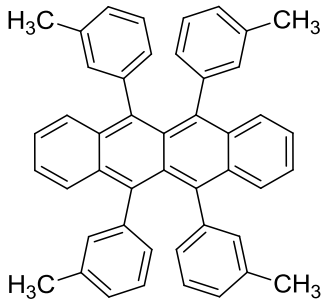

Rubrene **3.1b**. Following the general procedure using **3.8b** (0.100 g, 1.70 mmol), **3.1b** was obtained as an orange amorphous solid (0.093 g, 0.158 mmol, 93% crude); ^{1}H NMR (500 MHz, $CDCl_3$, rt) δ 2.17-2.19 (m, 6H), 2.22-2.25 (m, 6H), 6.64-6.72 (m, 8H), 6.87-7.07 (m, 8H), 7.10-7.12 (m, 4H), 7.39-7.43 (m, 4H); ^{13}C NMR (500 MHz, $CDCl_3$, rt) δ 21.0, 21.0,

21.1, 21.1, 21.1, 21.1, 21.2, 124.7, 126.3, 126.4, 126.5, 126.6, 126.7, 126.7, 126.8, 126.8, 126.9, 129.0, 129.1, 129.2, 129.2, 129.3, 129.4, 129.5, 130.0, 130.0, 130.1, 130.1, 132.8, 133.0, 133.2, 133.4, 135.7, 135.9, 135.9, 136.0, 136.2, 136.2, 137.1, 137.1, 141.5, 141.5, 141.5, 141.6 (peaks reported as observed); IR (thin film, $CDCl_3$) 3071, 3050, 3032, 2918, 2857, 1601, 1583, 1487, 1464 cm^{-1}; HRMS (EI) *m*/*z* calcd for $C_{46}H_{36}$ $[M]^+$ 588.2817, found 588.2816. The structure was confirmed by X-ray crystallography.

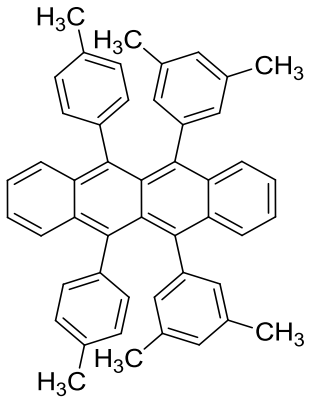

Rubrene **3.1c**. Following the general procedure using **3.8c** (1.03 g, 1.58 mmol with impurity), **3.1c** was obtained as red crystals (0.336 g, 0.550 mmol, 34%) was obtained. Tm[2] 319.96 °C; ^{1}H NMR (500 MHz, $CDCl_3$) δ 2.16 (s, 12H), 2.37 (s, 6H), 6.47 (s, 4H), 6.73-6.75 (m, 6H), 6.87 (d, J = 7.7 Hz, 4H), 7.09 (m, 4H), 7.41-7.45 (m, 4H); ^{13}C NMR (125 MHz, $CDCl_3$) δ 21.0, 21.2, 124.5, 124.6, 126.8, 127.1, 127.5, 129.4, 130.1, 130.2, 130.3, 132.0, 134.7, 136.2, 137.1, 137.2, 138.7, 141.6 (not all carbons resolved); IR (thin film, CH_2Cl_2) 3075,

[2] Melting point determined by TA Instruments Discovery DSC calibrated with indium; ramp 10.00 °C/min to 370.00 °C.

3025, 2916, 2860, 1599, 1512 cm^{-1}; HRMS (EI) *m/z* calcd for $C_{48}H_{40}$ $[M]^+$ 616.3130, found 616.3129. The structure was confirmed by X-ray crystallography.

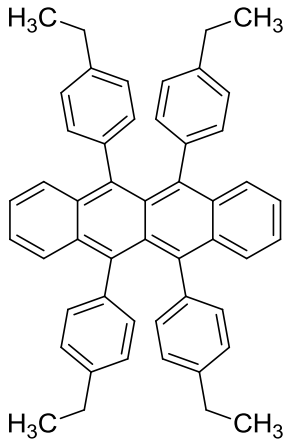

Rubrene **3.1d**. Following the general procedure using **3.8d** (3.50 g, 5.16 mmol), **3.1d** was obtained as red crystals (1.63 g, 2.53 mmol, 45%), mp 272-273 °C, ^{1}H NMR (300 MHz, $CDCl_3$) δ 1.33 (t, *J* = 7.5 Hz, 12 H), 2.65 (q, *J* = 7.6 Hz, 8 H), 6.76 (d, *J* = 8.0 Hz, 8 H), 6.87 (d, *J* = 7.9 Hz, 8 H), 7.09 (dd, *J* = 3.3, 7.1 Hz, 4 H), 7.42 (dd, *J* = 3.3, 7.1 Hz, 4 H); ^{13}C NMR (75 MHz, $CDCl_3$) δ 15.8, 28.7, 124.6, 126.5, 126.7, 129.6, 130.2, 132.0, 137.0, 139.2, 141.2; IR (thin film, CH_2Cl_2) 3072, 3049, 3023, 2962, 2927, 2870, 1511, 1460, 1397, 1260, 1111, 1020, 831, 760, 700 cm^{-1}, HRMS (EI) *m/z* calcd for $C_{50}H_{44}$ $[M]^+$ 644.3443, found 644.3481. Anal. Calcd for $C_{50}H_{44}$: C, 93.12; H, 6.88. Found: C, 92.87; H, 6.81.

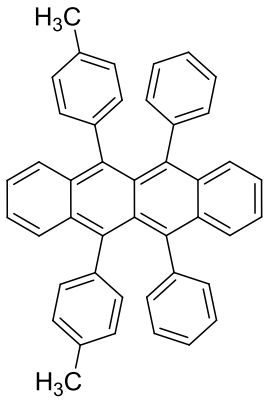

Rubrene **3.1e**. Following the general procedure using **3.8e** (0.614 g, 1.03 mmol), **3.1e** was obtained as red crystals (0.192 g, 0.340 mmol, 34%) was obtained after two batches of recrystallization (first batch: 0.170 g; second batch: 0.0220 g). ^{1}H NMR (500 MHz, $CDCl_3$) δ 2.35 (s, 6H), 6.74 (d, J = 7.9 Hz, 4H), 6.83-6.86 (m, 8H), 7.04 (t, J = 7.7 Hz, 4H), 7.08-7.14 (m, 6H), 7.35 (dd, J = 3.3, 7.1 Hz, 2H), 7.43 (dd, J = 3.2, 7.1 Hz, 2H); ^{13}C NMR (125 MHz, $CDCl_3$) δ 21.2, 124.7, 124.7, 125.5, 126.6, 126.7, 126.9, 127.9, 129.4, 130.2, 130.3, 132.0, 132.1, 135.1, 137.0, 137.1, 138.7, 142.0; IR (thin film, CH_2Cl_2) 3078, 3055, 3025, 2919, 1598, 1515 cm^{-1}; HRMS (EI) *m*/*z* calcd for $C_{44}H_{32}$ $[M]^+$ 560.2504, found 560.2481. Anal. Calcd for $C_{44}H_{32}$: C, 94.25; H, 5.75. Found: C, 94.01; H, 5.64. The structure was confirmed by X-ray crystallography.

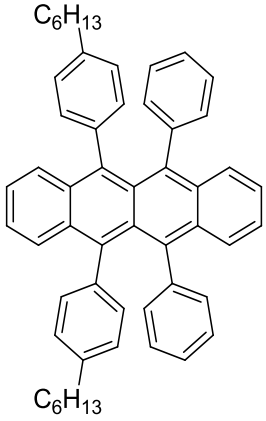

Rubrene **3.1f**. Following the general procedure using **3.8f** (0.228 g, 0.331 mmol), **3.1f** was obtained as a red amorphous solid (0.205 g, 0.293 mmol, 88% crude); ^{1}H NMR

(500 MHz, $CDCl_3$) δ 0.96-0.99 (m, 6H), 1.42-1.47 (m, 12H), 1.66-1.71 (m, 4H), 6.76 (d, J = 7.8 Hz, 4H), 6.86 (app t, J = 8.5 Hz, 8H), 7.04 (app t, J = 7.5 Hz, 4H), 7.09-7.11 (m, 6H), 7.36 (dd, J = 3.2, 7.1 Hz, 2H), 7.40 (dd, J = 3.2, 7.1 Hz, 2H); ^{13}C NMR (500 MHz, $CDCl_3$) δ 14.2, 22.8, 29.3, 31.6, 31.9, 35.8, 124.7, 124.7, 125.6, 125.9, 126.6, 126.7, 127.1, 127.2, 129.3, 130.1, 130.4, 132.0, 132.1, 137.0, 137.0, 138.9, 140.1, 141.9; IR (thin film, $CDCl_3$) 3053, 3022, 2954, 2926, 2854, 1598, 1511, 1464, 1440 cm^{-1}; HRMS (EI) m/z calcd for $C_{54}H_{52}$ $[M]^+$ 700.4069, found 700.4077.

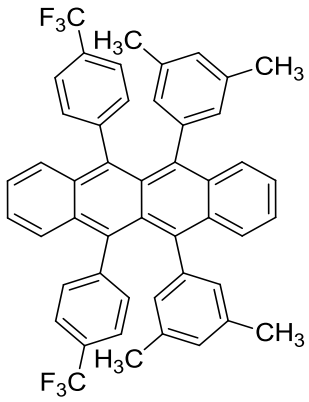

Rubrene **3.1g**. Following the general procedure using **3.8g** (1.90 g, 2.50 mmol), **3.1g** was obtained as red crystals (1.24 g, 1.71 mmol, 94%) was obtained. Mp 312-315 °C; ^{1}H NMR (500 MHz, $CDCl_3$) δ 2.17 (s, 12H), 6.51 (app s, 4H), 6.78 (app s, 2H), 7.03 (d, J = 7.9 Hz, 4H), 7.12-7.17 (m, 4H), 7.24 (dd, J = 3.3, 7.2 Hz, 2H), 7.36 (d, J = 8.0 Hz, 4H), 7.46 (dd, J = 3.3, 7.0 Hz, 2H); ^{13}C NMR (125 MHz, $CDCl_3$) δ 20.8, 123.5 (q, $J_{C\text{-}F}$ = 3.6 Hz), 124.5 (q, $J_{C\text{-}F}$ = 270.0 Hz), 125.2, 125.2, 126.2, 126.7, 127.7, (q, $J_{C\text{-}F}$ = 31.9 Hz), 128.0, 128.7, 129.8, 130.5, 130.6, 132.4, 136.1, 136.7, 137.0, 141.1, 145.3; ^{19}F NMR (470 MHz, $CDCl_3$) δ −63.46; IR (thin film, CH_2Cl_2) 3075, 3025, 2916, 2864, 1614, 1600 cm^{-1}; HRMS (EI) m/z calcd for $C_{48}H_{34}F_6$ $[M]^+$ 724.2565, found 724.2611. The structure was confirmed by X-ray crystallography.

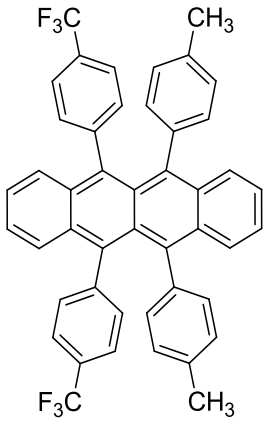

Rubrene **3.1h**. Following the general procedure using **3.8h** (1.72 g, 2.34 mmol), **3.1h** was obtained as red crystals (0.505 g, 0.725 mmol, 65%); Mp 333-335 °C; ^{1}H NMR (500 MHz, $CDCl_3$) δ 2.37 (s, 6H), 6.74 (d, J = 7.9 Hz, 4H), 6.87 (d, J = 7.7 Hz, 4H), 6.99 (d, J = 7.9 Hz, 4H), 7.13-7.16 (m, 4H), 7.25-7.27 (m, 2H), 7.32 (d, J = 8.0 Hz, 4H), 7.42 (dd, J = 3.3, 7.1 Hz, 2H); ^{13}C NMR (125 MHz, $CDCl_3$) δ 21.0, 123.9 (q, $J_{C\text{-}F}$ = 3.7 Hz), 124.5 (q, $J_{C\text{-}F}$ = 270.1 Hz), 125.3, 126.2, 126.7, 127.7 (q, $J_{C\text{-}F}$ = 32.0 Hz), 128.2, 129.0, 129.8, 130.8, 132.22, 132.23, 135.9, 136.0, 136.9, 138.3, 145.6 (not all carbons resolved); ^{19}F NMR (470 MHz, $CDCl_3$) δ −63.74; IR (thin film, CH_2Cl_2) 3074, 3029, 2926, 1614, 1508 cm^{-1}; HRMS (EI) *m*/*z* calcd for $C_{46}H_{30}F_6$ $[M]^+$ 696.2252, found 696.2264. The structure was confirmed by X-ray crystallography.

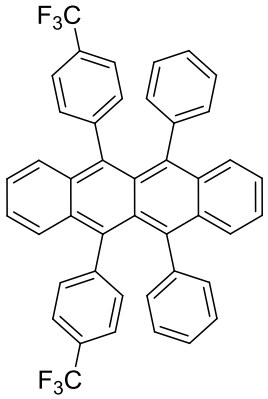

Rubrene **3.1i**. Following the general procedure using **3.8i** (1.85 g, 2.63 mmol) or **3.8l** (2.27 g, 3.23 mmol), **3.1h** was obtained as red crystals (0.961 g, 1.44 mmol, 55%

or 0.557 g, 0.833 mmol, 26% respectively); Mp 300-302 °C, ^{1}H NMR (500 MHz, $CDCl_3$) δ 6.86 (d, J = 7.0 Hz, 4H), 7.00 (d, J = 7.9 Hz, 4H), 7.08 (t, J = 7.7 Hz, 4H), 7.14-7.19 (m, 6H), 7.26-7.28 (m, 2H), 7.33 (d, J = 8.0 Hz, 4H), 7.36 (d, J = 3.3, 7.1 Hz, 2H); ^{13}C NMR (125 MHz, $CDCl_3$) δ 124.1 (q, $J_{C\text{-}F}$ = 3.6 Hz), 124.4 (q, $J_{C\text{-}F}$ = 270.0 Hz), 125.4, 125.5, 126.2, 126.3, 126.5, 127.5, 128.0 (q, $J_{C\text{-}F}$ = 32.1 Hz), 128.8, 129.8, 130.6, 132.3, 135.9, 136.9, 141.4, 145.4 (not all carbons resolved); ^{19}F NMR (470 MHz, $CDCl_3$) δ −63.88; IR (thin film, CH_2Cl_2) 3078, 3055, 1613 cm^{-1}; HRMS (EI) *m*/*z* calcd for $C_{44}H_{26}F_6$ $[M]^+$ 668.1939, found 668.1882. The structure was confirmed by X-ray crystallography.

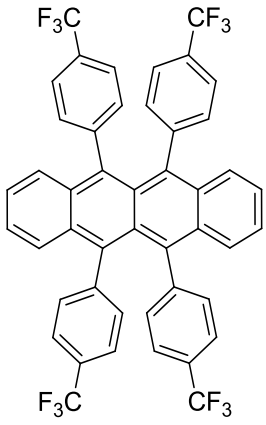

Rubrene **3.1j**. Following the general procedure using **3.8j** (0.879 g, 1.05 mmol), **3.1j** was obtained as orange crystals (0.148 g, 0.184 mmol, 18%); ^{1}H NMR (500 MHz, $CDCl_3$) δ 7.01 (d, *J* = 8.0 Hz, 8H), 7.20 (dd, *J* = 3.1, 7.1 Hz, 4H), 7.27 (dd, *J* = 3.3, 7.3, 4H), 7.36 (d, *J* = 8.1 Hz, 8H); ^{13}C NMR (500 MHz, $CDCl_3$) δ 124.1 (q, $J_{C\text{-}F}$ = 270.5 Hz), 124.3 (br, tentatively assigned as two carbons), 126.0, 128.4, 128.7 (q, $J_{C\text{-}F}$ = 32.5 Hz), 130.2, 132.4, 135.7, 145.0 (not all carbons resolved); ^{19}F NMR (282 MHz, $CDCl_3$) δ −65.98; IR (thin film, $CDCl_3$) 3075, 2928, 2855, 1615, 1572, 1466, 1407 cm^{-1}; HRMS (EI) *m*/*z* calcd for $C_{46}H_{24}F_{12}$ $[M]^+$ 804.1686, found 804.1635.

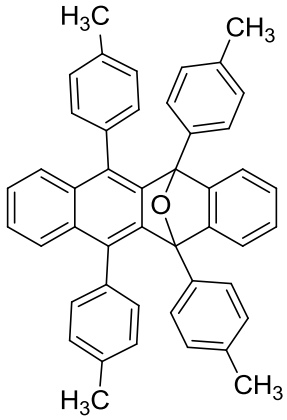

Byproduct **3.13**. While trying to form **3.1a** using **3.8a** (1.29 g, 2.07 mmol), **3.13** was obtained as a white solid (0.160 g, 0.265 mmol, 13%). ^{1}H NMR (500 MHz, $CDCl_3$) δ 2.27 (s, 6H), 2.35 (s, 6H), 6.86-6.89 (m, 6H), 6.97 (d, *J* = 7.7 Hz, 2H), 7.02 (d, *J* = 7.4 Hz, 2H), 7.23 (dd, *J* = 3.0, 5.4 Hz, 2H), 7.29 (dd, *J* = 3.3, 6.5 Hz, 2H), 7.45 (d, *J* = 8.1 Hz, 4H), 7.61 (dd, *J* = 3.4, 6.4 Hz, 2H), 7.75 (dd, *J* = 3.1, 5.3 Hz, 2H); ^{13}C NMR (500 MHz, $CDCl_3$) δ 21.1, 21.1, 90.6, 122.4, 125.7, 126.0, 126.4, 128.0, 128.0, 128.3, 128.5, 129.8, 131.0, 131.9, 132 .0, 132.2, 134.1, 136.4, 136.9, 145.0, 150.3; IR (thin film, $CDCl_3$) 3067, 3020, 2920, 2866, 1513, 1455 cm^{-1}; HRMS (ESI) *m*/*z* calcd for $C_{46}H_{36}O$ $[M+Na]^+$ 627.2664, found 627.2687.

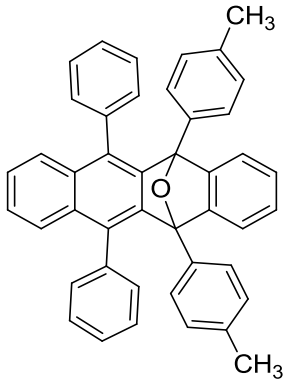

Byproduct **3.14**. While trying to form **3.1e** using **3.8k** (0.875 g, 1.47 mmol), **3.14** was obtained as a white solid (0.299 g, 0.519 mmol, 35%) ^{1}H NMR (500MHz, CD_2Cl_2) δ 2.27 (s, 6H), 6.91 (d, *J* = 8.0 Hz, 4H), 6.97 (d, *J* = 6.8 Hz, 2H), 7.18-7.25 (m, 8H),

7.26-7.29 (m, 4H), 7.44 (d, J = 8.1 Hz, 4H), 7.52 (dd, J = 3.4, 6.5 Hz, 2H), 7.77 (dd, J = 3.1, 5.4 Hz, 2H); ^{13}C NMR (300MHz, $CDCl_3$) δ 21.1, 90.6, 122.4, 125.8, 126.0, 126.3, 126.8, 127.3, 127.8, 128.1, 128.3, 128.5, 129.9, 131.1, 131.8, 131.9, 132.1, 137.0, 137.1, 145.0, 150.2 (not all peaks resolved); LRMS (EI) m/z 576.2 $(M)^+$, 558.2 $(M - H_2O)^+$, 484.2 $(M - C_7H_8)^+$.

3.6 REFERENCES

(1) Schuck, G.; Haas, S.; Stassen, A. F.; Berens, U.; Batlogg, B. *Acta Crystallogr. Sect. E Struct. Reports Online* **2007**, *E63*, o2894.

(2) Schuck, G.; Haas, S.; Stassen, A. F.; Kirner, H.-J.; Batlogg, B. *Acta Crystallogr. Sect. E Struct. Reports Online* **2007**, *E63*, o2893.

(3) Paraskar, A. S.; Reddy, A. R.; Patra, A.; Wijsboom, Y. H.; Gidron, O.; Shimon, L. J. W.; Leitus, G.; Bendikov, M. *Chem. – Eur. J.* **2008**, *14*, 10639–10647.

(4) Haas, S.; Stassen, A. F.; Schuck, G.; Pernstich, K. P.; Gundlach, D. J.; Batlogg, B.; Berens, U.; Kirner, H.-J. *Phys. Rev. B Condens. Matter Mater. Phys.* **2007**, *76*, 115203–6.

(5) Bergantin, S.; Moret, M. *Cryst. Growth Des.* **2012**, *12*, 6035–6041.

(6) Filho, D. A. da S.; Kim, E.-G.; Brédas, J.-L. *Adv. Mater.* **2005**, *17*, 1072–1076.

(7) Sundar, V. C.; Zaumseil, J.; Podzorov, V.; Menard, E.; Willett, R. L.; Someya, T.; Gershenson, M. E.; Rogers, J. A. *Science.* **2004**, *303*, 1644–1646.

(8) Minder, N. A.; Ono, S.; Chen, Z.; Facchetti, A.; Morpurgo, A. F. *Adv. Mater.* **2012**, *24*, 503–508.

(9) Dodge, J.; Bain, J. D.; Chamberlin, A. R. *J. Org. Chem.* **1990**, *55*, 4190–4198.

(10) Miyaura, N.; Suzuki, A. *J. Chem. Soc. Chem. Commun.* **1979**, 866–867.

(11) Miyaura, N.; Yamada, K.; Suzuki, A. *Tetrahedron Lett.* **1979**, *20*, 3437–3440.

(12) Miyaura, N.; Yanagi, T.; Suzuki, A. *Synth. Commun.* **1981**, *11*, 513–519.

(13) Yagodkin, E.; McGarry, K. A.; Douglas, C. J. *Org. Prep. Proced. Int.* **2011**, *43*, 360–363.

(14) Balodis, K. A.; Medne, R. S.; Neiland, O. Y.; Kozlova, L. M.; Klyavinya, Z. P.; Mazheika, I. B.; Gaukhman, A. P. *Zh. Org. Khim.* **1985**, *21*, 2423–2427.

(15) Yagodkin, E.; Xia, Y.; Kalihari, V.; Frisbie, C. D.; Douglas, C. J. *J. Phys. Chem. C* **2009**, *113*, 16544–16548.

(16) Sartori, G.; Casnati, G.; Bigi, F.; Robles, P. *Tetrahedron Lett.* **1987**, *28*, 1533–1536.

(17) Gabriel, S.; Leupold, E. *Berichte Dtsch. Chem. Ges.* **1897**, *31*, 1159–1174.

(18) Nathanson, F. *Berichte Dtsch. Chem. Ges.* **1893**, *26*, 2576–2582.

(19) Oatis, J. E.; Walle, T.; Daniell, H. B.; Gaffney, T. E.; Knapp, D. R. *J. Med. Chem.* **1985**, *28*, 822–824.

(20) Snelders, D. J. M.; Kreiter, R.; Firet, J. J.; van Koten, G.; Klein Gebbink, R. J. M. *Adv. Synth. Catal.* **2008**, *350*, 262–266.

(21) Peng, Z.; Gharavi, A. R.; Yu, L. *J. Am. Chem. Soc.* **1997**, *119*, 4622–4632.

(22) Hoye, T. R.; Eklov, B. M.; Voloshin, M. *Org. Lett.* **2004**, *6*, 2567–2570.

(23) Yagodkin, E. Electrical Properties and Synthesis of Tetracene and Rubrene Derivatives. Ph.D., University of Minnesota, 2010.

(24) Zeis, R.; Besnard, C.; Siegrist, T.; Schlockermann, C.; Chi, X.; Kloc, C. *Chem. Mater.* **2006**, *18*, 244–248.

(25) Cozzi, F.; Cinquini, M.; Annunziata, R.; Dwyer, T.; Siegel, J. S. *J. Am. Chem. Soc.* **1992**, *114*, 5729–5733.

(26) Cozzi, F.; Cinquini, M.; Annuziata, R.; Siegel, J. S. *J. Am. Chem. Soc.* **1993**, *115*, 5330–5331.

(27) Cozzi, F.; Ponzini, F.; Annunziata, R.; Cinquini, M.; Siegel, J. S. *Angew. Chem. Int. Ed. Engl.* **1995**, *34*, 1019–1020.

(28) Cozzi, F.; Siegel, J. S. *Pure Appl. Chem.* **1995**, *67*, 683–689.

(29) Thalladi, V. R.; Weiss, H.-C.; Bläser, D.; Boese, R.; Nangia, A.; Desiraju, G. R. *J. Am. Chem. Soc.* **1998**, *120*, 8702–8710.

(30) McGarry, K. A.; Xie, W.; Sutton, C.; Risko, C.; Wu, Y.; Young, V. G.; Brédas, J.-L.; Frisbie, C. D.; Douglas, C. J. *Chem. Mater.* **2013**.

(31) Cicoira, F.; Aguirre, C. M.; Martel, R. *ACS Nano* **2011**, *5*, 283–290.

(32) Gwinner, M. C.; Jakubka, F.; Gannott, F.; Sirringhaus, H.; Zaumseil, J. *ACS Nano* **2012**, *6*, 539–548.

(33) Kang, N.; Sarker, B. K.; Khondaker, S. I. *Appl. Phys. Lett.* **2012**, *101*, 233302.

(34) Xie, W.; Prabhumirashi, P. L.; Nakayama, Y.; McGarry, K. A.; Geier, M. L.; Uragami, Y.; Mase, K.; Douglas, C. J.; Ishii, H.; Hersam, M. C.; Frisbie, C. D. *ACS Nano* **2013**, *submitted for publication*.

(35) Tomura, M.; Yamaguchi, H.; Ono, K.; Saito, K. *Acta Crystallogr. Sect. E Struct. Reports Online* **2007**, *64*, o172–o173.

(36) Gerasimenko, Y. E.; Poteleshchenko, N. T.; Romanov, V. V. *Zhurnal Organicheskoĭ Khimii* **1980**, *16*, 1651–1656.

4 SYNTHETIC EFFORTS TOWARDS RUBRENE-F_{28}

4.1 BACKGROUND

Although organic semiconductors with p-type (hole) mobility currently dominate this class of materials, compounds that function with n-type (electron) mobility have begun to emerge.[1,2] Improved n-type organic semiconductors will allow for bipolar transistors and complementary circuits to be developed, which have advantages such as lower power dissipation, higher circuit speeds, and improved device stability.[3–7] In order for these devices to be realized, the library of n-type organic semiconductors as well as our understanding of electron transport in organic materials must be expanded. The ability to tune this class of compounds via synthesis presents the unique opportunity to enhance electron mobilities using molecular modifications.

Enhanced electron injection and transport have previously been achieved by decreasing the LUMO energy levels (< 4.0 eV) and incorporating electron withdrawing substituents on π-conjugated scaffolds.[7,8] Specifically, fluorination has proven to be a successful technique in providing air-stable n-type organic semicondcutors.[8–12] The transport of electrons in these materials has been attributed to the improved stability of the frontier molecular orbitals and the radical anion resulting from the inductive effect of the fluorine atoms.[13,14] The lowered HOMO-LUMO levels also improves electron charge injection and provides stability of the material towards oxidation, which will likely improve device lifetimes.[15] Another benefit to fluorination of π-conjugated materials is the effect on supramolecular organization. In the solid state, strong interactions between the electron rich non-fluorinated aromatic rings with the electron-deficient fluorinated aromatic rings will induce π-stacking,[15] a feature commonly associated with improved

charge transport. The similarity in size between hydrogen and fluorine also suggests that the solid-state packing may not be greatly disrupted by this molecular modification.

A benchmark carrier of holes, rubrene **1.1** would be an ideal material to examine the effects of fluorination on the charge carrier mobility of the molecule. The high degree of π-stacking in the solid-state structure of rubrene leads to the exceptional p-type charge carrier mobility observed and would potentially lead to high n-type mobility if the HOMO-LUMO levels could be lowered while the solid-state structure is preserved. The formation of rubrene-F_{28} (perfluororubrene, $C_{42}F_{28}$, **4.1**, Figure 4.1) appears to be an ideal way to achieve this goal. A literature search returns one recent report (2013) in which **4.1** and its optical properties are discussed;[16] however, the synthesis and common characterization details have not yet been reported. Therefore, our aim was to synthesize, characterize, and crystallize rubrene-F_{28} for analysis in single-crystal OFET. Herein, work towards this aim is described.

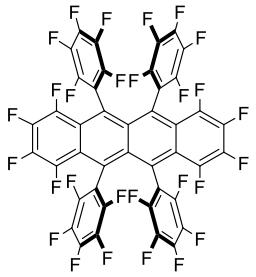

4.1

Figure 4.1. Molecular structure of rubrene-F_{28} **4.1**.

4.2 PROPOSED SYNTHESIS

As seen in Chapters 1 and 2, rubrene **1.1** is commonly made via a one-pot dimerization of 1,1,3-triphenyl propargyl alcohol **1.5** (Scheme 4.1a).[17–20] Initially, chloroallene **1.4** is formed, which then combines to form a bisallyl diradical **1.7**.[21,22] This intermediate can either recombine

with loss of Cl_2 to form the cyclobutene byproduct **1.8** (an impurity commonly found in commercial rubrene)[23] or propagate with loss of 2HCl to form rubrene **1.1**. We planned on utilizing this route to synthesize rubrene-F_{28} **4.1** (Scheme 4.1b).

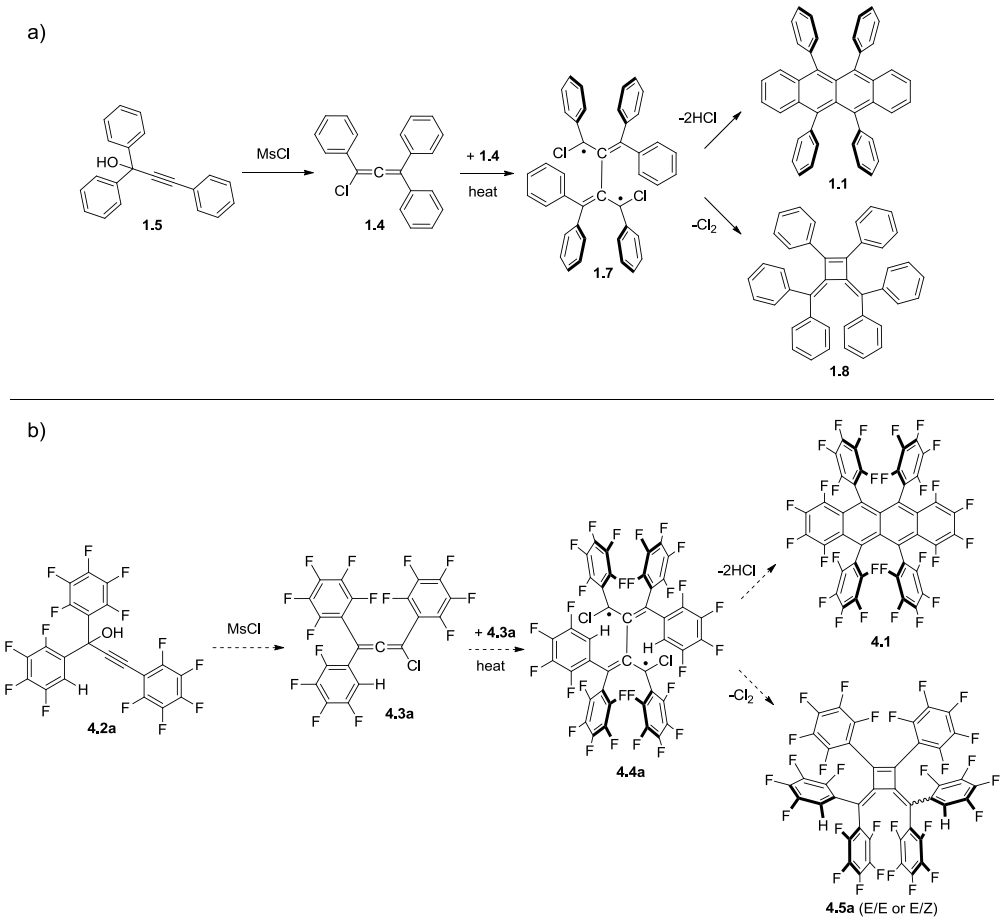

Scheme 4.1. a) Formation of rubrene **1.1** and cyclobutene **1.8** from propargyl alcohol **1.5**. **b**) Proposed formation of rubrene-F_{28} **4.1** and fluorinated cyclobutene **4.5a** from fluorinated propargyl alcohol **4.2a**.

Previous studies to rubrenes using this route indicated that the rubrene core might be favored to form over the cyclobutene byproduct through the presence of electron withdrawing subsituents.[20] Studies on the dimerization of fluorine-substituted allenes indicated that while the

ratios of products were influenced by the fluorine atoms, the expected rubrene products were still observed.[24,25] Both of these studies supported our plan to utilize this route to synthesize rubrene-F_{28}. Although the fluorine atoms would change the electrostatics of the aromatic rings, we did not anticipate their presence to impede the formation of bisallyl diradical **4.4a** or subsequent C–C bond formation. The fluorine atoms were also not anticipated to impede the final cyclization to form rubrene, provided the intermediate could lose HCl. Towards this end, we proposed synthesizing the fluorinated propargyl alcohol **4.2a**. We assumed that **4.2a** could be converted into the fluorinated chloroallene **4.3a** under standard conditions. The corresponding bisallyl diradical **4.4a** would form by heating **4.3a**, which could then recombine with loss of 2HCl to form rubrene-F_{28} **4.1** or with loss of Cl_2 to form the cyclobutene byproduct **4.5a**. Diastereomers of **4.5a** are likely to be observed since the two aryl hydrogen atoms would not be lost, leading to different geometries of the double bond. Studies on the thermal stability of methyl-substituted cyclobutanes lead us to postulate that these diastereomers may thermally interconvert to a mixture favoring the most stable isomer, although it is unclear which, if either, isomer that may be.[21,22] The synthesis of propargyl alcohol **4.2** (Scheme 4.2) was envisioned to come from the combination of benzophenone **4.6** with a perfluorophenyl alkynyl unit. Compound **4.6** could be synthesized using a Grignard addition between commercially available fluorinated bromobenzene **4.7** and benzaldehyde **4.8**. This route would allow for the synthesis of two series of intermediates **a** or **b** in which R = H or F respectively.

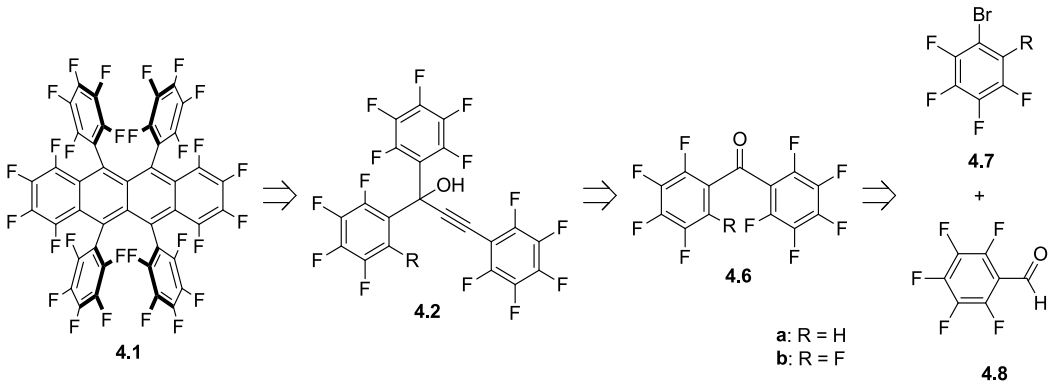

Scheme 4.2. Retrosynthetic analysis of rubrene-F_{28} **4.1**.

4.3 RESULTS AND DISCUSSION

4.3.1 Synthesis of fluorinated intermediates

Both partially and fully fluorinated intermediates were successfully prepared using the same synthetic route (Scheme 4.3). The synthesis commenced with formation of 2,3,4,5-tetrafluorophenyl magnesium bromide from 2,3,4,5-tetrafluorobromobenzene **4.7**, which was then added into fluorinated benzaldehyde **4.8** to form benzhydrol **4.9**. Both the partially and fully fluorinated benzhydrols were formed in high yields. Oxidation using pyridinium chlorochromate afforded the benzophenone **4.6** in moderate yield. Although initially we envisioned addition of pentafluorophenyl acetylide into the benzophenone intermediate, formation of the acetylene was found to be challenging by a previous Douglas group member, undergraduate Susie Krzmarzick. Thus, the alkynyl unit was installed by (trimethylsilyl)acetylide addition into the benzophenone to form TMS-protected propargyl alcohol **4.10** in high yield. This reaction proceeded very quickly as the starting material was consumed in 20 minutes and would lead to decomposition if allowed to proceed longer. Removal of the TMS group

employing KF in methanol provided the penultimate intermediate **4.11**, the deprotected propargyl alcohol, in good yield.

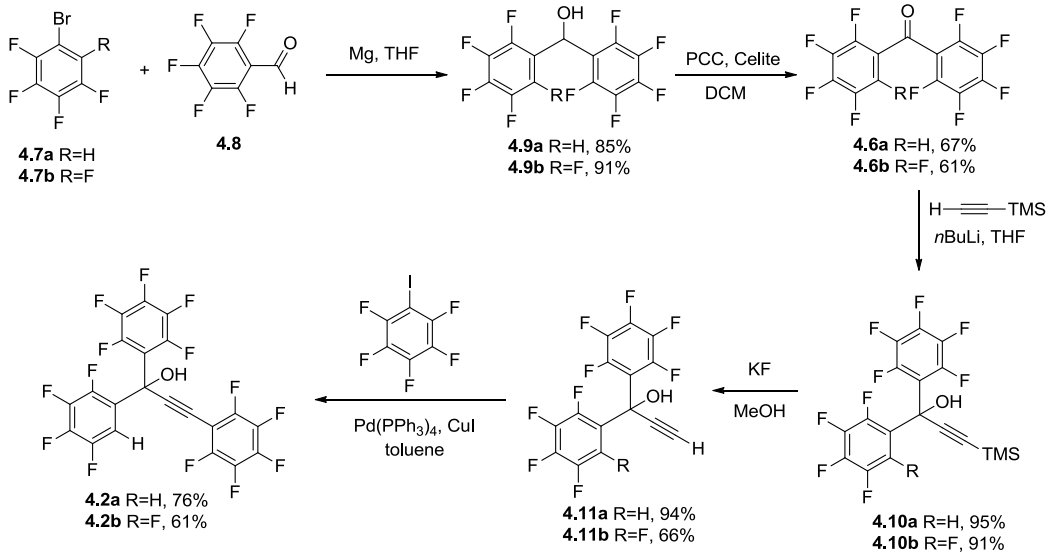

Scheme 4.3. Synthesis of fluorinated intermediates.

With alkyne **4.11** prepared, the Sonogashira coupling was attempted. Initial trials between alkyne **4.11** and bromopentafluorobenzene proved challenging and a series of conditions were screened in order to optimize the reaction (Scheme 4.4, Table 4.1). Early attempts yeielded no detectable amount of the desired product (Table 4.1, Entries 1-4). To conserve **4.11a**, a model substrate, propargyl alcohol **4.12**, was employed to examine further conditions (Table 4.1, Entries 5-11). A brief catalyst screen indicated that while $PdCl_2(PPh_3)_2$ provided product, $Pd(PPh_3)_4$ gave highest yield and PEPPSI-IPR[26] led to complex mixture (Table 4.1, Entries 5-8). Adjusting the method of addition of the alkyne **4.12** and the base did not appear to improve the yield nor did longer reaction times (Table 4.1, Entries 9-11). The model system yielded the highest amount of the product **4.13** under conditions of $Pd(PPh_3)_4$ (3 mol %) and CuI (9.5 mol %) using diisopropyl

amine (6.4 eq) at 80 °C for 7 h (Table 4.1, Entry 6). Adjusting these optimized conditions to include a bulkier amine base (diisopropylethyl amine) and double the reaction time, **4.11a** was subjected to the coupling conditions and desired **4.2** was afforded in 23% isolated yield (Table 4.1, Entry 12). Changing the coupling partner to pentafluoroiodobenzene and dropping the temperature to 60 °C successfully provided **4.2** in 51% yield after column chromatography (Table 4.1, Entry 13).

Table 4.1. Optimization of the Sonogashira coupling conditions.

Entry	Pd (mol %)	Cu (mol %)	Base (eq)	T (°C)	Time (h)	Results
1[a]	$Pd(PPh_3)_4$ (5)	CuBr (6.9)	TEA (3.5)	95	2.5	complex mixture
2[b]	$PdCl_2(PPh_3)_2$ (5)	CuI (10)	DIEA (4.0)	70	2	complex mixture
3[b]	$PdCl_2(PPh_3)_2$ (5)	CuI (10)	DIEA (4.0)	70	12	**4.2** observed, mixture
4[b]	$PdCl_2(PPh_3)_2$ (5)	CuI (10)	DIEA (4.0)	70	7	complex mixture
5[b,c]	$PdCl_2(PPh_3)_2$ (5)	CuI (10)	DIEA (4.0)	70	7	**4.13** (13%)
6[c]	$Pd(PPh_3)_4$ (3)	CuI (9.5)	DIPA (6.4)	80	7	**4.13** (53%)
7[c]	PEPPSI-IPR (3)	CuI (9.5)	DIPA (6.4)	80	23	complex mixture
8[c]	PEPPSI-IPR (3)	CuI (9.5)	Cs_2CO_3 (2.0)	80	20	complex mixture
9[c]	$Pd(PPh_3)_4$ (3)	CuI (9.5)	DIPA (6.4)[d]	80	7	**4.13** (43%)
10[c]	$Pd(PPh_3)_4$ (3)	CuI (9.5)	DIPA (6.4)[e]	80	46	**4.13** (31%)
11[c]	$Pd(PPh_3)_4$ (3)	CuI (9.5)	DIPA (6.4)[f]	80	46	**4.13** (23%)
12	$Pd(PPh_3)_4$ (3)	CuI (9.5)	DIEA (4.0)	80	16	**4.2** (23%)
13[g]	$Pd(PPh_3)_4$ (3)	CuI (9.5)	DIEA (4.0)	60	15	**4.2** (51%)

[a]Reaction run in toluene (0.25 M); [b]Reaction run in THF (0.5 M); [c]Reaction run with **4.12**; [d]DIPA added over 30 min while rxn was heating; [e]DIPA and propargyl alcohol added together over 5min; [f]DIPA and propargyl alcohol added over 30 min while rxn was heating; [g]Reaction run with iodopentafluorobenzene.

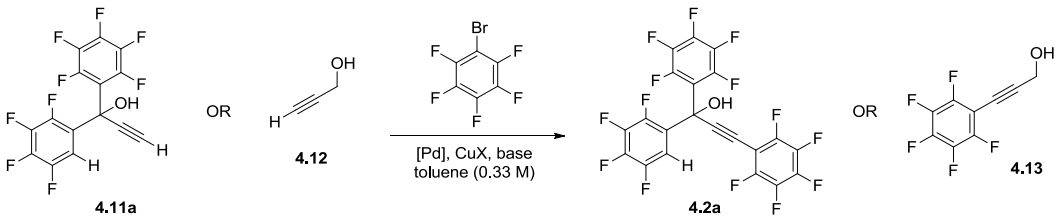

Scheme 4.4. Attempted conversion of **4.11a** to **4.2a** (or **4.12** to **4.13**) under various Sonogashira coupling conditions.

Although these intermediates are highly fluorinated, their solvation properties were not found to be affected at any step in the synthesis. Characterization of these intermediates utilized ^{19}F NMR in which fluorine-fluorine coupling was observed. While some coupling constants could be resolved, most of the fluorine peaks were denoted as multiplets due to the second order splitting, which arises from the magnetic nonequivalence of the fluorine atoms.[27] Fluorine-hydrogen coupling was observed for the aromatic hydrogen on all partially fluorinated intermediates. Surprisingly, fluorine-hydrogen coupling was observed in the ^{1}H NMR spectrum of fully fluorinated benzhydrol **4.9b** (Figure 4.2). The splitting pattern shows coupling between the bridging carbon hydrogen H_b and the alcohol proton H_a, providing a doublet at 6.50 ppm (J = 10.4 Hz). The alcohol proton H_a can be found at 3.29 ppm (confirmed by its disappearance when washing with D_2O). The splitting pattern indicates not only coupling to the bridging carbon hydrogen H_b (J = 10.4 Hz), but also long range, 5-bond, coupling between the alcohol proton H_a and the four *ortho* fluorine atoms (J = 2.1 Hz). Long range coupling between fluorine and hydrogen is common, yet the presence of 5-bond coupling while the 4-bond coupling between fluorine and H_b is absent is surprising. These long range couplings (both 4- and 5-bond) between hydrogen and fluorine have been found to be dependent on the internuclear distance.[27,28] It is likely that this coupling is observed due to the molecule adopting a conformation in which the

alcohol proton H_a is nearest to the *ortho* fluorine atoms, rather than the bridging carbon hydrogen H_b. Remarkably, this type of coupling was absent in the partially fluorinated benzhydrol **4.9a**.

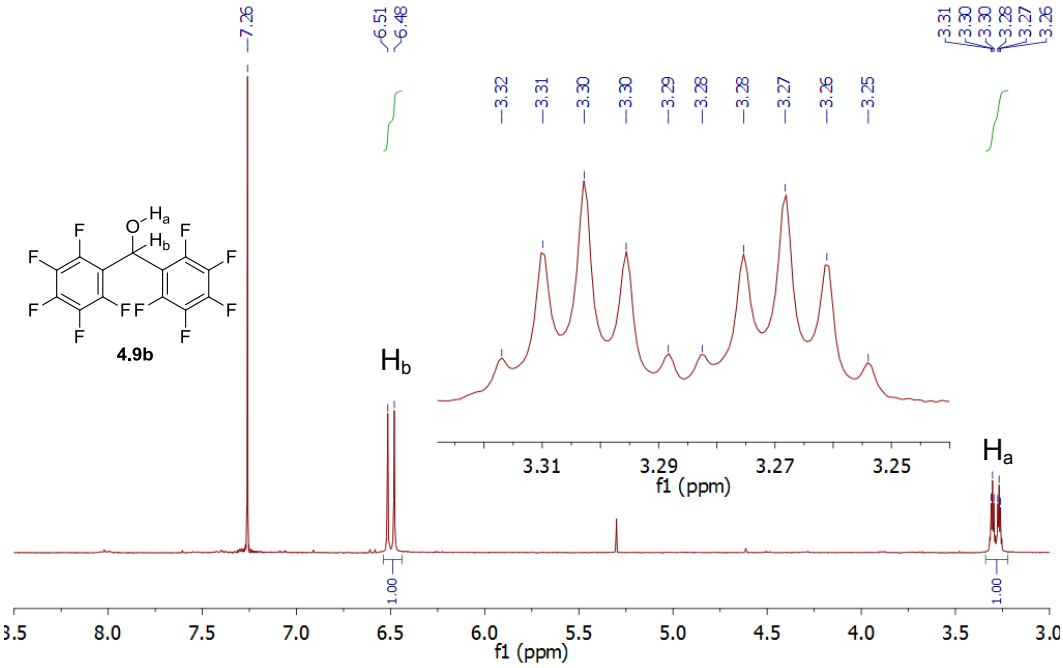

Figure 4.2. ^{1}H NMR spectrum of benzhydrol **4.9b**.

4.3.2 Synthetic efforts towards rubrene-F_{28}

With propargyl alcohol **4.2** in hand the dimerization reaction was attempted. We acknowledged that this reaction presented the potential for a mixture of compounds to form, which included regioisomers of cyclobutene **4.5**. The identification and isolation of our desired rubrene **4.1** might also be made difficult by the lack of characterization data on these compounds and further complicating matters is the moderate conversion to rubrene **1.1** (Figure 1.1, Chapter 1, page 1) under these conditions. In spite of these challenges, we began our investigations towards rubrene-F_{28} **4.1** (Scheme 4.5, Table 4.2).

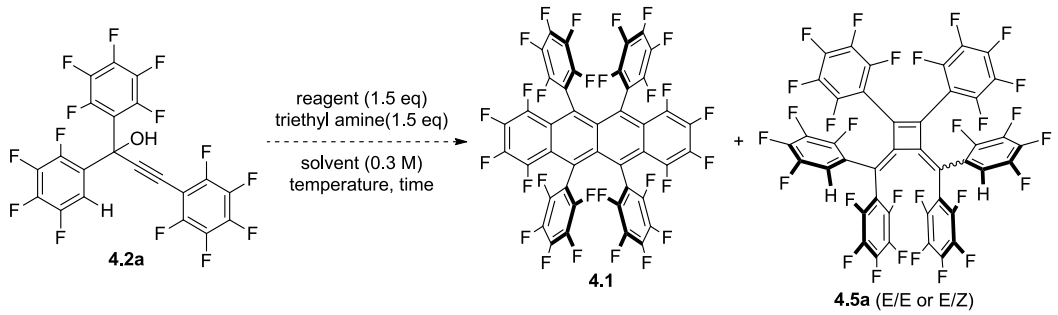

Scheme 4.5. Conversion of **4.2a** into desired rubrene **4.1** and one possible regioisomer of cyclobutene **4.5**.

Table 4.2. Reaction trials in the conversion of propargyl alcohol **4.2a** to rubrene **4.1**.

Entry	Reagent	Solvent	T (°C)	Time (h)	Results
1	MsCl	Tol	0-120	2	**4.1**[a], **4.1H**[a], **4.5a**[a,b], unidentified byproducts
2	MsCl	Tol	0-120	5	**4.5a**[b], unidentified byproducts
3	MsCl	Tol	0-70[c]; 120	1.5; 17	**4.5a**[d], unidentified byproducts
4	MsCl	Tol	130[e]; 120	20 min; 21	complex mixture
5[f]	MsCl	none	180	5 min	complex mixture
6	MsCl	Mes	0-165	2	complex mixture
7[g]	MsCl	Tol	0-110	3	complex mixture
8	MsCl	Tol	0-120	3	**4.14a**[a,h], **4.15a**[a,h]
9	Ms_2O	Tol	0-120	4	**4.14a** (69%)
10	Ms_2O	Mes	0-170	12	complex mixture
11	MsCl	Tol	0-rt	3	**4.14a** (91%)
12	MsCl	CH_2Cl_2	0-rt	1	**4.14a** (56%)

[a]Confirmed by LRMS; [b]Stereoisomers observed by ^{19}F NMR; [c]No change in reaction observed by TLC at this temperature; [d]Single stereoisomer observed by ^{19}F NMR; [e]Performed in microwave; [f]Performed in 0.05 M of triethylamine; [g]Used diisopropylethyl amine instead of triethylamine; [h]Obtained in a 1:1 ratio based on ^{1}H NMR.

Using the one pot conversion under standard conditions of methanesulfonyl chloride and triethylamine in toluene,[20,29] a mixture of compounds was obtained after heating for two hours (Table 4.2, Entry 1). Some of the compounds could be isolated by preparative TLC and their identities were confirmed to be desired **4.1** and expected **4.5a** by LRMS. Unexpected was the presence of rubrene **4.1H** (Figure 4.3), which was inseparable from **4.1**. In order for **4.1H** to form, a fluorine atom must have been lost; however, it is unclear by what mechanism this may

occur. The identification of this compound did inspire our later studies into whether the hydrogen atoms were necessary for the formation of **4.1** (*vide infra*). With these positive results, we attempted to optimize the reaction to favor **4.1**.

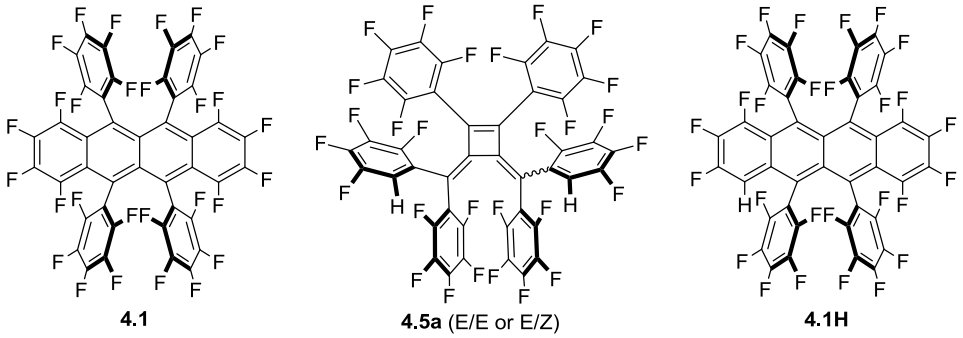

Figure 4.3. Products **4.1**, **4.5a**, and **4.1H** from the reaction of **4.2** with methanesulfonyl chloride confirmed by LRMS.

Longer reaction times appeared to favor the formation of **4.5a** (Table 4.2, Entries 2-3) and we were able to observe different ratios of the regioisomers (Figure 4.4). Heating at lower temperature did not appear to overcome the thermal barrier to dimerization (Table 4-2, Entry 3) and neither did heating in the microwave, although upon further heating without the microwave a complex mixture formed (Table 4.2, Entry 4). Use of triethylamine or mesitylene as the solvent gave a complex mixture with no indication of the desired product (Table 4.2, Entries 5-6). Use of a different amine base did not appear to improve the reaction (Table 4.2, Entry 7).

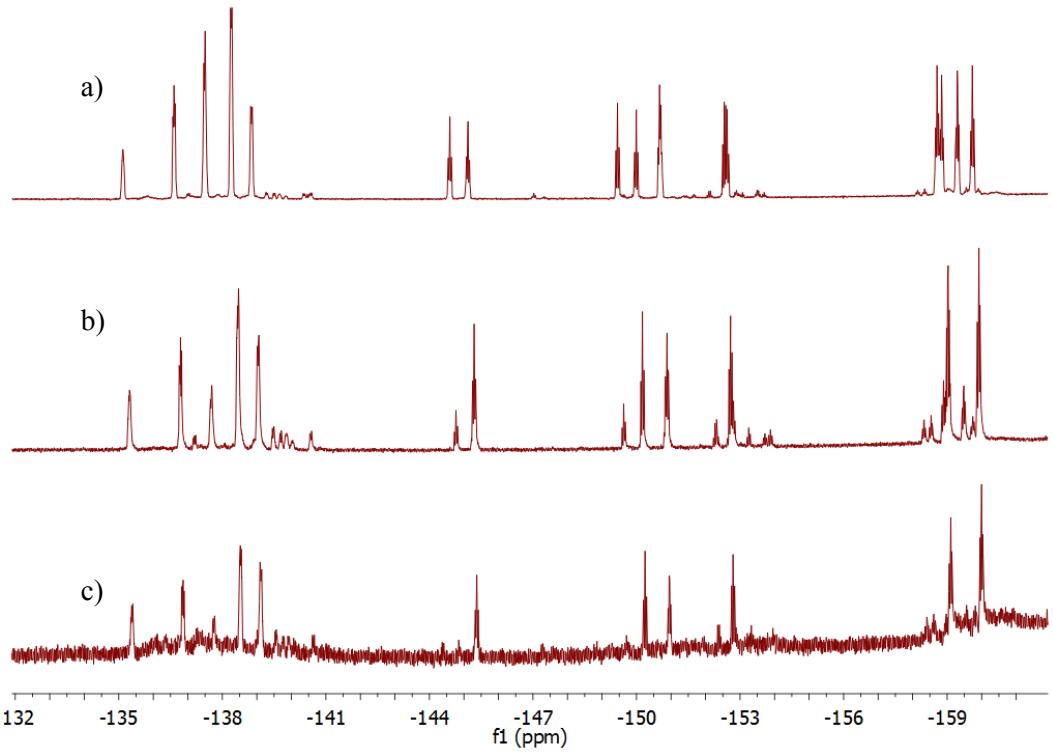

Figure 4.4. ^{19}F spectra of cyclobutene **4.5a** observed under conditions in Table 4.2 **a**) Entry 1, **b**) Entry 2, **c**) Entry 3. Smaller peaks due to an unidentified byproduct.

In an attempt to replicate the reaction using conditions from Entry 1 in Table 4.2, two new compounds were observed and isolated (Table 4.2, Entry 8). Based on LRMS of these compounds, these structures were proposed to be alkynyl mesylate **4.14a**, which would be the first intermediate formed in this reaction, and alkene **4.15a** (Figure 4.5). Alkene **4.15a** was also proposed based on the presence of a singlet in the ^{1}H NMR spectrum at 5.41 ppm and a singlet at 3.27 ppm corresponding to the mesyl group. The scale of this reaction required microliter quantities of base and it is possible that a lower amount of triethylamine was added than intended. Not having enough base to remove the HCl that is formed during the reaction might explain the

formation of **4.15a**. In light of this observation, a different mesylating agent was employed in order to avoid the formation of HCl. However, the use of methanesulfonic anhydride resulted in more of **4.14a** and higher temperatures did not appear to improve the reaction towards **4.1** (Table 4.2, Entries 9-10). We then found that formation of **4.14a** occurred at room temperature when either toluene or dichloromethane was used as the solvent (Table 4.2, Entries 11-12). Having little success with propargyl alcohol **4.2a**, we decided to look into the conversion of **4.2b** (Scheme 4.6).

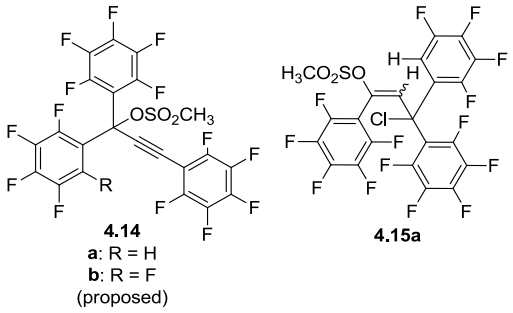

Figure 4.5. Compounds **4.14a** and **4.15** isolated and identified from one attempt to convert propargyl alcohol **4.2a** to rubrene **4.1**.

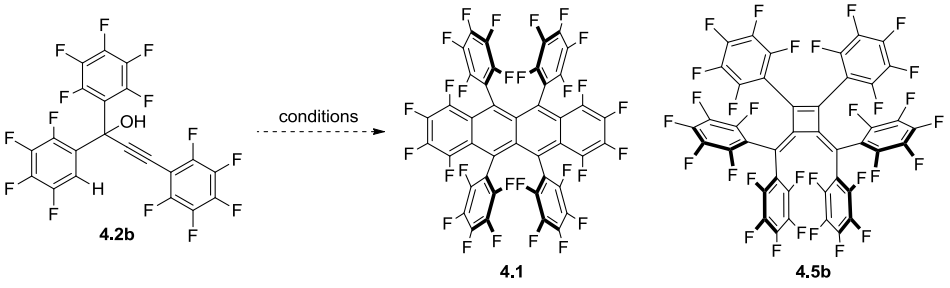

Scheme 4.6. Transformation of **4.2b** to rubrene **4.1** and byproduct **4.5b**.

Table 4.3. Reaction trials in the conversion of propargyl alcohol **4.2b** to rubrene **4.1**.

Entry	Reagent	Solvent	T (°C)	Time (h)	Results
1	MsCl	Tol	0-110	3	**4.5b**[a] (7%), **4.14b**[a] (65%)
2	MsCl	Tol	0-115	11	complex mixture
3[b]	MsCl	Tol	rt-100	1	**4.14b** immediately observed

[a]Confirmed by HRMS; [b]VT NMR study. Tol: toluene; MsCl: methanesulfonyl chloride

Standard conditions provided **4.5b** and **4.14b** (Figure 4.4) in 7 and 65 percent yield respectively, with no evidence for the desired rubrene **4.1** (Table 4.3, Entry 1). Longer reaction time led to a complex mixture (Table 4.3, Entry 2). In order to examine when the formation of **4.14b** occured and whether this compound converted into the other observed products, a variable temperature (VT) ^{19}F NMR study was performed on the reaction of **4.2b** (Table 4.3, Entry 3). Upon addition of the methanesulfonyl chloride, the spectrum immediately showed the presence of **4.14b** in full conversion (Figure 4.5a-b). Ramping the temperature by 20 °C per 10 minutes showed little reactivity until the reaction temperature had reached 100 °C (Figure 4.5c-f). A peak around −137 ppm appeared to become more intense while heating at 100 °C (Figure 4.5g-j); however, upon cooling to room temperature the peak disappeared and only peaks that could be attributed to the **4.14b** (confirmed by HRMS) and a minor unidentified byproduct were observed (Figure 4.5k). The mesylate **4.14** appears to be quite stable under these conditions, suggesting better ionization conditions were necessary. We decided to briefly explore treating **4.14a** with different additives.

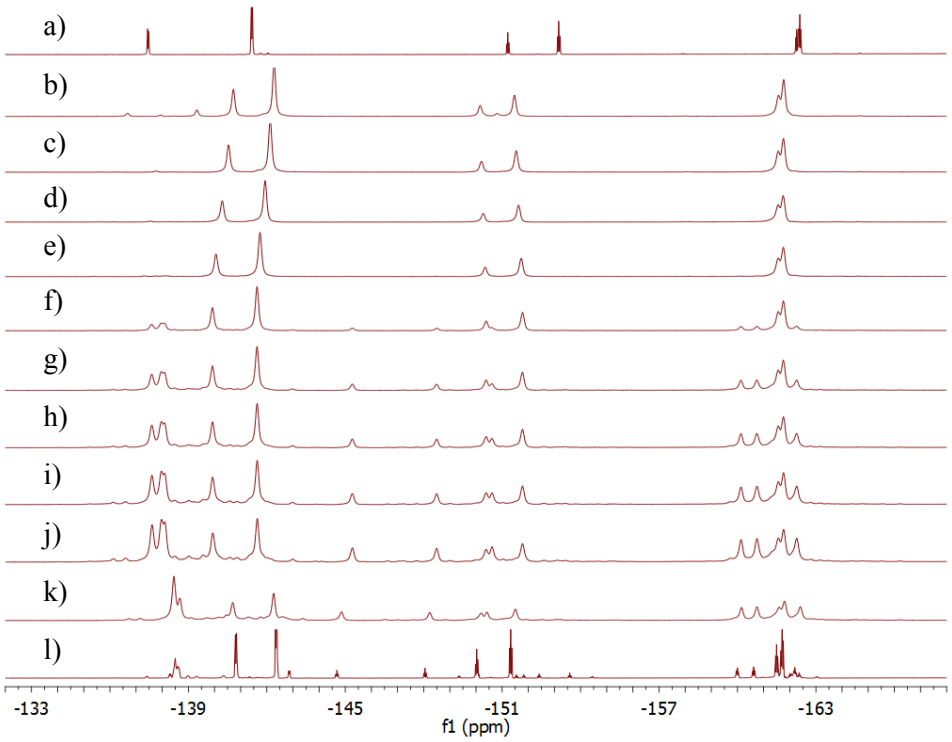

Figure 4.6. Variable temperature (VT) ^{19}F NMR data for the reaction of **4.2b** with methanesulfonyl chloride and triethylamine in toluene-d_8. Spectra are as follows: **a**) **4.2b** in toluene-d_8; reaction mixture at **b**) rt, **c**) 40 °C, **d**) 60 °C, **e**) 80 °C, **f**) 100 °C, 0 min, **g**) 100 °C, 15 min, **h**) 100 °C, 30 min, **i**) 100 °C, 45 min, **j**) 100 °C, 60 min, **k**) returned to rt; **l**) **4.14b**.

The next experiments briefly explored whether this isolated intermediate might still lead to rubrene **4.1** under different conditions (Scheme 4.7). Heating **4.14a** in toluene or neat without additives led to negligible formation of products (Table 4.4, Entries 1-3). One equivalent of a Lewis acid, $LiBF_4$, was employed to promote the loss of the mesylate in a variety of solvents but was found to be ineffective (Table 4.4, Entries 4-6). Increasing the amount of $LiBF_4$ to 2.4 equivalents did consume the starting material but the products did not match any previously observed structures nor were we able to identify them (Table 4.4, Entry 7). While the ionic

nature of the last reaction did appear to improve the reactivity of the intermediate, **4.14a** did not appear to be a viable intermediate to rubrene **4.1**.

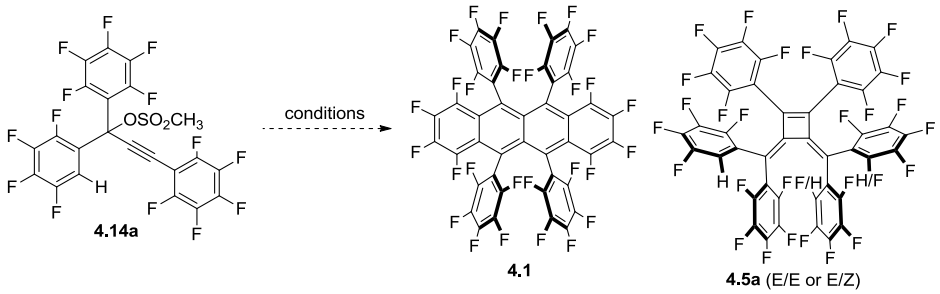

Scheme 4.7. Attempted conversion of allenyl mesylate **4.14a** to rubrene **4.1** and likely byproduct cyclobutene **4.5a**.

Table 4.4. Attempts to convert proposed alkynyl mesylate **4.14a** to rubrene **4.1**.

Entry	Additive	Solvent	T (°C)	Time (h)	Results
1	none	Tol	100	90	mostly starting material
2	none	Tol	150	24	mostly starting material
3	none	none	200	2	mostly starting material
4	$LiBF_4$[a]	Tol	150	16	mostly starting material
5	$LiBF_4$[b]	THF	80	18	mostly starting material
6	$LiBF_4$[a]	dioxane	120	18	mostly starting material
7	$LiBF_4$[c]	Tol	150	19	complex mixture

[a]1.0 equivalents; [b]1.2 equivalents; [c]2.4 equivalents.

The surprisingly low reactivity of **4.14a** led us to reassign the structure to the allenyl mesylate (**4.14a**, Figure 7) based on further characterization. Compared to the starting propargyl alcohol **4.2a**, the single aromatic proton in **4.14a** has shifted upfield significantly, indicating a dramatic change in structure. This structural change was reflected in the fluorine spectrum of **4.14a**, as compared to **4.2a**, in which peaks had resolved and shifted. The HRMS data corresponded to the correct mass of the allenyl mesylate, although this mass also corresponds to the previously proposed propargyl mesylate structure thus the data is supportive but not conclusive. A comparison of the IR spectra between **4.2a** and **4.14a** revealed that while **4.2a**

shows an alkynyl stretch at 2245 cm^{-1}, an allenyl stretch was seen at 1962 cm^{-1} for **4.14a** (Figure 4.6c-d). The ^{13}C NMR also confirmed the presence of the allene by an observed singlet at 203.6 ppm. The formation of this structure seems to indicate that, under the standard reaction conditions, the chloride ion is slower to attack the alkyne than the mesylate anion, and that once formed the allenyl mesylate is quite stable. This is strikingly different from the reactivity of the protonated propargyl alcohol **1.5** (Scheme 4.1) in which the corresponding allenyl mesylate has never been reported. The presence of the perfluoroaryl rings will certainly influence the electronics of the alkyne **4.2a**; the electron deficiency of the alkyne may explain the more favorable formation of the allenyl mesylate over the chloroallene **4.3a** (Scheme 4.1b) under these conditions.

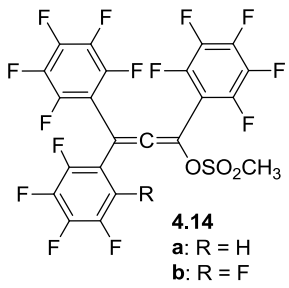

4.14
a: R = H
b: R = F

Figure 4.7. Revised structure of **4.14**.

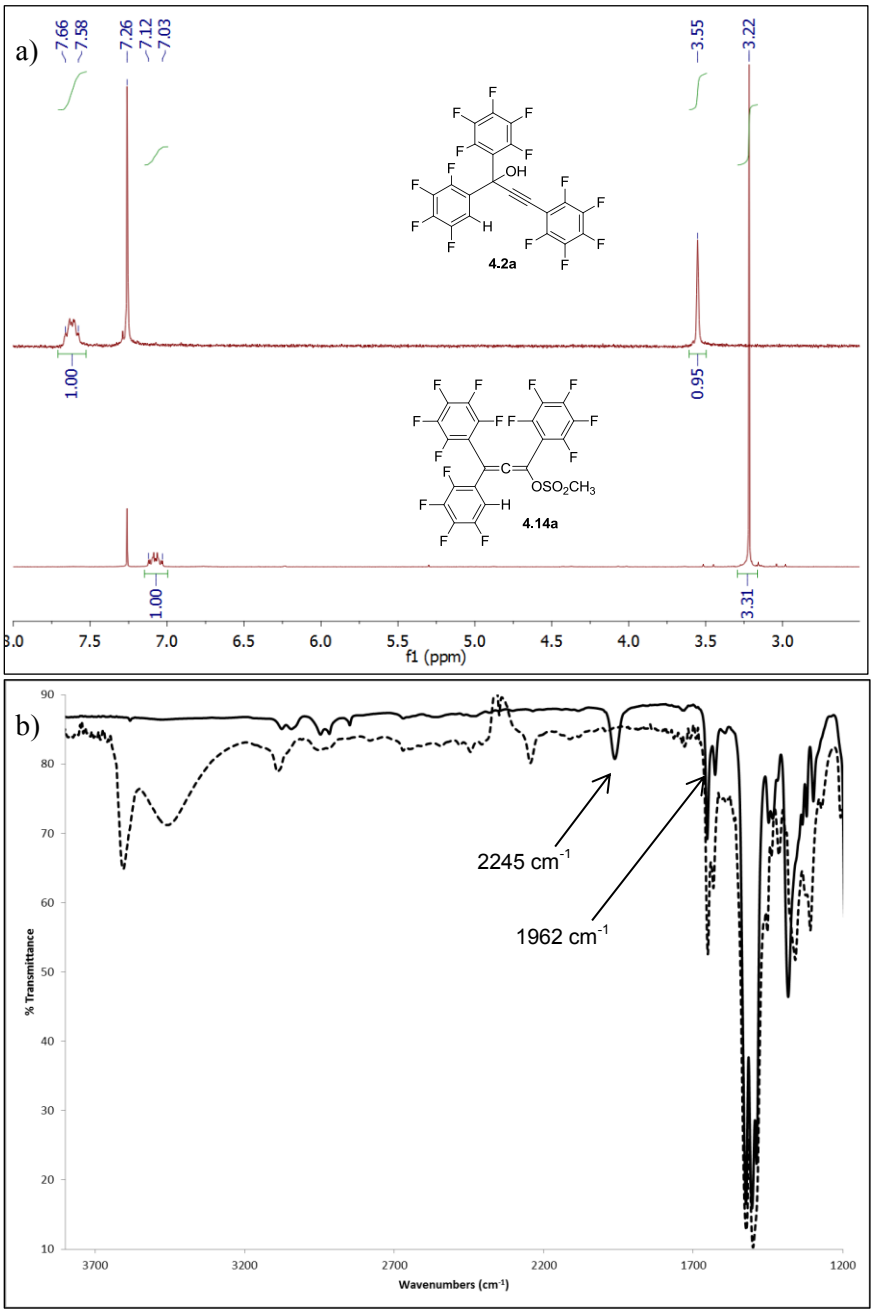

Figure 4.8. a) ^{1}H NMR spectra of propargyl alcohol **4.2a** (top) and allenyl mesylate **4.14a** (bottom). **b**) IR spectra (thin film, CH_2Cl_2) of **4.2a** (dashed line) and **4.14a** (solid line).

Based on the observed stability of allenyl mesylate **4.14a**, we decided to return to the propargyl alcohol **4.2a** and attempt to isolate the perceived reactive chloroallene **4.3a** (Scheme 4.8). Conversion to the chloroallene **4.3a** was first attempted by saturating the standard reaction conditions with chloride ion using tetrabutylammonium chloride (Table 4.5, Entries 1-2). The reaction did lead to a new product as observed by ^{19}F NMR, but this product would decompose when attempts were made to isolate it away from the ammonium salt. Immediately heating this intermediate without purification led to a complex mixture of products that were not able to be identified. Changing the chlorinating agent to thionyl chloride (Table 4.5, Entries 3-4) provided the desired product in 4 percent yield, in which much of the product was likely lost while screening work-up conditions. Having found suitable conditions, chloroallene **4.3a** could be isolated in 44 percent yield. The other recovered material was an unidentified mixture.

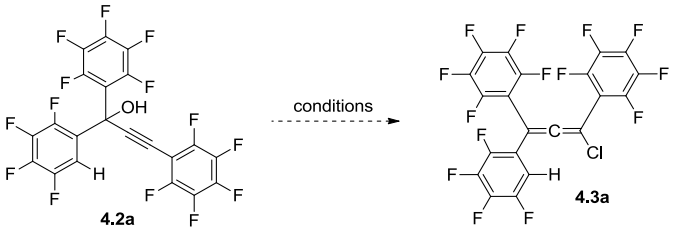

Scheme 4.8. Attempted conversion of propargyl alcohol **4.2b** into chloroallene **4.3a**.

Table 4.5. Attempts to isolate chloroallene **4.3a**.

Entry	Reagent	Base	Solvent	T (°C)	Time (h)	Results
1[a]	MsCl	TEA	CH_2Cl_2	0	1	unidentifed and unisolable pdt
2[a]	MsCl	TEA	CH_2Cl_2, then tol	0; 100	1; 2	complex mixture
3	$SOCl_2$	pyr	diethyl ether	0-rt	1	**4.3a** (10.9 mg, 4%)
4	$SOCl_2$	pyr	diethyl ether	0-rt	1	**4.3a** (113 mg, 44%)

[a]$N(C_4H_{10})_4Cl$ added.

Having successfully synthesized the fluorinated chloroallene **4.3a**, attempts were made to convert this isolated intermediate into rubrene **4.1** (Scheme 4.9). Heating the chloroallene with triethylamine in toluene at 120 °C led to a complex mixture in which a variety of ethyl peaks were observed and there was no evidence of perfluororubrene or cyclobutene **4.5a** (Table 4.6, Entry 1). Employing pyridine or 2,6-lutidine as the base instead of triethylamine in order to decrease the nucleophilicity of the base resulted in recovered starting material (Table 4.6, Entries 2-3). Going to higher temperature using mesitylene still did not appear to have overcome the thermal barrier to dimerization (Table 4.6, Entry 4). Postulating that perhaps there was a strong solvent effect, we changed the solvent to hexafluorobenzene (Table 4.6, Entry 5), but no reaction occurred. In an attempt to heat the intermediate as high as possible, **4.3a** was treated with imidazole and heated to 200 °C, but unfortunately this appeared to result in decomposition as no material could be recovered (Table 4.6, Entry 6).

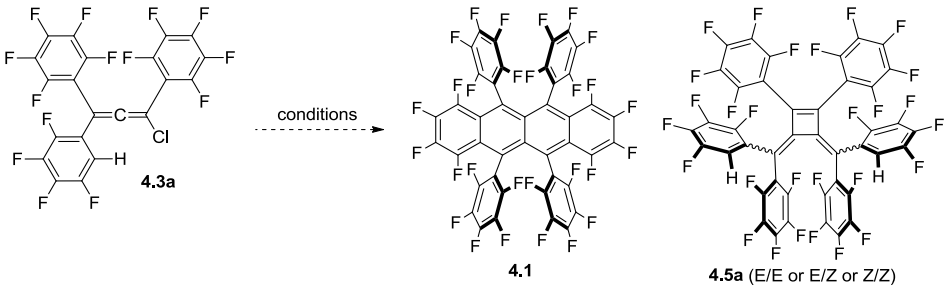

Scheme 4.9. Attempted conversion of chloroallene **4.3a** into rubrene **4.1** and likely byproduct cyclobutene **4.5a**.

Table 4.6. Reaction conditions used in the conversion of chloroallene **4.16** to rubrene **4.1**.

Entry	Reagent	Base	Solvent	T (°C)	Time (h)	Results
1	none	triethylamine	toluene	120	3	complex mixture
2	none	pyridine	toluene	120	3	recovered starting material
3	none	2,6-lutidine	toluene	120	4	recovered starting material
4	none	2,6-lutidine	mesitylene	180	14	mostly starting material
5	none	2,6-lutidine	C_6F_6	100	16	recovered starting material
6	none	imidazole	none	200	15min	no recoverable material

One final attempt was made to form desired perfluororubrene. Thionyl chloride was used in an attempt to convert the propargyl alcohol **4.2a** in one step to **4.1** in the presence of 3.5 equivalents of pyridine (Scheme 4.10). Following filtration and concentration, the reaction mixture was purified by column chromatography. Diastereomers of cyclobutene **4.5a** were isolated in a 9% yield and the stereoisomerism was enhanced by the purification (Figure 4.9). Isolation of these compounds from this reaction indicates that in the previous attempts to convert the chloroallene **4.3a**, the thermal barrier to dimerization was likely being reached. However, presumably the chloride ions, which are in solution during the one-pot reaction but not in the attempts to convert **4.3a**, play a role the closure to rubrene **4.1** or cyclobutene **4.5a**. Further examination of the medium effect and role of the chloride ion is needed in order to understand this transformation.

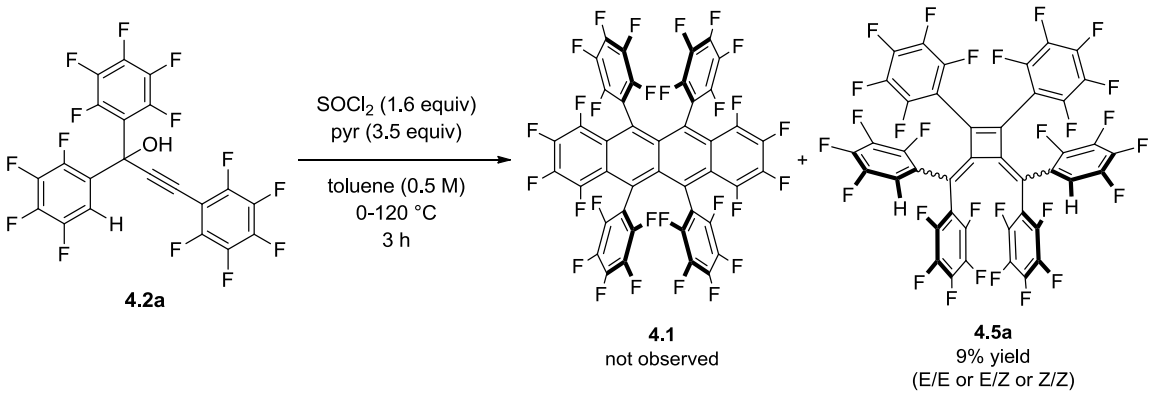

Scheme 4.10. One-pot conversion of propargyl alcohol **4.2a** gave **4.5a**.

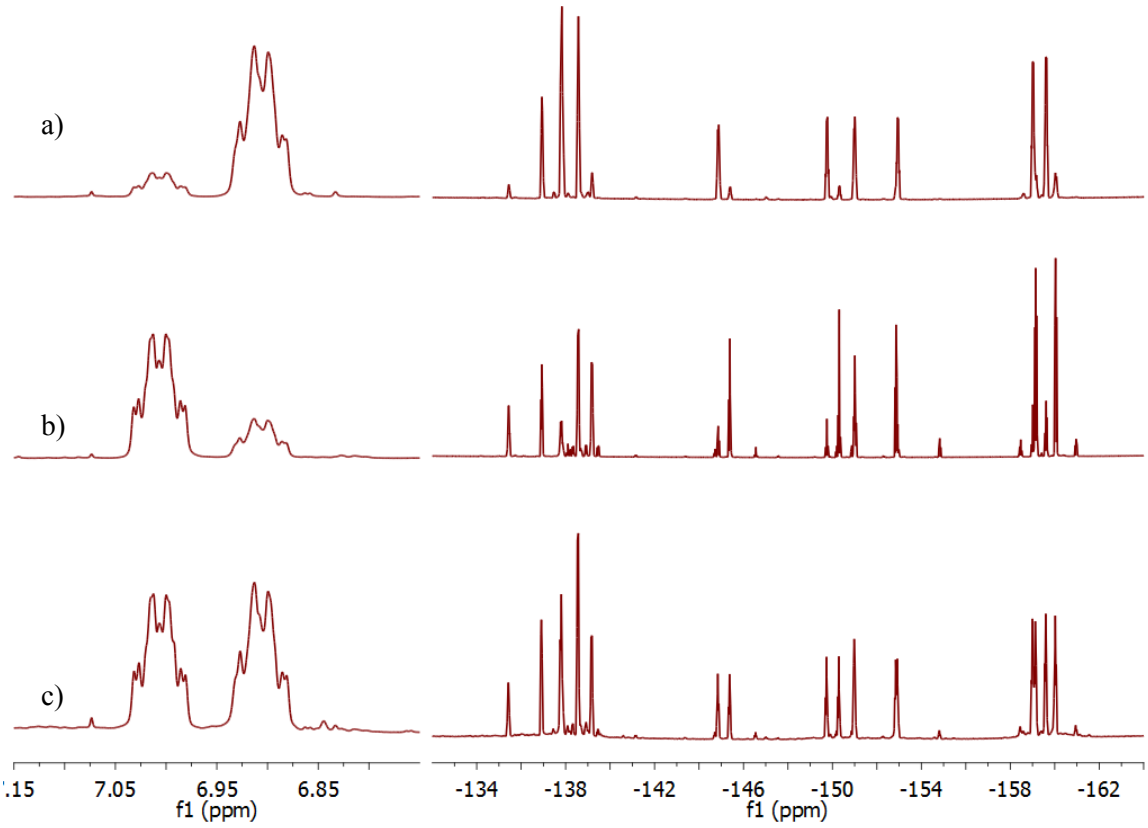

Figure 4.9. ^{1}H NMR (left) and ^{19}F NMR (right) spectra showing diastereomers of cyclobutene **4.5a a**)-**b**) enhanced in one stereoisomer and **c**) mixture of stereoisomers.

While preparative quantities and full characterization of rubrene-F_{28} **4.1** has not yet been achieved, this route may yet prove successful. Isolation and identification of allenyl mesylate **4.14a** was essential in understanding the reactivity of these intermediates. The observation and identification of cyclobutene **4.5** indicates that the formation of the bisallyl diradical **4.4a** does indeed form. Perhaps the barrier needed to be overcome is the potential resistance of fluorinated substrates to 6π-electrocyclization[30] (a necessary step in the formation of rubrene-F_{28} **4.1**); however, the carbons that would need to react to form **4.1** are not fluorinated, so this effect may

be minimal. Further examination of the reactivity of chloroallene **4.3a** will shed more light whether the classical route to rubrene **1.1** is a viable route to rubrene-F_{28} **4.1**.

4.4 FUTURE STUDIES

Efforts to convert the chloroallene **4.3a** to rubrene-F_{28} **4.1** may continue to be pursued; however, the challenges encountered while exploring this classical route have led us to propose other routes to the target molecule. The first alternative route utilizes a series of Diels-Alder reactions to form the tetracene core beginning from known α-keto acid **4.19**[31] and hydrazide **4.20**[32] (Scheme 4.10a). Similar to other routes to rubrene **1.1**, we envisioned building the tetracene core via a [4+2] cycloaddition between pyridazine **4.16** and benzyne precursor **4.17**. The latter intermediate could be synthesized from a Diels-Alder reaction between **4.16** and alkyne **4.21**. Pyridazine **4.16** could be synthesized from the [4+2] cycloaddition between cyclic ester **4.18** and the benzyne formed in situ from bromopentafluorobenzene. Oxadiazine **4.18** could be synthesized from known α-keto acid **4.19** and hydrazide **4.20**.[33] The protonated **4.18** is known to undergo inverse-electron-demand Diels-Alder reactions with benzyne intermediates and has been utilized in the successful formation of other acene cores.[34,35] The fluorination of the phenyls will undoubtedly make this cycloaddition more challenging, but likely still feasible under the right conditions.

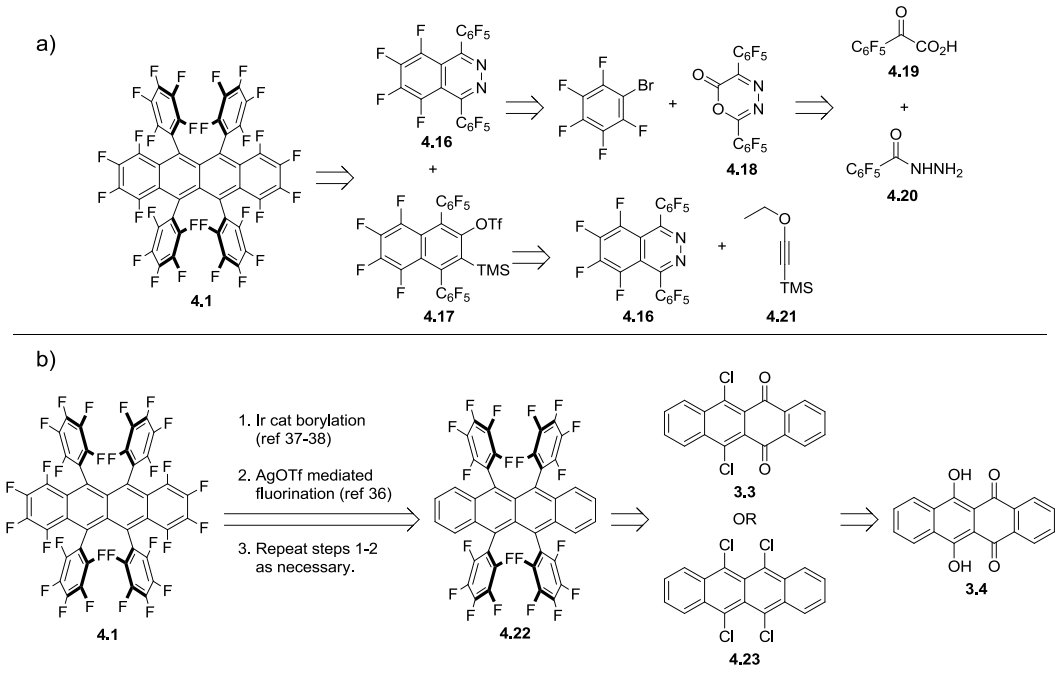

Scheme 4.11. Retrosynthetic analysis of **a**) the first alternative route to rubrene- F_{28} using Diels-Alder cyclizations and **b**) the second alternative route to rubrene- F_{28} using iterative borylation and fluorination.

The idea for second alternative route (Scheme 4.10b) came from the report by Furuya and Ritter in which they convert an aryl C–B bond into a C–F bond.[36] Aryl C–B bonds can be formed without prior functionalization from the C–H bond utilizing an iridium-catalyzed reaction.[37,38] This second route would employ iterative borylation and fluorination since the borylation would not convert all desired bonds at once. Beginning from a key intermediate seen in Chapter 3, **3.4** would be converted into either the chlorotetracenedione **3.3** or tetrachlorotetracene **4.16** in order to install the pentafluorophenyl side rings. In theory the second route could fluorinate the parent rubrene **1.1**, but we believe the *ortho* positions of the side phenyls will be rather challenging to borylate; therefore, we propose installing the fully fluorinated side phenyls first. Although the first steps in these routes were attempted, little progress was made in either synthesis.

4.5 EXPERIMENTALS

All reactions were carried out using flame-dried glassware under a nitrogen or argon atmosphere unless aqueous solutions were employed as reagents. Toluene was dried by distillation from CaH_2. Tetrahydrofuran (THF) was dried by distillation from benzophenone/sodium. Analytical thin layer chromatography (TLC) was carried out using 0.25 mm silica plates from Silicycle. Eluted plates were visualized first with UV light. Flash chromatography was performed using 230–400 mesh (particle size 0.04–0.063 mm) silica gel purchased from Silicycle. ^{1}H NMR (300 MHz), ^{13}C NMR (75 MHz), ^{2}H (46.1 MHz) spectra were obtained on Varian FT NMR or Bruker FT NMR instruments. NMR spectra were reported as δ values in ppm relative to chloroform for ^{1}H (7.26 ppm), chloroform for ^{13}C (77.00 ppm), and trifluorotoluene or hexafluorobenzene for ^{19}F (−63.72 or −164.9 ppm). ^{1}H and ^{13}C NMR coupling constants are reported in Hz; multiplicity was indicated as follows; s (singlet); d (doublet); t (triplet); q (quartet); quint (quintet); m (multiplet); dd (doublet of doublets); ddd (doublet of doublet of doublets); dddd (doublet of doublet of doublet of doublets); dt (doublet of triplets); td (triplet of doublets); tt (triplet of triplets); ddt (doublet of doublet of triplets); dtd (doublet of triplet of doublets); dquint (doublet of quintets); app (apparent); br (broad). Infrared (IR) spectra were obtained as films from CH_2Cl_2 on a Thermo Scientific FT-IR. Low-resolution mass spectra (LRMS) in EI experiments were performed on a Varian Saturn 2200 GC-MS system. Low-resolution mass spectra (LRMS) in EI or CI experiments were performed on a Varian Saturn 2200 GC-MS system. High-resolution mass spectra (HRMS) in EI experiments were performed on a Finnigan MAT 95 GC-MS system or in electrospray (ESI) experiments were performed on a Bruker BioTOF II. Elemental analysis was performed by Atlantic Microlab, Inc., 6180 Atlantic Blvd, Suite M, Norcross, GA 30071.

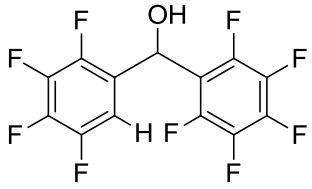

Benzhydrol **4.9a**: The compound was synthesized as reported in the literature.[39] Purification by column chromatography (1:1 CH_2Cl_2:hexanes) yielded **4.9a** as a cream-colored solid (5.57 g, 16.1 mmol, 85%). R_f = 0.17 (1:1 hexanes:CH_2Cl_2); ^{1}H NMR (300 MHz, $CDCl_3$) δ 2.69 (d, J = 5.9 Hz, 1H), 6.41 (d, J = 5.9 Hz, 1H), 7.42-7.49 (m, 1H); ^{19}F NMR (282 MHz, $CDCl_3$) δ −138.71 (ddd, J = 11.1, 17.9, 23.8 Hz, 1F), −143.26 (dt, J = 5.1, 19.5 Hz, 2F), −143.99-−144.14 (m, 1F), −153.35 (t, J = 20.8 Hz, 1F), −156.05-−156.23 (m, 2F), −161.43-−161.61 (m, 2F).

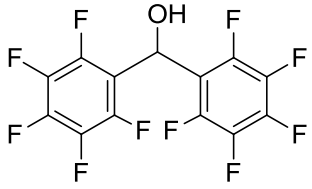

Benzhydrol **4.9b**: Following the same procedure as **4.9a** using pentafluorobenzaldehyde (2.00 g, 10.2 mmol) and bromopentafluorobenzene (2.93 mL, 23.5 mmol), **4.9b** was obtained without purification by column chromatography as a brown oil (3.43 g, 9.32 mmol, 91%). ^{1}H NMR (300 MHz, $CDCl_3$) δ 3.29 (dquint, J = 2.1, 10.4 Hz, 1H), 6.50 (d, J = 10.4 Hz, 1H); ^{19}F NMR (282 MHz, $CDCl_3$) δ −143.83-−143.88 (m, 4F), −153.25 (t, J = 20.9 Hz, 2F), −161.22-−161.34 (m, 4F).

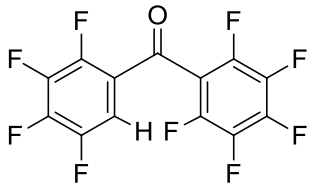

Benzophenone **4.6a**: To a 50 mL round-bottom flask was added **4.9a** (0.346 g, 1.00 mmol, 1.0 equiv.), pyridinium chlorochromate (PCC) (0.259 g, 1.20 mmol, 1.2

equiv.), celite (1 g), and CH_2Cl_2 (10 mL). The reaction was stirred at room temperature. The flask was recharged with PCC (0.020 g) after 19 h to try to improve the conversion. After stirring at room temperature for 1 h, the solvent was removed in vacuo, and the resulting solid was purified by column chromatography (1:1 CH_2Cl_2:hexanes) to afford **4.6a** as a colorless oil (0.281 g, 0.817 mmol, 82%). R_f = 0.75 (1:1 hexanes:CH_2Cl_2); ^{1}H NMR (300 MHz, $CDCl_3$) δ 7.58 (dddd, J = 2.5, 6.1, 8.4, 10.5 Hz, 1H); ^{19}F NMR (282 MHz, $CDCl_3$) δ −136.30-−136.47(m, 1F), −138.51-−138.68 (m, 1F), −141.76-−141.89 (m, 2F), −144.04 (ddd, J = 8.7, 19.0, 28.8 Hz, 1F), −148.21 (tt, J = 4.1, 20.9 Hz, 1F), −152.96 (app t, J = 20.4 Hz, 1F), −160.09 (dddd, J = 5.0, 11.3, 20.6, 25.3 Hz, 2F).

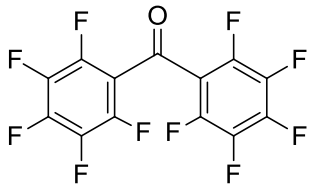

Benzophenone **4.6b**: Following the same procedure as **4.6a** using benzhydrol **4.9b** (1.05 g, 2.88 mmol), **4.6b** was obtained as a colorless solid (0.641 g, 1.77 mmol, 61%). ^{19}F NMR (282 MHz, $CDCl_3$) δ −143.83-−143.88 (m, 4F), −145.63 (app tt, J = 5.2, 20.8 Hz, 2F), −161.22-−161.34 (m, 4F).

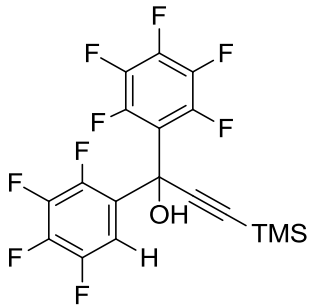

Compound **4.10a**: To a 50 mL round-bottom flask was added (trimethylsilyl)acetylene (1.18 mL, 8.30 mmol, 1.2 equiv.) and THF (7 mL). The solution was

cooled to −30 °C with a dry ice/acetonitrile bath. To the solution was added *n*-butyl lithium (2.5 M solution in hexanes, 0.80 mL, 2.0 mmol, 1.2 equiv.). A separate 50 mL round bottom flask was charged with **4.6a** (2.38 g, 6.92 mmol, 1.0 equiv) and THF (6.4 mL), then cooled to −30 °C. The organolithium solution was transferred dropwise via syringe into the second flask, and the reaction was stirred at −30 °C for 20 min. After warming to room temperature, the solution was extracted with saturated aqueous NH_4Cl (15 mL) and diethyl ether (2 × 15 mL). The organic layers were combined, dried over Na_2SO_4, filtered, and concentrated to provide **4.10a** as a tan-colored oil (2.89 g, 6.54 mmol, 95%). ^{1}H NMR (500 MHz, $CDCl_3$) δ 0.22 (s, 9H), 3.36 (s, 1H), 7.56-7.61 (m, 1H); ^{19}F NMR (282 MHz, $CDCl_3$) δ −139.25 (ddd, *J* = 11.3, 11.3, 22.0 Hz, 1F), −140.20-−140.25 (m, 3F), −154.10 (app t, *J* = 21.2 Hz, 1F), −155.01 (app dtd, *J* = 4.2, 8.1, 20.6 Hz, 1F), −155.34 (t, *J* = 20.4 Hz, 1F), −162.15 (app td, *J* = 6.0, 21.5 Hz, 2F); IR (thin film, CH_2Cl_2) 3607, 3468, 2964, 2903, 2172, 1651, 1632, 1524, 1487 cm^{-1}; HRMS (EI) *m*/*z* calcd for $C_{18}H_{11}F_9OSi$ [M−H]$^-$ 441.0363, found 441.0361.

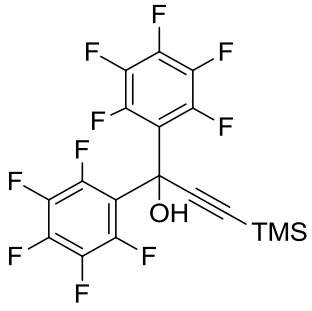

Compound **4.10b**: Following the same procedure as **4.10a** using benzophenone **4.6b** (0.876 g, 2.42 mmol), **4.10b** was obtained as a tan-colored oil (1.01 g, 2.20 mmol, 91%). ^{1}H NMR (300 MHz, $CDCl_3$) δ 0.20 (s, 9H), 3.65 (s, 1H); ^{19}F NMR (282 MHz, $CDCl_3$) δ −140.60-−140.67 (m, 4F), −153.71 (app t, *J* = 21.5 Hz, 2F), −161.75-−161.92 (m, 4F); IR (thin film, CH_2Cl_2) 3608, 3485, 2964, 2929, 2857, 1652, 1526, 1499 cm^{-1}.

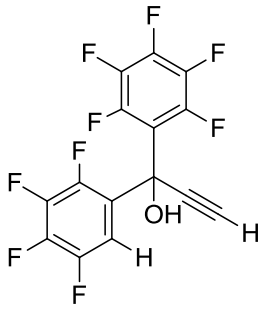

Compound **4.11a**: To a 100 mL round-bottom flask was added **4.10a** (2.89 g, 6.54 mmol, 1.0 equiv.), methanol (32.7 mL), and KF•H_2O (3.08 g, 32.7 mmol, 5.0 equiv.). The reaction was stirred at room temperature for 1 h, then poured into separatory funnel with saturated aqueous NH_4Cl (30 mL). The aqueous layer was extracted with diethyl ether (2 × 30 mL). The combined organic layers were dried over Na_2SO_4, filtered, and concentrated to give **4.11a** as a tan-colored oil (2.28 g, 6.15 mmol, 94%). ^{1}H NMR (500 MHz, $CDCl_3$) δ 3.00 (s, 1H), 3.43 (s, 1H), 7.58-7.64 (m, 1H); ^{19}F NMR (282 MHz, $CDCl_3$) δ −138.75 (ddd, J = 11.8, 11.8, 22.0 Hz, 1F), −139.92-−139.97 (m, 3F), −153.28 (app t, J = 21.2 Hz, 1F), −154.35 (app dtd, J = 4.6, 7.6, 20.1 Hz, 1F), −154.85 (t, J = 20.1 Hz, 1F), −161.60 (app td, J = 5.5, 20.8 Hz, 2F); IR (thin film, CH_2Cl_2) 3604, 3449, 3306, 3088, 2962, 2124, 1650, 1633, 1525, 1486 cm^{-1}; HRMS (CI) m/z calcd for $C_{15}H_3F_9O$ $[M]^+$ 370.0040, found 370.0281.

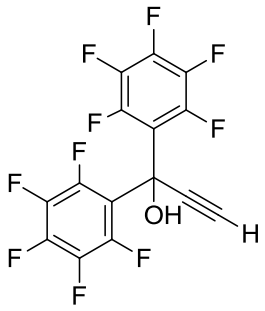

Compound **4.11b**: Following the same procedure as **4.11a** using **4.10b** (0.810 g, 1.76 mmol), **4.11b** was obtained as a tan-colored oil (0.450 g, 1.16 mmol, 66%) was obtained. ^{1}H NMR (300 MHz, $CDCl_3$) δ 2.99 (s, 1H), 3.60 (s, 1H); ^{19}F NMR (282 MHz, $CDCl_3$)

δ −140.54-−140.60 (m, 4F), −152.87-−153.05 (m, 2F), −161.25-−161.42 (m, 4F); IR (thin film, CH_2Cl_2) 3605, 3455, 3310, 2926, 2125, 1652, 1527, 1497 cm^{-1}; HRMS (EI) *m*/*z* calcd for $C_{15}H_2F_{10}O$ $[M]^+$ 387.9946, found 387.9939.

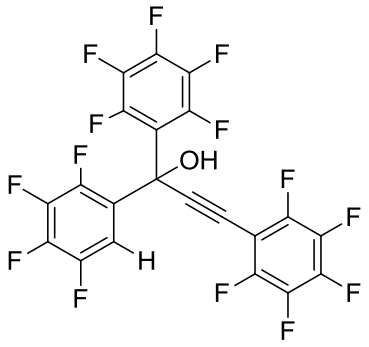

Propargyl alcohol **4.2a**: To a 100 mL round-bottom flask was added **4.11a** (2.41 g, 6.50 mmol, 1.0 equiv.), toluene (20.0 mL), pentafluoroiodobenzene (1.10 mL, 8.13 mmol, 1.3 equiv.), CuI (0.118 g, 0.618 mmol, 9.5 mol %), $Pd(PPh_3)_4$ (0.225 g, 0.195 mmol, 3 mol %), followed by Hünig's base (3.40 mL, 19.5 mmol, 3.0 equiv.). The reaction was heated to 70 °C under N_2 for 15 h, and then allowed to cool to room temperature, filtered through celite, concentrated onto celite and purified by column chromatography (3% ethyl acetate in hexanes) to provide **4.2a** as a brown oil (1.79 g, 3.33 mmol, 51%). R_f = 0.45 (5:1 hexanes:EtOAc); ^{1}H NMR (300 MHz, $CDCl_3$) δ 3.55 (s, 1H), 7.58-7.66 (m, 1H); ^{13}C NMR (125 MHz, $CDCl_3$)[3] δ 67.7 (s), 72.9 (s), 97.6 (m), 98.1 (dt, J_{C-F} = 3.8, 17.7 Hz), 108.9 (d, J_{C-F} = 22.0 Hz), 115.5-115.6 (m), 125.6 (app q, J_{C-F} = 5.3 Hz), 136.7-137.2 (m), 138.6-139.2 (m), 139.9-140.3 (m), 140.7 (app tt, J_{C-F} = 4.8, 13.1 Hz), 141.6 (app tt, J_{C-F} = 4.7, 13.4 Hz), 142.0-142.3 (m),

[3] Due to the high degree of splitting and resulting overlap between the signals, the J^1_{C-F} was not able to be resolved in all cases. The peaks and splitting patterns are reported as observed.

142.7 (app tt, $J_{C\text{-}F}$ = 4.9, 13.2 Hz), 143.6-143.9 (m), 144.1 (app dd, $J_{C\text{-}F}$ = 3.2, 11.5 Hz), 145.7-145.9 (m), 146.1 (app dd, $J_{C\text{-}F}$ = 3.1, 11.4 Hz), 146.6 (app dq, $J_{C\text{-}F}$ = 4.0, 12.0 Hz), 147.7 (app d, $J_{C\text{-}F}$ = 9.6 Hz), 148.6 (app dq, $J_{C\text{-}F}$ = 4.0, 12.1 Hz); ^{19}F NMR (282 MHz, $CDCl_3$) δ −136.01-−136.06 (m, 2F), −138.96 (ddd, J = 11.5, 11.5, 22.4 Hz, 1F), −140.31-−140.37 (m, 3F), −150.54 (app t, J = 20.8 Hz, 1F), −153.18 (app t, J = 21.2 Hz, 1F), −154.56 (app dtd, J = 4.0, 7.4, 19.9 Hz, 1F), −155.22 (t, J = 20.1 Hz, 1F), −161.76-−161.95 (m, 4F); IR (thin film, CH_2Cl_2) 3606, 3458, 3090, 2245, 1651, 1633, 1522, 1500 cm^{-1}; HRMS (EI) *m*/*z* calcd for $C_{21}H_2F_{14}O$ $[M]^+$ 536.2176, found 535.9873.

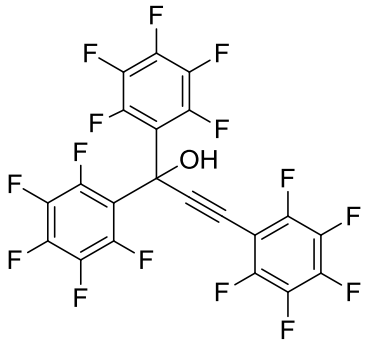

Propargyl alcohol **4.2b**: Following the same procedure as **4.2a** using **4.11b** (0.450 g, 1.16 mmol), **4.2b** was obtained as a tan-colored oil (0.145 g, 0.262 mmol, 23%). R_f = 0.65 (4:1 hexanes:EtOAc); ^{1}H NMR (300 MHz, $CDCl_3$) δ 3.80 (s, 1H); ^{19}F NMR (282 MHz, $CDCl_3$) δ −135.19-−135.25 (m, 2F), −140.44-−140.51 (m, 4F), −149.70-−149.85 (m, 1F), −152.13-−152.31 (m, 2F), −160.78-−160.98 (m, 4F), −160.02-−161.22 (m, 2F); IR (thin film, CH_2Cl_2) 3608, 3421, 2961, 2931, 2858, 2244, 1652, 1523, 1500 cm^{-1}; HRMS (ESI) *m*/*z* calcd for $C_{21}HF_{15}O$ $[M-H]^-$ 552.9715, found 552.9712.

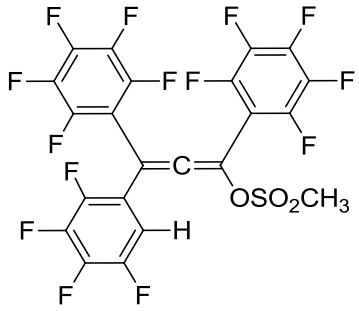

Allenyl mesylate **4.14a:** To a 10 mL round-bottom flask was added: **4.2a** (0.10 g, 0.19 mmol) and toluene (0.62 mL). The solution was cooled to 0 °C; triethylamine (39 μL, 0.28 mmol) and methanesulfonyl chloride (22 μL, 0.28 mmol) were added. Ice bath was removed. The reaction was allowed to warm to room temperature for 3.5 h, and then filtered through celite. The compound was loaded onto celite and purified by column chromatography (2:1 hexanes:CH_2Cl_2) to provide **4.14a** as a light yellow oil (0.10 g, 0.17 mmol, 91%). R_f = 0.41 (1:1 hexanes:CH_2Cl_2); ^{1}H NMR (300 MHz, $CDCl_3$) δ 3.22 (s, 3H), 7.08 (dddd, J = 2.5, 6.6, 7.8, 10.2 Hz, 1H); ^{13}C NMR (75 MHz, $CDCl_3$)[4] δ 39.0 (s), 106.0 (app dt, $J_{C\text{-}F}$ = 4.5, 15.4 Hz), 108.1 (app dt, $J_{C\text{-}F}$ = 3.5, 16.7 Hz), 111.1 (dd, $J_{C\text{-}F}$ = 2.3, 21.0 Hz), 113.7 (s), 116.6-116.9 (m), 136.0-136.4 (m), 139.4-140.0 (m), 140.2-141.2 (m), 142.5-143.4 (m), 143.6-144.7 (m), 145.6-145.7 (m), 145.9-146.2 (m), 147.5 (app dd, $J_{C\text{-}F}$ = 3.2, 12.3 Hz), 148.9-149.1 (m), 203.6 (s); ^{19}F NMR (282 MHz, $CDCl_3$) δ −137.68 (ddd, J = 10.3, 10.3, 21.0 Hz, 1F), −137.68 (app d, J = 18.2 Hz, 2F), −139.45 (br s, 1F), −140.25 (app d, J = 16.9 Hz, 2F), −149.76 (app t, J = 21.0 Hz, 1F), −151.04 (t, J = 21.0 Hz, 1F), −151.67 (tt, J = 6.6, 20.4 Hz, 1F), −153.96 (t, J = 19.7

[4] Not all signals may have been observed due to the low S/N ratio of the spectrum. Due to the high degree of splitting and resulting overlap between the signals, the $J^1_{C\text{-}F}$ was not able to be resolved in all cases. The peaks and splitting patterns are reported as observed.

Hz, 1F), −160.38-−160.66 (m, 4F); IR (thin film, CH_2Cl_2) 3044, 2946, 2849, 1962, 1653, 1627, 1524, 1503, 1448 cm^{-1}; HRMS (ESI) *m*/*z* calcd for $C_{22}H_4F_{14}O_3S$ $[M+Na]^+$ 636.9555, found 636.9570.

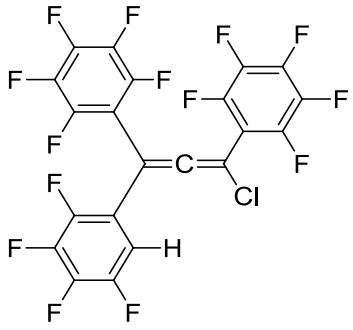

Chloroallene **4.3a**: To a 10 mL round-bottom flask was added **4.2a** (0.25 g, 0.47 mmol, 1 equiv.) and diethyl ether (0.47 mL) followed by pyridine (83 μL, 1.0 mmol, 2.2 equiv.). The solution was cooled to 0 °C; thionyl chloride (40 μL, 0.56 mmol, 1.2 equiv.) was added and stirred at 0 °C for 30 min. The ice bath was removed and the reaction stirred at room temperature for 30 min. The reaction mixture was treated with 1 M HCl (2 mL) and extracted with ethyl acetate (2 x 2 mL). The organic layer were combined, washed with brine (2 mL), dried over Na_2SO_4, filtered, and concentrated to give 0.22 g crude brown oil. The material was purified by column chromatography (100% hexanes) to provide **4.3a** as a colorless oil (0.11 g, 0.20 mmol, 44%). R_f = 0.40 (100% hexanes); ^{1}H NMR (300 MHz, $CDCl_3$) δ 6.78-6.87 (m, 1H); ^{13}C NMR (125 MHz, $CDCl_3$) δ 94.2 (s), 96.6 (s), 107.8 (app dt, J_{C-F} = 4.1, 16.7 Hz), 108.6 (app dt, J_{C-F} = 4.1, 16.7 Hz), 110.5 (dd, J_{C-F} = 2.7, 20.8 Hz), 116.6-116.8 (m), 136.8-137.2 (m), 138.8-139.2 (m), 140.1-140.5 (m), 141.2 (app dq, J_{C-F} = 4.9, 13.2 Hz), 141.5 (app dq, J_{C-F} = 4.8, 13.2 Hz), 142.4 (dddd, J_{C-F} = 3.9, 12.4, 12.4, 20.2 Hz), 143.1-143.7 (m), 145.3-145.6 (m), 145.8 (ddd, J_{C-F} = 3.1, 11.2, 252.8 Hz), 147.3 (ddd, J_{C-F} = 3.2, 10.4, 247.7 Hz), 207.7 (s); ^{19}F NMR (282 MHz, $CDCl_3$) δ −137.93 (ddd, *J* = 9.9, 9.9, 21.2 Hz, 1F), −138.88 (app d, *J* = 17.5 Hz, 2F), −138.98-−139.08 (m,

1F), −139.66 (app d, J = 15.7 Hz, 2F), −150.61 (app t, J = 20.8 Hz, 1F), −151.00 (app t, J = 20.8 Hz, 1F), −152.08 (tt, J = 6.4, 20.3 Hz, 1F), −153.67 (t, J = 19.8 Hz, 1F), −160.23-−160.68 (m, 4F); IR (thin film, CH_2Cl_2) 2917, 2849, 1959, 1652, 1626, 1522, 1488 cm^{-1}; HRMS (ESI) m/z calcd for $C_{21}H_4ClF_{14}$ $[M]^+$ 553.9543, found 553.9501.

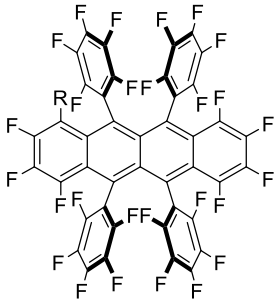

4.1 R = F
4.1H R = H

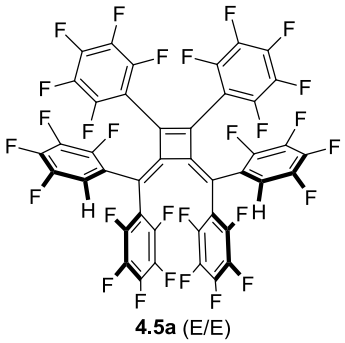

4.5a (E/E)

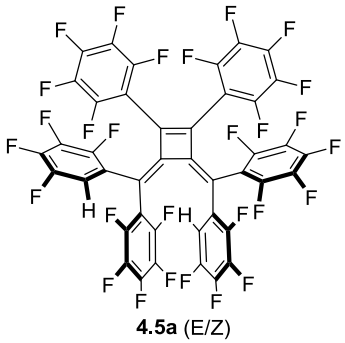

4.5a (E/Z)

Rubrene

4.1, **4.1H**, and cyclobutene **4.5a**: To a 10 mL 2 neck round-bottom flask was added **4.2a** (0.10 g, 0.19 mmol, 1.0 equiv.), toluene (0.62 mL), and triethylamine (0.039 mL, 0.28 mmol, 1.5 equiv.). The solution was cooled to 0 °C and methanesulfonyl chloride (0.022 mL, 0.28 mmol, 1.5 equiv.) was added. The reaction was stirred at 0 °C for 30 min, allowed to warm to room temperature and stirred for 30 minutes, then heated to 120 °C for 2 hours. The mixture was allowed to cool to room temperature, filtered through celite, and concentrated. The crude material was purified by preparative TLC (1:10 CH_2Cl_2:hexanes). Two fractions were isolated. Fraction 1 was a pink residue identified as a mixture of **4.1**and **4.1H**. Fraction 2 was a yellow residue identified as a mixture of diastereomers of **4.5a**. Diagnostic data[5] for the mixture of **4.1** and **4.1H**: ^{19}F NMR

[5] ^1H NMR was obtained and is included in Appendix 1; however, the low S/N of this spectrum prevented the assignment of peaks.

(470 MHz, $CDCl_3$)[6] δ −137.65-−137.74 (m, 1F), −138.11-−138.18 (m, 1F), −140.78 (d, *J* = 22.1 Hz, 3F), −140.89 (app d, *J* = 19.6 Hz, 2F), −149.74-−149.94 (m, 1F), −153.13 (d, *J* = 19.2 Hz, 1F), −153.74 (t, *J* = 20.3 Hz, 1F), −159.36-−159.25 (m, 3F), −160.16 (app dt, *J* = 6.5, 21.7 Hz, 3F) (peaks reported as observed); LRMS[7] (mixture of **4.1** and **4.1H**) (EI) *m*/*z* 1036.0 $(M)^+$, 1018.0 $(M - F + H)^+$. Diagnostic data for the two diastereomers of **4.5a**: ^1H NMR (500 MHz, $CDCl_3$) δ 6.86-690 (m, 2H), 6.96-7.00 (m, 2H); ^{19}F NMR (470 MHz, $CDCl_3$)[8] δ −135.38-−135.43 (m, 2F), −136.85-−136.93 (m, 4F), −137.75-−137.79 (m, 6F), −138.53-−138.57 (m, 8F), −139.11-−139.16 (m, 4F), −144.83-−144.92 (m, 2F), −145.35-−145.45 (m, 2F), −149.74 (t, *J* = 21.0 Hz, 2F), −150.28 (t, *J* = 20.7 Hz, 2F), −150.91-−151.04 (m, 4F), −152.79-−152.95 (m, 4F), −158.94-−159.19 (m, 8F), −159.54-−159.63 (m, 4F), −159.97-−160.07 (m, 4F); LRMS (EI) *m*/*z* 1038.0 $(M)^+$, 519.0 $(M - C_{21}HF_{14})^+$.

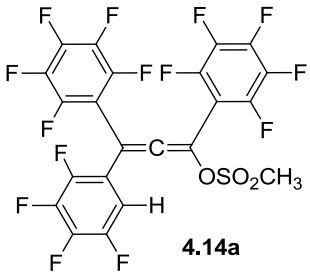

4.14a

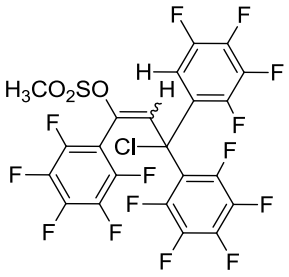

4.15a

Allenyl mesylate **4.14a** and compound **4.15a**: To a 10 mL 2 neck round-bottom flask was added **4.2a** (0.10 g, 0.19 mmol, 1.0 equiv.), toluene (0.62 mL), and triethylamine (0.039 mL, 0.28 mmol, 1.5 equiv.). The solution was

[6] Spectrum was unreferenced. Low S/N observed in the sample may impair the integral values; therefore, the integrals were reported as observed normalized to 1.
[7] (M)+ ion refers to $C_{42}F_{28}$ (1035.9553 g/mol).
[8] Spectrum was unreferenced.

cooled to 0 °C and methanesulfonyl chloride (0.022 mL, 0.28 mmol, 1.5 equiv.) was added. The reaction was then immediately heated to 120 °C for 3 hours. The mixture was allowed to cool to room temperature, filtered through celite, concentrated, and purified by preparative TLC (1:2 CH_2Cl_2:hexanes) to give a light yellow oil (0.0697 g) as a 1:1 mixture of **4.14a** and **4.15a**. Peaks corresponding to **4.14a** matched tabulated data above. Diagnostic data for **4.15a**: ^{1}H NMR (300 MHz, $CDCl_3$) δ 3.27 (s, 3H), 5.41 (s, 1H), 7.15-7.20 (m, 1H); ^{19}F NMR (282 MHz, $CDCl_3$)[9] δ −135.40-−135.45 (m, 1F), −135.62-−135.71 (m, 1F), −137.00 (dd, *J* = 11.8, 21.2 Hz, 1F), −139.61-−139.66 (m, 2F), −140.35-−140.42 (m, 1F), −146.15 (t, *J* = 20.9 Hz, 1F), −151.31 (t, *J* = 20.8 Hz, 1F), −153.80 (app dt, *J* = 3.3, 20.6 Hz, 1F), −154.03 (t, *J* = 20.0 Hz, 1F), −158.42 (app dt, *J* = 8.2, 22.1 Hz, 1F), −158.61 (app dt, *J* = 8.5, 21.7 Hz, 1F), −159.63-−159.89 (m, 2F)[10]; LRMS (EI) *m*/*z* 668.2 $(M + NH_4)^+$, 632.2 $(M + NH_4 - Cl)^+$, 519.1 $(M - C_3H_4SO_3Cl)^+$.

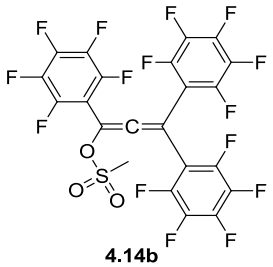

4.14b

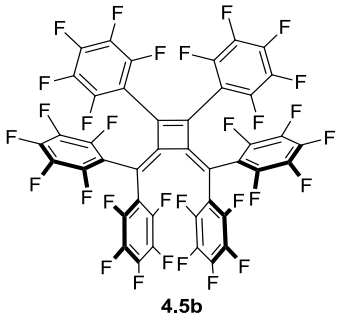

4.5b

Allenyl mesylate **4.14b** and cyclobutene **4.5b**: To a 10 mL 2 neck round-bottom flask was added **4.2b** (0.10 g, 0.18 mmol, 1.0 equiv.), toluene (0.55 mL). The solution was cooled to 0 °C then methanesulfonyl chloride (0.021 mL, 0.27 mmol, 1.5 equiv.) and triethylamine (0.050 mL, 0.36 mmol, 2.0 equiv.) were added. The

[9] Spectrum was unreferenced.
[10] Overlapped with **4.14a**.

reaction was stirred at 0 °C for 15 min, then allowed to warm to room temperature and stir for 15 minutes, followed by heating to 110 °C for 2 hours. The mixture was allowed to cool to room temperature, filtered through celite, concentrated then purified using column chromatography (2% ethyl acetate in hexanes) to afford **4.5b** as an amber oil (0.0067 g, 0.0062 mmol, 7%) and **4.14b** as a light orange oil (0.0744 g, 0.118 mmol, 65%). Diagnostic data for **4.5b**: R_f = 0.59 (20% ethyl acetate in hexanes); ^{19}F NMR (282 MHz, $CDCl_3$)[11] δ −139.86-−140.05 (m, 4F), −140.80 (d, *J* = 17.5 Hz, 2F), −141.20-−141.35 (m, 2F), −145.58 (app tt, *J* = 4.8, 20.9 Hz, 1F), −146.45 (app tt, *J* = 4.7, 20.7 Hz, 1F), −150.03 (t, *J* = 21.1 Hz, 1F), −151.52 (t, *J* = 20.7 Hz, 1F), −159.34-−159.65 (m, 3F), −160.12-−160.35 (m, 2F), −161.33-−161.53 (m, 1F); HRMS (EI) *m*/*z* calcd for $C_{42}F_{30}$ $[M]^+$ 1073.9521, found 1073.9486. Diagnostic data for **4.14b**[12]: R_f = 0.47 (20% ethyl acetate in hexanes); ^{1}H NMR (300 MHz, $CDCl_3$) δ 3.23 (s, 3H); ^{19}F NMR (282 MHz, $CDCl_3$) δ −139.29 (app d, *J* = 17.7 Hz, 2F), −141.19 (app d, *J* = 16.2 Hz, 4F), −149.50 (app tt, *J* = 3.8, 21.0 Hz, 2F), −150.96 (app t, *J* = 20.9 Hz, 4F), −160.44-−160.81 (m, 3F); IR (thin film, CH_2Cl_2) 3040, 2927, 2855, 1967, 1692, 1652 cm^{-1}; HRMS (ESI) *m*/*z* calcd for $C_{22}H_3F_{15}O_3S$ $[M+Na]^+$ 654.9456, found 654.9458.

[11] Sample contained unidentified and inseparable impurity. High intensity peaks reported; integrals reported as observed normalized to 1.
[12] Sample contained unidentified and inseparable impurity.

4.6 REFERENCES

(1) Facchetti, A. Semiconductors for organic transistors. *Mater. Today* **2007**, *10*, 28–37.

(2) Wang, C.; Dong, H.; Hu, W.; Liu, Y.; Zhu, D. Semiconducting π-Conjugated Systems in Field-Effect Transistors: A Material Odyssey of Organic Electronics. *Chem. Rev.* **2011**.

(3) Dodabalapur, A.; Katz, H. E.; Torsi, L.; Haddon, R. C. Organic Heterostructure Field-Effect Transistors. *Science* **1995**, *269*, 1560–1562.

(4) Dodabalapur, A.; Laquindanum, J.; Katz, H. E.; Bao, Z. Complementary circuits with organic transistors. *Appl. Phys. Lett.* **1996**, *69*, 4227–4229.

(5) Rost, C.; Gundlach, D. J.; Karg, S.; Rieß, W. Ambipolar organic field-effect transistor based on an organic heterostructure. *J. Appl. Phys.* **2004**, *95*, 5782–5787.

(6) Newman, C. R.; Frisbie, C. D.; da Silva Filho, D. A.; Bredas, J.-L.; Ewbank, P. C.; Mann, K. R. Introduction to Organic Thin Film Transistors and Design of n-Channel Organic Semiconductors. *Chem. Mater.* **2004**, *16*, 4436–4451.

(7) Usta, H.; Facchetti, A.; Marks, T. J. n-Channel Semiconductor Materials Design for Organic Complementary Circuits. *Accounts Chem. Res.* **2011**, *44*, 501–510.

(8) Mei, J.; Diao, Y.; Appleton, A. L.; Fang, L.; Bao, Z. Integrated Materials Design of Organic Semiconductors for Field-Effect Transistors. *J. Am. Chem. Soc.* **2013**, *135*, 6724–6746.

(9) Sakamoto, Y.; Suzuki, T.; Kobayashi, M.; Gao, Y.; Fukai, Y.; Inoue, Y.; Sato, F.; Tokito, S. Perfluoropentacene: High-Performance p−n Junctions and Complementary Circuits with Pentacene. *J. Am. Chem. Soc.* **2004**, *126*, 8138–8140.

(10) Heidenhain, S. B.; Sakamoto, Y.; Suzuki, T.; Miura, A.; Fujikawa, H.; Mori, T.; Tokito, S.; Taga, Y. Perfluorinated Oligo(p-Phenylene)s: Efficient n-Type Semiconductors for Organic Light-Emitting Diodes. *J. Am. Chem. Soc.* **2000**, *122*, 10240–10241.

(11) Liang, Z.; Tang, Q.; Liu, J.; Li, J.; Yan, F.; Miao, Q. N-Type Organic Semiconductors Based on π-Deficient Pentacenequinones: Synthesis, Electronic Structures, Molecular Packing, and Thin Film Transistors. *Chem. Mater.* **2010**, *22*, 6438–6443.

(12) Reddy, J. S.; Kale, T.; Balaji, G.; Chandrasekaran, A.; Thayumanavan, S. Cyclopentadithiophene-Based Organic Semiconductors: Effect of Fluorinated Substituents on Electrochemical and Charge Transport Properties. *J. Phys. Chem. Lett.* **2011**, *2*, 648–654.

(13) Delgado, M. C. R.; Pigg, K. R.; da Silva Filho, D. A.; Gruhn, N. E.; Sakamoto, Y.; Suzuki, T.; Osuna, R. M.; Casado, J.; Hernández, V.; Navarrete, J. T. L.; Martinelli, N. G.; Cornil, J.; Sánchez-Carrera, R. S.; Coropceanu, V.; Brédas, J.-L. Impact of Perfluorination on the Charge-Transport Parameters of Oligoacene Crystals. *J. Am. Chem. Soc.* **2009**, *131*, 1502–1512.

(14) Tang, M. L.; Bao, Z. Halogenated Materials as Organic Semiconductors†. *Chem. Mater.* **2011**, *23*, 446–455.

(15) Babudri, F.; Farinola, G. M.; Naso, F.; Ragni, R. Fluorinated organic materials for electronic and optoelectronic applications: the role of the fluorine atom. *Chem. Commun.* **2007**, 1003–1022.

(16) Anger, F.; Scholz, R.; Adamski, E.; Broch, K.; Gerlach, A.; Sakamoto, Y.; Suzuki, T.; Schreiber, F. Optical properties of fully and partially fluorinated rubrene in films and solution. *Appl. Phys. Lett.* **2013**, *102*, 013308.

(17) Moureu, C.; Dufraisse, C.; Dean, P. M. Chimie Organique. - Sur un hydrocarbure colore: le rubrene. *Comptes Rendus Hebd. Seances Acad. Sci.* **1926**, *182*, 1440–1443.

(18) Landor, P. D.; Landor, S. R. 503. Allenes. Part V. The reaction of aromatic tertiary acetylenic alcohols with thionyl chloride. *J. Chem. Soc. Resumed* **1963**, 2707–2711.

(19) Rigaudy, J.; Capdevielle, P. Dimerisation des polyphenyl-allenes—I : Chloropolyphenyl-allenes: mecanisme de la reaction "Rubrenique."*Tetrahedron.* **1977**, *33*, 767–773.

(20) Braga, D.; Jaafari, A.; Miozzo, L.; Moret, M.; Rizzato, S.; Papagni, A.; Yassar, A. The Rubrenic Synthesis: The Delicate Equilibrium between Tetracene and Cyclobutene. *Eur. J. Org. Chem.* **2011**, 4160–4169.

(21) Gajewski, J. J.; Shih, C. N. Tetramethylenethane. Degenerate thermal rearrangement of 1,2-dimethylenecyclobutane. *J. Am. Chem. Soc.* **1967**, *89*, 4532–4533.

(22) Gajewski, J. J.; Shih, C. N. Hydrocarbon thermal degenerate rearrangements. V. Stereochemistry of the 1,2-dimethylenecyclobutane self-interconversion and its relation to the allene dimerization and the rearrangements of other C6H8 isomers. *J. Am. Chem. Soc.* **1972**, *94*, 1675–1682.

(23) Zeis, R.; Besnard, C.; Siegrist, T.; Schlockermann, C.; Chi, X.; Kloc, C. Field Effect Studies on Rubrene and Impurities of Rubrene. *Chem. Mater.* **2006**, *18*, 244–248.

(24) Dolbier, W. R.; Burkholder, C. R. The [2 + 2] and [2 + 4] cycloadditions of fluorinated allenes. *J. Org. Chem.* **1984**, *49*, 2381–2386.

(25) Dolbier Jr., W. R.; Seabury, M. The effect of styrene α-substituents on the regiochemistry of [2+2] cycloadditions with difluoroallene. *Tetrahedron Lett.* **1987**, *28*, 1491–1492.

(26) Organ, M. G.; Avola, S.; Dubovyk, I.; Hadei, N.; Kantchev, E. A. B.; O'Brien, C. J.; Valente, C. A User-Friendly, All-Purpose Pd–NHC (NHC=N-Heterocyclic Carbene) Precatalyst for the Negishi Reaction: A Step Towards a Universal Cross-Coupling Catalyst. *Chem. – Eur. J.* **2006**, *12*, 4749–4755.

(27) Dolbier, W. R. *Guide to Fluorine NMR for Organic Chemists*; John Wiley & Sons, Inc: Hoboken, New Jersey, 2009.

(28) Myhre, P. C.; Edmonds, J. W.; Kruger, J. D. Long-Range Spin-Spin Coupling in Alkylfluorobenzenes. The Stereochemical Requirements for Coupling of Fluorine and Hydrogen Separated by Five Bonds1. *J. Am. Chem. Soc.* **1966**, *88*, 2459–2466.

(29) Begley, W. J.; Rajeswaran, M.; Andrievsky, N. Process for preparing triphenylnaphthacene compound. US 20060025642A1, February 2, 2006.

(30) Lam, Y.; Stanway, S. J.; Gouverneur, V. Recent progress in the use of fluoroorganic compounds in pericyclic reactions. *Tetrahedron* **2009**, *65*, 9905–9933.

(31) Kashiwabara, T.; Tanaka, M. Synthesis of 1,2-Diketones by the Transition Metal-Catalyst-Free Reaction of α-Oxo Acid Chlorides or Oxalyl Chloride with Organostannanes. *J. Org. Chem.* **2009**, *74*, 3958–3961.

(32) Prudchenko, A. T.; Vereshchagina, S. A.; Barkhash, V. A.; Vorozhtsov, N. N., Jr. Hydrazide of pentafluorobenzoic acid. *Zh. Obshch. Khim.* **1967**, *37*, 2195–2197.

(33) Steglich, W.; Buschmann, E.; Gansen, G.; Wilschowitz, L. Herstellung und Reaktionen von 2,5-Diphenyl-6-oxo-1,3,4-oxadiazin. *Synthesis.* **1977**, 252–253.

(34) Miao, Q.; Chi, X.; Xiao, S.; Zeis, R.; Lefenfeld, M.; Siegrist, T.; Steigerwald, M. L.; Nuckolls, C. Organization of Acenes with a Cruciform Assembly Motif. *J. Am. Chem. Soc.* **2006**, *128*, 1340–1345.

(35) Chun, D.; Cheng, Y.; Wudl, F. The Most Stable and Fully Characterized Functionalized Heptacene. *Angew. Chem. Int. Ed.* **2008**, *47*, 8380–8385.

(36) Furuya, T.; Ritter, T. Fluorination of Boronic Acids Mediated by Silver(I) Triflate. *Org. Lett.* **2009**, *11*, 2860–2863.

(37) Murphy, J. M.; Tzschucke, C. C.; Hartwig, J. F. One-Pot Synthesis of Arylboronic Acids and Aryl Trifluoroborates by Ir-Catalyzed Borylation of Arenes. *Org. Lett.* **2007**, *9*, 757–760.

(38) Kimoto, T.; Tanaka, K.; Sakai, Y.; Ohno, A.; Yoza, K.; Kobayashi, K. 2,8- and 2,9-Diboryltetracenes as Useful Building Blocks for Extended π-Conjugated Tetracenes. *Org. Lett.* **2009**, *11*, 3658–3661.

(39) Jenkins, C. M.; Pedler, A. E.; Tatlow, J. C. The electrochemical oxidation of polyfluoroaromatic amines—III : The synthesis of polyfluoroacridones. *Tetrahedron* **1971**, *27*, 2557–2560.

BIBLIOGRAPHY

Adam, Waldemar, O. Cueto, and F. Yany. “Cyclic Peroxides. 59. On the Mechanism of the Rubrene-enhanced Chemiluminescence of .alpha.-peroxylactones.” Journal of the American Chemical Society 100.8 (1978): 2587–2589. ACS Publications. Web. 24 July 2013.

Akopyan, R. L., A. I. Kitaigordskii, and Y. T. Struchkov. “Crystallographic Data on Some Sterically Strained Derivatives of Naphthacene.” Zhurnal Strukturnol Khimii 3 (1962): 602–605. Print.

Allen, C. F. H., and Lucius Gilman. “A Synthesis of Rubrene.” Journal of the American Chemical Society 58.6 (1936): 937–940. ACS Publications. Web. 1 Oct. 2009.

Awschalom, David D., and Michael E. Flatté. “Challenges for Semiconductor Spintronics.” Nature Physics 3.3 (2007): 153–159. www.nature.com.ezp1.lib.umn.edu. Web. 12 June 2013.

Balodis, K. A. et al. “Synthesis, Photooxidation and Mass Spectra of 5,6,11,12-tetrachlorotetracene.” Zhurnal Organicheskoi Khimii 21 (1985): 2423–2427. Print.

Begley, William J., Manju Rajeswaran, and Natasha Andrievsky. “Process for Preparing Triphenylnaphthacene Compound.” 2 Feb. 2006 : 1–10. Print.

Bergantin, Stefano, and Massimo Moret. “Rubrene Polymorphs and Derivatives: The Effect of Chemical Modification on the Crystal Structure.” Crystal Growth & Design 12.12 (2012): 6035–6041. ACS Publications. Web. 12 Dec. 2012.

Bhattacharya, Suman, and Binoy K. Saha. “Uniaxial Negative Thermal Expansion in an Organic Complex Caused by Sliding of Layers.” Crystal Growth & Design 12.10 (2012): 4716–4719. ACS Publications. Web. 7 May 2013.

Braga, Daniele et al. “The Rubrenic Synthesis: The Delicate Equilibrium Between Tetracene and Cyclobutene.” European Journal of Organic Chemistry 22 (2011): 4160–4169. onlinelibrary.wiley.com. Web. 6 Mar. 2012.

Braga, Daniele, and Gilles Horowitz. “High-Performance Organic Field-Effect Transistors.” Advanced Materials 21.14-15 (2009): 1473–1486. Wiley InterScience. Web. 22 Sept. 2009.

Brédas, J. L. et al. “Organic Semiconductors: A Theoretical Characterization of the Basic Parameters Governing Charge Transport.” Proceedings of the National Academy of Sciences 99.9 (2002): 5804–5809. www.pnas.org. Web. 5 June 2012.

Bulgarovskaya, I et al. “Growth, Structure and Optical Properties of Single Crystals of Rubrene.” Latvijas PSR Zinātņu akadēmijas vēstis. Fizikas un tehnisko zinātņu sērija 4 (1983): 53–59. Print.

Cicoira, Fabio, Carla M. Aguirre, and Richard Martel. “Making Contacts to n-Type Organic Transistors Using Carbon Nanotube Arrays.” ACS Nano 5.1 (2011): 283–290. ACS Publications. Web. 17 July 2013.

Corey, E. J., and P. L. Fuchs. “A Synthetic Method for Formyl - Ethynyl Conversion (RCHO - RCCH or RCCR’).” Tetrahedron Letters 13.36 (1972): 3769–3772. Print.

Cozzi, F., and J. S. Siegel. “Interaction Between Stacked Aryl Groups in 1,8-diarylnaphthalenes: Dominance of Polar/π over Charge-transfer Effects.” Pure and Applied Chemistry 67.5 (1995): 683–689. CrossRef. Web. 22 June 2012.

Cozzi, Franco, Mauro Cinquini, Rita Annuziata, et al. “Dominance of Polar/.pi. over Charge-transfer Effects in Stacked Phenyl Interactions.” Journal of the American Chemical Society 115.12 (1993): 5330–5331. ACS Publications. Web. 16 Feb. 2013.

Cozzi, Franco, Francesco Ponzini, et al. “Polar Interactions Between Stacked π Systems in Fluorinated 1,8-Diarylnaphthalenes: Importance of Quadrupole Moments in Molecular Recognition.” Angewandte Chemie International Edition in English 34.9 (1995): 1019–1020. Wiley Online Library. Web. 16 Feb. 2013.

Cozzi, Franco, Mauro Cinquini, Rita Annunziata, et al. “Polar/.pi. Interactions Between Stacked Aryls in 1,8-diarylnaphthalenes.” Journal of the American Chemical Society 114.14 (1992): 5729–5733. ACS Publications. Web. 16 Feb. 2013.

Curtis, M. David, Jie Cao, and Jeff W. Kampf. “Solid-State Packing of Conjugated Oligomers: From π-Stacks to the Herringbone Structure.” Journal of the American Chemical Society 126.13 (2004): 4318–4328. ACS Publications. Web.

De Boer, R. W. I. et al. “Organic Single-crystal Field-effect Transistors.” Phys. Status Solidi A 201.6 (2004): 1302–1331. onlinelibrary.wiley.com. Web. 29 May 2012.

Dediu, V. Alek et al. “Spin Routes in Organic Semiconductors.” Nature Materials 8.9 (2009): 707–716. www.nature.com.ezp2.lib.umn.edu. Web. 7 June 2013.

Ding, Huanjun, and Yongli Gao. “Electronic Structure at Rubrene Metal Interfaces.” Applied Physics A 95.1 (2009): 89–94. link.springer.com.ezp2.lib.umn.edu. Web. 10 June 2013.

Dodge, Jeffrey, J. D. Bain, and A. Richard Chamberlin. “Regioselective Synthesis of Substituted Rubrenes.” Journal of Organic Chemistry 55 (1990): 4190–4198. Print.

El Helou, Mira, Olaf Medenbach, and Gregor Witte. “Rubrene Microcrystals: A Route to Investigate Surface Morphology and Bulk Anisotropies of Organic Semiconductors.” Crystal Growth & Design 10.8 (2010): 3496–3501. ACS Publications. Web. 5 June 2013.

Fieser, Louis F. “Reduction Products of Naphthacenequinone.” Journal of the American Chemical Society 53.6 (1931): 2329–2341. ACS Publications. Web. 1 Oct. 2009.

Filho, D. A. da Silva, E.-G. Kim, and J.-L. Brédas. “Transport Properties in the Rubrene Crystal: Electronic Coupling and Vibrational Reorganization Energy.” Advanced Materials 17.8 (2005): 1072–1076. Wiley InterScience. Web. 15 Sept. 2009.

Fumagalli, Enrico et al. “Oxidation Dynamics of Epitaxial Rubrene Ultrathin Films.” Chemistry of Materials 23.13 (2011): 3246–3253. ACS Publications. Web. 5 June 2013.

Gabriel, Siegmund, and Ernst Leupold. “Transformation of Ethinediphthalide. I.” Berichte der Deutschen Chemischen Gesellschaft 31 (1897): 1159–1174. Print.

Gajewski, Joesph J., and Chung Nan Shih. “Hydrocarbon Thermal Degenerate Rearrangements. V. Stereochemistry of the 1,2-dimethylenecyclobutane Self-interconversion and Its Relation to the Allene Dimerization and the Rearrangements of Other C6H8 Isomers.” Journal of the American Chemical Society 94.5 (1972): 1675–1682. ACS Publications. Web. 3 Apr. 2013.

Gajewski, Joseph J., and Chung Nan. Shih. “Tetramethylenethane. Degenerate Thermal Rearrangement of 1,2-dimethylenecyclobutane.” Journal of the American Chemical Society 89.17 (1967): 4532–4533. ACS Publications. Web.

Garnier, Francis. “Thin-film Transistors Based on Organic Conjugated Semiconductors.” Chemical Physics 227.1-2 (1998): 253–262. ScienceDirect. Web. 22 Sept. 2009.

Gershenson, M. E., V. Podzorov, and A. F. Morpurgo. “Colloquium: Electronic Transport in Single-crystal Organic Transistors.” Reviews of Modern Physics 78.3 (2006): 973–989. APS. Web. 16 Mar. 2012.

Greene, Allison K., and Lawrence T. Scott. “Rapid, Microwave-Assisted Perdeuteration of Polycyclic Aromatic Hydrocarbons.” The Journal of Organic Chemistry 78.5 (2013): 2139–2143. ACS Publications. Web. 6 Sept. 2013.

---. “Rapid, Microwave-Assisted Perdeuteration of Polycyclic Aromatic Hydrocarbons.” The Journal of Organic Chemistry (2012): n. pag. ACS Publications. Web. 18 Dec. 2012.

Gwinner, Michael C. et al. “Enhanced Ambipolar Charge Injection with Semiconducting Polymer/Carbon Nanotube Thin Films for Light-Emitting Transistors.” ACS Nano 6.1 (2012): 539–548. ACS Publications. Web. 17 July 2013.

Haas, S. et al. “High Charge-carrier Mobility and Low Trap Density in a Rubrene Derivative.” Physical Review B (Condensed Matter and Materials Physics) 76.11 (2007): 115203–6. Scitation. Web. 23 Sept. 2009.

Henn, D. E., W. G. Williams, and D. J. Gibbons. “Crystallographic Data for an Orthorhombic Form of Rubrene.” Journal of Applied Crystallography 4.3 (1971): 256–256. CrossRef. Web. 17 Jan. 2012.

Hercules, David M. “Chemiluminescence Resulting from Electrochemically Generated Species.” Science 145.3634 (1964): 808–809. JSTOR. Web. 24 July 2013.

Horowitz, Gilles. “Organic Transistors.” Organic Electronics, Materials, Manufacturing and Applications. Weinheim: Wiley-VCH Verlag GmbH & Co. KGaA, 2006. 3–32. Print.

Hoye, Thomas R., Brian M. Eklov, and Mikhail Voloshin. “No-D NMR Spectroscopy as a Convenient Method for Titering Organolithium (RLi), RMgX, and LDA Solutions.” Organic Letters 6.15 (2004): 2567–2570. ACS Publications. Web. 21 June 2013.

Huang, Liwei et al. “Rubrene Micro-crystals from Solution Routes: Their Crystallography, Morphology and Optical Properties.” Journal of Materials Chemistry 20.1 (2009): 159–166. pubs.rsc.org. Web. 5 June 2013.

Jiang, Hui, and Christian Kloc. “Single-crystal Growth of Organic Semiconductors.” MRS Bulletin 38.01 (2013): 28–33. Cambridge Journals Online. Web.

Jurchescu, O. D., A. Meetsma, and T. T. M. Palstra. “Low-temperature Structure of Rubrene Single Crystals Grown by Vapor Transport.” Acta Crystallographica, Section B B62 (2006): 330–334. Print.

Kang, Narae, Biddut K. Sarker, and Saiful I. Khondaker. “The Effect of Carbon Nanotube/organic Semiconductor Interfacial Area on the Performance of Organic Transistors.” Applied Physics Letters 101.23 (2012): 233302. AIP. Web. 17 July 2013.

Kim, Kihyun et al. “New Growth Method of Rubrene Single Crystal for Organic Field-effect Transistor.” Synthetic Metals 157.10–12 (2007): 481–484. ScienceDirect. Web. 28 May 2013.

Kytka, M. et al. “Real-time Observation of Oxidation and Photo-oxidation of Rubrene Thin Films by Spectroscopic Ellipsometry.” Applied Physics Letters 90.13 (2007): 131911. AIP. Web. 5 June 2013.

Lam, Yu-hong, Steven J. Stanway, and Véronique Gouverneur. “Recent Progress in the Use of Fluoroorganic Compounds in Pericyclic Reactions.” Tetrahedron 65.48 (2009): 9905–9933. ScienceDirect. Web. 29 July 2013.

Landor, Phyllis D., and S. R. Landor. “503. Allenes. Part V. The Reaction of Aromatic Tertiary Acetylenic Alcohols with Thionyl Chloride.” Journal of the Chemical Society (Resumed) 0 (1963): 2707–2711. pubs.rsc.org. Web. 13 July 2013.

Larena, A, and J Martinez-Urreaga. “The Rubrene Character in Chemiluminescent Reactions Studied by V-UV Absorption Spectroscopy.” Spectroscopy Letters 18.6 (1985): 463–472. Print.

Laudise, R.A et al. “Physical Vapor Growth of Organic Semiconductors.” Journal of Crystal Growth 187.3–4 (1998): 449–454. ScienceDirect. Web. 14 Sept. 2012.

Lewis, Frederick D. et al. “Competitive 1,2- and 1,5-Hydrogen Shifts Following 2-Vinylbiphenyl Photocyclization.” Journal of Organic Chemistry 70.25 (2005): 10447–10452.

Li, Hu et al. “Synthesis of Fluorenone Derivatives through Pd-Catalyzed Dehydrogenative Cyclization.” Organic Letters 14.18 (2012): 4850–4853. ACS Publications. Web. 22 Feb. 2013.

Machida, Shin-ichi et al. “Highest-Occupied-Molecular-Orbital Band Dispersion of Rubrene Single Crystals as Observed by Angle-Resolved Ultraviolet Photoelectron Spectroscopy.” Physical Review Letters 104.15 (2010): 156401. APS. Web. 28 Oct. 2012.

Mas-Torrent, Marta, and Concepció Rovira. “Role of Molecular Order and Solid-State Structure in Organic Field-Effect Transistors.” Chemical Reviews 111.8 (2011): 4833–4856. ACS Publications. Web.

McGarry, Kathryn A. et al. “Rubrene-Based Single-Crystal Organic Semiconductors: Synthesis, Electronic Structure, and Charge-Transport Properties.” Chemistry of Materials (2013): n. pag. ACS Publications. Web. 6 June 2013.

Menard, E. et al. “High-Performance N- and p-Type Single-Crystal Organic Transistors with Free-Space Gate Dielectrics.” Advanced Materials 16.23-24 (2004): 2097–2101. Wiley Online Library. Web. 6 June 2012.

Minder, Nikolas A. et al. “Band-Like Electron Transport in Organic Transistors and Implication of the Molecular Structure for Performance Optimization.” Advanced Materials 24.4 (2012): 503–508. onlinelibrary.wiley.com. Web. 27 May 2012.

Miyaura, N., T. Yanagi, and A. Suzuki. “The Palladium-Catalyzed Cross-Coupling Reaction of Phenylboronic Acid with Haloarenes in the Presence of Bases.” Synthetic Communications 11.7 (1981): 513–519. Taylor and Francis+NEJM. Web. 8 Aug. 2013.

Miyaura, Norio, and Akira Suzuki. “Stereoselective Synthesis of Arylated (E)-alkenes by the Reaction of Alk-1-enylboranes with Aryl Halides in the Presence of Palladium Catalyst.” Journal of the Chemical Society, Chemical Communications 19 (1979): 866–867. pubs.rsc.org. Web. 8 Aug. 2013.

Miyaura, Norio, Kinji Yamada, and Akira Suzuki. “A New Stereospecific Cross-coupling by the Palladium-catalyzed Reaction of 1-alkenylboranes with 1-alkenyl or 1-alkynyl Halides.” Tetrahedron Letters 20.36 (1979): 3437–3440. ScienceDirect. Web. 8 Aug. 2013.

Moureu, C., C. Dufraisse, and P. M. Dean. “Chimie Organique. - Sur Un Hydrocarbure Colore: Le Rubrene.” Comptes rendus hebdomadaires des seances de l’Academie des sciences 182 (1926): 1440–1443. Print.

Naber, W. J. M., S. Faez, and W. G. van der Wiel. “Organic Spintronics.” Journal of Physics D: Applied Physics 40.12 (2007): R205. Institute of Physics. Web. 11 June 2013.

Nakayama, Yasuo, Shinichi Machida, et al. “Direct Observation of the Electronic States of Single Crystalline Rubrene Under Ambient Condition by Photoelectron Yield Spectroscopy.” Applied Physics Letters 93.17 (2008): 173305. AIP. Web. 11 June 2013.

Nakayama, Yasuo, Yuki Uragami, et al. “Full Picture of Valence Band Structure of Rubrene Single Crystals Probed by Angle-Resolved and Excitation-Energy-Dependent Photoelectron Spectroscopy.” Applied Physics Express 5.11 (2012): 111601. Institute of Pure and Applied Physics. Web. 11 June 2013.

Nathanson, F. “Intramolecular Change of Phthalides into Derivatives of Alpha,gamma-diketohydrindene.” Berichte der Deutschen Chemischen Gesellschaft 26 (1893): 2576–2582. Print.

Newman, Christopher R. et al. “Introduction to Organic Thin Film Transistors and Design of n-Channel Organic Semiconductors.” Chemistry of Materials 16.23 (2004): 4436–4451. ACS Publications. Web. 19 Sept. 2009.

Nguyen, Tho D. et al. “Isotope Effect in Spin Response of Π-conjugated Polymer Films and Devices.” Nature Materials 9.4 (2010): 345–352. www.nature.com.ezp2.lib.umn.edu. Web. 7 June 2013.

Oatis, John E. et al. “Synthesis of 4’-hydroxypropranolol Sulfate, a Major Non-.beta.-blocking Propranolol Metabolite in Man.” Journal of Medicinal Chemistry 28.6 (1985): 822–824. ACS Publications. Web. 8 Aug. 2013.

Ogata, Akitoshi et al. “Titanocene(II)-Promoted Stereoselective Alkenylation Utilizing (Z)-Alkenyl Sulfones.” The Journal of Organic Chemistry 72.10 (2007): 3816–3822. ACS Publications. Web. 11 June 2013.

Omer, Khalid M., and Allen J Bard. “Electrogenerated Chemiluminescence of Aromatic Hydrocarbon Nanoparticles in an Aqueous Solution†.” The Journal of Physical Chemistry C 113.27 (2009): 11575–11578. ACS Publications. Web. 5 June 2013.

Paraskar, Abhimanyu S. et al. “Rubrenes: Planar and Twisted.” Chemistry – A European Journal 14.34 (2008): 10639–10647. Wiley Online Library. Web. 11 May 2013.

Peña-López, Miguel et al. “Palladium-Catalyzed Cross-Coupling Reactions of Organogold(I) Reagents with Organic Electrophiles.” Chemistry – A European Journal 16.32 (2010): 9905–9909. Wiley Online Library. Web. 11 June 2013.

Peng, Zhonghua, Ali R. Gharavi, and Luping Yu. “Synthesis and Characterization of Photorefractive Polymers Containing Transition Metal Complexes as Photosensitizer.” Journal of the American Chemical Society 119.20 (1997): 4622–4632. ACS Publications. Web. 21 June 2013.

Perez, M. Dolores et al. “Molecular and Morphological Influences on the Open Circuit Voltages of Organic Photovoltaic Devices.” Journal of the American Chemical Society 131.26 (2009): 9281–9286. ACS Publications. Web. 6 June 2013.

Podzorov, V., E. Menard, J. A. Rogers, et al. “Hall Effect in the Accumulation Layers on the Surface of Organic Semiconductors.” Physical Review Letters 95.22 (2005): 226601. APS. Web. 28 Oct. 2012.

Podzorov, V., E. Menard, A. Borissov, et al. “Intrinsic Charge Transport on the Surface of Organic Semiconductors.” Physical Review Letters 93.8 (2004): 086602. PROLA. Web. 23 Sept. 2009.

Podzorov, V., V. M. Pudalov, and M. E. Gershenson. “Field-effect Transistors on Rubrene Single Crystals with Parylene Gate Insulator.” Applied Physics Letters 82.11 (2003): 1739–1741. AIP. Web. 25 May 2013.

Rauhut, M. M., B. G. Roberts, and A. M. Semsel. “A Study of Chemiluminescence from Reactions of Oxalyl Chloride, Hydrogen Peroxide, and Fluorescent Compounds1.” Journal of the American Chemical Society 88.15 (1966): 3604–3617. ACS Publications. Web. 24 July 2013.

Reese, Colin, and Zhenan Bao. “Organic Single-crystal Field-effect Transistors.” Materials Today 10.3 (2007): 20–27. ScienceDirect. Web. 16 Jan. 2012.

Ren, Z. Q. et al. “Molecular Motion and Mobility in an Organic Single Crystal: Raman Study and Model.” Physical Review B 80.24 (2009): 245211. APS. Web. 6 June 2013.

Rigaudy, J., and P. Capdevielle. “Dimerisation Des polyphenyl-allenes—I : Chloropolyphenyl-allenes: Mecanisme de La Reaction ‘Rubrenique’.” Tetrahedron 33.7 (1977): 767–773. ScienceDirect. Web. 6 Mar. 2012.

Rodríguez-López, Joaquín et al. “Scanning Electrochemical Microscopy Study of Ion Annihilation Electrogenerated Chemiluminescence of Rubrene and [Ru(bpy)3]2+.” Journal of the American Chemical Society 134.22 (2012): 9240–9250. ACS Publications. Web. 5 June 2013.

Ruden, P. P., and D. L. Smith. “Theory of Spin Injection into Conjugated Organic Semiconductors.” Journal of Applied Physics 95.9 (2004): 4898–4904. AIP. Web. 11 June 2013.

Sakamoto, Gosuke et al. “Significant Improvement of Device Durability in Organic Light-emitting Diodes by Doping Both Hole Transport and Emitter Layers with Rubrene Molecules.” Applied Physics Letters 75.6 (1999): 766–768. AIP. Web. 7 June 2013.

Sanvito, Stefano. “Organic Spintronics: Filtering Spins with Molecules.” Nature Materials 10.7 (2011): 484–485. www.nature.com.ezp1.lib.umn.edu. Web. 11 June 2013.

Sartori, Giovanni et al. “Metal Template Ortho-acylation of Phenols; A New General Approach to Anthracyclinones.” Tetrahedron Letters 28.14 (1987): 1533–1536. ScienceDirect. Web. 19 June 2013.

Schmidt, R., and H.-D. Brauer. “Comparison of the Photochemical and Thermal Rearrangement Reaction of Endoperoxides.” Journal of Photochemistry 34.1 (1986): 1–12. ScienceDirect. Web. 6 July 2013.

Schuck, Götz, Simon Haas, Arno F. Stassen, Ulrich Berens, et al. “5,11-Bis(4-tert-butylphenyl)-6,12-diphenylnaphthacene (form A).” Acta Crystallographica Section E Structure Reports Online E63.6 (2007): o2894. CrossRef. Web. 12 Dec. 2012.

Schuck, Götz, Simon Haas, Arno F. Stassen, Hans-Jörg Kirner, et al. “5,12-Bis(4-tert-butylphenyl)-6,11-diphenylnaphthacene.” Acta Crystallographica Section E Structure Reports Online E63.6 (2007): o2893. CrossRef. Web. 12 Dec. 2012.

Shim, J. H. et al. “Large Spin Diffusion Length in an Amorphous Organic Semiconductor.” Physical Review Letters 100.22 (2008): 226603. APS. Web. 12 June 2013.

Snelders, Dennis J. M et al. “Fast Suzuki–Miyaura Cross-Coupling Reaction with Hexacationic Triarylphosphine Bn-Dendriphos as Ligand.” Advanced Synthesis & Catalysis 350.2 (2008): 262–266. onlinelibrary.wiley.com. Web. 7 Mar. 2012.

Sundar, Vikram C. et al. “Elastomeric Transistor Stamps: Reversible Probing of ChargeTransport in Organic Crystals.” Science 303.5664 (2004): 1644–1646. EBSCOhost. Web. 15 Sept. 2009.

Taima, Tetsuya et al. “Doping Effects for Organic Photovoltaic Cells Based on Small-molecular-weight Semiconductors.” Solar Energy Materials and Solar Cells 93.6–7 (2009): 742–745. ScienceDirect. Web. 6 June 2013.

Taylor, W. H. “X-Ray Measurements on Diflavylene, Rubrene, and Related Compounds.” Zeitschrift fur Kristallographie, Kristallgeometrie, Kristallphysik, Kristallchemie 93 (1936): 151. Print.

Thalladi, Venkat R. et al. “C−H•••F Interactions in the Crystal Structures of Some Fluorobenzenes.” Journal of the American Chemical Society 120.34 (1998): 8702–8710. ACS Publications. Web. 16 Feb. 2013.

Uttiya, Sureeporn et al. “Stability to Photo-oxidation of Rubrene and Fluorine-substituted Rubrene.” Synthetic Metals 161.23–24 (2012): 2603–2606. ScienceDirect. Web. 28 Oct. 2012.

Vinyard, David J., Shujun Su, and Mark M. Richter. “Electrogenerated Chemiluminescence of 9,10-Diphenylanthracene, Rubrene, and Anthracene in Fluorinated Aromatic Solvents.” The Journal of Physical Chemistry A 112.37 (2008): 8529–8533. ACS Publications. Web. 5 June 2013.

Wang, Chengliang et al. “Semiconducting π-Conjugated Systems in Field-Effect Transistors: A Material Odyssey of Organic Electronics.” Chemical Reviews (2011): n. pag. ACS Publications. Web.

Wilson, Therese. “Fluorescence of Rubrene Excited by Energy Transfer from Singlet Oxygen. Temperature Dependence and Competition with Oxidation.” Journal of the American Chemical Society 91.9 (1969): 2387–2388. ACS Publications. Web. 7 June 2013.

Wittig, G., and D. Waldi. “Uber Eine Vereinfachte Darstellung von Rubren.” Journal fur praktische Chemie 160 (1942): 242–244. Print.

Xie, Wei, Kathryn A. McGarry, et al. “High-Mobility Transistors Based on Single Crystals of Isotopically Substituted Rubrene-d28.” The Journal of Physical Chemistry C 117.22 (2013): 11522–11529. ACS Publications. Web. 6 June 2013.

Xie, Wei, Pradyumna L. Prabhumirashi, et al. “Use of Carbon Nanotube Electrodes to Improve Charge Injection and Transport in Ambipolar Rubrene-Based Single Crystal Transistors.” ACS Nano submitted for publication (2013): n. pag. Print.

Xue, Qin et al. “White Organic Light-emitting Devices with a Bipolar Transport Layer Between Blue Fluorescent and Yellow Phosphor-sensitized-fluorescent Emitting Layers.” Synthetic Metals 160.7–8 (2010): 829–831. ScienceDirect. Web. 7 June 2013.

Yagodkin, Elisey. “Electrical Properties and Synthesis of Tetracene and Rubrene Derivatives.” Ph.D. University of Minnesota, 2010. Print.

---. “Synthesis, Solid State Properties, and Semiconductor Measurements of 5,6,11,12-Tetrachlorotetracene.” The Journal of Physical Chemistry C 113.37 (2009): 16544–16548. CrossRef. Web. 9 Aug. 2013.

Yagodkin, Elisey, Kathryn A. McGarry, and Christopher J. Douglas. “Preparation of 6,11-Dihydroxy-5,12-tetracenedione.” Organic Preparations and Procedures International 43.4 (2011): 360–363. Taylor&Francis. Web.

Yee, W. Atom et al. “Quenching of the Fluorescent State of Rubrene Directly to the Ground State.” Journal of the American Chemical Society 101.17 (1979): 5104–5106. ACS Publications. Web. 7 June 2013.

Yu, Zhi-Gang. “Spin-orbit Coupling, Spin Relaxation, and Spin Diffusion in Organic Solids.” Proceedings of SPIE 8333.Photonics and Optoelectronics Meetings (POEM) 2011: Optoelectronic Devices and Integration (2011): 83331A. Silverchair. Web. 12 June 2013.

Zeis, Roswitha et al. “Field Effect Studies on Rubrene and Impurities of Rubrene.” Chemistry of Materials 18.2 (2006): 244–248. ACS Publications. Web. 23 Sept. 2009.

Zhang, Yadong, and Jianxun Wen. “A Convenient Synthesis of Bis(polyfluorophenyl)butadiyne Monomers.” Synthesis 8 (1990): 727–728. Print.

Zheng, Chong, Heike Hofstetter, and Oliver Hofstetter. “Charge Density and Computational Study of Benzhydrol and Benzhydrol-d10.” Journal of Molecular Structure 875.1–3 (2008): 173–182. ScienceDirect. Web. 26 Feb. 2013.

Zhi-lin, Zhang et al. “The Effect of Rubrene as a Dopant on the Efficiency and Stability of Organic Thin Film Electroluminescent Devices.” Journal of Physics D: Applied Physics 31.1 (1998): 32. Institute of Physics. Web. 7 June 2013.

APPENDIX 1. CRYSTAL STRUCTURE REPORTS

The following crystal data collections and structure solutions were conducted at the X-Ray Crystallographic Laboratory, S146 Kolthoff Hall, Department of Chemistry, University of Minnesota. All crystals were grown by solution unless otherwise noted. All calculations were performed using Pentium computers using the current SHELXTL suite of programs. All publications arising from this report MUST either 1) include Kathryn A. McGarry as a coauthor or 2) acknowledge Kathryn A. McGarry, Victor G. Young, Jr., and the X-Ray Crystallographic Laboratory.

Some equations of interest:

$$R_{int} = \Sigma |F_o^2 - < F_o^2 >| / \Sigma |F_o^2|$$

$$R_1 = \Sigma ||F_o| - |F_c|| / \Sigma |F_o|$$

$$wR2 = [\Sigma [w(F_o^2 - F_c^2)^2] / \Sigma [w(F_o^2)^2]]^{1/2}$$

where $w = q / [\sigma^2 (F_o^2) + (a*P)^2 + b*P + d + e*\sin(\theta)]$

$$\text{GooF} = S = [\Sigma [w(F_o^2 - F_c^2)^2] / (n-p)]^{1/2}$$

A1.1. CHAPTER 2 CRYSTAL STRUCTURES

Crystal Structure Report for **1.1** at 100 K (project code: 13069)

Data collection: A crystal (approximate dimensions 0.20 x 0.16 x 0.04 mm^3) was placed onto the tip of a 0.1 mm diameter glass capillary and mounted on a Bruker Photon CCD diffractometer for a data collection at 100(2) K.[1] A preliminary set of cell constants was calculated from reflections harvested from three sets of 12 frames. These initial sets of frames were oriented such that orthogonal wedges of reciprocal space were surveyed. This produced initial orientation matrices determined from 112 reflections. The data collection was carried out using MoKα radiation (graphite monochromator) with a frame time of 60 seconds and a detector distance of 6.0 cm. A randomly oriented region of reciprocal space was surveyed to the extent of one sphere and to a resolution of 0.77 Å. Four major sections of frames were collected with 0.30º steps in ω at four different ϕ settings and a detector position of -28º in 2θ. The intensity data were corrected for absorption and decay (SADABS).[2] Final cell constants were calculated from the xyz centroids of 2976 strong reflections from the actual data collection after integration (SAINT).[3] Please refer to Table 1 for additional crystal and refinement information.

Structure solution and refinement: The structure was solved using SHELXS-97 (Sheldrick, 1990)[4] and refined using SHELXL-97 (Sheldrick, 1997).[4] The space group Cmca was determined based on systematic absences and intensity statistics. A direct-methods solution was calculated which provided most non-hydrogen atoms from the E-map. Full-matrix least squares / difference Fourier cycles were performed which located the remaining non-hydrogen atoms. All non-hydrogen atoms were refined with anisotropic displacement parameters. All hydrogen atoms were placed in ideal positions and refined as riding atoms with relative isotropic displacement parameters. The final full matrix least squares refinement converged to $R1 = 0.0342$ and $wR2 = 0.0955$ (F^2, all data).

Table A0.1. Atomic coordinates (x 10^4) and equivalent isotropic displacement parameters ($Å^2$x 10^3) for **1.1** at 100 K. Ueq is defined as one third of the trace of the orthogonalized Uij tensor.

Atom	x	y	z	Ueq
C1	265(1)	-895(2)	6754(1)	20(1)
C2	519(1)	525(2)	6341(1)	18(1)
C3	269(1)	2043(1)	5876(1)	16(1)

C4	532(1)	3556(1)	5490(1)	16(1)
C5	274(1)	5000	5000	15(1)
C6	1077(1)	3654(1)	5728(1)	16(1)
C7	1230(1)	4764(2)	6481(1)	20(1)
C8	1722(1)	4751(2)	6786(1)	25(1)
C9	2069(1)	3609(2)	6345(1)	25(1)
C10	1920(1)	2489(2)	5600(1)	23(1)
C11	1429(1)	2517(2)	5290(1)	19(1)

Table A0.2. Bond lengths (Å) and angles (°) for **1.1** at 100 K.

Atoms	Length	Atoms	Angle	Atoms	Angle
C(1)-C(2)	1.3571(16)	C(2)-C(1)-C(1)#1	120.09(6)	C(9)-C(8)-H(4)	120
C(1)-C(1)#1	1.419(2)	C(2)-C(1)-H(1)	120	C(7)-C(8)-H(4)	120
C(1)-H(1)	0.95	C(1)#1-C(1)-H(1)	120	C(10)-C(9)-C(8)	119.47(10)
C(2)-C(3)	1.4372(15)	C(1)-C(2)-C(3)	122.16(10)	C(10)-C(9)-H(5)	120.3
C(2)-H(2)	0.95	C(1)-C(2)-H(2)	118.9	C(8)-C(9)-H(5)	120.3
C(3)-C(4)	1.4029(14)	C(3)-C(2)-H(2)	118.9	C(11)-C(10)-C(9)	120.48(11)
C(3)-C(3)#1	1.443(2)	C(4)-C(3)-C(2)	122.03(10)	C(11)-C(10)-H(6)	119.8
C(4)-C(5)	1.4256(12)	C(4)-C(3)-C(3)#1	120.08(6)	C(9)-C(10)-H(6)	119.8
C(4)-C(6)	1.5006(14)	C(2)-C(3)-C(3)#1	117.73(6)	C(10)-C(11)-C(6)	120.60(11)
C(5)-C(4)#2	1.4256(12)	C(3)-C(4)-C(5)	120.52(10)	C(10)-C(11)-H(7)	119.7
C(5)-C(5)#3	1.466(3)	C(3)-C(4)-C(6)	115.84(9)	C(6)-C(11)-H(7)	119.7
C(6)-C(11)	1.3929(15)	C(5)-C(4)-C(6)	123.24(9)		
C(6)-C(7)	1.3936(15)	C(4)#2-C(5)-C(4)	121.98(13)		
C(7)-C(8)	1.3886(15)	C(4)#2-C(5)-C(5)#3	119.01(6)		
C(7)-H(3)	0.95	C(4)-C(5)-C(5)#3	119.01(7)		
C(8)-C(9)	1.3880(17)	C(11)-C(6)-C(7)	118.53(10)		
C(8)-H(4)	0.95	C(11)-C(6)-C(4)	122.09(9)		
C(9)-C(10)	1.3875(17)	C(7)-C(6)-C(4)	119.00(9)		
C(9)-H(5)	0.95	C(8)-C(7)-C(6)	120.95(10)		
C(10)-C(11)	1.3859(15)	C(8)-C(7)-H(3)	119.5		
C(10)-H(6)	0.95	C(6)-C(7)-H(3)	119.5		
C(11)-H(7)	0.95	C(9)-C(8)-C(7)	119.97(11)		

Symmetry transformations used to generate equivalent atoms: #1 -x,y,z #2 x,-y+1,-z+1 #3 -x,-y+1,-z+1

Table A0.3. Anisotropic displacement parameters ($Å^2$ x 10^3) for **1.1** at 100 K. The anisotropic displacement factor exponent takes the form: $-2\pi^2[h^2 a^{*2}U11 + ... + 2 h k a^* b^* U12]$.

Atom	U11	U22	U33	U23	U13	U12
C1	27(1)	16(1)	16(1)	1(1)	0(1)	4(1)

C2	20(1)	19(1)	16(1)	-1(1)	0(1)	4(1)
C3	20(1)	15(1)	11(1)	-2(1)	0(1)	1(1)
C4	18(1)	16(1)	12(1)	-2(1)	1(1)	1(1)
C5	17(1)	14(1)	13(1)	-2(1)	0	0
C6	18(1)	16(1)	15(1)	5(1)	0(1)	0(1)
C7	22(1)	22(1)	16(1)	1(1)	0(1)	2(1)
C8	25(1)	30(1)	19(1)	1(1)	-5(1)	-4(1)
C9	16(1)	33(1)	27(1)	8(1)	-3(1)	-1(1)
C10	19(1)	22(1)	29(1)	4(1)	5(1)	3(1)
C11	20(1)	17(1)	20(1)	2(1)	2(1)	0(1)

Table A0.4. Hydrogen coordinates (x 104) and isotropic displacement parameters (a2 x 103) for **1.1** at 100 K.

Atom	x	y	z	U(eq)
H1	442	-1890	7043	24
H2	874	516	6360	22
H3	993	5540	6790	24
H4	1821	5524	7296	30
H5	2407	3594	6553	30
H6	2156	1697	5299	28
H7	1332	1754	4774	23

Table A0.5. Torsion angles (°) for **1.1** at 100 K.

Atoms	Angle
C1#1-C1-C2-C3	-1.37(12)
C1-C2-C3-C4	176.81(10)
C1-C2-C3-C3#1	1.34(12)
C2-C3-C4-C5	177.43(8)
C3#1-C3-C4-C5	-7.21(10)
C2-C3-C4-C6	-9.66(14)
C3#1-C3-C4-C6	165.71(6)
C3-C4-C5-C4#2	-172.87(10)
C6-C4-C5-C4#2	14.76(7)
C3-C4-C5-C5#3	7.13(10)
C6-C4-C5-C5#3	-165.24(7)
C3-C4-C6-C11	77.22(13)
C5-C4-C6-C11	-110.08(11)
C3-C4-C6-C7	-95.58(11)
C5-C4-C6-C7	77.12(13)
C11-C6-C7-C8	0.42(16)

C4-C6-C7-C8	173.47(10)
C6-C7-C8-C9	-0.60(17)
C7-C8-C9-C10	0.13(17)
C8-C9-C10-C11	0.50(17)
C9-C10-C11-C6	-0.68(17)
C7-C6-C11-C10	0.22(16)
C4-C6-C11-C10	-172.61(10)

Symmetry transformations used to generate equivalent atoms: #1 -x,y,z #2 x,-y+1,-z+1 #3 -x,-y+1,-z+1

Crystal Structure Report for **1.1** at 150 K (project code: 13069)

Data collection: A crystal (approximate dimensions 0.20 x 0.16 x 0.04 mm^3) was placed onto the tip of a 0.1 mm diameter glass capillary and mounted on a Bruker Photon CCD diffractometer for a data collection at 150(2) K.[1] A preliminary set of cell constants was calculated from reflections harvested from three sets of 12 frames. These initial sets of frames were oriented such that orthogonal wedges of reciprocal space were surveyed. This produced initial orientation matrices determined from 112 reflections. The data collection was carried out using MoKα radiation (graphite monochromator) with a frame time of 60 seconds and a detector distance of 6.0 cm. A randomly oriented region of reciprocal space was surveyed to the extent of one sphere and to a resolution of 0.77 Å. Four major sections of frames were collected with 0.30º steps in ω at four different ϕ settings and a detector position of -28º in 2θ. The intensity data were corrected for absorption and decay (SADABS).[2] Final cell constants were calculated from the xyz centroids of 2980 strong reflections from the actual data collection after integration (SAINT).[3] Please refer to Table 1 for additional crystal and refinement information.

Structure solution and refinement: The structure was solved using SHELXS-97[4] and refined using SHELXL-97.[4] The space group Cmca was determined based on systematic absences and intensity statistics. A direct-methods solution was calculated which provided most non-hydrogen atoms from the E-map. Full-matrix least squares / difference Fourier cycles were performed which located the remaining non-hydrogen atoms. All non-hydrogen atoms were refined with anisotropic displacement parameters. All hydrogen atoms were placed in ideal positions and refined as riding atoms with relative isotropic displacement parameters. The final full matrix least squares refinement converged to $R1 = 0.0345$ and $wR2 = 0.0940$ (F^2, all data).

Table A0.6. Atomic coordinates (x 10^4) and equivalent isotropic displacement parameters ($Å^2$x 10^3) for **1.1** at 150 K. Ueq is defined as one third of the trace of the orthogonalized Uij tensor.

Atom	x	y	z	Ueq
C1	5264(1)	10880(2)	3248(1)	26(1)
C2	5518(1)	9465(2)	3660(1)	24(1)
C3	5269(1)	7951(1)	4124(1)	20(1)
C4	5531(1)	6442(1)	4509(1)	20(1)
C5	5274(1)	5000	5000	19(1)
C6	6076(1)	6342(1)	4272(1)	21(1)
C7	6227(1)	5235(2)	3523(1)	27(1)
C8	6719(1)	5248(2)	3219(1)	35(1)
C9	7065(1)	6382(2)	3658(1)	35(1)
C10	6917(1)	7498(2)	4399(1)	33(1)

C11	6428(1)	7473(2)	4708(1)	26(1)

Table A0.7. Bond lengths (Å) and angles (°) for **1.1** at 150 K.

Atoms	Length	Atoms	Angle	Atoms	Angle
C(1)-C(2)	1.3548(15)	C(2)-C(1)-C(1)#1	120.11(7)	C(9)-C(8)-H(4)	120
C(1)-C(1)#1	1.418(2)	C(2)-C(1)-H(1)	119.9	C(7)-C(8)-H(4)	120
C(1)-H(1)	0.95	C(1)#1-C(1)-H(1)	119.9	C(10)-C(9)-C(8)	119.47(10)
C(2)-C(3)	1.4362(14)	C(1)-C(2)-C(3)	122.14(10)	C(10)-C(9)-H(5)	120.3
C(2)-H(2)	0.95	C(1)-C(2)-H(2)	118.9	C(8)-C(9)-H(5)	120.3
C(3)-C(4)	1.4027(14)	C(3)-C(2)-H(2)	118.9	C(9)-C(10)-C(11)	120.52(11)
C(3)-C(3)#1	1.441(2)	C(4)-C(3)-C(2)	121.99(10)	C(9)-C(10)-H(6)	119.7
C(4)-C(5)	1.4260(12)	C(4)-C(3)-C(3)#1	120.12(6)	C(11)-C(10)-H(6)	119.7
C(4)-C(6)	1.5005(14)	C(2)-C(3)-C(3)#1	117.73(6)	C(10)-C(11)-C(6)	120.66(11)
C(5)-C(4)#2	1.4260(12)	C(3)-C(4)-C(5)	120.52(10)	C(10)-C(11)-H(7)	119.7
C(5)-C(5)#3	1.468(3)	C(3)-C(4)-C(6)	115.91(9)	C(6)-C(11)-H(7)	119.7
C(6)-C(7)	1.3914(16)	C(5)-C(4)-C(6)	123.16(9)		
C(6)-C(11)	1.3920(15)	C(4)-C(5)-C(4)#2	122.08(13)		
C(7)-C(8)	1.3876(16)	C(4)-C(5)-C(5)#3	118.96(6)		
C(7)-H(3)	0.95	C(4)#2-C(5)-C(5)#3	118.96(6)		
C(8)-C(9)	1.3845(18)	C(7)-C(6)-C(11)	118.37(10)		
C(8)-H(4)	0.95	C(7)-C(6)-C(4)	119.02(9)		
C(9)-C(10)	1.3823(18)	C(11)-C(6)-C(4)	122.23(9)		
C(9)-H(5)	0.95	C(8)-C(7)-C(6)	120.93(11)		
C(10)-C(11)	1.3838(15)	C(8)-C(7)-H(3)	119.5		
C(10)-H(6)	0.95	C(6)-C(7)-H(3)	119.5		
C(11)-H(7)	0.95	C(9)-C(8)-C(7)	120.04(11)		

Symmetry transformations used to generate equivalent atoms: #1 -x+1,y,z #2 x,-y+1,-z+1 #3 -x+1,-y+1,-z+1

Table A0.8. Anisotropic displacement parameters ($Å^2$ x 10^3) for **1.1** at 150 K. The anisotropic displacement factor exponent takes the form: $-2\pi^2[h^2 a^{*2}U11 + ... + 2 h k a^* b^* U12]$.

Atom	U11	U22	U33	U23	U13	U12
C1	36(1)	21(1)	22(1)	3(1)	0(1)	-5(1)
C2	26(1)	24(1)	21(1)	0(1)	-1(1)	-4(1)
C3	26(1)	20(1)	16(1)	-2(1)	-1(1)	-2(1)
C4	22(1)	21(1)	17(1)	-2(1)	-1(1)	-1(1)
C5	22(1)	19(1)	16(1)	-3(1)	0	0
C6	22(1)	21(1)	21(1)	5(1)	-1(1)	-1(1)
C7	28(1)	30(1)	23(1)	0(1)	0(1)	-2(1)
C8	33(1)	44(1)	26(1)	1(1)	8(1)	6(1)

C9	21(1)	46(1)	39(1)	11(1)	5(1)	1(1)
C10	24(1)	33(1)	41(1)	6(1)	-7(1)	-4(1)
C11	25(1)	24(1)	28(1)	1(1)	-3(1)	-1(1)

Table A0.9. Hydrogen coordinates (x 104) and isotropic displacement parameters (a2 x 103) for **1.1** at 150 K.

Atom	x	y	z	U(eq)
H1	5441	11874	2959	32
H2	5872	9474	3641	29
H3	5991	4459	3215	32
H4	6818	4477	2710	41
H5	7402	6394	3452	42
H6	7153	8287	4698	39
H7	6332	8235	5222	31

Table A0.10. Torsion angles (°) for **1.1** at 150 K.

Atoms	Angle
C1#1-C1-C2-C3	-1.40(12)
C1-C2-C3-C4	176.81(10)
C1-C2-C3-C3#1	1.37(12)
C2-C3-C4-C5	177.38(8)
C3#1-C3-C4-C5	-7.29(10)
C2-C3-C4-C6	-9.65(14)
C3#1-C3-C4-C6	165.68(6)
C3-C4-C5-C4#2	-172.80(10)
C6-C4-C5-C4#2	14.76(7)
C3-C4-C5-C5#3	7.21(10)
C6-C4-C5-C5#3	-165.24(7)
C3-C4-C6-C7	-95.42(11)
C5-C4-C6-C7	77.34(12)
C3-C4-C6-C11	77.35(13)
C5-C4-C6-C11	-109.88(11)
C11-C6-C7-C8	0.35(16)
C4-C6-C7-C8	173.40(10)
C6-C7-C8-C9	-0.47(18)
C7-C8-C9-C10	-0.01(19)
C8-C9-C10-C11	0.62(18)
C9-C10-C11-C6	-0.74(18)
C7-C6-C11-C10	0.26(16)

C4-C6-C11-C10	-172.56(10)

Symmetry transformations used to generate equivalent atoms: #1 -x+1,y,z #2 x,-y+1,-z+1 #3 -x+1,-y+1,-z+1

Crystal Structure Report for **1.1** at 200 K (project code: 13069)

Data collection: A crystal (approximate dimensions 0.20 x 0.16 x 0.04 mm^3) was placed onto the tip of a 0.1 mm diameter glass capillary and mounted on a Bruker Photon CCD diffractometer for a data collection at 200(2) K.[1] A preliminary set of cell constants was calculated from reflections harvested from three sets of 12 frames. These initial sets of frames were oriented such that orthogonal wedges of reciprocal space were surveyed. This produced initial orientation matrices determined from 112 reflections. The data collection was carried out using MoKα radiation (graphite monochromator) with a frame time of 60 seconds and a detector distance of 6.0 cm. A randomly oriented region of reciprocal space was surveyed to the extent of one sphere and to a resolution of 0.77 Å. Four major sections of frames were collected with 0.30º steps in ω at four different ϕ settings and a detector position of -28º in 2θ. The intensity data were corrected for absorption and decay (SADABS).[2] Final cell constants were calculated from the xyz centroids of 2994 strong reflections from the actual data collection after integration (SAINT).[3] Please refer to Table 1 for additional crystal and refinement information.

Structure solution and refinement: The structure was solved using SHELXS-97[4] and refined using SHELXL-97.[4] The space group Cmca was determined based on systematic absences and intensity statistics. A direct-methods solution was calculated which provided most non-hydrogen atoms from the E-map. Full-matrix least squares / difference Fourier cycles were performed which located the remaining non-hydrogen atoms. All non-hydrogen atoms were refined with anisotropic displacement parameters. All hydrogen atoms were placed in ideal positions and refined as riding atoms with relative isotropic displacement parameters. The final full matrix least squares refinement converged to $R1 = 0.0389$ and $wR2 = 0.1127$ (F^2, all data).

Table A0.11. Atomic coordinates (x 10^4) and equivalent isotropic displacement parameters ($Å^2$x 10^3) for **1.1** at 200 K. Ueq is defined as one third of the trace of the orthogonalized Uij tensor.

Atoms	x	y	z	Ueq
C1	9737(1)	4135(2)	3251(1)	34(1)
C2	9483(1)	5546(2)	3661(1)	31(1)
C3	9733(1)	7055(2)	4125(1)	26(1)
C4	9470(1)	8561(2)	4511(1)	25(1)
C5	9727(1)	10000	5000	24(1)
C6	8926(1)	8663(2)	4272(1)	27(1)
C7	8775(1)	9768(2)	3527(1)	35(1)
C8	8285(1)	9755(2)	3225(1)	45(1)
C9	7939(1)	8625(2)	3660(1)	47(1)
C10	8086(1)	7516(2)	4397(1)	43(1)
C11	8572(1)	7536(2)	4704(1)	33(1)

Table A0.12. Bond lengths (Å) and angles (°) for **1.1** at 200 K.

Atoms	Length	Atoms	Angle	Atoms	Angle
C(1)-C(2)	1.3545(18)	C(2)-C(1)-C(1)#1	120.22(7)	C(9)-C(8)-H(4)	119.9
C(1)-C(1)#1	1.412(3)	C(2)-C(1)-H(1)	119.9	C(7)-C(8)-H(4)	119.9

C(1)-H(1)	0.95	C(1)#1-C(1)-H(1)	119.9	C(10)-C(9)-C(8)	119.44(12)
C(2)-C(3)	1.4355(16)	C(1)-C(2)-C(3)	121.97(12)	C(10)-C(9)-H(5)	120.3
C(2)-H(2)	0.95	C(1)-C(2)-H(2)	119	C(8)-C(9)-H(5)	120.3
C(3)-C(4)	1.4038(16)	C(3)-C(2)-H(2)	119	C(9)-C(10)-C(11)	120.61(13)
C(3)-C(3)#1	1.436(2)	C(4)-C(3)-C(2)	121.83(11)	C(9)-C(10)-H(6)	119.7
C(4)-C(5)	1.4268(13)	C(4)-C(3)-C(3)#1	120.22(7)	C(11)-C(10)-H(6)	119.7
C(4)-C(6)	1.5008(16)	C(2)-C(3)-C(3)#1	117.80(7)	C(10)-C(11)-C(6)	120.73(13)
C(5)-C(4)#2	1.4269(13)	C(3)-C(4)-C(5)	120.37(11)	C(10)-C(11)-H(7)	119.6
C(5)-C(5)#3	1.465(3)	C(3)-C(4)-C(6)	115.96(10)	C(6)-C(11)-H(7)	119.6
C(6)-C(7)	1.3892(18)	C(5)-C(4)-C(6)	123.24(10)		
C(6)-C(11)	1.3922(17)	C(4)-C(5)-C(4)#2	121.96(14)		
C(7)-C(8)	1.3864(18)	C(4)-C(5)-C(5)#3	119.02(7)		
C(7)-H(3)	0.95	C(4)#2-C(5)-C(5)#3	119.02(7)		
C(8)-C(9)	1.382(2)	C(7)-C(6)-C(11)	118.23(11)		
C(8)-H(4)	0.95	C(7)-C(6)-C(4)	119.08(11)		
C(9)-C(10)	1.378(2)	C(11)-C(6)-C(4)	122.31(11)		
C(9)-H(5)	0.95	C(8)-C(7)-C(6)	120.89(13)		
C(10)-C(11)	1.3797(18)	C(8)-C(7)-H(3)	119.6		
C(10)-H(6)	0.95	C(6)-C(7)-H(3)	119.6		
C(11)-H(7)	0.95	C(9)-C(8)-C(7)	120.10(14)		

Symmetry transformations used to generate equivalent atoms: #1 -x+2,y,z #2 x,-y+2,-z+1 #3 -x+2,-y+2,-z+1

Table A0.13. Anisotropic displacement parameters ($Å^2$ x 10^3) for **1.1** at 200 K. The anisotropic displacement factor exponent takes the form: $-2\pi^2[h^2 a^{*2}U11 + ... + 2 h k a^* b^* U12]$.

Atom	U11	U22	U33	U23	U13	U12
C1	46(1)	27(1)	30(1)	-5(1)	-1(1)	-7(1)
C2	34(1)	31(1)	28(1)	-2(1)	1(1)	-6(1)
C3	32(1)	26(1)	20(1)	3(1)	0(1)	-3(1)
C4	28(1)	26(1)	22(1)	2(1)	1(1)	-2(1)
C5	27(1)	24(1)	22(1)	3(1)	0	0
C6	28(1)	27(1)	26(1)	-6(1)	1(1)	-2(1)
C7	35(1)	41(1)	29(1)	1(1)	-1(1)	-2(1)
C8	42(1)	59(1)	35(1)	-1(1)	-10(1)	7(1)
C9	27(1)	62(1)	52(1)	-14(1)	-6(1)	1(1)
C10	30(1)	44(1)	55(1)	-8(1)	9(1)	-6(1)
C11	31(1)	31(1)	38(1)	-1(1)	5(1)	-1(1)

Table A0.14. Hydrogen coordinates (x 10^4) and isotropic displacement parameters ($Å^2$ x 10^3) for **1.1** at 200 K.

Atom	x	y	z	U(eq)

H1	9561	3142	2962	41
H2	9130	5537	3642	37
H3	9011	10542	3221	42
H4	8186	10525	2717	54
H5	7603	8613	3454	56
H6	7849	6731	4695	51
H7	8667	6772	5216	40

Table A0.15. Torsion angles (°) for **1.1** at 200 K.

Atoms	Angle
C1#1-C1-C2-C3	-1.44(14)
C1-C2-C3-C4	176.87(11)
C1-C2-C3-C3#1	1.41(14)
C2-C3-C4-C5	177.43(9)
C3#1-C3-C4-C5	-7.21(11)
C2-C3-C4-C6	-9.82(15)
C3#1-C3-C4-C6	165.54(7)
C3-C4-C5-C4#2	-172.88(11)
C6-C4-C5-C4#2	14.92(8)
C3-C4-C5-C5#3	7.12(11)
C6-C4-C5-C5#3	-165.08(8)
C3-C4-C6-C7	-95.20(13)
C5-C4-C6-C7	77.31(14)
C3-C4-C6-C11	77.62(15)
C5-C4-C6-C11	-109.87(12)
C11-C6-C7-C8	0.32(19)
C4-C6-C7-C8	173.44(12)
C6-C7-C8-C9	-0.4(2)
C7-C8-C9-C10	0.1(2)
C8-C9-C10-C11	0.4(2)
C9-C10-C11-C6	-0.5(2)
C7-C6-C11-C10	0.16(19)
C4-C6-C11-C10	-172.71(11)
Symmetry transformations used to generate equivalent atoms: #1 -x+2,y,z #2 x,-y+2,-z+1 #3 -x+2,-y+2,-z+1	

Crystal Structure Report for **1.1** at 250 K (project code: 13069)

Data collection: A crystal (approximate dimensions 0.20 x 0.16 x 0.04 mm^3) was placed onto the tip of a 0.1 mm diameter glass capillary and mounted on a Bruker Photon CCD diffractometer for a data collection at 250(2) K.[1] A

preliminary set of cell constants was calculated from reflections harvested from three sets of 20 frames. These initial sets of frames were oriented such that orthogonal wedges of reciprocal space were surveyed. This produced initial orientation matrices determined from ?? reflections. The data collection was carried out using MoKα radiation (graphite monochromator) with a frame time of ?? seconds and a detector distance of ?? cm. A randomly oriented region of reciprocal space was surveyed to the extent of one sphere and to a resolution of 0.84 Å. Four major sections of frames were collected with 0.30º steps in ω at four different ϕ settings and a detector position of -28º in 2θ. The intensity data were corrected for absorption and decay (SADABS).[2] Final cell constants were calculated from the xyz centroids of 2975 strong reflections from the actual data collection after integration (SAINT).[3] Please refer to Table 1 for additional crystal and refinement information.

Structure solution and refinement: The structure was solved using SHELXS-97 (Sheldrick, 1990)[4] and refined using SHELXL-97 (Sheldrick, 1997).[4] The space group Cmca was determined based on systematic absences and intensity statistics. A direct-methods solution was calculated which provided most non-hydrogen atoms from the E-map. Full-matrix least squares / difference Fourier cycles were performed which located the remaining non-hydrogen atoms. All non-hydrogen atoms were refined with anisotropic displacement parameters. All hydrogen atoms were placed in ideal positions and refined as riding atoms with relative isotropic displacement parameters. The final full matrix least squares refinement converged to $R1 = 0.0397$ and $wR2 = 0.1156$ (F^2, all data).

Table A0.16. Atomic coordinates (x 10^4) and equivalent isotropic displacement parameters (Å^{2}x 10^3) for **1.1** at 250 K. Ueq is defined as one third of the trace of the orthogonalized Uij tensor.

Atom	x	y	z	Ueq
C1	5262(1)	4154(2)	6747(1)	42(1)
C2	5515(1)	5558(2)	6338(1)	38(1)
C3	5267(1)	7065(2)	5874(1)	31(1)
C4	5530(1)	8565(2)	5489(1)	31(1)
C5	5272(1)	10000	5000	29(1)
C6	6073(1)	8670(2)	5728(1)	33(1)
C7	6223(1)	9772(2)	6467(1)	43(1)
C8	6712(1)	9759(3)	6769(1)	57(1)
C9	7058(1)	8634(2)	6337(1)	59(1)
C10	6912(1)	7531(2)	5607(1)	53(1)
C11	6427(1)	7547(2)	5301(1)	41(1)

Table A0.17. Bond lengths (Å) and angles (°) for **1.1** at 250 K.

Atoms	Length	Atoms	Angle	Atoms	Angle
C(1)-C(2)	1.3520(18)	C(2)-C(1)-C(1)#1	120.27(8)	C(9)-C(8)-H(4)	119.9
C(1)-C(1)#1	1.409(3)	C(2)-C(1)-H(1)	119.9	C(7)-C(8)-H(4)	119.9
C(1)-H(1)	0.94	C(1)#1-C(1)-H(1)	119.9	C(10)-C(9)-C(8)	119.41(13)
C(2)-C(3)	1.4360(16)	C(1)-C(2)-C(3)	121.93(12)	C(10)-C(9)-H(5)	120.3
C(2)-H(2)	0.94	C(1)-C(2)-H(2)	119	C(8)-C(9)-H(5)	120.3
C(3)-C(4)	1.4027(16)	C(3)-C(2)-H(2)	119	C(9)-C(10)-C(11)	120.63(14)
C(3)-C(3)#1	1.433(2)	C(4)-C(3)-C(3)#1	120.30(7)	C(9)-C(10)-H(6)	119.7
C(4)-C(5)	1.4265(13)	C(4)-C(3)-C(2)	121.77(11)	C(11)-C(10)-H(6)	119.7

C(4)-C(6)	1.5014(16)	C(3)#1-C(3)-C(2)	117.78(7)	C(10)-C(11)-C(6)	120.81(13)
C(5)-C(4)#2	1.4265(13)	C(3)-C(4)-C(5)	120.31(11)	C(10)-C(11)-H(7)	119.6
C(5)-C(5)#3	1.465(3)	C(3)-C(4)-C(6)	116.02(10)	C(6)-C(11)-H(7)	119.6
C(6)-C(7)	1.3858(18)	C(5)-C(4)-C(6)	123.22(10)		
C(6)-C(11)	1.3907(17)	C(4)-C(5)-C(4)#2	121.98(14)		
C(7)-C(8)	1.3838(19)	C(4)-C(5)-C(5)#3	119.01(7)		
C(7)-H(3)	0.94	C(4)#2-C(5)-C(5)#3	119.01(7)		
C(8)-C(9)	1.380(2)	C(7)-C(6)-C(11)	118.05(11)		
C(8)-H(4)	0.94	C(7)-C(6)-C(4)	119.21(11)		
C(9)-C(10)	1.372(2)	C(11)-C(6)-C(4)	122.37(11)		
C(9)-H(5)	0.94	C(8)-C(7)-C(6)	120.93(13)		
C(10)-C(11)	1.3782(18)	C(8)-C(7)-H(3)	119.5		
C(10)-H(6)	0.94	C(6)-C(7)-H(3)	119.5		
C(11)-H(7)	0.94	C(9)-C(8)-C(7)	120.17(14)		

Symmetry transformations used to generate equivalent atoms: #1 -x+1,y,z #2 x,-y+2,-z+1 #3 -x+1,-y+2,-z+1

Table A0.18. Anisotropic displacement parameters ($Å^2$ x 10^3) for **1.1** at 250 K. The anisotropic displacement factor exponent takes the form: $-2\pi^2[h^2 a^{*2}U11 + ... + 2 h k a^* b^* U12]$.

Atom	U11	U22	U33	U23	U13	U12
C1	56(1)	33(1)	38(1)	7(1)	0(1)	7(1)
C2	41(1)	37(1)	35(1)	3(1)	1(1)	7(1)
C3	39(1)	30(1)	25(1)	-3(1)	1(1)	3(1)
C4	34(1)	31(1)	28(1)	-2(1)	1(1)	3(1)
C5	32(1)	28(1)	27(1)	-2(1)	0	0
C6	33(1)	33(1)	32(1)	6(1)	1(1)	2(1)
C7	43(1)	51(1)	36(1)	-2(1)	-1(1)	3(1)
C8	52(1)	76(1)	45(1)	1(1)	-14(1)	-10(1)
C9	33(1)	78(1)	65(1)	17(1)	-8(1)	-1(1)
C10	36(1)	56(1)	69(1)	11(1)	10(1)	8(1)
C11	38(1)	39(1)	48(1)	2(1)	7(1)	2(1)

Table A0.19. Hydrogen coordinates (x 10^4) and isotropic displacement parameters ($Å^2$ x 10^3) for **1.1** at 250 K.

Atom	x	y	z	U(eq)
H1	5436	3174	7033	51
H2	5865	5548	6357	45
H3	5990	10539	6768	52
H4	6808	10519	7270	69
H5	7390	8624	6541	70
H6	7146	6756	5314	64

H7	6334	6790	4796	50

Table A0.20. Torsion angles (°) for **1.1** at 250 K.

Atoms	Angle
C1#1-C1-C2-C3	-1.39(14)
C1-C2-C3-C4	176.89(11)
C1-C2-C3-C3#1	1.35(14)
C3#1-C3-C4-C5	-7.19(11)
C2-C3-C4-C5	177.38(9)
C3#1-C3-C4-C6	165.41(7)
C2-C3-C4-C6	-10.02(15)
C3-C4-C5-C4#2	-172.90(11)
C6-C4-C5-C4#2	15.05(8)
C3-C4-C5-C5#3	7.10(11)
C6-C4-C5-C5#3	-164.95(8)
C3-C4-C6-C7	-95.03(13)
C5-C4-C6-C7	77.34(14)
C3-C4-C6-C11	77.81(15)
C5-C4-C6-C11	-109.83(12)
C11-C6-C7-C8	0.2(2)
C4-C6-C7-C8	173.36(12)
C6-C7-C8-C9	-0.3(2)
C7-C8-C9-C10	0.0(2)
C8-C9-C10-C11	0.4(2)
C9-C10-C11-C6	-0.5(2)
C7-C6-C11-C10	0.18(19)
C4-C6-C11-C10	-172.73(12)
Symmetry transformations used to generate equivalent atoms: #1 -x+1,y,z #2 x,-y+2,-z+1 #3 -x+1,-y+2,-z+1	

Crystal Structure Report for **2.1** at 100 K (project code: 13065)

Data collection: A crystal (approximate dimensions 0.20 x 0.16 x 0.03 mm^3) was placed onto the tip of a 0.1 mm diameter glass capillary and mounted on a Bruker Photon CCD diffractometer for a data collection at 100(2) K.[1] A preliminary set of cell constants was calculated from reflections harvested from three sets of 12 frames. These initial sets of frames were oriented such that orthogonal wedges of reciprocal space were surveyed. This produced initial orientation matrices determined from 150 reflections. The data collection was carried out using MoKα radiation (graphite monochromator) with a frame time of 30 seconds and a detector distance of 6.0 cm. A randomly oriented region of reciprocal space was surveyed to the extent of one sphere and to a resolution of 0.77 Å. Four major sections of frames were collected with 0.30º steps in ω at four different ϕ settings and a detector position of -28º in 2θ. The intensity data were corrected for absorption and decay (SADABS).[2] Final cell constants were calculated from the xyz centroids of 2993 strong reflections from the actual data collection after integration (SAINT).[3] Please refer to Table 1

for additional crystal and refinement information.

Structure solution and refinement: The structure was solved using SHELXS-97[4] and refined using SHELXL-97.[4] The space group Cmca was determined based on systematic absences and intensity statistics. A direct-methods solution was calculated which provided most non-hydrogen atoms from the E-map. Full-matrix least squares / difference Fourier cycles were performed which located the remaining non-hydrogen atoms. All non-hydrogen atoms were refined with anisotropic displacement parameters. All hydrogen atoms were placed in ideal positions and refined as riding atoms with relative isotropic displacement parameters. The final full matrix least squares refinement converged to $R1 = 0.0326$ and $wR2 = 0.0853$ (F^2, all data).

Table A0.21. Atomic coordinates (x 10^4) and equivalent isotropic displacement parameters (Å^{2}x 10^3) for **2.1** at 100 K. Ueq is defined as one third of the trace of the orthogonalized Uij tensor.

Atom	x	y	z	Ueq
C1	264(1)	10896(2)	6757(1)	21(1)
D1	441	11892	7048	25
C2	519(1)	9476(2)	6342(1)	20(1)
D2	873	9486	6360	23
C3	269(1)	7958(2)	5877(1)	17(1)
C4	532(1)	6446(2)	5492(1)	17(1)
C5	273(1)	5000	5000	16(1)
C6	1078(1)	6348(2)	5730(1)	17(1)
C7	1231(1)	5235(2)	6481(1)	21(1)
D3	995	4456	6789	26
C8	1723(1)	5246(2)	6785(1)	26(1)
D4	1822	4471	7295	32
C9	2071(1)	6388(2)	6346(1)	27(1)
D5	2408	6400	6553	32
C10	1921(1)	7509(2)	5603(1)	25(1)
D6	2156	8303	5302	30
C11	1431(1)	7482(2)	5293(1)	21(1)
D7	1334	8246	4777	25

Table A0.22. Bond lengths (Å) and angles (°) for **2.1** at 100 K.

Atoms	Length	Atoms	Angle	Atoms	Angle
C(1)-C(2)	1.3570(16)	C(2)-C(1)-C(1)#1	120.14(7)	C(9)-C(8)-D(4)	120
C(1)-C(1)#1	1.417(2)	C(2)-C(1)-D(1)	119.9	C(7)-C(8)-D(4)	120
C(1)-D(1)	0.95	C(1)#1-C(1)-D(1)	119.9	C(10)-C(9)-C(8)	119.27(11)
C(2)-C(3)	1.4351(16)	C(1)-C(2)-C(3)	122.10(11)	C(10)-C(9)-D(5)	120.4
C(2)-D(2)	0.95	C(1)-C(2)-D(2)	119	C(8)-C(9)-D(5)	120.4
C(3)-C(4)	1.4009(16)	C(3)-C(2)-D(2)	119	C(9)-C(10)-C(11)	120.54(12)
C(3)-C(3)#1	1.444(2)	C(4)-C(3)-C(2)	121.94(10)	C(9)-C(10)-D(6)	119.7

C(4)-C(5)	1.4265(13)	C(4)-C(3)-C(3)#1	120.15(6)	C(11)-C(10)-D(6)	119.7
C(4)-C(6)	1.5033(16)	C(2)-C(3)-C(3)#1	117.75(7)	C(10)-C(11)-C(6)	120.76(11)
C(5)-C(4)#2	1.4265(13)	C(3)-C(4)-C(5)	120.40(11)	C(10)-C(11)-D(7)	119.6
C(5)-C(5)#3	1.465(3)	C(3)-C(4)-C(6)	115.90(10)	C(6)-C(11)-D(7)	119.6
C(6)-C(11)	1.3914(16)	C(5)-C(4)-C(6)	123.31(10)		
C(6)-C(7)	1.3915(16)	C(4)-C(5)-C(4)#2	121.89(14)		
C(7)-C(8)	1.3877(16)	C(4)-C(5)-C(5)#3	119.05(7)		
C(7)-D(3)	0.95	C(4)#2-C(5)-C(5)#3	119.06(7)		
C(8)-C(9)	1.3863(18)	C(11)-C(6)-C(7)	118.27(11)		
C(8)-D(4)	0.95	C(11)-C(6)-C(4)	122.26(10)		
C(9)-C(10)	1.3849(18)	C(7)-C(6)-C(4)	119.11(10)		
C(9)-D(5)	0.95	C(8)-C(7)-C(6)	121.07(11)		
C(10)-C(11)	1.3855(16)	C(8)-C(7)-D(3)	119.5		
C(10)-D(6)	0.95	C(6)-C(7)-D(3)	119.5		
C(11)-D(7)	0.95	C(9)-C(8)-C(7)	120.09(12)		

Symmetry transformations used to generate equivalent atoms: #1 -x,y,z #2 x,-y+1,-z+1 #3 -x,-y+1,-z+1

Table A0.23. Anisotropic displacement parameters ($Å^2$ x 10^3) for **2.1** at 100 K. The anisotropic displacement factor exponent takes the form: $-2\pi^2[h^2 a^{*2}U11 + ... + 2 h k a^* b^* U12]$.

Atom	U11	U22	U33	U23	U13	U12
C1	30(1)	17(1)	18(1)	-1(1)	0(1)	-4(1)
C2	23(1)	19(1)	16(1)	1(1)	1(1)	-4(1)
C3	22(1)	16(1)	13(1)	3(1)	0(1)	-1(1)
C4	20(1)	16(1)	14(1)	2(1)	1(1)	-1(1)
C5	20(1)	16(1)	13(1)	3(1)	0	0
C6	20(1)	16(1)	16(1)	-5(1)	0(1)	-1(1)
C7	24(1)	22(1)	18(1)	-1(1)	1(1)	-2(1)
C8	28(1)	32(1)	20(1)	-1(1)	-5(1)	4(1)
C9	19(1)	33(1)	29(1)	-8(1)	-3(1)	1(1)
C10	20(1)	24(1)	31(1)	-5(1)	6(1)	-3(1)
C11	23(1)	18(1)	21(1)	-2(1)	3(1)	0(1)

Table A0.24. Torsion angles (°) for **2.1** at 100 K.

Atoms	Angle
C1#1-C1-C2-C3	1.28(13)
C1-C2-C3-C4	-176.64(10)
C1-C2-C3-C3#1	-1.25(13)
C2-C3-C4-C5	-177.40(8)
C3#1-C3-C4-C5	7.32(11)

C2-C3-C4-C6	9.58(15)
C3#1-C3-C4-C6	-165.70(6)
C3-C4-C5-C4#2	172.76(11)
C6-C4-C5-C4#2	-14.76(7)
C3-C4-C5-C5#3	-7.24(11)
C6-C4-C5-C5#3	165.24(7)
C3-C4-C6-C11	-77.30(14)
C5-C4-C6-C11	109.91(12)
C3-C4-C6-C7	95.67(13)
C5-C4-C6-C7	-77.12(13)
C11-C6-C7-C8	-0.26(18)
C4-C6-C7-C8	-173.51(11)
C6-C7-C8-C9	0.49(19)
C7-C8-C9-C10	-0.06(19)
C8-C9-C10-C11	-0.59(19)
C9-C10-C11-C6	0.83(19)
C7-C6-C11-C10	-0.40(18)
C4-C6-C11-C10	172.63(11)

Symmetry transformations used to generate equivalent atoms: #1 -x,y,z #2 x,-y+1,-z+1 #3 -x,-y+1,-z+1

Crystal Structure Report for **2.1** at 150 K (project code: 13065)

Data collection: A crystal (approximate dimensions 0.20 x 0.16 x 0.03 mm^3) was placed onto the tip of a 0.1 mm diameter glass capillary and mounted on a Bruker Photon CCD diffractometer for a data collection at 150(2) K.[1] A preliminary set of cell constants was calculated from reflections harvested from three sets of 12 frames. These initial sets of frames were oriented such that orthogonal wedges of reciprocal space were surveyed. This produced initial orientation matrices determined from 150 reflections. The data collection was carried out using MoKα radiation (graphite monochromator) with a frame time of 30 seconds and a detector distance of 6.0 cm. A randomly oriented region of reciprocal space was surveyed to the extent of one sphere and to a resolution of 0.77 Å. Four major sections of frames were collected with 0.30º steps in ω at four different ϕ settings and a detector position of -28º in 2θ. The intensity data were corrected for absorption and decay (SADABS).[2] Final cell constants were calculated from the xyz centroids of 2992 strong reflections from the actual data collection after integration (SAINT).[3] Please refer to Table 1 for additional crystal and refinement information.

Structure solution and refinement: The structure was solved using SHELXS-97 (Sheldrick, 1990)[4] and refined using SHELXL-97 (Sheldrick, 1997).[4] The space group Cmca was determined based on systematic absences and intensity statistics. A direct-methods solution was calculated which provided most non-hydrogen atoms from the E-map. Full-matrix least squares / difference Fourier cycles were performed which located the remaining non-hydrogen atoms. All non-hydrogen atoms were refined with anisotropic displacement parameters. All hydrogen atoms were placed in ideal positions and refined as riding atoms with relative isotropic displacement parameters. The final full matrix least squares refinement converged to $R1 = 0.0345$ and $wR2 = 0.0921$ (F^2, all data).

Table A0.25. Atomic coordinates (x 10^4) and equivalent isotropic displacement parameters ($Å^2$x 10^3) for **2.1** at 150 K. Ueq is defined as one third of the trace of the orthogonalized Uij tensor.

Atom	x	y	z	Ueq
C1	4736(1)	-880(2)	6755(1)	27(1)
D1	4559	-1873	7045	33
C2	4483(1)	535(2)	6341(1)	25(1)
D2	4128	524	6358	30
C3	4731(1)	2047(2)	5877(1)	21(1)
C4	4469(1)	3558(2)	5491(1)	21(1)
C5	4727(1)	5000	5000	20(1)
C6	3924(1)	3658(2)	5729(1)	22(1)
C7	3772(1)	4770(2)	6476(1)	28(1)
D3	4007	5549	6783	34
C8	3280(1)	4756(2)	6779(1)	36(1)
D4	3182	5530	7288	43
C9	2933(1)	3621(2)	6344(1)	37(1)
D5	2597	3609	6551	44
C10	3081(1)	2504(2)	5605(1)	34(1)
D6	2845	1714	5306	40
C11	3571(1)	2525(2)	5296(1)	27(1)
D7	3666	1758	4782	32

Table A0.26. Bond lengths (Å) and angles (°) for **2.1** at 150 K.

Atoms	Length	Atoms	Angle	Atoms	Angle
C(1)-C(2)	1.3544(17)	C(2)-C(1)-C(1)#1	120.09(7)	C(9)-C(8)-D(4)	119.9
C(1)-C(1)#1	1.417(3)	C(2)-C(1)-D(1)	120	C(7)-C(8)-D(4)	119.9
C(1)-D(1)	0.95	C(1)#1-C(1)-D(1)	120	C(10)-C(9)-C(8)	119.33(12)
C(2)-C(3)	1.4320(17)	C(1)-C(2)-C(3)	122.19(12)	C(10)-C(9)-D(5)	120.3
C(2)-D(2)	0.95	C(1)-C(2)-D(2)	118.9	C(8)-C(9)-D(5)	120.3
C(3)-C(4)	1.4021(16)	C(3)-C(2)-D(2)	118.9	C(9)-C(10)-C(11)	120.60(13)
C(3)-C(3)#1	1.444(2)	C(4)-C(3)-C(2)	122.05(11)	C(9)-C(10)-D(6)	119.7
C(4)-C(5)	1.4260(14)	C(4)-C(3)-C(3)#1	120.08(7)	C(11)-C(10)-D(6)	119.7
C(4)-C(6)	1.5023(17)	C(2)-C(3)-C(3)#1	117.71(7)	C(10)-C(11)-C(6)	120.68(12)
C(5)-C(4)#2	1.4260(14)	C(3)-C(4)-C(5)	120.50(11)	C(10)-C(11)-D(7)	119.7
C(5)-C(5)#3	1.466(3)	C(3)-C(4)-C(6)	115.83(10)	C(6)-C(11)-D(7)	119.7
C(6)-C(7)	1.3908(18)	C(5)-C(4)-C(6)	123.25(11)		
C(6)-C(11)	1.3917(17)	C(4)-C(5)-C(4)#2	121.94(15)		
C(7)-C(8)	1.3866(18)	C(4)-C(5)-C(5)#3	119.03(7)		
C(7)-D(3)	0.95	C(4)#2-C(5)-C(5)#3	119.03(7)		

C(8)-C(9)	1.382(2)	C(7)-C(6)-C(11)	118.24(11)
C(8)-D(4)	0.95	C(7)-C(6)-C(4)	119.10(11)
C(9)-C(10)	1.380(2)	C(11)-C(6)-C(4)	122.28(11)
C(9)-D(5)	0.95	C(8)-C(7)-C(6)	120.92(12)
C(10)-C(11)	1.3846(17)	C(8)-C(7)-D(3)	119.5
C(10)-D(6)	0.95	C(6)-C(7)-D(3)	119.5
C(11)-D(7)	0.95	C(9)-C(8)-C(7)	120.23(13)

Symmetry transformations used to generate equivalent atoms: #1 -x+1,y,z #2 x,-y+1,-z+1 #3 -x+1,-y+1,-z+1

Table A0.27. Anisotropic displacement parameters ($Å^2$ x 10^3) for **2.1** at 150 K. The anisotropic displacement factor exponent takes the form: $-2\pi^2[h^2 a^{*2}U11 + ... + 2 h k a^* b^* U12]$.

Atom	U11	U22	U33	U23	U13	U12
C1	38(1)	21(1)	23(1)	3(1)	0(1)	-6(1)
C2	29(1)	25(1)	21(1)	1(1)	-1(1)	-5(1)
C3	27(1)	20(1)	16(1)	-2(1)	-1(1)	-2(1)
C4	25(1)	20(1)	17(1)	-1(1)	-2(1)	-1(1)
C5	24(1)	20(1)	17(1)	-3(1)	0	0
C6	24(1)	20(1)	21(1)	5(1)	-1(1)	-1(1)
C7	30(1)	31(1)	23(1)	0(1)	0(1)	-2(1)
C8	35(1)	44(1)	27(1)	1(1)	8(1)	5(1)
C9	23(1)	48(1)	39(1)	12(1)	4(1)	1(1)
C10	25(1)	34(1)	42(1)	6(1)	-7(1)	-3(1)
C11	28(1)	24(1)	28(1)	2(1)	-4(1)	-1(1)

Table A0.28. Torsion angles (°) for **2.1** at 150 K.

Atoms	Angle
C1#1-C1-C2-C3	1.23(14)
C1-C2-C3-C4	-176.71(11)
C1-C2-C3-C3#1	-1.20(13)
C2-C3-C4-C5	-177.39(9)
C3#1-C3-C4-C5	7.21(11)
C2-C3-C4-C6	9.77(15)
C3#1-C3-C4-C6	-165.64(7)
C3-C4-C5-C4#2	172.87(11)
C6-C4-C5-C4#2	-14.83(8)
C3-C4-C5-C5#3	-7.13(11)
C6-C4-C5-C5#3	165.17(8)
C3-C4-C6-C7	95.48(14)
C5-C4-C6-C7	-77.16(14)

C3-C4-C6-C11	-77.39(14)
C5-C4-C6-C11	109.98(13)
C11-C6-C7-C8	-0.28(19)
C4-C6-C7-C8	-173.44(12)
C6-C7-C8-C9	0.4(2)
C7-C8-C9-C10	0.0(2)
C8-C9-C10-C11	-0.5(2)
C9-C10-C11-C6	0.6(2)
C7-C6-C11-C10	-0.25(19)
C4-C6-C11-C10	172.67(11)

Symmetry transformations used to generate equivalent atoms: #1 -x+1,y,z #2 x,-y+1,-z+1 #3 -x+1,-y+1,-z+1

Crystal Structure Report for **2.1** at 200 K (project code: 13065)

Data collection: A crystal (approximate dimensions 0.20 x 0.16 x 0.03 mm^3) was placed onto the tip of a 0.1 mm diameter glass capillary and mounted on a Bruker Photon CCD diffractometer for a data collection at 200(2) K.[1] A preliminary set of cell constants was calculated from reflections harvested from three sets of 12 frames. These initial sets of frames were oriented such that orthogonal wedges of reciprocal space were surveyed. This produced initial orientation matrices determined from 150 reflections. The data collection was carried out using MoKα radiation (graphite monochromator) with a frame time of 30 seconds and a detector distance of 6.0 cm. A randomly oriented region of reciprocal space was surveyed to the extent of one sphere and to a resolution of 0.77 Å. Four major sections of frames were collected with 0.30º steps in ω at four different ϕ settings and a detector position of -28º in 2θ. The intensity data were corrected for absorption and decay (SADABS).[2] Final cell constants were calculated from the xyz centroids of 2991 strong reflections from the actual data collection after integration (SAINT).[3] Please refer to Table 1 for additional crystal and refinement information.

Structure solution and refinement: The structure was solved using SHELXS-97[4] and refined using SHELXL-97.[4] The space group Cmca was determined based on systematic absences and intensity statistics. A direct-methods solution was calculated which provided most non-hydrogen atoms from the E-map. Full-matrix least squares / difference Fourier cycles were performed which located the remaining non-hydrogen atoms. All non-hydrogen atoms were refined with anisotropic displacement parameters. All hydrogen atoms were placed in ideal positions and refined as riding atoms with relative isotropic displacement parameters. The final full matrix least squares refinement converged to $R1 = 0.0364$ and $wR2 = 0.0958$ (F^2, all data).

Table A0.29. Atomic coordinates (x 10^4) and equivalent isotropic displacement parameters ($Å^2$x 10^3) for **2.1** at 200 K. Ueq is defined as one third of the trace of the orthogonalized Uij tensor.

Atom	x	y	z	Ueq
C1	9736(1)	10863(2)	3247(1)	35(1)
D1	9560	11855	2957	42
C2	9484(1)	9453(2)	3660(1)	32(1)
D2	9130	9465	3642	38
C3	9732(1)	7943(2)	4123(1)	26(1)
C4	9470(1)	6440(2)	4510(1)	26(1)
C5	9727(1)	5000	5000	25(1)

C6	8925(1)	6334(2)	4271(1)	28(1)
C7	8774(1)	5228(2)	3529(1)	36(1)
D3	9009	4452	3223	44
C8	8283(1)	5238(2)	3226(1)	47(1)
D4	8185	4465	2720	56
C9	7938(1)	6369(2)	3659(1)	48(1)
D5	7601	6380	3452	57
C10	8084(1)	7482(2)	4392(1)	44(1)
D6	7848	8271	4688	53
C11	8571(1)	7463(2)	4701(1)	34(1)
D7	8666	8229	5213	41

Table A0.30. Bond lengths (Å) and angles (°) for **2.1** at 200 K.

Atoms	Length	Atoms	Angle	Atoms	Angle
C(1)-C(2)	1.3524(18)	C(2)-C(1)-C(1)#1	120.11(8)	C(9)-C(8)-D(4)	119.9
C(1)-C(1)#1	1.416(3)	C(2)-C(1)-D(1)	119.9	C(7)-C(8)-D(4)	119.9
C(1)-D(1)	0.95	C(1)#1-C(1)-D(1)	119.9	C(10)-C(9)-C(8)	119.40(12)
C(2)-C(3)	1.4331(17)	C(1)-C(2)-C(3)	122.20(12)	C(10)-C(9)-D(5)	120.3
C(2)-D(2)	0.95	C(1)-C(2)-D(2)	118.9	C(8)-C(9)-D(5)	120.3
C(3)-C(4)	1.4007(16)	C(3)-C(2)-D(2)	118.9	C(9)-C(10)-C(11)	120.69(13)
C(3)-C(3)#1	1.441(2)	C(4)-C(3)-C(2)	122.02(11)	C(9)-C(10)-D(6)	119.7
C(4)-C(5)	1.4258(14)	C(4)-C(3)-C(3)#1	120.16(7)	C(11)-C(10)-D(6)	119.7
C(4)-C(6)	1.5023(16)	C(2)-C(3)-C(3)#1	117.68(7)	C(10)-C(11)-C(6)	120.68(13)
C(5)-C(4)#2	1.4258(14)	C(3)-C(4)-C(5)	120.52(11)	C(10)-C(11)-D(7)	119.7
C(5)-C(5)#3	1.468(3)	C(3)-C(4)-C(6)	115.91(10)	C(6)-C(11)-D(7)	119.7
C(6)-C(7)	1.3872(18)	C(5)-C(4)-C(6)	123.12(11)		
C(6)-C(11)	1.3918(17)	C(4)#2-C(5)-C(4)	122.10(15)		
C(7)-C(8)	1.3865(18)	C(4)#2-C(5)-C(5)#3	118.95(7)		
C(7)-D(3)	0.95	C(4)-C(5)-C(5)#3	118.95(7)		
C(8)-C(9)	1.378(2)	C(7)-C(6)-C(11)	118.07(12)		
C(8)-D(4)	0.95	C(7)-C(6)-C(4)	119.28(11)		
C(9)-C(10)	1.376(2)	C(11)-C(6)-C(4)	122.27(11)		
C(9)-D(5)	0.95	C(8)-C(7)-C(6)	121.03(13)		
C(10)-C(11)	1.3803(18)	C(8)-C(7)-D(3)	119.5		
C(10)-D(6)	0.95	C(6)-C(7)-D(3)	119.5		
C(11)-D(7)	0.95	C(9)-C(8)-C(7)	120.11(14)		

Symmetry transformations used to generate equivalent atoms: #1 -x+2,y,z #2 x,-y+1,-z+1 #3 -x+2,-y+1,-z+1

Table A0.31. Anisotropic displacement parameters ($Å^2$ x 10^3) for **2.1** at 200 K. The anisotropic displacement factor exponent takes the form: $-2\pi^2[h^2 a^{*2}U11 + ... + 2 h k a^* b^* U12]$.

Atom	U11	U22	U33	U23	U13	U12
C1	47(1)	27(1)	31(1)	5(1)	0(1)	6(1)
C2	36(1)	31(1)	28(1)	2(1)	2(1)	6(1)
C3	33(1)	25(1)	21(1)	-2(1)	0(1)	2(1)
C4	29(1)	25(1)	23(1)	-2(1)	1(1)	2(1)
C5	29(1)	25(1)	22(1)	-2(1)	0	0
C6	29(1)	28(1)	27(1)	5(1)	1(1)	2(1)
C7	37(1)	42(1)	30(1)	-1(1)	-1(1)	3(1)
C8	44(1)	60(1)	37(1)	1(1)	-11(1)	-7(1)
C9	29(1)	62(1)	52(1)	14(1)	-6(1)	-1(1)
C10	31(1)	45(1)	56(1)	9(1)	8(1)	6(1)
C11	33(1)	32(1)	38(1)	1(1)	5(1)	2(1)

Table A0.32. Torsion angles (°) for **2.1** at 200 K.

Atoms	Angle
C1#1-C1-C2-C3	1.25(14)
C1-C2-C3-C4	-176.87(11)
C1-C2-C3-C3#1	-1.22(14)
C2-C3-C4-C5	-177.38(9)
C3#1-C3-C4-C5	7.07(11)
C2-C3-C4-C6	10.08(16)
C3#1-C3-C4-C6	-165.47(7)
C3-C4-C5-C4#2	173.01(11)
C6-C4-C5-C4#2	-15.00(8)
C3-C4-C5-C5#3	-6.99(11)
C6-C4-C5-C5#3	164.99(8)
C3-C4-C6-C7	95.08(14)
C5-C4-C6-C7	-77.25(14)
C3-C4-C6-C11	-77.74(14)
C5-C4-C6-C11	109.93(13)
C11-C6-C7-C8	-0.3(2)
C4-C6-C7-C8	-173.43(12)
C6-C7-C8-C9	0.5(2)
C7-C8-C9-C10	-0.1(2)
C8-C9-C10-C11	-0.5(2)
C9-C10-C11-C6	0.8(2)
C7-C6-C11-C10	-0.32(19)

C4-C6-C11-C10	172.59(12)

Symmetry transformations used to generate equivalent atoms: #1 -x+2,y,z #2 x,-y+1,-z+1 #3 -x+2,-y+1,-z+1

Crystal Structure Report for **2.1** at 250 K (project code: 13065)

Data collection: A crystal (approximate dimensions 0.20 x 0.16 x 0.03 mm^3) was placed onto the tip of a 0.1 mm diameter glass capillary and mounted on a Bruker Photon CCD diffractometer for a data collection at 250(2) K.[1] A preliminary set of cell constants was calculated from reflections harvested from three sets of 12 frames. These initial sets of frames were oriented such that orthogonal wedges of reciprocal space were surveyed. This produced initial orientation matrices determined from 150 reflections. The data collection was carried out using MoKα radiation (graphite monochromator) with a frame time of 30 seconds and a detector distance of 6.0 cm. A randomly oriented region of reciprocal space was surveyed to the extent of one sphere and to a resolution of 0.77 Å. Four major sections of frames were collected with 0.30º steps in ω at four different ϕ settings and a detector position of -28º in 2θ. The intensity data were corrected for absorption and decay (SADABS).[2] Final cell constants were calculated from the xyz centroids of 2987 strong reflections from the actual data collection after integration (SAINT).[3] Please refer to Table 1 for additional crystal and refinement information.

Structure solution and refinement: The structure was solved using SHELXS-97[4] and refined using SHELXL-97.[4] The space group Cmca was determined based on systematic absences and intensity statistics. A direct-methods solution was calculated which provided most non-hydrogen atoms from the E-map. Full-matrix least squares / difference Fourier cycles were performed which located the remaining non-hydrogen atoms. All non-hydrogen atoms were refined with anisotropic displacement parameters. All hydrogen atoms were placed in ideal positions and refined as riding atoms with relative isotropic displacement parameters. The final full matrix least squares refinement converged to $R1 = 0.0387$ and $wR2 = 0.1034$ (F^2, all data).

Table A0.33. Atomic coordinates (x 10^4) and equivalent isotropic displacement parameters ($Å^2$x 10^3) for **2.1** at 250 K. Ueq is defined as one third of the trace of the orthogonalized Uij tensor.

Atom	x	y	z	Ueq
C1	9737(1)	-846(2)	6750(1)	43(1)
D1	9563	-1825	7037	52
C2	9485(1)	555(2)	6340(1)	38(1)
D2	9135	543	6357	46
C3	9732(1)	2064(2)	5877(1)	32(1)
C4	9470(1)	3567(2)	5490(1)	31(1)
C5	9727(1)	5000	5000	30(1)
C6	8927(1)	3671(2)	5728(1)	33(1)
C7	8776(1)	4774(2)	6466(1)	44(1)
D3	9009	5541	6767	53
C8	8286(1)	4768(3)	6768(1)	59(1)
D4	8190	5533	7267	70
C9	7941(1)	3639(3)	6338(1)	60(1)
D5	7609	3626	6542	72
C10	8087(1)	2536(2)	5611(1)	55(1)
D6	7853	1761	5317	65

C11	8573(1)	2547(2)	5303(1)	42(1)
D7	8665	1786	4799	50

Table A0.34. Bond lengths (Å) and angles (°) for **2.1** at 250 K.

Atoms	Length	Atoms	Angle	Atoms	Angle
C(1)-C(2)	1.3483(19)	C(2)-C(1)-C(1)#1	120.17(8)	C(9)-C(8)-D(4)	120
C(1)-C(1)#1	1.413(3)	C(2)-C(1)-D(1)	119.9	C(7)-C(8)-D(4)	120
C(1)-D(1)	0.94	C(1)#1-C(1)-D(1)	119.9	C(10)-C(9)-C(8)	119.36(14)
C(2)-C(3)	1.4338(18)	C(1)-C(2)-C(3)	122.21(13)	C(10)-C(9)-D(5)	120.3
C(2)-D(2)	0.94	C(1)-C(2)-D(2)	118.9	C(8)-C(9)-D(5)	120.3
C(3)-C(4)	1.4029(17)	C(3)-C(2)-D(2)	118.9	C(9)-C(10)-C(11)	120.89(15)
C(3)-C(3)#1	1.439(2)	C(4)-C(3)-C(2)	122.09(12)	C(9)-C(10)-D(6)	119.6
C(4)-C(5)	1.4250(14)	C(4)-C(3)-C(3)#1	120.16(7)	C(11)-C(10)-D(6)	119.6
C(4)-C(6)	1.5018(18)	C(2)-C(3)-C(3)#1	117.61(8)	C(10)-C(11)-C(6)	120.64(14)
C(5)-C(4)#2	1.4251(14)	C(3)-C(4)-C(5)	120.46(12)	C(10)-C(11)-D(7)	119.7
C(5)-C(5)#3	1.467(3)	C(3)-C(4)-C(6)	115.86(11)	C(6)-C(11)-D(7)	119.7
C(6)-C(7)	1.3851(19)	C(5)-C(4)-C(6)	123.24(12)		
C(6)-C(11)	1.3885(18)	C(4)-C(5)-C(4)#2	122.01(15)		
C(7)-C(8)	1.384(2)	C(4)-C(5)-C(5)#3	118.99(8)		
C(7)-D(3)	0.94	C(4)#2-C(5)-C(5)#3	119.00(8)		
C(8)-C(9)	1.378(2)	C(7)-C(6)-C(11)	117.99(13)		
C(8)-D(4)	0.94	C(7)-C(6)-C(4)	119.23(12)		
C(9)-C(10)	1.369(2)	C(11)-C(6)-C(4)	122.41(12)		
C(9)-D(5)	0.94	C(8)-C(7)-C(6)	121.11(15)		
C(10)-C(11)	1.3781(19)	C(8)-C(7)-D(3)	119.4		
C(10)-D(6)	0.94	C(6)-C(7)-D(3)	119.4		
C(11)-D(7)	0.94	C(9)-C(8)-C(7)	120.00(16)		

Symmetry transformations used to generate equivalent atoms: #1 -x+2,y,z #2 x,-y+1,-z+1 #3 -x+2,-y+1,-z+1

Table A0.35. Anisotropic displacement parameters ($Å^2$ x 10^3) for **2.1** at 250 K. The anisotropic displacement factor exponent takes the form: $-2\pi^2[h^2 a^{*2}U11 + ... + 2 h k a^* b^* U12]$.

Atom	U11	U22	U33	U23	U13	U12
C1	56(1)	34(1)	39(1)	7(1)	0(1)	-7(1)
C2	43(1)	36(1)	36(1)	5(1)	-3(1)	-7(1)
C3	38(1)	30(1)	27(1)	-1(1)	0(1)	-2(1)
C4	34(1)	30(1)	29(1)	-1(1)	-2(1)	-2(1)
C5	33(1)	28(1)	28(1)	-1(1)	0	0
C6	34(1)	33(1)	33(1)	6(1)	-1(1)	-2(1)
C7	43(1)	52(1)	38(1)	-3(1)	2(1)	-3(1)

C8	53(1)	77(1)	46(1)	1(1)	14(1)	9(1)
C9	34(1)	79(1)	68(1)	18(1)	8(1)	0(1)
C10	37(1)	57(1)	70(1)	10(1)	-10(1)	-9(1)
C11	38(1)	40(1)	48(1)	2(1)	-6(1)	-4(1)

Table A0.36. Torsion angles (°) for **2.1** at 250 K.

Atoms	Angle
C1#1-C1-C2-C3	1.22(15)
C1-C2-C3-C4	-176.81(12)
C1-C2-C3-C3#1	-1.19(15)
C2-C3-C4-C5	-177.28(10)
C3#1-C3-C4-C5	7.21(12)
C2-C3-C4-C6	10.04(17)
C3#1-C3-C4-C6	-165.47(7)
C3-C4-C5-C4#2	172.87(12)
C6-C4-C5-C4#2	-15.01(8)
C3-C4-C5-C5#3	-7.13(12)
C6-C4-C5-C5#3	164.99(8)
C3-C4-C6-C7	95.04(15)
C5-C4-C6-C7	-77.42(15)
C3-C4-C6-C11	-77.77(16)
C5-C4-C6-C11	109.77(14)
C11-C6-C7-C8	-0.4(2)
C4-C6-C7-C8	-173.50(14)
C6-C7-C8-C9	0.5(3)
C7-C8-C9-C10	-0.2(3)
C8-C9-C10-C11	-0.2(3)
C9-C10-C11-C6	0.4(2)
C7-C6-C11-C10	-0.1(2)
C4-C6-C11-C10	172.79(13)

Symmetry transformations used to generate equivalent atoms: #1 -x+2,y,z #2 x,-y+1,-z+1 #3 -x+2,-y+1,-z+1

A1.2. CHAPTER 3 CRYSTAL STRUCTURES

Crystal Structure Report for **3.1a** (project code: 10132)

Data collection: A crystal (approximate dimensions 0.45 x 0.30 x 0.20 mm^3) was placed onto the tip of a 0.1 mm diameter glass capillary and mounted on a Siemens SMART Platform CCD diffractometer for a data collection at 173(2) K.[1] A preliminary set of cell constants was calculated from reflections harvested from three sets of 20 frames. These initial sets of frames were oriented such that orthogonal wedges of reciprocal space were surveyed. This

produced initial orientation matrices determined from 99 reflections. The data collection was carried out using MoKα radiation (graphite monochromator) with a frame time of 60 seconds and a detector distance of 4.8 cm. A randomly oriented region of reciprocal space was surveyed to the extent of one sphere and to a resolution of 0.84 Å. Four major sections of frames were collected with 0.30º steps in ω at four different ϕ settings and a detector position of -28º in 2θ. The intensity data were corrected for absorption and decay (SADABS).[2] Final cell constants were calculated from the xyz centroids of 4043 strong reflections from the actual data collection after integration (SAINT).[3] Please refer to Table 1 for additional crystal and refinement information.

Structure solution and refinement: The structure was solved using SHELXS-97[4] and refined using SHELXL-97.[4] The space group C2/c was determined based on systematic absences and intensity statistics. A direct-methods solution was calculated which provided most non-hydrogen atoms from the E-map. Full-matrix least squares / difference Fourier cycles were performed which located the remaining non-hydrogen atoms. All non-hydrogen atoms were refined with anisotropic displacement parameters. All hydrogen atoms were placed in ideal positions and refined as riding atoms with relative isotropic displacement parameters. The final full matrix least squares refinement converged to $R1$ = 0.0475 and $wR2$ = 0.1131 (F^2, all data).

Crystal and structure description: Twelve molecules exist in the unit cell. Of those twelve, 1.5 molecules are unique, indicating that one molecule lies on a general position and another lies on a special position, a symmetry element (2-fold rotation, symmetry operation: −x,y,1/2−z). Torsion angles for each ring in the tetracene backbone were calculated as well as the torsion angle across the entire tetracene backbone. [5] For the molecule on a general position, the angles for each ring are: 4.7, 12.7, 12.5, and 4.0 degrees. The torsion angle of the entire backbone is 33.9 degrees. For the molecule on a special position, the angles for each ring are: 6.3, 15.1, 15.2, and 6.3 degrees. The torsion angle of the entire backbone is 42.8 degrees.

Table A0.37. Atomic coordinates (x 10^4) and equivalent isotropic displacement parameters (Å^2 x 10^3) for **3.1a**. Ueq is defined as one third of the trace of the orthogonalized Uij tensor.

Atom	x	y	z	Ueq
C1	1849(1)	3168(2)	2291(1)	35(1)
C2	1902(1)	3137(2)	2875(1)	36(1)
C3	2046(1)	4214(2)	3200(1)	42(1)
C4	2106(1)	4150(2)	3764(1)	48(1)
C5	2030(1)	2998(2)	4053(1)	47(1)
C6	1886(1)	1965(2)	3767(1)	43(1)
C7	1803(1)	2003(2)	3173(1)	35(1)
C8	1613(1)	1021(2)	2886(1)	34(1)
C9	1529(1)	1105(2)	2296(1)	34(1)
C10	1292(1)	272(2)	1991(1)	35(1)
C11	1272(1)	227(2)	1407(1)	36(1)
C12	1042(1)	-613(2)	1084(1)	47(1)
C13	1050(1)	-780(2)	529(1)	55(1)
C14	1284(1)	-124(2)	249(1)	54(1)
C15	1495(1)	732(2)	528(1)	46(1)
C16	1492(1)	982(2)	1114(1)	38(1)
C17	1695(1)	1924(2)	1402(1)	35(1)
C18	1694(1)	2083(2)	1991(1)	34(1)

C19	1912(1)	4429(2)	2000(1)	37(1)
C20	1646(1)	5159(2)	1766(1)	40(1)
C21	1688(1)	6361(2)	1516(1)	49(1)
C22	1994(1)	6881(2)	1492(1)	55(1)
C23	2261(1)	6155(2)	1727(1)	55(1)
C24	2221(1)	4952(2)	1979(1)	44(1)
C25	1524(1)	-155(2)	3210(1)	37(1)
C26	1284(1)	-100(2)	3565(1)	48(1)
C27	1217(1)	-1184(2)	3874(1)	60(1)
C28	1390(1)	-2345(2)	3856(1)	59(1)
C29	1626(1)	-2401(2)	3500(1)	58(1)
C30	1694(1)	-1319(2)	3180(1)	47(1)
C31	1041(1)	-443(2)	2275(1)	35(1)
C32	1040(1)	-1803(2)	2343(1)	41(1)
C33	801(1)	-2411(2)	2606(1)	48(1)
C34	552(1)	-1705(2)	2802(1)	48(1)
C35	546(1)	-358(2)	2715(1)	55(1)
C36	788(1)	263(2)	2460(1)	46(1)
C37	1941(1)	2618(2)	1100(1)	39(1)
C38	1859(1)	3559(2)	688(1)	46(1)
C39	2093(1)	4151(2)	410(1)	50(1)
C40	2420(1)	3826(2)	529(1)	47(1)
C41	2501(1)	2876(2)	931(1)	49(1)
C42	2267(1)	2279(2)	1215(1)	45(1)
C43	2037(1)	8191(3)	1210(1)	98(1)
C44	1315(1)	-3499(3)	4212(1)	94(1)
C45	303(1)	-2391(3)	3111(1)	76(1)
C46	2677(1)	4484(2)	230(1)	67(1)
C47	410(1)	3727(2)	2245(1)	33(1)
C48	612(1)	3697(2)	2754(1)	34(1)
C49	953(1)	4001(2)	2796(1)	40(1)
C50	1150(1)	3851(2)	3281(1)	44(1)
C51	1027(1)	3343(2)	3760(1)	44(1)
C52	705(1)	3080(2)	3751(1)	40(1)
C53	481(1)	3326(2)	3259(1)	34(1)
C54	143(1)	3247(2)	3265(1)	34(1)
C55	-69(1)	3476(2)	2763(1)	33(1)
C56	548(1)	4173(2)	1730(1)	33(1)

C57	758(1)	3410(2)	1455(1)	37(1)
C58	876(1)	3863(2)	977(1)	40(1)
C59	796(1)	5103(2)	761(1)	40(1)
C60	595(1)	5876(2)	1045(1)	41(1)
C61	471(1)	5423(2)	1520(1)	38(1)
C62	13(1)	2789(2)	3785(1)	37(1)
C63	-129(1)	1552(2)	3797(1)	44(1)
C64	-247(1)	1093(2)	4273(1)	54(1)
C65	-230(1)	1841(3)	4753(1)	57(1)
C66	-80(1)	3059(2)	4748(1)	55(1)
C67	41(1)	3527(2)	4274(1)	45(1)
C68	920(1)	5573(2)	233(1)	62(1)
C69	-379(1)	1366(3)	5264(1)	91(1)

Table A0.38. Bond lengths (Å) and angles (°) for **3.1a.**

Bond	Length	Atoms	Angle	Atoms	Angle
C(1)-C(2)	1.398(3)	C(2)-C(1)-C(18)	119.88(16)	C(28)-C(44)-H(44C)	109.5
C(1)-C(18)	1.424(3)	C(2)-C(1)-C(19)	118.31(17)	H(44A)-C(44)-H(44C)	109.5
C(1)-C(19)	1.496(2)	C(18)-C(1)-C(19)	121.18(16)	H(44B)-C(44)-H(44C)	109.5
C(2)-C(3)	1.431(3)	C(1)-C(2)-C(3)	122.45(17)	C(34)-C(45)-H(45A)	109.5
C(2)-C(7)	1.439(3)	C(1)-C(2)-C(7)	119.86(17)	C(34)-C(45)-H(45B)	109.5
C(3)-C(4)	1.353(3)	C(3)-C(2)-C(7)	117.67(17)	H(45A)-C(45)-H(45B)	109.5
C(3)-H(3A)	0.95	C(4)-C(3)-C(2)	121.73(18)	C(34)-C(45)-H(45C)	109.5
C(4)-C(5)	1.413(3)	C(4)-C(3)-H(3A)	119.1	H(45A)-C(45)-H(45C)	109.5
C(4)-H(4A)	0.95	C(2)-C(3)-H(3A)	119.1	H(45B)-C(45)-H(45C)	109.5
C(5)-C(6)	1.353(3)	C(3)-C(4)-C(5)	120.47(19)	C(40)-C(46)-H(46A)	109.5
C(5)-H(5A)	0.95	C(3)-C(4)-H(4A)	119.8	C(40)-C(46)-H(46B)	109.5
C(6)-C(7)	1.430(3)	C(5)-C(4)-H(4A)	119.8	H(46A)-C(46)-H(46B)	109.5
C(6)-H(6A)	0.95	C(6)-C(5)-C(4)	120.09(19)	C(40)-C(46)-H(46C)	109.5
C(7)-C(8)	1.398(3)	C(6)-C(5)-H(5A)	120	H(46A)-C(46)-H(46C)	109.5
C(8)-C(9)	1.422(2)	C(4)-C(5)-H(5A)	120	H(46B)-C(46)-H(46C)	109.5
C(8)-C(25)	1.493(2)	C(5)-C(6)-C(7)	121.75(19)	C(48)-C(47)-C(55)#1	119.49(16)
C(9)-C(10)	1.428(2)	C(5)-C(6)-H(6A)	119.1	C(48)-C(47)-C(56)	119.26(16)
C(9)-C(18)	1.449(2)	C(7)-C(6)-H(6A)	119.1	C(55)#1-C(47)-C(56)	120.87(16)
C(10)-C(11)	1.398(2)	C(8)-C(7)-C(6)	121.91(17)	C(47)-C(48)-C(49)	122.35(17)
C(10)-C(31)	1.494(2)	C(8)-C(7)-C(2)	120.00(16)	C(47)-C(48)-C(53)	120.03(16)
C(11)-C(16)	1.433(3)	C(6)-C(7)-C(2)	117.97(17)	C(49)-C(48)-C(53)	117.61(17)
C(11)-C(12)	1.434(3)	C(7)-C(8)-C(9)	120.38(16)	C(50)-C(49)-C(48)	121.47(18)

C(12)-C(13)	1.349(3)	C(7)-C(8)-C(25)	117.99(16)	C(50)-C(49)-H(49A)	119.3
C(12)-H(12A)	0.95	C(9)-C(8)-C(25)	121.47(16)	C(48)-C(49)-H(49A)	119.3
C(13)-C(14)	1.409(3)	C(8)-C(9)-C(10)	123.18(16)	C(49)-C(50)-C(51)	120.62(18)
C(13)-H(13A)	0.95	C(8)-C(9)-C(18)	118.10(16)	C(49)-C(50)-H(50A)	119.7
C(14)-C(15)	1.350(3)	C(10)-C(9)-C(18)	118.72(16)	C(51)-C(50)-H(50A)	119.7
C(14)-H(14A)	0.95	C(11)-C(10)-C(9)	119.36(16)	C(52)-C(51)-C(50)	120.41(18)
C(15)-C(16)	1.433(3)	C(11)-C(10)-C(31)	118.73(16)	C(52)-C(51)-H(51A)	119.8
C(15)-H(15A)	0.95	C(9)-C(10)-C(31)	121.56(16)	C(50)-C(51)-H(51A)	119.8
C(16)-C(17)	1.398(3)	C(10)-C(11)-C(16)	120.67(17)	C(51)-C(52)-C(53)	121.11(18)
C(17)-C(18)	1.427(2)	C(10)-C(11)-C(12)	121.37(17)	C(51)-C(52)-H(52A)	119.4
C(17)-C(37)	1.493(2)	C(16)-C(11)-C(12)	117.91(17)	C(53)-C(52)-H(52A)	119.4
C(19)-C(20)	1.386(3)	C(13)-C(12)-C(11)	121.3(2)	C(54)-C(53)-C(48)	120.01(16)
C(19)-C(24)	1.388(3)	C(13)-C(12)-H(12A)	119.3	C(54)-C(53)-C(52)	121.93(17)
C(20)-C(21)	1.379(3)	C(11)-C(12)-H(12A)	119.3	C(48)-C(53)-C(52)	118.04(16)
C(20)-H(20A)	0.95	C(12)-C(13)-C(14)	120.6(2)	C(53)-C(54)-C(55)	119.67(16)
C(21)-C(22)	1.378(3)	C(12)-C(13)-H(13A)	119.7	C(53)-C(54)-C(62)	118.92(16)
C(21)-H(21A)	0.95	C(14)-C(13)-H(13A)	119.7	C(55)-C(54)-C(62)	121.10(16)
C(22)-C(23)	1.387(3)	C(15)-C(14)-C(13)	120.38(19)	C(54)-C(55)-C(47)#1	123.08(16)
C(22)-C(43)	1.511(3)	C(15)-C(14)-H(14A)	119.8	C(54)-C(55)-C(55)#1	118.40(19)
C(23)-C(24)	1.380(3)	C(13)-C(14)-H(14A)	119.8	C(47)#1-C(55)-C(55)#1	118.5(2)
C(23)-H(23A)	0.95	C(14)-C(15)-C(16)	121.5(2)	C(57)-C(56)-C(61)	117.86(17)
C(24)-H(24A)	0.95	C(14)-C(15)-H(15A)	119.3	C(57)-C(56)-C(47)	123.05(16)
C(25)-C(30)	1.380(3)	C(16)-C(15)-H(15A)	119.3	C(61)-C(56)-C(47)	119.06(16)
C(25)-C(26)	1.381(3)	C(17)-C(16)-C(11)	119.91(17)	C(58)-C(57)-C(56)	120.82(18)
C(26)-C(27)	1.375(3)	C(17)-C(16)-C(15)	122.19(18)	C(58)-C(57)-H(57A)	119.6
C(26)-H(26A)	0.95	C(11)-C(16)-C(15)	117.90(18)	C(56)-C(57)-H(57A)	119.6
C(27)-C(28)	1.380(3)	C(16)-C(17)-C(18)	119.88(16)	C(57)-C(58)-C(59)	121.54(18)
C(27)-H(27A)	0.95	C(16)-C(17)-C(37)	118.97(16)	C(57)-C(58)-H(58A)	119.2
C(28)-C(29)	1.373(3)	C(18)-C(17)-C(37)	120.62(17)	C(59)-C(58)-H(58A)	119.2
C(28)-C(44)	1.502(3)	C(1)-C(18)-C(17)	122.43(16)	C(60)-C(59)-C(58)	117.43(17)
C(29)-C(30)	1.389(3)	C(1)-C(18)-C(9)	118.91(16)	C(60)-C(59)-C(68)	121.55(19)
C(29)-H(29A)	0.95	C(17)-C(18)-C(9)	118.66(16)	C(58)-C(59)-C(68)	121.02(18)
C(30)-H(30A)	0.95	C(20)-C(19)-C(24)	117.85(18)	C(59)-C(60)-C(61)	121.49(18)
C(31)-C(36)	1.383(3)	C(20)-C(19)-C(1)	118.27(16)	C(59)-C(60)-H(60A)	119.3
C(31)-C(32)	1.390(3)	C(24)-C(19)-C(1)	123.77(17)	C(61)-C(60)-H(60A)	119.3
C(32)-C(33)	1.379(3)	C(21)-C(20)-C(19)	121.11(18)	C(60)-C(61)-C(56)	120.81(18)
C(32)-H(32A)	0.95	C(21)-C(20)-H(20A)	119.4	C(60)-C(61)-H(61A)	119.6
C(33)-C(34)	1.381(3)	C(19)-C(20)-H(20A)	119.4	C(56)-C(61)-H(61A)	119.6

C(33)-H(33A)	0.95	C(22)-C(21)-C(20)	121.23(19)	C(67)-C(62)-C(63)	117.62(18)
C(34)-C(35)	1.382(3)	C(22)-C(21)-H(21A)	119.4	C(67)-C(62)-C(54)	122.74(18)
C(34)-C(45)	1.508(3)	C(20)-C(21)-H(21A)	119.4	C(63)-C(62)-C(54)	119.58(17)
C(35)-C(36)	1.382(3)	C(21)-C(22)-C(23)	117.76(19)	C(64)-C(63)-C(62)	121.0(2)
C(35)-H(35A)	0.95	C(21)-C(22)-C(43)	120.8(2)	C(64)-C(63)-H(63A)	119.5
C(36)-H(36A)	0.95	C(23)-C(22)-C(43)	121.5(2)	C(62)-C(63)-H(63A)	119.5
C(37)-C(42)	1.386(3)	C(24)-C(23)-C(22)	121.38(19)	C(65)-C(64)-C(63)	121.5(2)
C(37)-C(38)	1.390(3)	C(24)-C(23)-H(23A)	119.3	C(65)-C(64)-H(64A)	119.3
C(38)-C(39)	1.377(3)	C(22)-C(23)-H(23A)	119.3	C(63)-C(64)-H(64A)	119.3
C(38)-H(38A)	0.95	C(23)-C(24)-C(19)	120.66(19)	C(64)-C(65)-C(66)	117.8(2)
C(39)-C(40)	1.384(3)	C(23)-C(24)-H(24A)	119.7	C(64)-C(65)-C(69)	121.2(2)
C(39)-H(39A)	0.95	C(19)-C(24)-H(24A)	119.7	C(66)-C(65)-C(69)	121.0(2)
C(40)-C(41)	1.379(3)	C(30)-C(25)-C(26)	118.17(18)	C(67)-C(66)-C(65)	121.2(2)
C(40)-C(46)	1.506(3)	C(30)-C(25)-C(8)	119.94(17)	C(67)-C(66)-H(66A)	119.4
C(41)-C(42)	1.385(3)	C(26)-C(25)-C(8)	121.81(17)	C(65)-C(66)-H(66A)	119.4
C(41)-H(41A)	0.95	C(27)-C(26)-C(25)	120.5(2)	C(66)-C(67)-C(62)	120.9(2)
C(42)-H(42A)	0.95	C(27)-C(26)-H(26A)	119.8	C(66)-C(67)-H(67A)	119.6
C(43)-H(43A)	0.98	C(25)-C(26)-H(26A)	119.8	C(62)-C(67)-H(67A)	119.6
C(43)-H(43B)	0.98	C(26)-C(27)-C(28)	121.9(2)	C(59)-C(68)-H(68A)	109.5
C(43)-H(43C)	0.98	C(26)-C(27)-H(27A)	119	C(59)-C(68)-H(68B)	109.5
C(44)-H(44A)	0.98	C(28)-C(27)-H(27A)	119	H(68A)-C(68)-H(68B)	109.5
C(44)-H(44B)	0.98	C(29)-C(28)-C(27)	117.5(2)	C(59)-C(68)-H(68C)	109.5
C(44)-H(44C)	0.98	C(29)-C(28)-C(44)	122.0(3)	H(68A)-C(68)-H(68C)	109.5
C(45)-H(45A)	0.98	C(27)-C(28)-C(44)	120.4(3)	H(68B)-C(68)-H(68C)	109.5
C(45)-H(45B)	0.98	C(28)-C(29)-C(30)	121.2(2)	C(65)-C(69)-H(69A)	109.5
C(45)-H(45C)	0.98	C(28)-C(29)-H(29A)	119.4	C(65)-C(69)-H(69B)	109.5
C(46)-H(46A)	0.98	C(30)-C(29)-H(29A)	119.4	H(69A)-C(69)-H(69B)	109.5
C(46)-H(46B)	0.98	C(25)-C(30)-C(29)	120.7(2)	C(65)-C(69)-H(69C)	109.5
C(46)-H(46C)	0.98	C(25)-C(30)-H(30A)	119.6	H(69A)-C(69)-H(69C)	109.5
C(47)-C(48)	1.398(2)	C(29)-C(30)-H(30A)	119.6	H(69B)-C(69)-H(69C)	109.5
C(47)-C(55)#1	1.429(2)	C(36)-C(31)-C(32)	117.64(18)		
C(47)-C(56)	1.493(2)	C(36)-C(31)-C(10)	119.16(17)		
C(48)-C(49)	1.434(2)	C(32)-C(31)-C(10)	123.14(17)		
C(48)-C(53)	1.435(2)	C(33)-C(32)-C(31)	120.64(19)		
C(49)-C(50)	1.349(3)	C(33)-C(32)-H(32A)	119.7		
C(49)-H(49A)	0.95	C(31)-C(32)-H(32A)	119.7		
C(50)-C(51)	1.410(3)	C(32)-C(33)-C(34)	121.74(19)		
C(50)-H(50A)	0.95	C(32)-C(33)-H(33A)	119.1		

C(51)-C(52)	1.352(3)	C(34)-C(33)-H(33A)	119.1
C(51)-H(51A)	0.95	C(33)-C(34)-C(35)	117.57(19)
C(52)-C(53)	1.436(3)	C(33)-C(34)-C(45)	120.4(2)
C(52)-H(52A)	0.95	C(35)-C(34)-C(45)	122.0(2)
C(53)-C(54)	1.397(2)	C(34)-C(35)-C(36)	121.1(2)
C(54)-C(55)	1.424(2)	C(34)-C(35)-H(35A)	119.5
C(54)-C(62)	1.490(2)	C(36)-C(35)-H(35A)	119.5
C(55)-C(47)#1	1.429(2)	C(35)-C(36)-C(31)	121.28(19)
C(55)-C(55)#1	1.444(3)	C(35)-C(36)-H(36A)	119.4
C(56)-C(57)	1.387(2)	C(31)-C(36)-H(36A)	119.4
C(56)-C(61)	1.388(3)	C(42)-C(37)-C(38)	117.57(18)
C(57)-C(58)	1.379(3)	C(42)-C(37)-C(17)	119.16(17)
C(57)-H(57A)	0.95	C(38)-C(37)-C(17)	123.21(17)
C(58)-C(59)	1.387(3)	C(39)-C(38)-C(37)	121.3(2)
C(58)-H(58A)	0.95	C(39)-C(38)-H(38A)	119.4
C(59)-C(60)	1.381(3)	C(37)-C(38)-H(38A)	119.4
C(59)-C(68)	1.500(3)	C(38)-C(39)-C(40)	121.2(2)
C(60)-C(61)	1.383(3)	C(38)-C(39)-H(39A)	119.4
C(60)-H(60A)	0.95	C(40)-C(39)-H(39A)	119.4
C(61)-H(61A)	0.95	C(41)-C(40)-C(39)	117.56(18)
C(62)-C(67)	1.387(3)	C(41)-C(40)-C(46)	121.2(2)
C(62)-C(63)	1.387(3)	C(39)-C(40)-C(46)	121.3(2)
C(63)-C(64)	1.376(3)	C(40)-C(41)-C(42)	121.7(2)
C(63)-H(63A)	0.95	C(40)-C(41)-H(41A)	119.2
C(64)-C(65)	1.375(3)	C(42)-C(41)-H(41A)	119.2
C(64)-H(64A)	0.95	C(41)-C(42)-C(37)	120.70(19)
C(65)-C(66)	1.383(3)	C(41)-C(42)-H(42A)	119.6
C(65)-C(69)	1.515(3)	C(37)-C(42)-H(42A)	119.6
C(66)-C(67)	1.380(3)	C(22)-C(43)-H(43A)	109.5
C(66)-H(66A)	0.95	C(22)-C(43)-H(43B)	109.5
C(67)-H(67A)	0.95	H(43A)-C(43)-H(43B)	109.5
C(68)-H(68A)	0.98	C(22)-C(43)-H(43C)	109.5
C(68)-H(68B)	0.98	H(43A)-C(43)-H(43C)	109.5
C(68)-H(68C)	0.98	H(43B)-C(43)-H(43C)	109.5
C(69)-H(69A)	0.98	C(28)-C(44)-H(44A)	109.5
C(69)-H(69B)	0.98	C(28)-C(44)-H(44B)	109.5
C(69)-H(69C)	0.98	H(44A)-C(44)-H(44B)	109.5

Symmetry transformations used to generate equivalent atoms: #1 -x,y,-z+1/2

Table A0.39. Anisotropic displacement parameters ($Å^2$ x 10^3) for **3.1a**. The anisotropic displacement factor exponent takes the form: $-2\pi^2[h^2 a^{*2}U11 + ... + 2 h k a^* b^* U12]$.

Atom	U11	U22	U33	U23	U13	U12
C1	30(1)	34(1)	43(1)	6(1)	10(1)	1(1)
C2	29(1)	35(1)	44(1)	3(1)	7(1)	2(1)
C3	39(1)	37(1)	51(1)	3(1)	5(1)	-4(1)
C4	44(1)	43(1)	54(1)	-6(1)	0(1)	-5(1)
C5	48(1)	49(1)	44(1)	1(1)	-1(1)	-4(1)
C6	44(1)	41(1)	42(1)	5(1)	2(1)	0(1)
C7	31(1)	36(1)	40(1)	3(1)	5(1)	3(1)
C8	33(1)	32(1)	39(1)	3(1)	8(1)	3(1)
C9	35(1)	31(1)	37(1)	3(1)	11(1)	4(1)
C10	38(1)	28(1)	39(1)	3(1)	7(1)	2(1)
C11	39(1)	31(1)	39(1)	3(1)	5(1)	3(1)
C12	55(1)	43(1)	42(1)	3(1)	4(1)	-8(1)
C13	75(2)	50(1)	40(1)	-1(1)	-1(1)	-9(1)
C14	79(2)	49(1)	35(1)	2(1)	6(1)	-2(1)
C15	57(1)	43(1)	38(1)	9(1)	10(1)	7(1)
C16	42(1)	35(1)	37(1)	7(1)	8(1)	7(1)
C17	33(1)	32(1)	40(1)	6(1)	9(1)	7(1)
C18	31(1)	34(1)	39(1)	5(1)	7(1)	4(1)
C19	34(1)	34(1)	44(1)	3(1)	10(1)	0(1)
C20	32(1)	40(1)	51(1)	6(1)	13(1)	-1(1)
C21	40(1)	42(1)	67(1)	13(1)	13(1)	8(1)
C22	47(1)	39(1)	83(2)	16(1)	21(1)	1(1)
C23	36(1)	44(1)	87(2)	12(1)	16(1)	-6(1)
C24	32(1)	41(1)	60(1)	8(1)	9(1)	1(1)
C25	44(1)	34(1)	31(1)	2(1)	2(1)	-4(1)
C26	66(2)	41(1)	39(1)	-7(1)	17(1)	-12(1)
C27	90(2)	57(2)	35(1)	-7(1)	19(1)	-34(1)
C28	88(2)	46(2)	37(1)	10(1)	-12(1)	-29(1)
C29	63(2)	40(1)	65(2)	15(1)	-14(1)	-6(1)
C30	45(1)	41(1)	54(1)	9(1)	2(1)	-2(1)
C31	39(1)	31(1)	35(1)	1(1)	5(1)	-3(1)
C32	51(1)	35(1)	40(1)	0(1)	8(1)	-4(1)
C33	63(2)	37(1)	42(1)	1(1)	5(1)	-15(1)
C34	45(1)	59(2)	41(1)	4(1)	5(1)	-18(1)
C35	43(1)	64(2)	59(1)	5(1)	17(1)	3(1)

C36	47(1)	38(1)	54(1)	5(1)	13(1)	2(1)
C37	37(1)	41(1)	39(1)	3(1)	11(1)	4(1)
C38	42(1)	52(1)	45(1)	9(1)	8(1)	1(1)
C39	56(2)	54(1)	40(1)	9(1)	12(1)	-11(1)
C40	50(1)	54(1)	39(1)	-11(1)	17(1)	-16(1)
C41	36(1)	59(1)	54(1)	-12(1)	13(1)	0(1)
C42	43(1)	47(1)	46(1)	1(1)	11(1)	6(1)
C43	71(2)	59(2)	166(3)	56(2)	30(2)	2(1)
C44	156(3)	67(2)	53(2)	23(1)	-14(2)	-54(2)
C45	68(2)	101(2)	60(2)	13(2)	16(1)	-35(2)
C46	69(2)	77(2)	59(2)	-18(1)	29(1)	-32(1)
C47	32(1)	30(1)	39(1)	-2(1)	10(1)	3(1)
C48	31(1)	32(1)	39(1)	-4(1)	10(1)	2(1)
C49	32(1)	42(1)	47(1)	-5(1)	11(1)	0(1)
C50	31(1)	48(1)	54(1)	-10(1)	5(1)	1(1)
C51	37(1)	50(1)	43(1)	-7(1)	-2(1)	5(1)
C52	39(1)	43(1)	38(1)	-3(1)	5(1)	3(1)
C53	33(1)	32(1)	37(1)	-6(1)	5(1)	2(1)
C54	35(1)	33(1)	35(1)	-3(1)	7(1)	0(1)
C55	30(1)	32(1)	36(1)	-1(1)	7(1)	-1(1)
C56	26(1)	36(1)	37(1)	-1(1)	8(1)	-3(1)
C57	33(1)	38(1)	40(1)	3(1)	8(1)	2(1)
C58	33(1)	45(1)	43(1)	-4(1)	12(1)	1(1)
C59	40(1)	43(1)	37(1)	-1(1)	10(1)	-7(1)
C60	46(1)	35(1)	43(1)	1(1)	9(1)	-2(1)
C61	37(1)	36(1)	43(1)	-4(1)	11(1)	1(1)
C62	32(1)	43(1)	36(1)	2(1)	5(1)	6(1)
C63	43(1)	45(1)	45(1)	5(1)	11(1)	3(1)
C64	50(1)	53(1)	61(2)	16(1)	17(1)	4(1)
C65	51(1)	77(2)	46(1)	20(1)	17(1)	18(1)
C66	53(1)	79(2)	35(1)	-3(1)	8(1)	15(1)
C67	40(1)	55(1)	40(1)	-4(1)	6(1)	3(1)
C68	81(2)	59(2)	52(1)	7(1)	28(1)	-1(1)
C69	90(2)	129(3)	61(2)	36(2)	35(2)	21(2)

Table A0.40. Hydrogen coordinates (x 10^4) and isotropic displacement parameters (Å^2 x 10^3) for **3.1a.**

Atom	x	y	z	U(eq)
H3A	2101	4994	3013	51

H4A	2200	4885	3968	57
H5A	2081	2950	4448	57
H6A	1839	1194	3966	51
H12A	881	-1060	1265	56
H13A	896	-1346	325	66
H14A	1294	-284	-138	65
H15A	1649	1178	332	55
H20A	1432	4825	1778	48
H21A	1502	6839	1358	59
H23A	2474	6492	1714	66
H24A	2408	4478	2139	53
H26A	1165	693	3595	57
H27A	1047	-1132	4108	72
H29A	1746	-3194	3473	69
H30A	1860	-1380	2938	57
H32A	1206	-2319	2208	50
H33A	807	-3341	2653	57
H35A	372	150	2832	65
H36A	780	1192	2412	55
H38A	1636	3799	596	55
H39A	2030	4795	131	60
H41A	2723	2625	1016	59
H42A	2331	1630	1491	54
H43A	1841	8387	951	146
H43B	2227	8149	1001	146
H43C	2070	8885	1494	146
H44A	1308	-3205	4599	141
H44B	1485	-4169	4203	141
H44C	1103	-3875	4066	141
H45A	103	-1859	3088	114
H45B	391	-2503	3505	114
H45C	252	-3257	2942	114
H46A	2893	4315	434	100
H46B	2637	5436	212	100
H46C	2669	4129	-151	100
H49A	1043	4316	2474	48
H50A	1374	4089	3300	53
H51A	1171	3185	4091	52

H52A	626	2726	4075	48
H57A	822	2565	1599	44
H58A	1015	3312	791	48
H60A	540	6739	912	50
H61A	331	5975	1705	46
H63A	-145	1013	3471	53
H64A	-342	240	4270	65
H66A	-60	3584	5077	66
H67A	144	4365	4283	54
H68A	781	6289	69	93
H68B	916	4842	-35	93
H68C	1144	5893	319	93
H69A	-357	406	5294	137
H69B	-610	1606	5227	137
H69C	-265	1779	5600	137

Table A0.41. Torsion angles (°) for **3.1a**

Atoms	Angle	Atoms	Angle
C18-C1-C2-C3	-177.85(17)	C26-C25-C30-C29	-0.3(3)
C19-C1-C2-C3	-6.8(3)	C8-C25-C30-C29	176.70(18)
C18-C1-C2-C7	0.6(3)	C28-C29-C30-C25	-0.2(3)
C19-C1-C2-C7	171.65(16)	C11-C10-C31-C36	-101.2(2)
C1-C2-C3-C4	-177.60(19)	C9-C10-C31-C36	72.1(2)
C7-C2-C3-C4	3.9(3)	C11-C10-C31-C32	76.0(2)
C2-C3-C4-C5	0.6(3)	C9-C10-C31-C32	-110.7(2)
C3-C4-C5-C6	-2.3(3)	C36-C31-C32-C33	-2.4(3)
C4-C5-C6-C7	-0.7(3)	C10-C31-C32-C33	-179.57(17)
C5-C6-C7-C8	-170.75(19)	C31-C32-C33-C34	1.0(3)
C5-C6-C7-C2	5.2(3)	C32-C33-C34-C35	1.4(3)
C1-C2-C7-C8	-9.1(3)	C32-C33-C34-C45	-177.02(19)
C3-C2-C7-C8	169.41(16)	C33-C34-C35-C36	-2.4(3)
C1-C2-C7-C6	174.85(17)	C45-C34-C35-C36	176.0(2)
C3-C2-C7-C6	-6.6(2)	C34-C35-C36-C31	1.1(3)
C6-C7-C8-C9	178.70(17)	C32-C31-C36-C35	1.3(3)
C2-C7-C8-C9	2.8(3)	C10-C31-C36-C35	178.66(18)
C6-C7-C8-C25	-5.9(3)	C16-C17-C37-C42	-105.5(2)
C2-C7-C8-C25	178.28(16)	C18-C17-C37-C42	66.1(2)
C7-C8-C9-C10	-168.81(17)	C16-C17-C37-C38	71.7(2)

C25-C8-C9-C10	15.9(3)	C18-C17-C37-C38	-116.7(2)
C7-C8-C9-C18	11.4(3)	C42-C37-C38-C39	-1.1(3)
C25-C8-C9-C18	-163.84(16)	C17-C37-C38-C39	-178.31(19)
C8-C9-C10-C11	-166.84(17)	C37-C38-C39-C40	0.3(3)
C18-C9-C10-C11	12.9(3)	C38-C39-C40-C41	0.8(3)
C8-C9-C10-C31	19.9(3)	C38-C39-C40-C46	-179.32(19)
C18-C9-C10-C31	-160.30(16)	C39-C40-C41-C42	-1.1(3)
C9-C10-C11-C16	1.6(3)	C46-C40-C41-C42	179.05(19)
C31-C10-C11-C16	174.97(16)	C40-C41-C42-C37	0.3(3)
C9-C10-C11-C12	178.87(17)	C38-C37-C42-C41	0.8(3)
C31-C10-C11-C12	-7.7(3)	C17-C37-C42-C41	178.15(18)
C10-C11-C12-C13	-171.66(19)	C55#1-C47-C48-C49	-176.96(16)
C16-C11-C12-C13	5.7(3)	C56-C47-C48-C49	-4.1(3)
C11-C12-C13-C14	-0.4(3)	C55#1-C47-C48-C53	4.3(3)
C12-C13-C14-C15	-3.2(3)	C56-C47-C48-C53	177.25(16)
C13-C14-C15-C16	1.1(3)	C47-C48-C49-C50	-173.84(18)
C10-C11-C16-C17	-9.9(3)	C53-C48-C49-C50	4.9(3)
C12-C11-C16-C17	172.70(17)	C48-C49-C50-C51	2.2(3)
C10-C11-C16-C15	169.94(17)	C49-C50-C51-C52	-4.3(3)
C12-C11-C16-C15	-7.5(3)	C50-C51-C52-C53	-0.9(3)
C14-C15-C16-C17	-175.93(19)	C47-C48-C53-C54	-12.6(3)
C14-C15-C16-C11	4.2(3)	C49-C48-C53-C54	168.64(16)
C11-C16-C17-C18	3.3(3)	C47-C48-C53-C52	169.02(16)
C15-C16-C17-C18	-176.58(17)	C49-C48-C53-C52	-9.7(2)
C11-C16-C17-C37	174.91(16)	C51-C52-C53-C54	-170.36(18)
C15-C16-C17-C37	-4.9(3)	C51-C52-C53-C48	8.0(3)
C2-C1-C18-C17	-166.45(17)	C48-C53-C54-C55	2.9(3)
C19-C1-C18-C17	22.8(3)	C52-C53-C54-C55	-178.74(17)
C2-C1-C18-C9	13.8(2)	C48-C53-C54-C62	176.68(16)
C19-C1-C18-C9	-157.01(16)	C52-C53-C54-C62	-5.0(3)
C16-C17-C18-C1	-168.61(17)	C53-C54-C55-C47#1	-164.54(17)
C37-C17-C18-C1	19.9(3)	C62-C54-C55-C47#1	21.9(3)
C16-C17-C18-C9	11.2(3)	C53-C54-C55-C55#1	14.4(2)
C37-C17-C18-C9	-160.34(16)	C62-C54-C55-C55#1	-159.24(13)
C8-C9-C18-C1	-19.7(2)	C48-C47-C56-C57	73.8(2)
C10-C9-C18-C1	160.50(16)	C55#1-C47-C56-C57	-113.4(2)
C8-C9-C18-C17	160.47(16)	C48-C47-C56-C61	-104.2(2)
C10-C9-C18-C17	-19.3(2)	C55#1-C47-C56-C61	68.6(2)

C2-C1-C19-C20	-106.3(2)	C61-C56-C57-C58	-2.7(3)
C18-C1-C19-C20	64.6(2)	C47-C56-C57-C58	179.33(17)
C2-C1-C19-C24	69.7(2)	C56-C57-C58-C59	1.7(3)
C18-C1-C19-C24	-119.4(2)	C57-C58-C59-C60	0.4(3)
C24-C19-C20-C21	0.5(3)	C57-C58-C59-C68	-178.73(19)
C1-C19-C20-C21	176.79(18)	C58-C59-C60-C61	-1.5(3)
C19-C20-C21-C22	-0.2(3)	C68-C59-C60-C61	177.60(19)
C20-C21-C22-C23	0.0(3)	C59-C60-C61-C56	0.6(3)
C20-C21-C22-C43	179.1(2)	C57-C56-C61-C60	1.5(3)
C21-C22-C23-C24	-0.1(4)	C47-C56-C61-C60	179.65(17)
C43-C22-C23-C24	-179.3(2)	C53-C54-C62-C67	68.9(2)
C22-C23-C24-C19	0.5(3)	C55-C54-C62-C67	-117.5(2)
C20-C19-C24-C23	-0.7(3)	C53-C54-C62-C63	-108.1(2)
C1-C19-C24-C23	-176.70(19)	C55-C54-C62-C63	65.5(2)
C7-C8-C25-C30	-100.7(2)	C67-C62-C63-C64	1.9(3)
C9-C8-C25-C30	74.6(2)	C54-C62-C63-C64	179.08(18)
C7-C8-C25-C26	76.1(2)	C62-C63-C64-C65	0.2(3)
C9-C8-C25-C26	-108.5(2)	C63-C64-C65-C66	-2.1(3)
C30-C25-C26-C27	-0.5(3)	C63-C64-C65-C69	176.2(2)
C8-C25-C26-C27	-177.39(18)	C64-C65-C66-C67	1.7(3)
C25-C26-C27-C28	1.8(3)	C69-C65-C66-C67	-176.5(2)
C26-C27-C28-C29	-2.2(3)	C65-C66-C67-C62	0.4(3)
C26-C27-C28-C44	178.4(2)	C63-C62-C67-C66	-2.2(3)
C27-C28-C29-C30	1.4(3)	C54-C62-C67-C66	-179.29(18)
C44-C28-C29-C30	-179.2(2)		

Symmetry transformations used to generate equivalent atoms: #1 -x,y,-z+1/2

Crystal Structure Report for **3.1b** (project code: 13167)

Data collection: A crystal (approximate dimensions 0.19 x 0.16 x 0.08 mm^3) was placed onto the tip of a 0.1 mm diameter glass capillary and mounted on a Bruker-AXS D8 Photon-100 diffractometer for a data collection at 173(2) K.[1] A preliminary set of cell constants was calculated from reflections harvested from three sets of 12 frames. These initial sets of frames were oriented such that orthogonal wedges of reciprocal space were surveyed. This produced initial orientation matrices determined from 129 reflections. The data collection was carried out using MoKα radiation (graphite monochromator) with a frame time of 40 seconds and a detector distance of 3.4 cm. A randomly oriented region of reciprocal space was surveyed to the extent of one sphere and to a resolution of 0.84 Å. Four major sections of frames were collected with 0.30º steps in ω at four different ϕ settings and a detector position of -28º in 2θ. The intensity data were corrected for absorption and decay (SADABS).[2] Final cell constants were calculated from the xyz centroids of 9967 strong reflections from the actual data collection after integration (SAINT).[3] Please refer to Table 1 for additional crystal and refinement information.

Structure solution and refinement: The structure was solved using SHELXS-97 (Sheldrick, 1990)[4] and refined using

SHELXL-97 (Sheldrick, 1997).[4] The space group P2(1)/n was determined based on systematic absences and intensity statistics. A direct-methods solution was calculated which provided most non-hydrogen atoms from the E-map. Full-matrix least squares / difference Fourier cycles were performed which located the remaining non-hydrogen atoms. All non-hydrogen atoms were refined with anisotropic displacement parameters. All hydrogen atoms were placed in ideal positions and refined as riding atoms with relative isotropic displacement parameters. The final full matrix least squares refinement converged to $R1 = 0.0648$ and $wR2 = 0.1881$ (F^2, all data).

Structure description: The structure contains one full rubrene molecule and a benzene molecule. The benzene is disordered and has been modeled as two full benzene molecules over two positions. Three of the side phenyl groups on the rubrene molecule are disordered and have been modeled over two positions. Two of the methyl groups have been modeled as ideally disordered groups.

Table A0.42. Atomic coordinantes (x 10^4) and equivalent isotropic displacement parameters (Å^2 x 10^3) for **3.1b**. Ueq is defined as one third of the trace of the orthogonalized Uij tensor.

Atom	x	y	z	Ueq
C1	2185(2)	15063(3)	-3216(1)	41(1)
C2	2862(2)	14092(3)	-3307(1)	37(1)
C3	3594(1)	13764(2)	-2971(1)	30(1)
C4	4274(1)	12709(3)	-3052(1)	30(1)
C5	4956(1)	12335(2)	-2694(1)	29(1)
C6	5520(1)	11017(3)	-2728(1)	31(1)
C7	6261(1)	10787(3)	-2405(1)	31(1)
C8	6845(2)	9470(3)	-2424(1)	40(1)
C9	7602(2)	9332(3)	-2137(1)	46(1)
C10	7826(2)	10486(3)	-1800(1)	47(1)
C11	7272(2)	11703(3)	-1752(1)	42(1)
C12	6453(1)	11899(3)	-2044(1)	32(1)
C13	5849(2)	13104(3)	-1976(1)	33(1)
C14	5058(1)	13306(2)	-2281(1)	30(1)
C15	4362(2)	14402(3)	-2207(1)	33(1)
C16	3620(1)	14573(3)	-2533(1)	31(1)
C17	2887(2)	15601(3)	-2458(1)	37(1)
C18	2193(1)	15816(3)	-2782(1)	39(1)
C19	4330(1)	12191(3)	-3542(1)	36(1)
C20	4979(1)	12865(3)	-3797(1)	45(1)
C21	5046(3)	12469(6)	-4261(1)	63(1)
C22	4459(4)	11389(9)	-4462(2)	75(2)
C23	3814(3)	10722(5)	-4214(1)	58(1)
C24	3739(3)	11126(5)	-3757(1)	43(1)
C43	5713(4)	13165(7)	-4528(2)	102(2)
C19'	4427(11)	12177(19)	-3546(5)	36(1)

C20'	3854(16)	11360(30)	-3867(6)	45(1)
C21'	4058(19)	11050(30)	-4316(7)	63(1)
C22'	4810(19)	11730(50)	-4457(8)	75(2)
C23'	5333(15)	12670(30)	-4157(6)	58(1)
C24'	5186(12)	12880(20)	-3702(6)	43(1)
C43'	3469(16)	9900(30)	-4564(7)	102(2)
C25	5271(2)	9741(3)	-3065(1)	33(1)
C26	5760(2)	9444(3)	-3446(1)	37(1)
C27	5520(2)	8247(3)	-3755(1)	42(1)
C28	4789(2)	7325(3)	-3666(1)	51(1)
C29	4313(2)	7582(3)	-3287(1)	51(1)
C30	4545(2)	8788(3)	-2987(1)	43(1)
C44	6026(2)	7993(4)	-4173(1)	61(1)
C31	6149(2)	14200(4)	-1594(1)	35(1)
C32	5977(3)	13868(4)	-1145(1)	43(1)
C33	6295(3)	14799(5)	-770(1)	53(1)
C34	6821(3)	16057(5)	-865(1)	55(1)
C35	7016(2)	16422(4)	-1313(1)	54(1)
C36	6669(2)	15496(4)	-1675(1)	44(1)
C45	6065(3)	14467(6)	-292(1)	81(1)
C31'	5928(12)	13890(20)	-1471(6)	35(1)
C32'	6530(10)	15096(16)	-1425(5)	43(1)
C33'	6774(15)	15890(20)	-1023(6)	53(1)
C34'	6444(13)	15220(20)	-636(6)	55(1)
C35'	5836(10)	13962(18)	-652(5)	54(1)
C36'	5585(11)	13254(18)	-1080(4)	39(3)
C45'	7426(2)	17168(3)	-986(1)	81(1)
C37	4319(2)	15328(3)	-1772(1)	30(1)
C38	3851(2)	14800(3)	-1407(1)	42(1)
C39	3784(2)	15755(4)	-1027(1)	49(1)
C40	4187(3)	17214(4)	-998(1)	48(1)
C41	4658(2)	17733(4)	-1365(1)	41(1)
C42	4703(2)	16804(3)	-1746(1)	32(1)
C46	5115(2)	19297(4)	-1333(1)	55(1)
C37'	4549(10)	15742(19)	-1843(5)	30(1)
C38'	5008(10)	17086(15)	-1952(5)	42(1)
C39'	5058(9)	18359(17)	-1670(4)	49(1)
C40'	4690(13)	18160(20)	-1246(5)	48(1)

C41'	4224(13)	16864(18)	-1126(5)	41(1)
C42'	4097(8)	15602(15)	-1454(4)	32(1)
C46'	3796(18)	16700(40)	-677(7)	129(12)
C47	6707(6)	10208(8)	-200(2)	93(2)
C48	7513(5)	10679(8)	17(2)	88(3)
C49	7827(3)	10003(10)	422(2)	79(2)
C50	7319(5)	8814(8)	609(2)	77(2)
C51	6500(5)	8398(8)	387(2)	75(2)
C52	6209(5)	9109(9)	-15(3)	83(2)
C47'	6250(20)	9940(60)	-165(13)	93(2)
C48'	7090(30)	10570(50)	-202(14)	88(3)
C49'	7680(30)	10540(50)	181(17)	79(2)
C50'	7610(30)	9260(50)	486(13)	77(2)
C51'	6810(30)	8440(50)	464(18)	75(2)
C52'	6140(30)	8810(60)	140(18)	83(2)

Table A0.43. Bond lengths (Å) and angles (°) for **3.1b**.

Atoms	Length	Atoms	Angles	Atoms	Angles
C(1)-C(2)	1.352(3)	C(2)-C(1)-C(18)	120.3(2)	C(36)-C(35)-C(34)	119.0(4)
C(1)-C(18)	1.416(3)	C(2)-C(1)-H(1A)	119.9	C(36)-C(35)-H(35A)	120.5
C(1)-H(1A)	0.95	C(18)-C(1)-H(1A)	119.9	C(34)-C(35)-H(35A)	120.5
C(2)-C(3)	1.430(3)	C(1)-C(2)-C(3)	121.9(2)	C(35)-C(36)-C(31)	121.0(3)
C(2)-H(2A)	0.95	C(1)-C(2)-H(2A)	119.1	C(35)-C(36)-H(36A)	119.5
C(3)-C(4)	1.395(3)	C(3)-C(2)-H(2A)	119.1	C(31)-C(36)-H(36A)	119.5
C(3)-C(16)	1.447(3)	C(4)-C(3)-C(2)	122.5(2)	C(33)-C(45)-H(45A)	109.5
C(4)-C(5)	1.428(3)	C(4)-C(3)-C(16)	119.61(19)	C(33)-C(45)-H(45B)	109.5
C(4)-C(19)	1.498(3)	C(2)-C(3)-C(16)	117.9(2)	H(45A)-C(45)-H(45B)	109.5
C(4)-C(19')	1.538(14)	C(3)-C(4)-C(5)	120.43(19)	C(33)-C(45)-H(45C)	109.5
C(5)-C(6)	1.422(3)	C(3)-C(4)-C(19)	116.80(18)	H(45A)-C(45)-H(45C)	109.5
C(5)-C(14)	1.460(3)	C(5)-C(4)-C(19)	122.14(19)	H(45B)-C(45)-H(45C)	109.5
C(6)-C(7)	1.402(3)	C(3)-C(4)-C(19')	121.0(6)	C(32')-C(31')-C(36')	119.8(16)
C(6)-C(25)	1.497(3)	C(5)-C(4)-C(19')	117.4(6)	C(32')-C(31')-C(13)	114.1(11)
C(7)-C(12)	1.433(3)	C(19)-C(4)-C(19')	5.3(6)	C(36')-C(31')-C(13)	124.7(12)
C(7)-C(8)	1.434(3)	C(6)-C(5)-C(4)	121.17(19)	C(31')-C(32')-C(33')	125.8(14)
C(8)-C(9)	1.350(3)	C(6)-C(5)-C(14)	119.58(19)	C(31')-C(32')-H(32B)	117.1
C(8)-H(8A)	0.95	C(4)-C(5)-C(14)	119.23(19)	C(33')-C(32')-H(32B)	117.1
C(9)-C(10)	1.417(4)	C(7)-C(6)-C(5)	120.2(2)	C(32')-C(33')-C(34')	113.2(13)
C(9)-H(9A)	0.95	C(7)-C(6)-C(25)	118.12(19)	C(32')-C(33')-C(45')	124.3(14)

C(10)-C(11)	1.349(3)	C(5)-C(6)-C(25)	121.17(18)	C(34')-C(33')-C(45')	121.9(12)
C(10)-H(10A)	0.95	C(6)-C(7)-C(12)	119.6(2)	C(33')-C(34')-C(35')	124.2(15)
C(11)-C(12)	1.435(3)	C(6)-C(7)-C(8)	122.2(2)	C(33')-C(34')-H(34B)	117.9
C(11)-H(11A)	0.95	C(12)-C(7)-C(8)	118.2(2)	C(35')-C(34')-H(34B)	117.9
C(12)-C(13)	1.398(3)	C(9)-C(8)-C(7)	121.6(2)	C(36')-C(35')-C(34')	119.1(15)
C(13)-C(14)	1.424(3)	C(9)-C(8)-H(8A)	119.2	C(36')-C(35')-H(35B)	120.5
C(13)-C(31)	1.497(4)	C(7)-C(8)-H(8A)	119.2	C(34')-C(35')-H(35B)	120.5
C(13)-C(31')	1.609(17)	C(8)-C(9)-C(10)	120.1(2)	C(31')-C(36')-C(35')	117.3(15)
C(14)-C(15)	1.431(3)	C(8)-C(9)-H(9A)	120	C(31')-C(36')-H(36B)	121.3
C(15)-C(16)	1.400(3)	C(10)-C(9)-H(9A)	120	C(35')-C(36')-H(36B)	121.3
C(15)-C(37)	1.498(3)	C(11)-C(10)-C(9)	120.4(2)	C(33')-C(45')-H(45D)	109.5
C(15)-C(37')	1.576(16)	C(11)-C(10)-H(10A)	119.8	C(33')-C(45')-H(45E)	109.5
C(16)-C(17)	1.436(3)	C(9)-C(10)-H(10A)	119.8	H(45D)-C(45')-H(45E)	109.5
C(17)-C(18)	1.351(3)	C(10)-C(11)-C(12)	121.9(2)	C(33')-C(45')-H(45F)	109.5
C(17)-H(17A)	0.95	C(10)-C(11)-H(11A)	119.1	H(45D)-C(45')-H(45F)	109.5
C(18)-H(18A)	0.95	C(12)-C(11)-H(11A)	119.1	H(45E)-C(45')-H(45F)	109.5
C(19)-C(24)	1.385(4)	C(13)-C(12)-C(7)	120.56(19)	C(38)-C(37)-C(42)	118.96(15)
C(19)-C(20)	1.3898	C(13)-C(12)-C(11)	121.9(2)	C(38)-C(37)-C(15)	121.61(12)
C(20)-C(21)	1.399(5)	C(7)-C(12)-C(11)	117.5(2)	C(42)-C(37)-C(15)	119.3(2)
C(20)-H(20A)	0.95	C(12)-C(13)-C(14)	120.8(2)	C(39)-C(38)-C(37)	118.93(17)
C(21)-C(22)	1.374(8)	C(12)-C(13)-C(31)	114.7(2)	C(39)-C(38)-H(38A)	120.5
C(21)-C(43)	1.437(7)	C(14)-C(13)-C(31)	124.3(2)	C(37)-C(38)-H(38A)	120.5
C(22)-C(23)	1.371(7)	C(12)-C(13)-C(31')	116.2(8)	C(38)-C(39)-C(40)	121.8(3)
C(22)-H(22A)	0.95	C(14)-C(13)-C(31')	120.6(7)	C(38)-C(39)-H(39A)	119.1
C(23)-C(24)	1.383(5)	C(31)-C(13)-C(31')	20.7(5)	C(40)-C(39)-H(39A)	119.1
C(23)-H(23A)	0.95	C(13)-C(14)-C(15)	124.06(19)	C(39)-C(40)-C(41)	118.9(3)
C(24)-H(24A)	0.95	C(13)-C(14)-C(5)	117.76(19)	C(39)-C(40)-H(40A)	120.6
C(43)-H(43A)	0.98	C(15)-C(14)-C(5)	118.19(19)	C(41)-C(40)-H(40A)	120.6
C(43)-H(43B)	0.98	C(16)-C(15)-C(14)	120.6(2)	C(42)-C(41)-C(40)	119.2(3)
C(43)-H(43C)	0.98	C(16)-C(15)-C(37)	115.29(19)	C(42)-C(41)-C(46)	121.4(3)
C(19')-C(24')	1.388(16)	C(14)-C(15)-C(37)	123.88(19)	C(40)-C(41)-C(46)	119.4(3)
C(19')-C(20')	1.401(17)	C(16)-C(15)-C(37')	117.5(6)	C(41)-C(42)-C(37)	122.2(3)
C(20')-C(21')	1.387(17)	C(14)-C(15)-C(37')	119.6(6)	C(41)-C(42)-H(42A)	118.9
C(20')-H(20B)	0.95	C(37)-C(15)-C(37')	20.2(4)	C(37)-C(42)-H(42A)	118.9
C(21')-C(22')	1.355(19)	C(15)-C(16)-C(17)	121.9(2)	C(42')-C(37')-C(38')	123.0(14)
C(21')-C(43')	1.475(18)	C(15)-C(16)-C(3)	120.4(2)	C(42')-C(37')-C(15)	114.6(10)
C(22')-C(23')	1.382(18)	C(17)-C(16)-C(3)	117.63(19)	C(38')-C(37')-C(15)	121.4(11)
C(22')-H(22B)	0.95	C(18)-C(17)-C(16)	121.7(2)	C(39')-C(38')-C(37')	122.4(14)

C(23')-C(24')	1.365(17)	C(18)-C(17)-H(17A)	119.1	C(39')-C(38')-H(38B)	118.8
C(23')-H(23B)	0.95	C(16)-C(17)-H(17A)	119.1	C(37')-C(38')-H(38B)	118.8
C(24')-H(20A)	0.7159	C(17)-C(18)-C(1)	120.5(2)	C(38')-C(39')-C(40')	115.1(13)
C(24')-H(24B)	0.95	C(17)-C(18)-H(18A)	119.8	C(38')-C(39')-H(39B)	122.5
C(43')-H(43D)	0.98	C(1)-C(18)-H(18A)	119.8	C(40')-C(39')-H(39B)	122.5
C(43')-H(43E)	0.98	C(24)-C(19)-C(20)	118.77(18)	C(41')-C(40')-C(39')	124.2(14)
C(43')-H(43F)	0.98	C(24)-C(19)-C(4)	122.9(2)	C(41')-C(40')-H(40B)	117.9
C(25)-C(30)	1.390(3)	C(20)-C(19)-C(4)	118.30(12)	C(39')-C(40')-H(40B)	117.9
C(25)-C(26)	1.395(3)	C(19)-C(20)-C(21)	121.0(2)	C(40')-C(41')-C(42')	119.2(13)
C(26)-C(27)	1.395(3)	C(19)-C(20)-H(20A)	120	C(40')-C(41')-C(46')	123.5(16)
C(26)-H(26A)	0.95	C(21)-C(20)-H(20A)	118.9	C(42')-C(41')-C(46')	117.2(16)
C(27)-C(28)	1.388(4)	C(22)-C(21)-C(20)	118.8(4)	C(37')-C(42')-C(41')	115.4(12)
C(27)-C(44)	1.493(4)	C(22)-C(21)-C(43)	119.8(5)	C(37')-C(42')-H(42B)	122.3
C(28)-C(29)	1.373(4)	C(20)-C(21)-C(43)	121.4(5)	C(41')-C(42')-H(42B)	122.3
C(28)-H(28A)	0.95	C(23)-C(22)-C(21)	120.6(4)	C(41')-C(46')-H(46G)	109.5
C(29)-C(30)	1.383(4)	C(23)-C(22)-H(22A)	119.7	C(41')-C(46')-H(46H)	109.5
C(29)-H(29A)	0.95	C(21)-C(22)-H(22A)	119.7	H(46G)-C(46')-H(46H)	109.5
C(30)-H(30A)	0.95	C(22)-C(23)-C(24)	120.8(4)	C(41')-C(46')-H(46I)	109.5
C(44)-H(44A)	0.98	C(22)-C(23)-H(23A)	119.6	H(46G)-C(46')-H(46I)	109.5
C(44)-H(44B)	0.98	C(24)-C(23)-H(23A)	119.6	H(46H)-C(46')-H(46I)	109.5
C(44)-H(44C)	0.98	C(23)-C(24)-C(19)	120.0(4)	C(52)-C(47)-C(48)	121.1(6)
C(44)-H(44F)	0.98	C(23)-C(24)-H(24A)	120	C(52)-C(47)-H(47A)	119.4
C(44)-H(44E)	0.98	C(19)-C(24)-H(24A)	120	C(48)-C(47)-H(47A)	119.4
C(44)-H(44D)	0.98	C(21)-C(43)-H(43A)	109.5	C(49)-C(48)-C(47)	119.8(6)
C(31)-C(32)	1.377(5)	C(21)-C(43)-H(43B)	109.5	C(49)-C(48)-H(48A)	120.1
C(31)-C(36)	1.390(4)	H(43A)-C(43)-H(43B)	109.5	C(47)-C(48)-H(48A)	120.1
C(32)-C(33)	1.403(5)	C(21)-C(43)-H(43C)	109.5	C(48)-C(49)-C(50)	119.1(5)
C(32)-H(32A)	0.95	H(43A)-C(43)-H(43C)	109.5	C(48)-C(49)-H(49A)	120.5
C(33)-C(34)	1.379(5)	H(43B)-C(43)-H(43C)	109.5	C(50)-C(49)-H(49A)	120.5
C(33)-C(45)	1.482(6)	C(24')-C(19')-C(20')	118.1(14)	C(51)-C(50)-C(49)	119.5(5)
C(34)-C(35)	1.388(5)	C(24')-C(19')-C(4)	111.0(11)	C(51)-C(50)-H(50A)	120.2
C(34)-H(34A)	0.95	C(20')-C(19')-C(4)	129.9(13)	C(49)-C(50)-H(50A)	120.2
C(35)-C(36)	1.385(4)	C(21')-C(20')-C(19')	123.5(17)	C(52)-C(51)-C(50)	119.5(5)
C(35)-H(35A)	0.95	C(21')-C(20')-H(20B)	118.2	C(52)-C(51)-H(51A)	120.3
C(36)-H(36A)	0.95	C(19')-C(20')-H(20B)	118.2	C(50)-C(51)-H(51A)	120.3
C(45)-H(45A)	0.98	C(22')-C(21')-C(20')	116.6(17)	C(47)-C(52)-C(51)	121.0(6)
C(45)-H(45B)	0.98	C(22')-C(21')-C(43')	128.3(17)	C(47)-C(52)-H(52A)	119.5
C(45)-H(45C)	0.98	C(20')-C(21')-C(43')	114.8(17)	C(51)-C(52)-H(52A)	119.5

C(31')-C(32')	1.372(15)	C(21')-C(22')-C(23')	120.1(18)	C(52')-C(47')-C(48')	120(2)
C(31')-C(36')	1.394(15)	C(21')-C(22')-H(22B)	119.9	C(52')-C(47')-H(47B)	119.9
C(32')-C(33')	1.376(16)	C(23')-C(22')-H(22B)	119.9	C(48')-C(47')-H(47B)	119.9
C(32')-H(32B)	0.95	C(24')-C(23')-C(22')	124(2)	C(49')-C(48')-C(47')	117(3)
C(33')-C(34')	1.384(16)	C(24')-C(23')-H(23B)	118	C(49')-C(48')-H(48B)	121.4
C(33')-C(45')	1.468(15)	C(22')-C(23')-H(23B)	118	C(47')-C(48')-H(48B)	121.4
C(34')-C(35')	1.412(15)	C(23')-C(24')-C(19')	117.1(16)	C(48')-C(49')-C(50')	117(2)
C(34')-H(34B)	0.95	C(23')-C(24')-H(20A)	101.1	C(48')-C(49')-H(49B)	121.6
C(35')-C(36')	1.406(15)	C(19')-C(24')-H(20A)	131	C(50')-C(49')-H(49B)	121.6
C(35')-H(35B)	0.95	C(23')-C(24')-H(24B)	121.5	C(51')-C(50')-C(49')	118(2)
C(36')-H(36B)	0.95	C(19')-C(24')-H(24B)	121.5	C(51')-C(50')-H(50B)	120.9
C(45')-H(45D)	0.98	H(20A)-C(24')-H(24B)	35.7	C(49')-C(50')-H(50B)	120.9
C(45')-H(45E)	0.98	C(21')-C(43')-H(43D)	109.5	C(52')-C(51')-C(50')	120(2)
C(45')-H(45F)	0.98	C(21')-C(43')-H(43E)	109.5	C(52')-C(51')-H(51B)	120.2
C(37)-C(38)	1.3901	H(43D)-C(43')-H(43E)	109.5	C(50')-C(51')-H(51B)	120.2
C(37)-C(42)	1.395(4)	C(21')-C(43')-H(43F)	109.5	C(47')-C(52')-C(51')	121(2)
C(38)-C(39)	1.386(4)	H(43D)-C(43')-H(43F)	109.5	C(47')-C(52')-H(52B)	119.6
C(38)-H(38A)	0.95	H(43E)-C(43')-H(43F)	109.5	C(51')-C(52')-H(52B)	119.6
C(39)-C(40)	1.394(5)	C(30)-C(25)-C(26)	118.8(2)		
C(39)-H(39A)	0.95	C(30)-C(25)-C(6)	118.9(2)		
C(40)-C(41)	1.395(5)	C(26)-C(25)-C(6)	122.3(2)		
C(40)-H(40A)	0.95	C(25)-C(26)-C(27)	121.5(2)		
C(41)-C(42)	1.370(4)	C(25)-C(26)-H(26A)	119.3		
C(41)-C(46)	1.511(5)	C(27)-C(26)-H(26A)	119.3		
C(42)-H(42A)	0.95	C(28)-C(27)-C(26)	118.0(2)		
C(46)-H(46A)	0.98	C(28)-C(27)-C(44)	121.3(2)		
C(46)-H(46B)	0.98	C(26)-C(27)-C(44)	120.7(3)		
C(46)-H(46C)	0.98	C(29)-C(28)-C(27)	121.2(2)		
C(46)-H(46D)	0.98	C(29)-C(28)-H(28A)	119.4		
C(46)-H(46E)	0.98	C(27)-C(28)-H(28A)	119.4		
C(46)-H(46F)	0.98	C(28)-C(29)-C(30)	120.5(3)		
C(37')-C(42')	1.362(13)	C(28)-C(29)-H(29A)	119.8		
C(37')-C(38')	1.395(15)	C(30)-C(29)-H(29A)	119.8		
C(38')-C(39')	1.369(15)	C(29)-C(30)-C(25)	120.1(2)		
C(38')-H(38B)	0.95	C(29)-C(30)-H(30A)	120		
C(39')-C(40')	1.393(15)	C(25)-C(30)-H(30A)	120		
C(39')-H(39B)	0.95	C(27)-C(44)-H(44A)	109.5		
C(40')-C(41')	1.378(16)	C(27)-C(44)-H(44B)	109.5		

C(40')-H(40B)	0.95	H(44A)-C(44)-H(44B)	109.5
C(41')-C(42')	1.448(15)	C(27)-C(44)-H(44C)	109.5
C(41')-C(46')	1.501(16)	H(44A)-C(44)-H(44C)	109.5
C(42')-H(42B)	0.95	H(44B)-C(44)-H(44C)	109.5
C(46')-H(46G)	0.98	C(27)-C(44)-H(44F)	109.5
C(46')-H(46H)	0.98	H(44A)-C(44)-H(44F)	141.1
C(46')-H(46I)	0.98	H(44B)-C(44)-H(44F)	56.3
C(47)-C(52)	1.341(9)	H(44C)-C(44)-H(44F)	56.3
C(47)-C(48)	1.371(8)	C(27)-C(44)-H(44E)	109.5
C(47)-H(47A)	0.95	H(44A)-C(44)-H(44E)	56.3
C(48)-C(49)	1.360(8)	H(44B)-C(44)-H(44E)	141.1
C(48)-H(48A)	0.95	H(44C)-C(44)-H(44E)	56.3
C(49)-C(50)	1.408(8)	H(44F)-C(44)-H(44E)	109.5
C(49)-H(49A)	0.95	C(27)-C(44)-H(44D)	109.5
C(50)-C(51)	1.378(7)	H(44A)-C(44)-H(44D)	56.3
C(50)-H(50A)	0.95	H(44B)-C(44)-H(44D)	56.3
C(51)-C(52)	1.356(7)	H(44C)-C(44)-H(44D)	141.1
C(51)-H(51A)	0.95	H(44F)-C(44)-H(44D)	109.5
C(52)-H(52A)	0.95	H(44E)-C(44)-H(44D)	109.5
C(47')-C(52')	1.335(19)	C(32)-C(31)-C(36)	118.4(3)
C(47')-C(48')	1.37(2)	C(32)-C(31)-C(13)	120.0(3)
C(47')-H(47B)	0.95	C(36)-C(31)-C(13)	121.4(3)
C(48')-C(49')	1.36(2)	C(31)-C(32)-C(33)	122.4(4)
C(48')-H(48B)	0.95	C(31)-C(32)-H(32A)	118.8
C(49')-C(50')	1.42(2)	C(33)-C(32)-H(32A)	118.8
C(49')-H(49B)	0.95	C(34)-C(33)-C(32)	117.2(4)
C(50')-C(51')	1.385(19)	C(34)-C(33)-C(45)	121.1(3)
C(50')-H(50B)	0.95	C(32)-C(33)-C(45)	121.7(4)
C(51')-C(52')	1.349(19)	C(33)-C(34)-C(35)	122.0(3)
C(51')-H(51B)	0.95	C(33)-C(34)-H(34A)	119
C(52')-H(52B)	0.95	C(35)-C(34)-H(34A)	119

Table A0.44. Anisotropic displacement parameters ($Å^2$ x 10^3) for **3.1b**. The anisotropic displacement factor exponent takes the form: $-2\pi^2[h^2 a^{*2}U11 + ... + 2 h k a^* b^* U12]$.

Atom	U11	U22	U33	U23	U13	U12
C1	32(1)	41(1)	47(1)	-3(1)	-7(1)	3(1)
C2	34(1)	37(1)	38(1)	-6(1)	-4(1)	0(1)
C3	28(1)	27(1)	34(1)	-1(1)	2(1)	-3(1)

C4	30(1)	28(1)	32(1)	-3(1)	1(1)	-3(1)
C5	29(1)	29(1)	30(1)	0(1)	3(1)	-2(1)
C6	30(1)	31(1)	31(1)	-2(1)	5(1)	-1(1)
C7	31(1)	30(1)	33(1)	0(1)	3(1)	0(1)
C8	44(1)	37(1)	38(1)	-7(1)	-1(1)	8(1)
C9	45(1)	41(1)	49(2)	-5(1)	-5(1)	15(1)
C10	41(1)	45(2)	52(2)	-5(1)	-14(1)	9(1)
C11	42(1)	38(1)	45(1)	-8(1)	-10(1)	5(1)
C12	32(1)	30(1)	33(1)	0(1)	-1(1)	-1(1)
C13	34(1)	30(1)	35(1)	-3(1)	-2(1)	-2(1)
C14	31(1)	28(1)	31(1)	-2(1)	2(1)	-1(1)
C15	35(1)	31(1)	32(1)	-3(1)	1(1)	1(1)
C16	32(1)	27(1)	34(1)	-1(1)	3(1)	1(1)
C17	36(1)	39(1)	35(1)	-6(1)	4(1)	6(1)
C18	34(1)	39(1)	45(1)	-4(1)	2(1)	6(1)
C19	37(1)	37(1)	32(1)	-3(1)	-2(1)	11(1)
C20	56(2)	47(2)	33(2)	6(2)	5(2)	12(2)
C21	91(4)	68(3)	32(2)	12(2)	21(2)	25(3)
C22	118(6)	75(5)	29(2)	-12(2)	-9(3)	43(4)
C23	80(3)	56(3)	33(2)	-20(2)	-22(2)	26(2)
C24	47(2)	45(2)	34(2)	-9(2)	-14(2)	13(2)
C43	123(4)	108(4)	78(3)	4(3)	38(3)	-6(4)
C19'	37(1)	37(1)	32(1)	-3(1)	-2(1)	11(1)
C20'	56(2)	47(2)	33(2)	6(2)	5(2)	12(2)
C21'	91(4)	68(3)	32(2)	12(2)	21(2)	25(3)
C22'	118(6)	75(5)	29(2)	-12(2)	-9(3)	43(4)
C23'	80(3)	56(3)	33(2)	-20(2)	-22(2)	26(2)
C24'	47(2)	45(2)	34(2)	-9(2)	-14(2)	13(2)
C43'	123(4)	108(4)	78(3)	4(3)	38(3)	-6(4)
C25	34(1)	30(1)	34(1)	-3(1)	-2(1)	5(1)
C26	35(1)	37(1)	37(1)	-1(1)	-1(1)	5(1)
C27	48(1)	42(1)	35(1)	-6(1)	-6(1)	15(1)
C28	64(2)	37(1)	50(2)	-8(1)	-12(1)	3(1)
C29	56(2)	37(1)	59(2)	-3(1)	-1(1)	-13(1)
C30	44(1)	39(1)	45(1)	-1(1)	2(1)	-5(1)
C44	68(2)	74(2)	40(2)	-15(1)	-3(1)	22(2)
C31	30(2)	37(2)	37(2)	-9(2)	-3(1)	6(1)
C32	46(2)	41(2)	39(2)	-3(2)	-4(2)	5(2)

C33	56(2)	58(2)	42(2)	-15(2)	-12(2)	14(2)
C34	48(2)	61(2)	56(3)	-21(2)	-9(2)	4(2)
C35	43(2)	50(2)	68(2)	-22(2)	1(2)	-7(2)
C36	37(2)	37(2)	56(2)	-10(2)	2(2)	1(1)
C45	108(3)	88(3)	45(2)	-15(2)	-5(2)	2(3)
C31'	30(2)	37(2)	37(2)	-9(2)	-3(1)	6(1)
C32'	46(2)	41(2)	39(2)	-3(2)	-4(2)	5(2)
C33'	56(2)	58(2)	42(2)	-15(2)	-12(2)	14(2)
C34'	48(2)	61(2)	56(3)	-21(2)	-9(2)	4(2)
C35'	43(2)	50(2)	68(2)	-22(2)	1(2)	-7(2)
C36'	53(10)	42(9)	23(7)	6(6)	4(6)	7(7)
C45'	108(3)	88(3)	45(2)	-15(2)	-5(2)	2(3)
C37	26(2)	35(2)	30(2)	0(1)	2(1)	2(1)
C38	43(2)	44(2)	38(2)	2(1)	4(1)	-11(2)
C39	46(2)	74(2)	29(2)	-5(2)	8(1)	2(2)
C40	45(2)	62(3)	37(2)	-25(2)	-3(2)	10(2)
C41	39(2)	42(2)	42(2)	-20(1)	-4(2)	12(2)
C42	31(1)	33(2)	32(1)	-2(1)	3(1)	2(1)
C46	50(2)	44(2)	69(2)	-21(2)	-5(2)	3(2)
C37'	26(2)	35(2)	30(2)	0(1)	2(1)	2(1)
C38'	43(2)	44(2)	38(2)	2(1)	4(1)	-11(2)
C39'	46(2)	74(2)	29(2)	-5(2)	8(1)	2(2)
C40'	45(2)	62(3)	37(2)	-25(2)	-3(2)	10(2)
C41'	39(2)	42(2)	42(2)	-20(1)	-4(2)	12(2)
C42'	31(1)	33(2)	32(1)	-2(1)	3(1)	2(1)
C46'	120(20)	210(30)	64(14)	-22(18)	24(14)	40(20)
C47	125(8)	74(5)	75(3)	-3(3)	-25(5)	11(5)
C48	119(6)	94(4)	53(5)	-1(3)	10(4)	-29(4)
C49	71(3)	92(5)	71(4)	-1(4)	-6(2)	-15(3)
C50	100(5)	82(4)	48(3)	-4(2)	1(3)	-12(3)
C51	84(6)	68(2)	74(4)	-16(3)	10(4)	-13(4)
C52	85(3)	58(5)	101(6)	-16(4)	-21(4)	3(2)
C47'	125(8)	74(5)	75(3)	-3(3)	-25(5)	11(5)
C48'	119(6)	94(4)	53(5)	-1(3)	10(4)	-29(4)
C49'	71(3)	92(5)	71(4)	-1(4)	-6(2)	-15(3)
C50'	100(5)	82(4)	48(3)	-4(2)	1(3)	-12(3)
C51'	84(6)	68(2)	74(4)	-16(3)	10(4)	-13(4)
C52'	85(3)	58(5)	101(6)	-16(4)	-21(4)	3(2)

Table A0.45. Hydrogen coordinates (x 10^4) and isotropic displacement parameters (Å^2 x 10^3) for **3.1b**.

Atom	x	y	z	U(eq)	Atom	x	y	z	U(eq)
H1A	1701	15239	-3445	49	H45B	6292	13439	-198	122
H2A	2851	13615	-3603	44	H45C	5408	14492	-280	122
H8A	6696	8676	-2644	48	H32B	6803	15411	-1695	51
H9A	7986	8460	-2161	55	H34B	6639	15637	-342	66
H10A	8370	10402	-1606	56	H35B	5600	13598	-377	65
H11A	7429	12452	-1520	51	H36B	5199	12377	-1101	47
H17A	2889	16144	-2173	44	H45D	7515	17509	-663	122
H18A	1708	16479	-2718	47	H45E	7195	18034	-1180	122
H20A	5372	13635	-3660	54	H45F	8002	16817	-1090	122
H22A	4499	11103	-4776	89	H38A	3582	13802	-1418	50
H23A	3415	9974	-4357	69	H39A	3454	15405	-780	59
H24A	3281	10672	-3590	52	H40A	4141	17844	-732	58
H43A	5654	12746	-4843	153	H42A	5006	17177	-2000	39
H43B	6317	12934	-4384	153	H46A	5069	19790	-1638	82
H43C	5623	14289	-4539	153	H46B	5752	19164	-1225	82
H20B	3296	10989	-3771	54	H46C	4820	19952	-1113	82
H22B	4977	11568	-4762	89	H46D	5359	19481	-1013	82
H23B	5825	13206	-4274	69	H46E	4675	20107	-1426	82
H24B	5586	13475	-3501	52	H46F	5607	19318	-1538	82
H43D	3620	9826	-4886	153	H38B	5295	17120	-2233	50
H43E	2837	10213	-4556	153	H39B	5324	19306	-1756	59
H43F	3558	8885	-4414	153	H40B	4766	18979	-1026	58
H26A	6268	10072	-3497	44	H42B	3725	14736	-1402	39
H28A	4614	6501	-3872	61	H46G	3917	17633	-490	193
H29A	3820	6927	-3230	61	H46H	4050	15795	-509	193
H30A	4208	8966	-2727	51	H46I	3143	16566	-740	193
H44A	5746	7145	-4358	91	H47A	6497	10667	-486	111
H44B	6654	7725	-4077	91	H48A	7852	11475	-115	106
H44C	6011	8942	-4359	91	H49A	8382	10328	577	94
H44F	6528	8730	-4171	91	H50A	7538	8302	885	92
H44E	5620	8150	-4453	91	H51A	6142	7619	514	91
H44D	6263	6933	-4170	91	H52A	5644	8825	-168	99
H32A	5629	12976	-1087	51	H47B	5746	10309	-356	111
H34A	7057	16693	-617	66	H48B	7250	11010	-484	106
H35A	7381	17293	-1370	65	H49B	8111	11336	242	94
H36A	6788	15751	-1983	52	H50B	8101	8982	699	92

H45A	6342	15251	-81	122	H51B	6728	7619	676	91
					H52B	5586	8255	127	99

Table A0.46. Torsion angles (°) for **3.1b**.

Atoms	Angle	Atoms	Angle	Atoms	Angle
C18-C1-C2-C3	1.4(4)	C2-C3-C16-C17	2.7(3)	C32-C31-C36-C35	0.9(5)
C1-C2-C3-C4	176.8(2)	C15-C16-C17-C18	176.9(2)	C13-C31-C36-C35	-173.8(3)
C1-C2-C3-C16	-3.4(3)	C3-C16-C17-C18	-0.1(3)	C12-C13-C31'-C32'	88.3(15)
C2-C3-C4-C5	-175.5(2)	C16-C17-C18-C1	-2.0(4)	C14-C13-C31'-C32'	-109.3(14)
C16-C3-C4-C5	4.8(3)	C2-C1-C18-C17	1.4(4)	C31-C13-C31'-C32'	-2.5(12)
C2-C3-C4-C19	13.5(3)	C3-C4-C19-C24	-76.3(4)	C12-C13-C31'-C36'	-78.3(18)
C16-C3-C4-C19	-166.3(2)	C5-C4-C19-C24	112.8(3)	C14-C13-C31'-C36'	84.1(19)
C2-C3-C4-C19'	17.1(8)	C19'-C4-C19-C24	140(8)	C31-C13-C31'-C36'	-169(4)
C16-C3-C4-C19'	-162.6(7)	C3-C4-C19-C20	100.76(17)	C36'-C31'-C32'-C33'	-8(3)
C3-C4-C5-C6	164.8(2)	C5-C4-C19-C20	-70.2(2)	C13-C31'-C32'-C33'	-174.9(17)
C19-C4-C5-C6	-24.6(3)	C19'-C4-C19-C20	-43(7)	C31'-C32'-C33'-C34'	8(3)
C19'-C4-C5-C6	-27.3(8)	C24-C19-C20-C21	-0.7(3)	C31'-C32'-C33'-C45'	179.6(18)
C3-C4-C5-C14	-13.7(3)	C4-C19-C20-C21	-177.9(3)	C32'-C33'-C34'-C35'	-7(4)
C19-C4-C5-C14	156.9(2)	C19-C20-C21-C22	-0.3(6)	C45'-C33'-C34'-C35'	-178.2(16)
C19'-C4-C5-C14	154.1(7)	C19-C20-C21-C43	179.7(4)	C33'-C34'-C35'-C36'	4(3)
C4-C5-C6-C7	171.4(2)	C20-C21-C22-C23	0.5(9)	C32'-C31'-C36'-C35'	4(3)
C14-C5-C6-C7	-10.1(3)	C43-C21-C22-C23	-179.5(6)	C13-C31'-C36'-C35'	170.0(14)
C4-C5-C6-C25	-17.2(3)	C21-C22-C23-C24	0.3(9)	C34'-C35'-C36'-C31'	-3(2)
C14-C5-C6-C25	161.3(2)	C22-C23-C24-C19	-1.4(7)	C16-C15-C37-C38	83.2(2)
C5-C6-C7-C12	-0.9(3)	C20-C19-C24-C23	1.5(5)	C14-C15-C37-C38	-91.4(2)
C25-C6-C7-C12	-172.6(2)	C4-C19-C24-C23	178.5(3)	C37'-C15-C37-C38	-175.5(19)
C5-C6-C7-C8	179.6(2)	C3-C4-C19'-C24'	104.9(12)	C16-C15-C37-C42	-92.1(3)
C25-C6-C7-C8	7.9(3)	C5-C4-C19'-C24'	-62.9(13)	C14-C15-C37-C42	93.3(3)
C6-C7-C8-C9	173.9(2)	C19-C4-C19'-C24'	143(8)	C37'-C15-C37-C42	9.2(18)
C12-C7-C8-C9	-5.7(4)	C3-C4-C19'-C20'	-63(2)	C42-C37-C38-C39	-0.2(2)
C7-C8-C9-C10	1.5(4)	C5-C4-C19'-C20'	129(2)	C15-C37-C38-C39	-175.6(3)
C8-C9-C10-C11	2.1(4)	C19-C4-C19'-C20'	-25(6)	C37-C38-C39-C40	-1.3(4)
C9-C10-C11-C12	-1.3(4)	C24'-C19'-C20'-C21'	8(4)	C38-C39-C40-C41	1.0(5)
C6-C7-C12-C13	8.0(3)	C4-C19'-C20'-C21'	175(2)	C39-C40-C41-C42	0.7(6)
C8-C7-C12-C13	-172.5(2)	C19'-C20'-C21'-C22'	-7(5)	C39-C40-C41-C46	-178.6(3)
C6-C7-C12-C11	-173.3(2)	C19'-C20'-C21'-C43'	167(3)	C40-C41-C42-C37	-2.2(5)
C8-C7-C12-C11	6.2(3)	C20'-C21'-C22'-C23'	0(6)	C46-C41-C42-C37	177.1(3)
C10-C11-C12-C13	175.7(2)	C43'-C21'-C22'-C23'	-173(3)	C38-C37-C42-C41	2.0(3)

C10-C11-C12-C7	-2.9(4)	C21'-C22'-C23'-C24'	5(6)	C15-C37-C42-C41	177.5(3)
C7-C12-C13-C14	-3.8(3)	C22'-C23'-C24'-C19'	-4(4)	C16-C15-C37'-C42'	87.2(12)
C11-C12-C13-C14	177.6(2)	C20'-C19'-C24'-C23'	-2(3)	C14-C15-C37'-C42'	-109.9(11)
C7-C12-C13-C31	-178.5(2)	C4-C19'-C24'-C23'	-171.5(17)	C37-C15-C37'-C42'	-1.6(10)
C11-C12-C13-C31	2.9(3)	C7-C6-C25-C30	101.8(3)	C16-C15-C37'-C38'	-81.7(14)
C7-C12-C13-C31'	158.6(6)	C5-C6-C25-C30	-69.8(3)	C14-C15-C37'-C38'	81.2(15)
C11-C12-C13-C31'	-20.0(6)	C7-C6-C25-C26	-76.1(3)	C37-C15-C37'-C38'	-171(3)
C12-C13-C14-C15	173.1(2)	C5-C6-C25-C26	112.3(2)	C42'-C37'-C38'-C39'	2(2)
C31-C13-C14-C15	-12.7(4)	C30-C25-C26-C27	1.8(3)	C15-C37'-C38'-C39'	169.7(13)
C31'-C13-C14-C15	11.5(7)	C6-C25-C26-C27	179.8(2)	C37'-C38'-C39'-C40'	6(2)
C12-C13-C14-C5	-7.1(3)	C25-C26-C27-C28	-1.6(3)	C38'-C39'-C40'-C41'	-6(3)
C31-C13-C14-C5	167.1(2)	C25-C26-C27-C44	177.2(2)	C39'-C40'-C41'-C42'	0(3)
C31'-C13-C14-C5	-168.6(6)	C26-C27-C28-C29	0.2(4)	C39'-C40'-C41'-C46'	-177.2(19)
C6-C5-C14-C13	14.0(3)	C44-C27-C28-C29	-178.6(3)	C38'-C37'-C42'-C41'	-8(2)
C4-C5-C14-C13	-167.4(2)	C27-C28-C29-C30	1.0(4)	C15-C37'-C42'-C41'	-176.8(13)
C6-C5-C14-C15	-166.2(2)	C28-C29-C30-C25	-0.7(4)	C40'-C41'-C42'-C37'	7(3)
C4-C5-C14-C15	12.4(3)	C26-C25-C30-C29	-0.7(3)	C46'-C41'-C42'-C37'	-175.4(18)
C13-C14-C15-C16	177.5(2)	C6-C25-C30-C29	-178.7(2)	C52-C47-C48-C49	1.4(11)
C5-C14-C15-C16	-2.3(3)	C12-C13-C31-C32	-85.6(3)	C47-C48-C49-C50	0.7(10)
C13-C14-C15-C37	-8.2(4)	C14-C13-C31-C32	99.9(4)	C48-C49-C50-C51	-2.3(9)
C5-C14-C15-C37	172.0(2)	C31'-C13-C31-C32	14(2)	C49-C50-C51-C52	1.9(11)
C13-C14-C15-C37'	15.1(6)	C12-C13-C31-C36	88.9(4)	C48-C47-C52-C51	-1.9(13)
C5-C14-C15-C37'	-164.7(6)	C14-C13-C31-C36	-85.6(4)	C50-C51-C52-C47	0.2(14)
C14-C15-C16-C17	176.5(2)	C31'-C13-C31-C36	-172(3)	C52'-C47'-C48'-C49'	-28(8)
C37-C15-C16-C17	1.8(3)	C36-C31-C32-C33	0.9(5)	C47'-C48'-C49'-C50'	32(7)
C37'-C15-C16-C17	-20.7(6)	C13-C31-C32-C33	175.6(3)	C48'-C49'-C50'-C51'	-21(6)
C14-C15-C16-C3	-6.6(3)	C31-C32-C33-C34	-2.0(6)	C49'-C50'-C51'-C52'	4(8)
C37-C15-C16-C3	178.62(19)	C31-C32-C33-C45	177.0(4)	C48'-C47'-C52'-C51'	11(10)
C37'-C15-C16-C3	156.1(5)	C32-C33-C34-C35	1.5(6)	C50'-C51'-C52'-C47'	1(10)
C4-C3-C16-C15	5.5(3)	C45-C33-C34-C35	-177.5(4)		
C2-C3-C16-C15	-174.3(2)	C33-C34-C35-C36	0.2(6)		
C4-C3-C16-C17	-177.5(2)	C34-C35-C36-C31	-1.4(5)		

Crystal Structure Report for **3.1c** (project code: 10150)

Data collection: A crystal (approximate dimensions 0.50 x 0.25 x 0.03 mm^3) was placed onto the tip of a 0.1 mm diameter glass capillary and mounted on a Bruker SMART Platform CCD diffractometer for a data collection at 173(2) K.[1] A preliminary set of cell constants was calculated from reflections harvested from three sets of 20 frames. These initial sets of frames were oriented such that orthogonal wedges of reciprocal space were surveyed. This produced initial orientation matrices determined from 4060 reflections. The data collection was carried out using MoKα radiation (graphite monochromator) with a frame time of 60 seconds and a detector distance of 4.8 cm. A randomly

oriented region of reciprocal space was surveyed to the extent of one sphere and to a resolution of 0.80 Å. Four major sections of frames were collected with 0.30º steps in ω at four different ϕ settings and a detector position of -28º in 2θ. The intensity data were corrected for absorption and decay (SADABS).[2] Final cell constants were calculated from the xyz centroids of 4060 strong reflections from the actual data collection after integration (SAINT).[3] Please refer to Table 1 for additional crystal and refinement information.

Structure solution and refinement: The structure was solved using SHELXS-97[4] and refined using SHELXL-97.[4] The space group $P2_1$ was determined based on systematic absences and intensity statistics. A direct-methods solution was calculated which provided most non-hydrogen atoms from the E-map. Full-matrix least squares / difference Fourier cycles were performed which located the remaining non-hydrogen atoms. All non-hydrogen atoms were refined with anisotropic displacement parameters. All hydrogen atoms were placed in ideal positions and refined as riding atoms with relative isotropic displacement parameters. The final full matrix least squares refinement converged to $R1$ = 0.0431 and $wR2$ = 0.1051 (F^2, all data).

Structure description: Two molecules exist in the unit cell, only one of which is unique. Twisting occurs in the tetracene backbone; however, the twisting is not consistent along the backbone, most likely due to the two different phenyl groups. Torsion angles for each ring in the backbone beginning at the *p*-methyl phenyl substituent side are as follows: 2.5, 11.4, 12.3, 4.1 degrees. The end-to-end twist of the backbone is 30.3 degrees.

Table A0.47. Atomic coordinates (x 10^4) and equivalent isotropic displacement parameters (Å^2 x 10^3) for **3.1c.** Ueq is defined as one third of the trace of the orthogonalized Uij tensor.

Atom	x	y	z	Ueq	Atom	x	y	z	Ueq
C1	8486(2)	784(2)	3716(1)	29(1)	C25	11061(2)	2606(2)	2484(1)	29(1)
C2	9544(2)	659(2)	4159(1)	31(1)	C26	11671(2)	3770(2)	2817(1)	35(1)
C3	9839(2)	-86(2)	5024(2)	39(1)	C27	12531(2)	4182(3)	2406(1)	41(1)
C4	10865(2)	-313(2)	5398(2)	42(1)	C28	12816(2)	3432(2)	1666(2)	42(1)
C5	11692(2)	217(2)	4951(2)	39(1)	C29	12221(2)	2244(2)	1350(2)	42(1)
C6	11458(2)	963(2)	4151(1)	33(1)	C30	11354(2)	1841(2)	1751(1)	37(1)
C7	10385(2)	1253(2)	3730(1)	29(1)	C31	9466(2)	4451(2)	1532(1)	33(1)
C8	10140(2)	2096(2)	2924(1)	28(1)	C32	9593(2)	5646(2)	2090(2)	41(1)
C9	9062(2)	2309(2)	2499(1)	28(1)	C33	10253(2)	6745(3)	1918(2)	52(1)
C10	8746(2)	3279(2)	1745(1)	30(1)	C34	10795(2)	6623(3)	1176(2)	56(1)
C11	7726(2)	3196(2)	1210(1)	32(1)	C35	10675(2)	5443(3)	590(2)	46(1)
C12	7412(2)	4094(2)	413(1)	39(1)	C36	9986(2)	4375(2)	765(1)	38(1)
C13	6488(2)	3866(3)	-183(2)	46(1)	C37	6487(2)	147(2)	2380(1)	31(1)
C14	5808(2)	2744(3)	-24(2)	46(1)	C38	6765(2)	-1250(2)	2212(1)	36(1)
C15	6046(2)	1907(3)	750(1)	39(1)	C39	6090(2)	-2370(2)	2321(2)	40(1)
C16	6995(2)	2122(2)	1411(1)	32(1)	C40	5122(2)	-2070(3)	2596(2)	41(1)
C17	7244(2)	1311(2)	2235(1)	30(1)	C41	4815(2)	-693(3)	2761(1)	40(1)
C18	8241(2)	1460(2)	2823(1)	28(1)	C42	5507(2)	417(2)	2643(1)	35(1)
C19	7625(2)	337(2)	4242(1)	30(1)	C43	5148(2)	-700(3)	5841(2)	50(1)
C20	7382(2)	-1067(2)	4408(1)	33(1)	C44	13750(2)	3903(3)	1222(2)	64(1)
C21	6583(2)	-1396(2)	4920(1)	35(1)	C45	10400(3)	8034(3)	2557(2)	85(1)

C22	6020(2)	-345(2)	5292(1)	37(1)	C46	11289(2)	5273(4)	-208(2)	67(1)
C23	6290(2)	1048(3)	5158(2)	42(1)	C47	6425(2)	-3876(3)	2177(2)	59(1)
C24	7070(2)	1396(2)	4631(2)	39(1)	C48	3770(2)	-383(3)	3074(2)	57(1)

Table A0.48. Bond lengths (Å) and angles (°) for **3.1c**.

Bond	Length	Atoms	Angle	Atoms	Angle
C(1)-C(2)	1.399(3)	C(46)-H(46A)	0.98	C(27)-C(26)-H(26A)	119.7
C(1)-C(18)	1.430(3)	C(46)-H(46B)	0.98	C(28)-C(27)-C(26)	121.3(2)
C(1)-C(19)	1.498(3)	C(46)-H(46C)	0.98	C(28)-C(27)-H(27A)	119.4
C(2)-C(3)	1.432(3)	C(47)-H(47A)	0.98	C(26)-C(27)-H(27A)	119.4
C(2)-C(7)	1.439(3)	C(47)-H(47B)	0.98	C(27)-C(28)-C(29)	118.0(2)
C(3)-C(4)	1.347(3)	C(47)-H(47C)	0.98	C(27)-C(28)-C(44)	120.6(2)
C(3)-H(3A)	0.95	C(48)-H(48A)	0.98	C(29)-C(28)-C(44)	121.5(2)
C(4)-C(5)	1.416(3)	C(48)-H(48B)	0.98	C(30)-C(29)-C(28)	120.9(2)
C(4)-H(4A)	0.95	C(48)-H(48C)	0.98	C(30)-C(29)-H(29A)	119.6
C(5)-C(6)	1.347(3)	C(2)-C(1)-C(18)	120.17(17)	C(28)-C(29)-H(29A)	119.6
C(5)-H(5A)	0.95	C(2)-C(1)-C(19)	118.36(16)	C(29)-C(30)-C(25)	121.0(2)
C(6)-C(7)	1.429(3)	C(18)-C(1)-C(19)	121.15(17)	C(29)-C(30)-H(30A)	119.5
C(6)-H(6A)	0.95	C(1)-C(2)-C(3)	122.43(18)	C(25)-C(30)-H(30A)	119.5
C(7)-C(8)	1.404(3)	C(1)-C(2)-C(7)	119.95(17)	C(32)-C(31)-C(36)	119.2(2)
C(8)-C(9)	1.424(3)	C(3)-C(2)-C(7)	117.59(18)	C(32)-C(31)-C(10)	119.63(18)
C(8)-C(25)	1.504(3)	C(4)-C(3)-C(2)	121.73(19)	C(36)-C(31)-C(10)	121.16(19)
C(9)-C(10)	1.430(3)	C(4)-C(3)-H(3A)	119.1	C(31)-C(32)-C(33)	121.3(2)
C(9)-C(18)	1.456(3)	C(2)-C(3)-H(3A)	119.1	C(31)-C(32)-H(32A)	119.4
C(10)-C(11)	1.401(3)	C(3)-C(4)-C(5)	120.46(19)	C(33)-C(32)-H(32A)	119.4
C(10)-C(31)	1.501(3)	C(3)-C(4)-H(4A)	119.8	C(34)-C(33)-C(32)	118.6(2)
C(11)-C(12)	1.434(3)	C(5)-C(4)-H(4A)	119.8	C(34)-C(33)-C(45)	121.1(2)
C(11)-C(16)	1.437(3)	C(6)-C(5)-C(4)	120.2(2)	C(32)-C(33)-C(45)	120.3(2)
C(12)-C(13)	1.358(3)	C(6)-C(5)-H(5A)	119.9	C(33)-C(34)-C(35)	121.7(2)
C(12)-H(12A)	0.95	C(4)-C(5)-H(5A)	119.9	C(33)-C(34)-H(34A)	119.1
C(13)-C(14)	1.409(3)	C(5)-C(6)-C(7)	121.79(19)	C(35)-C(34)-H(34A)	119.1
C(13)-H(13A)	0.95	C(5)-C(6)-H(6A)	119.1	C(36)-C(35)-C(34)	118.4(2)
C(14)-C(15)	1.364(3)	C(7)-C(6)-H(6A)	119.1	C(36)-C(35)-C(46)	119.3(3)
C(14)-H(14A)	0.95	C(8)-C(7)-C(6)	121.88(17)	C(34)-C(35)-C(46)	122.3(2)
C(15)-C(16)	1.429(3)	C(8)-C(7)-C(2)	120.07(17)	C(35)-C(36)-C(31)	120.7(2)
C(15)-H(15A)	0.95	C(6)-C(7)-C(2)	118.05(17)	C(35)-C(36)-H(36A)	119.6
C(16)-C(17)	1.408(3)	C(7)-C(8)-C(9)	120.32(17)	C(31)-C(36)-H(36A)	119.6
C(17)-C(18)	1.415(3)	C(7)-C(8)-C(25)	116.89(17)	C(42)-C(37)-C(38)	119.09(19)

C(17)-C(37)	1.497(3)	C(9)-C(8)-C(25)	122.43(16)	C(42)-C(37)-C(17)	122.32(19)
C(19)-C(20)	1.388(3)	C(8)-C(9)-C(10)	123.38(17)	C(38)-C(37)-C(17)	118.56(18)
C(19)-C(24)	1.394(3)	C(8)-C(9)-C(18)	118.50(16)	C(39)-C(38)-C(37)	121.2(2)
C(20)-C(21)	1.391(3)	C(10)-C(9)-C(18)	118.08(17)	C(39)-C(38)-H(38A)	119.4
C(20)-H(20A)	0.95	C(11)-C(10)-C(9)	120.39(18)	C(37)-C(38)-H(38A)	119.4
C(21)-C(22)	1.384(3)	C(11)-C(10)-C(31)	118.00(17)	C(38)-C(39)-C(40)	118.5(2)
C(21)-H(21A)	0.95	C(9)-C(10)-C(31)	121.54(18)	C(38)-C(39)-C(47)	120.3(2)
C(22)-C(23)	1.378(3)	C(10)-C(11)-C(12)	121.52(19)	C(40)-C(39)-C(47)	121.2(2)
C(22)-C(43)	1.508(3)	C(10)-C(11)-C(16)	119.96(18)	C(41)-C(40)-C(39)	122.0(2)
C(23)-C(24)	1.390(3)	C(12)-C(11)-C(16)	118.35(19)	C(41)-C(40)-H(40A)	119
C(23)-H(23A)	0.95	C(13)-C(12)-C(11)	121.1(2)	C(39)-C(40)-H(40A)	119
C(24)-H(24A)	0.95	C(13)-C(12)-H(12A)	119.5	C(40)-C(41)-C(42)	118.4(2)
C(25)-C(26)	1.383(3)	C(11)-C(12)-H(12A)	119.5	C(40)-C(41)-C(48)	121.5(2)
C(25)-C(30)	1.387(3)	C(12)-C(13)-C(14)	120.4(2)	C(42)-C(41)-C(48)	120.0(2)
C(26)-C(27)	1.389(3)	C(12)-C(13)-H(13A)	119.8	C(37)-C(42)-C(41)	120.8(2)
C(26)-H(26A)	0.95	C(14)-C(13)-H(13A)	119.8	C(37)-C(42)-H(42A)	119.6
C(27)-C(28)	1.382(3)	C(15)-C(14)-C(13)	120.6(2)	C(41)-C(42)-H(42A)	119.6
C(27)-H(27A)	0.95	C(15)-C(14)-H(14A)	119.7	C(22)-C(43)-H(43A)	109.5
C(28)-C(29)	1.386(3)	C(13)-C(14)-H(14A)	119.7	C(22)-C(43)-H(43B)	109.5
C(28)-C(44)	1.511(3)	C(14)-C(15)-C(16)	121.3(2)	H(43A)-C(43)-H(43B)	109.5
C(29)-C(30)	1.385(3)	C(14)-C(15)-H(15A)	119.4	C(22)-C(43)-H(43C)	109.5
C(29)-H(29A)	0.95	C(16)-C(15)-H(15A)	119.4	H(43A)-C(43)-H(43C)	109.5
C(30)-H(30A)	0.95	C(17)-C(16)-C(15)	122.59(19)	H(43B)-C(43)-H(43C)	109.5
C(31)-C(32)	1.380(3)	C(17)-C(16)-C(11)	119.46(18)	C(28)-C(44)-H(44A)	109.5
C(31)-C(36)	1.388(3)	C(15)-C(16)-C(11)	117.94(18)	C(28)-C(44)-H(44B)	109.5
C(32)-C(33)	1.383(3)	C(16)-C(17)-C(18)	120.67(18)	H(44A)-C(44)-H(44B)	109.5
C(32)-H(32A)	0.95	C(16)-C(17)-C(37)	117.17(18)	C(28)-C(44)-H(44C)	109.5
C(33)-C(34)	1.377(4)	C(18)-C(17)-C(37)	121.52(17)	H(44A)-C(44)-H(44C)	109.5
C(33)-C(45)	1.519(4)	C(17)-C(18)-C(1)	122.77(17)	H(44B)-C(44)-H(44C)	109.5
C(34)-C(35)	1.392(4)	C(17)-C(18)-C(9)	118.81(16)	C(33)-C(45)-H(45A)	109.5
C(34)-H(34A)	0.95	C(1)-C(18)-C(9)	118.40(17)	C(33)-C(45)-H(45B)	109.5
C(35)-C(36)	1.386(3)	C(20)-C(19)-C(24)	117.85(18)	H(45A)-C(45)-H(45B)	109.5
C(35)-C(46)	1.510(3)	C(20)-C(19)-C(1)	124.05(18)	C(33)-C(45)-H(45C)	109.5
C(36)-H(36A)	0.95	C(24)-C(19)-C(1)	118.00(18)	H(45A)-C(45)-H(45C)	109.5
C(37)-C(42)	1.390(3)	C(19)-C(20)-C(21)	120.62(19)	H(45B)-C(45)-H(45C)	109.5
C(37)-C(38)	1.394(3)	C(19)-C(20)-H(20A)	119.7	C(35)-C(46)-H(46A)	109.5
C(38)-C(39)	1.386(3)	C(21)-C(20)-H(20A)	119.7	C(35)-C(46)-H(46B)	109.5
C(38)-H(38A)	0.95	C(22)-C(21)-C(20)	121.50(19)	H(46A)-C(46)-H(46B)	109.5

C(39)-C(40)	1.388(3)	C(22)-C(21)-H(21A)	119.3	C(35)-C(46)-H(46C)	109.5
C(39)-C(47)	1.505(3)	C(20)-C(21)-H(21A)	119.3	H(46A)-C(46)-H(46C)	109.5
C(40)-C(41)	1.387(3)	C(23)-C(22)-C(21)	117.82(19)	H(46B)-C(46)-H(46C)	109.5
C(40)-H(40A)	0.95	C(23)-C(22)-C(43)	120.6(2)	C(39)-C(47)-H(47A)	109.5
C(41)-C(42)	1.396(3)	C(21)-C(22)-C(43)	121.6(2)	C(39)-C(47)-H(47B)	109.5
C(41)-C(48)	1.506(3)	C(22)-C(23)-C(24)	121.4(2)	H(47A)-C(47)-H(47B)	109.5
C(42)-H(42A)	0.95	C(22)-C(23)-H(23A)	119.3	C(39)-C(47)-H(47C)	109.5
C(43)-H(43A)	0.98	C(24)-C(23)-H(23A)	119.3	H(47A)-C(47)-H(47C)	109.5
C(43)-H(43B)	0.98	C(23)-C(24)-C(19)	120.8(2)	H(47B)-C(47)-H(47C)	109.5
C(43)-H(43C)	0.98	C(23)-C(24)-H(24A)	119.6	C(41)-C(48)-H(48A)	109.5
C(44)-H(44A)	0.98	C(19)-C(24)-H(24A)	119.6	C(41)-C(48)-H(48B)	109.5
C(44)-H(44B)	0.98	C(26)-C(25)-C(30)	118.13(18)	H(48A)-C(48)-H(48B)	109.5
C(44)-H(44C)	0.98	C(26)-C(25)-C(8)	122.56(17)	C(41)-C(48)-H(48C)	109.5
C(45)-H(45A)	0.98	C(30)-C(25)-C(8)	119.21(18)	H(48A)-C(48)-H(48C)	109.5
C(45)-H(45B)	0.98	C(25)-C(26)-C(27)	120.7(2)	H(48B)-C(48)-H(48C)	109.5
C(45)-H(45C)	0.98	C(25)-C(26)-H(26A)	119.7		

Table A0.49. Anisotropic displacement parameters ($Å^2$ x 10^3) for **3.1c**. The anisotropic displacement factor exponent takes the form: $-2\pi^2[h^2 a^{*2}U11 + ... + 2 h k a^* b^* U12]$.

Atom	U11	U22	U33	U23	U13	U12
C1	33(1)	25(1)	31(1)	0(1)	12(1)	-1(1)
C2	36(1)	27(1)	30(1)	-1(1)	9(1)	0(1)
C3	39(1)	43(1)	35(1)	13(1)	11(1)	-1(1)
C4	45(1)	45(1)	35(1)	14(1)	4(1)	3(1)
C5	34(1)	37(1)	45(1)	6(1)	2(1)	1(1)
C6	34(1)	30(1)	37(1)	4(1)	8(1)	-2(1)
C7	32(1)	24(1)	31(1)	-3(1)	9(1)	-1(1)
C8	33(1)	25(1)	28(1)	-3(1)	10(1)	-4(1)
C9	35(1)	24(1)	27(1)	-4(1)	9(1)	-1(1)
C10	36(1)	26(1)	28(1)	-1(1)	11(1)	1(1)
C11	36(1)	31(1)	29(1)	0(1)	9(1)	6(1)
C12	44(1)	38(1)	36(1)	6(1)	12(1)	4(1)
C13	43(1)	59(2)	34(1)	12(1)	4(1)	8(1)
C14	35(1)	66(2)	35(1)	3(1)	3(1)	6(1)
C15	32(1)	49(1)	37(1)	-1(1)	10(1)	-1(1)
C16	30(1)	36(1)	30(1)	-3(1)	10(1)	4(1)
C17	30(1)	32(1)	29(1)	-2(1)	12(1)	3(1)
C18	31(1)	25(1)	29(1)	0(1)	10(1)	2(1)

C19	30(1)	34(1)	28(1)	2(1)	8(1)	-2(1)
C20	33(1)	35(1)	32(1)	3(1)	6(1)	2(1)
C21	34(1)	34(1)	36(1)	4(1)	6(1)	-9(1)
C22	32(1)	50(1)	30(1)	3(1)	7(1)	-8(1)
C23	43(1)	43(1)	44(1)	-6(1)	20(1)	1(1)
C24	46(1)	31(1)	45(1)	1(1)	20(1)	-1(1)
C25	30(1)	32(1)	27(1)	5(1)	5(1)	1(1)
C26	35(1)	39(1)	31(1)	1(1)	6(1)	-3(1)
C27	36(1)	44(1)	41(1)	6(1)	3(1)	-9(1)
C28	35(1)	47(1)	47(1)	12(1)	12(1)	0(1)
C29	47(1)	41(1)	42(1)	3(1)	20(1)	10(1)
C30	41(1)	30(1)	40(1)	1(1)	12(1)	-2(1)
C31	37(1)	29(1)	33(1)	6(1)	4(1)	3(1)
C32	45(1)	32(1)	46(1)	2(1)	5(1)	2(1)
C33	57(2)	32(1)	64(2)	3(1)	3(1)	-3(1)
C34	52(2)	40(1)	73(2)	24(1)	1(1)	-12(1)
C35	40(1)	50(1)	49(1)	24(1)	6(1)	0(1)
C36	40(1)	42(1)	32(1)	9(1)	5(1)	-2(1)
C37	30(1)	37(1)	26(1)	0(1)	4(1)	-3(1)
C38	32(1)	42(1)	34(1)	-6(1)	10(1)	-1(1)
C39	40(1)	41(1)	39(1)	-5(1)	4(1)	-6(1)
C40	35(1)	45(1)	42(1)	3(1)	6(1)	-10(1)
C41	29(1)	56(1)	35(1)	8(1)	5(1)	0(1)
C42	32(1)	40(1)	34(1)	3(1)	7(1)	5(1)
C43	41(1)	66(2)	47(1)	-4(1)	19(1)	-13(1)
C44	42(2)	83(2)	72(2)	15(2)	28(1)	-2(2)
C45	105(3)	40(2)	107(3)	-18(2)	10(2)	-18(2)
C46	55(2)	91(2)	56(2)	36(2)	18(1)	-3(2)
C47	61(2)	40(1)	79(2)	-16(1)	21(2)	-7(1)
C48	31(1)	77(2)	67(2)	21(1)	18(1)	7(1)

Table A0.50. Hydrogen coordinates (x 10^4) and isotropic displacement parameters (Å^2 x 10^3) for **3.1c**.

Atom	x	y	z	U(eq)
H3A	9297	-429	5343	46
H4A	11036	-832	5965	50
H5A	12413	46	5217	47
H6A	12022	1306	3859	40
H12A	7858	4862	301	47

H13A	6299	4466	-712	55
H14A	5178	2570	-460	55
H15A	5571	1168	851	47
H20A	7765	-1810	4170	40
H21A	6421	-2364	5016	42
H23A	5937	1786	5431	50
H24A	7227	2366	4536	47
H26A	11499	4292	3332	42
H27A	12932	4995	2637	49
H29A	12410	1699	851	50
H30A	10953	1027	1520	44
H32A	9219	5715	2603	50
H34A	11262	7363	1061	67
H36A	9869	3581	356	46
H38A	7428	-1438	2019	43
H40A	4656	-2832	2674	49
H42A	5305	1368	2745	42
H43A	5374	-1495	6264	75
H43B	4503	-967	5409	75
H43C	5000	130	6206	75
H44A	13738	4938	1155	96
H44B	13704	3461	605	96
H44C	14414	3613	1619	96
H45A	10476	7724	3210	128
H45B	9780	8658	2411	128
H45C	11041	8552	2462	128
H46A	12002	5677	-30	100
H46B	10916	5769	-761	100
H46C	11347	4261	-352	100
H47A	5818	-4410	1843	88
H47B	6671	-4321	2785	88
H47C	7003	-3877	1808	88
H48A	3328	-1241	3008	86
H48B	3401	378	2688	86
H48C	3900	-85	3731	86

Table A0.51. Torsion angles (°) for **3.1c**.

Atoms	Angle	Atoms	Angle

C18-C1-C2-C3	-175.93(18)	C18-C1-C19-C20	112.4(2)
C19-C1-C2-C3	10.4(3)	C2-C1-C19-C24	102.3(2)
C18-C1-C2-C7	2.0(3)	C18-C1-C19-C24	-71.2(3)
C19-C1-C2-C7	-171.57(17)	C24-C19-C20-C21	2.3(3)
C1-C2-C3-C4	173.6(2)	C1-C19-C20-C21	178.66(18)
C7-C2-C3-C4	-4.4(3)	C19-C20-C21-C22	-1.1(3)
C2-C3-C4-C5	1.6(3)	C20-C21-C22-C23	-1.4(3)
C3-C4-C5-C6	0.5(3)	C20-C21-C22-C43	179.51(19)
C4-C5-C6-C7	0.4(3)	C21-C22-C23-C24	2.8(3)
C5-C6-C7-C8	176.46(19)	C43-C22-C23-C24	-178.1(2)
C5-C6-C7-C2	-3.2(3)	C22-C23-C24-C19	-1.7(3)
C1-C2-C7-C8	7.3(3)	C20-C19-C24-C23	-0.9(3)
C3-C2-C7-C8	-174.64(18)	C1-C19-C24-C23	-177.48(19)
C1-C2-C7-C6	-173.02(18)	C7-C8-C25-C26	-80.8(2)
C3-C2-C7-C6	5.1(3)	C9-C8-C25-C26	106.1(2)
C6-C7-C8-C9	177.13(18)	C7-C8-C25-C30	95.4(2)
C2-C7-C8-C9	-3.2(3)	C9-C8-C25-C30	-77.7(2)
C6-C7-C8-C25	3.8(3)	C30-C25-C26-C27	2.0(3)
C2-C7-C8-C25	-176.49(17)	C8-C25-C26-C27	178.24(19)
C7-C8-C9-C10	172.57(17)	C25-C26-C27-C28	-1.2(3)
C25-C8-C9-C10	-14.5(3)	C26-C27-C28-C29	-0.6(3)
C7-C8-C9-C18	-9.8(3)	C26-C27-C28-C44	179.5(2)
C25-C8-C9-C18	163.12(17)	C27-C28-C29-C30	1.4(3)
C8-C9-C10-C11	164.36(18)	C44-C28-C29-C30	-178.7(2)
C18-C9-C10-C11	-13.3(3)	C28-C29-C30-C25	-0.5(3)
C8-C9-C10-C31	-18.7(3)	C26-C25-C30-C29	-1.2(3)
C18-C9-C10-C31	163.69(17)	C8-C25-C30-C29	-177.55(19)
C9-C10-C11-C12	-175.90(18)	C11-C10-C31-C32	100.9(2)
C31-C10-C11-C12	7.0(3)	C9-C10-C31-C32	-76.1(3)
C9-C10-C11-C16	-0.7(3)	C11-C10-C31-C36	-77.3(2)
C31-C10-C11-C16	-177.79(17)	C9-C10-C31-C36	105.7(2)
C10-C11-C12-C13	169.8(2)	C36-C31-C32-C33	-2.1(3)
C16-C11-C12-C13	-5.4(3)	C10-C31-C32-C33	179.7(2)
C11-C12-C13-C14	0.8(3)	C31-C32-C33-C34	-0.5(4)
C12-C13-C14-C15	2.6(3)	C31-C32-C33-C45	-178.5(3)
C13-C14-C15-C16	-1.2(3)	C32-C33-C34-C35	1.4(4)
C14-C15-C16-C17	177.5(2)	C45-C33-C34-C35	179.4(3)
C14-C15-C16-C11	-3.5(3)	C33-C34-C35-C36	0.2(4)

C10-C11-C16-C17	10.3(3)	C33-C34-C35-C46	-178.1(2)
C12-C11-C16-C17	-174.37(18)	C34-C35-C36-C31	-2.9(3)
C10-C11-C16-C15	-168.71(18)	C46-C35-C36-C31	175.5(2)
C12-C11-C16-C15	6.6(3)	C32-C31-C36-C35	3.8(3)
C15-C16-C17-C18	173.58(18)	C10-C31-C36-C35	-178.0(2)
C11-C16-C17-C18	-5.4(3)	C16-C17-C37-C42	-75.0(2)
C15-C16-C17-C37	2.6(3)	C18-C17-C37-C42	114.2(2)
C11-C16-C17-C37	-176.30(17)	C16-C17-C37-C38	102.8(2)
C16-C17-C18-C1	172.75(17)	C18-C17-C37-C38	-68.0(2)
C37-C17-C18-C1	-16.7(3)	C42-C37-C38-C39	-1.2(3)
C16-C17-C18-C9	-8.7(3)	C17-C37-C38-C39	-179.09(19)
C37-C17-C18-C9	161.79(17)	C37-C38-C39-C40	0.5(3)
C2-C1-C18-C17	163.54(17)	C37-C38-C39-C47	-177.4(2)
C19-C1-C18-C17	-23.0(3)	C38-C39-C40-C41	0.1(3)
C2-C1-C18-C9	-15.0(3)	C47-C39-C40-C41	178.0(2)
C19-C1-C18-C9	158.46(18)	C39-C40-C41-C42	0.1(3)
C8-C9-C18-C17	-159.79(17)	C39-C40-C41-C48	-179.0(2)
C10-C9-C18-C17	18.0(2)	C38-C37-C42-C41	1.4(3)
C8-C9-C18-C1	18.8(2)	C17-C37-C42-C41	179.17(18)
C10-C9-C18-C1	-163.45(17)	C40-C41-C42-C37	-0.8(3)
C2-C1-C19-C20	-74.1(3)	C48-C41-C42-C37	178.2(2)

Crystal Structure Report for **3.1d** (project code: 11007)

Data collection: A crystal (approximate dimensions 0.50 x 0.25 x 0.25 mm^3) was placed onto the tip of a 0.1 mm diameter glass capillary and mounted on a Bruker SMART Platform CCD diffractometer for a data collection at 123(2) K.[1] A preliminary set of cell constants was calculated from reflections harvested from three sets of 20 frames. These initial sets of frames were oriented such that orthogonal wedges of reciprocal space were surveyed. This produced initial orientation matrices determined from 200 reflections. The data collection was carried out using MoKα radiation (graphite monochromator) with a frame time of 30 seconds and a detector distance of 4.8 cm. A randomly oriented region of reciprocal space was surveyed to the extent of one sphere and to a resolution of 0.84 Å. Four major sections of frames were collected with 0.30º steps in ω at four different ϕ settings and a detector position of -28º in 2θ. The intensity data were corrected for absorption and decay (SADABS).[2] Final cell constants were calculated from the xyz centroids of 4088 strong reflections from the actual data collection after integration (SAINT).[3] Please refer to Table 1 for additional crystal and refinement information.

Structure solution and refinement: The structure was solved using SHELXS-97[4] and refined using SHELXL-97.[4] The space group P-1 was determined based on systematic absences and intensity statistics. A direct-methods solution was calculated which provided most non-hydrogen atoms from the E-map. Full-matrix least squares / difference Fourier cycles were performed which located the remaining non-hydrogen atoms. All non-hydrogen atoms were refined with anisotropic displacement parameters. All hydrogen atoms were placed in ideal positions and refined as riding atoms with relative isotropic displacement parameters. The final full matrix least squares refinement converged to $R1$ = 0.0599 and $wR2$ = 0.1564 (F^2, all data).

Structure description: The structure exhibits disorder in the ethyl groups which was found to be best not modeled.

There are three unique molecules in the unit cell. This compound likely went through a phase transition to the twinned triclinic cell during cooling as suggested by the unit cell being close to twice the volume of a C-centered cell.

Table A0.52. Atomic coordinates (x 10^4) and equivalent isotropic displacement parameters (Å^2 x 10^3) for **3.1d.** Ueq is defined as one third of the trace of the orthogonalized Uij tensor.

Atom	x	y	z	Ueq	Atom	x	y	z	Ueq
C1	5296(3)	1779(1)	3134(1)	31(1)	C76	9238(3)	8720(1)	14009(1)	32(1)
C2	4494(3)	1422(1)	3420(1)	31(1)	C77	8455(3)	9189(1)	14282(1)	38(1)
C3	4559(3)	1320(1)	3978(1)	38(1)	C78	8550(3)	9816(1)	14186(1)	39(1)
C4	3693(3)	1029(2)	4253(1)	42(1)	C79	9468(3)	9951(1)	13816(1)	38(1)
C5	2689(3)	810(1)	3994(1)	41(1)	C80	10254(3)	9487(1)	13543(1)	31(1)
C6	2601(3)	878(1)	3465(1)	35(1)	C81	8332(3)	8784(1)	12809(1)	25(1)
C7	3524(3)	1165(1)	3155(1)	31(1)	C82	7747(3)	8297(1)	13009(1)	30(1)
C8	3500(3)	1201(1)	2610(1)	30(1)	C83	6490(3)	8419(1)	13244(1)	34(1)
C9	4419(3)	1506(1)	2313(1)	28(1)	C84	5758(3)	9040(1)	13286(1)	34(1)
C10	4613(3)	1463(1)	1771(1)	31(1)	C85	6350(3)	9524(1)	13084(1)	32(1)
C11	5349(3)	1849(1)	1484(1)	30(1)	C86	7602(3)	9405(1)	12845(1)	27(1)
C12	5606(3)	1807(1)	937(1)	36(1)	C87	13317(3)	7929(1)	11665(1)	25(1)
C13	6187(3)	2222(1)	652(1)	42(1)	C88	14369(3)	8223(1)	11747(1)	29(1)
C14	6571(3)	2716(1)	892(1)	40(1)	C89	15538(3)	8106(1)	11448(1)	33(1)
C15	6413(3)	2761(1)	1410(1)	35(1)	C90	15688(3)	7703(1)	11053(1)	35(1)
C16	5842(3)	2318(1)	1737(1)	30(1)	C91	14640(3)	7401(1)	10983(1)	34(1)
C17	5774(3)	2320(1)	2276(1)	29(1)	C92	13478(3)	7507(1)	11279(1)	31(1)
C18	5181(3)	1874(1)	2580(1)	28(1)	C93	16680(5)	5475(2)	11840(2)	70(1)
C19	6368(3)	1990(1)	3413(1)	38(1)	C94	17124(7)	5661(2)	11330(2)	116(3)
C20	7712(3)	1694(2)	3354(2)	51(1)	C95	7668(4)	10330(2)	14475(2)	63(1)
C21	8737(4)	1871(2)	3629(2)	77(2)	C96	8361(5)	10682(2)	14785(2)	78(1)
C22	8431(5)	2350(2)	3968(2)	76(2)	C97	4422(3)	9168(2)	13566(1)	46(1)
C23	7099(4)	2631(2)	4017(1)	63(1)	C98	4597(4)	9192(2)	14151(1)	59(1)
C24	6071(4)	2466(2)	3754(1)	47(1)	C99	16903(3)	7625(2)	10700(1)	49(1)
C25	2349(3)	1017(1)	2353(1)	31(1)	C100	16685(4)	8122(2)	10245(1)	66(1)
C26	2262(3)	391(1)	2326(1)	34(1)	C101	8563(3)	5275(1)	6873(1)	30(1)
C27	1109(3)	260(1)	2117(1)	37(1)	C102	8313(3)	5933(1)	6863(1)	31(1)
C28	21(3)	733(1)	1937(1)	39(1)	C103	7854(3)	6340(1)	6400(1)	36(1)
C29	106(3)	1358(1)	1965(1)	42(1)	C104	7749(3)	6972(1)	6386(1)	40(1)
C30	1259(3)	1493(1)	2168(1)	39(1)	C105	8109(3)	7246(1)	6823(1)	39(1)
C31	4179(3)	970(1)	1490(1)	30(1)	C106	8482(3)	6887(1)	7278(1)	34(1)
C32	4916(3)	348(1)	1556(1)	32(1)	C107	8526(3)	6223(1)	7326(1)	30(1)
C33	4576(3)	-108(1)	1273(1)	34(1)	C108	8715(3)	5865(1)	7806(1)	31(1)

C34	3497(3)	38(1)	931(1)	35(1)	C109	8804(3)	5200(1)	7831(1)	29(1)
C35	2751(3)	669(1)	865(1)	40(1)	C110	8719(3)	4827(1)	8306(1)	29(1)
C36	3101(3)	1122(1)	1139(1)	38(1)	C111	9147(3)	4170(1)	8328(1)	27(1)
C37	6165(3)	2861(1)	2508(1)	29(1)	C112	9092(3)	3768(1)	8796(1)	31(1)
C38	5144(3)	3353(1)	2654(1)	33(1)	C113	9658(3)	3140(1)	8824(1)	32(1)
C39	5446(3)	3888(1)	2828(1)	38(1)	C114	10299(3)	2862(1)	8379(1)	31(1)
C40	6783(3)	3943(1)	2863(1)	35(1)	C115	10293(3)	3212(1)	7919(1)	28(1)
C41	7802(3)	3453(1)	2721(1)	37(1)	C116	9669(3)	3876(1)	7863(1)	26(1)
C42	7511(3)	2920(1)	2541(1)	35(1)	C117	9533(3)	4232(1)	7379(1)	27(1)
C43	9564(6)	2516(3)	4246(2)	133(3)	C118	8971(3)	4897(1)	7351(1)	27(1)
C44	10262(5)	2079(2)	4632(2)	85(2)	C119	8228(3)	4985(1)	6405(1)	32(1)
C45	-1223(3)	591(2)	1695(1)	51(1)	C120	8945(3)	4995(1)	5939(1)	39(1)
C46	-1147(4)	627(2)	1111(2)	59(1)	C121	8571(4)	4718(2)	5518(1)	47(1)
C47	3120(4)	-458(2)	629(1)	51(1)	C122	7473(4)	4434(2)	5543(1)	47(1)
C48	3414(8)	-398(2)	65(2)	110(2)	C123	6740(3)	4441(1)	6000(1)	42(1)
C49	7140(4)	4514(2)	3073(1)	50(1)	C124	7115(3)	4708(1)	6426(1)	35(1)
C50	7445(8)	4410(2)	3642(2)	109(2)	C125	9000(3)	6167(1)	8279(1)	32(1)
C51	13078(3)	7537(1)	12802(1)	26(1)	C126	8018(3)	6618(1)	8513(1)	35(1)
C52	13141(3)	7531(1)	13344(1)	27(1)	C127	8337(3)	6876(1)	8951(1)	38(1)
C53	14173(3)	7090(1)	13650(1)	37(1)	C128	9643(3)	6706(1)	9172(1)	38(1)
C54	14302(3)	7130(2)	14167(1)	44(1)	C129	10624(3)	6275(1)	8928(1)	38(1)
C55	13428(3)	7611(2)	14423(1)	40(1)	C130	10307(3)	6010(1)	8489(1)	36(1)
C56	12402(3)	8021(1)	14159(1)	34(1)	C131	7994(3)	5130(1)	8760(1)	31(1)
C57	12182(3)	7984(1)	13612(1)	26(1)	C132	6611(3)	5415(1)	8696(1)	31(1)
C58	11054(3)	8369(1)	13345(1)	25(1)	C133	5878(3)	5716(1)	9093(1)	36(1)
C59	10888(3)	8332(1)	12801(1)	23(1)	C134	6481(3)	5749(1)	9567(1)	37(1)
C60	9654(3)	8620(1)	12527(1)	25(1)	C135	7839(3)	5449(1)	9635(1)	40(1)
C61	9634(3)	8675(1)	11983(1)	24(1)	C136	8592(3)	5142(1)	9238(1)	37(1)
C62	8407(3)	8948(1)	11692(1)	28(1)	C137	10116(3)	3916(1)	6909(1)	26(1)
C63	8411(3)	9041(1)	11163(1)	31(1)	C138	11335(3)	4030(1)	6704(1)	30(1)
C64	9638(3)	8865(1)	10885(1)	32(1)	C139	11938(3)	3729(1)	6285(1)	32(1)
C65	10814(3)	8585(1)	11142(1)	29(1)	C140	11347(3)	3307(1)	6047(1)	31(1)
C66	10862(3)	8457(1)	11698(1)	24(1)	C141	10145(3)	3192(1)	6254(1)	31(1)
C67	12035(3)	8105(1)	11962(1)	24(1)	C142	9529(3)	3486(1)	6678(1)	30(1)
C68	12024(2)	7984(1)	12517(1)	23(1)	C143	7142(5)	4086(2)	5092(1)	72(1)
C69	14014(3)	7023(1)	12540(1)	26(1)	C144	5673(7)	4246(4)	4903(2)	128(2)
C70	15411(3)	6972(1)	12508(1)	32(1)	C145	9969(4)	6979(1)	9661(1)	44(1)
C71	16245(3)	6474(1)	12283(1)	39(1)	C146	10079(4)	7666(2)	9564(1)	48(1)

C72	15732(3)	6005(1)	12094(1)	44(1)	C147	5690(4)	6119(2)	9984(1)	46(1)
C73	14347(3)	6049(1)	12128(1)	43(1)	C148	4449(5)	5879(2)	10182(2)	69(1)
C74	13491(3)	6557(1)	12343(1)	32(1)	C149	12014(4)	2980(1)	5587(1)	41(1)
C75	10143(3)	8864(1)	13632(1)	27(1)	C150	12075(5)	3429(2)	5105(1)	65(1)

Table A0.53. Bond lengths (Å) and angles (°) for **3.1d**.

Atoms	Length	Atoms	Angle	Atoms	Angle
C(1)-C(2)	1.405(4)	C(142)-H(14T)	0.95	C(76)-C(77)-C(78)	121.1(3)
C(1)-C(18)	1.427(4)	C(143)-C(144)	1.522(8)	C(76)-C(77)-H(77A)	119.4
C(1)-C(19)	1.489(4)	C(143)-H(14A)	0.99	C(78)-C(77)-H(77A)	119.4
C(2)-C(3)	1.434(4)	C(143)-H(14B)	0.99	C(79)-C(78)-C(77)	117.8(3)
C(2)-C(7)	1.444(4)	C(144)-H(14I)	0.98	C(79)-C(78)-C(95)	121.1(3)
C(3)-C(4)	1.353(4)	C(144)-H(14J)	0.98	C(77)-C(78)-C(95)	121.1(3)
C(3)-H(3A)	0.95	C(144)-H(14K)	0.98	C(80)-C(79)-C(78)	121.4(3)
C(4)-C(5)	1.415(4)	C(145)-C(146)	1.528(4)	C(80)-C(79)-H(79A)	119.3
C(4)-H(4A)	0.95	C(145)-H(14C)	0.99	C(78)-C(79)-H(79A)	119.3
C(5)-C(6)	1.358(4)	C(145)-H(14D)	0.99	C(79)-C(80)-C(75)	120.8(3)
C(5)-H(5A)	0.95	C(146)-H(14L)	0.98	C(79)-C(80)-H(80A)	119.6
C(6)-C(7)	1.434(4)	C(146)-H(14M)	0.98	C(75)-C(80)-H(80A)	119.6
C(6)-H(6A)	0.95	C(146)-H(14N)	0.98	C(82)-C(81)-C(86)	118.2(2)
C(7)-C(8)	1.398(4)	C(147)-C(148)	1.531(5)	C(82)-C(81)-C(60)	118.4(2)
C(8)-C(9)	1.435(4)	C(147)-H(14E)	0.99	C(86)-C(81)-C(60)	123.3(2)
C(8)-C(25)	1.496(4)	C(147)-H(14F)	0.99	C(83)-C(82)-C(81)	121.1(2)
C(9)-C(10)	1.415(4)	C(148)-H(14O)	0.98	C(83)-C(82)-H(82A)	119.5
C(9)-C(18)	1.452(4)	C(148)-H(14P)	0.98	C(81)-C(82)-H(82A)	119.5
C(10)-C(11)	1.404(4)	C(148)-H(14Q)	0.98	C(82)-C(83)-C(84)	121.1(2)
C(10)-C(31)	1.498(4)	C(149)-C(150)	1.521(4)	C(82)-C(83)-H(83A)	119.5
C(11)-C(12)	1.435(4)	C(149)-H(14G)	0.99	C(84)-C(83)-H(83A)	119.5
C(11)-C(16)	1.444(4)	C(149)-H(14H)	0.99	C(85)-C(84)-C(83)	117.4(2)
C(12)-C(13)	1.347(4)	C(150)-H(15A)	0.98	C(85)-C(84)-C(97)	121.9(2)
C(12)-H(12A)	0.95	C(150)-H(15B)	0.98	C(83)-C(84)-C(97)	120.7(3)
C(13)-C(14)	1.421(4)	C(150)-H(15C)	0.98	C(86)-C(85)-C(84)	121.9(2)
C(13)-H(13A)	0.95	C(2)-C(1)-C(18)	120.2(2)	C(86)-C(85)-H(85A)	119.1
C(14)-C(15)	1.351(4)	C(2)-C(1)-C(19)	118.7(2)	C(84)-C(85)-H(85A)	119.1
C(14)-H(14R)	0.95	C(18)-C(1)-C(19)	120.8(2)	C(85)-C(86)-C(81)	120.4(2)
C(15)-C(16)	1.440(4)	C(1)-C(2)-C(3)	122.3(3)	C(85)-C(86)-H(86A)	119.8
C(15)-H(15D)	0.95	C(1)-C(2)-C(7)	120.0(3)	C(81)-C(86)-H(86A)	119.8
C(16)-C(17)	1.390(4)	C(3)-C(2)-C(7)	117.7(2)	C(88)-C(87)-C(92)	118.2(2)

C(17)-C(18)	1.426(4)	C(4)-C(3)-C(2)	121.8(3)	C(88)-C(87)-C(67)	119.1(2)
C(17)-C(37)	1.504(4)	C(4)-C(3)-H(3A)	119.1	C(92)-C(87)-C(67)	122.6(2)
C(19)-C(20)	1.379(4)	C(2)-C(3)-H(3A)	119.1	C(89)-C(88)-C(87)	120.7(2)
C(19)-C(24)	1.398(5)	C(3)-C(4)-C(5)	120.4(3)	C(89)-C(88)-H(88A)	119.6
C(20)-C(21)	1.408(5)	C(3)-C(4)-H(4A)	119.8	C(87)-C(88)-H(88A)	119.6
C(20)-H(20A)	0.95	C(5)-C(4)-H(4A)	119.8	C(88)-C(89)-C(90)	121.4(3)
C(21)-C(22)	1.399(7)	C(6)-C(5)-C(4)	120.4(3)	C(88)-C(89)-H(89A)	119.3
C(21)-H(21A)	0.95	C(6)-C(5)-H(5A)	119.8	C(90)-C(89)-H(89A)	119.3
C(22)-C(23)	1.355(7)	C(4)-C(5)-H(5A)	119.8	C(89)-C(90)-C(91)	117.3(2)
C(22)-C(43)	1.490(5)	C(5)-C(6)-C(7)	121.3(3)	C(89)-C(90)-C(99)	121.0(3)
C(23)-C(24)	1.381(5)	C(5)-C(6)-H(6A)	119.3	C(91)-C(90)-C(99)	121.7(3)
C(23)-H(23A)	0.95	C(7)-C(6)-H(6A)	119.3	C(92)-C(91)-C(90)	122.0(3)
C(24)-H(24A)	0.95	C(8)-C(7)-C(6)	121.8(3)	C(92)-C(91)-H(91A)	119
C(25)-C(30)	1.387(4)	C(8)-C(7)-C(2)	120.0(2)	C(90)-C(91)-H(91A)	119
C(25)-C(26)	1.398(4)	C(6)-C(7)-C(2)	118.1(3)	C(91)-C(92)-C(87)	120.4(3)
C(26)-C(27)	1.389(4)	C(7)-C(8)-C(9)	120.1(2)	C(91)-C(92)-H(92A)	119.8
C(26)-H(26A)	0.95	C(7)-C(8)-C(25)	117.8(2)	C(87)-C(92)-H(92A)	119.8
C(27)-C(28)	1.381(4)	C(9)-C(8)-C(25)	121.2(2)	C(94)-C(93)-C(72)	113.7(3)
C(27)-H(27A)	0.95	C(10)-C(9)-C(8)	122.7(2)	C(94)-C(93)-H(93A)	108.8
C(28)-C(29)	1.395(4)	C(10)-C(9)-C(18)	118.6(2)	C(72)-C(93)-H(93A)	108.8
C(28)-C(45)	1.517(4)	C(8)-C(9)-C(18)	118.7(2)	C(94)-C(93)-H(93B)	108.8
C(29)-C(30)	1.387(4)	C(11)-C(10)-C(9)	120.3(2)	C(72)-C(93)-H(93B)	108.8
C(29)-H(29A)	0.95	C(11)-C(10)-C(31)	117.0(2)	H(93A)-C(93)-H(93B)	107.7
C(30)-H(30A)	0.95	C(9)-C(10)-C(31)	122.4(2)	C(93)-C(94)-H(94A)	109.5
C(31)-C(36)	1.387(4)	C(10)-C(11)-C(12)	122.1(2)	C(93)-C(94)-H(94B)	109.5
C(31)-C(32)	1.390(4)	C(10)-C(11)-C(16)	119.7(2)	H(94A)-C(94)-H(94B)	109.5
C(32)-C(33)	1.391(4)	C(12)-C(11)-C(16)	118.2(2)	C(93)-C(94)-H(94C)	109.5
C(32)-H(32A)	0.95	C(13)-C(12)-C(11)	121.8(3)	H(94A)-C(94)-H(94C)	109.5
C(33)-C(34)	1.373(4)	C(13)-C(12)-H(12A)	119.1	H(94B)-C(94)-H(94C)	109.5
C(33)-H(33A)	0.95	C(11)-C(12)-H(12A)	119.1	C(96)-C(95)-C(78)	116.9(3)
C(34)-C(35)	1.410(4)	C(12)-C(13)-C(14)	120.1(3)	C(96)-C(95)-H(95A)	108.1
C(34)-C(47)	1.506(4)	C(12)-C(13)-H(13A)	120	C(78)-C(95)-H(95A)	108.1
C(35)-C(36)	1.376(4)	C(14)-C(13)-H(13A)	120	C(96)-C(95)-H(95B)	108.1
C(35)-H(35A)	0.95	C(15)-C(14)-C(13)	120.7(3)	C(78)-C(95)-H(95B)	108.1
C(36)-H(36A)	0.95	C(15)-C(14)-H(14R)	119.6	H(95A)-C(95)-H(95B)	107.3
C(37)-C(38)	1.385(4)	C(13)-C(14)-H(14R)	119.6	C(95)-C(96)-H(96A)	109.5
C(37)-C(42)	1.399(4)	C(14)-C(15)-C(16)	121.6(3)	C(95)-C(96)-H(96B)	109.5
C(38)-C(39)	1.386(4)	C(14)-C(15)-H(15D)	119.2	H(96A)-C(96)-H(96B)	109.5

C(38)-H(38A)	0.95	C(16)-C(15)-H(15D)	119.2	C(95)-C(96)-H(96C)	109.5
C(39)-C(40)	1.390(4)	C(17)-C(16)-C(15)	122.8(2)	H(96A)-C(96)-H(96C)	109.5
C(39)-H(39A)	0.95	C(17)-C(16)-C(11)	119.8(2)	H(96B)-C(96)-H(96C)	109.5
C(40)-C(41)	1.379(4)	C(15)-C(16)-C(11)	117.3(2)	C(84)-C(97)-C(98)	112.3(3)
C(40)-C(49)	1.521(4)	C(16)-C(17)-C(18)	120.3(2)	C(84)-C(97)-H(97A)	109.2
C(41)-C(42)	1.384(4)	C(16)-C(17)-C(37)	116.9(2)	C(98)-C(97)-H(97A)	109.2
C(41)-H(41A)	0.95	C(18)-C(17)-C(37)	122.2(2)	C(84)-C(97)-H(97B)	109.2
C(42)-H(42A)	0.95	C(17)-C(18)-C(1)	122.7(2)	C(98)-C(97)-H(97B)	109.2
C(43)-C(44)	1.391(6)	C(17)-C(18)-C(9)	118.6(2)	H(97A)-C(97)-H(97B)	107.9
C(43)-H(43A)	0.99	C(1)-C(18)-C(9)	118.7(2)	C(97)-C(98)-H(98A)	109.5
C(43)-H(43B)	0.99	C(20)-C(19)-C(24)	117.7(3)	C(97)-C(98)-H(98B)	109.5
C(44)-H(44A)	0.98	C(20)-C(19)-C(1)	119.4(3)	H(98A)-C(98)-H(98B)	109.5
C(44)-H(44B)	0.98	C(24)-C(19)-C(1)	122.8(3)	C(97)-C(98)-H(98C)	109.5
C(44)-H(44C)	0.98	C(19)-C(20)-C(21)	120.3(4)	H(98A)-C(98)-H(98C)	109.5
C(45)-C(46)	1.502(5)	C(19)-C(20)-H(20A)	119.9	H(98B)-C(98)-H(98C)	109.5
C(45)-H(45A)	0.99	C(21)-C(20)-H(20A)	119.9	C(90)-C(99)-C(100)	111.6(3)
C(45)-H(45B)	0.99	C(22)-C(21)-C(20)	121.6(4)	C(90)-C(99)-H(99A)	109.3
C(46)-H(46A)	0.98	C(22)-C(21)-H(21A)	119.2	C(100)-C(99)-H(99A)	109.3
C(46)-H(46B)	0.98	C(20)-C(21)-H(21A)	119.2	C(90)-C(99)-H(99B)	109.3
C(46)-H(46C)	0.98	C(23)-C(22)-C(21)	116.6(3)	C(100)-C(99)-H(99B)	109.3
C(47)-C(48)	1.481(6)	C(23)-C(22)-C(43)	124.6(6)	H(99A)-C(99)-H(99B)	108
C(47)-H(47A)	0.99	C(21)-C(22)-C(43)	118.8(5)	C(99)-C(100)-H(10A)	109.5
C(47)-H(47B)	0.99	C(22)-C(23)-C(24)	123.2(4)	C(99)-C(100)-H(10B)	109.5
C(48)-H(48A)	0.98	C(22)-C(23)-H(23A)	118.4	H(10A)-C(100)-H(10B)	109.5
C(48)-H(48B)	0.98	C(24)-C(23)-H(23A)	118.4	C(99)-C(100)-H(10C)	109.5
C(48)-H(48C)	0.98	C(23)-C(24)-C(19)	120.6(4)	H(10A)-C(100)-H(10C)	109.5
C(49)-C(50)	1.488(5)	C(23)-C(24)-H(24A)	119.7	H(10B)-C(100)-H(10C)	109.5
C(49)-H(49A)	0.99	C(19)-C(24)-H(24A)	119.7	C(102)-C(101)-C(118)	119.5(2)
C(49)-H(49B)	0.99	C(30)-C(25)-C(26)	118.2(3)	C(102)-C(101)-C(119)	119.2(2)
C(50)-H(50A)	0.98	C(30)-C(25)-C(8)	118.1(2)	C(118)-C(101)-C(119)	120.7(2)
C(50)-H(50B)	0.98	C(26)-C(25)-C(8)	123.6(3)	C(101)-C(102)-C(103)	122.3(3)
C(50)-H(50C)	0.98	C(27)-C(26)-C(25)	120.0(3)	C(101)-C(102)-C(107)	120.0(2)
C(51)-C(52)	1.396(4)	C(27)-C(26)-H(26A)	120	C(103)-C(102)-C(107)	117.8(2)
C(51)-C(68)	1.431(4)	C(25)-C(26)-H(26A)	120	C(104)-C(103)-C(102)	120.9(3)
C(51)-C(69)	1.500(3)	C(28)-C(27)-C(26)	121.8(3)	C(104)-C(103)-H(10D)	119.5
C(52)-C(53)	1.437(4)	C(28)-C(27)-H(27A)	119.1	C(102)-C(103)-H(10D)	119.5
C(52)-C(57)	1.437(4)	C(26)-C(27)-H(27A)	119.1	C(103)-C(104)-C(105)	121.0(3)
C(53)-C(54)	1.353(4)	C(27)-C(28)-C(29)	118.2(3)	C(103)-C(104)-H(10E)	119.5

C(53)-H(53A)	0.95	C(27)-C(28)-C(45)	121.8(3)	C(105)-C(104)-H(10E)	119.5
C(54)-C(55)	1.416(4)	C(29)-C(28)-C(45)	120.0(3)	C(106)-C(105)-C(104)	120.5(3)
C(54)-H(54A)	0.95	C(30)-C(29)-C(28)	120.3(3)	C(106)-C(105)-H(10F)	119.8
C(55)-C(56)	1.351(4)	C(30)-C(29)-H(29A)	119.8	C(104)-C(105)-H(10F)	119.8
C(55)-H(55A)	0.95	C(28)-C(29)-H(29A)	119.8	C(105)-C(106)-C(107)	121.0(3)
C(56)-C(57)	1.441(4)	C(25)-C(30)-C(29)	121.5(3)	C(105)-C(106)-H(10G)	119.5
C(56)-H(56A)	0.95	C(25)-C(30)-H(30A)	119.3	C(107)-C(106)-H(10G)	119.5
C(57)-C(58)	1.401(4)	C(29)-C(30)-H(30A)	119.3	C(108)-C(107)-C(106)	121.9(2)
C(58)-C(59)	1.424(3)	C(36)-C(31)-C(32)	118.4(2)	C(108)-C(107)-C(102)	119.9(2)
C(58)-C(75)	1.496(3)	C(36)-C(31)-C(10)	121.8(2)	C(106)-C(107)-C(102)	118.2(2)
C(59)-C(60)	1.427(4)	C(32)-C(31)-C(10)	119.8(2)	C(107)-C(108)-C(109)	119.8(2)
C(59)-C(68)	1.452(3)	C(31)-C(32)-C(33)	120.4(3)	C(107)-C(108)-C(125)	119.1(2)
C(60)-C(61)	1.396(4)	C(31)-C(32)-H(32A)	119.8	C(109)-C(108)-C(125)	120.6(2)
C(60)-C(81)	1.498(3)	C(33)-C(32)-H(32A)	119.8	C(110)-C(109)-C(108)	122.8(2)
C(61)-C(62)	1.436(4)	C(34)-C(33)-C(32)	121.5(3)	C(110)-C(109)-C(118)	118.6(2)
C(61)-C(66)	1.440(3)	C(34)-C(33)-H(33A)	119.2	C(108)-C(109)-C(118)	118.6(2)
C(62)-C(63)	1.358(4)	C(32)-C(33)-H(33A)	119.2	C(111)-C(110)-C(109)	120.0(2)
C(62)-H(62A)	0.95	C(33)-C(34)-C(35)	118.0(2)	C(111)-C(110)-C(131)	119.9(2)
C(63)-C(64)	1.416(4)	C(33)-C(34)-C(47)	121.4(3)	C(109)-C(110)-C(131)	119.6(2)
C(63)-H(63A)	0.95	C(35)-C(34)-C(47)	120.6(3)	C(110)-C(111)-C(112)	122.6(2)
C(64)-C(65)	1.357(4)	C(36)-C(35)-C(34)	120.5(3)	C(110)-C(111)-C(116)	119.5(2)
C(64)-H(64A)	0.95	C(36)-C(35)-H(35A)	119.8	C(112)-C(111)-C(116)	117.9(2)
C(65)-C(66)	1.433(4)	C(34)-C(35)-H(35A)	119.8	C(113)-C(112)-C(111)	121.5(2)
C(65)-H(65A)	0.95	C(35)-C(36)-C(31)	121.3(3)	C(113)-C(112)-H(11A)	119.3
C(66)-C(67)	1.405(4)	C(35)-C(36)-H(36A)	119.4	C(111)-C(112)-H(11A)	119.3
C(67)-C(68)	1.430(3)	C(31)-C(36)-H(36A)	119.4	C(112)-C(113)-C(114)	120.2(2)
C(67)-C(87)	1.486(3)	C(38)-C(37)-C(42)	118.1(3)	C(112)-C(113)-H(11B)	119.9
C(69)-C(74)	1.386(4)	C(38)-C(37)-C(17)	118.6(2)	C(114)-C(113)-H(11B)	119.9
C(69)-C(70)	1.392(4)	C(42)-C(37)-C(17)	123.0(3)	C(115)-C(114)-C(113)	120.5(2)
C(70)-C(71)	1.382(4)	C(37)-C(38)-C(39)	121.0(3)	C(115)-C(114)-H(11C)	119.8
C(70)-H(70A)	0.95	C(37)-C(38)-H(38A)	119.5	C(113)-C(114)-H(11C)	119.8
C(71)-C(72)	1.379(5)	C(39)-C(38)-H(38A)	119.5	C(114)-C(115)-C(116)	121.6(2)
C(71)-H(71A)	0.95	C(38)-C(39)-C(40)	120.8(3)	C(114)-C(115)-H(11D)	119.2
C(72)-C(73)	1.383(5)	C(38)-C(39)-H(39A)	119.6	C(116)-C(115)-H(11D)	119.2
C(72)-C(93)	1.516(4)	C(40)-C(39)-H(39A)	119.6	C(117)-C(116)-C(115)	122.3(2)
C(73)-C(74)	1.396(4)	C(41)-C(40)-C(39)	118.3(3)	C(117)-C(116)-C(111)	120.0(2)
C(73)-H(73A)	0.95	C(41)-C(40)-C(49)	120.0(3)	C(115)-C(116)-C(111)	117.7(2)
C(74)-H(74A)	0.95	C(39)-C(40)-C(49)	121.6(3)	C(116)-C(117)-C(118)	119.7(2)

C(75)-C(76)	1.387(4)	C(40)-C(41)-C(42)	121.4(3)	C(116)-C(117)-C(137)	118.6(2)
C(75)-C(80)	1.391(4)	C(40)-C(41)-H(41A)	119.3	C(118)-C(117)-C(137)	121.4(2)
C(76)-C(77)	1.384(4)	C(42)-C(41)-H(41A)	119.3	C(101)-C(118)-C(117)	123.3(2)
C(76)-H(76A)	0.95	C(41)-C(42)-C(37)	120.4(3)	C(101)-C(118)-C(109)	118.4(2)
C(77)-C(78)	1.394(4)	C(41)-C(42)-H(42A)	119.8	C(117)-C(118)-C(109)	118.3(2)
C(77)-H(77A)	0.95	C(37)-C(42)-H(42A)	119.8	C(124)-C(119)-C(120)	118.0(3)
C(78)-C(79)	1.380(4)	C(44)-C(43)-C(22)	118.2(4)	C(124)-C(119)-C(101)	118.6(2)
C(78)-C(95)	1.514(4)	C(44)-C(43)-H(43A)	107.8	C(120)-C(119)-C(101)	123.4(3)
C(79)-C(80)	1.378(4)	C(22)-C(43)-H(43A)	107.8	C(121)-C(120)-C(119)	120.2(3)
C(79)-H(79A)	0.95	C(44)-C(43)-H(43B)	107.8	C(121)-C(120)-H(12B)	119.9
C(80)-H(80A)	0.95	C(22)-C(43)-H(43B)	107.8	C(119)-C(120)-H(12B)	119.9
C(81)-C(82)	1.388(4)	H(43A)-C(43)-H(43B)	107.1	C(120)-C(121)-C(122)	121.5(3)
C(81)-C(86)	1.400(3)	C(43)-C(44)-H(44A)	109.5	C(120)-C(121)-H(12C)	119.3
C(82)-C(83)	1.381(4)	C(43)-C(44)-H(44B)	109.5	C(122)-C(121)-H(12C)	119.3
C(82)-H(82A)	0.95	H(44A)-C(44)-H(44B)	109.5	C(123)-C(122)-C(121)	118.1(3)
C(83)-C(84)	1.404(4)	C(43)-C(44)-H(44C)	109.5	C(123)-C(122)-C(143)	120.9(3)
C(83)-H(83A)	0.95	H(44A)-C(44)-H(44C)	109.5	C(121)-C(122)-C(143)	120.8(3)
C(84)-C(85)	1.388(4)	H(44B)-C(44)-H(44C)	109.5	C(122)-C(123)-C(124)	120.9(3)
C(84)-C(97)	1.502(4)	C(46)-C(45)-C(28)	111.9(3)	C(122)-C(123)-H(12D)	119.6
C(85)-C(86)	1.380(4)	C(46)-C(45)-H(45A)	109.2	C(124)-C(123)-H(12D)	119.6
C(85)-H(85A)	0.95	C(28)-C(45)-H(45A)	109.2	C(123)-C(124)-C(119)	121.2(3)
C(86)-H(86A)	0.95	C(46)-C(45)-H(45B)	109.2	C(123)-C(124)-H(12E)	119.4
C(87)-C(88)	1.390(4)	C(28)-C(45)-H(45B)	109.2	C(119)-C(124)-H(12E)	119.4
C(87)-C(92)	1.399(3)	H(45A)-C(45)-H(45B)	107.9	C(130)-C(125)-C(126)	118.0(3)
C(88)-C(89)	1.388(4)	C(45)-C(46)-H(46A)	109.5	C(130)-C(125)-C(108)	119.0(2)
C(88)-H(88A)	0.95	C(45)-C(46)-H(46B)	109.5	C(126)-C(125)-C(108)	123.0(3)
C(89)-C(90)	1.389(4)	H(46A)-C(46)-H(46B)	109.5	C(127)-C(126)-C(125)	120.4(3)
C(89)-H(89A)	0.95	C(45)-C(46)-H(46C)	109.5	C(127)-C(126)-H(12F)	119.8
C(90)-C(91)	1.392(4)	H(46A)-C(46)-H(46C)	109.5	C(125)-C(126)-H(12F)	119.8
C(90)-C(99)	1.504(4)	H(46B)-C(46)-H(46C)	109.5	C(126)-C(127)-C(128)	121.7(3)
C(91)-C(92)	1.378(4)	C(48)-C(47)-C(34)	114.6(3)	C(126)-C(127)-H(12G)	119.2
C(91)-H(91A)	0.95	C(48)-C(47)-H(47A)	108.6	C(128)-C(127)-H(12G)	119.2
C(92)-H(92A)	0.95	C(34)-C(47)-H(47A)	108.6	C(129)-C(128)-C(127)	117.6(3)
C(93)-C(94)	1.437(6)	C(48)-C(47)-H(47B)	108.6	C(129)-C(128)-C(145)	121.2(3)
C(93)-H(93A)	0.99	C(34)-C(47)-H(47B)	108.6	C(127)-C(128)-C(145)	121.2(3)
C(93)-H(93B)	0.99	H(47A)-C(47)-H(47B)	107.6	C(128)-C(129)-C(130)	120.9(3)
C(94)-H(94A)	0.98	C(47)-C(48)-H(48A)	109.5	C(128)-C(129)-H(12H)	119.5
C(94)-H(94B)	0.98	C(47)-C(48)-H(48B)	109.5	C(130)-C(129)-H(12H)	119.5

C(94)-H(94C)	0.98	H(48A)-C(48)-H(48B)	109.5	C(129)-C(130)-C(125)	121.3(3)
C(95)-C(96)	1.448(5)	C(47)-C(48)-H(48C)	109.5	C(129)-C(130)-H(13B)	119.3
C(95)-H(95A)	0.99	H(48A)-C(48)-H(48C)	109.5	C(125)-C(130)-H(13B)	119.3
C(95)-H(95B)	0.99	H(48B)-C(48)-H(48C)	109.5	C(136)-C(131)-C(132)	118.1(3)
C(96)-H(96A)	0.98	C(50)-C(49)-C(40)	112.2(3)	C(136)-C(131)-C(110)	124.5(3)
C(96)-H(96B)	0.98	C(50)-C(49)-H(49A)	109.2	C(132)-C(131)-C(110)	117.4(2)
C(96)-H(96C)	0.98	C(40)-C(49)-H(49A)	109.2	C(133)-C(132)-C(131)	120.9(3)
C(97)-C(98)	1.526(5)	C(50)-C(49)-H(49B)	109.2	C(133)-C(132)-H(13C)	119.6
C(97)-H(97A)	0.99	C(40)-C(49)-H(49B)	109.2	C(131)-C(132)-H(13C)	119.6
C(97)-H(97B)	0.99	H(49A)-C(49)-H(49B)	107.9	C(132)-C(133)-C(134)	121.4(3)
C(98)-H(98A)	0.98	C(49)-C(50)-H(50A)	109.5	C(132)-C(133)-H(13D)	119.3
C(98)-H(98B)	0.98	C(49)-C(50)-H(50B)	109.5	C(134)-C(133)-H(13D)	119.3
C(98)-H(98C)	0.98	H(50A)-C(50)-H(50B)	109.5	C(135)-C(134)-C(133)	117.5(3)
C(99)-C(100)	1.506(5)	C(49)-C(50)-H(50C)	109.5	C(135)-C(134)-C(147)	121.6(3)
C(99)-H(99A)	0.99	H(50A)-C(50)-H(50C)	109.5	C(133)-C(134)-C(147)	120.8(3)
C(99)-H(99B)	0.99	H(50B)-C(50)-H(50C)	109.5	C(134)-C(135)-C(136)	121.6(3)
C(100)-H(10A)	0.98	C(52)-C(51)-C(68)	119.6(2)	C(134)-C(135)-H(13E)	119.2
C(100)-H(10B)	0.98	C(52)-C(51)-C(69)	118.8(2)	C(136)-C(135)-H(13E)	119.2
C(100)-H(10C)	0.98	C(68)-C(51)-C(69)	121.2(2)	C(131)-C(136)-C(135)	120.4(3)
C(101)-C(102)	1.400(3)	C(51)-C(52)-C(53)	121.9(2)	C(131)-C(136)-H(13F)	119.8
C(101)-C(118)	1.429(4)	C(51)-C(52)-C(57)	120.2(2)	C(135)-C(136)-H(13F)	119.8
C(101)-C(119)	1.489(4)	C(53)-C(52)-C(57)	117.8(2)	C(142)-C(137)-C(138)	118.1(2)
C(102)-C(103)	1.436(4)	C(54)-C(53)-C(52)	121.1(3)	C(142)-C(137)-C(117)	122.9(2)
C(102)-C(107)	1.443(4)	C(54)-C(53)-H(53A)	119.4	C(138)-C(137)-C(117)	118.9(2)
C(103)-C(104)	1.359(4)	C(52)-C(53)-H(53A)	119.4	C(139)-C(138)-C(137)	121.0(2)
C(103)-H(10D)	0.95	C(53)-C(54)-C(55)	120.9(3)	C(139)-C(138)-H(13G)	119.5
C(104)-C(105)	1.410(4)	C(53)-C(54)-H(54A)	119.5	C(137)-C(138)-H(13G)	119.5
C(104)-H(10E)	0.95	C(55)-C(54)-H(54A)	119.5	C(138)-C(139)-C(140)	121.2(3)
C(105)-C(106)	1.357(4)	C(56)-C(55)-C(54)	120.4(3)	C(138)-C(139)-H(13H)	119.4
C(105)-H(10F)	0.95	C(56)-C(55)-H(55A)	119.8	C(140)-C(139)-H(13H)	119.4
C(106)-C(107)	1.436(3)	C(54)-C(55)-H(55A)	119.8	C(141)-C(140)-C(139)	117.6(2)
C(106)-H(10G)	0.95	C(55)-C(56)-C(57)	121.0(3)	C(141)-C(140)-C(149)	121.6(3)
C(107)-C(108)	1.393(4)	C(55)-C(56)-H(56A)	119.5	C(139)-C(140)-C(149)	120.9(3)
C(108)-C(109)	1.430(3)	C(57)-C(56)-H(56A)	119.5	C(140)-C(141)-C(142)	122.0(2)
C(108)-C(125)	1.498(4)	C(58)-C(57)-C(52)	120.1(2)	C(140)-C(141)-H(14S)	119
C(109)-C(110)	1.421(4)	C(58)-C(57)-C(56)	121.6(2)	C(142)-C(141)-H(14S)	119
C(109)-C(118)	1.445(4)	C(52)-C(57)-C(56)	118.3(2)	C(141)-C(142)-C(137)	120.1(3)
C(110)-C(111)	1.398(3)	C(57)-C(58)-C(59)	120.1(2)	C(141)-C(142)-H(14T)	120

C(110)-C(131)	1.494(4)	C(57)-C(58)-C(75)	117.8(2)	C(137)-C(142)-H(14T)	120
C(111)-C(112)	1.435(4)	C(59)-C(58)-C(75)	121.7(2)	C(144)-C(143)-C(122)	116.9(4)
C(111)-C(116)	1.446(4)	C(58)-C(59)-C(60)	122.7(2)	C(144)-C(143)-H(14A)	108.1
C(112)-C(113)	1.357(4)	C(58)-C(59)-C(68)	118.3(2)	C(122)-C(143)-H(14A)	108.1
C(112)-H(11A)	0.95	C(60)-C(59)-C(68)	119.0(2)	C(144)-C(143)-H(14B)	108.1
C(113)-C(114)	1.423(4)	C(61)-C(60)-C(59)	119.9(2)	C(122)-C(143)-H(14B)	108.1
C(113)-H(11B)	0.95	C(61)-C(60)-C(81)	118.5(2)	H(14A)-C(143)-H(14B)	107.3
C(114)-C(115)	1.351(4)	C(59)-C(60)-C(81)	121.1(2)	C(143)-C(144)-H(14I)	109.5
C(114)-H(11C)	0.95	C(60)-C(61)-C(62)	121.6(2)	C(143)-C(144)-H(14J)	109.5
C(115)-C(116)	1.438(3)	C(60)-C(61)-C(66)	120.1(2)	H(14I)-C(144)-H(14J)	109.5
C(115)-H(11D)	0.95	C(62)-C(61)-C(66)	118.2(2)	C(143)-C(144)-H(14K)	109.5
C(116)-C(117)	1.399(4)	C(63)-C(62)-C(61)	121.3(2)	H(14I)-C(144)-H(14K)	109.5
C(117)-C(118)	1.430(3)	C(63)-C(62)-H(62A)	119.3	H(14J)-C(144)-H(14K)	109.5
C(117)-C(137)	1.495(3)	C(61)-C(62)-H(62A)	119.3	C(128)-C(145)-C(146)	113.0(3)
C(119)-C(124)	1.392(4)	C(62)-C(63)-C(64)	120.3(3)	C(128)-C(145)-H(14C)	109
C(119)-C(120)	1.393(4)	C(62)-C(63)-H(63A)	119.9	C(146)-C(145)-H(14C)	109
C(120)-C(121)	1.387(4)	C(64)-C(63)-H(63A)	119.9	C(128)-C(145)-H(14D)	109
C(120)-H(12B)	0.95	C(65)-C(64)-C(63)	120.5(2)	C(146)-C(145)-H(14D)	109
C(121)-C(122)	1.389(5)	C(65)-C(64)-H(64A)	119.7	H(14C)-C(145)-H(14D)	107.8
C(121)-H(12C)	0.95	C(63)-C(64)-H(64A)	119.7	C(145)-C(146)-H(14L)	109.5
C(122)-C(123)	1.380(5)	C(64)-C(65)-C(66)	121.7(2)	C(145)-C(146)-H(14M)	109.5
C(122)-C(143)	1.525(5)	C(64)-C(65)-H(65A)	119.2	H(14L)-C(146)-H(14M)	109.5
C(123)-C(124)	1.385(4)	C(66)-C(65)-H(65A)	119.2	C(145)-C(146)-H(14N)	109.5
C(123)-H(12D)	0.95	C(67)-C(66)-C(65)	122.2(2)	H(14L)-C(146)-H(14N)	109.5
C(124)-H(12E)	0.95	C(67)-C(66)-C(61)	120.0(2)	H(14M)-C(146)-H(14N)	109.5
C(125)-C(130)	1.391(4)	C(65)-C(66)-C(61)	117.7(2)	C(134)-C(147)-C(148)	114.3(3)
C(125)-C(126)	1.401(4)	C(66)-C(67)-C(68)	119.9(2)	C(134)-C(147)-H(14E)	108.7
C(126)-C(127)	1.381(4)	C(66)-C(67)-C(87)	118.9(2)	C(148)-C(147)-H(14E)	108.7
C(126)-H(12F)	0.95	C(68)-C(67)-C(87)	120.8(2)	C(134)-C(147)-H(14F)	108.7
C(127)-C(128)	1.401(4)	C(67)-C(68)-C(51)	122.9(2)	C(148)-C(147)-H(14F)	108.7
C(127)-H(12G)	0.95	C(67)-C(68)-C(59)	118.2(2)	H(14E)-C(147)-H(14F)	107.6
C(128)-C(129)	1.390(4)	C(51)-C(68)-C(59)	118.9(2)	C(147)-C(148)-H(14O)	109.5
C(128)-C(145)	1.512(4)	C(74)-C(69)-C(70)	117.9(2)	C(147)-C(148)-H(14P)	109.5
C(129)-C(130)	1.390(4)	C(74)-C(69)-C(51)	119.2(2)	H(14O)-C(148)-H(14P)	109.5
C(129)-H(12H)	0.95	C(70)-C(69)-C(51)	122.8(2)	C(147)-C(148)-H(14Q)	109.5
C(130)-H(13B)	0.95	C(71)-C(70)-C(69)	120.9(3)	H(14O)-C(148)-H(14Q)	109.5
C(131)-C(136)	1.384(4)	C(71)-C(70)-H(70A)	119.5	H(14P)-C(148)-H(14Q)	109.5
C(131)-C(132)	1.400(4)	C(69)-C(70)-H(70A)	119.5	C(140)-C(149)-C(150)	113.5(3)

C(132)-C(133)	1.381(4)	C(72)-C(71)-C(70)	121.3(3)	C(140)-C(149)-H(14G)	108.9
C(132)-H(13C)	0.95	C(72)-C(71)-H(71A)	119.3	C(150)-C(149)-H(14G)	108.9
C(133)-C(134)	1.387(4)	C(70)-C(71)-H(71A)	119.3	C(140)-C(149)-H(14H)	108.9
C(133)-H(13D)	0.95	C(71)-C(72)-C(73)	118.1(3)	C(150)-C(149)-H(14H)	108.9
C(134)-C(135)	1.386(5)	C(71)-C(72)-C(93)	119.6(3)	H(14G)-C(149)-H(14H)	107.7
C(134)-C(147)	1.512(4)	C(73)-C(72)-C(93)	122.3(3)	C(149)-C(150)-H(15A)	109.5
C(135)-C(136)	1.395(4)	C(72)-C(73)-C(74)	121.0(3)	C(149)-C(150)-H(15B)	109.5
C(135)-H(13E)	0.95	C(72)-C(73)-H(73A)	119.5	H(15A)-C(150)-H(15B)	109.5
C(136)-H(13F)	0.95	C(74)-C(73)-H(73A)	119.5	C(149)-C(150)-H(15C)	109.5
C(137)-C(142)	1.397(4)	C(69)-C(74)-C(73)	120.7(3)	H(15A)-C(150)-H(15C)	109.5
C(137)-C(138)	1.399(4)	C(69)-C(74)-H(74A)	119.7	H(15B)-C(150)-H(15C)	109.5
C(138)-C(139)	1.377(4)	C(73)-C(74)-H(74A)	119.7		
C(138)-H(13G)	0.95	C(76)-C(75)-C(80)	118.3(2)		
C(139)-C(140)	1.397(4)	C(76)-C(75)-C(58)	122.5(2)		
C(139)-H(13H)	0.95	C(80)-C(75)-C(58)	119.2(2)		
C(140)-C(141)	1.385(4)	C(77)-C(76)-C(75)	120.6(3)		
C(140)-C(149)	1.508(4)	C(77)-C(76)-H(76A)	119.7		
C(141)-C(142)	1.385(4)	C(75)-C(76)-H(76A)	119.7		
C(141)-H(14S)	0.95				

Table A0.54. Anisotropic displacement parameters ($Å^2 x\ 10^3$) for **3.1d**. The anisotropic displacement factor exponent takes the form: $-2\pi^2[\ h^2\ a^{*2}U11 + ...\ + 2\ h\ k\ a^*\ b^*\ U12\ ]$

Atom	U11	U22	U33	U23	U13	U12
C1	22(1)	26(1)	43(2)	-1(1)	-5(1)	-4(1)
C2	22(1)	25(1)	44(2)	0(1)	-2(1)	-1(1)
C3	27(1)	37(2)	46(2)	3(1)	-5(1)	-3(1)
C4	38(2)	48(2)	40(2)	4(1)	-1(1)	-11(1)
C5	37(2)	38(2)	51(2)	-4(1)	11(1)	-13(1)
C6	29(1)	27(1)	53(2)	-8(1)	6(1)	-9(1)
C7	23(1)	19(1)	48(2)	-3(1)	-1(1)	0(1)
C8	23(1)	17(1)	48(2)	-4(1)	-1(1)	-2(1)
C9	22(1)	19(1)	42(2)	0(1)	-6(1)	-2(1)
C10	26(1)	22(1)	44(2)	-1(1)	-6(1)	-3(1)
C11	25(1)	23(1)	39(1)	-2(1)	-4(1)	-1(1)
C12	35(2)	33(1)	41(2)	-3(1)	-5(1)	-9(1)
C13	41(2)	44(2)	41(2)	-2(1)	-1(1)	-12(1)
C14	40(2)	37(2)	45(2)	4(1)	0(1)	-16(1)
C15	31(2)	30(1)	46(2)	-1(1)	-2(1)	-12(1)

C16	23(1)	22(1)	43(2)	-1(1)	-2(1)	-3(1)
C17	21(1)	24(1)	42(2)	-3(1)	-4(1)	-4(1)
C18	18(1)	24(1)	41(1)	-1(1)	-4(1)	-1(1)
C19	31(2)	43(2)	41(2)	15(1)	-9(1)	-16(1)
C20	31(2)	47(2)	72(2)	23(2)	-13(2)	-13(1)
C21	31(2)	80(3)	116(4)	63(3)	-35(2)	-29(2)
C22	84(3)	84(3)	75(3)	45(2)	-46(2)	-67(3)
C23	75(3)	85(3)	45(2)	20(2)	-22(2)	-59(2)
C24	52(2)	58(2)	37(2)	3(1)	-6(2)	-30(2)
C25	26(1)	27(1)	42(2)	-7(1)	5(1)	-10(1)
C26	34(2)	26(1)	43(2)	-2(1)	2(1)	-9(1)
C27	38(2)	28(1)	49(2)	-8(1)	5(1)	-15(1)
C28	28(2)	40(2)	53(2)	-13(1)	5(1)	-13(1)
C29	28(2)	35(2)	64(2)	-15(1)	-7(1)	-2(1)
C30	29(2)	27(1)	64(2)	-15(1)	-3(1)	-8(1)
C31	29(1)	25(1)	37(1)	-2(1)	-2(1)	-8(1)
C32	28(1)	29(1)	39(2)	-2(1)	1(1)	-6(1)
C33	32(2)	26(1)	43(2)	-4(1)	7(1)	-7(1)
C34	43(2)	31(1)	35(1)	-4(1)	6(1)	-19(1)
C35	44(2)	40(2)	38(2)	2(1)	-10(1)	-18(1)
C36	41(2)	26(1)	48(2)	1(1)	-8(1)	-11(1)
C37	26(1)	26(1)	35(1)	0(1)	-1(1)	-9(1)
C38	22(1)	33(1)	43(2)	-5(1)	-2(1)	-7(1)
C39	35(2)	29(1)	49(2)	-7(1)	1(1)	-3(1)
C40	43(2)	30(1)	35(1)	-1(1)	-3(1)	-15(1)
C41	30(2)	38(2)	48(2)	-1(1)	-2(1)	-18(1)
C42	25(1)	33(1)	49(2)	-4(1)	1(1)	-9(1)
C43	130(5)	185(6)	114(4)	91(4)	-87(4)	-138(5)
C44	106(4)	62(2)	86(3)	-13(2)	-64(3)	-10(2)
C45	36(2)	45(2)	77(2)	-17(2)	-6(2)	-15(2)
C46	56(2)	49(2)	75(2)	0(2)	-26(2)	-22(2)
C47	61(2)	44(2)	55(2)	-13(2)	0(2)	-24(2)
C48	203(7)	73(3)	61(3)	-21(2)	-39(4)	-35(4)
C49	66(2)	38(2)	53(2)	-7(1)	-6(2)	-25(2)
C50	221(7)	82(3)	55(2)	-2(2)	-25(3)	-96(4)
C51	21(1)	25(1)	32(1)	-5(1)	4(1)	-7(1)
C52	22(1)	29(1)	31(1)	-3(1)	3(1)	-8(1)
C53	28(2)	44(2)	34(1)	-1(1)	5(1)	0(1)

C54	33(2)	60(2)	33(2)	3(1)	-2(1)	-1(2)
C55	36(2)	56(2)	26(1)	-5(1)	2(1)	-7(1)
C56	34(2)	39(2)	31(1)	-9(1)	5(1)	-12(1)
C57	26(1)	29(1)	27(1)	-4(1)	5(1)	-12(1)
C58	24(1)	24(1)	29(1)	-5(1)	6(1)	-9(1)
C59	24(1)	20(1)	29(1)	-3(1)	5(1)	-9(1)
C60	21(1)	19(1)	35(1)	-6(1)	6(1)	-6(1)
C61	23(1)	18(1)	33(1)	-5(1)	3(1)	-7(1)
C62	25(1)	22(1)	38(1)	-4(1)	1(1)	-6(1)
C63	27(1)	30(1)	35(1)	-1(1)	-5(1)	-5(1)
C64	33(2)	34(1)	30(1)	-2(1)	-1(1)	-9(1)
C65	27(1)	28(1)	33(1)	-3(1)	6(1)	-9(1)
C66	22(1)	22(1)	30(1)	-4(1)	3(1)	-10(1)
C67	22(1)	23(1)	31(1)	-5(1)	4(1)	-8(1)
C68	20(1)	22(1)	29(1)	-6(1)	3(1)	-8(1)
C69	22(1)	26(1)	26(1)	0(1)	6(1)	-1(1)
C70	23(1)	38(1)	34(1)	-2(1)	5(1)	-4(1)
C71	24(1)	45(2)	41(2)	5(1)	8(1)	3(1)
C72	49(2)	29(1)	47(2)	0(1)	23(2)	3(1)
C73	50(2)	28(1)	53(2)	-9(1)	18(2)	-10(1)
C74	29(1)	31(1)	38(1)	-5(1)	9(1)	-10(1)
C75	28(1)	26(1)	25(1)	-6(1)	2(1)	-4(1)
C76	36(2)	32(1)	30(1)	-5(1)	5(1)	-7(1)
C77	32(2)	49(2)	29(1)	-7(1)	6(1)	-1(1)
C78	33(2)	43(2)	39(2)	-21(1)	-8(1)	5(1)
C79	37(2)	29(1)	48(2)	-12(1)	-7(1)	-4(1)
C80	31(1)	31(1)	34(1)	-7(1)	0(1)	-8(1)
C81	20(1)	26(1)	28(1)	-5(1)	2(1)	-3(1)
C82	29(1)	24(1)	37(1)	-7(1)	7(1)	-5(1)
C83	33(2)	29(1)	44(2)	-8(1)	12(1)	-14(1)
C84	22(1)	35(1)	42(2)	-10(1)	8(1)	-4(1)
C85	26(1)	29(1)	38(1)	-9(1)	5(1)	-1(1)
C86	27(1)	22(1)	33(1)	-4(1)	4(1)	-5(1)
C87	24(1)	28(1)	23(1)	-2(1)	5(1)	-6(1)
C88	28(1)	31(1)	31(1)	-4(1)	5(1)	-12(1)
C89	23(1)	33(1)	42(2)	6(1)	4(1)	-8(1)
C90	26(1)	37(2)	33(1)	10(1)	8(1)	2(1)
C91	33(2)	36(1)	31(1)	-7(1)	8(1)	-2(1)

C92	30(1)	33(1)	31(1)	-6(1)	2(1)	-8(1)
C93	77(3)	41(2)	78(3)	-8(2)	41(2)	10(2)
C94	168(6)	84(3)	58(3)	-2(2)	50(3)	45(4)
C95	50(2)	66(2)	63(2)	-37(2)	-8(2)	21(2)
C96	110(4)	66(2)	77(3)	-48(2)	54(3)	-45(3)
C97	29(2)	43(2)	67(2)	-14(2)	20(2)	-11(1)
C98	54(2)	62(2)	61(2)	-15(2)	35(2)	-14(2)
C99	32(2)	63(2)	44(2)	4(2)	16(1)	-2(2)
C100	49(2)	106(3)	41(2)	12(2)	14(2)	-25(2)
C101	30(1)	26(1)	33(1)	-2(1)	7(1)	-5(1)
C102	25(1)	24(1)	40(1)	0(1)	7(1)	-4(1)
C103	34(2)	31(1)	43(2)	1(1)	6(1)	-7(1)
C104	35(2)	27(1)	51(2)	10(1)	3(1)	0(1)
C105	34(2)	22(1)	57(2)	0(1)	4(1)	-1(1)
C106	27(1)	23(1)	51(2)	-6(1)	3(1)	-2(1)
C107	24(1)	24(1)	42(2)	-4(1)	6(1)	-4(1)
C108	26(1)	23(1)	42(2)	-6(1)	7(1)	-1(1)
C109	27(1)	23(1)	37(1)	-5(1)	4(1)	-3(1)
C110	26(1)	27(1)	35(1)	-6(1)	3(1)	-6(1)
C111	24(1)	27(1)	31(1)	-1(1)	0(1)	-6(1)
C112	29(1)	32(1)	32(1)	-2(1)	2(1)	-8(1)
C113	34(2)	30(1)	32(1)	3(1)	-4(1)	-11(1)
C114	31(1)	22(1)	42(2)	-2(1)	-5(1)	-9(1)
C115	26(1)	24(1)	35(1)	-6(1)	0(1)	-7(1)
C116	24(1)	21(1)	33(1)	-5(1)	1(1)	-7(1)
C117	25(1)	25(1)	32(1)	-6(1)	3(1)	-7(1)
C118	26(1)	25(1)	32(1)	-4(1)	7(1)	-7(1)
C119	37(2)	22(1)	34(1)	3(1)	1(1)	0(1)
C120	44(2)	33(1)	36(2)	5(1)	5(1)	-3(1)
C121	51(2)	52(2)	28(1)	2(1)	5(1)	4(2)
C122	44(2)	54(2)	36(2)	-2(1)	-11(2)	3(2)
C123	37(2)	43(2)	43(2)	-8(1)	-5(1)	-1(1)
C124	36(2)	32(1)	34(1)	-1(1)	2(1)	-1(1)
C125	35(2)	23(1)	39(1)	-4(1)	6(1)	-5(1)
C126	30(1)	27(1)	45(2)	-6(1)	5(1)	-2(1)
C127	40(2)	27(1)	47(2)	-11(1)	10(1)	-5(1)
C128	41(2)	32(1)	43(2)	-7(1)	5(1)	-13(1)
C129	30(2)	38(2)	48(2)	-10(1)	2(1)	-9(1)

C130	30(2)	29(1)	47(2)	-10(1)	8(1)	-2(1)
C131	34(2)	25(1)	33(1)	-4(1)	6(1)	-6(1)
C132	34(2)	28(1)	32(1)	-4(1)	4(1)	-7(1)
C133	34(2)	32(1)	40(2)	-5(1)	7(1)	-2(1)
C134	45(2)	30(1)	36(2)	-6(1)	11(1)	-9(1)
C135	53(2)	36(2)	31(1)	-6(1)	-2(1)	-8(1)
C136	38(2)	32(1)	39(2)	-4(1)	-1(1)	-3(1)
C137	29(1)	19(1)	30(1)	1(1)	0(1)	-3(1)
C138	33(2)	23(1)	35(1)	-5(1)	-1(1)	-6(1)
C139	28(1)	32(1)	37(1)	-5(1)	5(1)	-7(1)
C140	34(2)	26(1)	30(1)	-2(1)	2(1)	-4(1)
C141	39(2)	26(1)	31(1)	-2(1)	-3(1)	-12(1)
C142	35(2)	25(1)	32(1)	0(1)	2(1)	-11(1)
C143	66(3)	109(3)	39(2)	-17(2)	-14(2)	-13(2)
C144	109(5)	174(6)	97(4)	-29(4)	-32(4)	-15(5)
C145	47(2)	43(2)	44(2)	-11(1)	5(2)	-14(2)
C146	47(2)	43(2)	57(2)	-16(2)	-1(2)	-9(2)
C147	55(2)	43(2)	40(2)	-13(1)	12(2)	-10(2)
C148	88(3)	58(2)	68(2)	-23(2)	47(2)	-27(2)
C149	48(2)	43(2)	36(2)	-12(1)	10(1)	-12(1)
C150	93(3)	62(2)	36(2)	-8(2)	19(2)	-10(2)

Table A0.55. Hydrogen coordinates (x 10^4) and isotropic displacement parameters (Å^2 x 10^3) for **3.1d.**

Atom	x	y	z	U(eq)	Atom	x	y	z	U(eq)
H3A	5229	1461	4159	45	H91A	14727	7114	10722	41
H4A	3759	970	4623	51	H92A	12784	7292	11222	37
H5A	2071	615	4191	50	H93A	17487	5310	12068	83
H6A	1916	731	3298	42	H93B	16211	5127	11814	83
H12A	5359	1477	772	43	H94A	17822	5315	11209	174
H13A	6339	2184	290	50	H94B	17504	6034	11345	174
H14R	6944	3018	686	48	H94C	16350	5762	11088	174
H15D	6684	3094	1562	42	H95A	7087	10633	14216	76
H20A	7948	1368	3126	61	H95B	7058	10137	14707	76
H21A	9658	1662	3584	93	H96A	7703	11043	14906	117
H23A	6862	2958	4243	76	H96B	9053	10834	14573	117
H24A	5153	2677	3805	56	H96C	8796	10408	15087	117
H26A	2993	56	2451	41	H97A	3938	8834	13508	55
H27A	1069	-167	2098	44	H97B	3854	9576	13418	55

H29A	-630	1692	1843	51	H98A	3703	9278	14317	88
H30A	1304	1920	2182	47	H98B	5062	9527	14210	88
H32A	5657	233	1795	39	H98C	5140	8786	14301	88
H33A	5102	-529	1317	40	H99A	17080	7202	10569	58
H35A	2003	784	629	48	H99B	17711	7653	10902	58
H36A	2594	1546	1087	46	H10A	17518	8078	10039	98
H38A	4223	3324	2634	39	H10B	16455	8541	10374	98
H39A	4729	4221	2924	46	H10C	15940	8070	10027	98
H41A	8722	3481	2746	45	H10D	7620	6165	6099	43
H42A	8230	2591	2439	42	H10E	7429	7234	6078	47
H43A	10233	2605	3982	159	H10F	8090	7684	6798	46
H43B	9191	2913	4407	159	H10G	8716	7079	7570	41
H44A	10920	2264	4803	128	H11A	8651	3946	9094	37
H44B	10743	1700	4474	128	H11B	9625	2885	9141	38
H44C	9617	1967	4891	128	H11C	10734	2426	8407	37
H45A	-1307	162	1830	61	H11D	10710	3016	7625	33
H45B	-2045	895	1800	61	H12B	9692	5192	5910	47
H46A	-1968	535	970	88	H12C	9078	4723	5204	56
H46B	-347	319	1006	88	H12D	5967	4261	6022	50
H46C	-1076	1052	975	88	H12E	6603	4703	6738	42
H47A	3617	-879	781	61	H12F	7128	6746	8369	41
H47B	2136	-437	674	61	H12G	7654	7177	9107	45
H48A	3062	-711	-107	166	H12H	11525	6160	9063	46
H48B	4398	-471	13	166	H13B	10996	5717	8329	43
H48C	2976	26	-86	166	H13C	6172	5401	8375	37
H49A	7940	4609	2885	60	H13D	4940	5905	9040	43
H49B	6371	4884	3006	60	H13E	8268	5452	9960	48
H50A	7665	4789	3761	164	H13F	9522	4940	9295	44
H50B	8220	4051	3709	164	H13G	11753	4318	6857	36
H50C	6650	4323	3831	164	H13H	12771	3811	6155	39
H53A	14774	6764	13486	44	H14S	9731	2903	6100	37
H54A	14989	6831	14362	53	H14T	8707	3396	6811	36
H55A	13564	7646	14782	48	H14A	7722	4172	4793	86
H56A	11817	8338	14337	41	H14B	7402	3628	5198	86
H62A	7575	9066	11873	34	H14I	5529	3923	4684	192
H63A	7588	9224	10979	37	H14J	5478	4658	4700	192
H64A	9637	8944	10516	39	H14K	5066	4261	5204	192
H65A	11626	8471	10948	35	H14C	10839	6722	9809	53

H70A	15796	7283	12643	39	H14D	9251	6951	9922	53
H71A	17192	6456	12258	47	H14L	10282	7818	9893	72
H73A	13972	5729	12002	52	H14M	9217	7924	9421	72
H74A	12540	6583	12356	38	H14N	10809	7694	9315	72
H76A	9155	8296	14080	39	H14E	5384	6565	9843	55
H77A	7843	9082	14539	45	H14F	6305	6105	10283	55
H79A	9561	10374	13748	46	H14O	3952	6160	10430	104
H80A	10878	9595	13291	38	H14P	4747	5452	10356	104
H82A	8220	7872	12982	36	H14Q	3853	5870	9887	104
H83A	6116	8077	13380	41	H14G	11507	2665	5501	50
H85A	5879	9949	13110	38	H14H	12950	2750	5688	50
H86A	7971	9747	12705	33	H15A	12560	3192	4827	98
H88A	14287	8506	12010	35	H15B	12554	3750	5189	98
H89A	16252	8306	11515	40	H15C	11150	3634	4986	98

Table A0.56. Torsion angles (°) for **3.1d**.

Atoms	Angle	Atoms	Angle	Atoms	Angle
C18-C1-C2-C3	-179.2(2)	C59-C60-C61-C62	178.5(2)	C110-C109-C118-C101	157.1(2)
C19-C1-C2-C3	7.7(4)	C81-C60-C61-C62	7.0(3)	C108-C109-C118-C101	-22.1(4)
C18-C1-C2-C7	-1.6(4)	C59-C60-C61-C66	-1.8(3)	C110-C109-C118-C117	-22.7(4)
C19-C1-C2-C7	-174.8(2)	C81-C60-C61-C66	-173.2(2)	C108-C109-C118-C117	158.1(2)
C1-C2-C3-C4	173.5(3)	C60-C61-C62-C63	175.3(2)	C102-C101-C119-C124	-107.8(3)
C7-C2-C3-C4	-4.0(4)	C66-C61-C62-C63	-4.5(3)	C118-C101-C119-C124	64.3(4)
C2-C3-C4-C5	0.3(5)	C61-C62-C63-C64	0.3(4)	C102-C101-C119-C120	69.9(4)
C3-C4-C5-C6	1.5(5)	C62-C63-C64-C65	2.0(4)	C118-C101-C119-C120	-118.0(3)
C4-C5-C6-C7	0.6(4)	C63-C64-C65-C66	0.0(4)	C124-C119-C120-C121	-1.9(4)
C5-C6-C7-C8	175.9(3)	C64-C65-C66-C67	172.7(2)	C101-C119-C120-C121	-179.6(3)
C5-C6-C7-C2	-4.3(4)	C64-C65-C66-C61	-4.2(4)	C119-C120-C121-C122	0.9(5)
C1-C2-C7-C8	8.1(4)	C60-C61-C66-C67	9.6(3)	C120-C121-C122-C123	1.0(5)
C3-C2-C7-C8	-174.3(2)	C62-C61-C66-C67	-170.7(2)	C120-C121-C122-C143	-175.2(3)
C1-C2-C7-C6	-171.8(2)	C60-C61-C66-C65	-173.5(2)	C121-C122-C123-C124	-1.9(5)
C3-C2-C7-C6	5.9(4)	C62-C61-C66-C65	6.2(3)	C143-C122-C123-C124	174.2(3)
C6-C7-C8-C9	178.5(2)	C65-C66-C67-C68	-179.2(2)	C122-C123-C124-C119	0.9(4)
C2-C7-C8-C9	-1.3(4)	C61-C66-C67-C68	-2.4(3)	C120-C119-C124-C123	1.0(4)
C6-C7-C8-C25	8.8(4)	C65-C66-C67-C87	7.9(3)	C101-C119-C124-C123	178.8(3)
C2-C7-C8-C25	-171.0(2)	C61-C66-C67-C87	-175.4(2)	C107-C108-C125-C130	-106.8(3)
C7-C8-C9-C10	168.6(2)	C66-C67-C68-C51	168.0(2)	C109-C108-C125-C130	65.3(4)
C25-C8-C9-C10	-22.0(4)	C87-C67-C68-C51	-19.1(3)	C107-C108-C125-C126	71.1(4)

C7-C8-C9-C18	-11.5(4)	C66-C67-C68-C59	-12.0(3)	C109-C108-C125-C126	-116.8(3)
C25-C8-C9-C18	157.9(2)	C87-C67-C68-C59	160.9(2)	C130-C125-C126-C127	-2.6(4)
C8-C9-C10-C11	169.6(2)	C52-C51-C68-C67	167.5(2)	C108-C125-C126-C127	179.5(3)
C18-C9-C10-C11	-10.3(4)	C69-C51-C68-C67	-20.1(4)	C125-C126-C127-C128	0.9(4)
C8-C9-C10-C31	-16.7(4)	C52-C51-C68-C59	-12.5(3)	C126-C127-C128-C129	1.3(4)
C18-C9-C10-C31	163.4(2)	C69-C51-C68-C59	159.9(2)	C126-C127-C128-C145	-178.3(3)
C9-C10-C11-C12	178.0(2)	C58-C59-C68-C67	-160.6(2)	C127-C128-C129-C130	-1.7(4)
C31-C10-C11-C12	4.0(4)	C60-C59-C68-C67	19.6(3)	C145-C128-C129-C130	177.8(3)
C9-C10-C11-C16	-3.7(4)	C58-C59-C68-C51	19.4(3)	C128-C129-C130-C125	0.0(4)
C31-C10-C11-C16	-177.7(2)	C60-C59-C68-C51	-160.4(2)	C126-C125-C130-C129	2.2(4)
C10-C11-C12-C13	172.9(3)	C52-C51-C69-C74	106.6(3)	C108-C125-C130-C129	-179.8(3)
C16-C11-C12-C13	-5.5(4)	C68-C51-C69-C74	-65.9(3)	C111-C110-C131-C136	69.2(4)
C11-C12-C13-C14	0.4(5)	C52-C51-C69-C70	-69.8(3)	C109-C110-C131-C136	-119.4(3)
C12-C13-C14-C15	2.7(5)	C68-C51-C69-C70	117.8(3)	C111-C110-C131-C132	-110.1(3)
C13-C14-C15-C16	-0.5(5)	C74-C69-C70-C71	0.7(4)	C109-C110-C131-C132	61.3(3)
C14-C15-C16-C17	174.3(3)	C51-C69-C70-C71	177.1(2)	C136-C131-C132-C133	2.0(4)
C14-C15-C16-C11	-4.5(4)	C69-C70-C71-C72	-1.6(4)	C110-C131-C132-C133	-178.7(2)
C10-C11-C16-C17	10.1(4)	C70-C71-C72-C73	1.0(5)	C131-C132-C133-C134	0.2(4)
C12-C11-C16-C17	-171.5(3)	C70-C71-C72-C93	178.9(3)	C132-C133-C134-C135	-2.2(4)
C10-C11-C16-C15	-171.1(2)	C71-C72-C73-C74	0.5(5)	C132-C133-C134-C147	175.7(3)
C12-C11-C16-C15	7.3(4)	C93-C72-C73-C74	-177.3(3)	C133-C134-C135-C136	2.1(4)
C15-C16-C17-C18	179.2(2)	C70-C69-C74-C73	0.8(4)	C147-C134-C135-C136	-175.8(3)
C11-C16-C17-C18	-2.0(4)	C51-C69-C74-C73	-175.7(2)	C132-C131-C136-C135	-2.1(4)
C15-C16-C17-C37	7.5(4)	C72-C73-C74-C69	-1.4(5)	C110-C131-C136-C135	178.6(3)
C11-C16-C17-C37	-173.7(2)	C57-C58-C75-C76	-74.6(3)	C134-C135-C136-C131	0.0(4)
C16-C17-C18-C1	168.6(2)	C59-C58-C75-C76	112.5(3)	C116-C117-C137-C142	73.4(3)
C37-C17-C18-C1	-20.2(4)	C57-C58-C75-C80	101.6(3)	C118-C117-C137-C142	-113.0(3)
C16-C17-C18-C9	-11.9(4)	C59-C58-C75-C80	-71.3(3)	C116-C117-C137-C138	-103.6(3)
C37-C17-C18-C9	159.2(2)	C80-C75-C76-C77	0.9(4)	C118-C117-C137-C138	70.0(3)
C2-C1-C18-C17	168.3(2)	C58-C75-C76-C77	177.2(3)	C142-C137-C138-C139	0.3(4)
C19-C1-C18-C17	-18.7(4)	C75-C76-C77-C78	0.2(4)	C117-C137-C138-C139	177.4(2)
C2-C1-C18-C9	-11.1(4)	C76-C77-C78-C79	-1.2(4)	C137-C138-C139-C140	0.7(4)
C19-C1-C18-C9	161.9(2)	C76-C77-C78-C95	178.5(3)	C138-C139-C140-C141	-1.1(4)
C10-C9-C18-C17	18.1(4)	C77-C78-C79-C80	1.1(4)	C138-C139-C140-C149	180.0(3)
C8-C9-C18-C17	-161.8(2)	C95-C78-C79-C80	-178.6(3)	C139-C140-C141-C142	0.6(4)
C10-C9-C18-C1	-162.5(2)	C78-C79-C80-C75	0.0(4)	C149-C140-C141-C142	179.5(3)
C8-C9-C18-C1	17.6(3)	C76-C75-C80-C79	-1.1(4)	C140-C141-C142-C137	0.3(4)
C2-C1-C19-C20	105.3(3)	C58-C75-C80-C79	-177.4(3)	C138-C137-C142-C141	-0.7(4)

C18-C1-C19-C20	-67.9(4)	C61-C60-C81-C82	99.7(3)	C117-C137-C142-C141	-177.7(2)
C2-C1-C19-C24	-72.1(4)	C59-C60-C81-C82	-71.6(3)	C123-C122-C143-C144	52.7(6)
C18-C1-C19-C24	114.8(3)	C61-C60-C81-C86	-74.9(3)	C121-C122-C143-C144	-131.3(5)
C24-C19-C20-C21	-0.2(4)	C59-C60-C81-C86	113.7(3)	C129-C128-C145-C146	106.3(3)
C1-C19-C20-C21	-177.7(3)	C86-C81-C82-C83	-1.1(4)	C127-C128-C145-C146	-74.1(4)
C19-C20-C21-C22	-0.1(5)	C60-C81-C82-C83	-176.0(2)	C135-C134-C147-C148	-120.6(4)
C20-C21-C22-C23	0.1(5)	C81-C82-C83-C84	0.5(4)	C133-C134-C147-C148	61.5(4)
C20-C21-C22-C43	-179.9(3)	C82-C83-C84-C85	-0.3(4)	C141-C140-C149-C150	115.9(3)
C21-C22-C23-C24	0.2(5)	C82-C83-C84-C97	-177.1(3)	C139-C140-C149-C150	-65.2(4)
C43-C22-C23-C24	-179.8(3)	C83-C84-C85-C86	0.6(4)		
C22-C23-C24-C19	-0.5(5)	C97-C84-C85-C86	177.4(3)		
C20-C19-C24-C23	0.5(4)	C84-C85-C86-C81	-1.2(4)		
C1-C19-C24-C23	177.9(3)	C82-C81-C86-C85	1.4(4)		
C7-C8-C25-C30	98.1(3)	C60-C81-C86-C85	176.1(2)		
C9-C8-C25-C30	-71.5(3)	C66-C67-C87-C88	108.7(3)		
C7-C8-C25-C26	-76.7(3)	C68-C67-C87-C88	-64.2(3)		
C9-C8-C25-C26	113.7(3)	C66-C67-C87-C92	-67.1(3)		
C30-C25-C26-C27	0.1(4)	C68-C67-C87-C92	120.0(3)		
C8-C25-C26-C27	174.9(3)	C92-C87-C88-C89	0.9(4)		
C25-C26-C27-C28	-0.6(4)	C67-C87-C88-C89	-175.0(2)		
C26-C27-C28-C29	0.5(5)	C87-C88-C89-C90	1.2(4)		
C26-C27-C28-C45	178.3(3)	C88-C89-C90-C91	-2.5(4)		
C27-C28-C29-C30	0.1(5)	C88-C89-C90-C99	174.4(3)		
C45-C28-C29-C30	-177.8(3)	C89-C90-C91-C92	1.8(4)		
C26-C25-C30-C29	0.4(5)	C99-C90-C91-C92	-175.1(3)		
C8-C25-C30-C29	-174.6(3)	C90-C91-C92-C87	0.3(4)		
C28-C29-C30-C25	-0.5(5)	C88-C87-C92-C91	-1.6(4)		
C11-C10-C31-C36	-75.9(4)	C67-C87-C92-C91	174.2(2)		
C9-C10-C31-C36	110.2(3)	C71-C72-C93-C94	-73.6(6)		
C11-C10-C31-C32	100.2(3)	C73-C72-C93-C94	104.2(5)		
C9-C10-C31-C32	-73.6(4)	C79-C78-C95-C96	-60.5(5)		
C36-C31-C32-C33	0.2(4)	C77-C78-C95-C96	119.8(4)		
C10-C31-C32-C33	-176.0(2)	C85-C84-C97-C98	-89.9(4)		
C31-C32-C33-C34	-1.3(4)	C83-C84-C97-C98	86.8(4)		
C32-C33-C34-C35	1.3(4)	C89-C90-C99-C100	-86.0(4)		
C32-C33-C34-C47	-179.3(3)	C91-C90-C99-C100	90.8(4)		
C33-C34-C35-C36	-0.3(4)	C118-C101-C102-C103	-177.7(3)		
C47-C34-C35-C36	-179.8(3)	C119-C101-C102-C103	-5.6(4)		

C34-C35-C36-C31	-0.7(5)	C118-C101-C102-C107	2.8(4)
C32-C31-C36-C35	0.7(4)	C119-C101-C102-C107	175.0(2)
C10-C31-C36-C35	176.9(3)	C101-C102-C103-C104	-173.4(3)
C16-C17-C37-C38	100.6(3)	C107-C102-C103-C104	6.1(4)
C18-C17-C37-C38	-70.9(3)	C102-C103-C104-C105	1.0(4)
C16-C17-C37-C42	-73.6(4)	C103-C104-C105-C106	-4.4(5)
C18-C17-C37-C42	115.0(3)	C104-C105-C106-C107	0.4(4)
C42-C37-C38-C39	0.0(4)	C105-C106-C107-C108	-170.7(3)
C17-C37-C38-C39	-174.5(3)	C105-C106-C107-C102	6.8(4)
C37-C38-C39-C40	-0.4(4)	C101-C102-C107-C108	-12.8(4)
C38-C39-C40-C41	0.1(5)	C103-C102-C107-C108	167.7(3)
C38-C39-C40-C49	-177.6(3)	C101-C102-C107-C106	169.7(2)
C39-C40-C41-C42	0.7(4)	C103-C102-C107-C106	-9.8(4)
C49-C40-C41-C42	178.4(3)	C106-C107-C108-C109	-177.6(3)
C40-C41-C42-C37	-1.1(5)	C102-C107-C108-C109	5.0(4)
C38-C37-C42-C41	0.8(4)	C106-C107-C108-C125	-5.4(4)
C17-C37-C42-C41	175.0(3)	C102-C107-C108-C125	177.2(2)
C23-C22-C43-C44	110.8(7)	C107-C108-C109-C110	-166.8(3)
C21-C22-C43-C44	-69.2(7)	C125-C108-C109-C110	21.1(4)
C27-C28-C45-C46	-95.8(4)	C107-C108-C109-C118	12.3(4)
C29-C28-C45-C46	81.9(4)	C125-C108-C109-C118	-159.8(3)
C33-C34-C47-C48	-109.0(4)	C108-C109-C110-C111	-163.9(3)
C35-C34-C47-C48	70.4(5)	C118-C109-C110-C111	16.9(4)
C41-C40-C49-C50	-84.2(5)	C108-C109-C110-C131	24.7(4)
C39-C40-C49-C50	93.4(5)	C118-C109-C110-C131	-154.5(3)
C68-C51-C52-C53	179.6(2)	C109-C110-C111-C112	179.7(3)
C69-C51-C52-C53	7.0(4)	C131-C110-C111-C112	-9.0(4)
C68-C51-C52-C57	-2.1(4)	C109-C110-C111-C116	-0.2(4)
C69-C51-C52-C57	-174.7(2)	C131-C110-C111-C116	171.1(2)
C51-C52-C53-C54	173.4(3)	C110-C111-C112-C113	-172.2(3)
C57-C52-C53-C54	-5.0(4)	C116-C111-C112-C113	7.7(4)
C52-C53-C54-C55	-0.3(5)	C111-C112-C113-C114	-1.3(4)
C53-C54-C55-C56	3.3(5)	C112-C113-C114-C115	-3.3(4)
C54-C55-C56-C57	-0.8(5)	C113-C114-C115-C116	1.3(4)
C51-C52-C57-C58	9.9(4)	C114-C115-C116-C117	-173.4(3)
C53-C52-C57-C58	-171.7(2)	C114-C115-C116-C111	5.2(4)
C51-C52-C57-C56	-171.1(2)	C110-C111-C116-C117	-10.9(4)
C53-C52-C57-C56	7.3(4)	C112-C111-C116-C117	169.2(2)

C55-C56-C57-C58	174.4(3)	C110-C111-C116-C115	170.5(2)
C55-C56-C57-C52	-4.6(4)	C112-C111-C116-C115	-9.4(4)
C52-C57-C58-C59	-2.7(4)	C115-C116-C117-C118	-176.6(2)
C56-C57-C58-C59	178.3(2)	C111-C116-C117-C118	4.8(4)
C52-C57-C58-C75	-175.8(2)	C115-C116-C117-C137	-2.9(4)
C56-C57-C58-C75	5.3(4)	C111-C116-C117-C137	178.5(2)
C57-C58-C59-C60	168.1(2)	C102-C101-C118-C117	-165.7(3)
C75-C58-C59-C60	-19.2(4)	C119-C101-C118-C117	22.2(4)
C57-C58-C59-C68	-11.8(3)	C102-C101-C118-C109	14.4(4)
C75-C58-C59-C68	161.0(2)	C119-C101-C118-C109	-157.6(3)
C58-C59-C60-C61	167.4(2)	C116-C117-C118-C101	-168.0(2)
C68-C59-C60-C61	-12.8(3)	C137-C117-C118-C101	18.5(4)
C58-C59-C60-C81	-21.3(3)	C116-C117-C118-C109	11.8(4)
C68-C59-C60-C81	158.5(2)	C137-C117-C118-C109	-161.7(2)

Crystal Structure Report for **3.1e** (project code: 11253)

Data collection: A crystal (approximate dimensions 0.15 x 0.13 x 0.13 mm^3) was placed onto the tip of a 0.1 mm diameter glass capillary and mounted on a Bruker APEX II Platform CCD diffractometer for a data collection at 173(2) K.[1] A preliminary set of cell constants was calculated from reflections harvested from three sets of 12 frames. These initial sets of frames were oriented such that orthogonal wedges of reciprocal space were surveyed. This produced initial orientation matrices determined from 406 reflections. The data collection was carried out using MoKα radiation (graphite monochromator) with a frame time of 60 seconds and a detector distance of 6.0 cm. A randomly oriented region of reciprocal space was surveyed to the extent of one sphere and to a resolution of 0.84 Å. Four major sections of frames were collected with 0.30º steps in ω at four different ϕ settings and a detector position of -28º in 2θ. The intensity data were corrected for absorption and decay (SADABS).[2] Final cell constants were calculated from the xyz centroids of 6686 strong reflections from the actual data collection after integration (SAINT).[3] Please refer to Table 1 for additional crystal and refinement information.

Structure solution and refinement: The structure was solved using SHELXS-97[4] and refined using SHELXL-97.[4] The space group $Pna2_1$ was determined based on systematic absences and intensity statistics. A direct-methods solution was calculated which provided most non-hydrogen atoms from the E-map. Full-matrix least squares / difference Fourier cycles were performed which located the remaining non-hydrogen atoms. All non-hydrogen atoms were refined with anisotropic displacement parameters. All hydrogen atoms were placed in ideal positions and refined as riding atoms with relative isotropic displacement parameters. The final full matrix least squares refinement converged to $R1 = 0.0421$ and $wR2 = 0.0964$ (F^2, all data).

Structure description: The molecule does not lie on a special position; therefore, one whole molecule is unique.

Table A0.57. Atomic coordinates (x 10^4) and equivalent isotropic displacement parameters (Å^2 x 10^3) for **3.1e**. Ueq is defined as one third as one third of the trace of the orthogonalized Uij tensor.

Atom	x	y	z	Ueq
C1	1890(1)	3425(2)	8292(2)	28(1)
C2	1226(1)	2864(2)	7883(2)	28(1)
C3	799(2)	2097(2)	8368(2)	35(1)

C4	109(2)	1625(2)	7988(2)	39(1)
C5	-216(2)	1890(2)	7100(2)	39(1)
C6	194(1)	2576(2)	6590(2)	35(1)
C7	958(1)	3061(2)	6936(2)	28(1)
C8	1448(1)	3686(2)	6376(2)	27(1)
C9	2208(1)	4154(2)	6756(2)	25(1)
C10	2859(1)	4614(2)	6196(2)	26(1)
C11	3509(1)	5178(2)	6618(2)	27(1)
C12	4218(1)	5587(2)	6093(2)	33(1)
C13	4796(2)	6204(2)	6488(2)	37(1)
C14	4694(2)	6476(2)	7429(2)	37(1)
C15	4061(1)	6081(2)	7975(2)	32(1)
C16	3471(1)	5366(2)	7606(2)	26(1)
C17	2890(1)	4849(2)	8167(2)	25(1)
C18	2327(1)	4146(2)	7753(1)	25(1)
C19	2239(1)	3141(2)	9234(2)	27(1)
C20	1757(2)	3179(2)	10052(2)	35(1)
C21	2089(2)	2817(2)	10878(2)	38(1)
C22	2915(2)	2399(2)	10914(2)	34(1)
C23	3410(2)	2386(2)	10105(2)	33(1)
C24	3076(1)	2743(2)	9273(2)	30(1)
C25	1130(1)	3920(2)	5418(2)	29(1)
C26	1191(2)	3286(2)	4675(2)	36(1)
C27	917(2)	3559(2)	3791(2)	41(1)
C28	553(2)	4456(2)	3621(2)	37(1)
C29	457(2)	5076(2)	4372(2)	38(1)
C30	749(2)	4816(2)	5257(2)	33(1)
C31	2941(1)	4418(2)	5175(2)	28(1)
C32	3247(2)	3523(2)	4890(2)	36(1)
C33	3385(2)	3330(2)	3954(2)	47(1)
C34	3209(2)	4031(2)	3286(2)	44(1)
C35	2909(2)	4916(2)	3563(2)	41(1)
C36	2789(2)	5116(2)	4506(2)	33(1)
C37	2762(1)	5135(2)	9169(2)	29(1)
C38	3416(2)	5101(2)	9845(2)	36(1)
C39	3271(2)	5441(2)	10739(2)	46(1)
C40	2462(2)	5822(2)	10976(2)	49(1)
C41	1795(2)	5847(2)	10319(2)	44(1)

C42	1948(2)	5512(2)	9423(2)	35(1)
C43	3246(2)	1935(2)	11801(2)	45(1)
C44	284(2)	4754(2)	2645(2)	55(1)

Table A0.58. Bond lengths (Å) and angles (°) for **3.1e**.

Atoms	Length	Atoms	Angle	Atoms	Angle
C(1)-C(2)	1.404(3)	C(2)-C(1)-C(18)	119.95(19)	C(25)-C(26)-C(27)	120.4(2)
C(1)-C(18)	1.429(3)	C(2)-C(1)-C(19)	118.82(19)	C(28)-C(27)-C(26)	121.8(2)
C(1)-C(19)	1.501(3)	C(18)-C(1)-C(19)	120.35(18)	C(27)-C(28)-C(29)	117.8(2)
C(2)-C(3)	1.428(3)	C(1)-C(2)-C(3)	122.6(2)	C(27)-C(28)-C(44)	121.1(2)
C(2)-C(7)	1.442(3)	C(1)-C(2)-C(7)	119.3(2)	C(29)-C(28)-C(44)	121.1(2)
C(3)-C(4)	1.352(3)	C(3)-C(2)-C(7)	118.1(2)	C(28)-C(29)-C(30)	120.7(2)
C(4)-C(5)	1.412(3)	C(4)-C(3)-C(2)	121.3(2)	C(29)-C(30)-C(25)	121.1(2)
C(5)-C(6)	1.352(3)	C(3)-C(4)-C(5)	120.4(2)	C(36)-C(31)-C(32)	118.7(2)
C(6)-C(7)	1.432(3)	C(6)-C(5)-C(4)	120.6(2)	C(36)-C(31)-C(10)	122.4(2)
C(7)-C(8)	1.397(3)	C(5)-C(6)-C(7)	121.3(2)	C(32)-C(31)-C(10)	118.7(2)
C(8)-C(9)	1.433(3)	C(8)-C(7)-C(6)	121.9(2)	C(33)-C(32)-C(31)	120.6(2)
C(8)-C(25)	1.490(3)	C(8)-C(7)-C(2)	120.48(19)	C(32)-C(33)-C(34)	120.1(2)
C(9)-C(10)	1.426(3)	C(6)-C(7)-C(2)	117.6(2)	C(35)-C(34)-C(33)	119.6(2)
C(9)-C(18)	1.439(3)	C(7)-C(8)-C(9)	119.61(19)	C(34)-C(35)-C(36)	120.3(2)
C(10)-C(11)	1.398(3)	C(7)-C(8)-C(25)	119.37(19)	C(31)-C(36)-C(35)	120.7(2)
C(10)-C(31)	1.491(3)	C(9)-C(8)-C(25)	120.82(19)	C(38)-C(37)-C(42)	117.9(2)
C(11)-C(12)	1.431(3)	C(10)-C(9)-C(8)	123.38(19)	C(38)-C(37)-C(17)	124.3(2)
C(11)-C(16)	1.439(3)	C(10)-C(9)-C(18)	118.25(18)	C(42)-C(37)-C(17)	117.7(2)
C(12)-C(13)	1.352(3)	C(8)-C(9)-C(18)	118.36(18)	C(39)-C(38)-C(37)	121.3(2)
C(13)-C(14)	1.408(3)	C(11)-C(10)-C(9)	119.99(19)	C(38)-C(39)-C(40)	120.0(2)
C(14)-C(15)	1.355(3)	C(11)-C(10)-C(31)	117.82(19)	C(39)-C(40)-C(41)	119.7(2)
C(15)-C(16)	1.439(3)	C(9)-C(10)-C(31)	121.76(19)	C(42)-C(41)-C(40)	119.8(2)
C(16)-C(17)	1.394(3)	C(10)-C(11)-C(12)	121.9(2)	C(41)-C(42)-C(37)	121.3(2)
C(17)-C(18)	1.427(3)	C(10)-C(11)-C(16)	119.8(2)		
C(17)-C(37)	1.500(3)	C(12)-C(11)-C(16)	118.3(2)		
C(19)-C(20)	1.382(3)	C(13)-C(12)-C(11)	121.5(2)		
C(19)-C(24)	1.389(3)	C(12)-C(13)-C(14)	119.9(2)		
C(20)-C(21)	1.380(3)	C(15)-C(14)-C(13)	121.4(2)		
C(21)-C(22)	1.385(3)	C(14)-C(15)-C(16)	120.7(2)		
C(22)-C(23)	1.382(3)	C(17)-C(16)-C(11)	119.87(19)		
C(22)-C(43)	1.509(3)	C(17)-C(16)-C(15)	122.7(2)		
C(23)-C(24)	1.387(3)	C(11)-C(16)-C(15)	117.5(2)		

C(25)-C(26)	1.384(3)	C(16)-C(17)-C(18)	119.59(19)
C(25)-C(30)	1.393(3)	C(16)-C(17)-C(37)	119.75(19)
C(26)-C(27)	1.386(3)	C(18)-C(17)-C(37)	120.02(19)
C(27)-C(28)	1.385(3)	C(17)-C(18)-C(1)	122.33(19)
C(28)-C(29)	1.386(3)	C(17)-C(18)-C(9)	118.85(19)
C(28)-C(44)	1.514(3)	C(1)-C(18)-C(9)	118.82(19)
C(29)-C(30)	1.389(3)	C(20)-C(19)-C(24)	117.9(2)
C(31)-C(36)	1.383(3)	C(20)-C(19)-C(1)	124.24(19)
C(31)-C(32)	1.390(3)	C(24)-C(19)-C(1)	117.68(19)
C(32)-C(33)	1.381(3)	C(21)-C(20)-C(19)	121.1(2)
C(33)-C(34)	1.391(4)	C(20)-C(21)-C(22)	121.2(2)
C(34)-C(35)	1.370(4)	C(23)-C(22)-C(21)	117.9(2)
C(35)-C(36)	1.389(3)	C(23)-C(22)-C(43)	121.1(2)
C(37)-C(38)	1.388(3)	C(21)-C(22)-C(43)	120.9(2)
C(37)-C(42)	1.392(3)	C(22)-C(23)-C(24)	121.0(2)
C(38)-C(39)	1.382(3)	C(23)-C(24)-C(19)	120.9(2)
C(39)-C(40)	1.382(4)	C(26)-C(25)-C(30)	118.1(2)
C(40)-C(41)	1.384(4)	C(26)-C(25)-C(8)	123.1(2)
C(41)-C(42)	1.383(3)	C(30)-C(25)-C(8)	118.8(2)

Table A0.59. Atomic coordinates (x 10^4) and equivalent isotropic displacement parameters (Å^2 x 10^3) for **3.1e.** Ueq is defined as one third of the trace of the orthogonalized Uij tensor.

	U11	U22	U33	U23	U13	U12
C1	25(1)	30(1)	28(1)	3(1)	0(1)	1(1)
C2	24(1)	27(1)	33(1)	1(1)	0(1)	0(1)
C3	31(1)	33(1)	40(1)	6(1)	-1(1)	-4(1)
C4	36(1)	31(1)	48(2)	8(1)	0(1)	-10(1)
C5	31(1)	35(1)	51(2)	2(1)	-8(1)	-10(1)
C6	31(1)	35(1)	38(1)	1(1)	-8(1)	-5(1)
C7	26(1)	24(1)	34(1)	-2(1)	-1(1)	0(1)
C8	27(1)	25(1)	29(1)	-2(1)	-3(1)	0(1)
C9	25(1)	22(1)	27(1)	0(1)	0(1)	0(1)
C10	25(1)	22(1)	30(1)	0(1)	1(1)	3(1)
C11	24(1)	22(1)	34(1)	0(1)	1(1)	2(1)
C12	29(1)	35(1)	36(1)	1(1)	4(1)	0(1)
C13	30(1)	36(1)	46(2)	0(1)	6(1)	-7(1)
C14	28(1)	33(1)	50(2)	-4(1)	-1(1)	-8(1)
C15	30(1)	31(1)	35(1)	-4(1)	1(1)	-4(1)

C16	21(1)	24(1)	31(1)	-2(1)	-1(1)	0(1)
C17	23(1)	24(1)	28(1)	-1(1)	-4(1)	2(1)
C18	23(1)	24(1)	28(1)	-2(1)	-1(1)	1(1)
C19	29(1)	26(1)	27(1)	0(1)	-2(1)	-7(1)
C20	31(1)	43(2)	32(1)	4(1)	1(1)	0(1)
C21	43(1)	40(2)	30(1)	5(1)	1(1)	-7(1)
C22	45(1)	25(1)	32(1)	2(1)	-10(1)	-9(1)
C23	33(1)	27(1)	37(1)	1(1)	-6(1)	-3(1)
C24	32(1)	27(1)	31(1)	1(1)	0(1)	-5(1)
C25	26(1)	31(1)	30(1)	1(1)	-4(1)	-6(1)
C26	46(2)	29(1)	34(1)	-3(1)	-8(1)	-1(1)
C27	52(2)	36(2)	34(1)	-5(1)	-9(1)	-9(1)
C28	37(1)	42(2)	33(1)	3(1)	-9(1)	-5(1)
C29	33(1)	40(2)	41(2)	6(1)	-6(1)	5(1)
C30	31(1)	32(1)	34(1)	-3(1)	-2(1)	3(1)
C31	28(1)	28(1)	27(1)	0(1)	0(1)	0(1)
C32	44(1)	33(1)	30(1)	0(1)	1(1)	6(1)
C33	57(2)	46(2)	38(2)	-11(1)	5(1)	13(1)
C34	53(2)	50(2)	29(1)	-3(1)	4(1)	5(1)
C35	45(2)	45(2)	33(2)	8(1)	0(1)	-1(1)
C36	38(1)	30(1)	30(1)	1(1)	2(1)	1(1)
C37	31(1)	26(1)	29(1)	1(1)	1(1)	0(1)
C38	37(1)	35(1)	35(1)	-1(1)	-4(1)	-2(1)
C39	58(2)	49(2)	32(1)	-2(1)	-10(1)	-3(1)
C40	71(2)	46(2)	31(1)	-6(1)	5(1)	3(2)
C41	56(2)	39(2)	38(2)	-1(1)	10(1)	9(1)
C42	35(1)	38(1)	33(1)	2(1)	0(1)	3(1)
C43	59(2)	38(2)	39(2)	4(1)	-14(1)	-9(1)
C44	67(2)	60(2)	38(2)	11(1)	-15(1)	0(2)

Table A0.60. Hydrogen coordinates (x 10^4) and isotropic displacement parameters (Å^2 x 10^3) for **3.1e**.

Atom	x	y	z	U(eq)
H3A	1004	1915	8970	42
H4A	-160	1111	8320	46
H5A	-726	1584	6858	47
H6A	-31	2739	5991	42
H12A	4283	5422	5452	40
H13A	5271	6453	6131	45

H14A	5077	6946	7688	44
H15A	4006	6279	8608	38
H20A	1187	3459	10045	42
H21A	1745	2855	11430	45
H23A	3989	2128	10118	39
H24A	3424	2716	8722	36
H26A	1423	2659	4772	44
H27A	979	3120	3287	49
H29A	188	5686	4282	45
H30A	687	5256	5760	39
H32A	3363	3039	5342	43
H33A	3600	2718	3767	56
H34A	3296	3897	2642	53
H35A	2784	5395	3109	49
H36A	2599	5738	4692	39
H38A	3974	4838	9690	43
H39A	3728	5413	11191	55
H40A	2363	6065	11588	59
H41A	1233	6094	10482	53
H42A	1490	5540	8973	42
H43A	2809	2019	12298	68
H43B	3800	2239	11988	68
H43C	3344	1248	11692	68
H44A	401	4226	2209	82
H44B	621	5322	2456	82
H44C	-345	4907	2637	82

Table A0.61. Torsion angles (°) for **3.1e**.

Atoms	Angle	Atoms	Angle
C18-C1-C2-C3	176.5(2)	C8-C9-C18-C17	-159.57(19)
C19-C1-C2-C3	7.2(3)	C10-C9-C18-C1	-157.49(19)
C18-C1-C2-C7	-3.5(3)	C8-C9-C18-C1	21.6(3)
C19-C1-C2-C7	-172.80(19)	C2-C1-C19-C20	-67.4(3)
C1-C2-C3-C4	174.0(2)	C18-C1-C19-C20	123.4(2)
C7-C2-C3-C4	-6.0(3)	C2-C1-C19-C24	107.3(2)
C2-C3-C4-C5	-0.8(4)	C18-C1-C19-C24	-61.9(3)
C3-C4-C5-C6	4.4(4)	C24-C19-C20-C21	-1.2(3)
C4-C5-C6-C7	-0.8(4)	C1-C19-C20-C21	173.5(2)

C5-C6-C7-C8	172.2(2)	C19-C20-C21-C22	-0.3(4)
C5-C6-C7-C2	-6.1(3)	C20-C21-C22-C23	2.3(3)
C1-C2-C7-C8	10.9(3)	C20-C21-C22-C43	-175.2(2)
C3-C2-C7-C8	-169.06(19)	C21-C22-C23-C24	-2.7(3)
C1-C2-C7-C6	-170.8(2)	C43-C22-C23-C24	174.8(2)
C3-C2-C7-C6	9.3(3)	C22-C23-C24-C19	1.2(3)
C6-C7-C8-C9	180.0(2)	C20-C19-C24-C23	0.8(3)
C2-C7-C8-C9	-1.7(3)	C1-C19-C24-C23	-174.2(2)
C6-C7-C8-C25	5.1(3)	C7-C8-C25-C26	-75.1(3)
C2-C7-C8-C25	-176.7(2)	C9-C8-C25-C26	110.0(3)
C7-C8-C9-C10	164.62(19)	C7-C8-C25-C30	104.6(2)
C25-C8-C9-C10	-20.5(3)	C9-C8-C25-C30	-70.2(3)
C7-C8-C9-C18	-14.4(3)	C30-C25-C26-C27	2.9(3)
C25-C8-C9-C18	160.4(2)	C8-C25-C26-C27	-177.3(2)
C8-C9-C10-C11	170.3(2)	C25-C26-C27-C28	-1.7(4)
C18-C9-C10-C11	-10.7(3)	C26-C27-C28-C29	-1.0(4)
C8-C9-C10-C31	-17.4(3)	C26-C27-C28-C44	178.0(3)
C18-C9-C10-C31	161.6(2)	C27-C28-C29-C30	2.5(3)
C9-C10-C11-C12	174.7(2)	C44-C28-C29-C30	-176.5(2)
C31-C10-C11-C12	2.1(3)	C28-C29-C30-C25	-1.2(3)
C9-C10-C11-C16	-5.8(3)	C26-C25-C30-C29	-1.5(3)
C31-C10-C11-C16	-178.39(19)	C8-C25-C30-C29	178.8(2)
C10-C11-C12-C13	173.7(2)	C11-C10-C31-C36	-72.3(3)
C16-C11-C12-C13	-5.7(3)	C9-C10-C31-C36	115.2(2)
C11-C12-C13-C14	-1.7(4)	C11-C10-C31-C32	102.5(2)
C12-C13-C14-C15	4.7(4)	C9-C10-C31-C32	-70.0(3)
C13-C14-C15-C16	0.1(4)	C36-C31-C32-C33	-0.9(4)
C10-C11-C16-C17	11.8(3)	C10-C31-C32-C33	-176.0(2)
C12-C11-C16-C17	-168.7(2)	C31-C32-C33-C34	-0.6(4)
C10-C11-C16-C15	-169.39(19)	C32-C33-C34-C35	0.8(4)
C12-C11-C16-C15	10.1(3)	C33-C34-C35-C36	0.5(4)
C14-C15-C16-C17	171.3(2)	C32-C31-C36-C35	2.3(3)
C14-C15-C16-C11	-7.5(3)	C10-C31-C36-C35	177.1(2)
C11-C16-C17-C18	-1.0(3)	C34-C35-C36-C31	-2.1(4)
C15-C16-C17-C18	-179.7(2)	C16-C17-C37-C38	-64.0(3)
C11-C16-C17-C37	-171.72(19)	C18-C17-C37-C38	125.3(2)
C15-C16-C17-C37	9.6(3)	C16-C17-C37-C42	112.1(2)
C16-C17-C18-C1	163.2(2)	C18-C17-C37-C42	-58.6(3)

C37-C17-C18-C1	-26.0(3)	C42-C37-C38-C39	-0.9(3)
C16-C17-C18-C9	-15.6(3)	C17-C37-C38-C39	175.2(2)
C37-C17-C18-C9	155.16(19)	C37-C38-C39-C40	0.3(4)
C2-C1-C18-C17	168.6(2)	C38-C39-C40-C41	0.9(4)
C19-C1-C18-C17	-22.3(3)	C39-C40-C41-C42	-1.5(4)
C2-C1-C18-C9	-12.6(3)	C40-C41-C42-C37	0.8(4)
C19-C1-C18-C9	156.5(2)	C38-C37-C42-C41	0.3(3)
C10-C9-C18-C17	21.4(3)	C17-C37-C42-C41	-176.0(2)

Crystal Structure Report for **3.1g** (project code: 11008)

Data collection: A crystal (approximate dimensions 0.50 x 0.25 x 0.03 mm^3) was placed onto the tip of a 0.1 mm diameter glass capillary and mounted on a Bruker SMART Platform CCD diffractometer for a data collection at 123(2) K.[1] A preliminary set of cell constants was calculated from reflections harvested from three sets of 20 frames. These initial sets of frames were oriented such that orthogonal wedges of reciprocal space were surveyed. This produced initial orientation matrices determined from 157 reflections. The data collection was carried out using MoKα radiation (graphite monochromator) with a frame time of 60 seconds and a detector distance of 4.8 cm. A randomly oriented region of reciprocal space was surveyed to the extent of one sphere and to a resolution of 0.84 Å. Four major sections of frames were collected with 0.30º steps in ω at four different ϕ settings and a detector position of -28º in 2θ. The intensity data were corrected for absorption and decay (SADABS).[2] Final cell constants were calculated from the xyz centroids of 2577 strong reflections from the actual data collection after integration (SAINT).[3] Please refer to Table 1 for additional crystal and refinement information.

Structure solution and refinement: The structure was solved using SHELXS-97[4] and refined using SHELXL-97.[4] The space group Pbcm was determined based on systematic absences and intensity statistics. A direct-methods solution was calculated which provided most non-hydrogen atoms from the E-map. Full-matrix least squares / difference Fourier cycles were performed which located the remaining non-hydrogen atoms. All non-hydrogen atoms were refined with anisotropic displacement parameters. All hydrogen atoms were placed in ideal positions and refined as riding atoms with relative isotropic displacement parameters. The final full matrix least squares refinement converged to $R1 = 0.0761$ and $wR2 = 0.2221$ (F^2, all data).

Structure description: Structure is on special position making only half of the molecule unique. The trifluoro-methyl group is correctly described as three unique fluorines although they appear prolated.

Table A0.62. Atomic coordinates (x 10^4) and equivalent isotropic displacement parameters (Å^2 x 10^3) for **3.1g**. Ueq is defined as one third of the trace of the orthogonalized Uij tensor.

Atom	x	y	z	Ueq
C1	-3353(4)	2592(2)	7062(1)	25(1)
C2	-4822(4)	2932(2)	7277(1)	26(1)
C3	-6317(5)	3342(2)	7072(1)	30(1)
C4	-7703(5)	3700(2)	7281(1)	33(1)
C5	3731(5)	494(2)	7281(1)	34(1)
C6	2364(5)	880(2)	7072(1)	32(1)
C7	910(4)	1315(2)	7278(1)	26(1)
C8	-548(4)	1682(2)	7063(1)	26(1)
C9	-1946(4)	2138(2)	7273(1)	25(1)

C10	-3207(4)	2868(2)	6617(1)	27(1)
C11	-2233(5)	3656(2)	6530(1)	31(1)
C12	-2102(5)	3987(3)	6133(1)	38(1)
C13	-2936(5)	3524(3)	5813(1)	40(1)
C14	-3913(5)	2742(3)	5894(1)	37(1)
C15	-4065(5)	2424(2)	6295(1)	31(1)
C16	-654(4)	1447(2)	6613(1)	26(1)
C17	367(4)	1879(2)	6314(1)	28(1)
C18	305(5)	1605(2)	5904(1)	30(1)
C19	-817(5)	883(2)	5797(1)	32(1)
C20	-1822(5)	432(2)	6088(1)	33(1)
C21	-1721(5)	715(2)	6497(1)	30(1)
C22	-2779(7)	3889(4)	5383(1)	63(1)
F1	-3057(6)	4769(3)	5356(1)	102(1)
F2	-3933(8)	3545(3)	5130(1)	145(2)
F3	-1201(7)	3810(5)	5237(1)	208(4)
C23	1424(6)	2063(3)	5578(1)	43(1)
C24	-2998(6)	-358(3)	5968(1)	53(1)

Table A0.63. Bond lengths (Å) and angles (°) for **3.1g**.

Atoms	Length	Atoms	Angle	Atoms	Angle
C(1)-C(2)	1.399(5)	C(2)-C(1)-C(9)	121.0(3)	C(18)-C(17)-H(17)	119.4
C(1)-C(9)	1.426(4)	C(2)-C(1)-C(10)	116.1(3)	C(17)-C(18)-C(19)	118.3(3)
C(1)-C(10)	1.505(4)	C(9)-C(1)-C(10)	122.1(3)	C(17)-C(18)-C(23)	121.6(3)
C(2)-C(3)	1.439(5)	C(1)-C(2)-C(3)	122.5(3)	C(19)-C(18)-C(23)	120.1(3)
C(2)-C(2)#1	1.447(6)	C(1)-C(2)-C(2)#1	119.85(18)	C(20)-C(19)-C(18)	121.8(3)
C(3)-C(4)	1.352(5)	C(3)-C(2)-C(2)#1	117.57(18)	C(20)-C(19)-H(19)	119.1
C(3)-H(3)	0.95	C(4)-C(3)-C(2)	122.2(3)	C(18)-C(19)-H(19)	119.1
C(4)-C(4)#1	1.418(7)	C(4)-C(3)-H(3)	118.9	C(19)-C(20)-C(21)	118.6(3)
C(4)-H(4)	0.95	C(2)-C(3)-H(3)	118.9	C(19)-C(20)-C(24)	121.0(3)
C(5)-C(6)	1.356(5)	C(3)-C(4)-C(4)#1	120.2(2)	C(21)-C(20)-C(24)	120.4(3)
C(5)-C(5)#1	1.422(7)	C(3)-C(4)-H(4)	119.9	C(16)-C(21)-C(20)	121.2(3)
C(5)-H(5)	0.95	C(4)#1-C(4)-H(4)	119.9	C(16)-C(21)-H(21)	119.4
C(6)-C(7)	1.433(5)	C(6)-C(5)-C(5)#1	120.0(2)	C(20)-C(21)-H(21)	119.4
C(6)-H(6)	0.95	C(6)-C(5)-H(5)	120	F(3)-C(22)-F(2)	110.5(5)
C(7)-C(8)	1.408(5)	C(5)#1-C(5)-H(5)	120	F(3)-C(22)-F(1)	102.2(5)
C(7)-C(7)#1	1.437(6)	C(5)-C(6)-C(7)	122.1(3)	F(2)-C(22)-F(1)	103.4(4)
C(8)-C(9)	1.421(5)	C(5)-C(6)-H(6)	118.9	F(3)-C(22)-C(13)	112.6(4)

C(8)-C(16)	1.501(4)	C(7)-C(6)-H(6)	118.9	F(2)-C(22)-C(13)	113.5(5)
C(9)-C(9)#1	1.470(6)	C(8)-C(7)-C(6)	122.2(3)	F(1)-C(22)-C(13)	113.7(4)
C(10)-C(15)	1.387(5)	C(8)-C(7)-C(7)#1	119.76(18)	C(18)-C(23)-H(23A)	109.5
C(10)-C(11)	1.395(5)	C(6)-C(7)-C(7)#1	117.87(19)	C(18)-C(23)-H(23B)	109.5
C(11)-C(12)	1.382(5)	C(7)-C(8)-C(9)	121.2(3)	H(23A)-C(23)-H(23B)	109.5
C(11)-H(11)	0.95	C(7)-C(8)-C(16)	115.9(3)	C(18)-C(23)-H(23C)	109.5
C(12)-C(13)	1.389(6)	C(9)-C(8)-C(16)	122.3(3)	H(23A)-C(23)-H(23C)	109.5
C(12)-H(12)	0.95	C(8)-C(9)-C(1)	122.6(3)	H(23B)-C(23)-H(23C)	109.5
C(13)-C(14)	1.386(6)	C(8)-C(9)-C(9)#1	118.70(18)	C(20)-C(24)-H(24A)	109.5
C(13)-C(22)	1.496(5)	C(1)-C(9)-C(9)#1	118.69(18)	C(20)-C(24)-H(24B)	109.5
C(14)-C(15)	1.387(5)	C(15)-C(10)-C(11)	118.8(3)	H(24A)-C(24)-H(24B)	109.5
C(14)-H(14)	0.95	C(15)-C(10)-C(1)	124.2(3)	C(20)-C(24)-H(24C)	109.5
C(15)-H(15)	0.95	C(11)-C(10)-C(1)	116.9(3)	H(24A)-C(24)-H(24C)	109.5
C(16)-C(17)	1.389(4)	C(12)-C(11)-C(10)	121.0(3)	H(24B)-C(24)-H(24C)	109.5
C(16)-C(21)	1.390(5)	C(12)-C(11)-H(11)	119.5		
C(17)-C(18)	1.391(4)	C(10)-C(11)-H(11)	119.5		
C(17)-H(17)	0.95	C(11)-C(12)-C(13)	119.6(4)		
C(18)-C(19)	1.396(5)	C(11)-C(12)-H(12)	120.2		
C(18)-C(23)	1.510(5)	C(13)-C(12)-H(12)	120.2		
C(19)-C(20)	1.377(5)	C(14)-C(13)-C(12)	120.0(3)		
C(19)-H(19)	0.95	C(14)-C(13)-C(22)	120.9(4)		
C(20)-C(21)	1.392(5)	C(12)-C(13)-C(22)	119.1(4)		
C(20)-C(24)	1.507(5)	C(13)-C(14)-C(15)	120.0(3)		
C(21)-H(21)	0.95	C(13)-C(14)-H(14)	120		
C(22)-F(3)	1.285(6)	C(15)-C(14)-H(14)	120		
C(22)-F(2)	1.298(6)	C(14)-C(15)-C(10)	120.6(3)		
C(22)-F(1)	1.308(6)	C(14)-C(15)-H(15)	119.7		
C(23)-H(23A)	0.98	C(10)-C(15)-H(15)	119.7		
C(23)-H(23B)	0.98	C(17)-C(16)-C(21)	118.8(3)		
C(23)-H(23C)	0.98	C(17)-C(16)-C(8)	122.9(3)		
C(24)-H(24A)	0.98	C(21)-C(16)-C(8)	118.0(3)		
C(24)-H(24B)	0.98	C(16)-C(17)-C(18)	121.2(3)		
C(24)-H(24C)	0.98	C(16)-C(17)-H(17)	119.4		

Symmetry transformations used to generate equivalent atoms: #1 x,y,-z+3/2

Table A0.64. Atomic coordinates (x 10^4) and equivalent isotropic displacement parameters (Å^2 x 10^3) for **3.1g.** Ueq is defined as one third of the trace of the orthogonalized Uij tensor.

Atom	U11	U22	U33	U23	U13	U12

C1	29(2)	23(2)	23(2)	-2(1)	-1(1)	-3(1)
C2	27(2)	23(2)	26(2)	0(1)	-3(1)	-5(1)
C3	30(2)	30(2)	28(2)	0(1)	-3(1)	-2(1)
C4	28(2)	34(2)	37(2)	4(2)	-5(2)	1(2)
C5	32(2)	32(2)	38(2)	-3(2)	2(2)	7(2)
C6	35(2)	32(2)	28(2)	-2(1)	3(2)	3(2)
C7	29(2)	24(2)	27(2)	-1(1)	1(1)	-1(1)
C8	29(2)	25(2)	25(2)	1(1)	2(1)	-2(1)
C9	29(2)	24(2)	22(2)	2(1)	-1(1)	-3(1)
C10	26(2)	31(2)	25(2)	2(1)	1(1)	6(1)
C11	31(2)	33(2)	30(2)	0(1)	-1(1)	2(2)
C12	39(2)	37(2)	37(2)	10(2)	7(2)	6(2)
C13	43(2)	50(2)	28(2)	9(2)	4(2)	15(2)
C14	35(2)	53(2)	24(2)	-6(2)	-4(2)	10(2)
C15	29(2)	36(2)	28(2)	-1(1)	-2(1)	2(2)
C16	28(2)	27(2)	24(2)	-1(1)	-1(1)	4(1)
C17	27(2)	30(2)	26(2)	-2(1)	1(1)	-2(1)
C18	31(2)	35(2)	25(2)	2(1)	2(1)	3(2)
C19	38(2)	34(2)	25(2)	-4(1)	-4(2)	4(2)
C20	37(2)	31(2)	30(2)	-4(1)	-3(2)	-3(2)
C21	32(2)	27(2)	31(2)	4(1)	1(2)	0(1)
C22	73(3)	84(4)	32(2)	14(2)	8(2)	27(3)
F1	140(3)	101(3)	66(2)	53(2)	-13(2)	-10(2)
F2	281(6)	121(3)	31(2)	22(2)	-47(3)	-79(4)
F3	152(4)	388(9)	83(3)	135(4)	83(3)	163(5)
C23	45(2)	56(2)	28(2)	0(2)	4(2)	-10(2)
C24	67(3)	50(2)	43(2)	-8(2)	1(2)	-23(2)

Table A0.65. Hydrogen coordinates (x 10^4) and isotropic displacement parameters (Å^2 x 10^3) for **3.1g**.

Atom	x	y	z	U(eq)
H3	-6330	3361	6779	35
H4	-8680	3953	7135	39
H5	4688	223	7134	41
H6	2371	862	6779	38
H11	-1652	3970	6749	38
H12	-1445	4528	6078	45
H14	-4479	2425	5675	45
H15	-4763	1897	6351	37

H17	1121	2370	6392	33
H19	-890	698	5517	39
H21	-2394	403	6701	36
H23A	1930	2628	5689	64
H23B	683	2206	5338	64
H23C	2386	1652	5494	64
H24A	-3184	-353	5669	80
H24B	-4145	-301	6109	80
H24C	-2431	-933	6049	80

Table A0.66. Torsion angles (°) for **3.1g**.

Atoms	Angle	Atoms	Angle
C9-C1-C2-C3	-175.9(3)	C11-C12-C13-C14	0.9(6)
C10-C1-C2-C3	13.8(4)	C11-C12-C13-C22	-179.8(4)
C9-C1-C2-C2#1	8.1(4)	C12-C13-C14-C15	0.3(5)
C10-C1-C2-C2#1	-162.21(19)	C22-C13-C14-C15	-179.0(4)
C1-C2-C3-C4	-177.4(3)	C13-C14-C15-C10	-1.7(5)
C2#1-C2-C3-C4	-1.4(4)	C11-C10-C15-C14	1.9(5)
C2-C3-C4-C4#1	1.4(4)	C1-C10-C15-C14	177.6(3)
C5#1-C5-C6-C7	1.4(4)	C7-C8-C16-C17	-78.7(4)
C5-C6-C7-C8	-177.3(3)	C9-C8-C16-C17	109.9(4)
C5-C6-C7-C7#1	-1.4(4)	C7-C8-C16-C21	96.2(4)
C6-C7-C8-C9	-177.9(3)	C9-C8-C16-C21	-75.3(4)
C7#1-C7-C8-C9	6.3(4)	C21-C16-C17-C18	1.4(5)
C6-C7-C8-C16	10.6(5)	C8-C16-C17-C18	176.2(3)
C7#1-C7-C8-C16	-165.22(19)	C16-C17-C18-C19	0.2(5)
C7-C8-C9-C1	173.9(3)	C16-C17-C18-C23	-179.3(3)
C16-C8-C9-C1	-15.1(5)	C17-C18-C19-C20	-1.3(5)
C7-C8-C9-C9#1	-6.3(4)	C23-C18-C19-C20	178.2(3)
C16-C8-C9-C9#1	164.7(2)	C18-C19-C20-C21	0.8(5)
C2-C1-C9-C8	171.8(3)	C18-C19-C20-C24	-178.8(4)
C10-C1-C9-C8	-18.4(5)	C17-C16-C21-C20	-2.0(5)
C2-C1-C9-C9#1	-8.0(4)	C8-C16-C21-C20	-177.1(3)
C10-C1-C9-C9#1	161.7(2)	C19-C20-C21-C16	1.0(5)
C2-C1-C10-C15	-84.1(4)	C24-C20-C21-C16	-179.5(3)
C9-C1-C10-C15	105.6(4)	C14-C13-C22-F3	-111.4(6)
C2-C1-C10-C11	91.6(4)	C12-C13-C22-F3	69.3(7)
C9-C1-C10-C11	-78.6(4)	C14-C13-C22-F2	15.1(6)

C15-C10-C11-C12	-0.8(5)	C12-C13-C22-F2	-164.2(4)
C1-C10-C11-C12	-176.7(3)	C14-C13-C22-F1	132.9(5)
C10-C11-C12-C13	-0.6(5)	C12-C13-C22-F1	-46.4(6)

Symmetry transformations used to generate equivalent atoms: #1 x,y,-z+3/2

Crystal Structure Report for **3.1h** (project code: 11079)

Data collection: A crystal (approximate dimensions 0.25 x 0.25 x 0.05 mm^3) was placed onto the tip of a 0.1 mm diameter glass capillary and mounted on a Bruker Apex II Platform CCD diffractometer for a data collection at 123(2) K.[1] A preliminary set of cell constants was calculated from reflections harvested from three sets of 20 frames. These initial sets of frames were oriented such that orthogonal wedges of reciprocal space were surveyed. This produced initial orientation matrices determined from 152 reflections. The data collection was carried out using MoKα radiation (graphite monochromator) with a frame time of 40 seconds and a detector distance of 4.8 cm. A randomly oriented region of reciprocal space was surveyed to the extent of one sphere and to a resolution of 0.77 Å. Four major sections of frames were collected with 0.30º steps in ω at four different ϕ settings and a detector position of -28º in 2θ. The intensity data were corrected for absorption and decay (SADABS).[2] Final cell constants were calculated from the xyz centroids of 4714 strong reflections from the actual data collection after integration (SAINT).[3] Please refer to Table 1 for additional crystal and refinement information.

Structure solution and refinement: The structure was solved using SHELXS-97[4] and refined using SHELXL-97.[4] The space group Pbcm was determined based on systematic absences and intensity statistics. A direct-methods solution was calculated which provided most non-hydrogen atoms from the E-map. Full-matrix least squares / difference Fourier cycles were performed which located the remaining non-hydrogen atoms. All non-hydrogen atoms were refined with anisotropic displacement parameters. All hydrogen atoms were placed in ideal positions and refined as riding atoms with relative isotropic displacement parameters. The final full matrix least squares refinement converged to $R1 = 0.0952$ and $wR2 = 0.2828$ (F^2, all data).

Structure description: Structure is on special position making only half of the molecule unique. The trifluoro-methyl groups are modeled as ideally disordered (rotational) trifluoromethyl groups. The methyl groups are modeled as ideally disordered (rotational) methyl groups.

Table A0.67. Atomic coordinates (x 10^4) and equivalent isotropic displacement parameters ($Å^2$ x 10^3) for **3.1h**. Ueq is defined as one third of the trace of the orthogonalized Uij tensor.

Atom	x	y	z	Ueq
C1	3934(6)	4719(3)	7084(1)	20(1)
C2	5452(5)	4335(3)	7290(1)	19(1)
C3	6993(6)	3891(3)	7093(1)	23(1)
C4	8433(6)	3492(3)	7293(1)	26(1)
C5	-3531(6)	6886(3)	7295(1)	28(1)
C6	-2083(6)	6497(3)	7094(1)	25(1)
C7	-531(5)	6054(3)	7290(1)	21(1)
C8	980(6)	5674(3)	7083(1)	20(1)
C9	2456(5)	5196(3)	7285(1)	19(1)
C10	3860(6)	4494(3)	6655(1)	21(1)
C11	4833(6)	5014(3)	6373(1)	26(1)

C12	4821(7)	4731(4)	5985(1)	35(1)
C13	3856(7)	3921(4)	5871(1)	39(1)
C14	2901(7)	3393(3)	6150(1)	36(1)
C15	2905(6)	3676(3)	6537(1)	31(1)
C16	1059(6)	5901(3)	6653(1)	24(1)
C17	2012(6)	6709(3)	6531(1)	27(1)
C18	2035(7)	6981(4)	6142(1)	40(1)
C19	1085(7)	6450(4)	5860(1)	44(1)
C20	107(7)	5657(4)	5985(1)	39(1)
C21	80(6)	5392(4)	6374(1)	29(1)
C22	3804(5)	3611(3)	5442(1)	63(2)
F1	5360(6)	3895(4)	5263(1)	117(3)
F2	2327(7)	4000(4)	5267(1)	136(3)
F3	3678(9)	2667(3)	5423(1)	119(3)
F1'	2217(6)	3146(5)	5372(1)	117(3)
F2'	5250(6)	3042(4)	5368(1)	136(3)
F3'	3899(9)	4374(3)	5212(1)	119(3)
C23	1140(10)	6741(6)	5432(2)	68(2)

Table A0.68. Bond lengths (Å) and angles (°) for **3.1h**.

Atoms	Length	Atoms	Angle	Atoms	Angle
C(1)-C(2)	1.401(6)	C(2)-C(1)-C(9)	120.8(4)	C(17)-C(16)-C(8)	119.0(4)
C(1)-C(9)	1.427(6)	C(2)-C(1)-C(10)	115.9(4)	C(18)-C(17)-C(16)	121.3(4)
C(1)-C(10)	1.497(6)	C(9)-C(1)-C(10)	122.9(4)	C(18)-C(17)-H(17A)	119.4
C(2)-C(3)	1.433(6)	C(1)-C(2)-C(3)	121.8(4)	C(16)-C(17)-H(17A)	119.4
C(2)-C(2)#1	1.436(8)	C(1)-C(2)-C(2)#1	120.2(2)	C(17)-C(18)-C(19)	120.7(5)
C(3)-C(4)	1.356(6)	C(3)-C(2)-C(2)#1	118.0(2)	C(17)-C(18)-H(18A)	119.7
C(3)-H(3A)	0.95	C(4)-C(3)-C(2)	121.8(4)	C(19)-C(18)-H(18A)	119.7
C(4)-C(4)#1	1.416(9)	C(4)-C(3)-H(3A)	119.1	C(20)-C(19)-C(18)	117.7(4)
C(4)-H(4A)	0.95	C(2)-C(3)-H(3A)	119.1	C(20)-C(19)-C(23)	121.8(5)
C(5)-C(6)	1.355(6)	C(3)-C(4)-C(4)#1	120.2(3)	C(18)-C(19)-C(23)	120.5(5)
C(5)-C(5)#1	1.403(9)	C(3)-C(4)-H(4A)	119.9	C(21)-C(20)-C(19)	121.4(5)
C(5)-H(5A)	0.95	C(4)#1-C(4)-H(4A)	119.9	C(21)-C(20)-H(20A)	119.3
C(6)-C(7)	1.437(6)	C(6)-C(5)-C(5)#1	120.3(3)	C(19)-C(20)-H(20A)	119.3
C(6)-H(6A)	0.95	C(6)-C(5)-H(5A)	119.8	C(20)-C(21)-C(16)	121.1(5)
C(7)-C(8)	1.397(6)	C(5)#1-C(5)-H(5A)	119.8	C(20)-C(21)-H(21A)	119.4
C(7)-C(7)#1	1.433(8)	C(5)-C(6)-C(7)	121.9(4)	C(16)-C(21)-H(21A)	119.4
C(8)-C(9)	1.428(5)	C(5)-C(6)-H(6A)	119.1	C(19)-C(23)-H(23A)	109.5

C(8)-C(16)	1.503(6)	C(7)-C(6)-H(6A)	119.1	C(19)-C(23)-H(23B)	109.5
C(9)-C(9)#1	1.469(7)	C(8)-C(7)-C(7)#1	120.4(2)	H(23A)-C(23)-H(23B)	109.5
C(10)-C(11)	1.395(6)	C(8)-C(7)-C(6)	121.7(4)	C(19)-C(23)-H(23C)	109.5
C(10)-C(15)	1.396(6)	C(7)#1-C(7)-C(6)	117.8(2)	H(23A)-C(23)-H(23C)	109.5
C(11)-C(12)	1.384(6)	C(7)-C(8)-C(9)	120.4(4)	H(23B)-C(23)-H(23C)	109.5
C(11)-H(11A)	0.95	C(7)-C(8)-C(16)	116.3(4)	C(19)-C(23)-H(23D)	109.5
C(12)-C(13)	1.387(7)	C(9)-C(8)-C(16)	122.9(4)	H(23A)-C(23)-H(23D)	141.1
C(12)-H(12A)	0.95	C(1)-C(9)-C(8)	122.3(3)	H(23B)-C(23)-H(23D)	56.3
C(13)-C(14)	1.388(7)	C(1)-C(9)-C(9)#1	118.8(2)	H(23C)-C(23)-H(23D)	56.3
C(13)-C(22)	1.528(5)	C(8)-C(9)-C(9)#1	118.9(2)	C(19)-C(23)-H(23E)	109.5
C(14)-C(15)	1.379(6)	C(11)-C(10)-C(15)	118.4(4)	H(23A)-C(23)-H(23E)	56.3
C(14)-H(14A)	0.95	C(11)-C(10)-C(1)	123.2(4)	H(23B)-C(23)-H(23E)	141.1
C(15)-H(15A)	0.95	C(15)-C(10)-C(1)	118.2(4)	H(23C)-C(23)-H(23E)	56.3
C(16)-C(21)	1.382(6)	C(12)-C(11)-C(10)	120.5(4)	H(23D)-C(23)-H(23E)	109.5
C(16)-C(17)	1.388(6)	C(12)-C(11)-H(11A)	119.7	C(19)-C(23)-H(23F)	109.5
C(17)-C(18)	1.384(6)	C(10)-C(11)-H(11A)	119.7	H(23A)-C(23)-H(23F)	56.3
C(17)-H(17A)	0.95	C(11)-C(12)-C(13)	120.6(4)	H(23B)-C(23)-H(23F)	56.3
C(18)-C(19)	1.395(8)	C(11)-C(12)-H(12A)	119.7	H(23C)-C(23)-H(23F)	141.1
C(18)-H(18A)	0.95	C(13)-C(12)-H(12A)	119.7	H(23D)-C(23)-H(23F)	109.5
C(19)-C(20)	1.382(8)	C(12)-C(13)-C(14)	119.2(4)	H(23E)-C(23)-H(23F)	109.5
C(19)-C(23)	1.517(7)	C(12)-C(13)-C(22)	121.1(4)		
C(20)-C(21)	1.381(6)	C(14)-C(13)-C(22)	119.7(4)		
C(20)-H(20A)	0.95	C(15)-C(14)-C(13)	120.3(5)		
C(21)-H(21A)	0.95	C(15)-C(14)-H(14A)	119.9		
C(23)-H(23A)	0.98	C(13)-C(14)-H(14A)	119.9		
C(23)-H(23B)	0.98	C(14)-C(15)-C(10)	121.0(4)		
C(23)-H(23C)	0.98	C(14)-C(15)-H(15A)	119.5		
C(23)-H(23D)	0.98	C(10)-C(15)-H(15A)	119.5		
C(23)-H(23E)	0.98	C(21)-C(16)-C(17)	117.8(4)		
C(23)-H(23F)	0.98	C(21)-C(16)-C(8)	123.0(4)		

Symmetry transformations used to generate equivalent atoms: #1 x,y,-z+3/2

Table A0.69. Atomic coordinates (x 10^4) and equivalent isotropic displacement parameters (Å^2 x 10^3) for **3.1h.** Ueq is defined as one third of the trace of the orthogonalized Uij tensor.

Atom	U11	U22	U33	U23	U13	U12
C1	17(2)	19(2)	23(2)	0(2)	1(2)	-5(2)
C2	16(2)	15(2)	26(2)	-1(2)	2(2)	-4(2)
C3	20(2)	19(2)	30(2)	0(2)	4(2)	-2(2)

C4	20(2)	18(2)	40(2)	-2(2)	6(2)	1(2)
C5	17(2)	28(2)	40(2)	2(2)	-5(2)	0(2)
C6	23(2)	25(2)	26(2)	0(2)	-3(2)	-2(2)
C7	18(2)	18(2)	25(2)	0(2)	0(2)	-3(2)
C8	18(2)	20(2)	23(2)	0(2)	-2(2)	-2(2)
C9	16(2)	21(2)	19(2)	-1(2)	-1(2)	-3(2)
C10	18(2)	20(2)	24(2)	0(2)	1(2)	2(2)
C11	20(2)	34(3)	26(2)	0(2)	3(2)	-2(2)
C12	27(2)	55(3)	24(2)	5(2)	5(2)	0(2)
C13	36(3)	54(3)	28(2)	-11(2)	-1(2)	4(2)
C14	41(3)	31(3)	36(3)	-12(2)	-2(2)	-2(2)
C15	25(2)	38(3)	28(2)	-1(2)	1(2)	-1(2)
C16	17(2)	32(2)	21(2)	0(2)	-2(2)	4(2)
C17	33(2)	19(2)	29(2)	2(2)	0(2)	-1(2)
C18	44(3)	43(3)	34(3)	10(2)	5(2)	2(2)
C19	41(3)	65(4)	25(2)	9(2)	1(2)	12(3)
C20	26(2)	64(4)	25(2)	-4(2)	-3(2)	-1(2)
C21	20(2)	43(3)	23(2)	-2(2)	0(2)	-2(2)
C22	55(4)	94(6)	41(3)	-16(3)	3(3)	-3(4)
F1	118(5)	182(7)	50(3)	-33(3)	35(3)	-18(5)
F2	127(5)	236(9)	46(3)	-33(4)	-35(3)	58(6)
F3	173(7)	110(5)	74(3)	-56(3)	16(4)	-12(5)
F1'	118(5)	182(7)	50(3)	-33(3)	35(3)	-18(5)
F2'	127(5)	236(9)	46(3)	-33(4)	-35(3)	58(6)
F3'	173(7)	110(5)	74(3)	-56(3)	16(4)	-12(5)
C23	73(4)	100(6)	32(3)	16(3)	-1(3)	4(4)

Table A0.70. Hydrogen coordinates (x 10^4) and isotropic displacement parameters (Å^2 x 10^3) for **3.1h**.

Atom	x	Y	z	U(eq)
H3A	7006	3876	6815	28
H4A	9445	3211	7154	31
H5A	-4550	7160	7156	34
H6A	-2095	6518	6816	29
H11A	5508	5567	6448	32
H12A	5480	5094	5795	42
H14A	2242	2836	6075	43
H15A	2249	3309	6726	37
H17A	2660	7084	6719	33

H18A	2706	7535	6066	48
H20A	-562	5287	5798	46
H21A	-623	4849	6451	35
H23A	-67	6596	5309	102
H23B	2136	6389	5298	102
H23C	1385	7426	5413	102
H23D	2370	7011	5371	102
H23E	167	7218	5382	102
H23F	918	6182	5267	102

Table A0.71. Torsion angles (°) for **3.1h**.

Atoms	Angle	Atoms	Angle
C9-C1-C2-C3	-177.2(4)	C9-C1-C10-C15	-82.8(5)
C10-C1-C2-C3	10.0(6)	C15-C10-C11-C12	1.0(6)
C9-C1-C2-C2#1	6.0(4)	C1-C10-C11-C12	175.2(4)
C10-C1-C2-C2#1	-166.9(2)	C10-C11-C12-C13	-0.6(7)
C1-C2-C3-C4	-177.8(4)	C11-C12-C13-C14	-0.1(7)
C2#1-C2-C3-C4	-0.9(5)	C11-C12-C13-C22	178.9(4)
C2-C3-C4-C4#1	0.9(5)	C12-C13-C14-C15	0.4(8)
C5#1-C5-C6-C7	1.5(5)	C22-C13-C14-C15	-178.7(4)
C5-C6-C7-C8	-178.4(4)	C13-C14-C15-C10	0.1(7)
C5-C6-C7-C7#1	-1.5(5)	C11-C10-C15-C14	-0.8(7)
C7#1-C7-C8-C9	6.2(5)	C1-C10-C15-C14	-175.3(4)
C6-C7-C8-C9	-176.9(4)	C7-C8-C16-C21	-83.6(5)
C7#1-C7-C8-C16	-166.6(2)	C9-C8-C16-C21	103.7(5)
C6-C7-C8-C16	10.3(6)	C7-C8-C16-C17	90.2(5)
C2-C1-C9-C8	173.9(4)	C9-C8-C16-C17	-82.5(5)
C10-C1-C9-C8	-13.7(6)	C21-C16-C17-C18	-2.1(7)
C2-C1-C9-C9#1	-6.0(4)	C8-C16-C17-C18	-176.2(4)
C10-C1-C9-C9#1	166.4(3)	C16-C17-C18-C19	0.5(7)
C7-C8-C9-C1	174.0(4)	C17-C18-C19-C20	0.9(8)
C16-C8-C9-C1	-13.6(6)	C17-C18-C19-C23	-179.0(5)
C7-C8-C9-C9#1	-6.1(5)	C18-C19-C20-C21	-0.6(8)
C16-C8-C9-C9#1	166.2(3)	C23-C19-C20-C21	179.3(5)
C2-C1-C10-C11	-84.2(5)	C19-C20-C21-C16	-1.1(8)
C9-C1-C10-C11	103.1(5)	C17-C16-C21-C20	2.4(7)
C2-C1-C10-C15	89.9(5)	C8-C16-C21-C20	176.2(4)

Symmetry transformations used to generate equivalent atoms: #1 x,y,-z+3/2

Crystal Structure Report for **3.1i** (project code: 11080)

Data collection: A crystal (approximate dimensions 0.25 x 0.20 x 0.13 mm^3) was placed onto the tip of a 0.1 mm diameter glass capillary and mounted on a Bruker SMART Platform CCD diffractometer for a data collection at 123(2) K.[1] A preliminary set of cell constants was calculated from reflections harvested from three sets of 20 frames. These initial sets of frames were oriented such that orthogonal wedges of reciprocal space were surveyed. This produced initial orientation matrices determined from 222 reflections. The data collection was carried out using MoKα radiation (graphite monochromator) with a frame time of 40 seconds and a detector distance of 4.8 cm. A randomly oriented region of reciprocal space was surveyed to the extent of one sphere and to a resolution of 0.77 Å. Four major sections of frames were collected with 0.30º steps in ω at four different ϕ settings and a detector position of -28º in 2θ. The intensity data were corrected for absorption and decay (SADABS).[2] Final cell constants were calculated from the xyz centroids of 6220 strong reflections from the actual data collection after integration (SAINT).[3] Please refer to Table 1 for additional crystal and refinement information.

Structure solution and refinement: The structure was solved using SHELXS-97[4] and refined using SHELXL-97.[4] The space group Pnma was determined based on systematic absences and intensity statistics. A direct-methods solution was calculated which provided most non-hydrogen atoms from the E-map. Full-matrix least squares / difference Fourier cycles were performed which located the remaining non-hydrogen atoms. All non-hydrogen atoms were refined with anisotropic displacement parameters. All hydrogen atoms were placed in ideal positions and refined as riding atoms with relative isotropic displacement parameters. The final full matrix least squares refinement converged to $R1 = 0.0459$ and $wR2 = 0.1477$ (F^2, all data).

Structure description: he structure lies on a special position making only half of the molecule unique. No disorder of the trifluoromethyl groups was detected.

Table A0.72. Atomic coordinates (x 10^4) and equivalent isotropic displacement parameters (Å^2 x 10^3) for **3.1i**. Ueq is defined as one third of the trace of the orthogonalized Uij tensor.

Atom	x	y	z	Ueq
C1	1065(2)	7044(1)	5479(1)	17(1)
C2	-453(2)	7270(1)	5865(1)	17(1)
C3	-2002(2)	7054(1)	6310(1)	20(1)
C4	-3455(2)	7273(1)	6703(1)	23(1)
C5	8513(2)	7273(1)	3291(1)	26(1)
C6	7063(2)	7053(1)	3686(1)	22(1)
C7	5522(2)	7270(1)	4132(1)	19(1)
C8	4003(2)	7043(1)	4516(1)	18(1)
C9	2534(2)	7265(1)	4996(1)	17(1)
C10	1119(2)	6573(1)	5695(1)	19(1)
C11	2046(2)	6438(1)	6506(1)	24(1)
C12	2037(3)	6010(1)	6775(1)	31(1)
C13	1085(3)	5714(1)	6225(1)	30(1)
C14	138(2)	5842(1)	5424(1)	28(1)
C15	146(2)	6270(1)	5166(1)	23(1)
C16	3944(2)	6571(1)	4300(1)	20(1)

C17	4932(2)	6269(1)	4826(1)	25(1)
C18	4942(3)	5840(1)	4564(2)	33(1)
C19	3985(3)	5708(1)	3765(1)	38(1)
C20	3020(3)	6006(1)	3226(1)	36(1)
C21	3002(3)	6435(1)	3493(1)	27(1)
C22	1143(4)	5248(1)	6480(2)	49(1)
F1	1318(4)	5185(1)	7391(1)	103(1)
F2	-383(2)	5035(1)	6209(1)	72(1)
F3	2544(3)	5042(1)	6059(2)	98(1)

Table A0.73. Bond lengths (Å) and angles (°) for **3.1i**.

Atoms	Length	Atoms	Angle	Atoms	Angle
C(1)-C(2)	1.401(2)	C(2)-C(1)-C(9)	120.73(13)	C(21)-C(16)-C(8)	118.69(14)
C(1)-C(9)	1.427(2)	C(2)-C(1)-C(10)	115.53(13)	C(18)-C(17)-C(16)	120.73(16)
C(1)-C(10)	1.5012(19)	C(9)-C(1)-C(10)	123.45(13)	C(19)-C(18)-C(17)	120.11(17)
C(2)-C(2)#1	1.435(3)	C(1)-C(2)-C(2)#1	120.15(8)	C(20)-C(19)-C(18)	119.92(16)
C(2)-C(3)	1.438(2)	C(1)-C(2)-C(3)	121.90(13)	C(19)-C(20)-C(21)	119.86(17)
C(3)-C(4)	1.359(2)	C(2)#1-C(2)-C(3)	117.88(8)	C(20)-C(21)-C(16)	120.89(17)
C(4)-C(4)#1	1.415(3)	C(4)-C(3)-C(2)	121.95(14)	F(1)-C(22)-F(3)	107.4(2)
C(5)-C(6)	1.359(2)	C(3)-C(4)-C(4)#1	120.16(9)	F(1)-C(22)-F(2)	106.6(2)
C(5)-C(5)#1	1.415(3)	C(6)-C(5)-C(5)#1	120.25(10)	F(3)-C(22)-F(2)	103.95(18)
C(6)-C(7)	1.435(2)	C(5)-C(6)-C(7)	121.72(15)	F(1)-C(22)-C(13)	112.72(18)
C(7)-C(8)	1.402(2)	C(8)-C(7)-C(6)	121.64(14)	F(3)-C(22)-C(13)	112.37(18)
C(7)-C(7)#1	1.437(3)	C(8)-C(7)-C(7)#1	120.26(8)	F(2)-C(22)-C(13)	113.14(19)
C(8)-C(9)	1.427(2)	C(6)-C(7)-C(7)#1	118.01(9)		
C(8)-C(16)	1.5023(19)	C(7)-C(8)-C(9)	120.44(13)		
C(9)-C(9)#1	1.467(3)	C(7)-C(8)-C(16)	115.80(13)		
C(10)-C(11)	1.392(2)	C(9)-C(8)-C(16)	123.46(14)		
C(10)-C(15)	1.392(2)	C(1)-C(9)-C(8)	122.20(13)		
C(11)-C(12)	1.389(2)	C(1)-C(9)-C(9)#1	118.81(8)		
C(12)-C(13)	1.388(3)	C(8)-C(9)-C(9)#1	118.99(8)		
C(13)-C(14)	1.382(3)	C(11)-C(10)-C(15)	118.54(14)		
C(13)-C(22)	1.497(2)	C(11)-C(10)-C(1)	118.52(13)		
C(14)-C(15)	1.385(2)	C(15)-C(10)-C(1)	122.69(14)		
C(16)-C(17)	1.393(2)	C(12)-C(11)-C(10)	121.08(15)		
C(16)-C(21)	1.394(2)	C(13)-C(12)-C(11)	119.16(16)		
C(17)-C(18)	1.390(2)	C(14)-C(13)-C(12)	120.65(15)		
C(18)-C(19)	1.386(3)	C(14)-C(13)-C(22)	119.54(17)		

C(19)-C(20)	1.384(3)	C(12)-C(13)-C(22)	119.76(18)
C(20)-C(21)	1.392(2)	C(13)-C(14)-C(15)	119.64(16)
C(22)-F(1)	1.316(3)	C(14)-C(15)-C(10)	120.90(15)
C(22)-F(3)	1.327(3)	C(17)-C(16)-C(21)	118.48(14)
C(22)-F(2)	1.330(3)	C(17)-C(16)-C(8)	122.56(14)

Symmetry transformations used to generate equivalent atoms: #1 x,-y+3/2,z

Table A0.74. Atomic coordinates (x 10^4) and equivalent isotropic displacement parameters (Å^2 x 10^3) for **3.1i.** Ueq is defined as one third of the trace of the orthogonalized Uij tensor.

Atom	U11	U22	U33	U23	U13	U12
C1	20(1)	16(1)	16(1)	0(1)	-2(1)	-1(1)
C2	19(1)	19(1)	15(1)	0(1)	-1(1)	-2(1)
C3	22(1)	19(1)	20(1)	0(1)	1(1)	-3(1)
C4	21(1)	28(1)	20(1)	2(1)	3(1)	-4(1)
C5	20(1)	36(1)	21(1)	-2(1)	3(1)	5(1)
C6	22(1)	25(1)	20(1)	-1(1)	0(1)	5(1)
C7	18(1)	23(1)	15(1)	0(1)	-1(1)	1(1)
C8	19(1)	19(1)	17(1)	-1(1)	-2(1)	3(1)
C9	18(1)	16(1)	16(1)	0(1)	-1(1)	0(1)
C10	20(1)	15(1)	21(1)	0(1)	2(1)	-1(1)
C11	30(1)	21(1)	22(1)	0(1)	-1(1)	0(1)
C12	41(1)	25(1)	26(1)	5(1)	-2(1)	5(1)
C13	35(1)	17(1)	38(1)	4(1)	7(1)	1(1)
C14	26(1)	18(1)	40(1)	-5(1)	0(1)	-3(1)
C15	21(1)	19(1)	29(1)	-2(1)	-1(1)	0(1)
C16	19(1)	19(1)	22(1)	-3(1)	4(1)	1(1)
C17	23(1)	21(1)	31(1)	-1(1)	-2(1)	2(1)
C18	30(1)	22(1)	49(1)	0(1)	2(1)	6(1)
C19	41(1)	21(1)	51(1)	-12(1)	10(1)	0(1)
C20	42(1)	34(1)	31(1)	-13(1)	2(1)	-6(1)
C21	31(1)	27(1)	23(1)	-2(1)	1(1)	-1(1)
C22	62(2)	23(1)	62(1)	9(1)	2(1)	-1(1)
F1	196(2)	39(1)	74(1)	34(1)	-32(1)	-20(1)
F2	83(1)	24(1)	108(1)	11(1)	-1(1)	-16(1)
F3	92(1)	30(1)	172(2)	17(1)	37(1)	28(1)

Table A0.75. Hydrogen coordinates (x 10^4) and isotropic displacement parameters (Å^2 x 10^3) for **3.1i**.

Atom	x	y	z	U(eq)
H3A	-2010	6750	6330	24

H4A	-4473	7121	6979	28
H5A	9530	7121	3014	31
H6A	7071	6749	3666	27
H11A	2695	6643	6881	29
H12A	2674	5922	7330	37
H14A	-514	5637	5051	34
H15A	-522	6359	4620	27
H17A	5607	6358	5369	30
H18A	5606	5636	4933	40
H19A	3991	5415	3587	45
H20A	2371	5917	2675	43
H21A	2340	6638	3121	33

Table A0.76. Torsion angles (°) for **3.1i**.

Atoms	Angle	Atoms	Angle
C9-C1-C2-C2#1	-6.43(17)	C1-C10-C11-C12	175.71(16)
C10-C1-C2-C2#1	167.55(9)	C10-C11-C12-C13	0.0(3)
C9-C1-C2-C3	176.60(14)	C11-C12-C13-C14	-0.7(3)
C10-C1-C2-C3	-9.4(2)	C11-C12-C13-C22	176.93(19)
C1-C2-C3-C4	178.51(14)	C12-C13-C14-C15	0.2(3)
C2#1-C2-C3-C4	1.48(18)	C22-C13-C14-C15	-177.42(18)
C2-C3-C4-C4#1	-1.51(18)	C13-C14-C15-C10	1.0(3)
C5#1-C5-C6-C7	-1.55(18)	C11-C10-C15-C14	-1.7(3)
C5-C6-C7-C8	178.25(15)	C1-C10-C15-C14	-175.96(15)
C5-C6-C7-C7#1	1.52(18)	C7-C8-C16-C17	84.42(19)
C6-C7-C8-C9	176.93(14)	C9-C8-C16-C17	-101.88(19)
C7#1-C7-C8-C9	-6.41(17)	C7-C8-C16-C21	-89.65(18)
C6-C7-C8-C16	-9.2(2)	C9-C8-C16-C21	84.1(2)
C7#1-C7-C8-C16	167.49(9)	C21-C16-C17-C18	-1.5(3)
C2-C1-C9-C8	-173.77(13)	C8-C16-C17-C18	-175.58(16)
C10-C1-C9-C8	12.7(2)	C16-C17-C18-C19	0.9(3)
C2-C1-C9-C9#1	6.34(16)	C17-C18-C19-C20	0.1(3)
C10-C1-C9-C9#1	-167.14(10)	C18-C19-C20-C21	-0.5(3)
C7-C8-C9-C1	-173.55(13)	C19-C20-C21-C16	-0.1(3)
C16-C8-C9-C1	13.0(2)	C17-C16-C21-C20	1.1(3)
C7-C8-C9-C9#1	6.33(17)	C8-C16-C21-C20	175.41(16)
C16-C8-C9-C9#1	-167.08(11)	C14-C13-C22-F1	-152.2(2)
C2-C1-C10-C11	-89.08(18)	C12-C13-C22-F1	30.1(3)

C9-C1-C10-C11	84.72(19)	C14-C13-C22-F3	86.2(3)
C2-C1-C10-C15	85.17(19)	C12-C13-C22-F3	-91.4(2)
C9-C1-C10-C15	-101.04(19)	C14-C13-C22-F2	-31.1(3)
C15-C10-C11-C12	1.2(3)	C12-C13-C22-F2	151.21(19)

Symmetry transformations used to generate equivalent atoms: #1 x,-y+3/2,z

Crystal Structure Report for **3.1j** (project code: 11217)

Data collection: A crystal (approximate dimensions 0.50 x 0.25 x 0.20 mm^3) was placed onto the tip of a 0.1 mm diameter glass capillary and mounted on a Burker APEX II Platform CCD diffractometer for a data collection at 123(2) K.[1] A preliminary set of cell constants was calculated from reflections harvested from three sets of 12 frames. These initial sets of frames were oriented such that orthogonal wedges of reciprocal space were surveyed. This produced initial orientation matrices determined from 221 reflections. The data collection was carried out using MoKα radiation (graphite monochromator) with a frame time of 30 seconds and a detector distance of 6.0 cm. A randomly oriented region of reciprocal space was surveyed to the extent of one sphere and to a resolution of 0.77 Å. Four major sections of frames were collected with 0.30º steps in ω at four different ϕ settings and a detector position of -28º in 2θ. The intensity data were corrected for absorption and decay (SADABS).[2] Final cell constants were calculated from the xyz centroids of 7587 strong reflections from the actual data collection after integration (SAINT).[3] Please refer to Table 1 for additional crystal and refinement information.

Structure solution and refinement: The structure was solved using SHELXS-97[4] and refined using SHELXL-97.[4] The space group C2/c was determined based on systematic absences and intensity statistics. A direct-methods solution was calculated which provided most non-hydrogen atoms from the E-map. Full-matrix least squares / difference Fourier cycles were performed which located the remaining non-hydrogen atoms. All non-hydrogen atoms were refined with anisotropic displacement parameters. All hydrogen atoms were placed in ideal positions and refined as riding atoms with relative isotropic displacement parameters. The final full matrix least squares refinement converged to $R1$ = 0.0713 and $wR2$ = 0.2058 (F^2, all data).

Structure description: Structure is on special position making only half of the molecule unique. The trifluoro-methyl groups are correctly described as three unique fluorines, although they appear to be prolated.

Table A0.77. Atomic coordinates (x 10^4) and equivalent isotropic displacement parameters ($Å^2$x 10^3) for **3.1j**. Ueq is defined as one third of the trace of the orthogonalized Uij tensor.

Atom	x	y	z	Ueq
C1	717(2)	5110(2)	8695(2)	19(1)
C2	369(2)	5852(2)	8101(2)	19(1)
C3	724(2)	6626(2)	8665(2)	21(1)
C4	370(2)	7339(2)	8094(2)	23(1)
C5	253(2)	1359(2)	8110(2)	25(1)
C6	519(2)	2075(2)	8697(2)	22(1)
C7	291(2)	2850(2)	8118(2)	19(1)
C8	625(2)	3586(2)	8717(2)	19(1)
C9	350(2)	4351(1)	8124(2)	18(1)
C10	1533(2)	5198(1)	9927(2)	22(1)

C11	1445(2)	5303(2)	10813(2)	26(1)
C12	2205(2)	5461(2)	11924(2)	34(1)
C13	3049(2)	5526(2)	12151(2)	36(1)
C14	3148(2)	5440(2)	11277(3)	35(1)
C15	2389(2)	5276(2)	10169(2)	28(1)
C16	1259(2)	3503(1)	9996(2)	19(1)
C17	915(2)	3452(2)	10632(2)	23(1)
C18	1489(2)	3301(2)	11805(2)	25(1)
C19	2409(2)	3190(2)	12343(2)	23(1)
C20	2762(2)	3223(2)	11720(2)	25(1)
C21	2187(2)	3378(2)	10552(2)	23(1)
C22	3871(2)	5716(2)	13352(3)	49(1)
F1	3751(3)	5554(3)	14138(2)	154(2)
F2	4054(2)	6484(2)	13524(2)	93(1)
F3	4573(3)	5363(3)	13628(3)	226(4)
C23	3039(2)	3026(2)	13604(2)	32(1)
F4	3450(2)	3699(2)	14212(2)	75(1)
F5	3706(1)	2513(2)	13887(2)	53(1)
F6	2626(1)	2710(2)	14023(2)	66(1)

Table A0.78. Bond lengths (Å) and angles (°) for **3.1j**.

Atoms	Length	Atoms	Angle	Atoms	Angle
C(1)-C(2)	1.404(3)	C(2)-C(1)-C(9)	121.1(2)	C(18)-C(19)-C(23)	120.5(2)
C(1)-C(9)	1.423(3)	C(2)-C(1)-C(10)	114.3(2)	C(20)-C(19)-C(23)	119.0(2)
C(1)-C(10)	1.506(3)	C(9)-C(1)-C(10)	124.4(2)	C(21)-C(20)-C(19)	119.6(2)
C(2)-C(2)#1	1.436(4)	C(1)-C(2)-C(2)#1	119.98(13)	C(20)-C(21)-C(16)	120.7(2)
C(2)-C(3)	1.439(3)	C(1)-C(2)-C(3)	122.0(2)	F(3)-C(22)-F(2)	107.1(5)
C(3)-C(4)	1.354(3)	C(2)#1-C(2)-C(3)	118.03(13)	F(3)-C(22)-F(1)	107.5(4)
C(4)-C(4)#1	1.423(5)	C(4)-C(3)-C(2)	121.7(2)	F(2)-C(22)-F(1)	100.9(4)
C(5)-C(6)	1.359(4)	C(3)-C(4)-C(4)#1	120.26(15)	F(3)-C(22)-C(13)	114.0(3)
C(5)-C(5)#1	1.426(5)	C(6)-C(5)-C(5)#1	120.19(15)	F(2)-C(22)-C(13)	113.0(3)
C(6)-C(7)	1.441(3)	C(5)-C(6)-C(7)	121.7(2)	F(1)-C(22)-C(13)	113.3(3)
C(7)-C(8)	1.397(3)	C(8)-C(7)-C(6)	122.1(2)	F(6)-C(23)-F(4)	105.9(3)
C(7)-C(7)#1	1.441(5)	C(8)-C(7)-C(7)#1	119.93(13)	F(6)-C(23)-F(5)	106.2(2)
C(8)-C(9)	1.431(3)	C(6)-C(7)-C(7)#1	117.91(14)	F(4)-C(23)-F(5)	105.5(3)
C(8)-C(16)	1.497(3)	C(7)-C(8)-C(9)	121.1(2)	F(6)-C(23)-C(19)	113.3(2)
C(9)-C(9)#1	1.468(4)	C(7)-C(8)-C(16)	114.9(2)	F(4)-C(23)-C(19)	112.5(2)
C(10)-C(15)	1.391(4)	C(9)-C(8)-C(16)	124.0(2)	F(5)-C(23)-C(19)	112.8(2)

C(10)-C(11)	1.395(4)	C(1)-C(9)-C(8)	122.8(2)
C(11)-C(12)	1.389(4)	C(1)-C(9)-C(9)#1	118.70(13)
C(12)-C(13)	1.378(5)	C(8)-C(9)-C(9)#1	118.48(13)
C(13)-C(14)	1.388(5)	C(15)-C(10)-C(11)	119.0(2)
C(13)-C(22)	1.509(4)	C(15)-C(10)-C(1)	118.7(2)
C(14)-C(15)	1.388(4)	C(11)-C(10)-C(1)	121.9(2)
C(16)-C(17)	1.393(3)	C(12)-C(11)-C(10)	120.4(3)
C(16)-C(21)	1.395(3)	C(13)-C(12)-C(11)	119.8(3)
C(17)-C(18)	1.389(3)	C(12)-C(13)-C(14)	120.6(3)
C(18)-C(19)	1.383(4)	C(12)-C(13)-C(22)	119.8(3)
C(19)-C(20)	1.388(4)	C(14)-C(13)-C(22)	119.5(3)
C(19)-C(23)	1.495(3)	C(13)-C(14)-C(15)	119.5(3)
C(20)-C(21)	1.385(3)	C(14)-C(15)-C(10)	120.6(3)
C(22)-F(3)	1.236(5)	C(17)-C(16)-C(21)	118.8(2)
C(22)-F(2)	1.288(4)	C(17)-C(16)-C(8)	120.2(2)
C(22)-F(1)	1.308(5)	C(21)-C(16)-C(8)	120.6(2)
C(23)-F(6)	1.322(3)	C(18)-C(17)-C(16)	120.7(2)
C(23)-F(4)	1.330(4)	C(19)-C(18)-C(17)	119.6(2)
C(23)-F(5)	1.331(3)	C(18)-C(19)-C(20)	120.5(2)

Symmetry transformations used to generate equivalent atoms: #1 -x,y,-z+3/2

Table A0.79. Atomic coordinates (x 10^4) and equivalent isotropic displacement parameters ($Å^2$ x 10^3) for **3.1j.** Ueq is defined as one third of the trace of the orthogonalized Uij tensor.

Atom	U11	U22	U33	U23	U13	U12
C1	19(1)	23(1)	14(1)	0(1)	9(1)	1(1)
C2	19(1)	21(1)	16(1)	0(1)	11(1)	0(1)
C3	22(1)	23(1)	17(1)	-3(1)	11(1)	-1(1)
C4	27(1)	21(1)	23(1)	-4(1)	16(1)	-2(1)
C5	25(1)	21(1)	30(1)	5(1)	17(1)	2(1)
C6	20(1)	24(1)	21(1)	3(1)	11(1)	2(1)
C7	19(1)	21(1)	19(1)	1(1)	12(1)	1(1)
C8	18(1)	22(1)	16(1)	1(1)	10(1)	2(1)
C9	19(1)	21(1)	16(1)	0(1)	10(1)	1(1)
C10	23(1)	17(1)	16(1)	1(1)	7(1)	2(1)
C11	31(1)	25(1)	17(1)	0(1)	11(1)	2(1)
C12	43(2)	28(1)	16(1)	0(1)	10(1)	2(1)
C13	36(2)	20(1)	21(1)	0(1)	1(1)	1(1)
C14	23(1)	26(1)	34(2)	-1(1)	5(1)	-1(1)

C15	25(1)	25(1)	25(1)	-2(1)	10(1)	-2(1)
C16	22(1)	18(1)	17(1)	2(1)	11(1)	1(1)
C17	20(1)	26(1)	20(1)	5(1)	11(1)	3(1)
C18	26(1)	30(1)	22(1)	4(1)	16(1)	2(1)
C19	25(1)	24(1)	17(1)	4(1)	11(1)	2(1)
C20	19(1)	32(1)	21(1)	4(1)	10(1)	3(1)
C21	23(1)	27(1)	19(1)	4(1)	13(1)	3(1)
C22	46(2)	33(2)	24(2)	0(1)	-2(1)	3(1)
F1	135(3)	218(5)	22(1)	3(2)	0(2)	-109(3)
F2	90(2)	58(2)	45(1)	-13(1)	-6(1)	-23(1)
F3	93(3)	280(6)	84(2)	-123(3)	-67(2)	129(3)
C23	30(1)	42(2)	21(1)	8(1)	14(1)	8(1)
F4	95(2)	61(2)	22(1)	-6(1)	9(1)	-3(1)
F5	42(1)	83(2)	29(1)	26(1)	18(1)	34(1)
F6	40(1)	127(2)	35(1)	44(1)	24(1)	21(1)

Table A0.80. Hydrogen coordinates (x 10^4) and isotropic displacement parameters (Å^2 x 10^3) for **3.1j**.

Atom	x	y	z	U(eq)
H3A	1219	6637	9457	25
H4A	618	7841	8489	28
H5A	403	857	8512	30
H6A	865	2064	9511	27
H11A	862	5266	10654	32
H12A	2142	5524	12526	41
H14A	3731	5493	11436	41
H15A	2455	5217	9569	33
H17A	281	3520	10260	27
H18A	1250	3275	12235	29
H20A	3394	3141	12093	30
H21A	2428	3398	10124	27

Table A0.81. Torsion angles (°) for **3.1j**.

Atoms	Angle	Atoms	Angle
C9-C1-C2-C2#1	-0.1(4)	C12-C13-C14-C15	-0.9(4)
C10-C1-C2-C2#1	175.7(3)	C22-C13-C14-C15	-179.1(3)
C9-C1-C2-C3	179.2(2)	C13-C14-C15-C10	0.0(4)
C10-C1-C2-C3	-4.9(3)	C11-C10-C15-C14	1.3(4)
C1-C2-C3-C4	-178.3(2)	C1-C10-C15-C14	173.5(2)
C2#1-C2-C3-C4	1.0(4)	C7-C8-C16-C17	-85.9(3)

C2-C3-C4-C4#1	-0.1(4)	C9-C8-C16-C17	92.7(3)
C5#1-C5-C6-C7	1.2(4)	C7-C8-C16-C21	86.2(3)
C5-C6-C7-C8	-174.5(2)	C9-C8-C16-C21	-95.2(3)
C5-C6-C7-C7#1	4.5(4)	C21-C16-C17-C18	1.9(4)
C6-C7-C8-C9	-176.6(2)	C8-C16-C17-C18	174.1(2)
C7#1-C7-C8-C9	4.3(4)	C16-C17-C18-C19	-1.0(4)
C6-C7-C8-C16	2.0(3)	C17-C18-C19-C20	-0.3(4)
C7#1-C7-C8-C16	-177.0(3)	C17-C18-C19-C23	-179.9(2)
C2-C1-C9-C8	-173.9(2)	C18-C19-C20-C21	0.6(4)
C10-C1-C9-C8	10.7(4)	C23-C19-C20-C21	-179.7(3)
C2-C1-C9-C9#1	5.5(4)	C19-C20-C21-C16	0.3(4)
C10-C1-C9-C9#1	-170.0(3)	C17-C16-C21-C20	-1.5(4)
C7-C8-C9-C1	-175.8(2)	C8-C16-C21-C20	-173.8(2)
C16-C8-C9-C1	5.7(4)	C12-C13-C22-F3	143.6(5)
C7-C8-C9-C9#1	4.8(4)	C14-C13-C22-F3	-38.2(6)
C16-C8-C9-C9#1	-173.7(2)	C12-C13-C22-F2	-93.8(4)
C2-C1-C10-C15	-83.5(3)	C14-C13-C22-F2	84.5(4)
C9-C1-C10-C15	92.2(3)	C12-C13-C22-F1	20.2(5)
C2-C1-C10-C11	88.5(3)	C14-C13-C22-F1	-161.6(4)
C9-C1-C10-C11	-95.8(3)	C18-C19-C23-F6	23.7(4)
C15-C10-C11-C12	-1.8(4)	C20-C19-C23-F6	-156.0(3)
C1-C10-C11-C12	-173.8(2)	C18-C19-C23-F4	-96.4(3)
C10-C11-C12-C13	1.0(4)	C20-C19-C23-F4	83.9(3)
C11-C12-C13-C14	0.4(4)	C18-C19-C23-F5	144.4(3)
C11-C12-C13-C22	178.6(3)	C20-C19-C23-F5	-35.3(4)

Symmetry transformations used to generate equivalent atoms: #1 -x,y,-z+3/2

Crystal Structure Report for **3.1h** (crystal grown by vapor diffusion; project code: 11199)

Data collection: A crystal (approximate dimensions 0.15 x 0.14 x 0.05 mm^3) was placed onto the tip of a 0.1 mm diameter glass capillary and mounted on a Bruker SMART Platform CCD diffractometer for a data collection at 173(2) K.[1] A preliminary set of cell constants was calculated from reflections harvested from three sets of 20 frames. These initial sets of frames were oriented such that orthogonal wedges of reciprocal space were surveyed. This produced initial orientation matrices determined from 200 reflections. The data collection was carried out using MoKα radiation (graphite monochromator) with a frame time of 45 seconds and a detector distance of 4.8 cm. A randomly oriented region of reciprocal space was surveyed to the extent of one sphere and to a resolution of 0.80 Å. Four major sections of frames were collected with 0.30º steps in ω at four different ϕ settings and a detector position of -28º in 2θ. The intensity data were corrected for absorption and decay (SADABS).[2] Final cell constants were calculated from the xyz centroids of 2998 strong reflections from the actual data collection after integration (SAINT).[3] Please refer to Table 1 for additional crystal and refinement information.

Structure solution and refinement: The structure was solved using SHELXS-97[4] and refined using SHELXL-97.[4] The

space group Cmca was determined based on systematic absences and intensity statistics. A direct-methods solution was calculated which provided most non-hydrogen atoms from the E-map. Full-matrix least squares / difference Fourier cycles were performed which located the remaining non-hydrogen atoms. All non-hydrogen atoms were refined with anisotropic displacement parameters. All hydrogen atoms were placed in ideal positions and refined as riding atoms with relative isotropic displacement parameters. The final full matrix least squares refinement converged to $R1 = 0.0527$ and $wR2 = 0.1560$ (F^2, all data).

Structure description: In this setting, the structure is centered about an inversion center, which suggests a higher level of symmetry in the molecule than actually exists. This was modeled by the fluorine and methyl hydrogen atoms being at half occupancy.

Table A0.82. Atomic coordinates (x 10^4) and equivalent isotropic displacement parameters (Å^2 x 10^3) for **3.1h**. Ueq is defined as one third of the trace of the orthogonalized Uij tensor.

Atom	x	y	z	Ueq
C1	4786(1)	0	0	31(1)
C2	4585(1)	1469(2)	476(1)	31(1)
C3	4790(1)	2978(2)	860(1)	32(1)
C4	4595(1)	4518(3)	1300(2)	37(1)
C5	4793(1)	5958(3)	1694(2)	41(1)
C6	4156(1)	1410(3)	698(2)	36(1)
C7	4035(1)	478(3)	1511(2)	46(1)
C8	3647(1)	469(4)	1782(2)	60(1)
C9	3372(1)	1415(4)	1246(2)	63(1)
C10	3491(1)	2370(3)	443(2)	58(1)
C11	3879(1)	2376(3)	177(2)	45(1)
C12	2950(1)	1381(5)	1522(3)	104(1)
F1	2772(1)	59(9)	1128(5)	252(5)
F2	2774(1)	2788(7)	1250(5)	234(5)
F3	2908(1)	1226(10)	2362(3)	204(4)

Table A0.83. Bond lengths (Å) and angles (°) for **3.1h**.

Atoms	Length	Atoms	Angle	Atoms	Angle
C(1)-C(2)#1	1.424(2)	C(2)#1-C(1)-C(2)	122.2(2)	C(10)-C(9)-C(12)	120.3(3)
C(1)-C(2)	1.424(2)	C(2)#1-C(1)-C(1)#2	118.91(12)	C(8)-C(9)-C(12)	120.6(3)
C(1)-C(1)#2	1.461(5)	C(2)-C(1)-C(1)#2	118.91(12)	C(11)-C(10)-C(9)	120.5(2)
C(2)-C(3)	1.396(3)	C(3)-C(2)-C(1)	120.70(17)	C(11)-C(10)-H(10A)	119.8
C(2)-C(6)	1.499(3)	C(3)-C(2)-C(6)	115.61(17)	C(9)-C(10)-H(10A)	119.8
C(3)-C(4)	1.429(3)	C(1)-C(2)-C(6)	123.33(17)	C(10)-C(11)-C(6)	120.9(2)
C(3)-C(3)#3	1.437(4)	C(2)-C(3)-C(4)	122.01(17)	C(10)-C(11)-H(11A)	119.5
C(4)-C(5)	1.352(3)	C(2)-C(3)-C(3)#3	120.13(11)	C(6)-C(11)-H(11A)	119.5
C(4)-H(4A)	0.95	C(4)-C(3)-C(3)#3	117.80(11)	C(9)-C(12)-H(12A)	109.5
C(5)-C(5)#3	1.413(4)	C(5)-C(4)-C(3)	122.08(19)	C(9)-C(12)-H(12B)	109.5

C(5)-H(5A)	0.95	C(5)-C(4)-H(4A)	119	H(12A)-C(12)-H(12B)	109.5
C(6)-C(11)	1.384(3)	C(3)-C(4)-H(4A)	119	C(9)-C(12)-H(12C)	109.5
C(6)-C(7)	1.387(3)	C(4)-C(5)-C(5)#3	120.10(12)	H(12A)-C(12)-H(12C)	109.5
C(7)-C(8)	1.380(3)	C(4)-C(5)-H(5A)	119.9	H(12B)-C(12)-H(12C)	109.5
C(7)-H(7A)	0.95	C(5)#3-C(5)-H(5A)	119.9		
C(8)-C(9)	1.382(4)	C(11)-C(6)-C(7)	118.11(19)		
C(8)-H(8A)	0.95	C(11)-C(6)-C(2)	123.11(19)		
C(9)-C(10)	1.380(4)	C(7)-C(6)-C(2)	118.54(18)		
C(9)-C(12)	1.495(3)	C(8)-C(7)-C(6)	121.1(2)		
C(10)-C(11)	1.379(3)	C(8)-C(7)-H(7A)	119.4		
C(10)-H(10A)	0.95	C(6)-C(7)-H(7A)	119.4		
C(11)-H(11A)	0.95	C(7)-C(8)-C(9)	120.2(3)		
C(12)-H(12A)	0.98	C(7)-C(8)-H(8A)	119.9		
C(12)-H(12B)	0.98	C(9)-C(8)-H(8A)	119.9		
C(12)-H(12C)	0.98	C(10)-C(9)-C(8)	119.2(2)		

Symmetry transformations used to generate equivalent atoms: #1 x,-y,-z #2 -x+1,-y,-z #3 -x+1,y,z

Table A0.84. Atomic coordinates (x 10^4) and equivalent isotropic displacement parameters (Å^2 x 10^3) for **3.1h.** Ueq is defined as one third of the trace of the orthogonalized Uij tensor.

	U11	U22	U33	U23	U13	U12
C1	29(1)	21(1)	42(2)	6(1)	0	0
C2	30(1)	22(1)	42(1)	5(1)	-1(1)	2(1)
C3	34(1)	22(1)	38(1)	7(1)	0(1)	2(1)
C4	40(1)	26(1)	45(1)	2(1)	1(1)	5(1)
C5	54(1)	25(1)	44(1)	-2(1)	1(1)	7(1)
C6	33(1)	22(1)	52(1)	0(1)	1(1)	2(1)
C7	40(1)	42(1)	56(2)	4(1)	3(1)	-1(1)
C8	49(1)	60(2)	69(2)	1(1)	17(1)	-7(1)
C9	36(1)	51(2)	103(2)	-10(2)	15(1)	1(1)
C10	35(1)	35(1)	105(2)	2(1)	-4(1)	6(1)
C11	36(1)	26(1)	74(2)	7(1)	-3(1)	2(1)
C12	45(2)	98(3)	168(4)	-4(3)	33(2)	-2(2)
F1	66(3)	261(8)	428(13)	-176(9)	95(5)	-80(5)
F2	70(3)	215(7)	418(12)	122(8)	108(5)	74(4)
F3	79(3)	342(10)	191(6)	39(7)	86(4)	23(5)

Table A0.85. Hydrogen coordinates (x 10^4) and isotropic displacement parameters (Å^2 x 10^3) for **3.1h**.

Atom	x	y	z	U(eq)
H4A	4317	4532	1316	45

H5A	4655	6971	1972	49
H7A	4222	-166	1888	55
H8A	3569	-189	2337	71
H10A	3304	3027	72	70
H11A	3957	3054	-373	54
H12A	2799	2152	1077	155
H12B	2920	1876	2168	155
H12C	2853	93	1501	155

Table A0.86. Torsion angles (°) for **3.1h**.

Atoms	Angle	Atoms	Angle
C2#1-C1-C2-C3	-174.0(2)	C3-C2-C6-C7	-89.8(2)
C1#2-C1-C2-C3	6.0(2)	C1-C2-C6-C7	83.3(2)
C2#1-C1-C2-C6	13.18(14)	C11-C6-C7-C8	1.7(3)
C1#2-C1-C2-C6	-166.82(14)	C2-C6-C7-C8	176.2(2)
C1-C2-C3-C4	176.80(16)	C6-C7-C8-C9	-0.7(4)
C6-C2-C3-C4	-9.9(3)	C7-C8-C9-C10	-0.2(4)
C1-C2-C3-C3#3	-6.0(2)	C7-C8-C9-C12	178.7(3)
C6-C2-C3-C3#3	167.28(11)	C8-C9-C10-C11	0.1(4)
C2-C3-C4-C5	178.2(2)	C12-C9-C10-C11	-178.8(3)
C3#3-C3-C4-C5	1.0(2)	C9-C10-C11-C6	0.9(4)
C3-C4-C5-C5#3	-1.0(3)	C7-C6-C11-C10	-1.8(3)
C3-C2-C6-C11	84.4(3)	C2-C6-C11-C10	-176.0(2)
C1-C2-C6-C11	-102.5(2)		

Symmetry transformations used to generate equivalent atoms: #1 x,-y,-z #2 -x+1,-y,-z #3 -x+1,y,z

A1.3. REFERENCES

(1) SMART V5.054, Bruker Analytical X-ray Systems, Madison, WI (2001).
(2) An empirical correction for absorption anisotropy, R. Blessing, *Acta Cryst.* **A51**, 33-38 (1995).
(3) SAINT+ V6.45, Bruker Analytical X-Ray Systems, Madison, WI (2003).
(4) SHELXTL V6.14, Bruker Analytical X-Ray Systems, Madison, WI (2000).
(5) Calculations performed using: Mercury Cambridge Structural Database 2.3, Cambridge Crystallographic Data Centre, Cambridge, UK (2009).

APPENDIX 2. NMR SPECTRA

A2.1. CHAPTER 2 SPECTRA

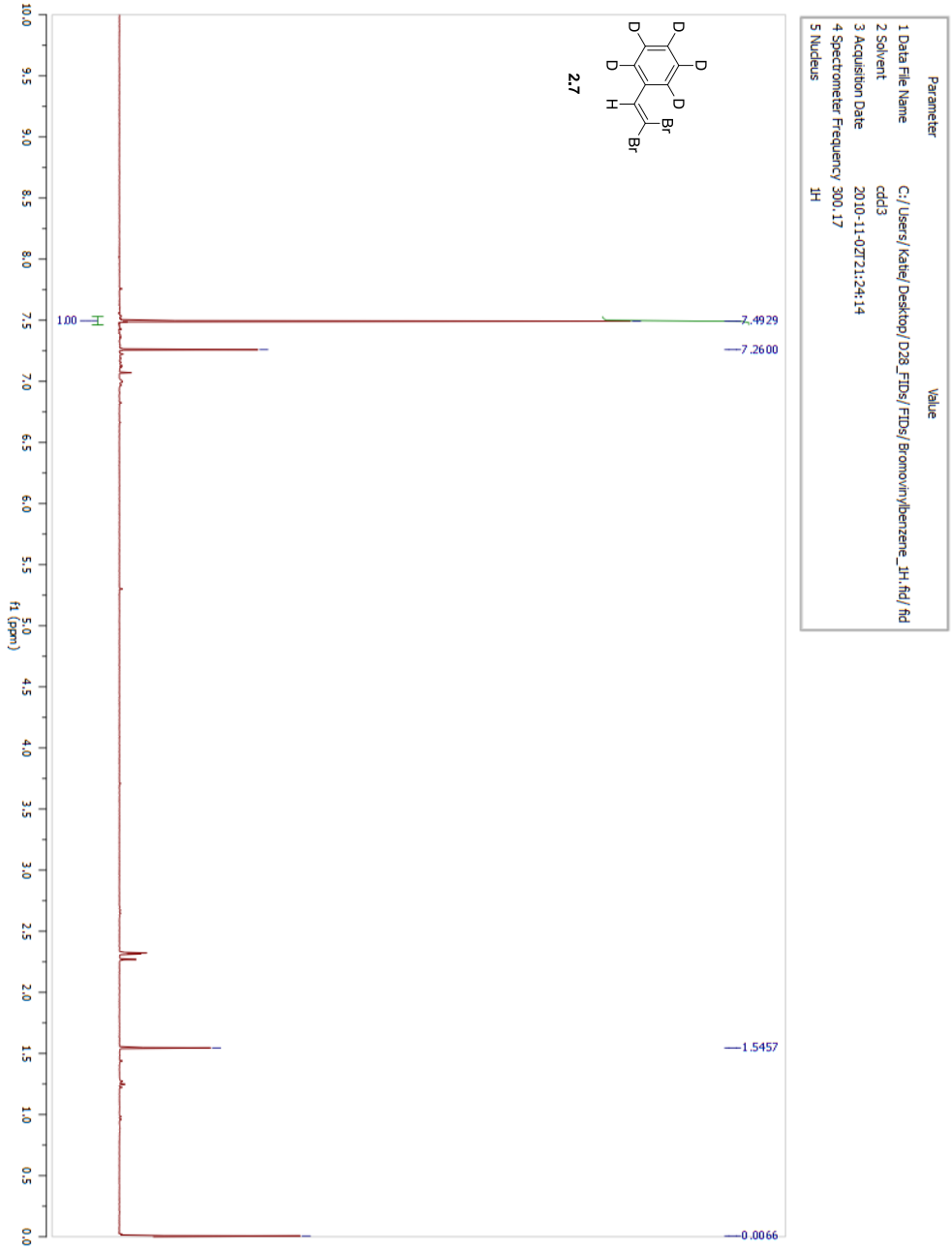

Parameter	Value
1 Data File Name	C:/ Users/ Katie/ Desktop/ D28_FIDs/ FIDs/ Bromovinylbenzene_2H.fid/ fid
2 Solvent	c6d6
3 Acquisition Date	2009-07-08T16:39:19
4 Spectrometer Frequency	46.08
5 Nucleus	2H

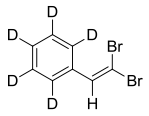

2.7

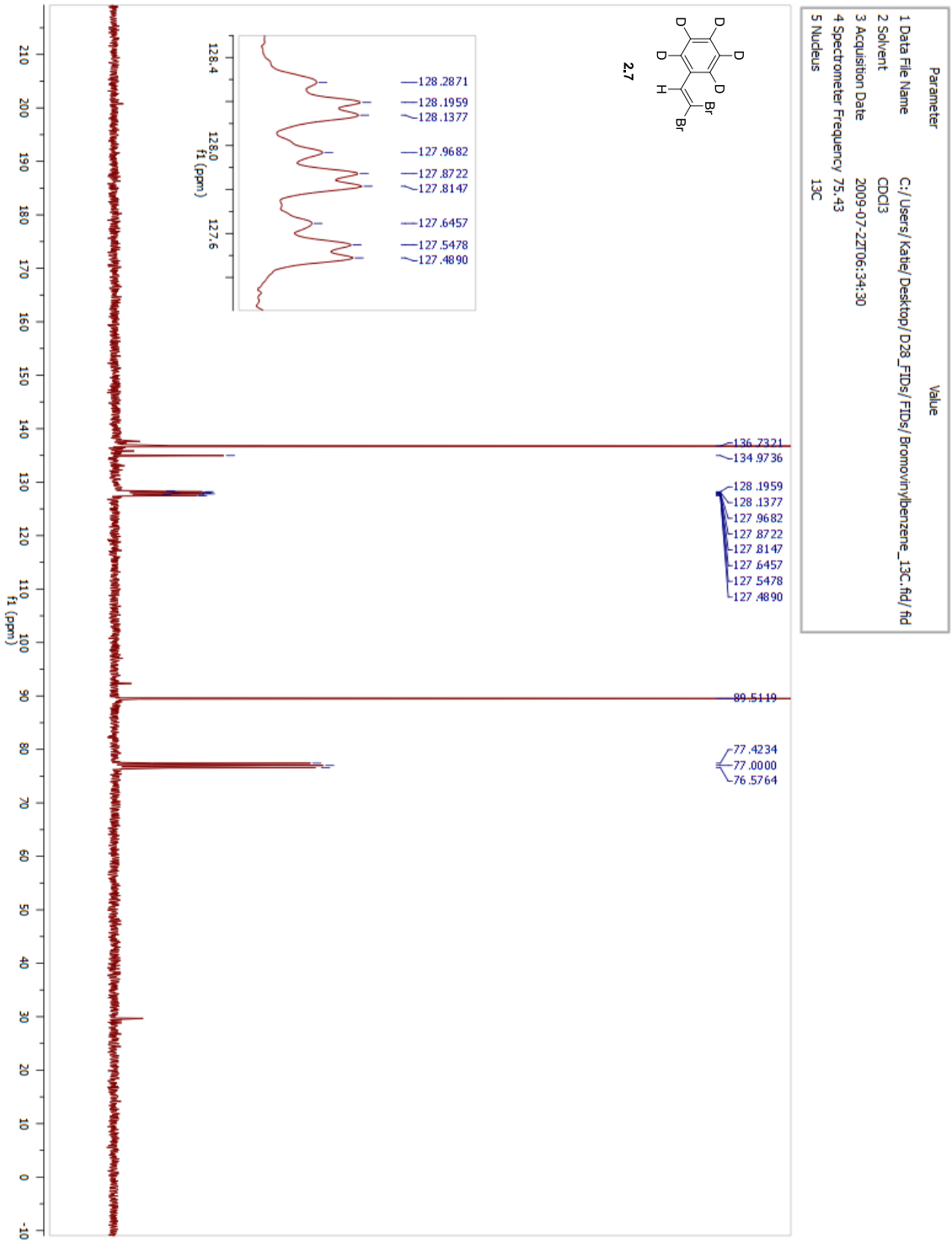
Parameter
Value
1 Data File Name
C:/Users/Katie/Desktop/D28_FIDs/FIDs/Bromovinylbenzene_13C.fid/fid
2 Solvent
CDCl3
3 Acquisition Date
2009-07-22T06:34:30
4 Spectrometer Frequency
75.43
5 Nucleus
13C
2.7
136.7321
134.9736
128.1959
128.1377
127.9682
127.8722
127.8147
127.6457
127.5478
127.4890
89.5119
77.4234
77.0000
76.5764
128.2871
128.1959
128.1377
127.9682
127.8722
127.8147
127.6457
127.5478
127.4890
f1 (ppm)

Parameter	Value
1 Data File Name	C:/ Users/ Katie/ Dropbox/ ChemResearch/ NMR data/ dRubrene/ Files_022613/ KAMi-73-2H.fid/ fid
2 Solvent	c6d6
3 Acquisition Date	2009-06-25T20:52:35
4 Spectrometer Frequency	46.08
5 Nucleus	2H

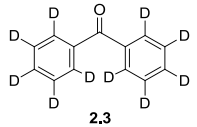

2.3

Parameter	Value
1 Data File Name	C:/ Users/ Katie/ Dropbox/ ChemResearch/ NMR data/ dRubrene/ Files_022613/ 090719v3_0603.fid/ fid
2 Solvent	CDCl3
3 Acquisition Date	2009-07-19T23:13:00
4 Spectrometer Frequency	75.43
5 Nucleus	13C

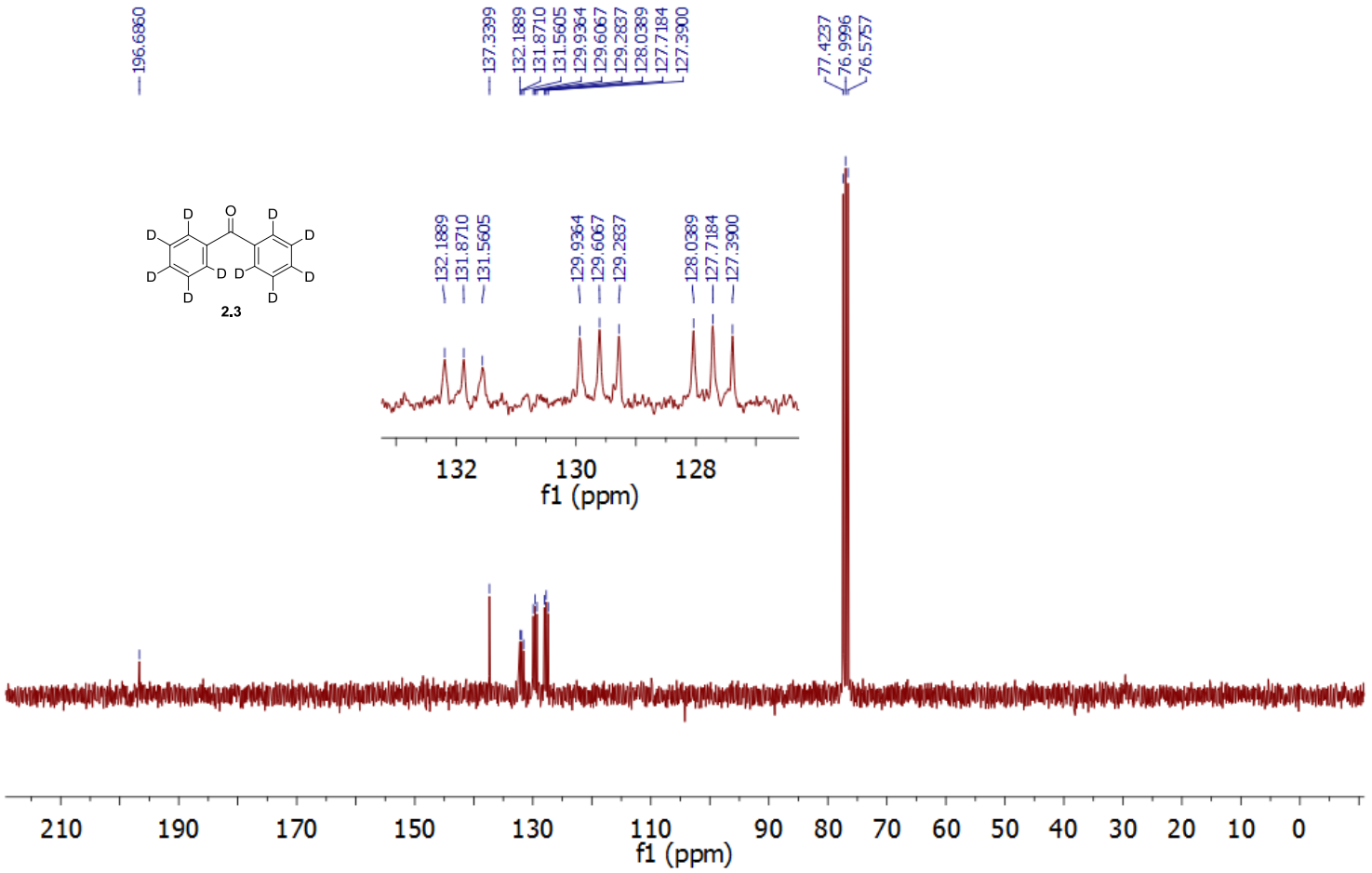

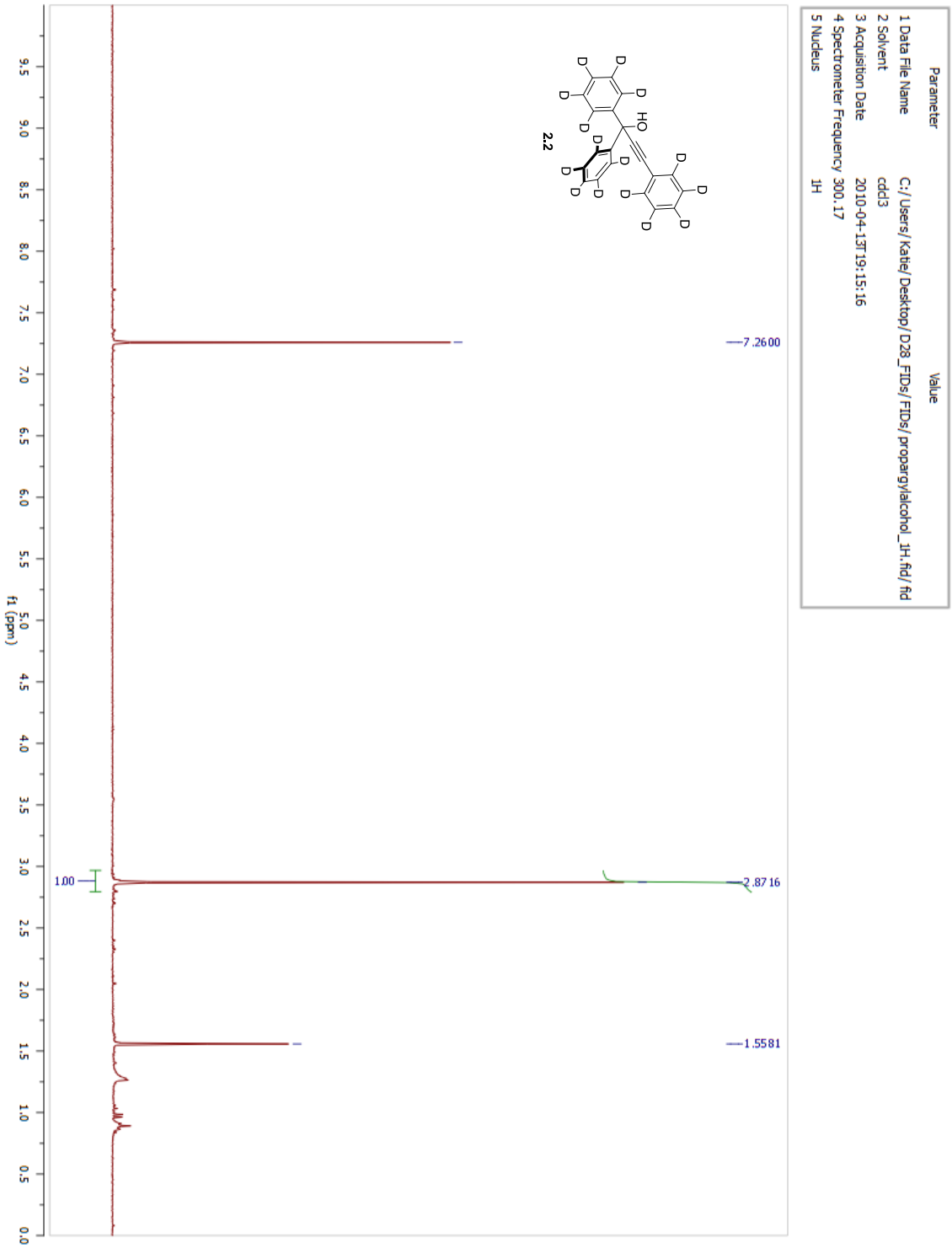
Parameter
Value
1 Data File Name
C:/Users/Katie/Desktop/D28_FIDs/FIDs/propargylalcohol_1H.fid/fid
2 Solvent
cdcl3
3 Acquisition Date
2010-04-13T19:15:16
4 Spectrometer Frequency
300.17
5 Nucleus
1H
2.2
HO
7.2600
2.8716
1.5581
1.00
f1 (ppm)

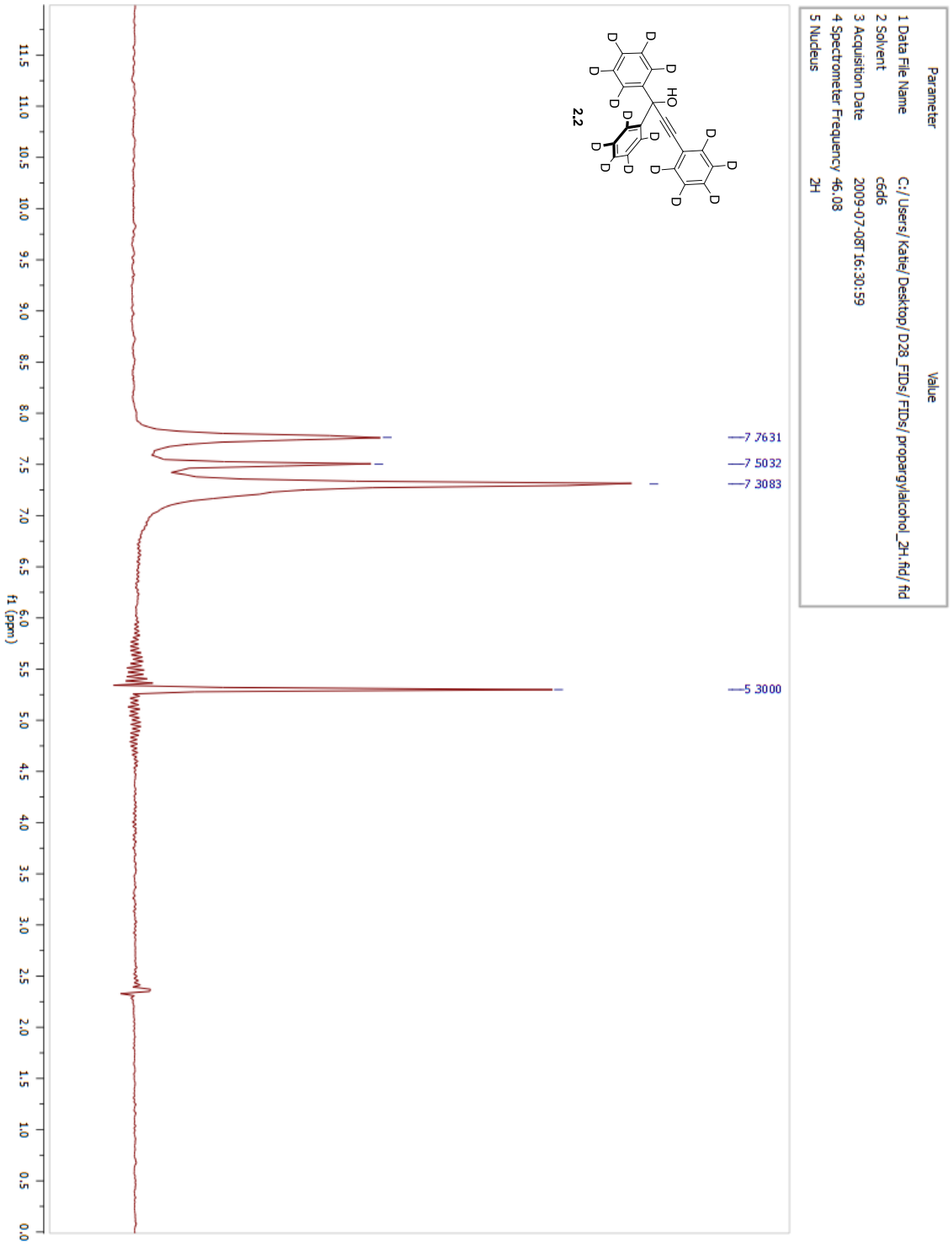
Parameter
Value
1 Data File Name
C:/Users/Katie/Desktop/D28_FIDs/FIDs/propargylalcohol_2H.fid/fid
2 Solvent
c6d6
3 Acquisition Date
2009-07-08T16:30:59
4 Spectrometer Frequency
46.08
5 Nucleus
2H
2.2
HO
7.7631
7.5032
7.3083
5.3000
f1 (ppm)

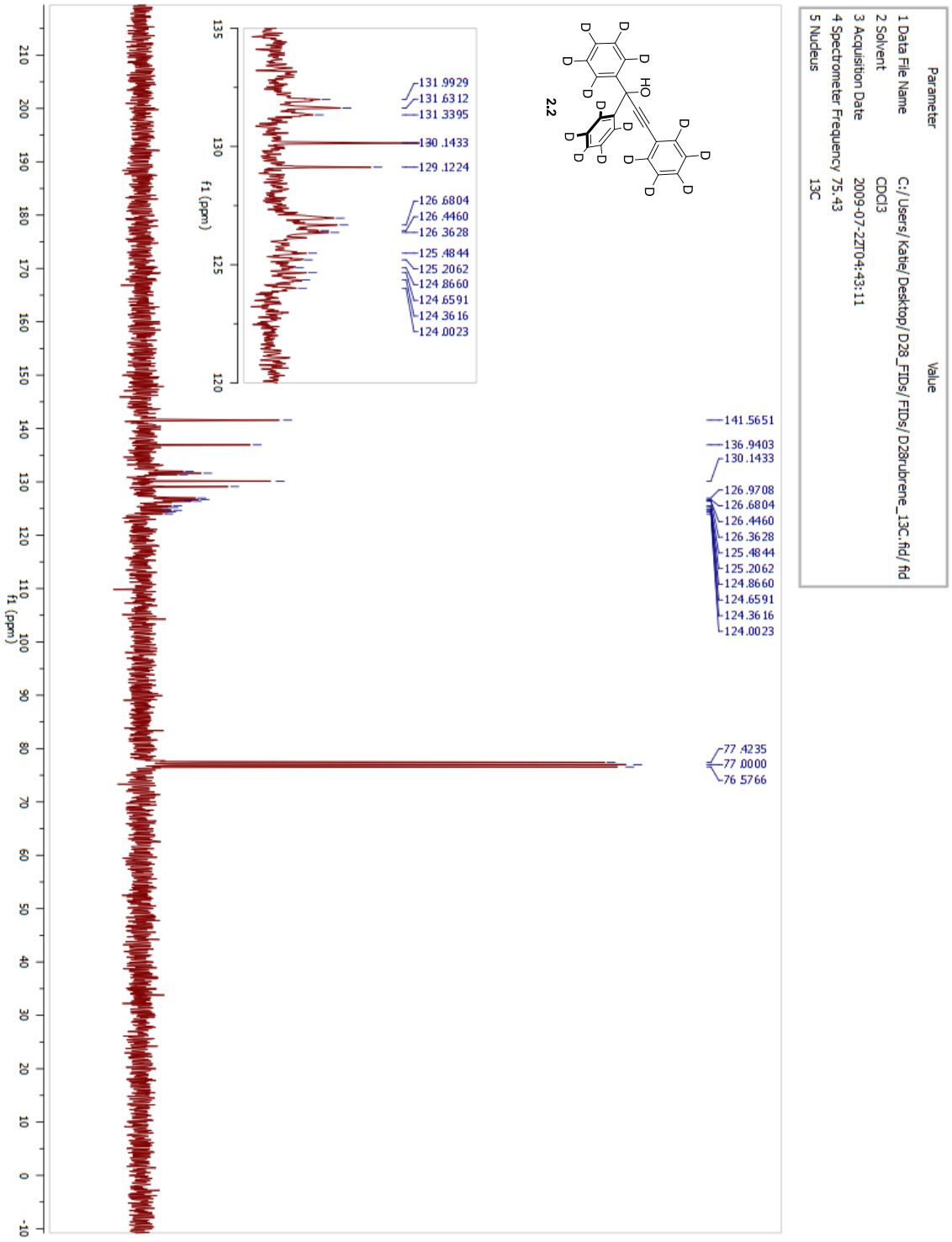
Parameter
Value
1 Data File Name
C:/Users/Katie/Desktop/D28_FIDs/FIDs/D28rubrene_13C.fid/fid
2 Solvent
CDCl3
3 Acquisition Date
2009-07-22T04:43:11
4 Spectrometer Frequency
75.43
5 Nucleus
13C
2.2
HO
D
141.5651
136.9403
130.1433
126.9708
126.6804
126.4460
126.3628
125.4844
125.2062
124.8660
124.6591
124.3616
124.0023
77.4235
77.0000
76.5766
131.9929
131.6312
131.3395
130.1433
129.1224
126.6804
126.4460
126.3628
125.4844
125.2062
124.8660
124.6591
124.3616
124.0023
f1 (ppm)

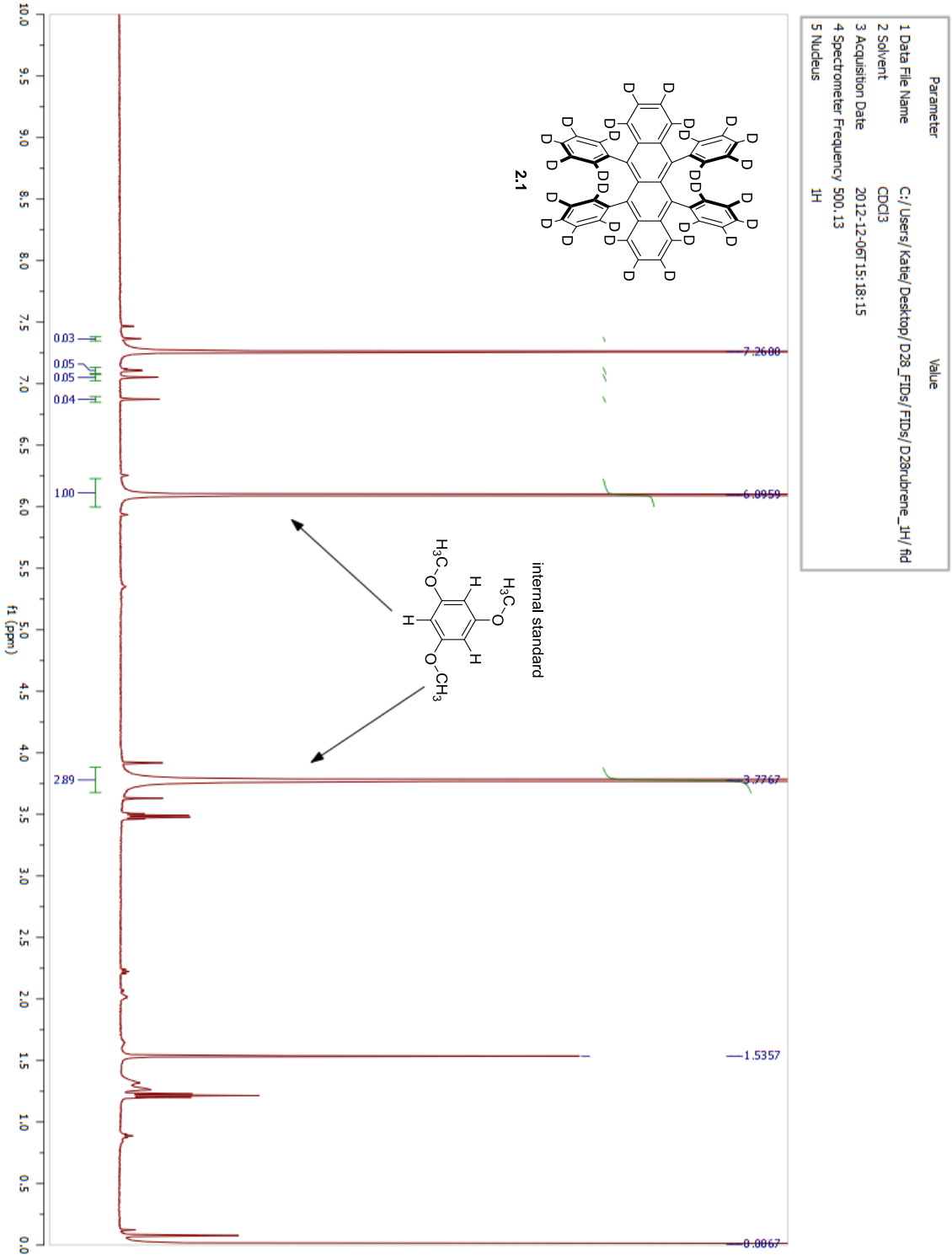
Parameter
Value
1 Data File Name
C:/Users/Katie/Desktop/D28_FIDs/FIDs/D28rubrene_1H/fid
2 Solvent
CDCl3
3 Acquisition Date
2012-12-06T15:18:15
4 Spectrometer Frequency
500.13
5 Nucleus
1H
2:1
internal standard
0.03
0.05
0.05
0.04
1.00
2.89
7.2600
6.0959
3.7767
1.5357
0.0067
f1 (ppm)

Parameter	Value
1 Data File Name	C:/ Users/ Katie/ Desktop/ D28_FIDs/ FIDs/ D28rubrene_2H.fid/ fid
2 Solvent	c6d6
3 Acquisition Date	2009-07-08T17:49:01
4 Spectrometer Frequency	46.08
5 Nucleus	2H

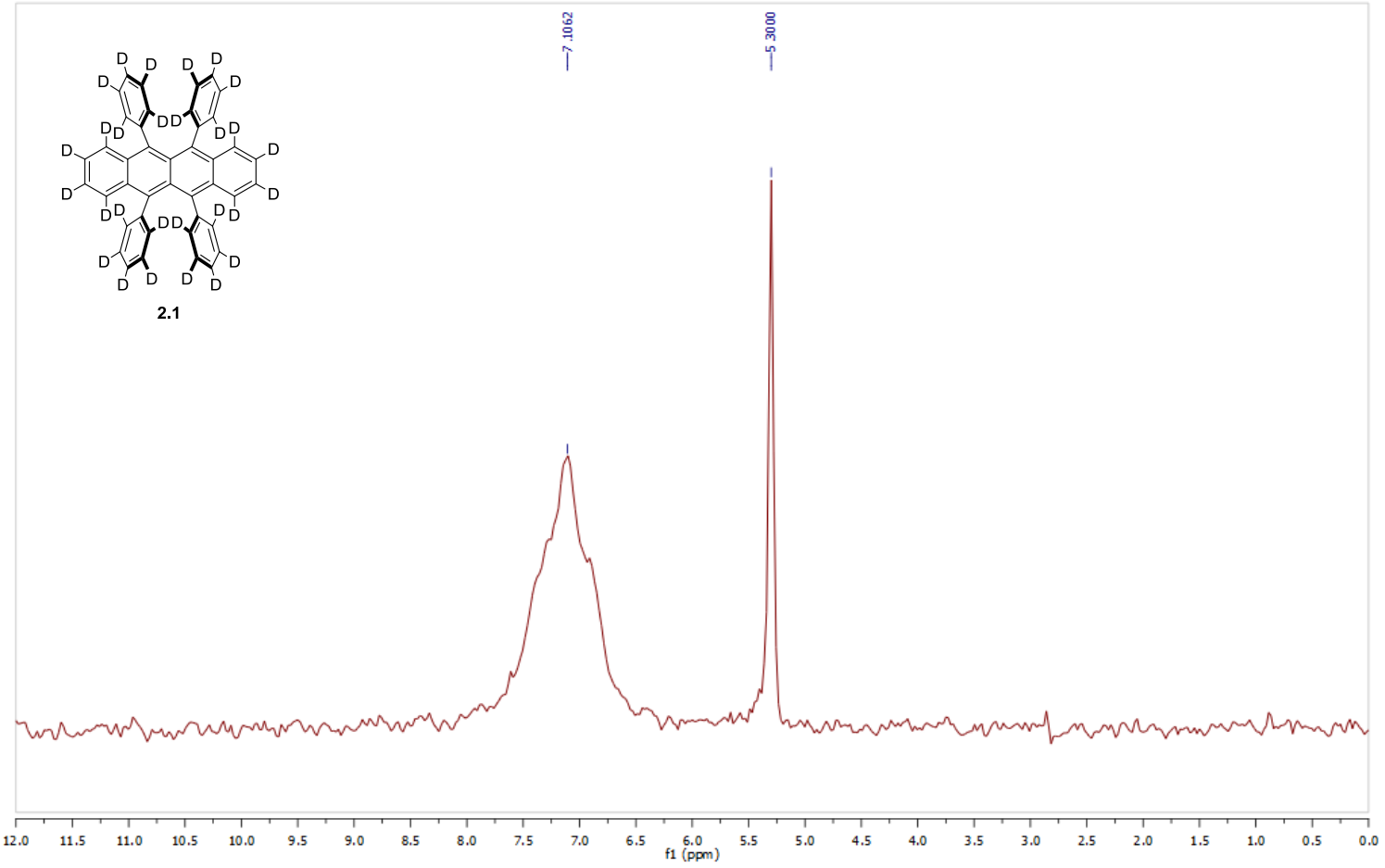

2.1

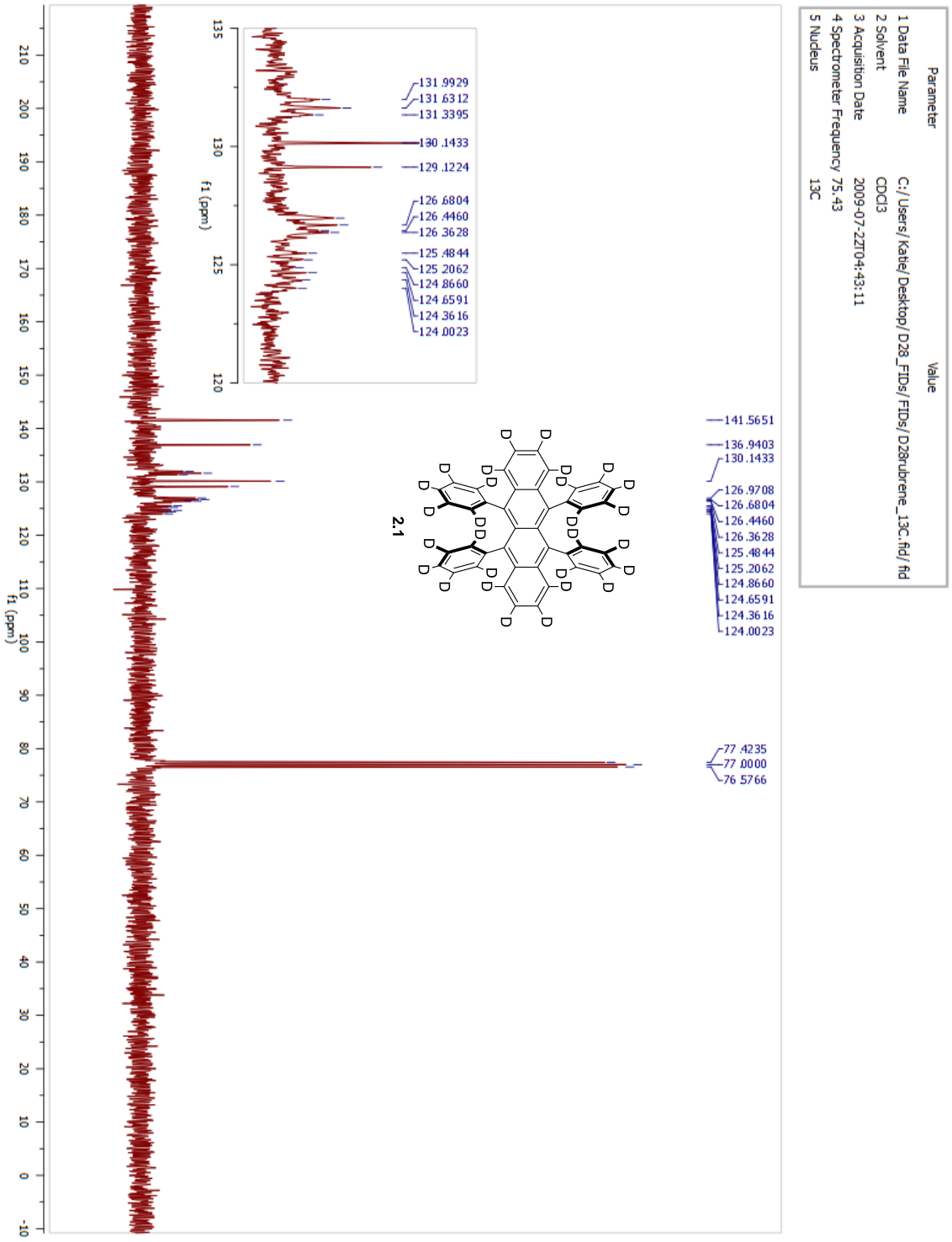
Parameter
Value
1 Data File Name
C:/Users/Katie/Desktop/D28_FIDs/FIDs/D28rubrene_13C.fid/fid
2 Solvent
CDCl3
3 Acquisition Date
2009-07-22T04:43:11
4 Spectrometer Frequency
75.43
5 Nucleus
13C
131.9929
131.6312
131.3395
130.1433
129.1224
126.6804
126.4460
126.3628
125.4844
125.2062
124.8660
124.6591
124.3616
124.0023
141.5651
136.9403
130.1433
126.9708
126.6804
126.4460
126.3628
125.4844
125.2062
124.8660
124.6591
124.3616
124.0023
77.4235
77.0000
76.5766
2.1
f1 (ppm)

A2.2. CHATPER 3 SPECTRA

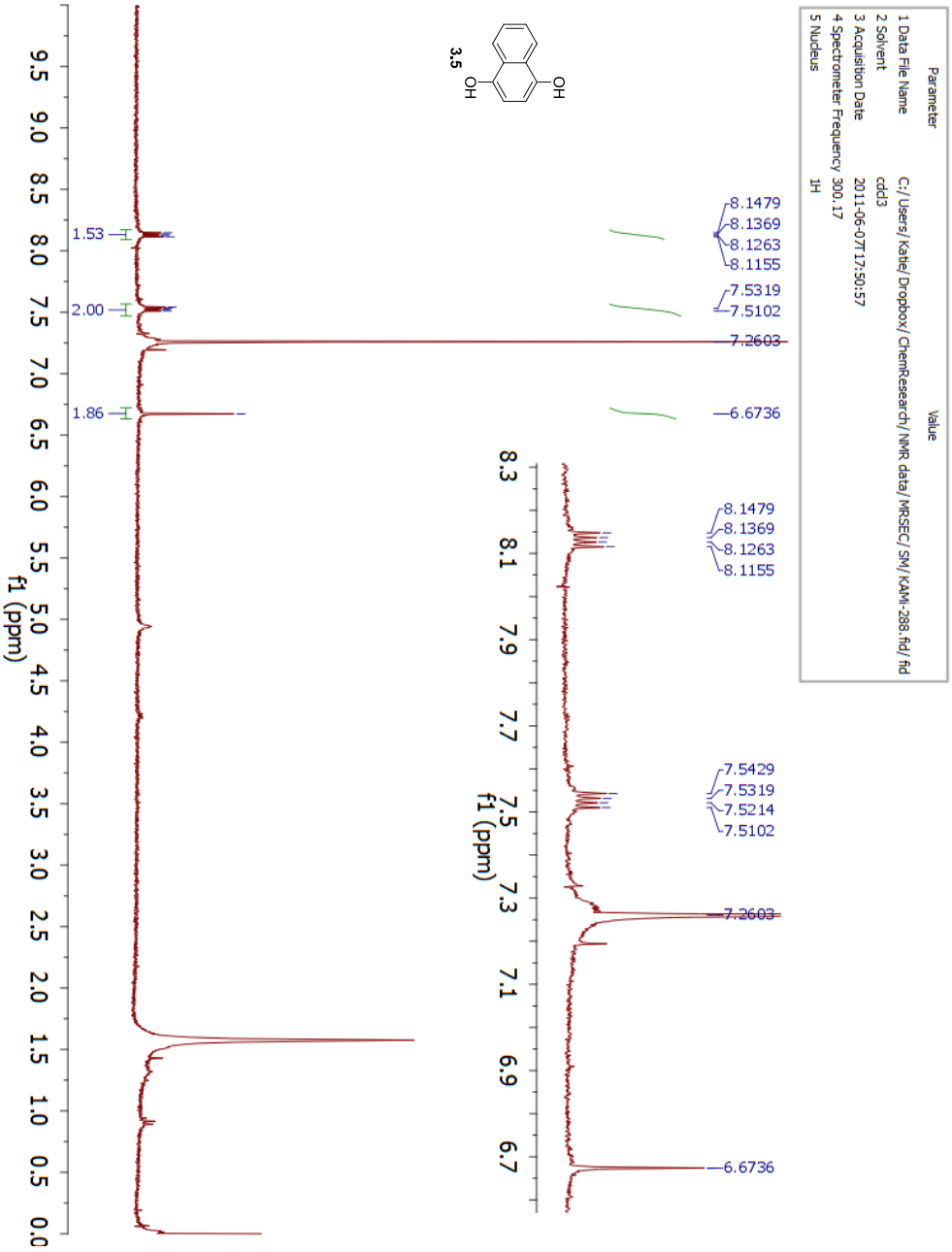

Parameter	Value
1 Data File Name	C:/ Users/ Katie/ Dropbox/ ChemResearch/ NMR data/ SynPrep/ KAMi-125.fid/ fid
2 Solvent	cdcl3
3 Acquisition Date	2010-04-26T23:16:46
4 Spectrometer Frequency	300.17
5 Nucleus	1H

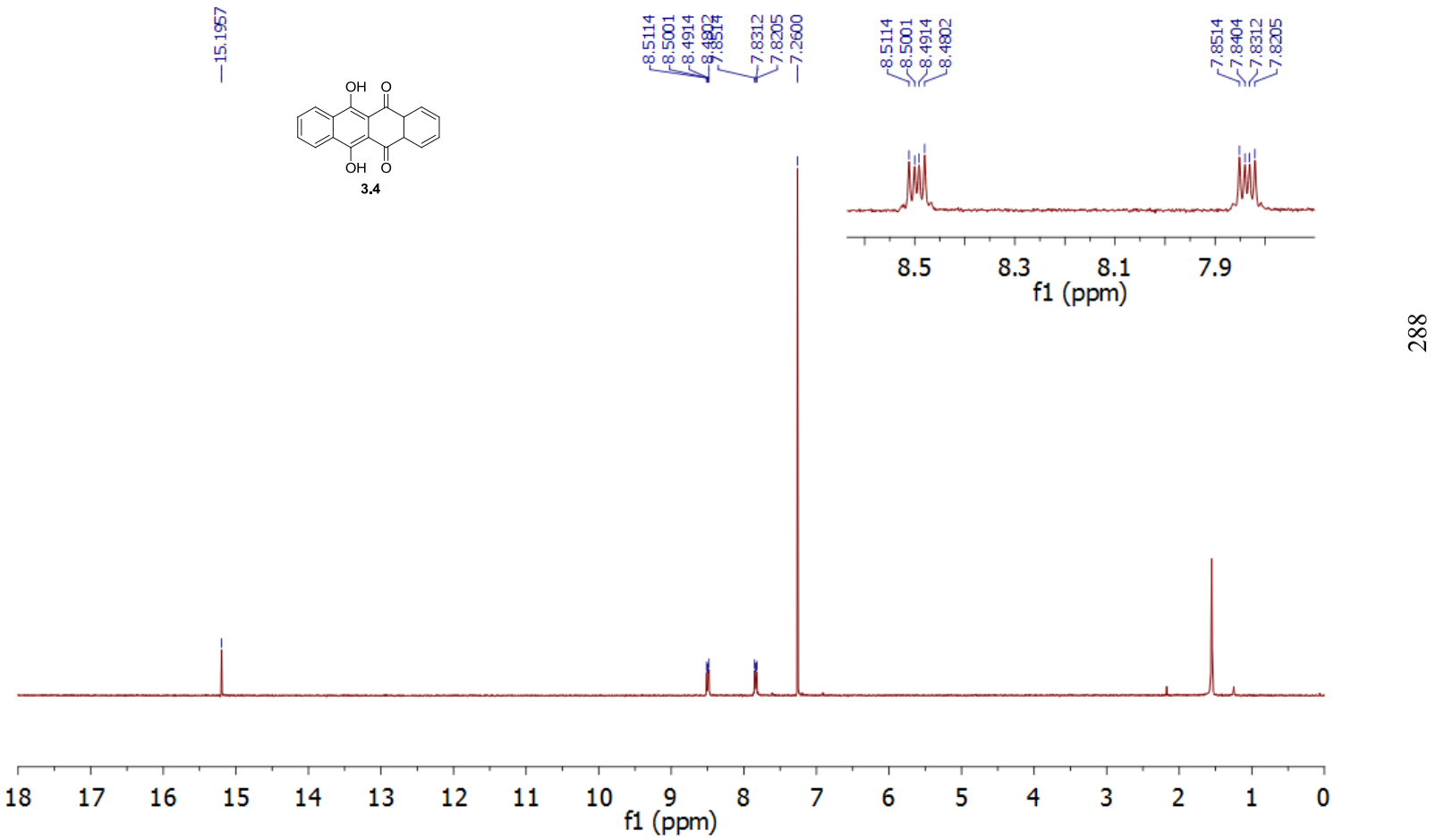

Parameter	Value
1 Data File Name	C:/ Users/ Katie/ Dropbox/ ChemResearch/ NMR data/ MRSEC/ SM/ KAMii-91/ 1/ fid
2 Solvent	CDCl3
3 Acquisition Date	2012-01-11T16:17:21
4 Spectrometer Frequency	500.13
5 Nucleus	1H

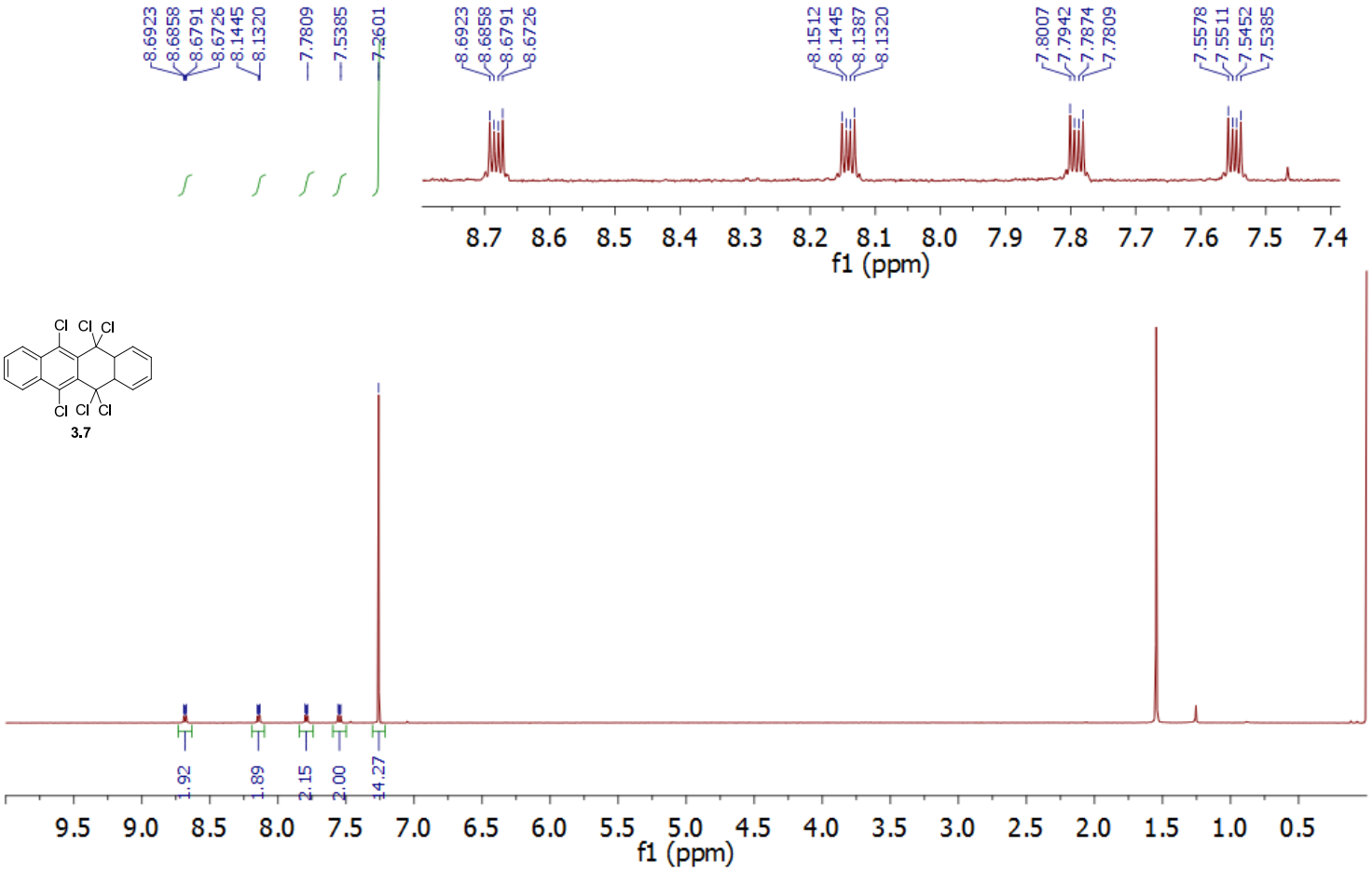

Parameter	Value
1 Data File Name	C:/ Users/ Katie/ Dropbox/ ChemResearch/ NMR data/ MRSEC/ SM/ KAMi-216-pure.fid/ fid
2 Solvent	cdcl3
3 Acquisition Date	2010-11-30T01:00:12
4 Spectrometer Frequency	299.83
5 Nucleus	1H

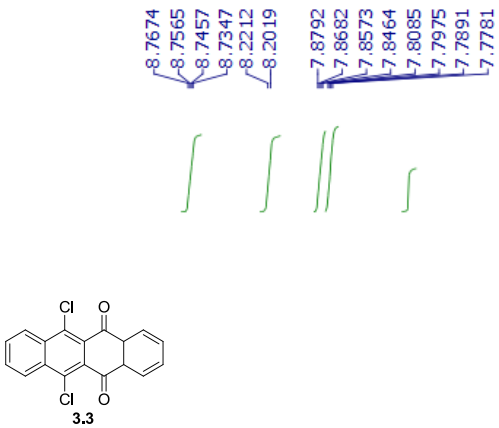

3.3

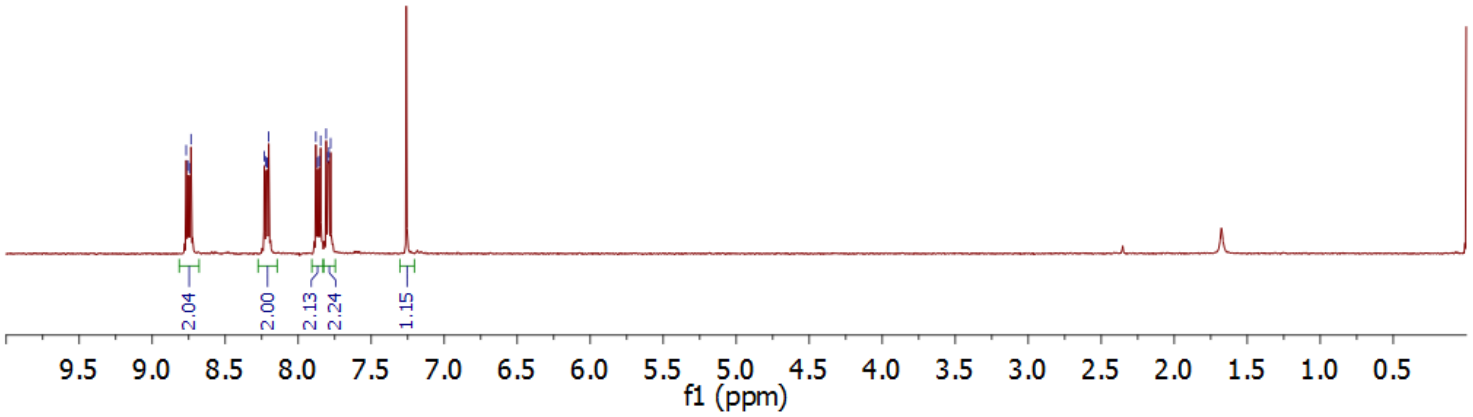

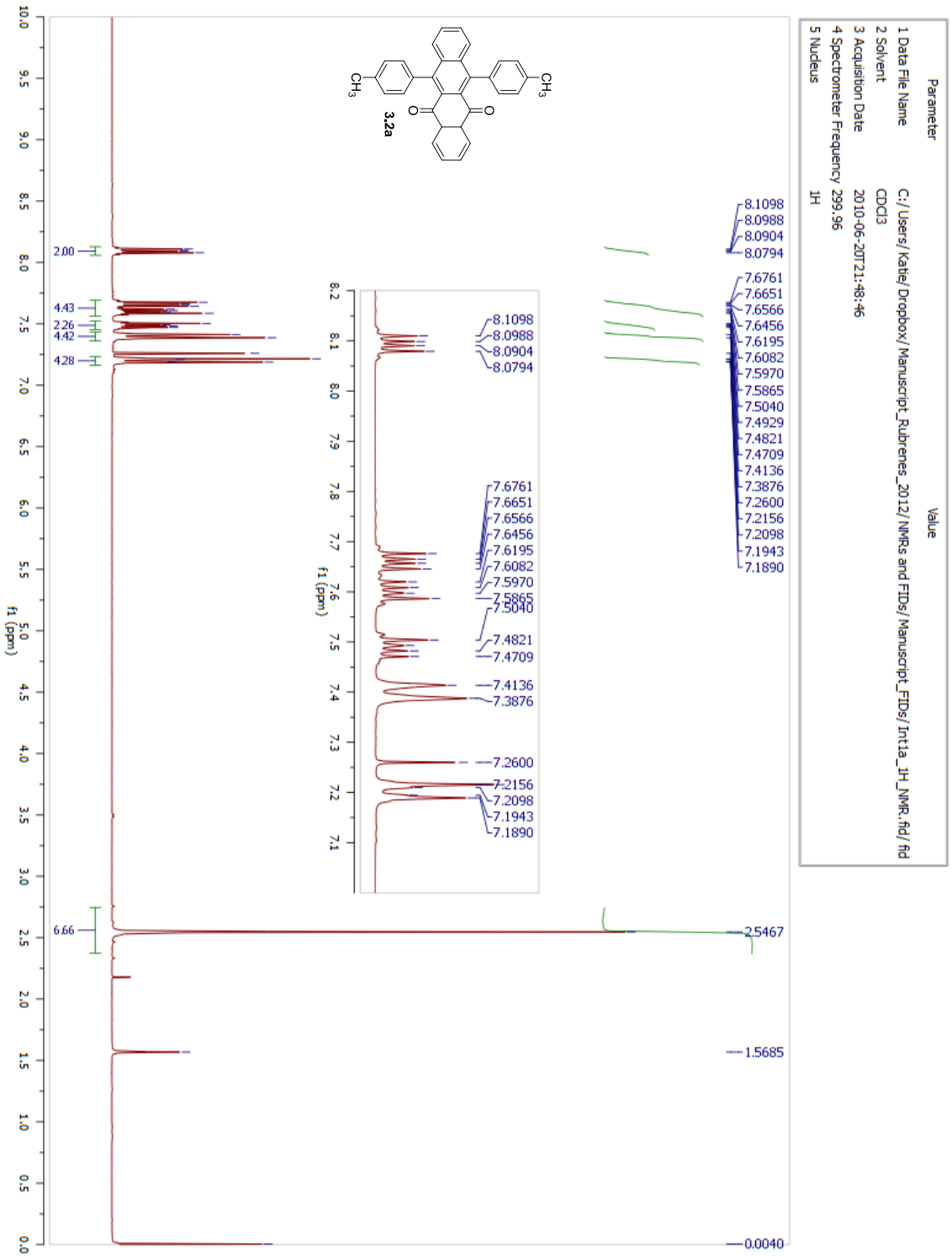
Parameter
Value
1 Data File Name
C:/Users/Katie/Dropbox/Manuscript_Rubrenes_2012/NMRs and FIDs/Manuscript_FIDs/Int1a_1H_NMR.fid/fid
2 Solvent
CDCl3
3 Acquisition Date
2010-06-20T21:48:46
4 Spectrometer Frequency
299.96
5 Nucleus
1H
3.2a
CH3
CH3
O
O
8.1098
8.0988
8.0904
8.0794
7.6761
7.6651
7.6566
7.6456
7.6195
7.6082
7.5970
7.5865
7.5040
7.4929
7.4821
7.4709
7.4136
7.3876
7.2600
7.2156
7.2098
7.1943
7.1890
2.5467
1.5685
0.0040
2.00
4.43
2.26
4.42
4.28
6.66
f1 (ppm)

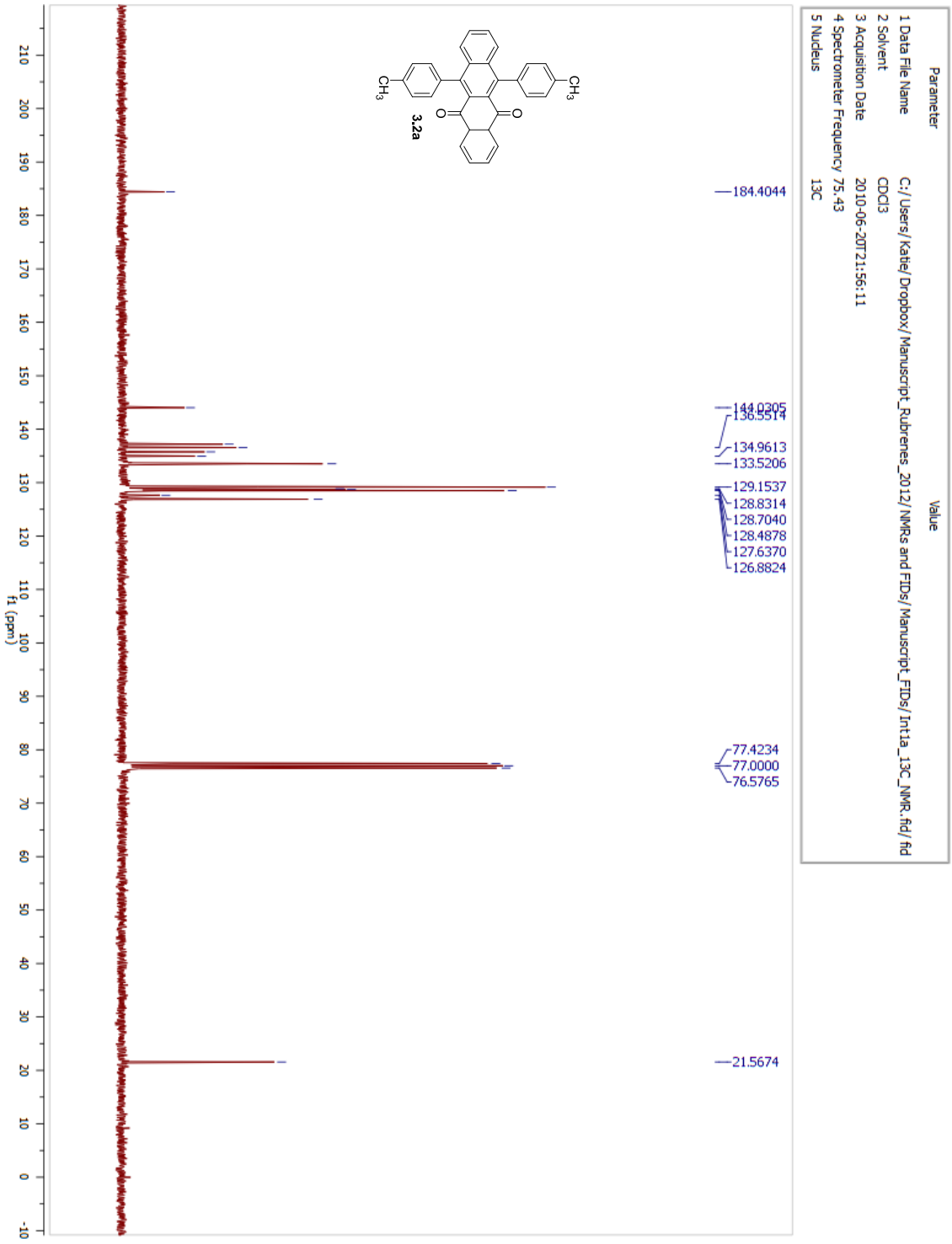
Parameter
Value
1 Data File Name
C:/Users/Katie/Dropbox/Manuscript_Rubrenes_2012/NMRs and FIDs/Manuscript_FIDs/Int1a_13C_NMR.fid/fid
2 Solvent
CDCl3
3 Acquisition Date
2010-06-20T21:56:11
4 Spectrometer Frequency
75.43
5 Nucleus
13C
3.2a
184.4044
144.0305
136.5514
134.9613
133.5206
129.1537
128.8314
128.7040
128.4878
127.6370
126.8824
77.4234
77.0000
76.5765
21.5674
f1 (ppm)

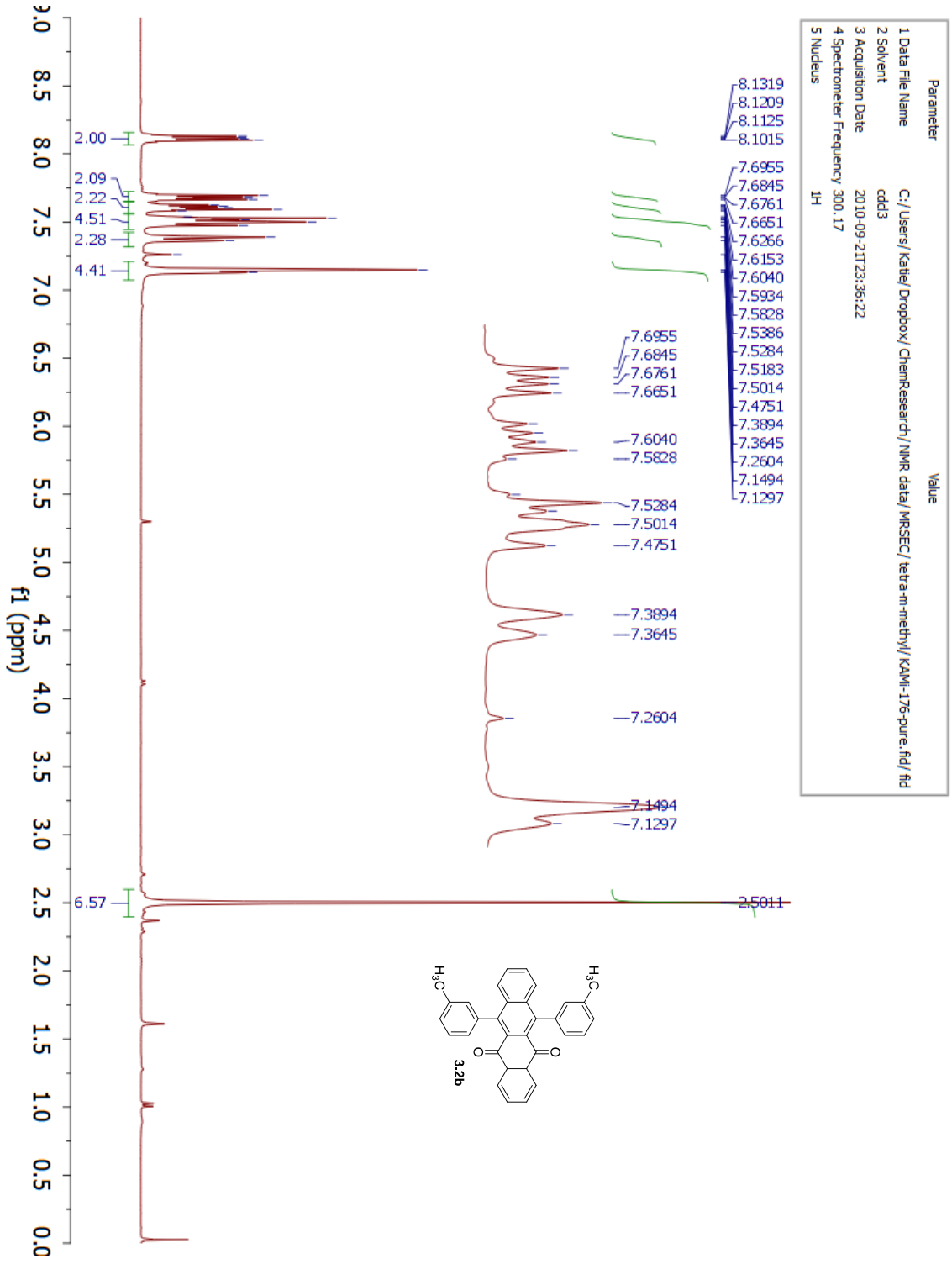
Parameter
Value
1 Data File Name
C:/Users/Katie/Dropbox/ChemResearch/NMR data/MRSEC/tetra-m-methyl/KAMI-176-pure.fid/fid
2 Solvent
cdcl3
3 Acquisition Date
2010-09-21T23:36:22
4 Spectrometer Frequency 300.17
5 Nucleus
1H
8.1319
8.1209
8.1125
8.1015
7.6955
7.6845
7.6761
7.6651
7.6266
7.6153
7.6040
7.5934
7.5828
7.5386
7.5284
7.5183
7.5014
7.4751
7.3894
7.3645
7.2604
7.1494
7.1297
2.5011
2.00
2.09
2.22
4.51
2.28
4.41
6.57
f1 (ppm)
3.2b

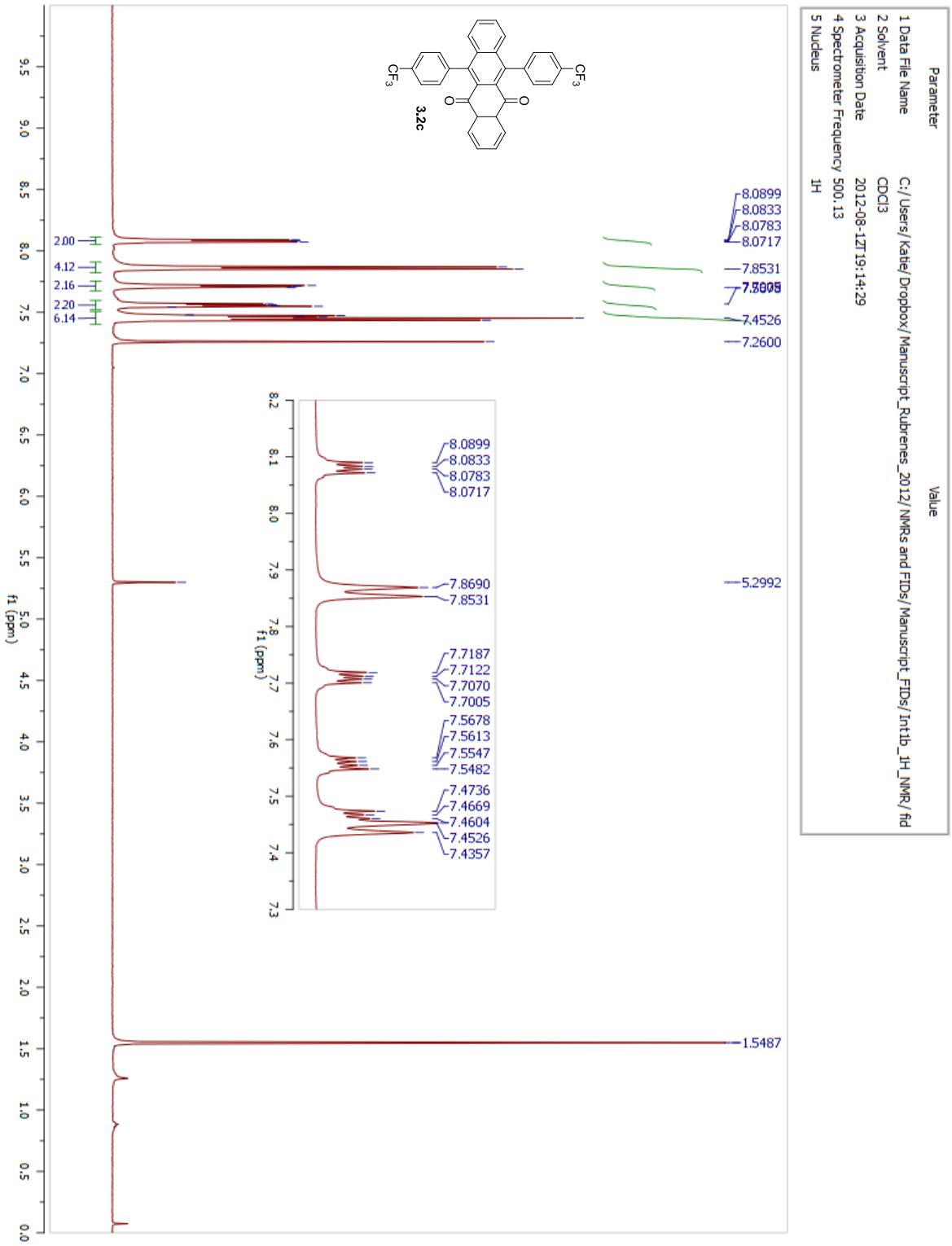
Parameter
Value
1 Data File Name
C:/Users/Katie/Dropbox/Manuscript_Rubrenes_2012/NMRs and FIDs/Manuscript_FIDs/Int1b_1H_NMR/fid
2 Solvent
CDCl3
3 Acquisition Date
2012-08-12T19:14:29
4 Spectrometer Frequency
500.13
5 Nucleus
1H
3.2c
CF3
CF3
O
O
2.00
4.12
2.16
2.20
6.14
8.0899
8.0833
8.0783
8.0717
7.8531
7.4526
7.2600
5.2992
1.5487
7.8690
7.8531
7.7187
7.7122
7.7070
7.7005
7.5678
7.5613
7.5547
7.5482
7.4736
7.4669
7.4604
7.4526
7.4357
f1 (ppm)

Parameter	Value
1 Data File Name	C:/Users/Katie/Dropbox/Manuscript_Rubrenes_2012/NMRs and FIDs/Manuscript_FIDs/Int1b_13C_NMR/fid
2 Solvent	CDCl3
3 Acquisition Date	2012-08-12T19:55:35
4 Spectrometer Frequency	125.76
5 Nucleus	13C

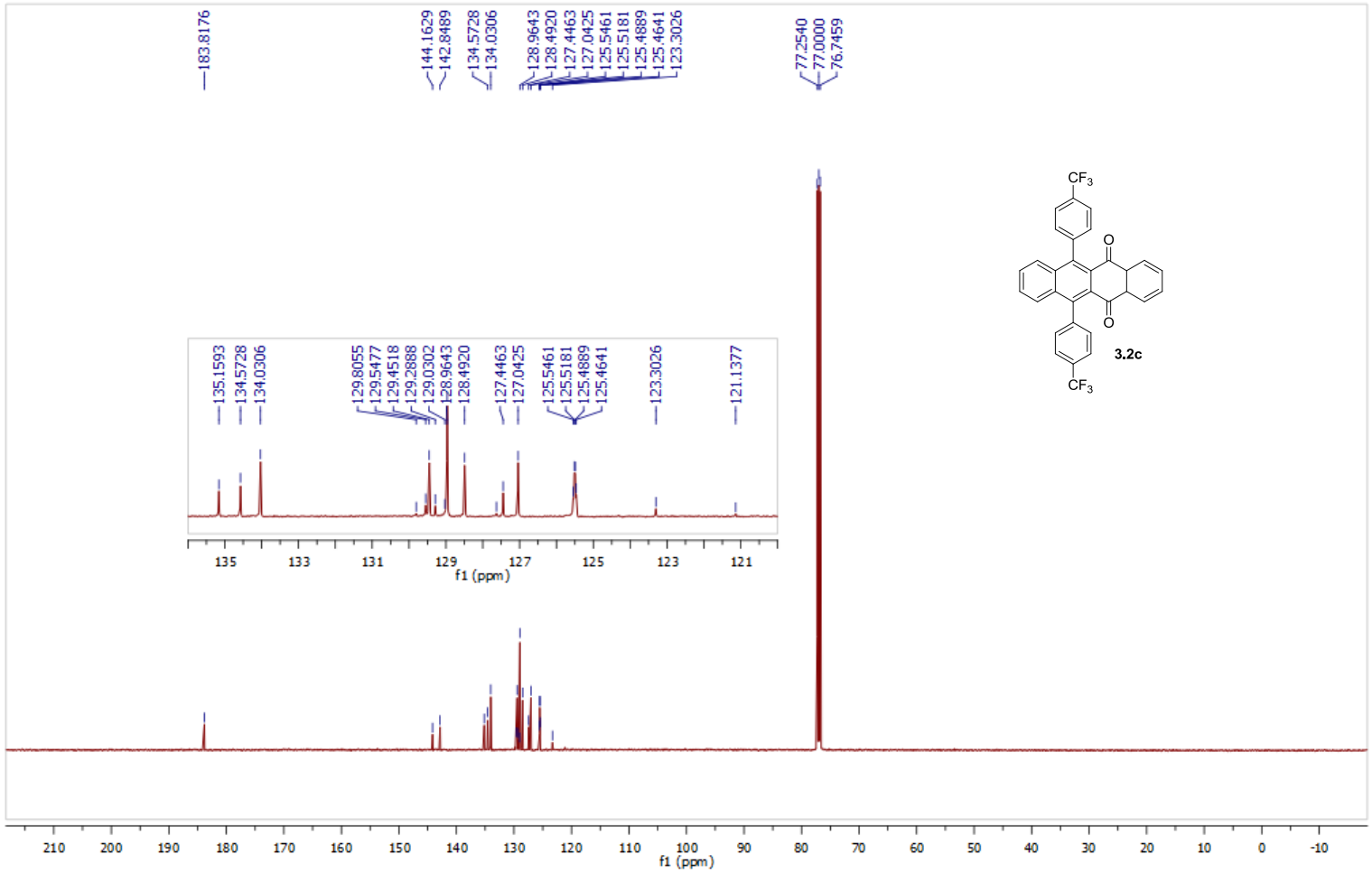

Parameter	Value
1 Data File Name	C:/ Users/ Katie/ Dropbox/ Manuscript_Rubrenes_2012/ NMRs and FIDs/ Manuscript_FIDs/ Int1b_19F_NMR/ fid
2 Solvent	CDCl3
3 Acquisition Date	2012-08-0ZT22:02:45
4 Spectrometer Frequency	470.59
5 Nucleus	19F

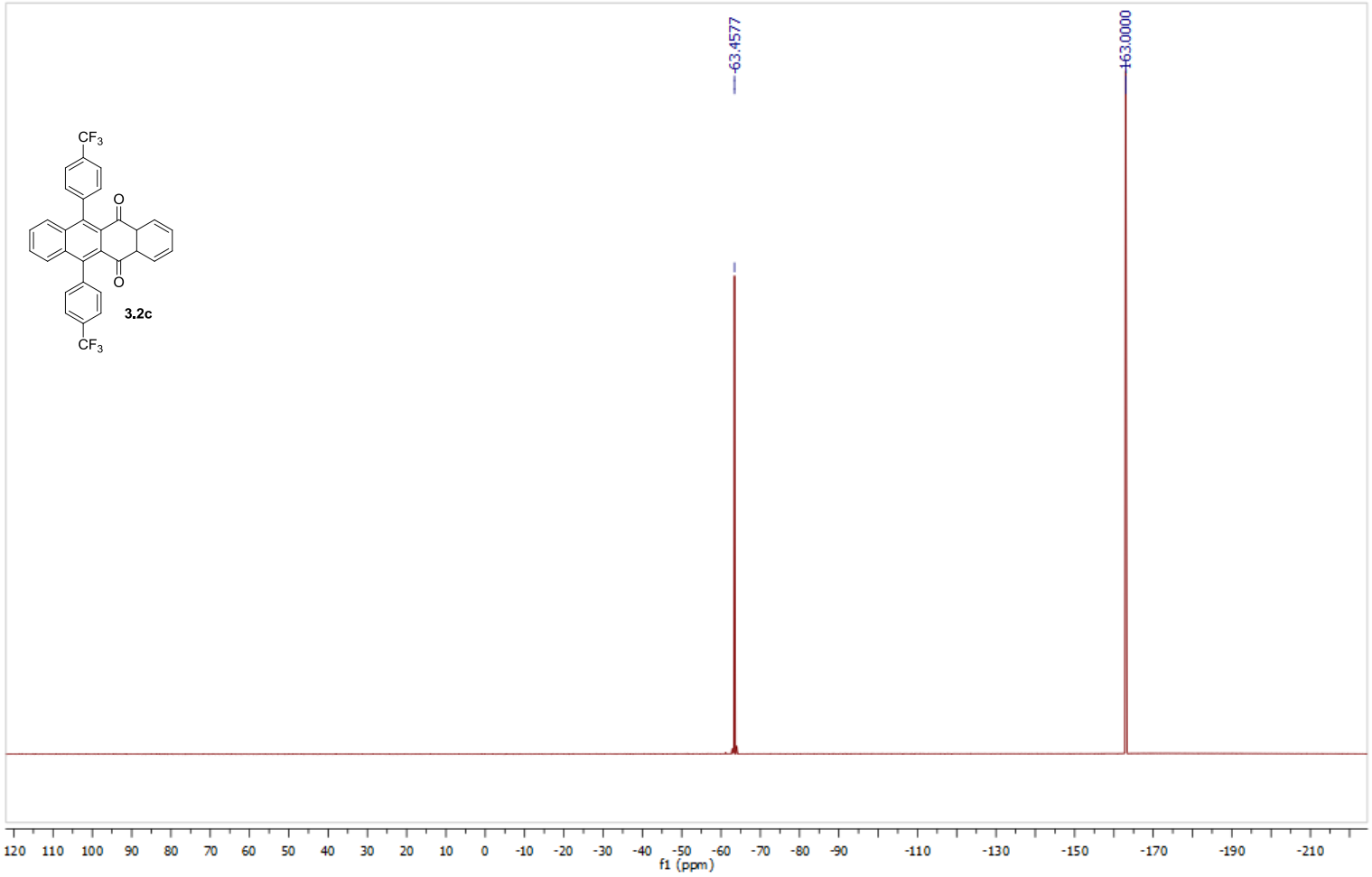

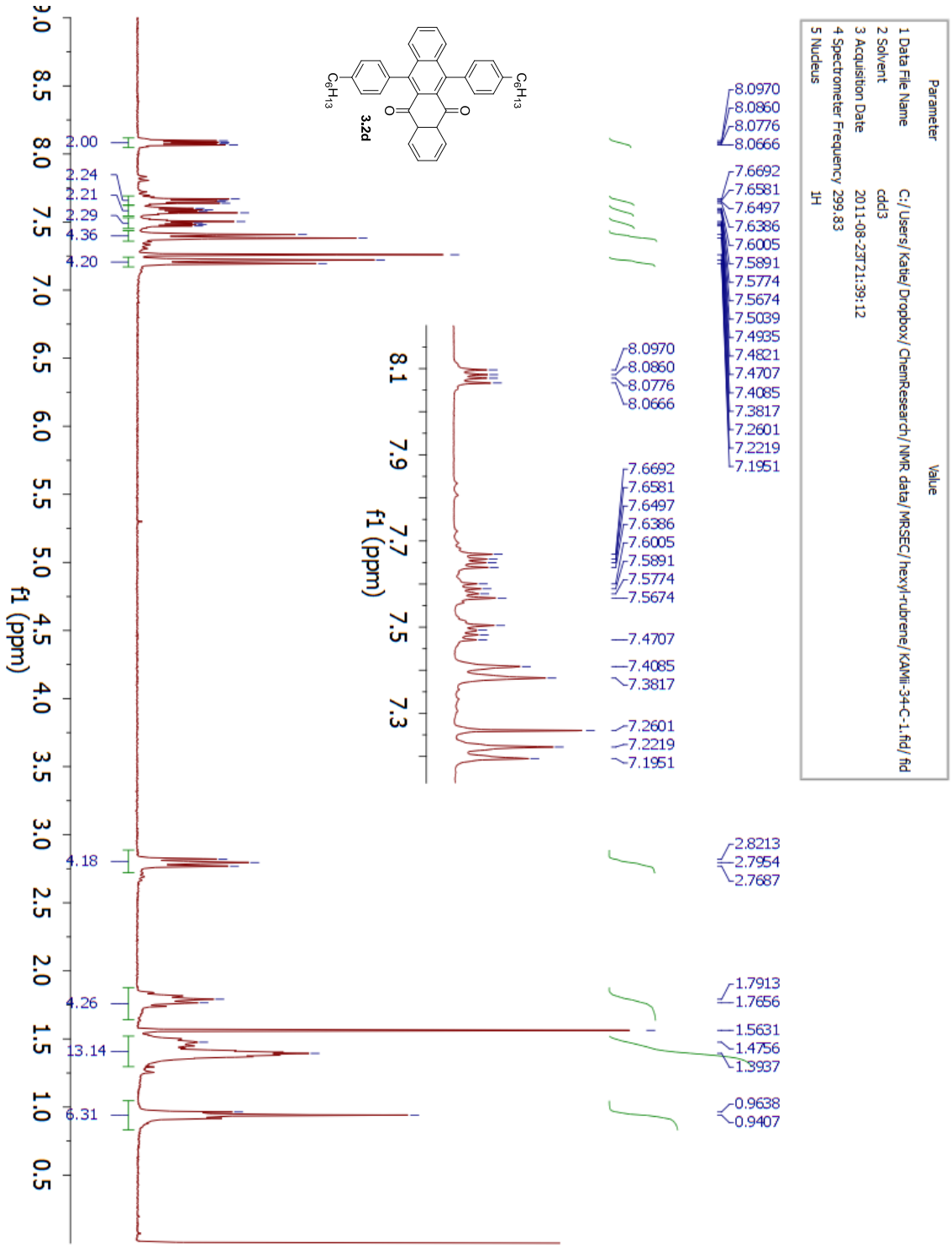
Parameter
Value
1 Data File Name
C:/Users/Katie/Dropbox/ChemResearch/NMR data/MRSEC/hexyl-rubrene/KAMii-34-C-1.fid/ fid
2 Solvent
cdcl3
3 Acquisition Date
2011-08-23T21:39:12
4 Spectrometer Frequency 299.83
5 Nucleus
1H
3.2d
f1 (ppm)
2.00
2.24
2.21
2.29
4.36
4.20
4.18
4.26
13.14
6.31
8.0970
8.0860
8.0776
8.0666
7.6692
7.6581
7.6497
7.6386
7.6005
7.5891
7.5774
7.5674
7.5039
7.4935
7.4821
7.4707
7.4085
7.3817
7.2601
7.2219
7.1951
2.8213
2.7954
2.7687
1.7913
1.7656
1.5631
1.4756
1.3937
0.9638
0.9407

Parameter	Value
1 Data File Name	C:/ Users/ Katie/ Dropbox/ ChemResearch/ NMR data/ MRSEC/ tetra-p-ethyl/ KAMi-227-pure.fid/ fid
2 Solvent	cdcl3
3 Acquisition Date	2010-12-21T18:37:34
4 Spectrometer Frequency	300.17
5 Nucleus	1H

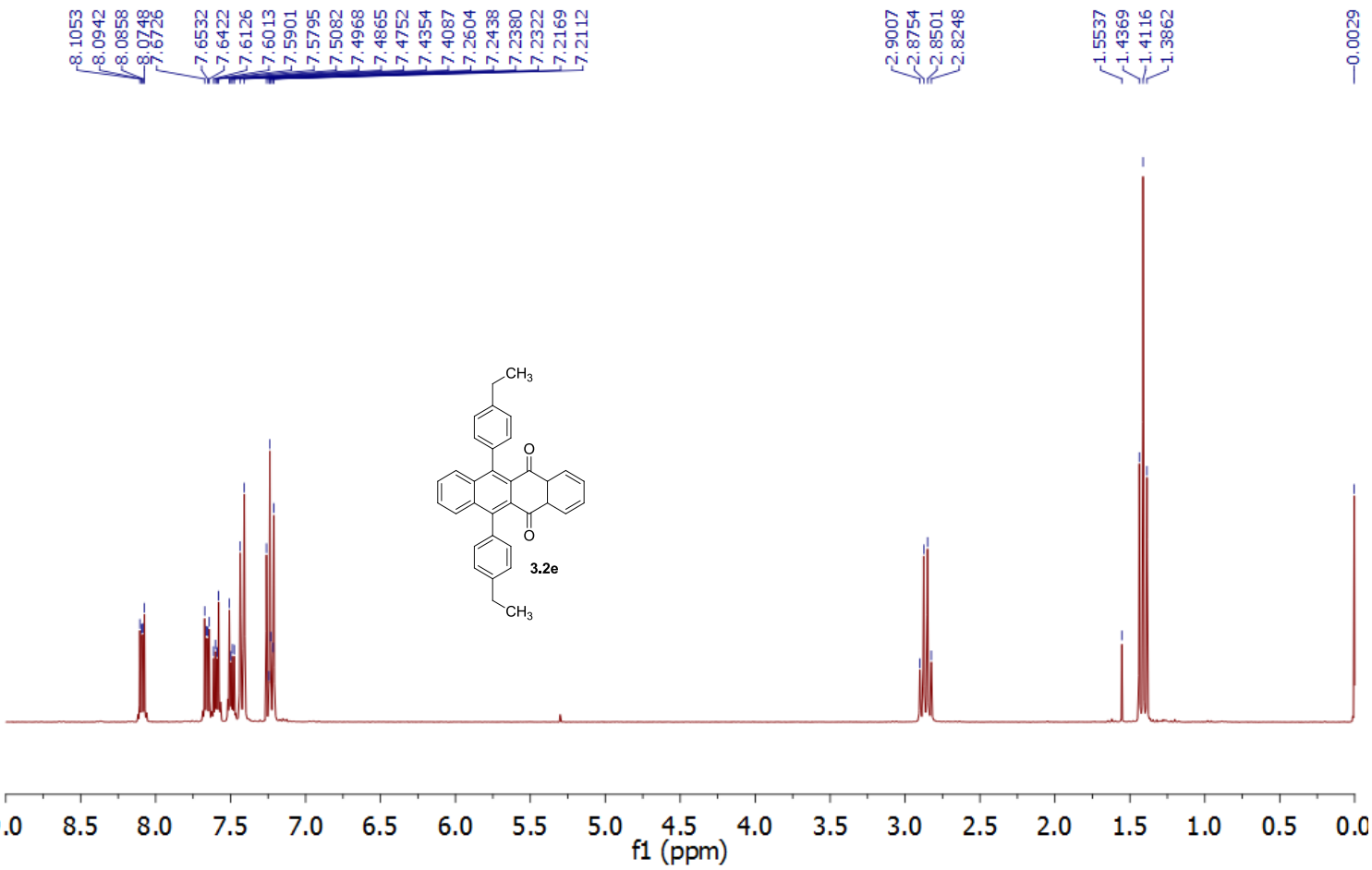

Parameter	Value
1 Data File Name	C:/Users/Katie/Dropbox/ChemResearch/NMR data/MRSEC/tetra-p-ethyl/KAMi-227-13C.fid/fid
2 Solvent	cdcl3
3 Acquisition Date	2010-12-21T18:38:03
4 Spectrometer Frequency	75.49
5 Nucleus	13C

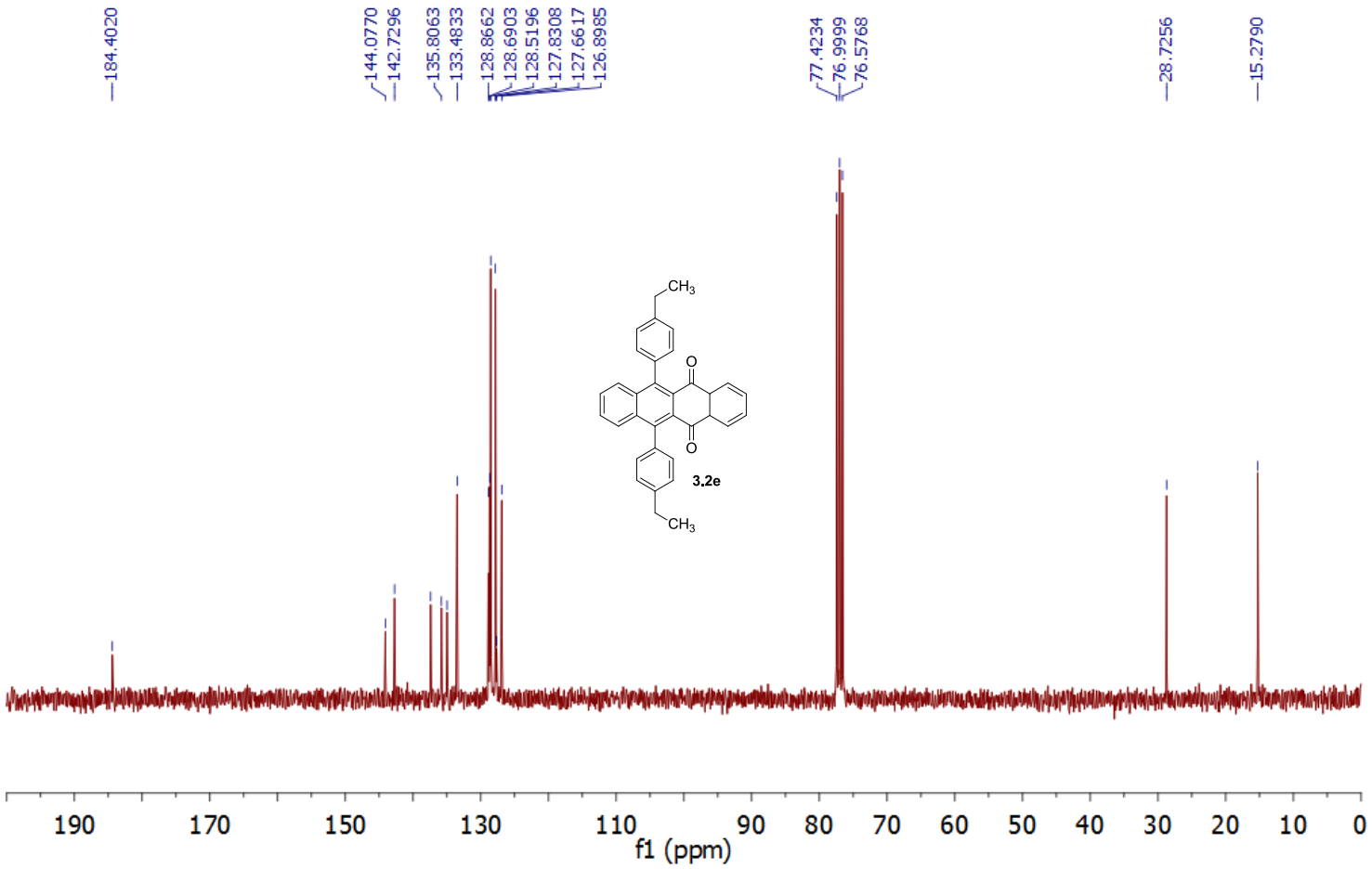

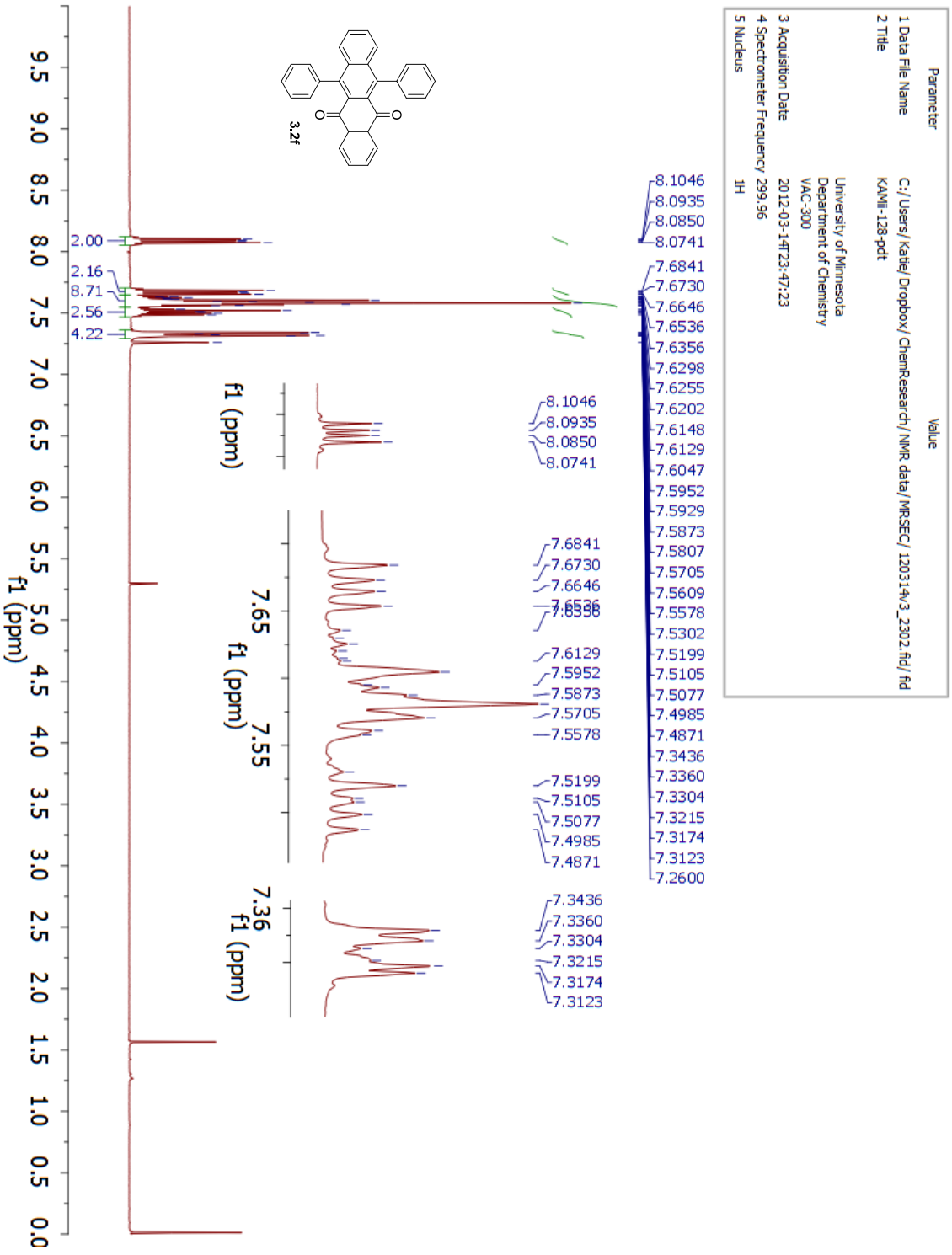
Parameter
Value
1 Data File Name
C:/Users/Katie/Dropbox/ChemResearch/NMR data/MRSEC/120314v3_2302.fid/fid
2 Title
KAMii-128-pdt
University of Minnesota
Department of Chemistry
VAC-300
3 Acquisition Date
2012-03-14T23:47:23
4 Spectrometer Frequency
299.96
5 Nucleus
1H
3.2f
2.00
2.16
8.71
2.56
4.22
8.1046
8.0935
8.0850
8.0741
7.6841
7.6730
7.6646
7.6536
7.6356
7.6298
7.6255
7.6202
7.6148
7.6129
7.6047
7.5952
7.5929
7.5873
7.5807
7.5705
7.5609
7.5578
7.5302
7.5199
7.5105
7.5077
7.4985
7.4871
7.3436
7.3360
7.3304
7.3215
7.3174
7.3123
7.2600
f1 (ppm)
7.65
7.55
7.36

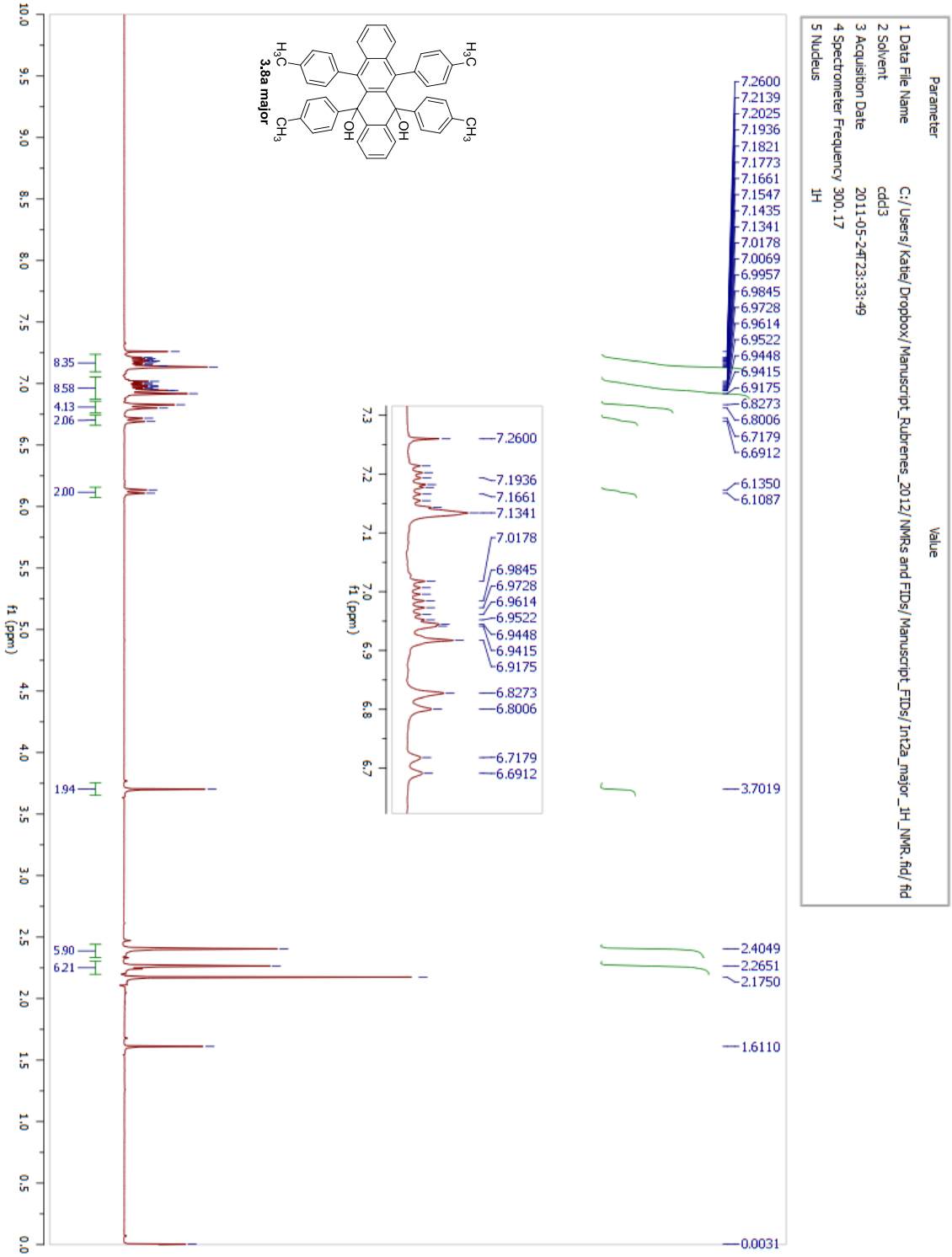
Parameter
Value
1 Data File Name
C:/Users/Katie/Dropbox/Manuscript_Rubrenes_2012/NMRs and FIDs/Manuscript_FIDs/Int2a_major_1H_NMR.fid/fid
2 Solvent
cdcl3
3 Acquisition Date
2011-05-24T23:33:49
4 Spectrometer Frequency
300.17
5 Nucleus
1H
3.8a major
f1 (ppm)
8.35
8.58
4.13
2.06
2.00
1.94
5.90
6.21
7.2600
7.2139
7.2025
7.1936
7.1821
7.1773
7.1661
7.1547
7.1435
7.1341
7.0178
7.0069
6.9957
6.9845
6.9728
6.9614
6.9522
6.9448
6.9415
6.9175
6.8273
6.8006
6.7179
6.6912
6.1350
6.1087
3.7019
2.4049
2.2651
2.1750
1.6110
0.0031

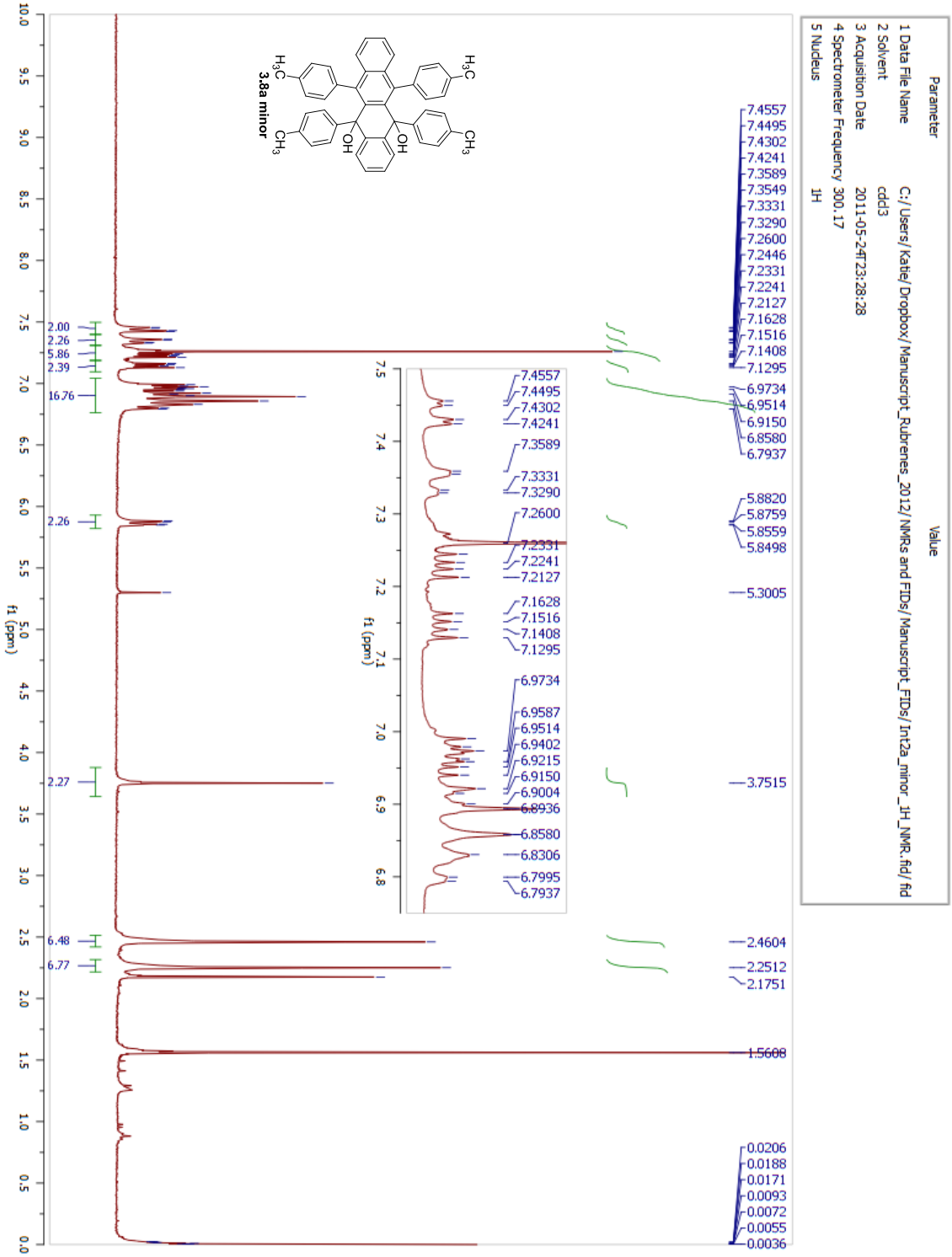
Parameter
Value
1 Data File Name
C:/Users/Katie/Dropbox/Manuscript_Rubrenes_2012/NMRs and FIDs/Manuscript_FIDs/Int2a_minor_1H_NMR.fid/fid
2 Solvent
cdcl3
3 Acquisition Date
2011-05-24T23:28:28
4 Spectrometer Frequency
300.17
5 Nucleus
1H
3.8a minor
f1 (ppm)

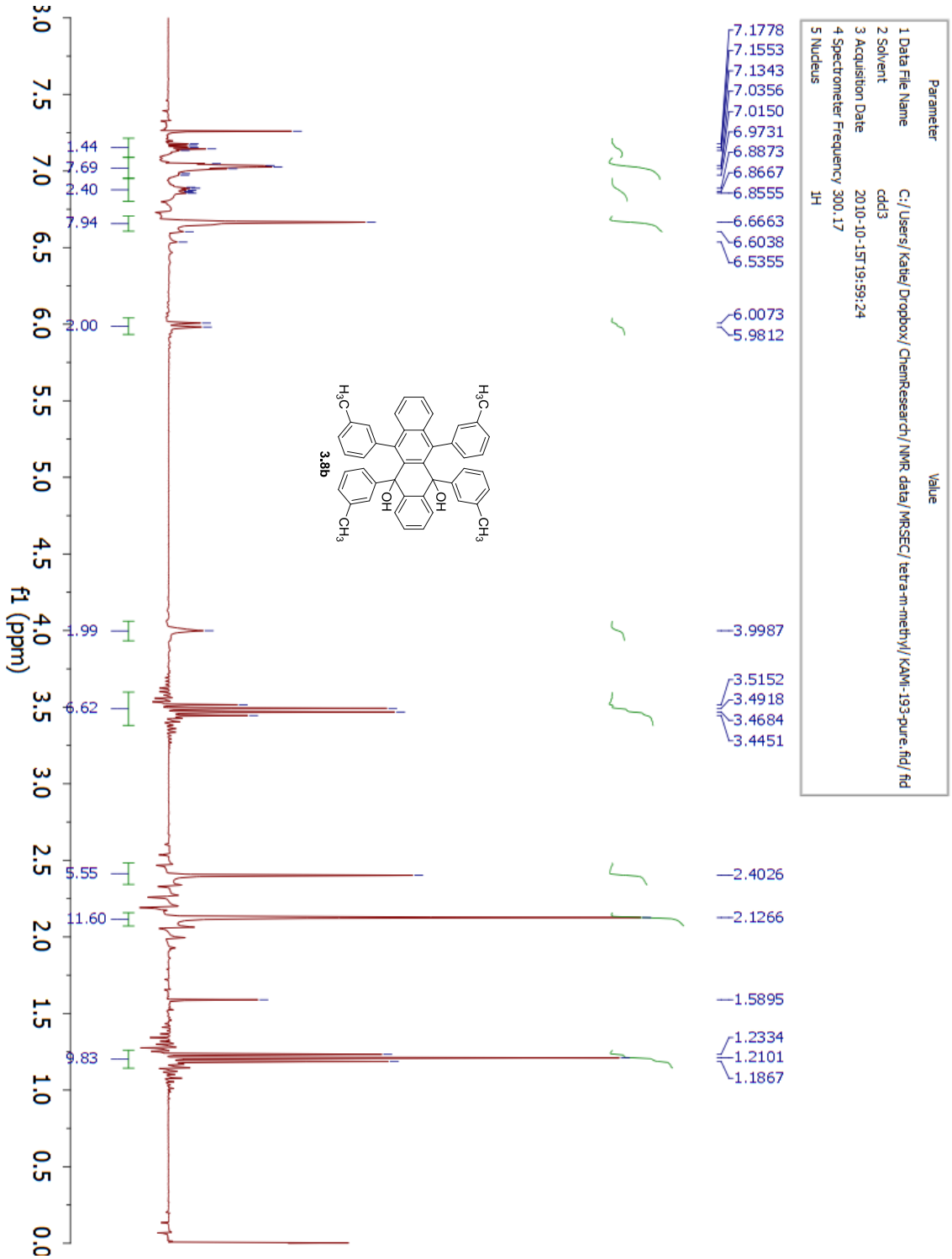
Parameter
Value
1 Data File Name
C:/Users/Katie/Dropbox/ChemResearch/NMR data/MRSEC/tetra-m-methyl/KAMI-193-pure.fid/fid
2 Solvent
cdcl3
3 Acquisition Date
2010-10-15T19:59:24
4 Spectrometer Frequency
300.17
5 Nucleus
1H
7.1778
7.1553
7.1343
7.0356
7.0150
6.9731
6.8873
6.8667
6.8555
6.6663
6.6038
6.5355
6.0073
5.9812
3.9987
3.5152
3.4918
3.4684
3.4451
2.4026
2.1266
1.5895
1.2334
1.2101
1.1867
1.44
7.69
2.40
7.94
2.00
1.99
6.62
5.55
11.60
9.83
3.8b
H3C
CH3
OH
f1 (ppm)

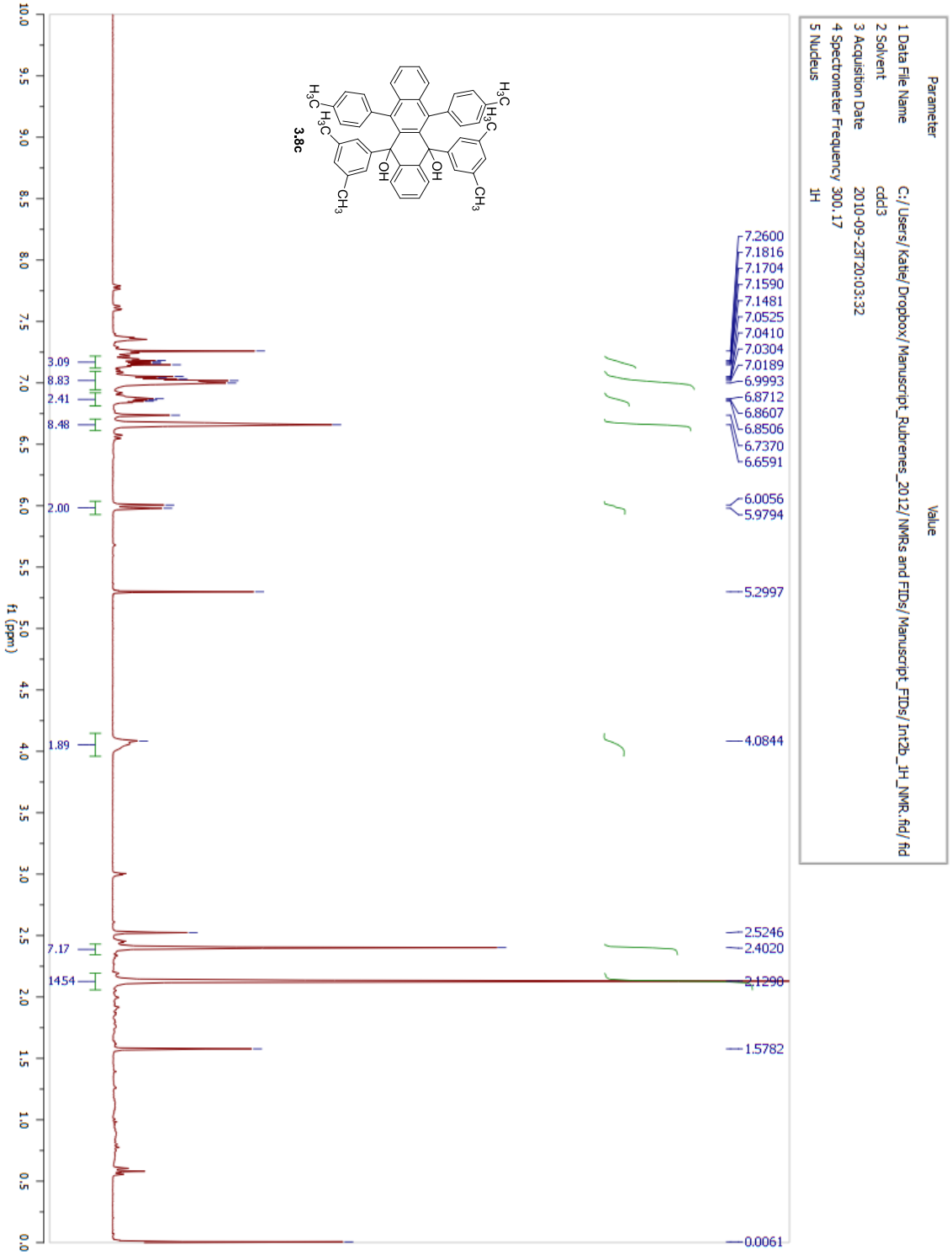
Parameter
Value
1 Data File Name
C:/Users/Katie/Dropbox/Manuscript_Rubrenes_2012/NMRs and FIDs/Manuscript_FIDs/Int2b_1H_NMR.fid/fid
2 Solvent
cdcl3
3 Acquisition Date
2010-09-23T20:03:32
4 Spectrometer Frequency
300.17
5 Nucleus
1H
3.8c
OH
OH
CH3
H3C
f1 (ppm)
7.2600
7.1816
7.1704
7.1590
7.1481
7.0525
7.0410
7.0304
7.0189
6.9993
6.8712
6.8607
6.8506
6.7370
6.6591
6.0056
5.9794
5.2997
4.0844
2.5246
2.4020
2.1290
1.5782
0.0061
3.09
8.83
2.41
8.48
2.00
1.89
7.17
14.54

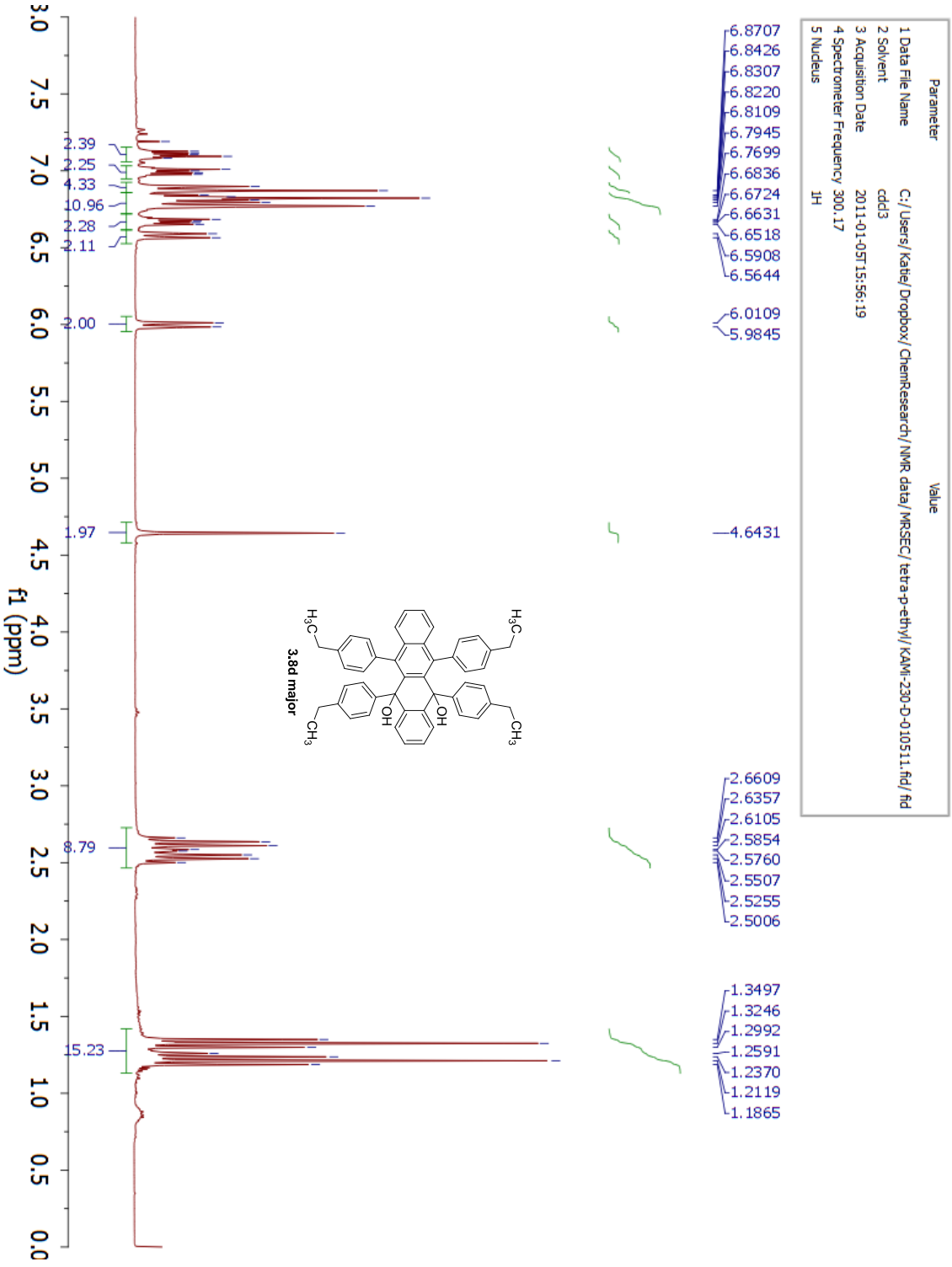
Parameter
Value
1 Data File Name
C:/Users/Katie/Dropbox/ChemResearch/NMR data/MRSEC/tetra-p-ethyl/KAMI-230-D-010511.fid/fid
2 Solvent
cdcl3
3 Acquisition Date
2011-01-05T15:56:19
4 Spectrometer Frequency
300.17
5 Nucleus
1H
6.8707
6.8426
6.8307
6.8220
6.8109
6.7945
6.7699
6.6836
6.6724
6.6631
6.6518
6.5908
6.5644
6.0109
5.9845
4.6431
2.6609
2.6357
2.6105
2.5854
2.5760
2.5507
2.5255
2.5006
1.3497
1.3246
1.2992
1.2591
1.2370
1.2119
1.1865
2.39
2.25
4.33
10.96
2.28
2.11
2.00
1.97
8.79
15.23
3.8d major
H3C
CH3
OH
f1 (ppm)

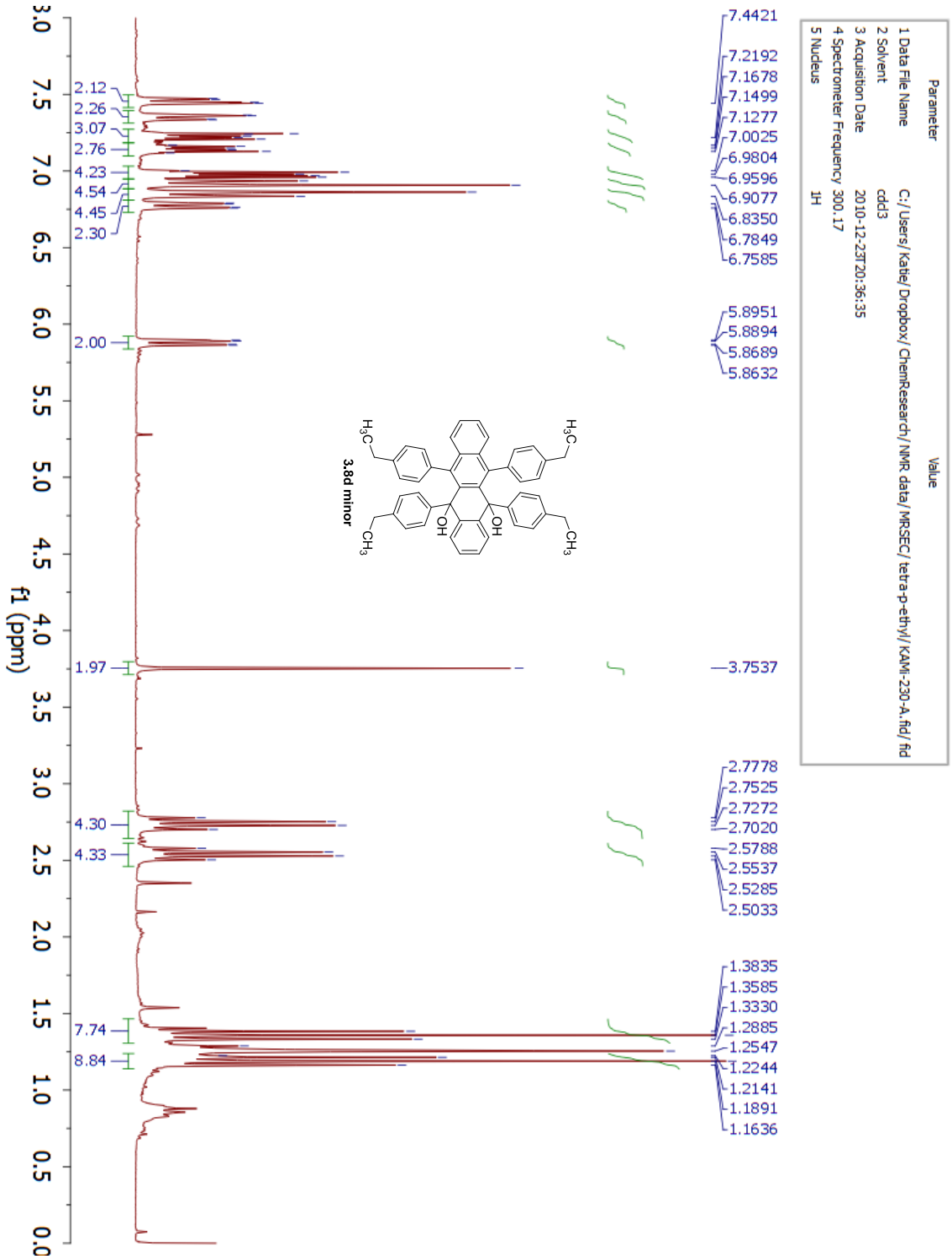
Parameter
Value
1 Data File Name
C:/Users/Katie/Dropbox/ChemResearch/NMR data/MRSEC/tetra-p-ethyl/KAMI-230-A.fid/fid
2 Solvent
cdcl3
3 Acquisition Date
2010-12-23T20:36:35
4 Spectrometer Frequency
300.17
5 Nucleus
1H
3.8d minor
f1 (ppm)

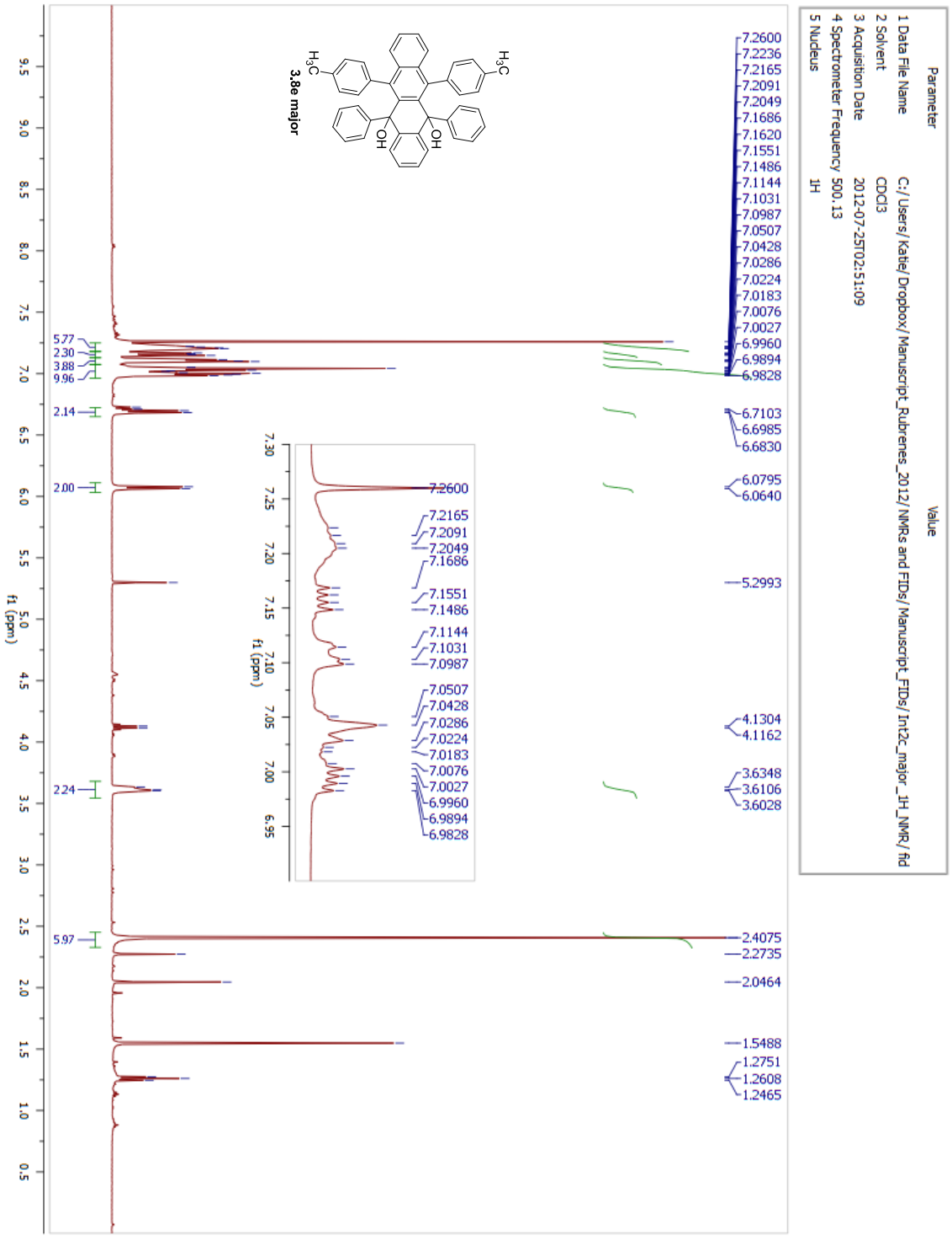
Parameter
Value
1 Data File Name
C:/Users/Katie/Dropbox/Manuscript_Rubrenes_2012/NMRs and FIDs/Manuscript_FIDs/Int2c_major_1H_NMR/fid
2 Solvent
CDCl3
3 Acquisition Date
2012-07-25T02:51:09
4 Spectrometer Frequency
500.13
5 Nucleus
1H
3.8e major
f1 (ppm)

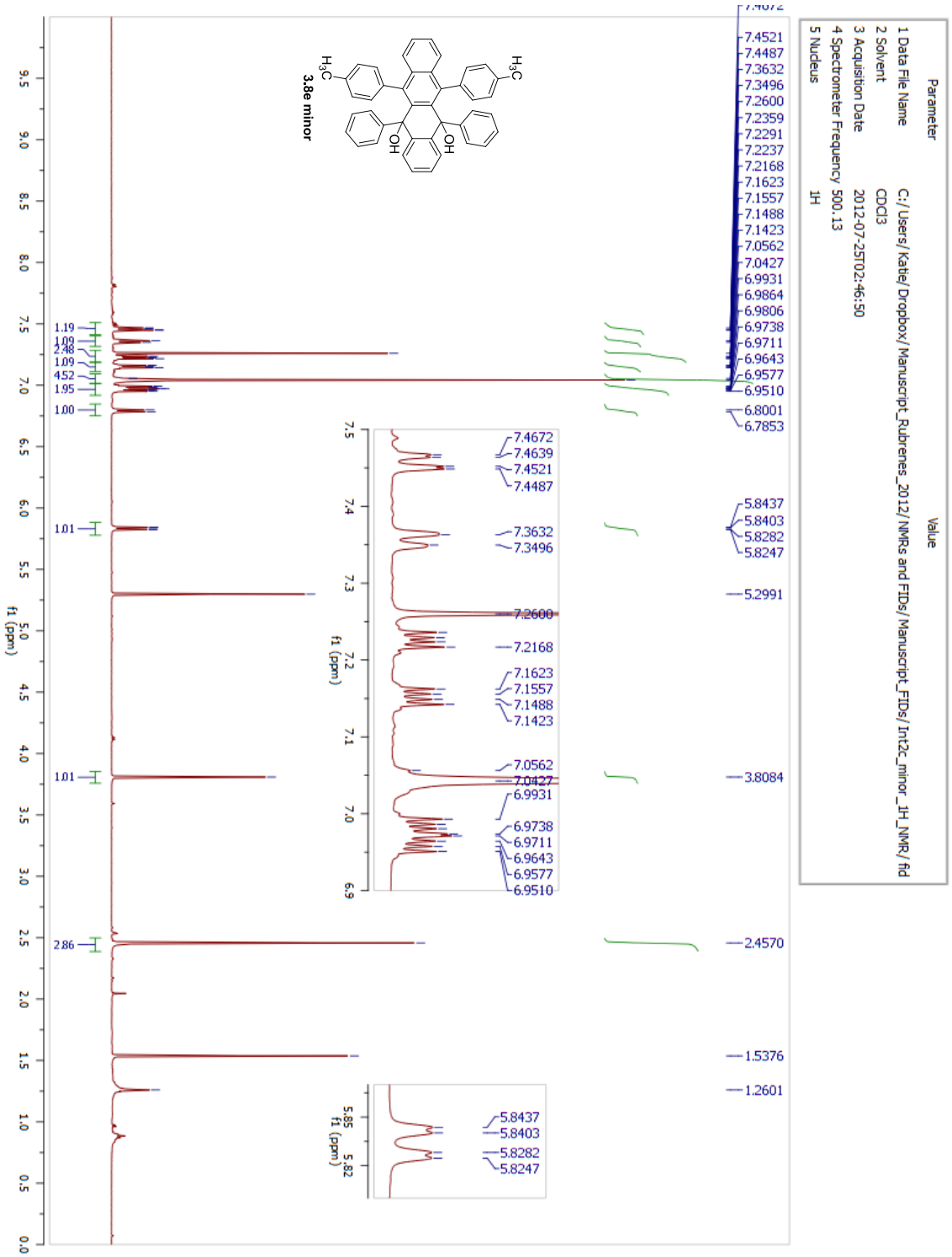
3.8e minor
H3C
CH3
OH
OH
Parameter
Value
1 Data File Name
C:/Users/Katie/Dropbox/Manuscript_Rubrenes_2012/NMRs and FIDs/Manuscript_FIDs/Int2c_minor_1H_NMR/fid
2 Solvent
CDCl3
3 Acquisition Date
2012-07-25T02:46:50
4 Spectrometer Frequency
500.13
5 Nucleus
1H
f1 (ppm)
1.19
1.00
2.48
1.09
4.52
1.95
1.00
1.01
1.01
2.86
7.4672
7.4639
7.4521
7.4487
7.3632
7.3496
7.2600
7.2168
7.1623
7.1557
7.1488
7.1423
7.0562
7.0427
6.9931
6.9738
6.9711
6.9643
6.9577
6.9510
6.8001
6.7853
5.8437
5.8403
5.8282
5.8247
5.2991
3.8084
2.4570
1.5376
1.2601

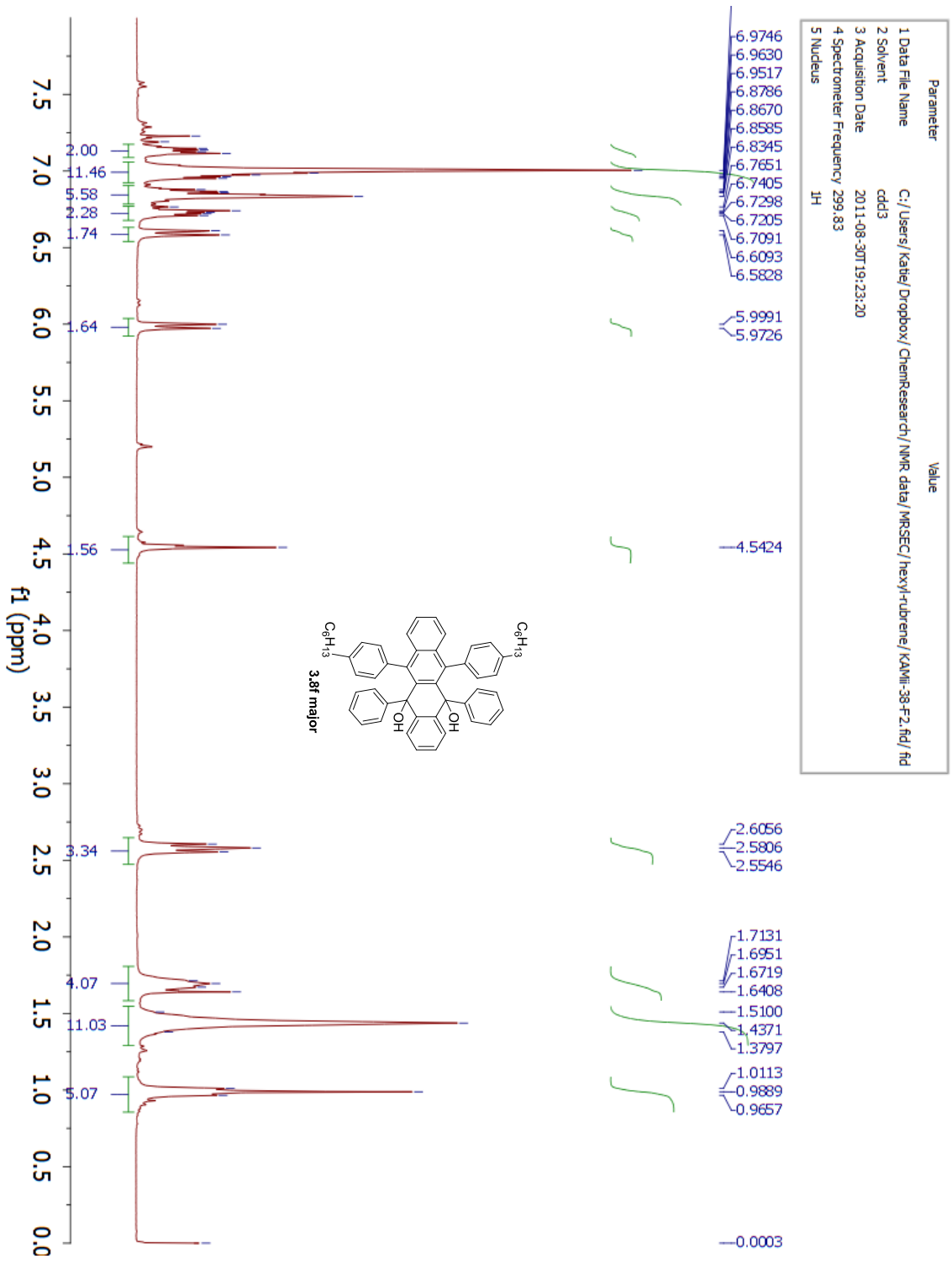
Parameter
Value
1 Data File Name
C:/Users/Katie/Dropbox/ChemResearch/NMR data/MRSEC/hexyl-rubrene/KAMii-38-F2.fid/fid
2 Solvent
cdcl3
3 Acquisition Date
2011-08-30T19:23:20
4 Spectrometer Frequency 299.83
5 Nucleus
1H
6.9746
6.9630
6.9517
6.8786
6.8670
6.8585
6.8345
6.7651
6.7405
6.7298
6.7205
6.7091
6.6093
6.5828
5.9991
5.9726
4.5424
2.6056
2.5806
2.5546
1.7131
1.6951
1.6719
1.6408
1.5100
1.4371
1.3797
1.0113
0.9889
0.9657
0.0003
2.00
11.46
5.58
2.28
1.74
1.64
1.56
3.34
4.07
11.03
5.07
C6H13
C6H13
OH
OH
3.8f major
f1 (ppm)
7.5
7.0
6.5
6.0
5.5
5.0
4.5
4.0
3.5
3.0
2.5
2.0
1.5
1.0
0.5
0.0

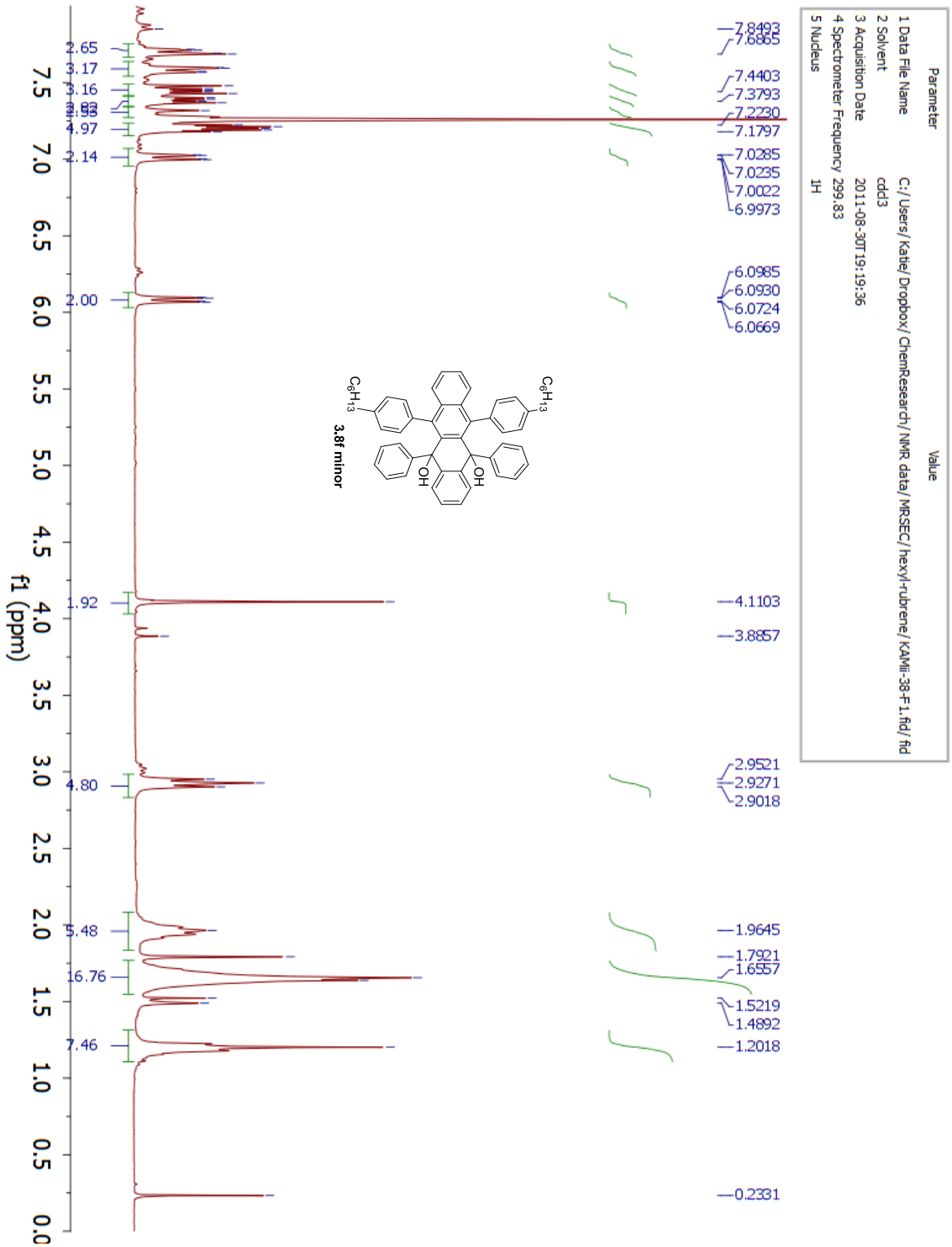
Parameter
Value
1 Data File Name
C:/Users/Katie/Dropbox/ChemResearch/NMR data/MRSEC/hexyl-rubrene/KAMii-38-F1.fid/fid
2 Solvent
cdcl3
3 Acquisition Date
2011-08-30T19:19:36
4 Spectrometer Frequency 299.83
5 Nucleus
1H
7.8493
7.6865
7.4403
7.3793
7.2230
7.1797
7.0285
7.0235
7.0022
6.9973
6.0985
6.0930
6.0724
6.0669
4.1103
3.8857
2.9521
2.9271
2.9018
1.9645
1.7921
1.6557
1.5219
1.4892
1.2018
0.2331
2.65
3.17
3.16
4.97
2.14
2.00
1.92
4.80
5.48
16.76
7.46
C6H13
C6H13
OH
OH
3.8f minor
f1 (ppm)

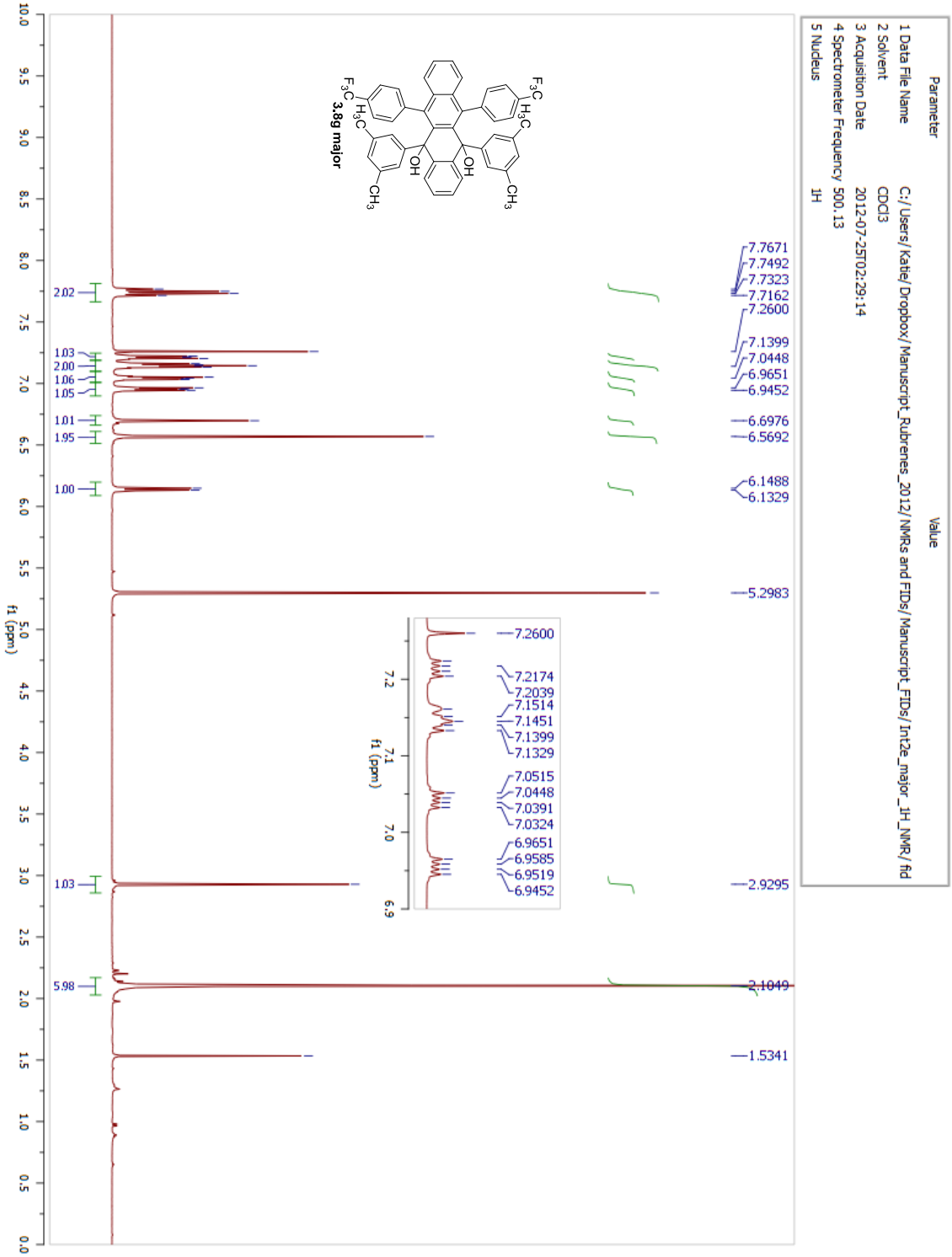
Parameter
Value
1 Data File Name C:/Users/Katie/Dropbox/Manuscript_Rubrenes_2012/NMRs and FIDs/Manuscript_FIDs/Int2e_major_1H_NMR/fid
2 Solvent CDCl3
3 Acquisition Date 2012-07-25T02:29:14
4 Spectrometer Frequency 500.13
5 Nucleus 1H
3.8g major
7.7671
7.7492
7.7323
7.7162
7.2600
7.1399
7.0448
6.9651
6.9452
6.6976
6.5692
6.1488
6.1329
5.2983
2.9295
2.1049
1.5341
2.02
1.03
2.00
1.06
1.05
1.01
1.95
1.00
1.03
5.98
f1 (ppm)

Parameter	Value
1 Data File Name	C:/ Users/ Katie/ Dropbox/ Manuscript_Rubrenes_2012/ NMRs and FIDs/ Manuscript_FIDs/ Int2e_major_19F_NMR/ fid
2 Solvent	CDCl3
3 Acquisition Date	2012-07-25T02:31:56
4 Spectrometer Frequency	470.59
5 Nucleus	19F

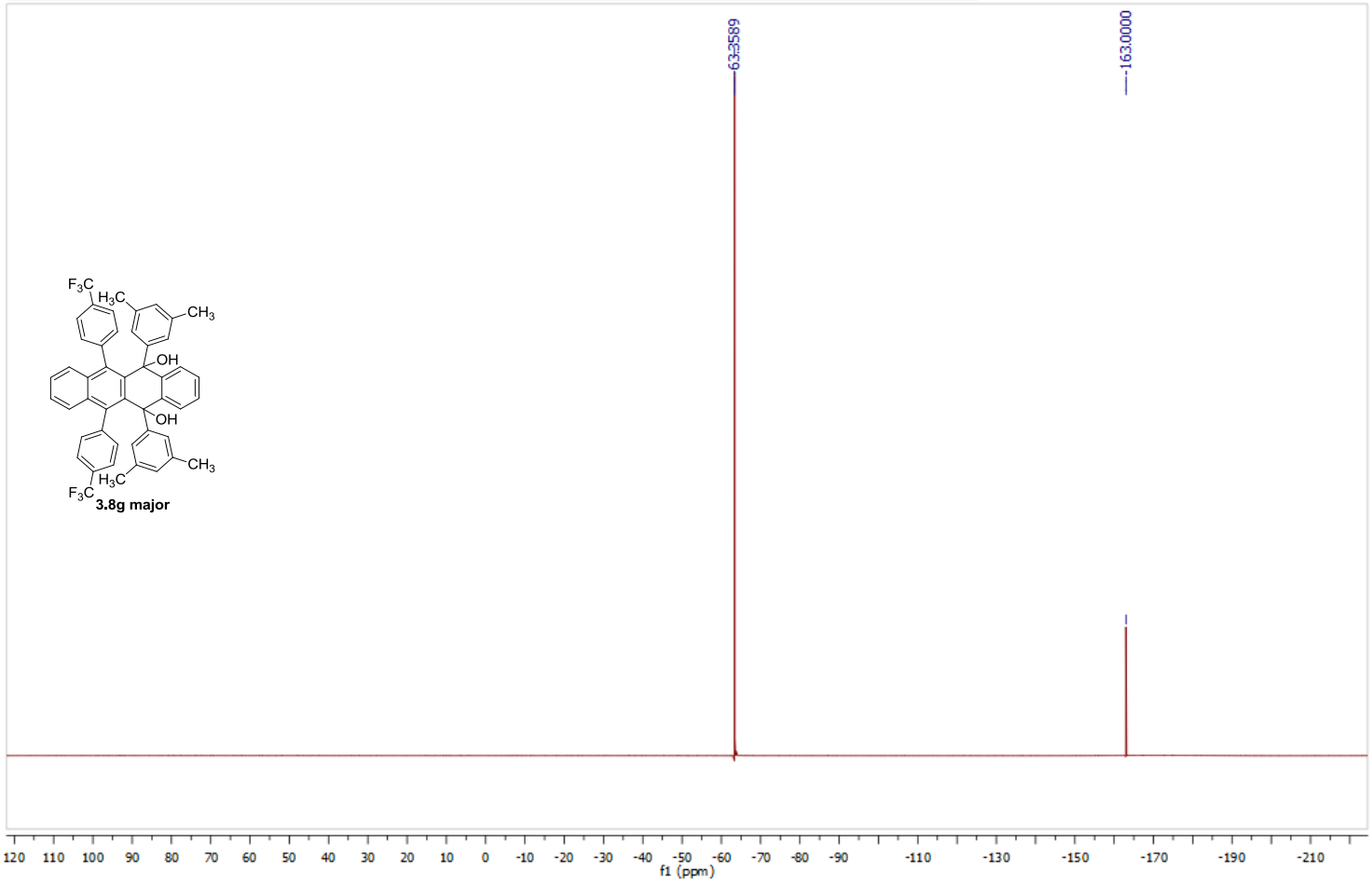

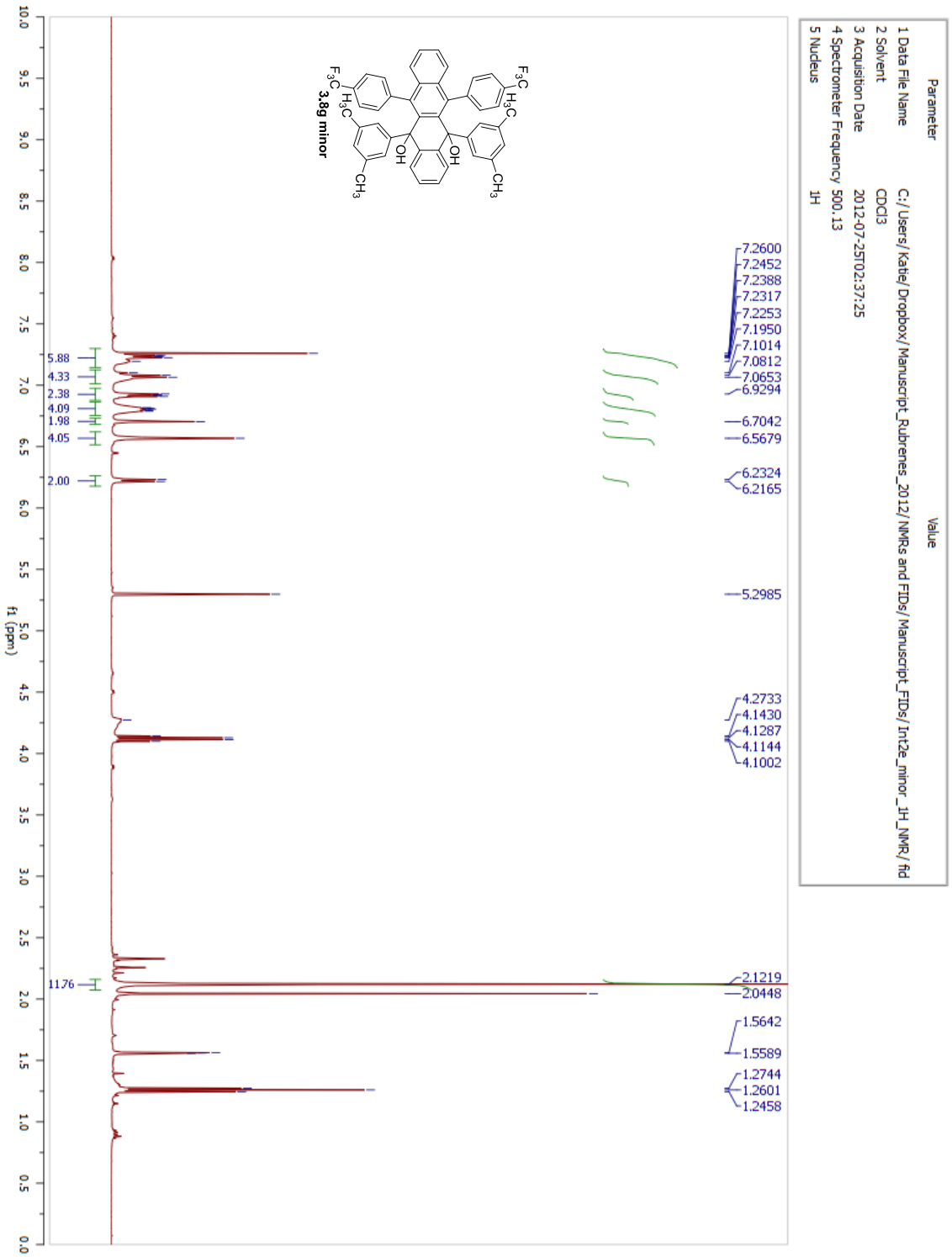
Parameter
Value
1 Data File Name C:/Users/Katie/Dropbox/Manuscript_Rubrenes_2012/NMRs and FIDs/Manuscript_FIDs/Int2e_minor_1H_NMR/fid
2 Solvent CDCl3
3 Acquisition Date 2012-07-25T02:37:25
4 Spectrometer Frequency 500.13
5 Nucleus 1H
3.8g minor
OH
OH
CH3
F3C
H3C
7.2600
7.2452
7.2388
7.2317
7.2253
7.1950
7.1014
7.0812
7.0653
6.9294
6.7042
6.5679
6.2324
6.2165
5.2985
4.2733
4.1430
4.1287
4.1144
4.1002
2.1219
2.0448
1.5642
1.5589
1.2744
1.2601
1.2458
5.88
4.33
2.38
4.09
1.98
4.05
2.00
11.76
f1 (ppm)

Parameter	Value
1 Data File Name	C:/ Users/ Katie/ Dropbox/ Manuscript_Rubrenes_2012/ NMRs and FIDs/ Manuscript_FIDs/ Int2e_minor_19F_NMR/ fid
2 Solvent	CDCl3
3 Acquisition Date	2012-07-25T02:39:57
4 Spectrometer Frequency	470.59
5 Nucleus	19F

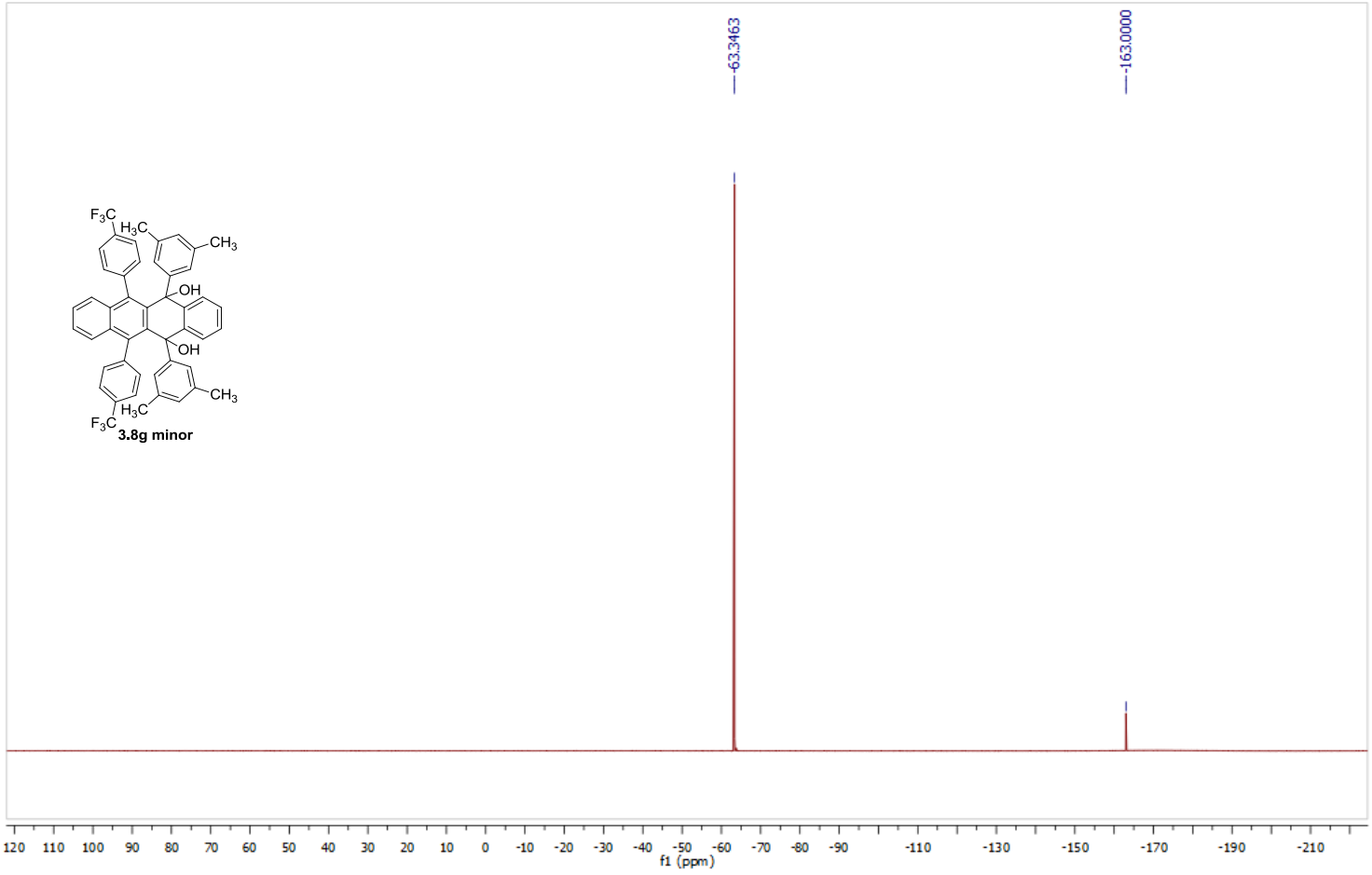

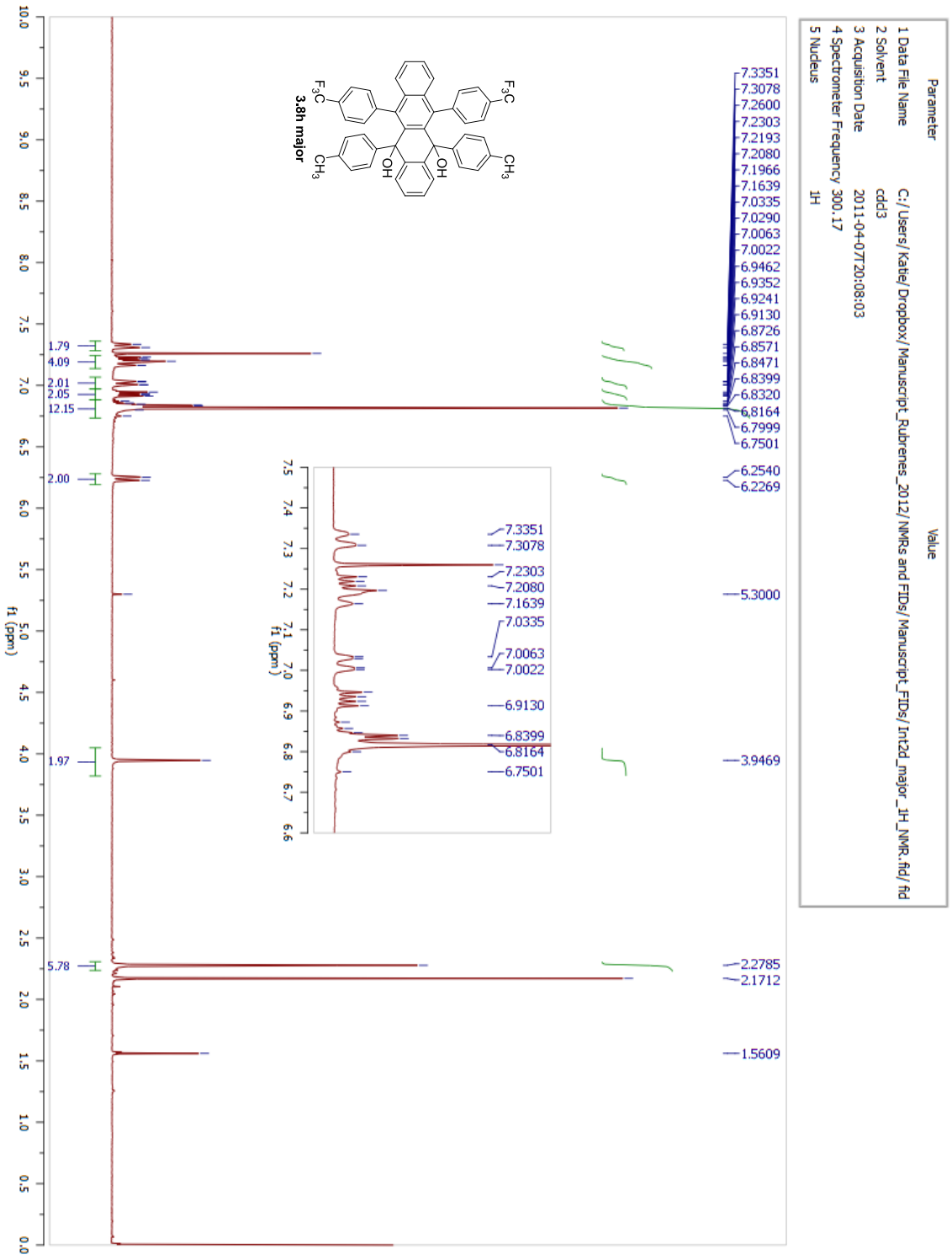
Parameter
Value
1 Data File Name
C:/Users/Katie/Dropbox/Manuscript_Rubrenes_2012/NMRs and FIDs/Manuscript_FIDs/Int2d_major_1H_NMR.fid/fid
2 Solvent
cdcl3
3 Acquisition Date
2011-04-07T20:08:03
4 Spectrometer Frequency
300.17
5 Nucleus
1H
3.8h major
F3C
CH3
OH
7.3351
7.3078
7.2600
7.2303
7.2193
7.2080
7.1966
7.1639
7.0335
7.0290
7.0063
7.0022
6.9462
6.9352
6.9241
6.9130
6.8726
6.8571
6.8471
6.8399
6.8320
6.8164
6.7999
6.7501
6.2540
6.2269
5.3000
3.9469
2.2785
2.1712
1.5609
1.79
4.09
2.01
2.05
12.15
2.00
1.97
5.78
f1 (ppm)

Parameter	Value
1 Data File Name	C:/ Users/ Katie/ Dropbox/ Manuscript_Rubrenes_2012/ NMRs and FIDs/ Manuscript_FIDs/ Int2d_major_19F_NMR.fid/ fid
2 Solvent	cdcl3
3 Acquisition Date	2012-08-08T18:50:09
4 Spectrometer Frequency	282.11
5 Nucleus	19F

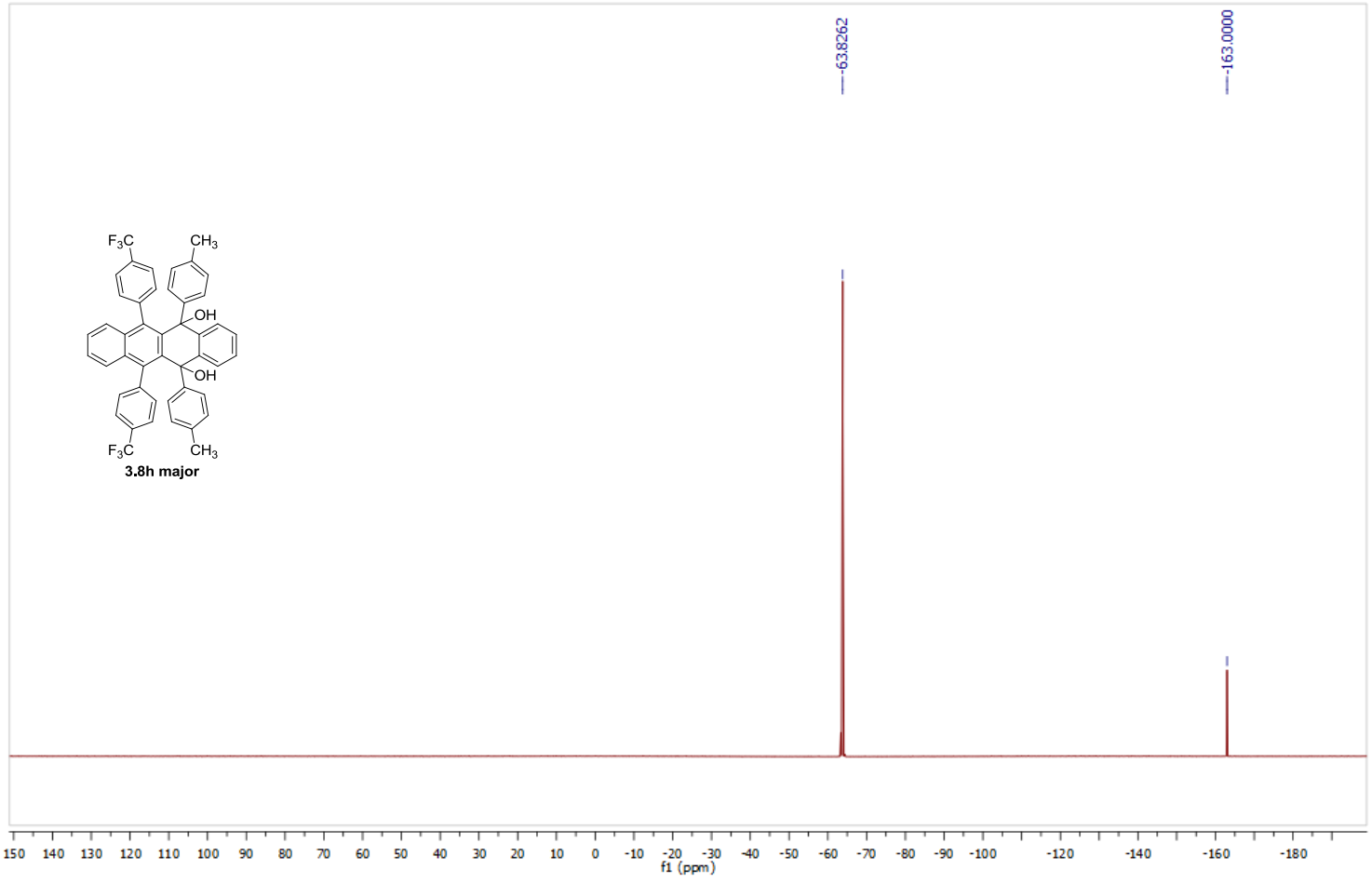

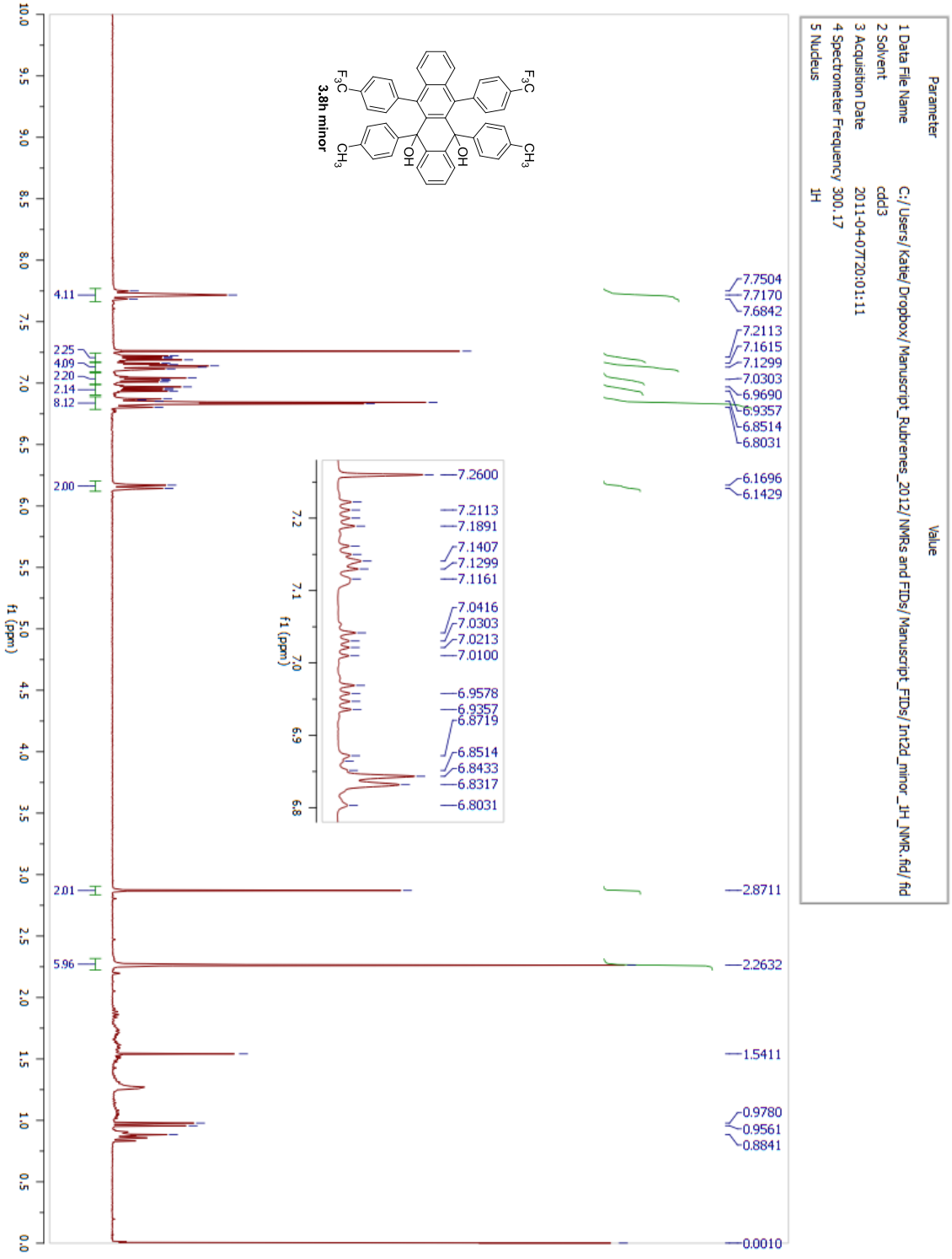
Parameter
Value
1 Data File Name
C:/Users/Katie/Dropbox/Manuscript_Rubrenes_2012/NMRs and FIDs/Manuscript_FIDs/Int2d_minor_1H_NMR.fid/fid
2 Solvent
cdcl3
3 Acquisition Date
2011-04-07T20:01:11
4 Spectrometer Frequency
300.17
5 Nucleus
1H
3.8h minor
F3C
CH3
OH
4.11
2.25
4.09
2.20
2.14
8.12
2.00
2.01
5.96
7.7504
7.7170
7.6842
7.2113
7.1615
7.1299
7.0303
6.9690
6.9357
6.8514
6.8031
6.1696
6.1429
2.8711
2.2632
1.5411
0.9780
0.9561
0.8841
0.0010
7.2600
7.2113
7.1891
7.1407
7.1299
7.1161
7.0416
7.0303
7.0213
7.0100
6.9578
6.9357
6.8719
6.8514
6.8433
6.8317
6.8031
f1 (ppm)

Parameter	Value
1 Data File Name	C:/ Users/ Katie/ Dropbox/ Manuscript_Rubrenes_2012/ NMRs and FIDs/ Manuscript_FIDs/ Int2d_minor_19F_NMR.fid/ fid
2 Owner	cdokam
3 Acquisition Date	2012-08-08T18:38:28
4 Spectrometer Frequency	282.11
5 Nucleus	19F

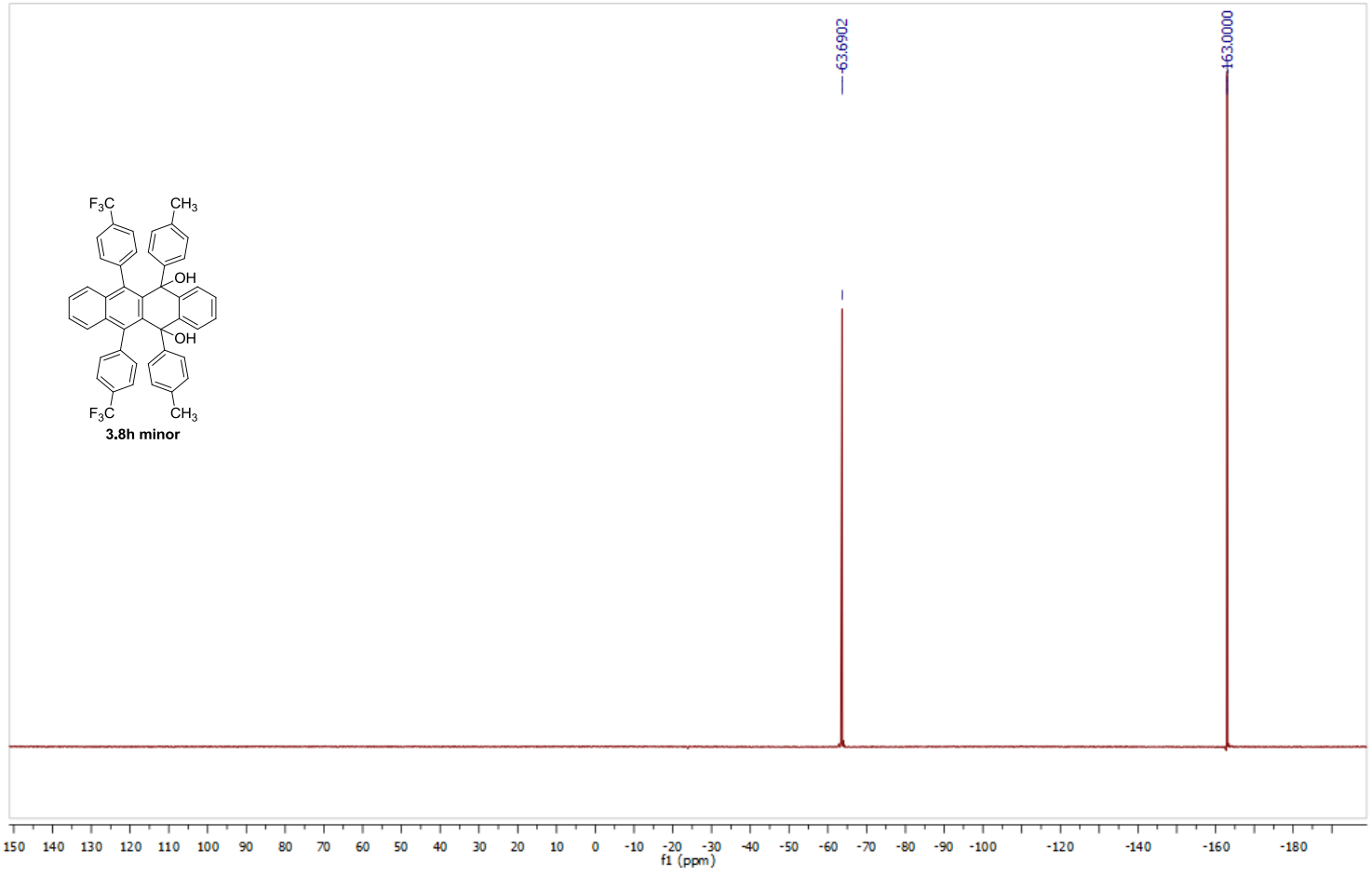

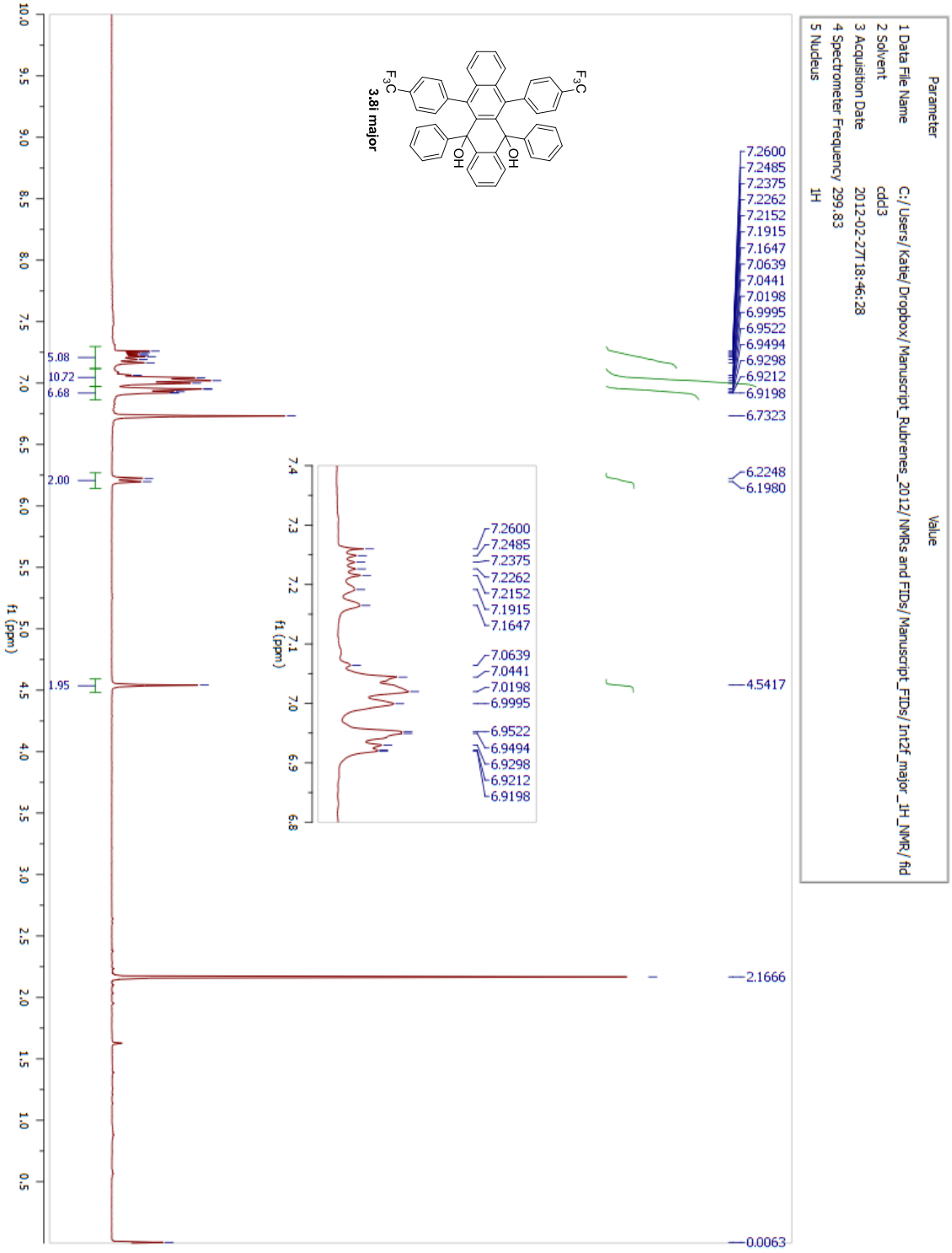
Parameter
Value
1 Data File Name
C:/Users/Katie/Dropbox/Manuscript_Rubrenes_2012/NMRs and FIDs/Manuscript_FIDs/Int2f_major_1H_NMR/fid
2 Solvent
cdcl3
3 Acquisition Date
2012-02-27T18:46:28
4 Spectrometer Frequency
299.83
5 Nucleus
1H
3.8i major
F3C
CF3
OH
OH
7.2600
7.2485
7.2375
7.2262
7.2152
7.1915
7.1647
7.0639
7.0441
7.0198
6.9995
6.9522
6.9494
6.9298
6.9212
6.9198
6.7323
6.2248
6.1980
4.5417
2.1666
0.0063
5.08
10.72
6.68
2.00
1.95
f1 (ppm)

Parameter	Value
1 Data File Name	C:/ Users/ Katie/ Dropbox/ Manuscript_Rubrenes_2012/ NMRs and FIDs/ Manuscript_FIDs/ Int2f_major_19F_NMR.fid/ fid
2 Solvent	cdcl3
3 Acquisition Date	2012-08-08T18:53:31
4 Spectrometer Frequency	282.11
5 Nucleus	19F

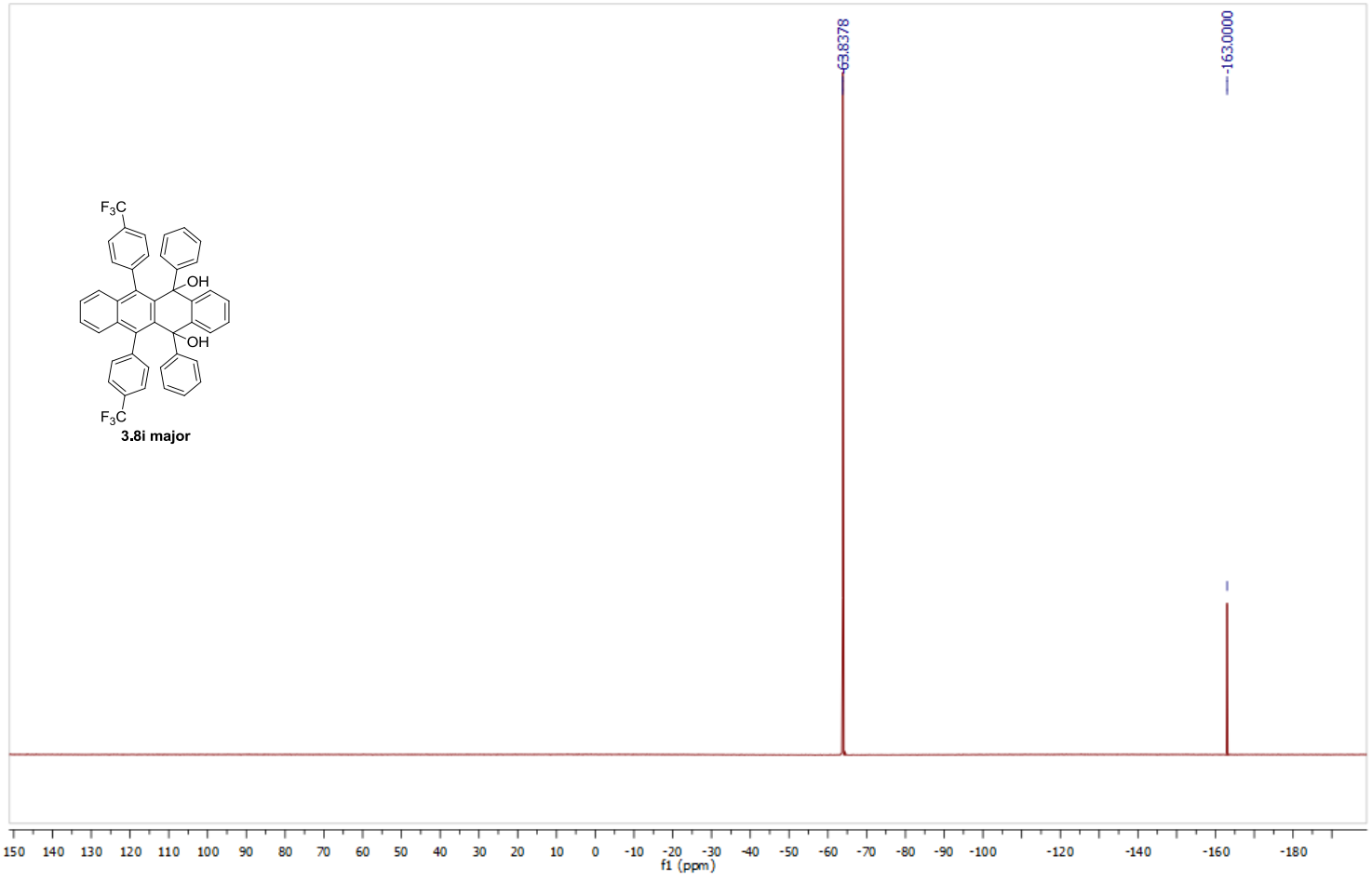

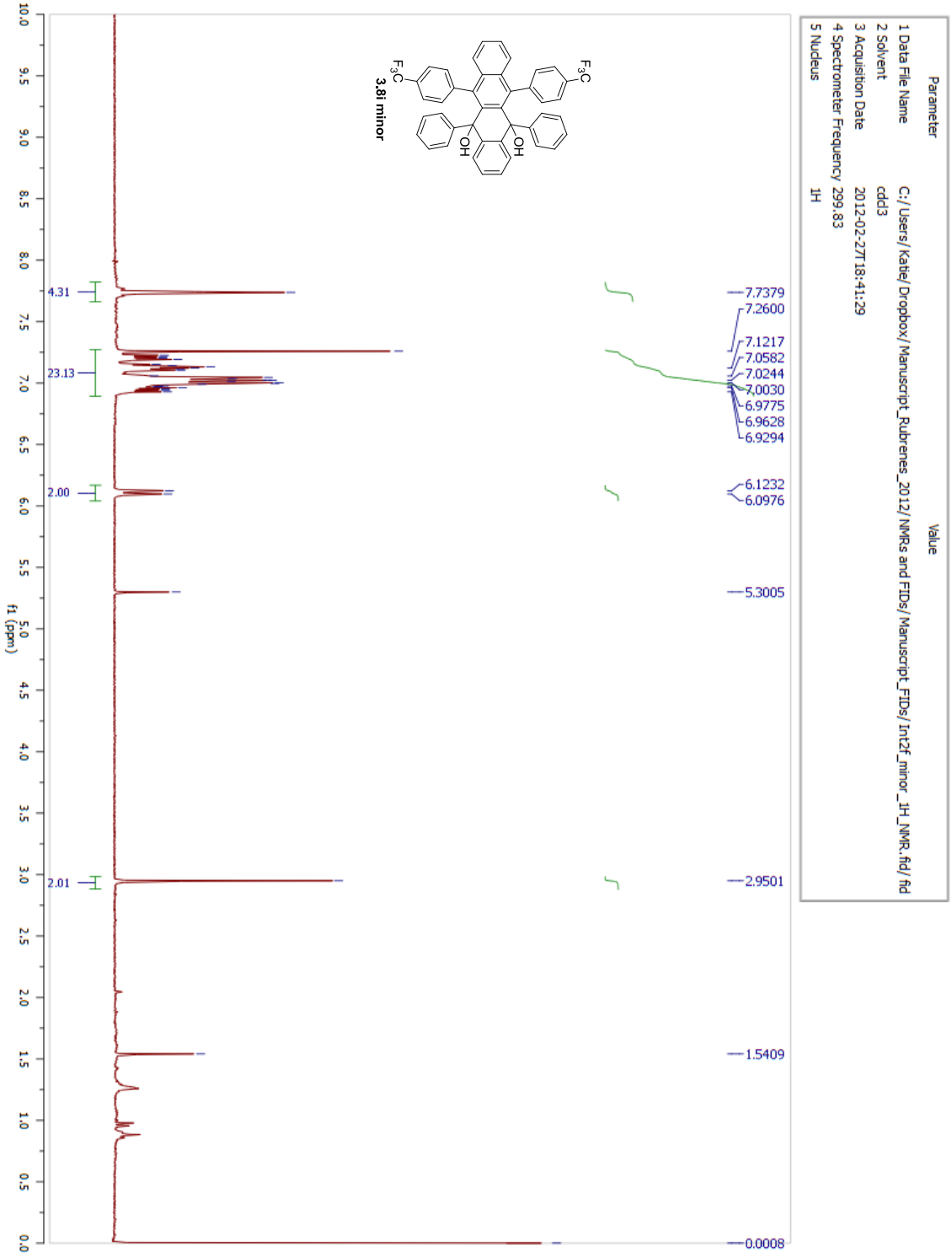
Parameter
Value
1 Data File Name
C:/Users/Katie/Dropbox/Manuscript_Rubrenes_2012/NMRs and FIDs/Manuscript_FIDs/Int2f_minor_1H_NMR.fid/fid
2 Solvent
cdcl3
3 Acquisition Date
2012-02-27T18:41:29
4 Spectrometer Frequency
299.83
5 Nucleus
1H
3.8i minor
F3C
CF3
OH
OH
4.31
23.13
2.00
2.01
7.7379
7.2600
7.1217
7.0582
7.0244
7.0030
6.9775
6.9628
6.9294
6.1232
6.0976
5.3005
2.9501
1.5409
0.0008
f1 (ppm)

Parameter	Value
1 Data File Name	C:/ Users/ Katie/ Dropbox/ Manuscript_Rubrenes_2012/ NMRs and FIDs/ Manuscript_FIDs/ Int2f_minor_19F_NMR.fid/ fid
2 Solvent	cdcl3
3 Acquisition Date	2012-02-27T18:41:51
4 Spectrometer Frequency	282.11
5 Nucleus	19F

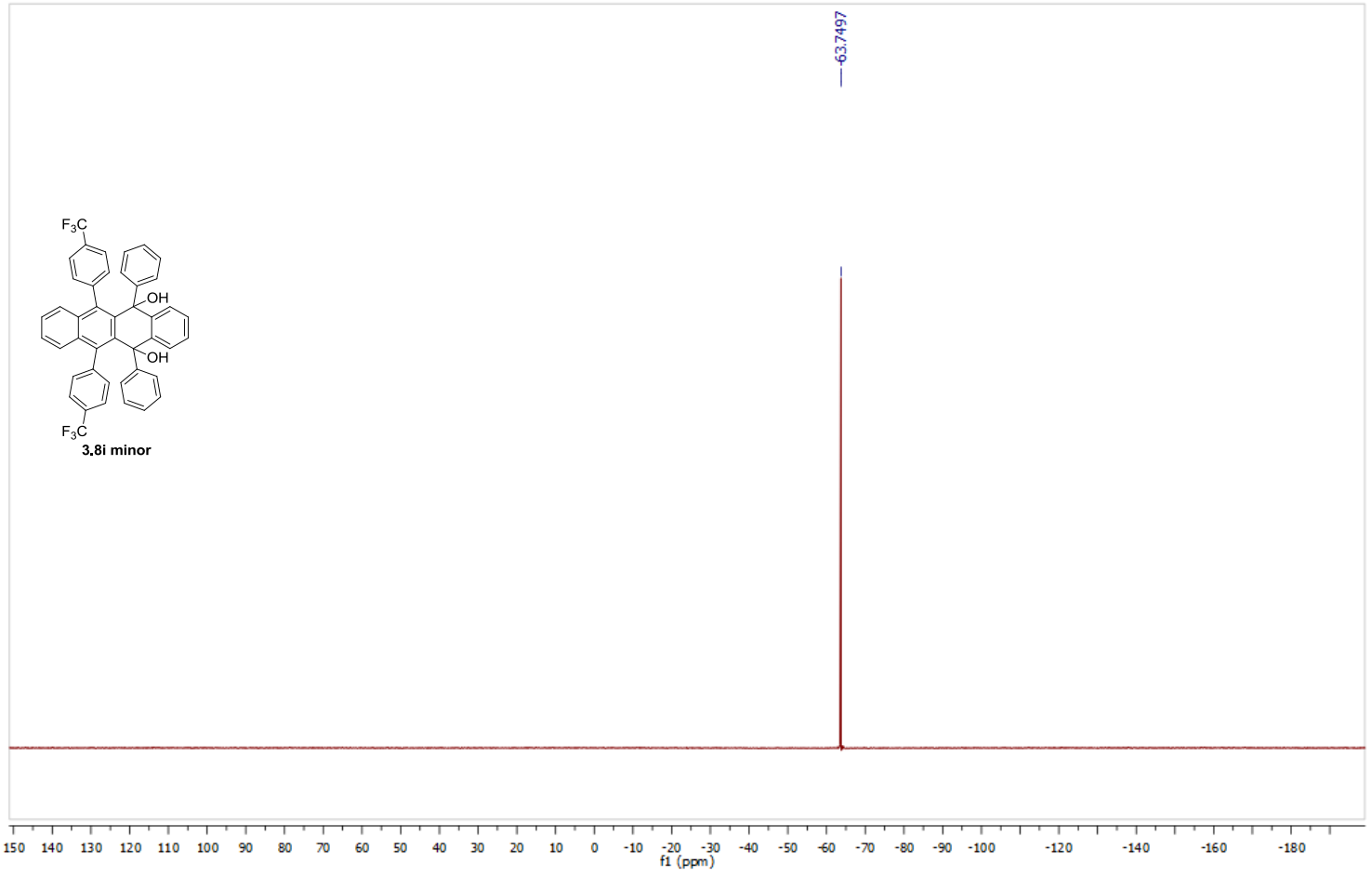

3.8i minor

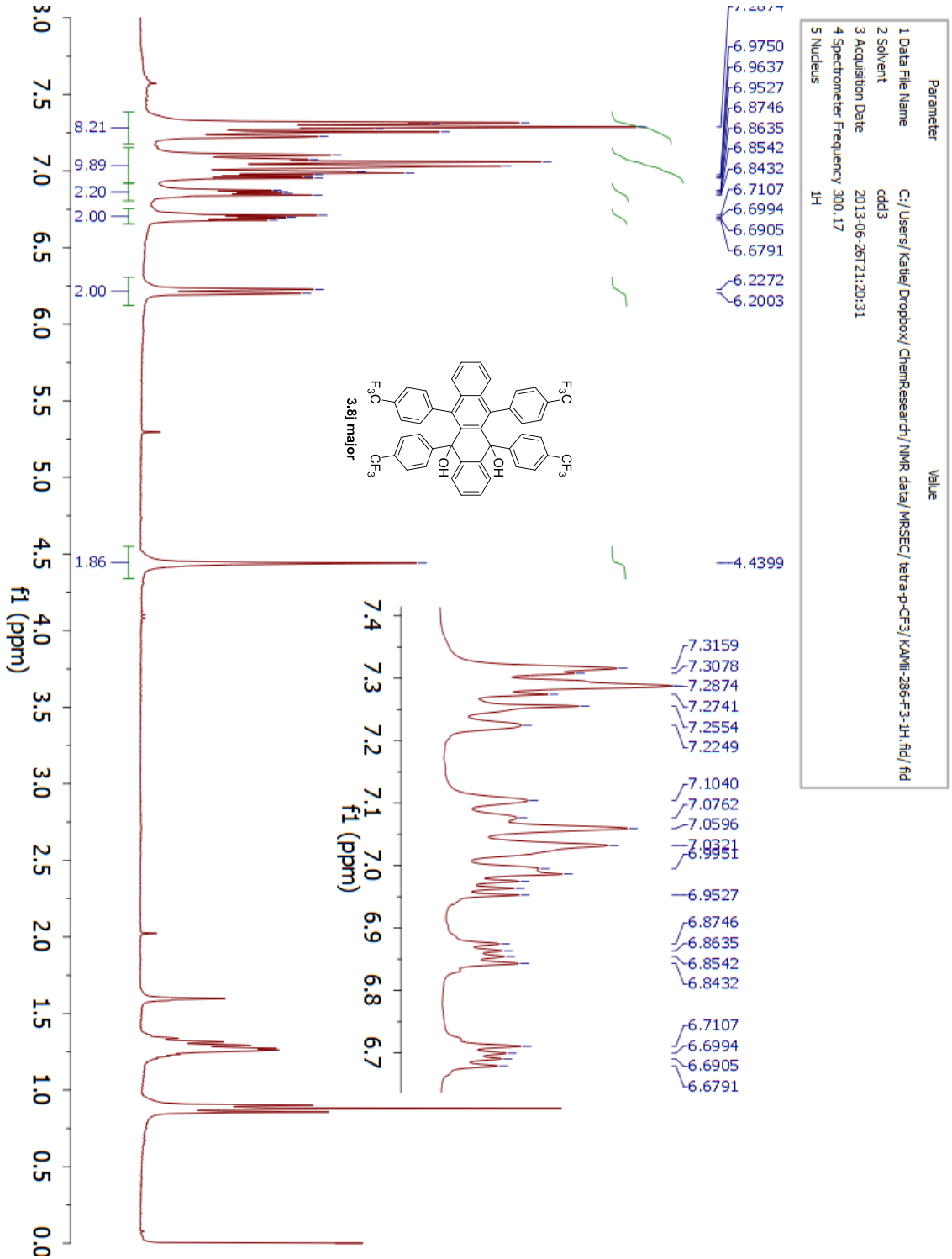
Parameter
Value
1 Data File Name
C:/Users/Katie/Dropbox/ChemResearch/NMR data/MRSEC/tetra-p-CF3/KAMii-286-F3-1H.fid/fid
2 Solvent
cdcl3
3 Acquisition Date
2013-06-26T21:20:31
4 Spectrometer Frequency
300.17
5 Nucleus
1H
3.8j major
8.21
9.89
2.20
2.00
2.00
1.86
6.9750
6.9637
6.9527
6.8746
6.8635
6.8542
6.8432
6.7107
6.6994
6.6905
6.6791
6.2272
6.2003
4.4399
7.3159
7.3078
7.2874
7.2741
7.2554
7.2249
7.1040
7.0762
7.0596
7.0321
6.9951
6.9527
6.8746
6.8635
6.8542
6.8432
6.7107
6.6994
6.6905
6.6791
f1 (ppm)
f1 (ppm)

Parameter	Value
1 Data File Name	C:/ Users/ Katie/ Dropbox/ ChemResearch/ NMR data/ MRSEC/ tetra-p-CF3/ KAMii-286-F3-F19.fid/ fid
2 Owner	cdokam
3 Acquisition Date	2013-06-26T21:21:29
4 Spectrometer Frequency	282.43
5 Nucleus	19F

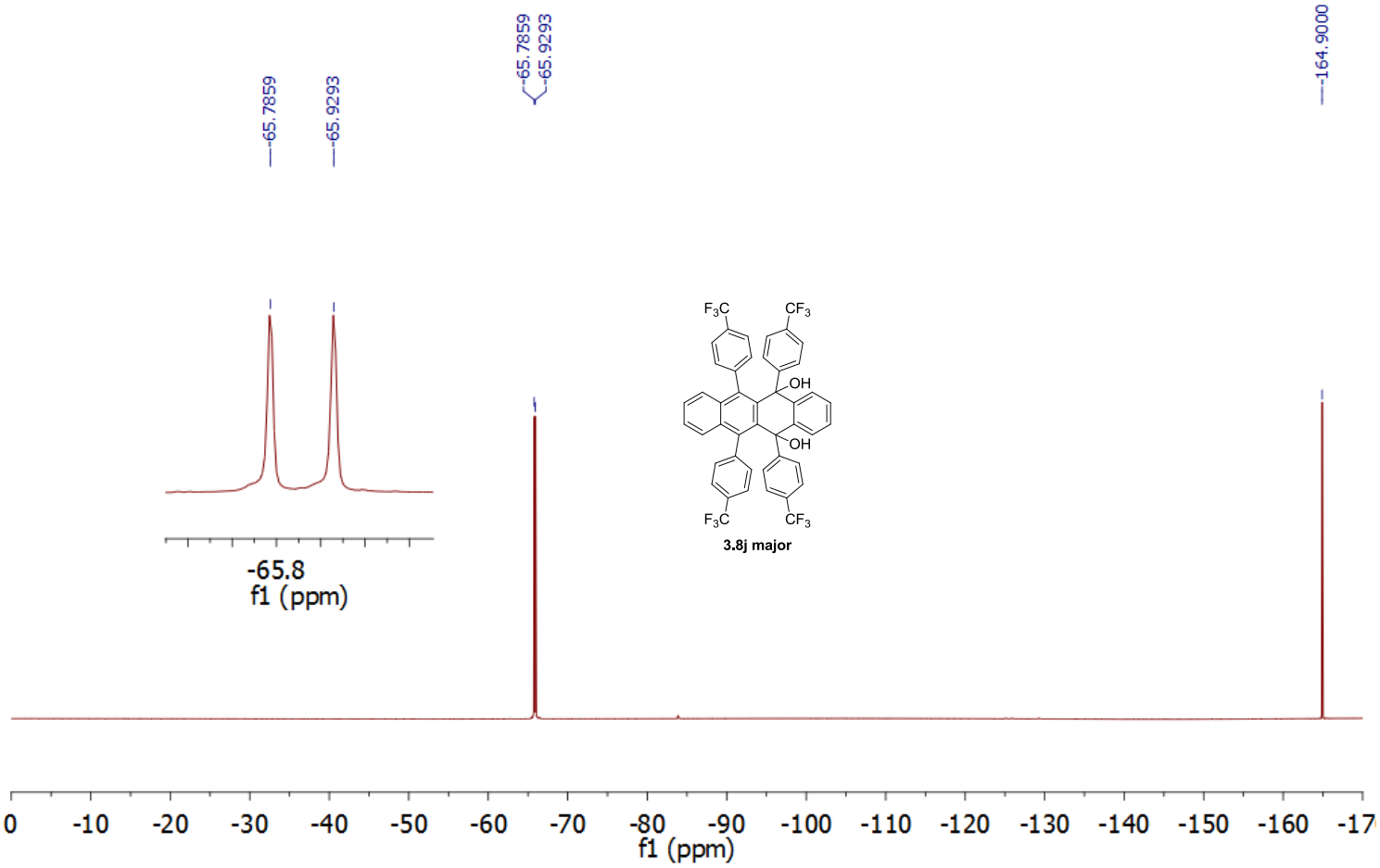

Parameter	Value
1 Data File Name	C:/ Users/ Katie/ Dropbox/ ChemResearch/ NMR data/ MRSEC/ tetra-p-CF3/ KAMii-286-F2-1H.fid/ fid
2 Solvent	cdcl3
3 Acquisition Date	2013-06-26T21:15:53
4 Spectrometer Frequency	300.17
5 Nucleus	1H

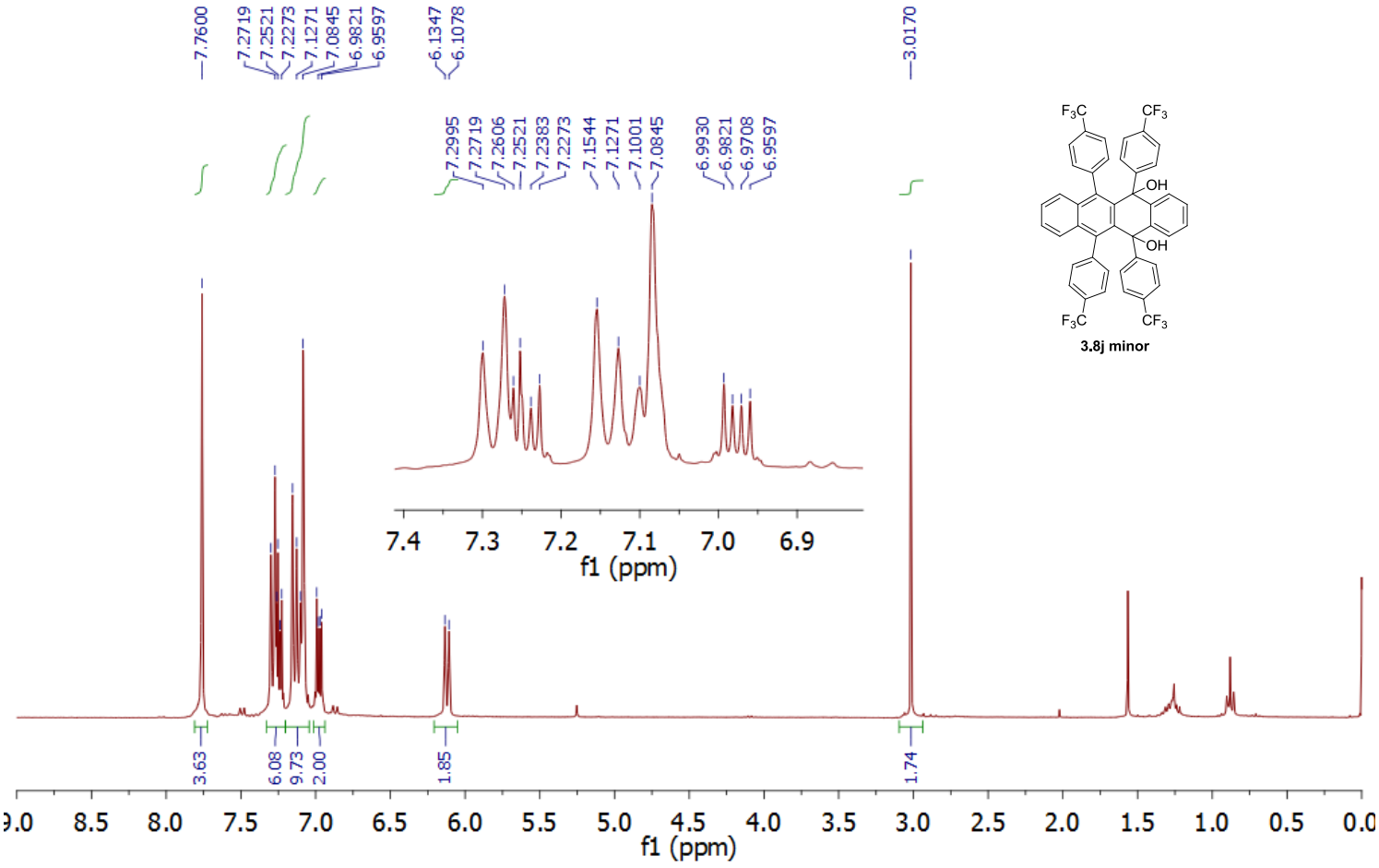

3.8j minor

Parameter	Value
1 Data File Name	C:/ Users/ Katie/ Dropbox/ ChemResearch/ NMR data/ MRSEC/ tetra-p-CF3/ KAMii-286-F2-F19.fid/ fid
2 Solvent	cdcl3
3 Acquisition Date	2013-06-26T21:16:51
4 Spectrometer Frequency	282.43
5 Nucleus	19F

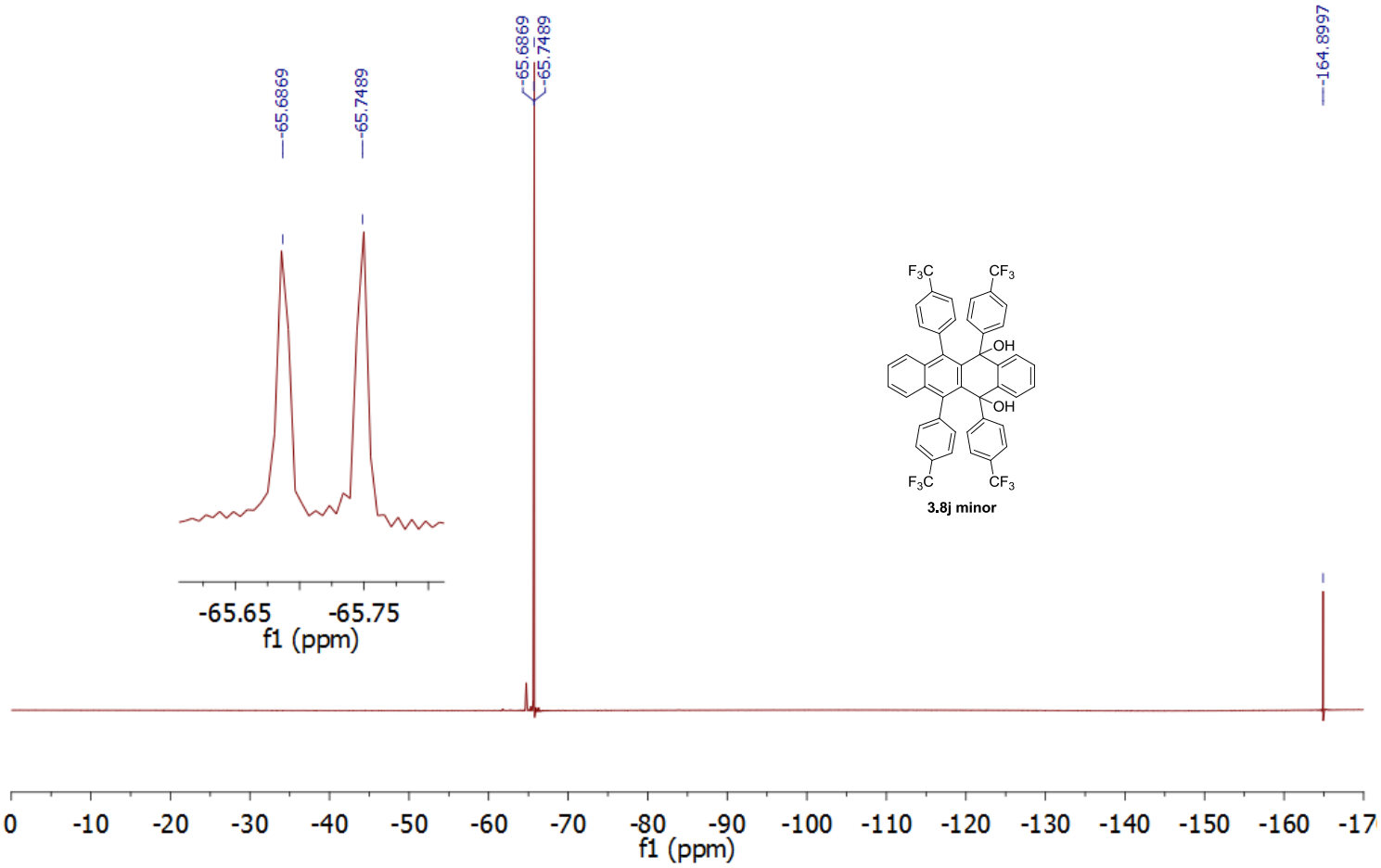

3.8j minor

Parameter	Value
1 Data File Name	C:/ Users/ Katie/ Dropbox/ ChemResearch/ NMR data/ MRSEC/ di-p-CH3/ KAMii-71-F2.fid/ fid
2 Solvent	cdcl3
3 Acquisition Date	2011-11-15T21:19:09
4 Spectrometer Frequency	300.17
5 Nucleus	1H

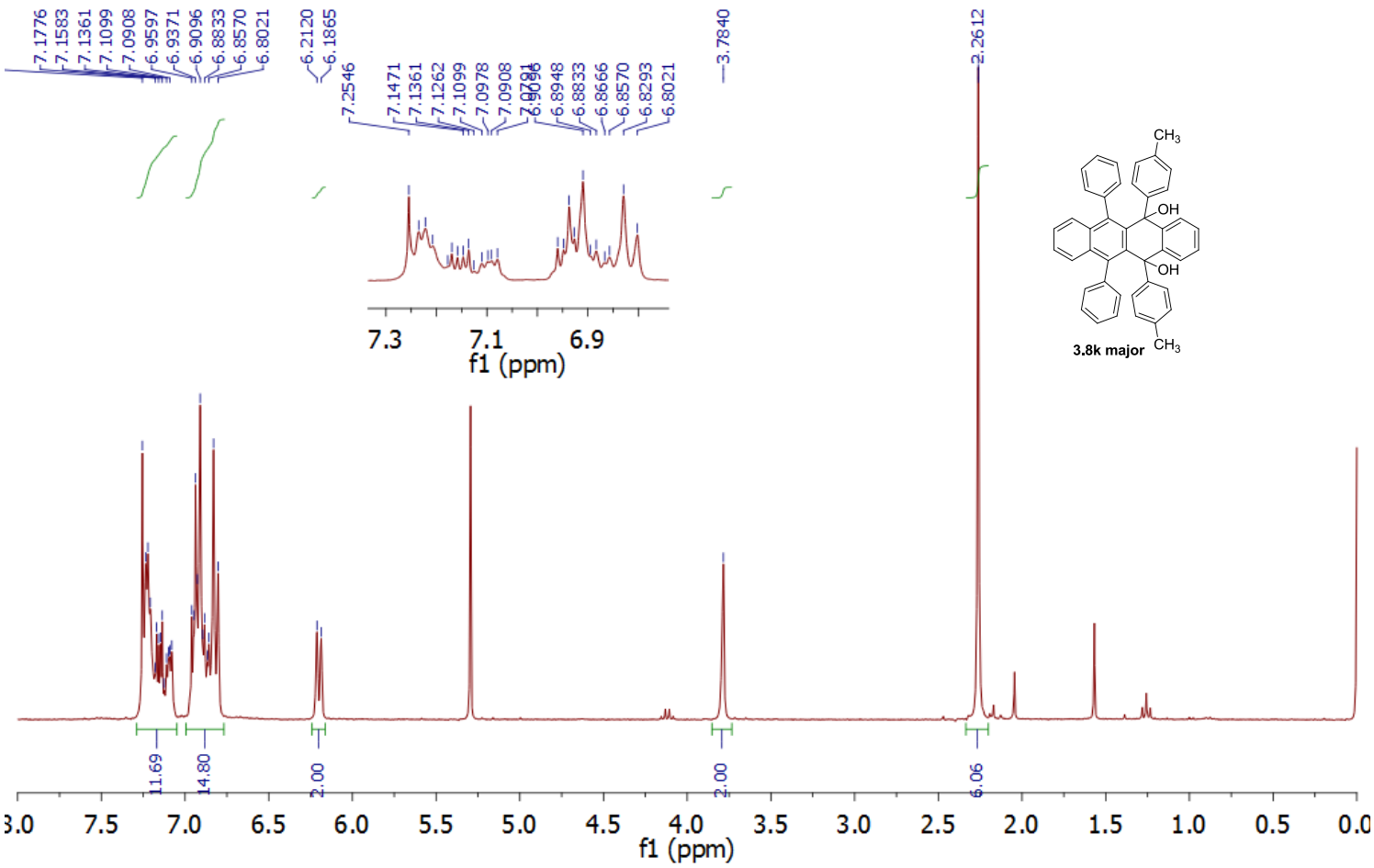

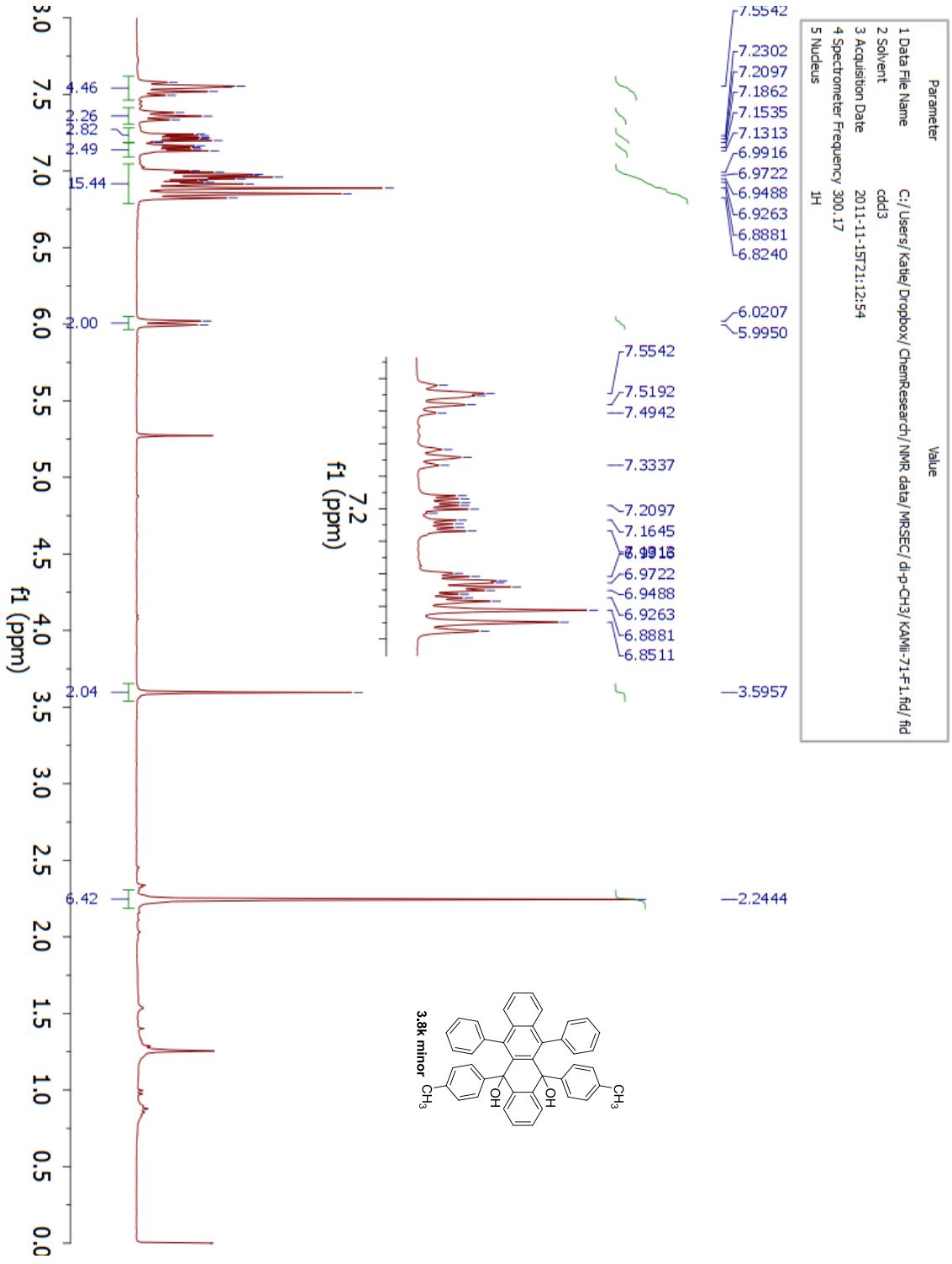
Parameter
Value
1 Data File Name
C:/Users/Katie/Dropbox/ChemResearch/NMR data/MRSEC/di-p-CH3/KAMii-71-F1.fid/fid
2 Solvent
cdcl3
3 Acquisition Date
2011-11-15T21:12:54
4 Spectrometer Frequency
300.17
5 Nucleus
1H
7.5542
7.2302
7.2097
7.1862
7.1535
7.1313
6.9916
6.9722
6.9488
6.9263
6.8881
6.8240
6.0207
5.9950
3.5957
2.2444
4.46
2.26
2.82
2.49
15.44
2.00
2.04
6.42
f1 (ppm)
7.2
3.8k minor
CH3
OH
OH
CH3

Parameter	Value
1 Data File Name	C:/ Users/ Katie/ Dropbox/ ChemResearch/ NMR data/ MRSEC/ di-p-CF3/ KAMii-130-F3-hexwash-040412.fid/ fid
2 Solvent	cdcl3
3 Acquisition Date	2012-04-04T16:57:00
4 Spectrometer Frequency	300.17
5 Nucleus	1H

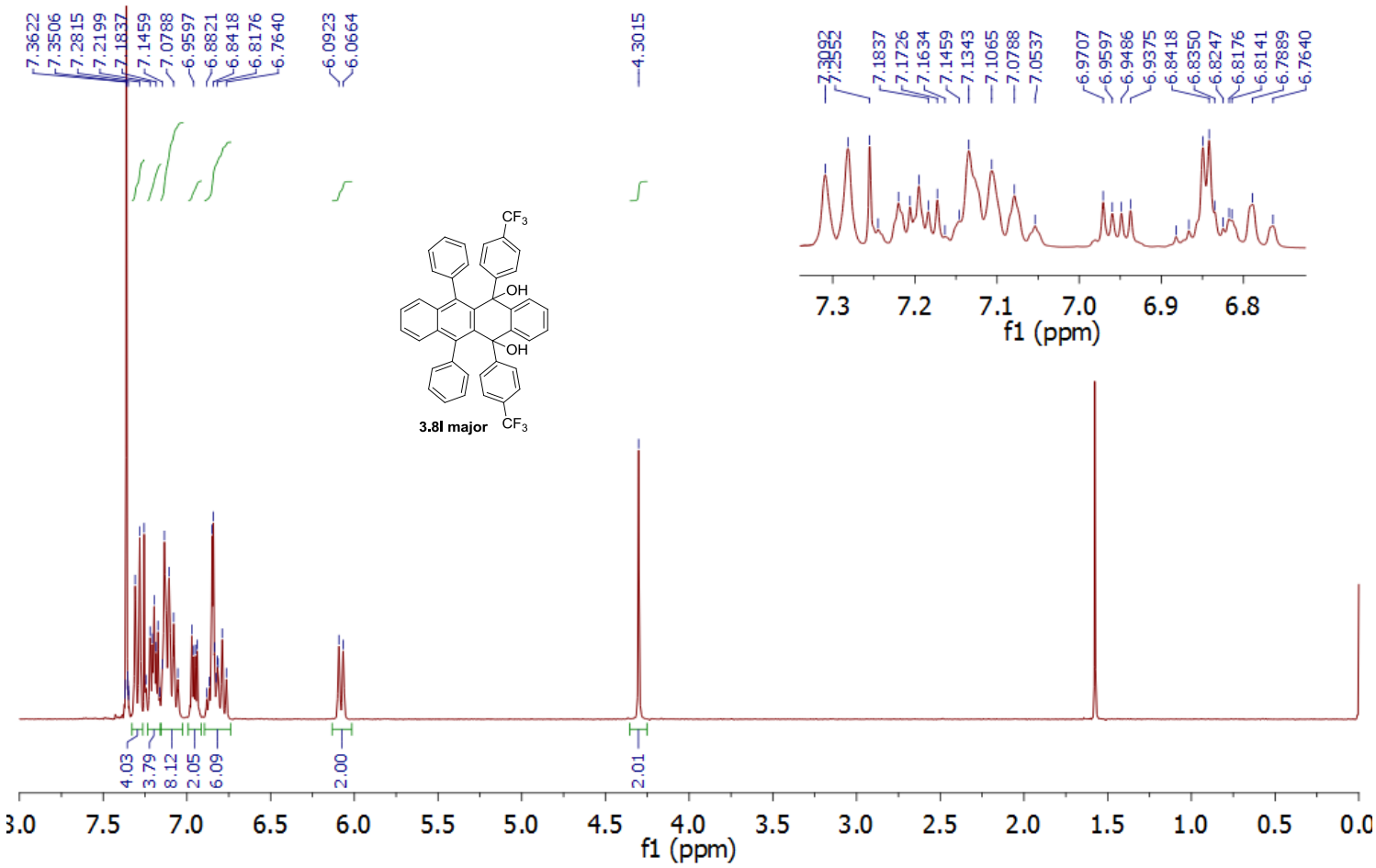

Parameter	Value
1 Data File Name	C:/ Users/ Katie/ Dropbox/ ChemResearch/ NMR data/ MRSEC/ di-p-CF3/ KAMii-130-F2-hexwash-040412.fid/ fid
2 Solvent	cdcl3
3 Acquisition Date	2012-04-04T17:01:17
4 Spectrometer Frequency	300.17
5 Nucleus	1H

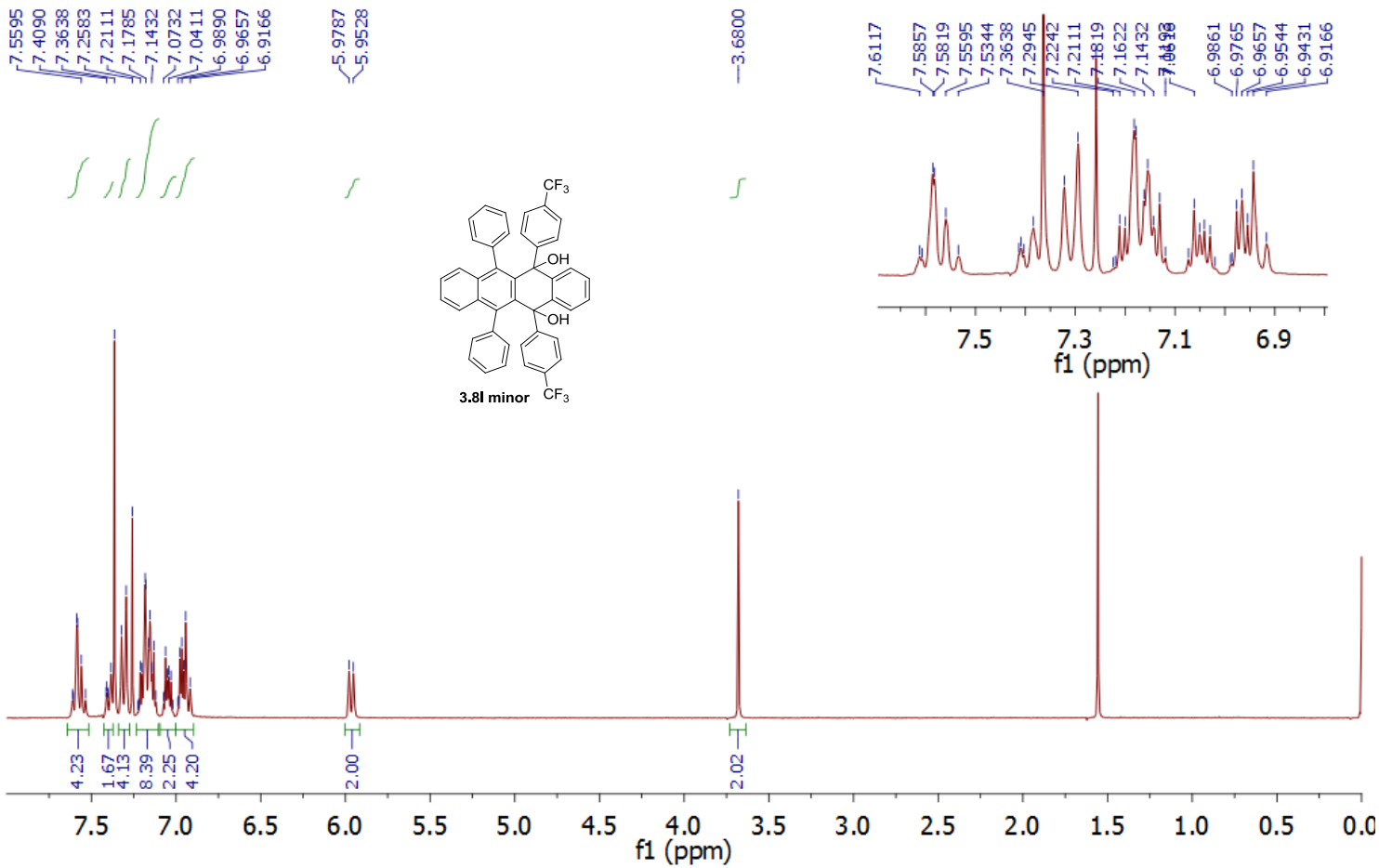

Parameter	Value
1 Data File Name	C:/ Users/ Katie/ Dropbox/ ChemResearch/ NMR data/ MRSEC/ tetra-p-ethyl/ KAMi-211-c1f1.fid/ fid
2 Solvent	cdcl3
3 Acquisition Date	2010-11-11T23:32:52
4 Spectrometer Frequency	300.17
5 Nucleus	1H

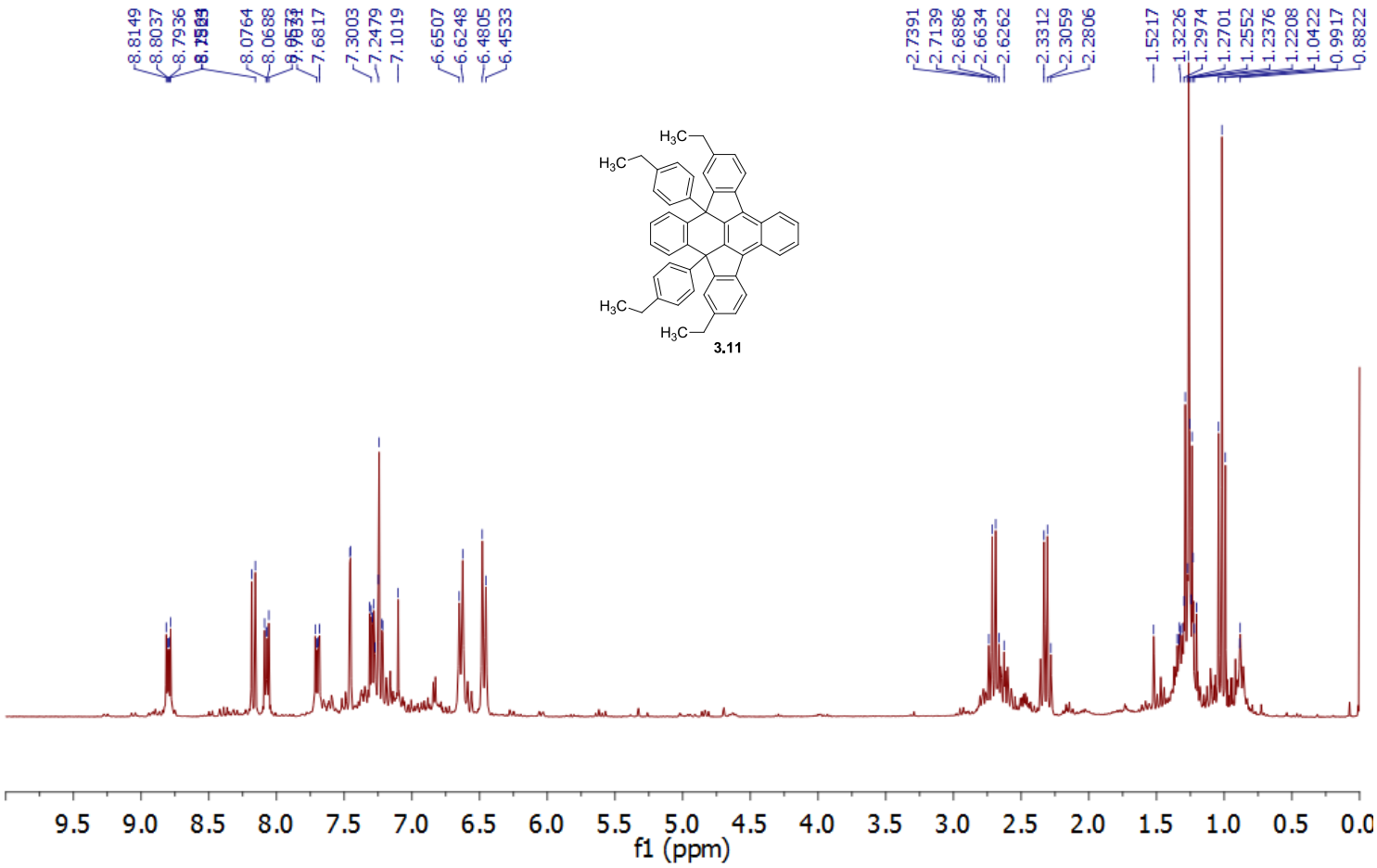

Parameter	Value
1 Data File Name	C:/ Users/ Katie/ Dropbox/ ChemResearch/ NMR data/ MRSEC/ Unknown/ KAMi-211c-1H.fid/ fid
2 Solvent	cdcl3
3 Acquisition Date	2010-12-14T14:24:01
4 Spectrometer Frequency	499.87
5 Nucleus	1H

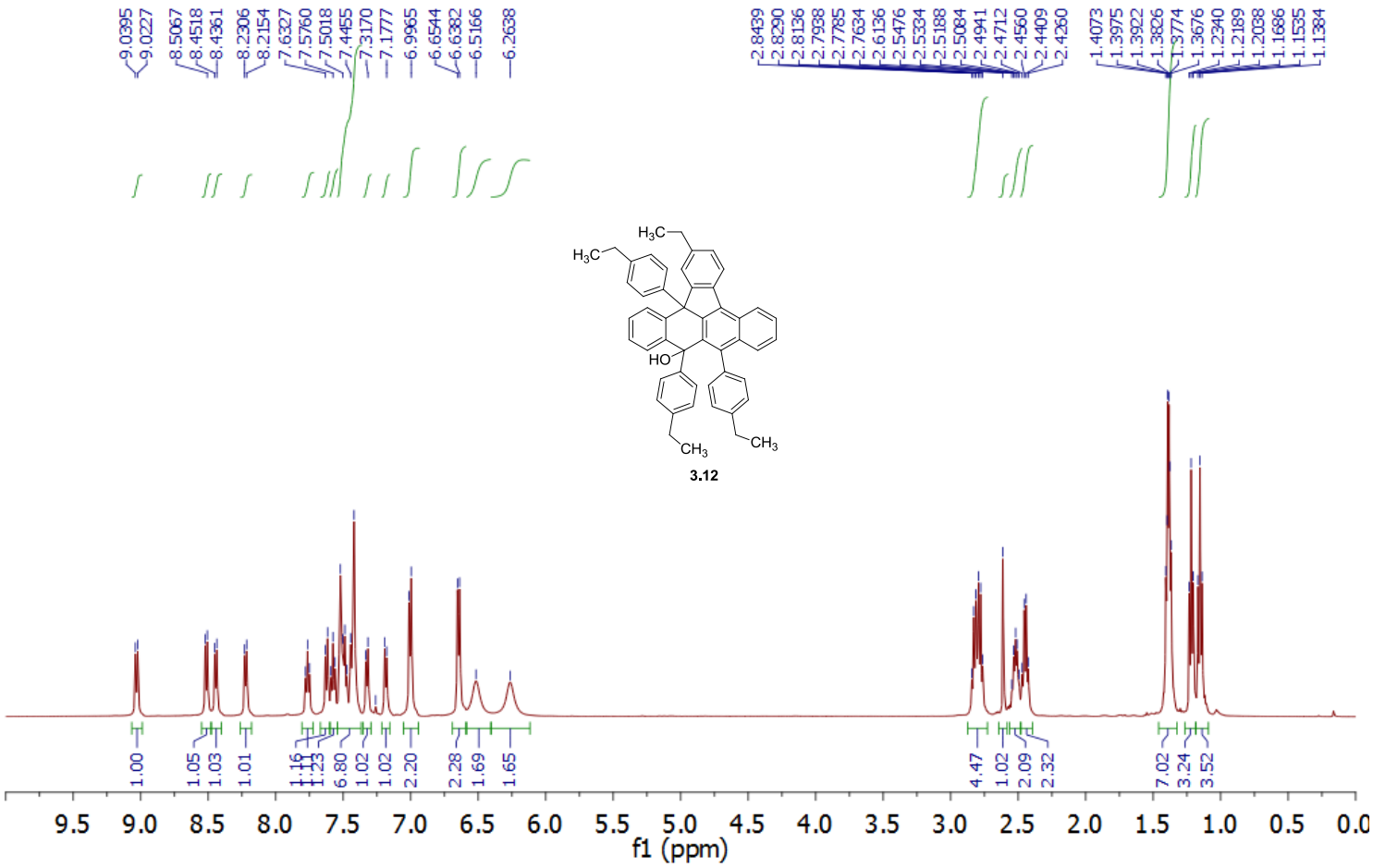

Parameter	Value
1 Data File Name	C:/ Users/ Katie/ Dropbox/ ChemResearch/ NMR data/ MRSEC/ Unknown/ KAMi-211c-13C.fid/ fid
2 Solvent	cdcl3
3 Acquisition Date	2010-12-14T14:24:32
4 Spectrometer Frequency	125.70
5 Nucleus	13C

153.3389
146.6547
137.2412
136.0653
134.8275
127.0202
126.8319
126.6921
126.6392
126.5766
126.2200
126.1264
125.1454
123.6473
123.1250
78.8256
77.2544
77.0000
76.7456
59.5570
28.9245
28.4685
28.1518
27.9906
15.6532
15.1877
15.1558

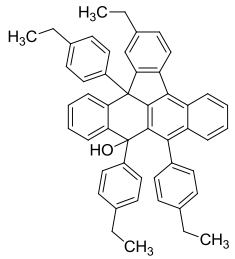

3.12

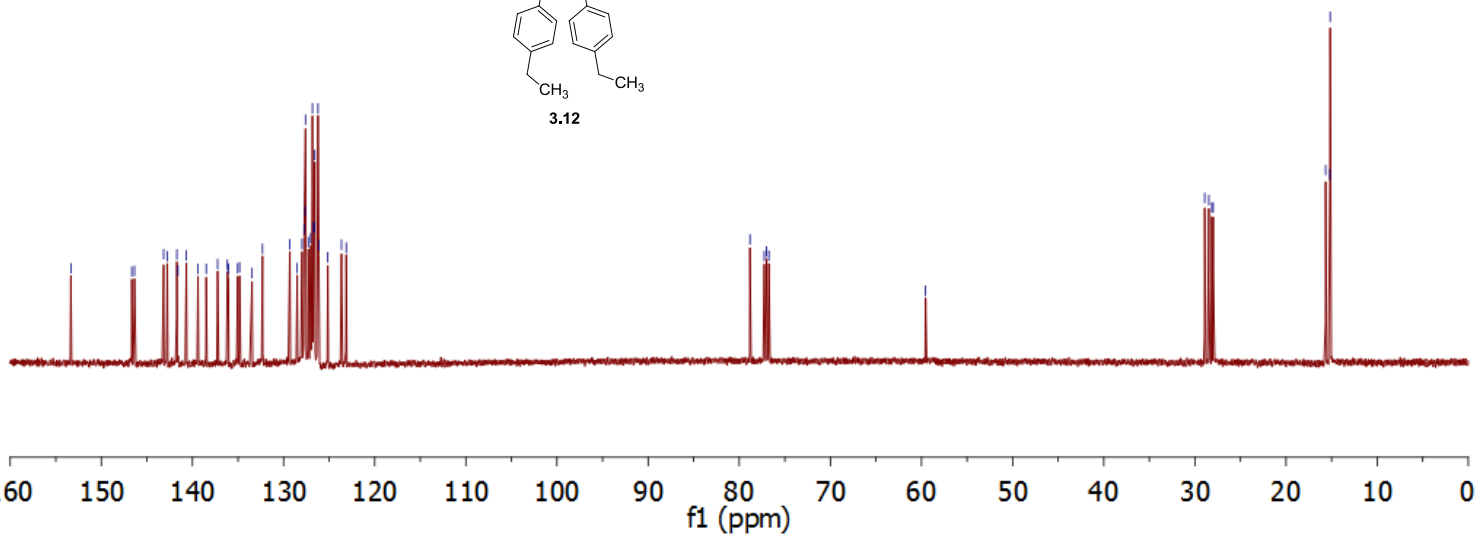

COSY

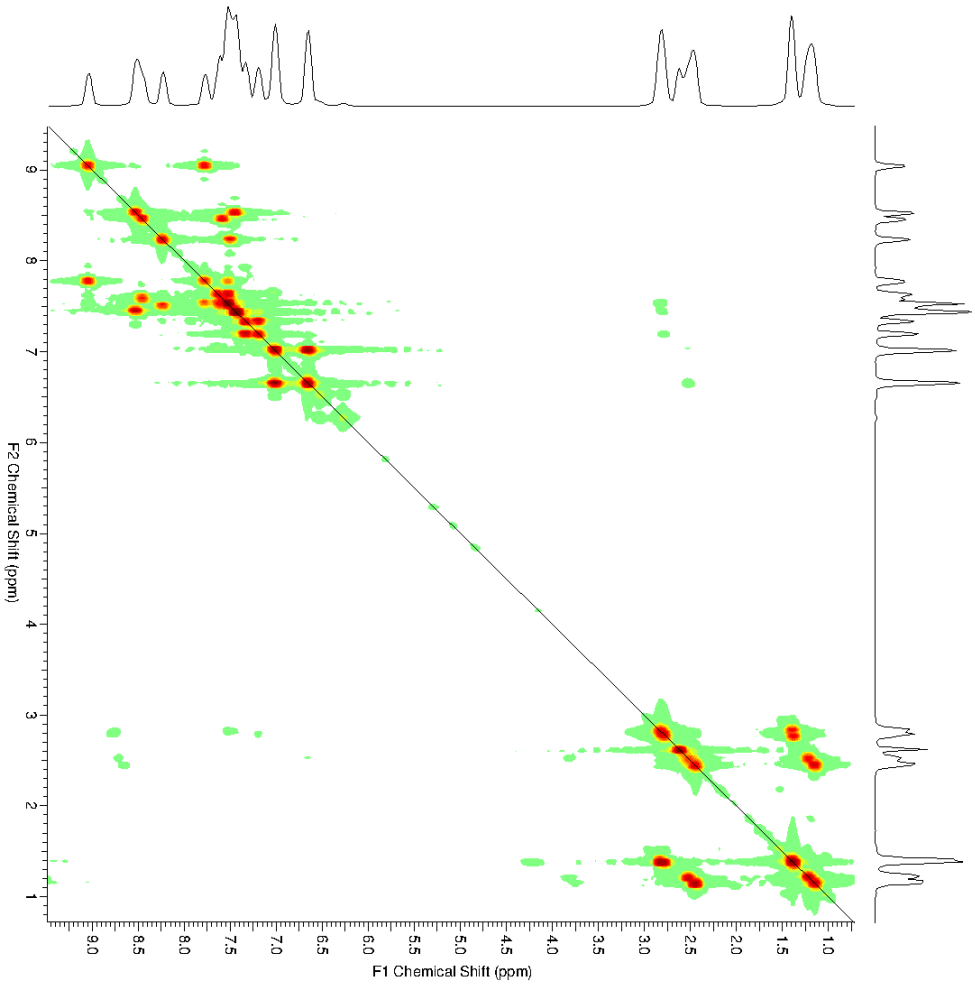
F2 Chemical Shift (ppm)
F1 Chemical Shift (ppm)
HO
CH3
CH3
H3C
H3C

3.12

HMQC

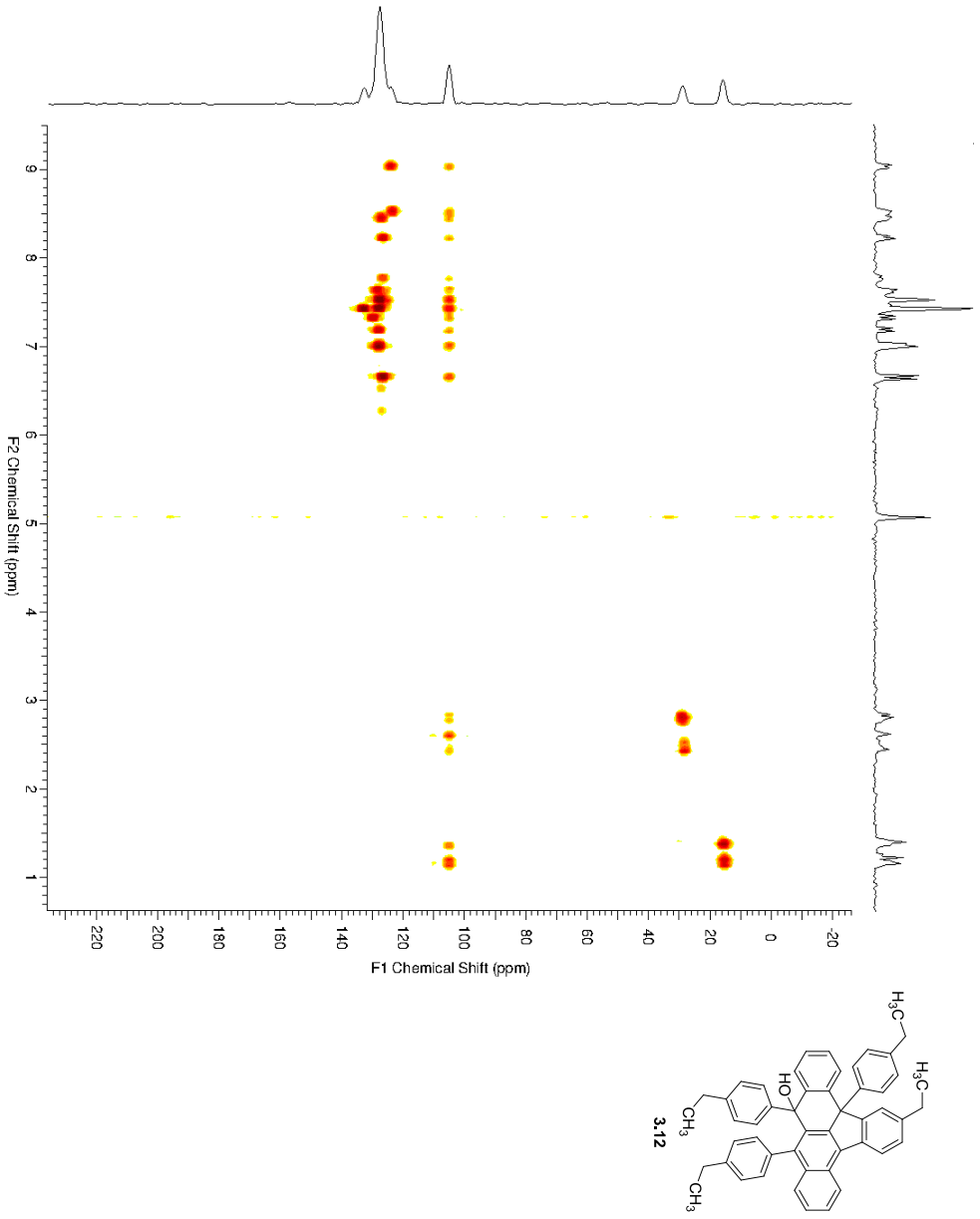
F2 Chemical Shift (ppm)
F1 Chemical Shift (ppm)
HO
H3C
H3C
CH3
CH3
3.12

DEPT

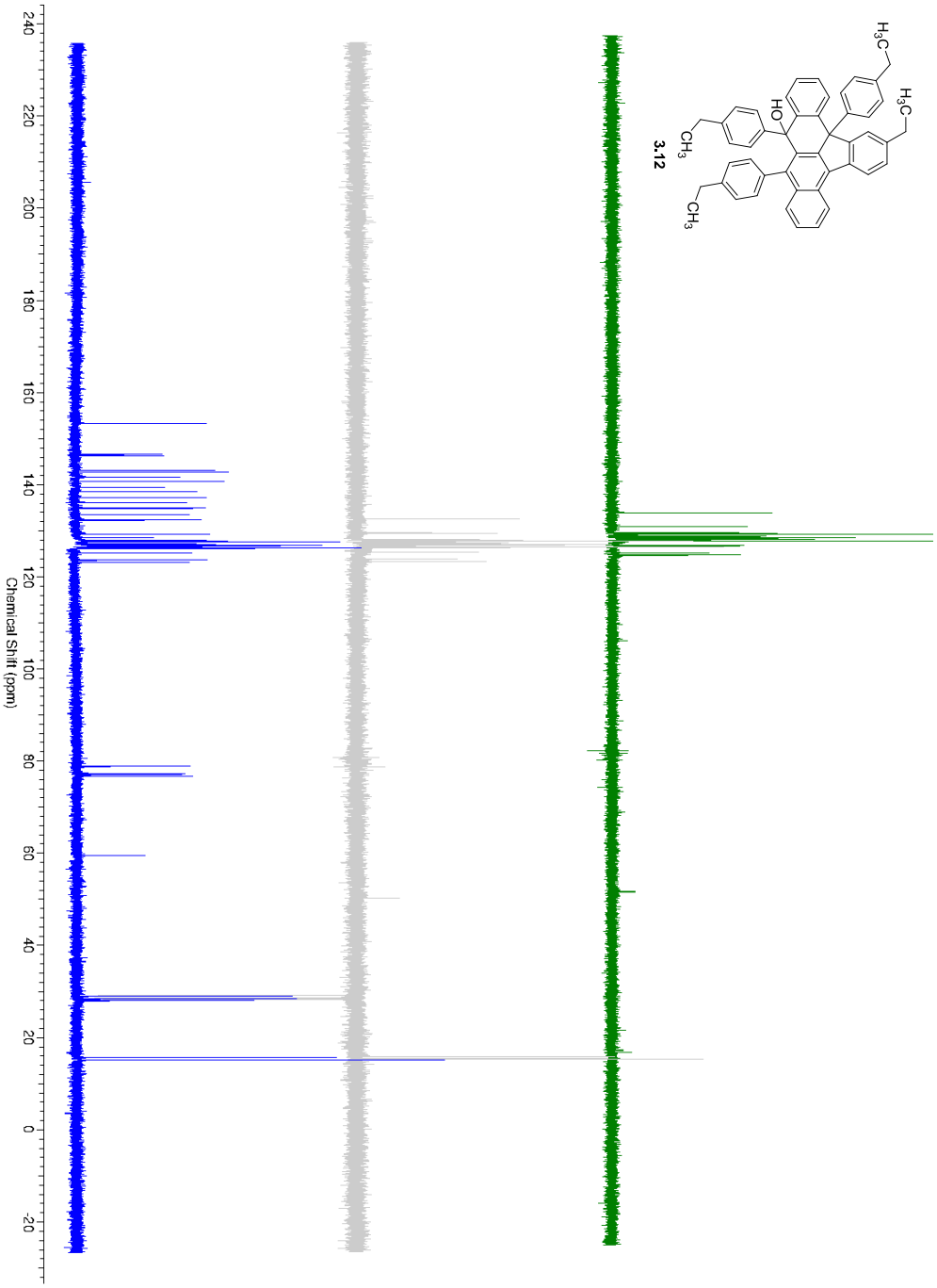
Chemical Shift (ppm)
240
220
200
180
160
140
120
100
80
60
40
20
0
-20
HO
CH3
CH3
H3C
H3C
3.12

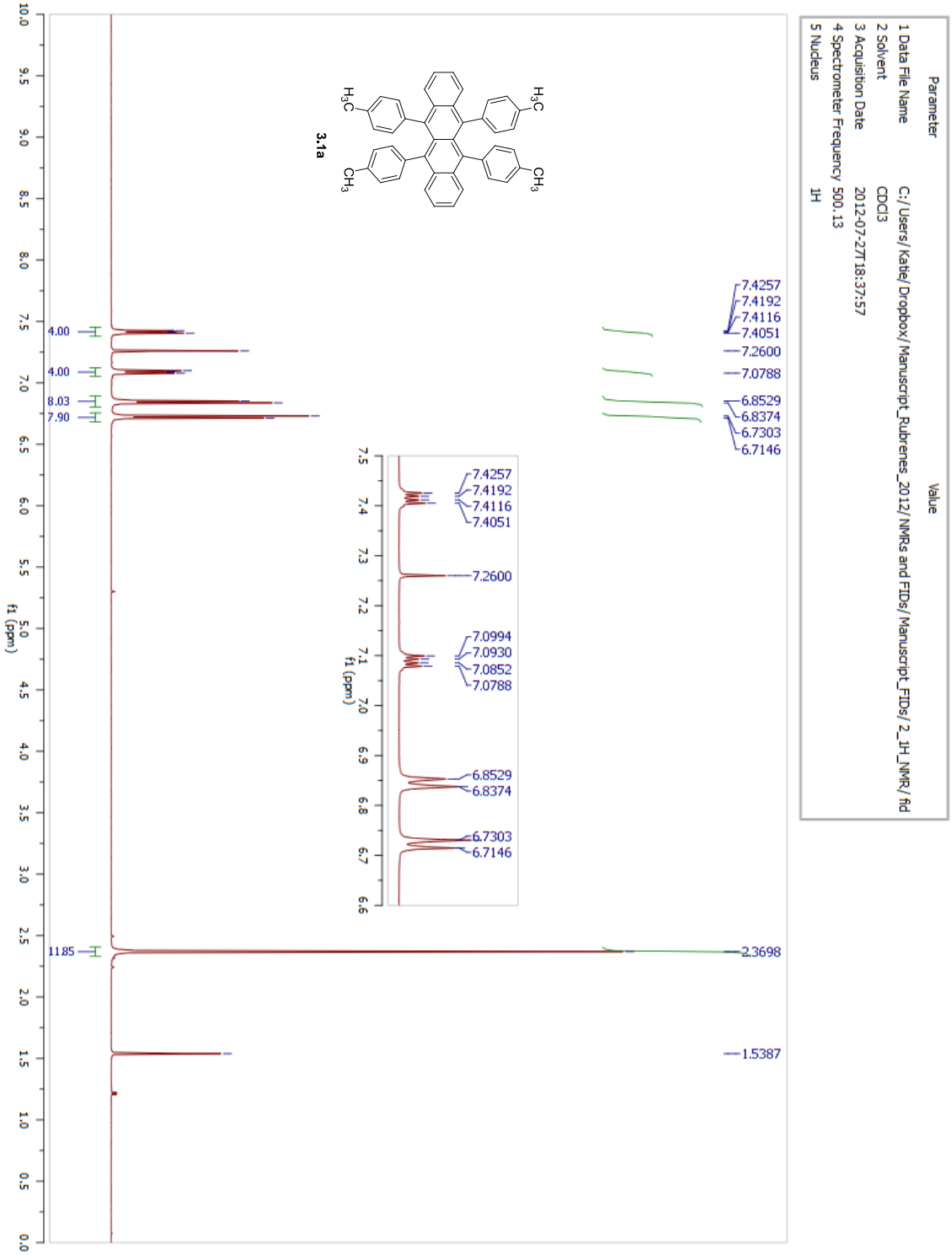
Parameter
Value
1 Data File Name
C:/Users/Katie/Dropbox/Manuscript_Rubrenes_2012/NMRs and FIDs/Manuscript_FIDs/2_1H_NMR/fid
2 Solvent
CDCl3
3 Acquisition Date
2012-07-27T18:37:57
4 Spectrometer Frequency
500.13
5 Nucleus
1H
3.1a
H3C
CH3
7.4257
7.4192
7.4116
7.4051
7.2600
7.0788
6.8529
6.8374
6.7303
6.7146
7.0994
7.0930
7.0852
4.00
4.00
8.03
7.90
11.85
2.3698
1.5387
f1 (ppm)

Parameter	Value
1 Data File Name	C:/ Users/ Katie/ Dropbox/ Manuscript_Rubrenes_2012/ NMRs and FIDs/ Manuscript_FIDs/ 2_13C_NMR/ fid
2 Solvent	CDCl3
3 Acquisition Date	2012-07-27T18:41:03
4 Spectrometer Frequency	125.76
5 Nucleus	13C

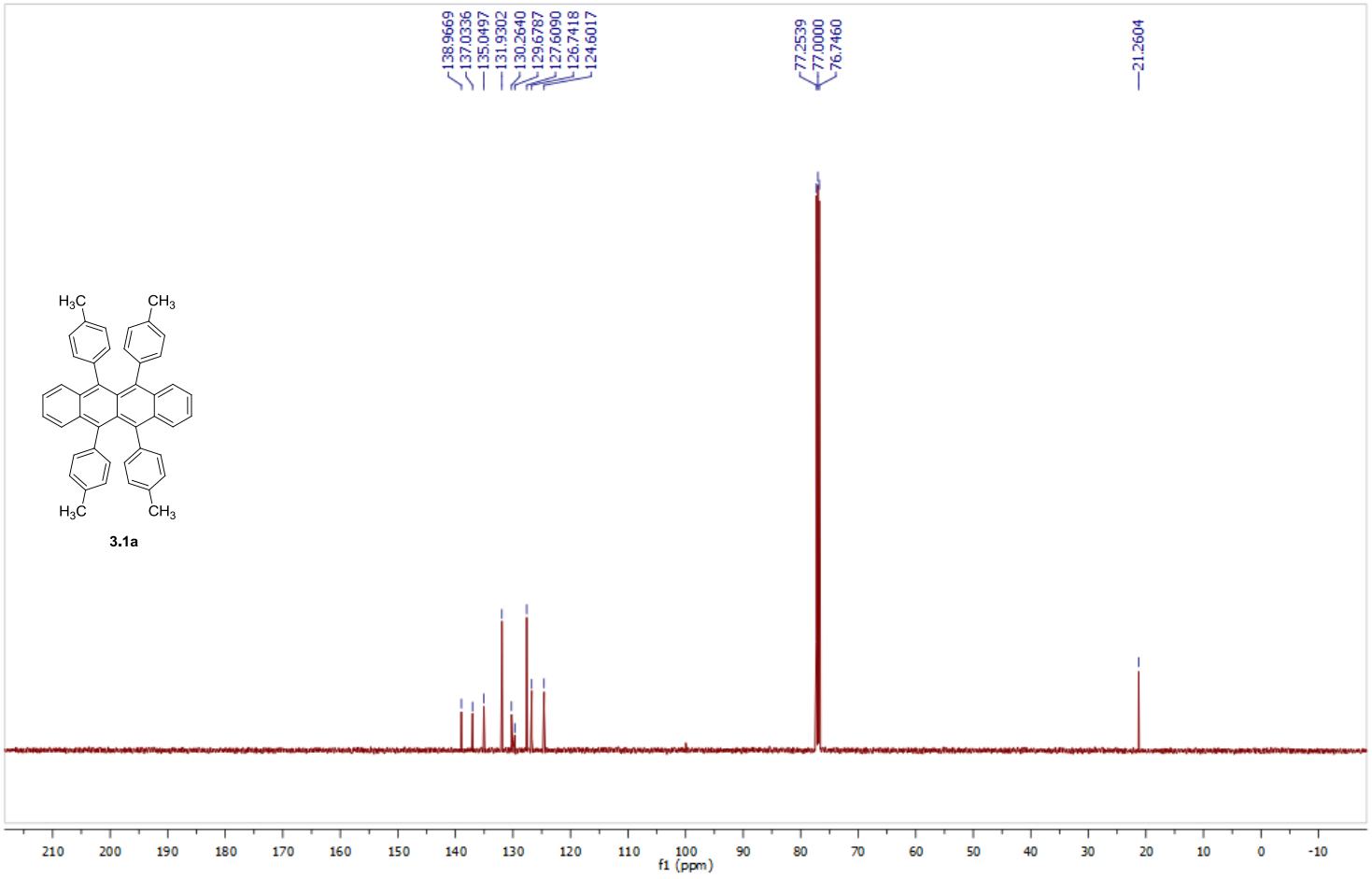

Parameter	Value
1 Data File Name	C:/ Users/ Katie/ Dropbox/ ChemResearch/ NMR data/ MRSEC/ tetra-m-methyl/ KAM-mMR-062313/ 2/ fid
2 Solvent	CDCl3
3 Acquisition Date	2013-06-23T15:20:41
4 Spectrometer Frequency	500.13
5 Nucleus	1H

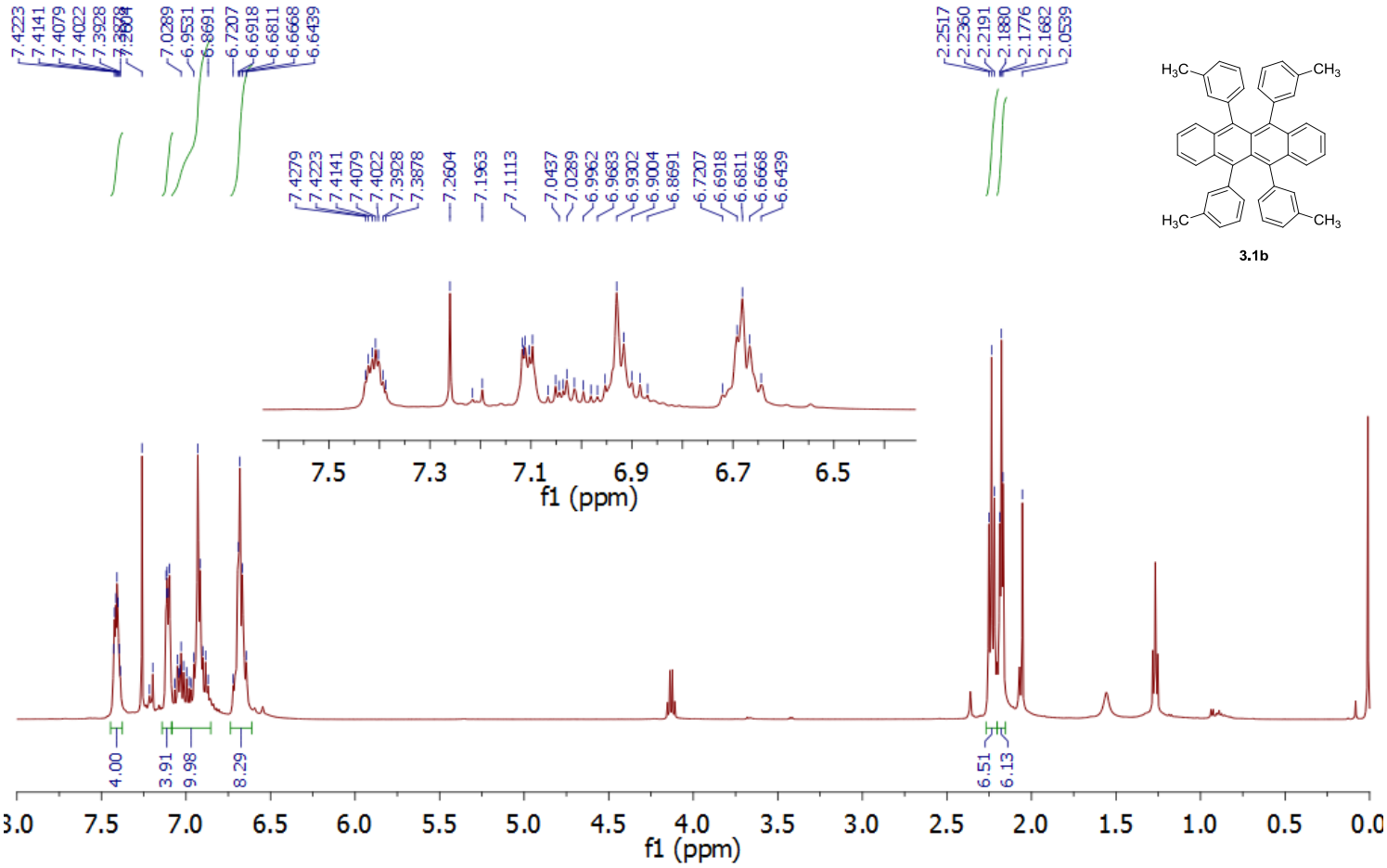

3.1b

Parameter	Value
1 Data File Name	C:/ Users/ Katie/ Dropbox/ ChemResearch/ NMR data/ MRSEC/ tetra-m-methyl/ KAM-mMR-062313/ 3/ fid
2 Solvent	CDCl3
3 Acquisition Date	2013-06-23T15:23:19
4 Spectrometer Frequency	125.76
5 Nucleus	13C

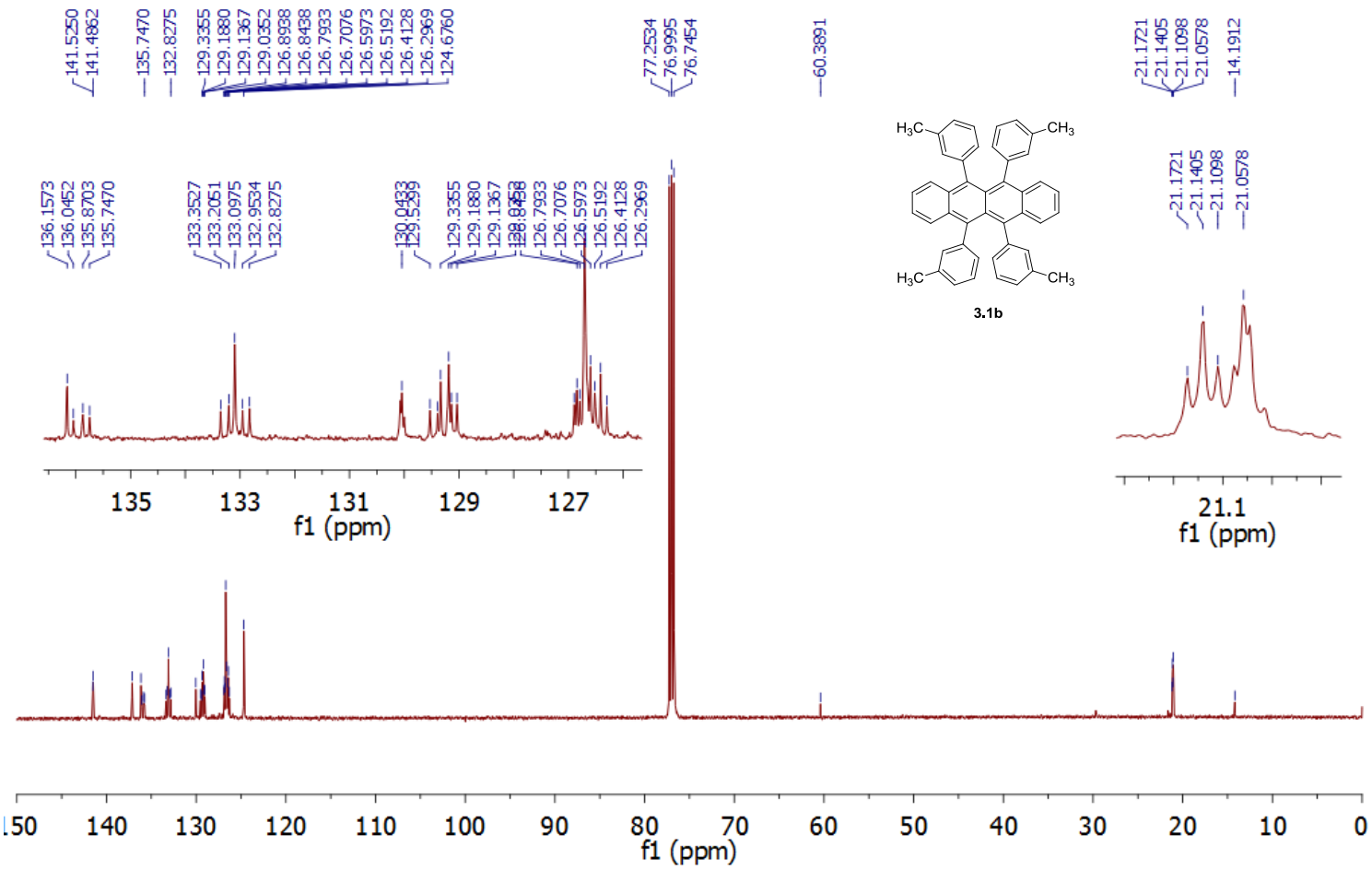

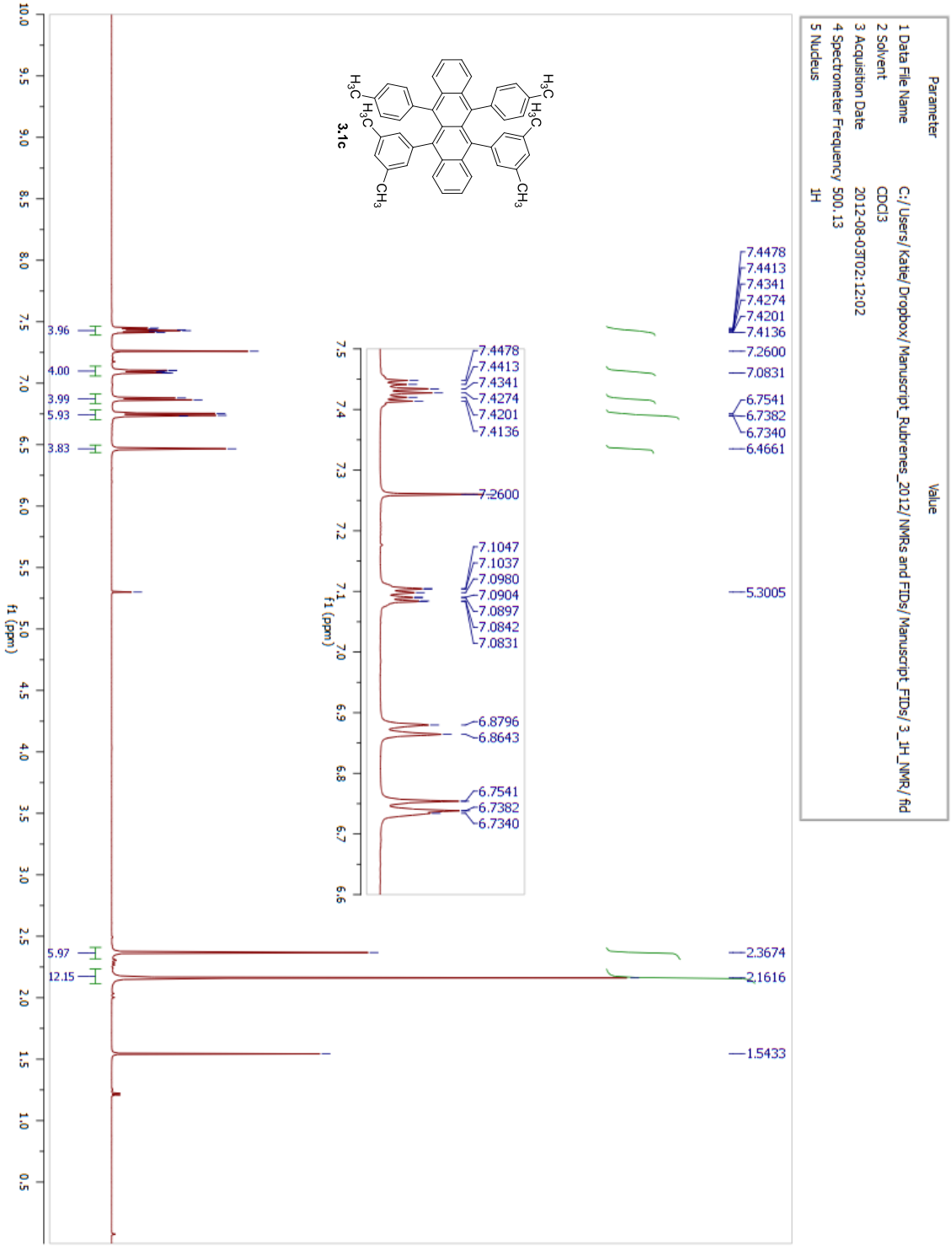
Parameter
Value
1 Data File Name
C:/Users/Katie/Dropbox/Manuscript_Rubrenes_2012/NMRs and FIDs/Manuscript_FIDs/3_1H_NMR/fid
2 Solvent
CDCl3
3 Acquisition Date
2012-08-03T02:12:02
4 Spectrometer Frequency
500.13
5 Nucleus
1H
3.1c
f1 (ppm)
7.4478
7.4413
7.4341
7.4274
7.4201
7.4136
7.2600
7.0831
6.7541
6.7382
6.7340
6.4661
5.3005
2.3674
2.1616
1.5433
7.1047
7.1037
7.0980
7.0904
7.0897
7.0842
7.0831
6.8796
6.8643
3.96
4.00
3.99
5.93
3.83
5.97
12.15

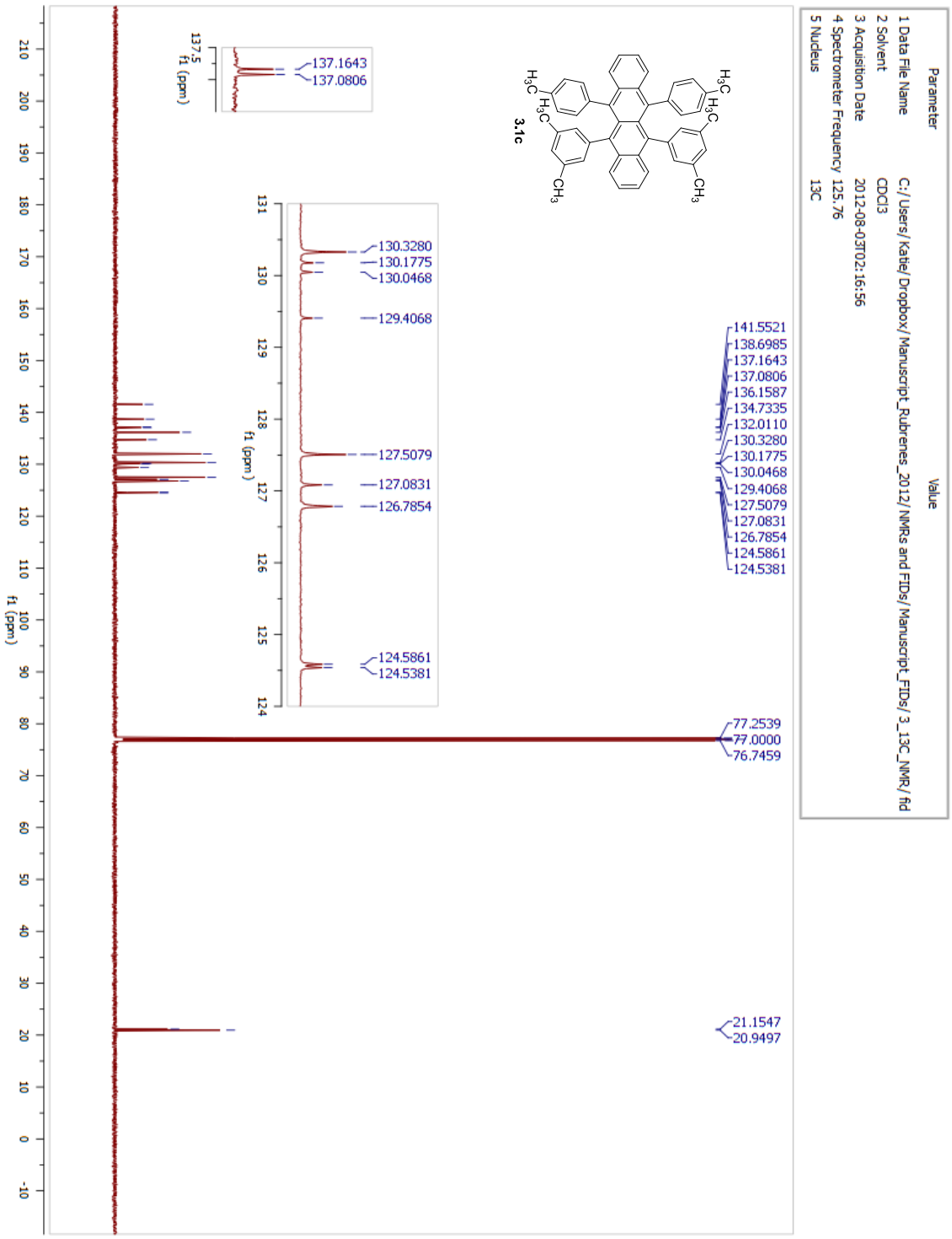
Parameter
Value
1 Data File Name
C:/Users/Katie/Dropbox/Manuscript_Rubrenes_2012/NMRs and FIDs/Manuscript_FIDs/3_13C_NMR/fid
2 Solvent
CDCl3
3 Acquisition Date
2012-08-03T02:16:56
4 Spectrometer Frequency
125.76
5 Nucleus
13C
3.1c
141.5521
138.6985
137.1643
137.0806
136.1587
134.7335
132.0110
130.3280
130.1775
130.0468
129.4068
127.5079
127.0831
126.7854
124.5861
124.5381
77.2539
77.0000
76.7459
21.1547
20.9497
f1 (ppm)

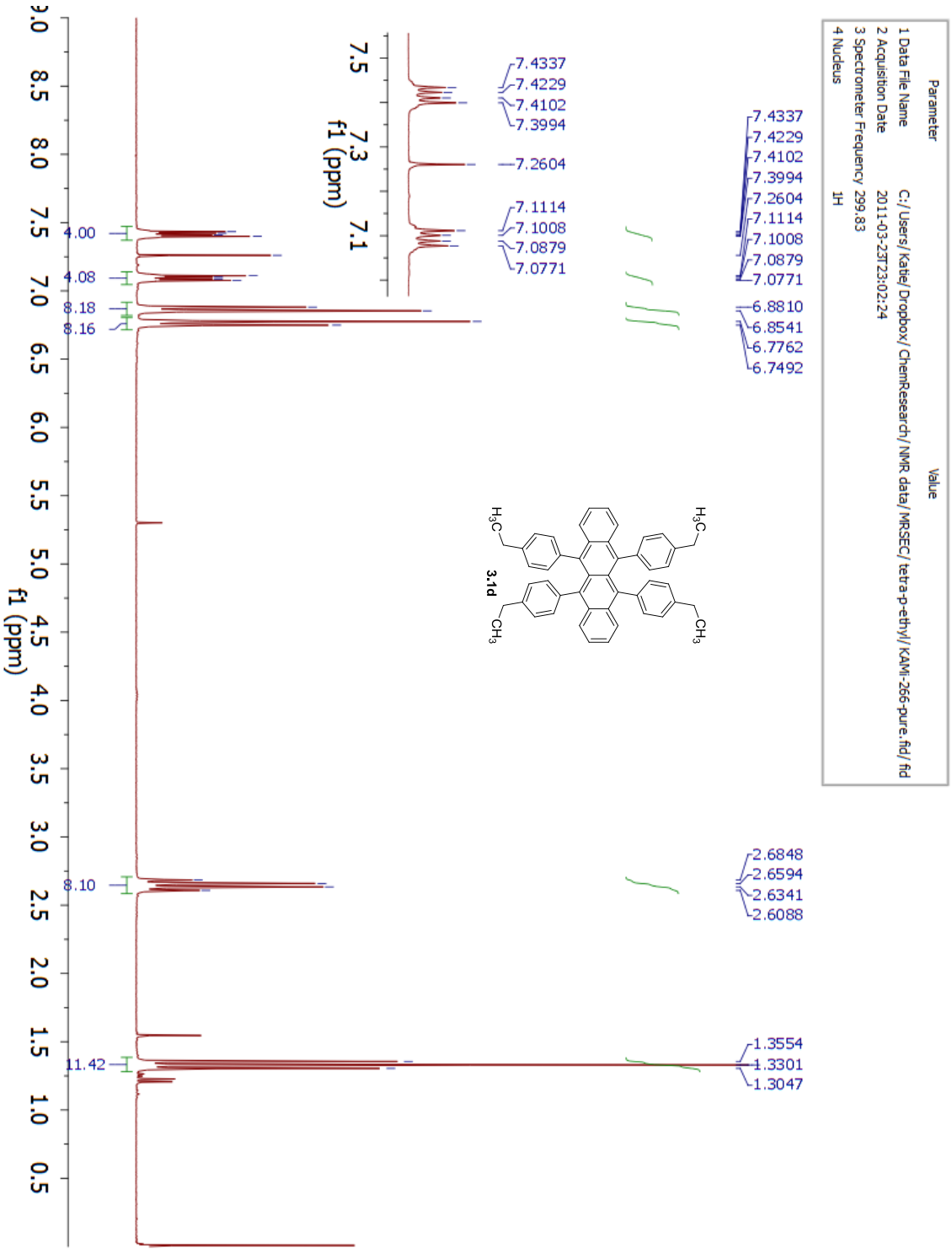
Parameter
Value
1 Data File Name
C:/Users/Katie/Dropbox/ChemResearch/NMR data/MRSEC/tetra-p-ethyl/KAMI-266-pure.fid/fid
2 Acquisition Date
2011-03-23T23:02:24
3 Spectrometer Frequency 299.83
4 Nucleus
1H
7.4337
7.4229
7.4102
7.3994
7.2604
7.1114
7.1008
7.0879
7.0771
6.8810
6.8541
6.7762
6.7492
2.6848
2.6594
2.6341
2.6088
1.3554
1.3301
1.3047
4.00
4.08
8.18
8.16
8.10
11.42
f1 (ppm)
3.1d

Parameter	Value
1 Data File Name	C:/ Users/ Katie/ Dropbox/ ChemResearch/ NMR data/ MRSEC/ tetra-p-ethyl/ KAMi-231-13C.fid/ fid
2 Solvent	cdcl3
3 Acquisition Date	2011-01-07T23:46:56
4 Spectrometer Frequency	75.49
5 Nucleus	13C

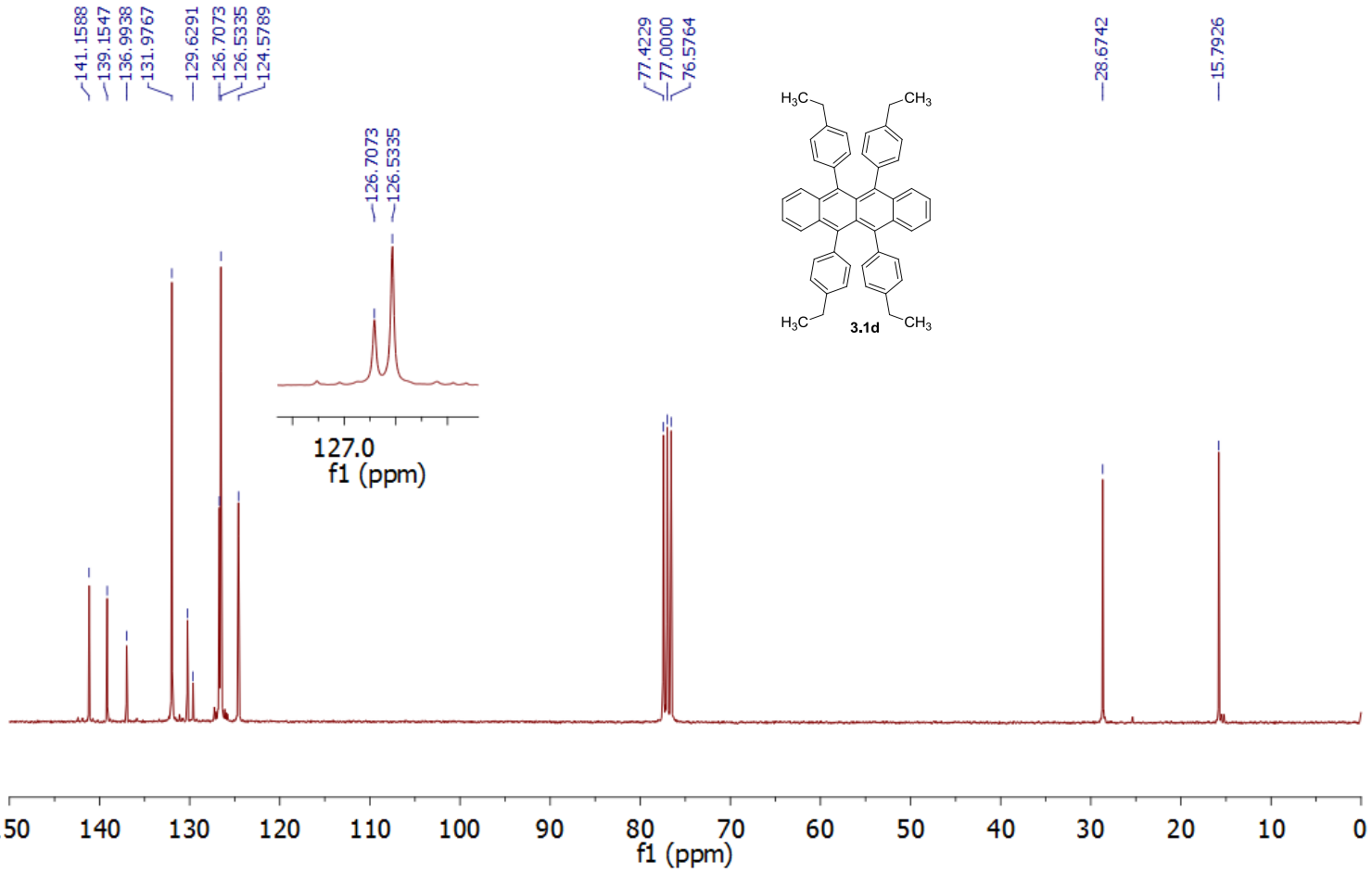

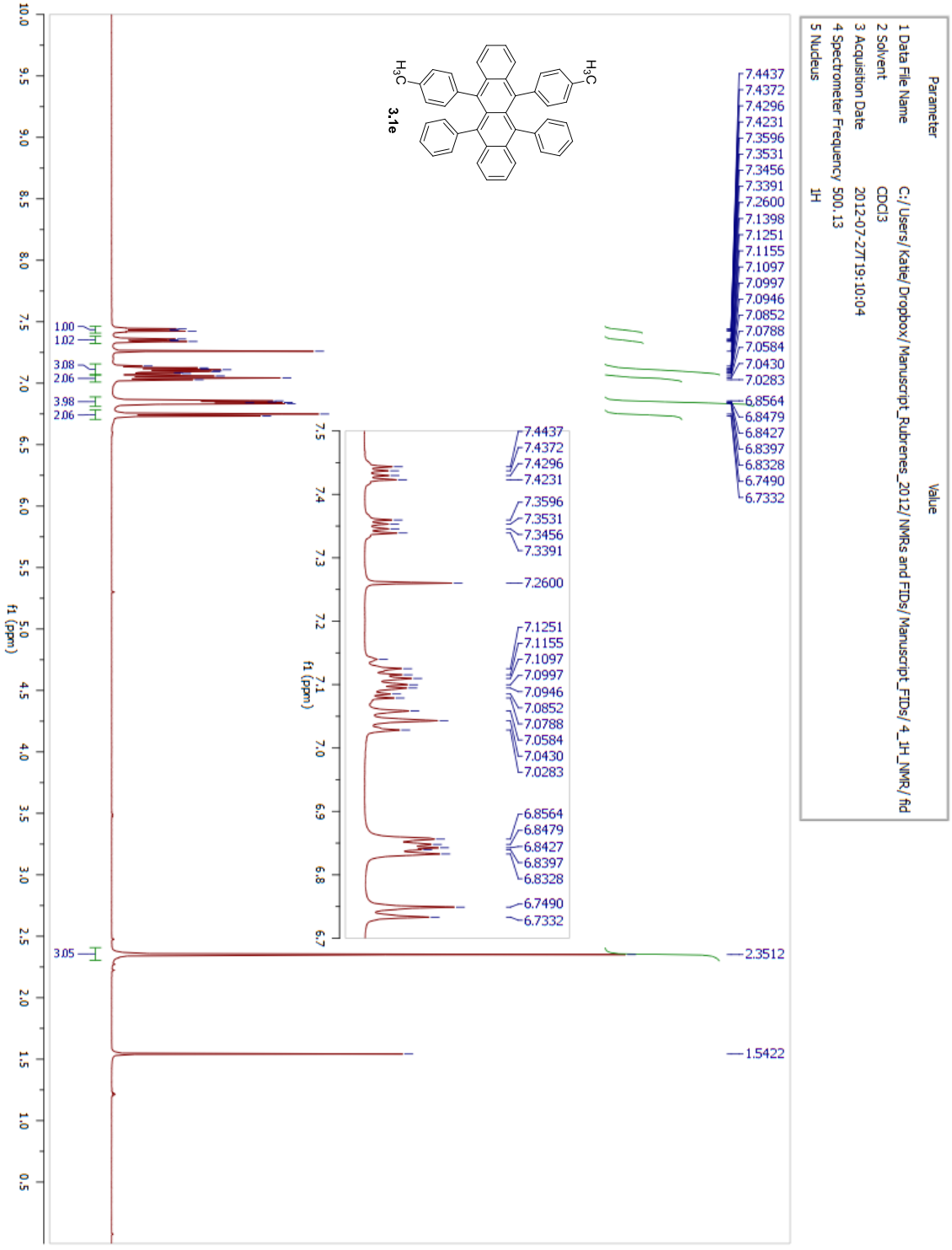
Parameter
Value
1 Data File Name
C:/Users/Katie/Dropbox/Manuscript_Rubrenes_2012/NMRs and FIDs/Manuscript_FIDs/4_1H_NMR/fid
2 Solvent
CDCl3
3 Acquisition Date
2012-07-27T19:10:04
4 Spectrometer Frequency
500.13
5 Nucleus
1H
3.1e
H3C
CH3
7.4437
7.4372
7.4296
7.4231
7.3596
7.3531
7.3456
7.3391
7.2600
7.1398
7.1251
7.1155
7.1097
7.0997
7.0946
7.0852
7.0788
7.0584
7.0430
7.0283
6.8564
6.8479
6.8427
6.8397
6.8328
6.7490
6.7332
1.00
1.02
3.08
2.06
3.98
2.06
3.05
2.3512
1.5422
f1 (ppm)

Parameter	Value
1 Data File Name	C:/ Users/ Katie/ Dropbox/ Manuscript_Rubrenes_2012/ NMRs and FIDs/ Manuscript_FIDs/ 4_13C_NMR/ fid
2 Solvent	CDCl3
3 Acquisition Date	2012-07-27T19:12:36
4 Spectrometer Frequency	125.76
5 Nucleus	13C

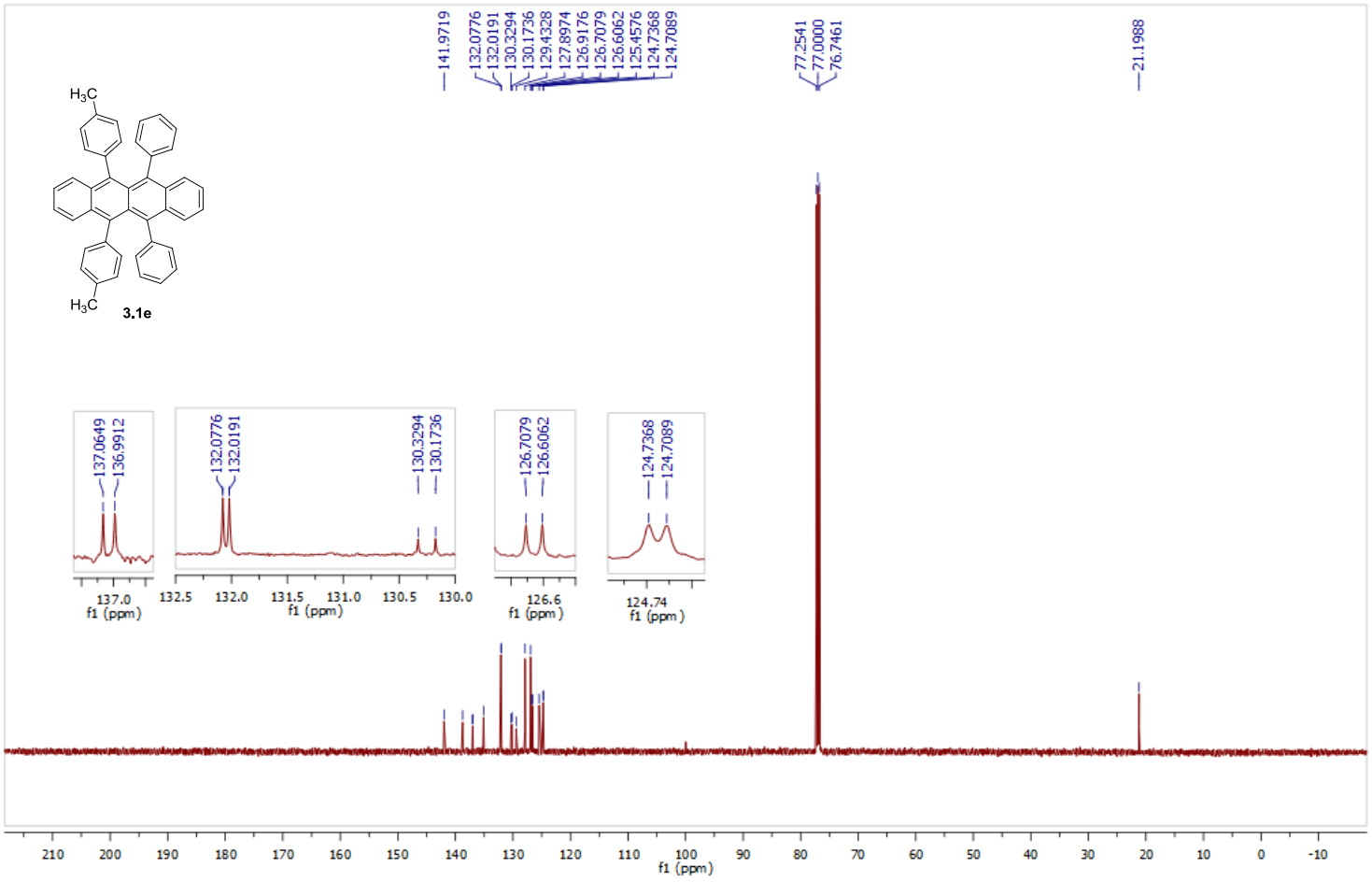

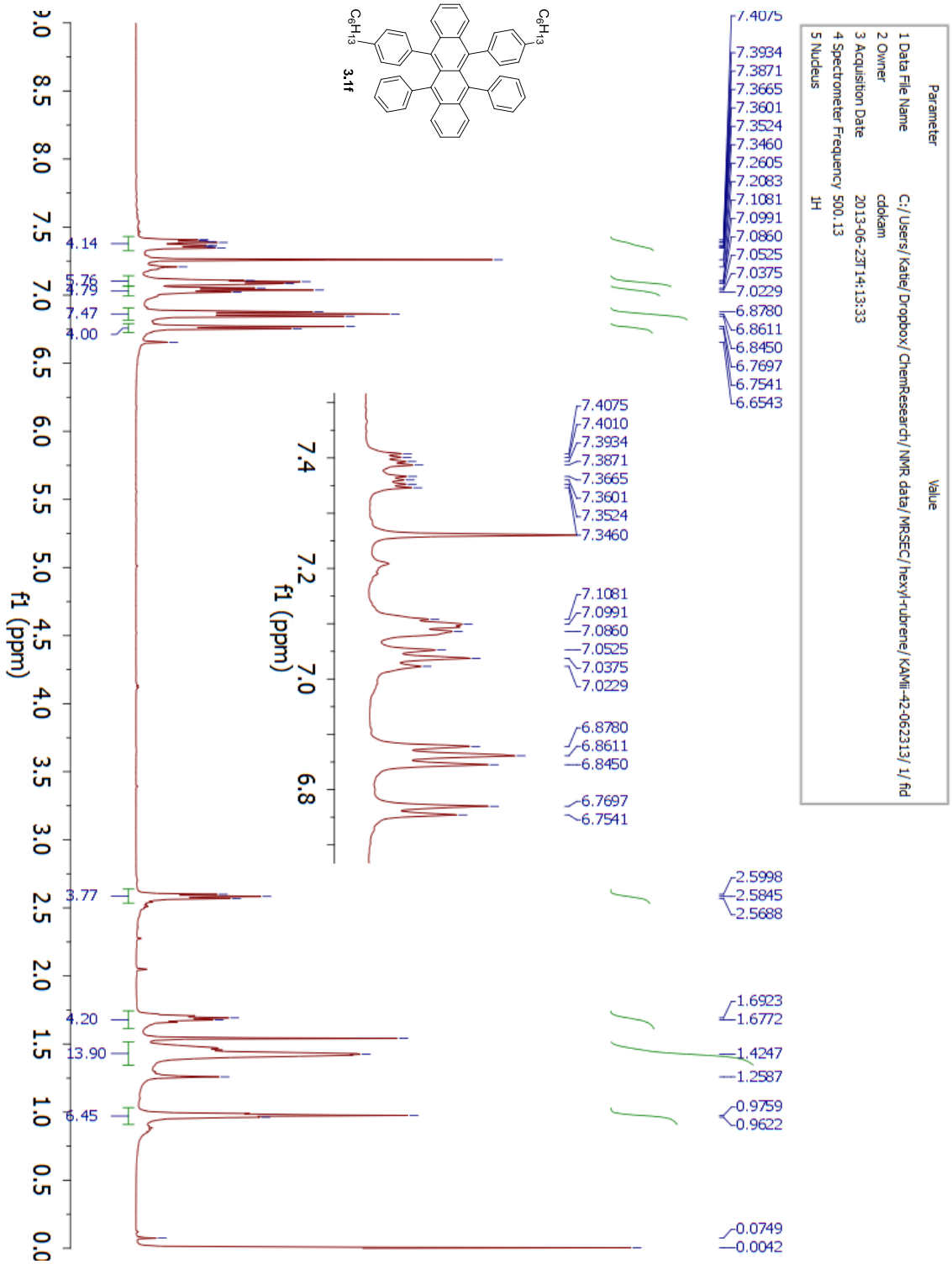
Parameter
Value
1 Data File Name C:/Users/Katie/Dropbox/ChemResearch/NMR data/MRSEC/hexyl-rubrene/KAMii-42-062313/1/fid
2 Owner cdokam
3 Acquisition Date 2013-06-23T14:13:33
4 Spectrometer Frequency 500.13
5 Nucleus 1H
3.1f
C6H13
C6H13
f1 (ppm)
4.14
5.76
4.79
7.47
4.00
3.77
4.20
13.90
6.45
7.4075
7.4010
7.3934
7.3871
7.3665
7.3601
7.3524
7.3460
7.1081
7.0991
7.0860
7.0525
7.0375
7.0229
6.8780
6.8611
6.8450
6.7697
6.7541
2.5998
2.5845
2.5688
1.6923
1.6772
1.4247
1.2587
0.9759
0.9622
0.0749
0.0042

Parameter	Value
1 Data File Name	C:/ Users/ Katie/ Dropbox/ ChemResearch/ NMR data/ MRSEC/ hexyl-rubrene/ KAMii-42-062313/ 2/ fid
2 Solvent	CDCl3
3 Acquisition Date	2013-06-23T14:16:40
4 Spectrometer Frequency	125.76
5 Nucleus	13C

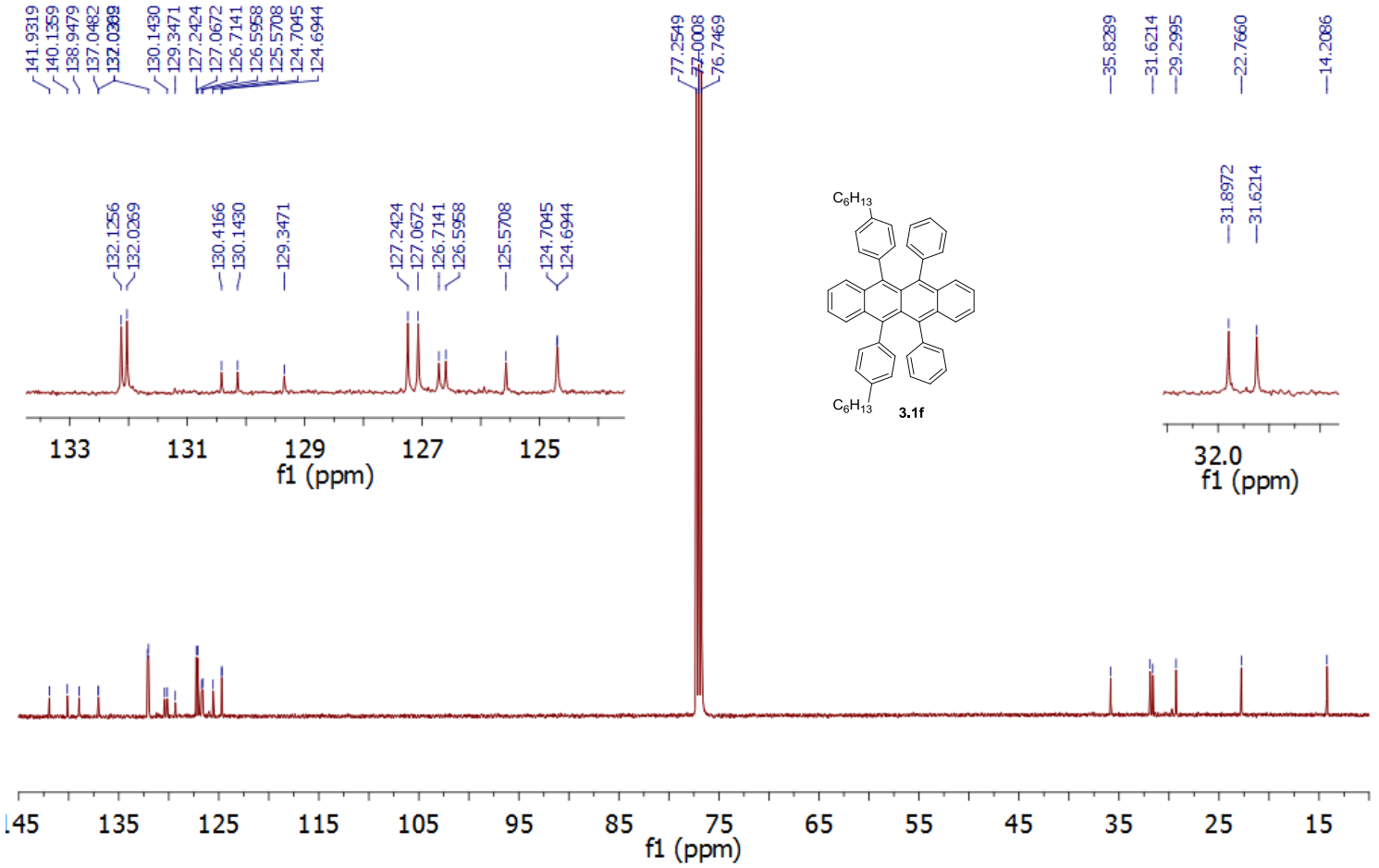

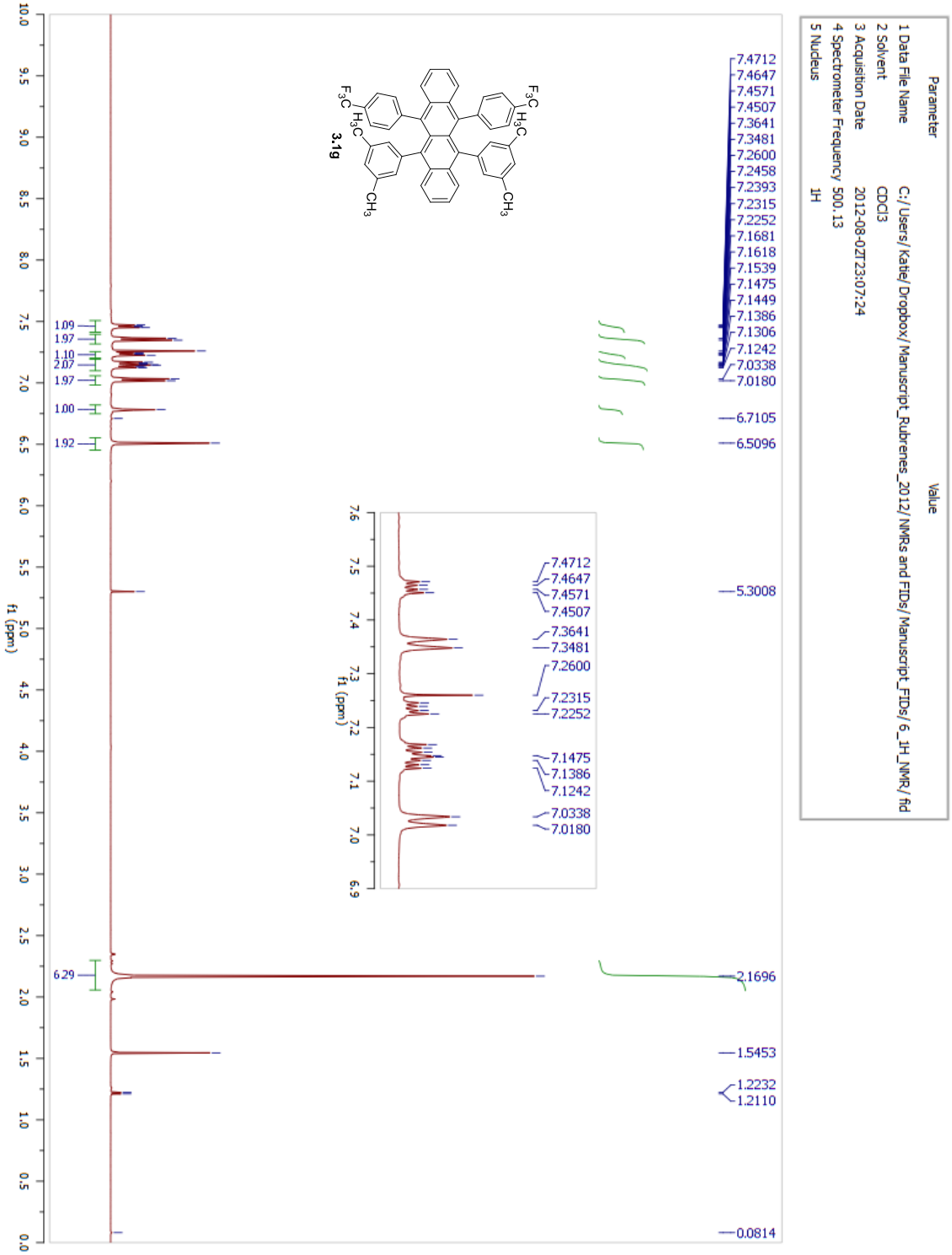
Parameter
Value
1 Data File Name
C:/Users/Katie/Dropbox/Manuscript_Rubrenes_2012/NMRs and FIDs/Manuscript_FIDs/6_1H_NMR/fid
2 Solvent
CDCl3
3 Acquisition Date
2012-08-02T23:07:24
4 Spectrometer Frequency
500.13
5 Nucleus
1H
3.1g
7.4712
7.4647
7.4571
7.4507
7.3641
7.3481
7.2600
7.2458
7.2393
7.2315
7.2252
7.1681
7.1618
7.1539
7.1475
7.1449
7.1386
7.1306
7.1242
7.0338
7.0180
6.7105
6.5096
5.3008
2.1696
1.5453
1.2232
1.2110
0.0814
1.09
1.97
1.10
2.07
1.97
1.00
1.92
6.29
f1 (ppm)

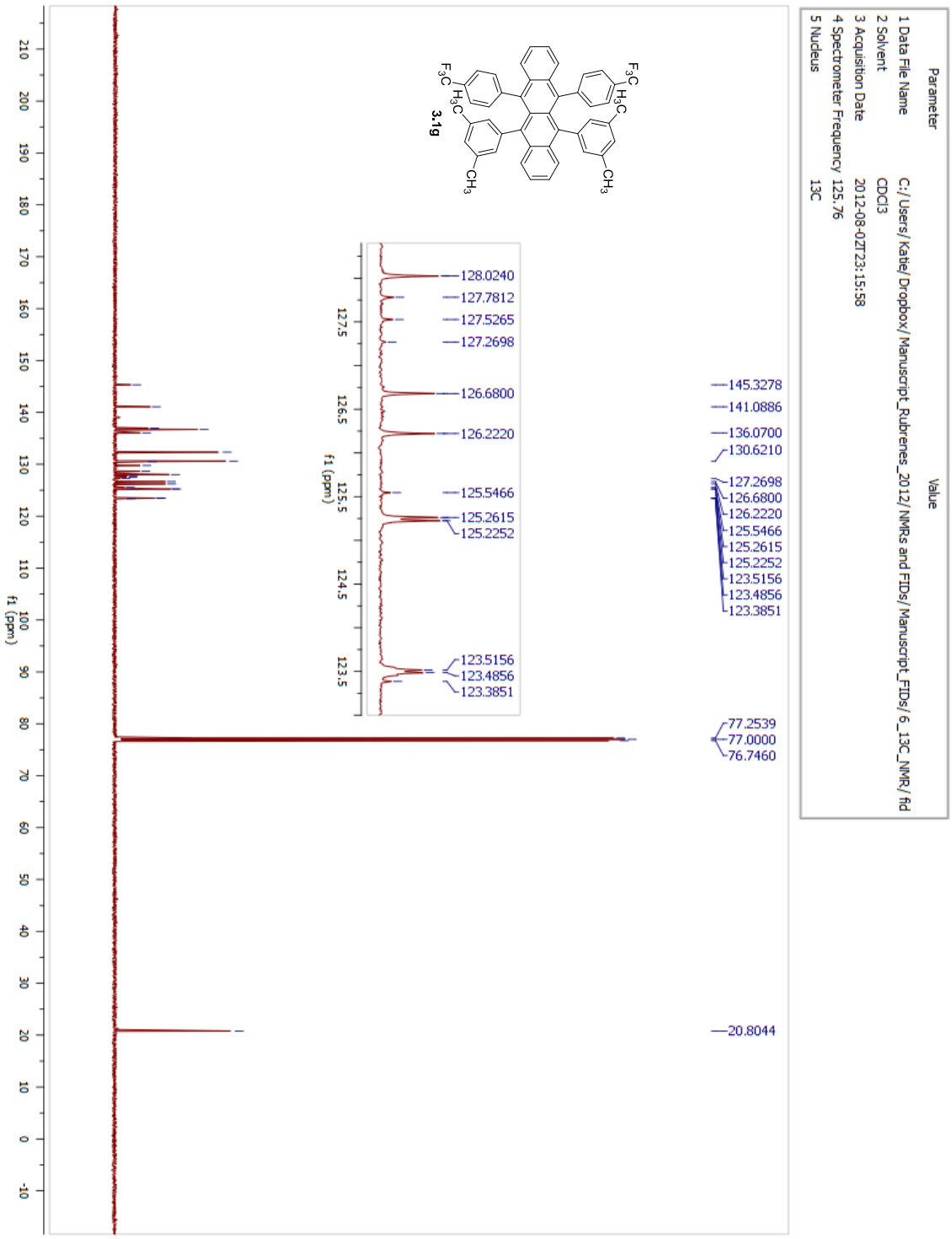
Parameter
Value
1 Data File Name
C:/Users/Katie/Dropbox/Manuscript_Rubrenes_2012/NMRs and FIDs/Manuscript_FIDs/6_13C_NMR/fid
2 Solvent
CDCl3
3 Acquisition Date
2012-08-02T23:15:58
4 Spectrometer Frequency
125.76
5 Nucleus
13C
3.1g
F3C
H3C
CH3
128.0240
127.7812
127.5265
127.2698
126.6800
126.2220
125.5466
125.2615
125.2252
123.5156
123.4856
123.3851
145.3278
141.0886
136.0700
130.6210
77.2539
77.0000
76.7460
20.8044
f1 (ppm)

Parameter	Value
1 Data File Name	C:/ Users/ Katie/ Dropbox/ Manuscript_Rubrenes_2012/ NMRs and FIDs/ Manuscript_FIDs/ 6_19F_NMR/ fid
2 Solvent	CDCl3
3 Acquisition Date	2012-08-02T23:11:46
4 Spectrometer Frequency	470.59
5 Nucleus	19F

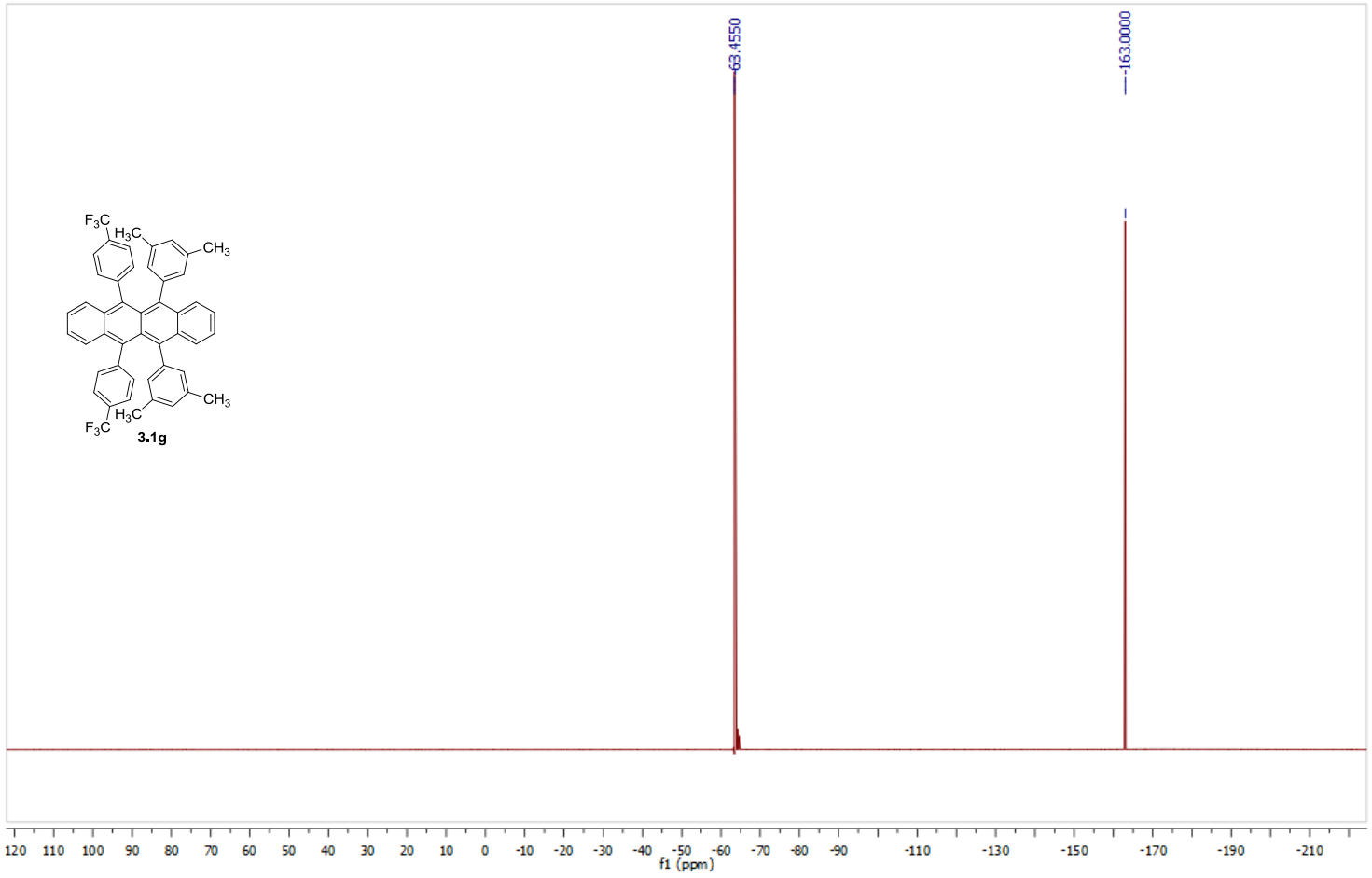

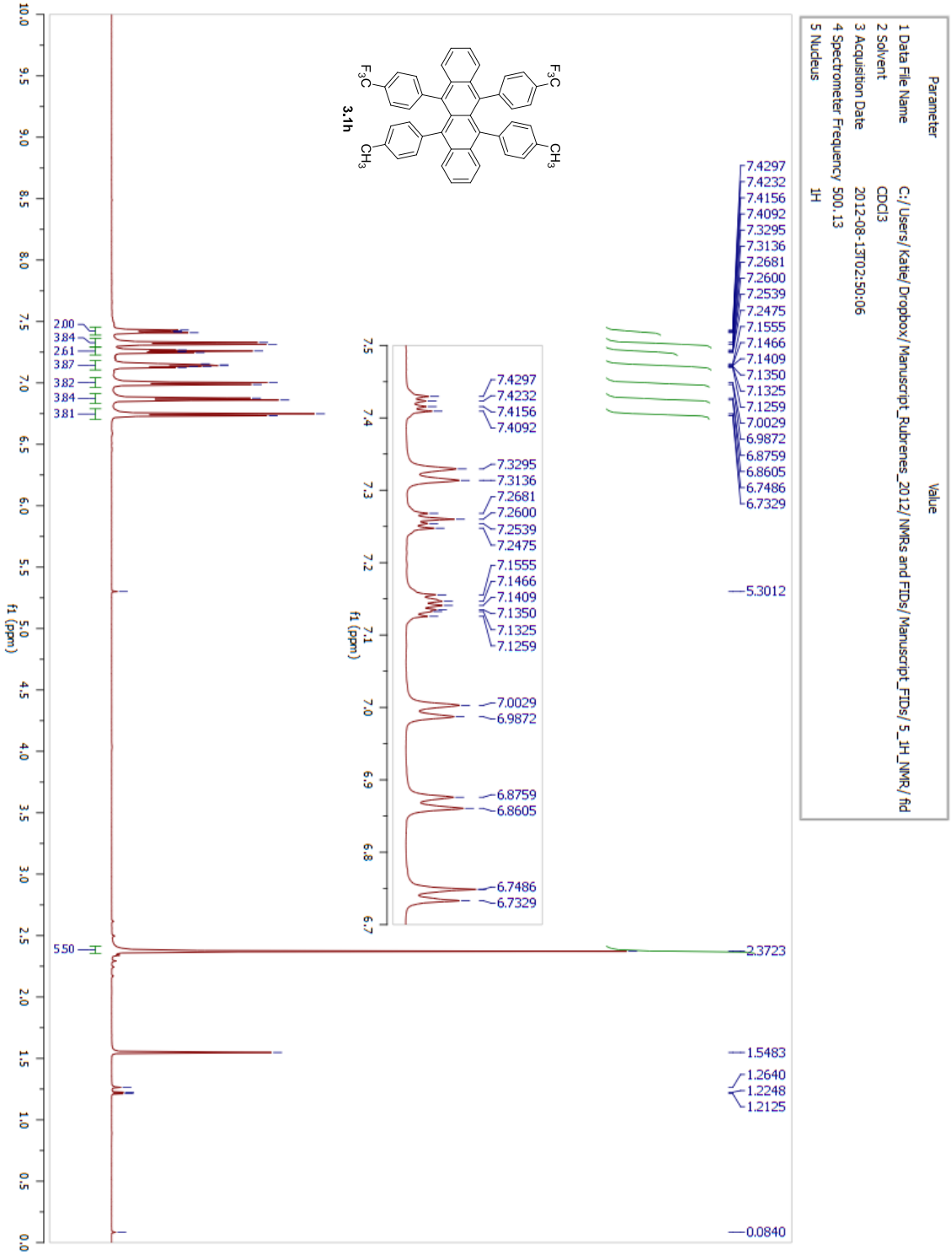
Parameter
Value
1 Data File Name
C:/Users/Katie/Dropbox/Manuscript_Rubrenes_2012/NMRs and FIDs/Manuscript_FIDs/5_1H_NMR/fid
2 Solvent
CDCl3
3 Acquisition Date
2012-08-13T02:50:06
4 Spectrometer Frequency
500.13
5 Nucleus
1H
3.1h
F3C
CH3
f1 (ppm)
2.00
3.84
2.61
3.87
3.82
3.84
3.81
5.50
7.4297
7.4232
7.4156
7.4092
7.3295
7.3136
7.2681
7.2600
7.2539
7.2475
7.1555
7.1466
7.1409
7.1350
7.1325
7.1259
7.0029
6.9872
6.8759
6.8605
6.7486
6.7329
5.3012
2.3723
1.5483
1.2640
1.2248
1.2125
0.0840

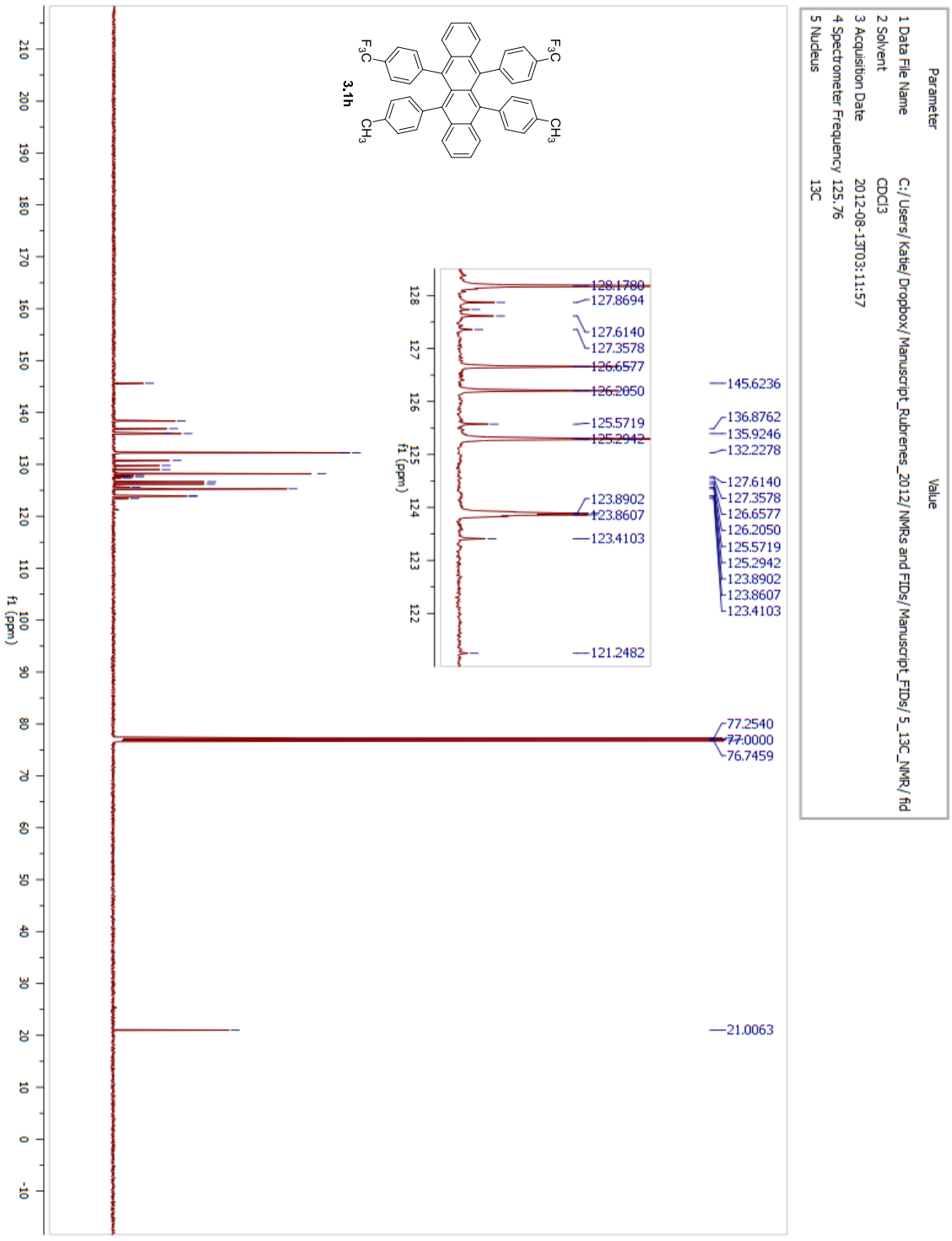
Parameter
Value
1 Data File Name
C:/Users/Katie/Dropbox/Manuscript_Rubrenes_2012/NMRs and FIDs/Manuscript_FIDs/5_13C_NMR/fid
2 Solvent
CDCl3
3 Acquisition Date
2012-08-13T03:11:57
4 Spectrometer Frequency
125.76
5 Nucleus
13C
3.1h
F3C
CH3
128.1780
127.8694
127.6140
127.3578
126.6577
126.2050
125.5719
125.2942
123.8902
123.8607
123.4103
121.2482
145.6236
136.8762
135.9246
132.2278
77.2540
77.0000
76.7459
21.0063
f1 (ppm)

Parameter	Value
1 Data File Name	C:/ Users/ Katie/ Dropbox/ Manuscript_Rubrenes_2012/ NMRs and FIDs/ Manuscript_FIDs/ 5_19F_NMR/ fid
2 Solvent	CDCl3
3 Acquisition Date	2012-08-13T05:35:55
4 Spectrometer Frequency	470.59
5 Nucleus	19F

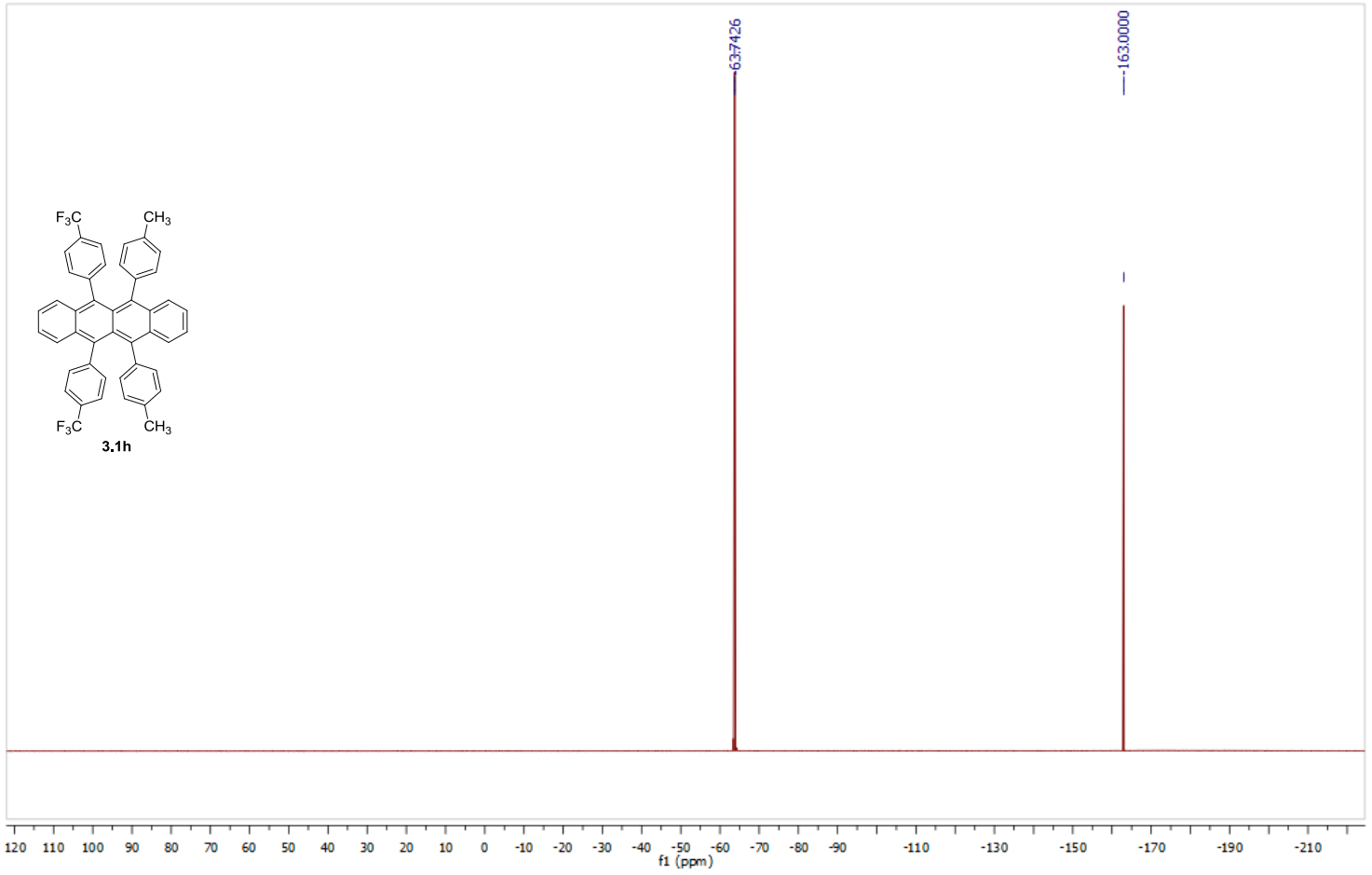

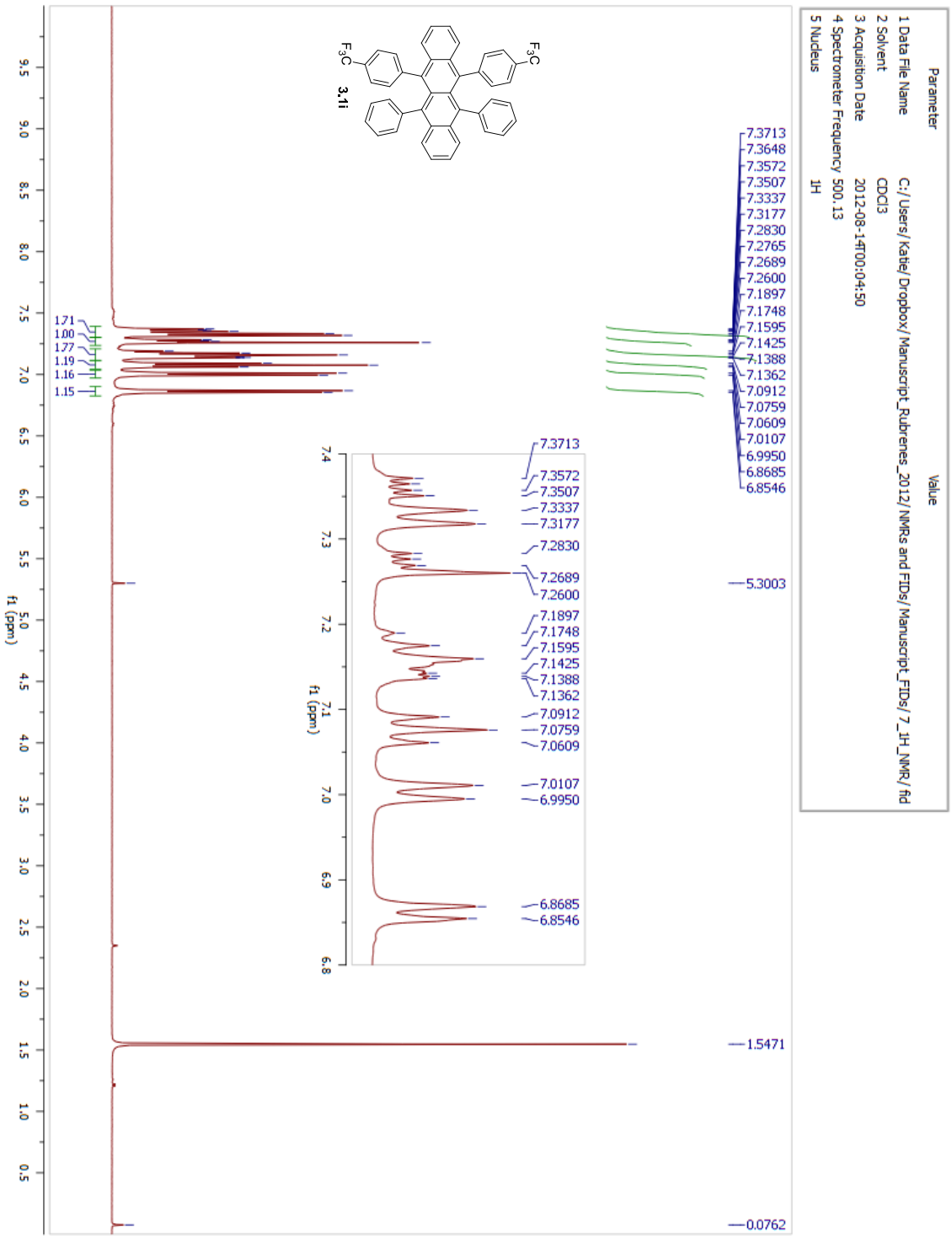
Parameter
Value
1 Data File Name
C:/Users/Katie/Dropbox/Manuscript_Rubrenes_2012/NMRs and FIDs/Manuscript_FIDs/7_1H_NMR/fid
2 Solvent
CDCl3
3 Acquisition Date
2012-08-14T00:04:50
4 Spectrometer Frequency
500.13
5 Nucleus
1H
3.1i
F3C
CF3
7.3713
7.3648
7.3572
7.3507
7.3337
7.3177
7.2830
7.2765
7.2689
7.2600
7.1897
7.1748
7.1595
7.1425
7.1388
7.1362
7.0912
7.0759
7.0609
7.0107
6.9950
6.8685
6.8546
5.3003
1.5471
0.0762
1.71
1.00
1.77
1.19
1.16
1.15
f1 (ppm)

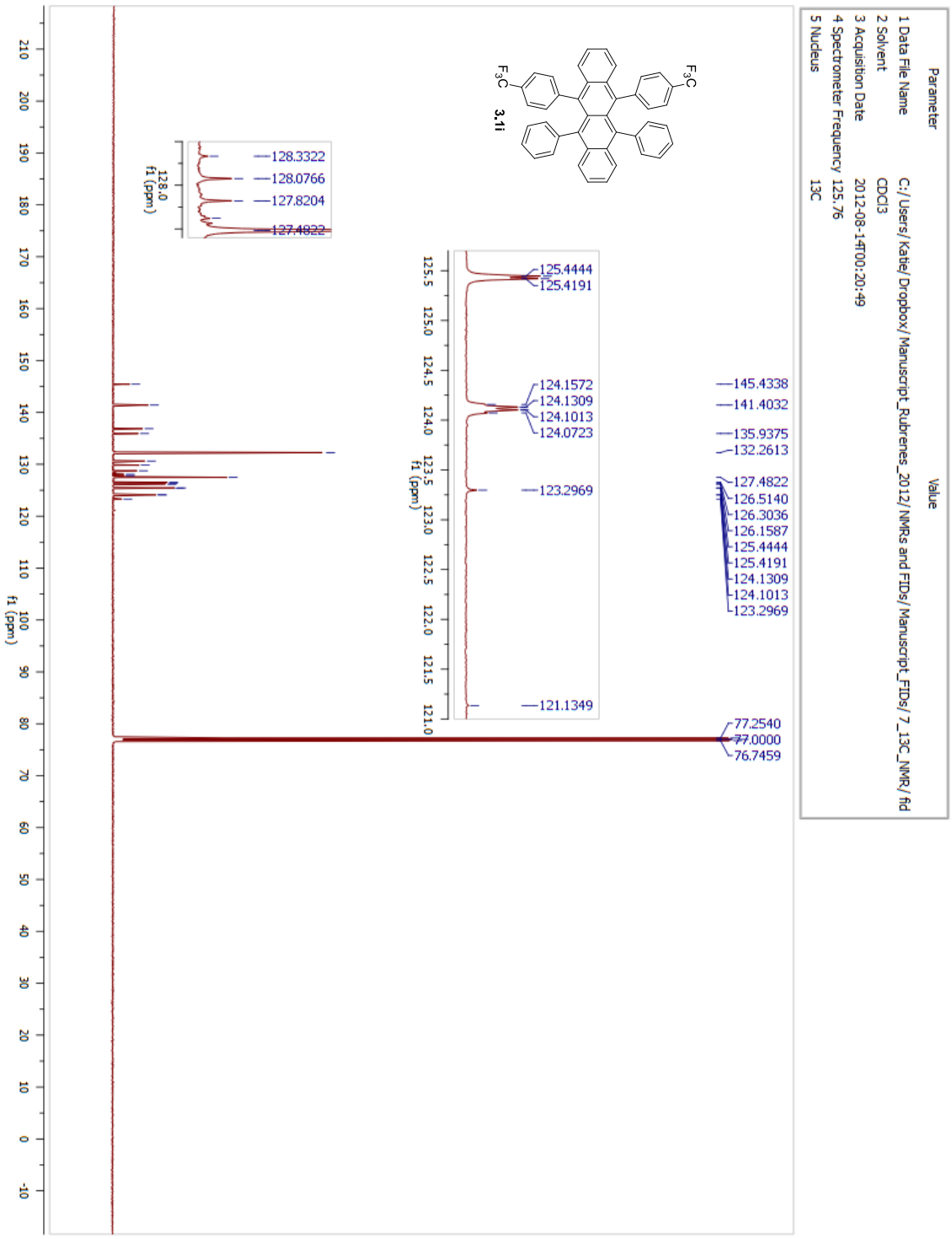
Parameter
Value
1 Data File Name
C:/Users/Katie/Dropbox/Manuscript_Rubrenes_2012/NMRs and FIDs/Manuscript_FIDs/7_13C_NMR/fid
2 Solvent
CDCl3
3 Acquisition Date
2012-08-14T00:20:49
4 Spectrometer Frequency
125.76
5 Nucleus
13C
F3C
F3C
3.1i
128.3322
128.0766
127.8204
127.4822
125.4444
125.4191
124.1572
124.1309
124.1013
124.0723
123.2969
121.1349
145.4338
141.4032
135.9375
132.2613
127.4822
126.5140
126.3036
126.1587
125.4444
125.4191
124.1309
124.1013
123.2969
77.2540
77.0000
76.7459
f1 (ppm)

Parameter	Value
1 Data File Name	C:/ Users/ Katie/ Dropbox/ Manuscript_Rubrenes_2012/ NMRs and FIDs/ Manuscript_FIDs/ 7_19F_NMR/ fid
2 Solvent	CDCl3
3 Acquisition Date	2012-08-14T12:29:25
4 Spectrometer Frequency	470.59
5 Nucleus	19F

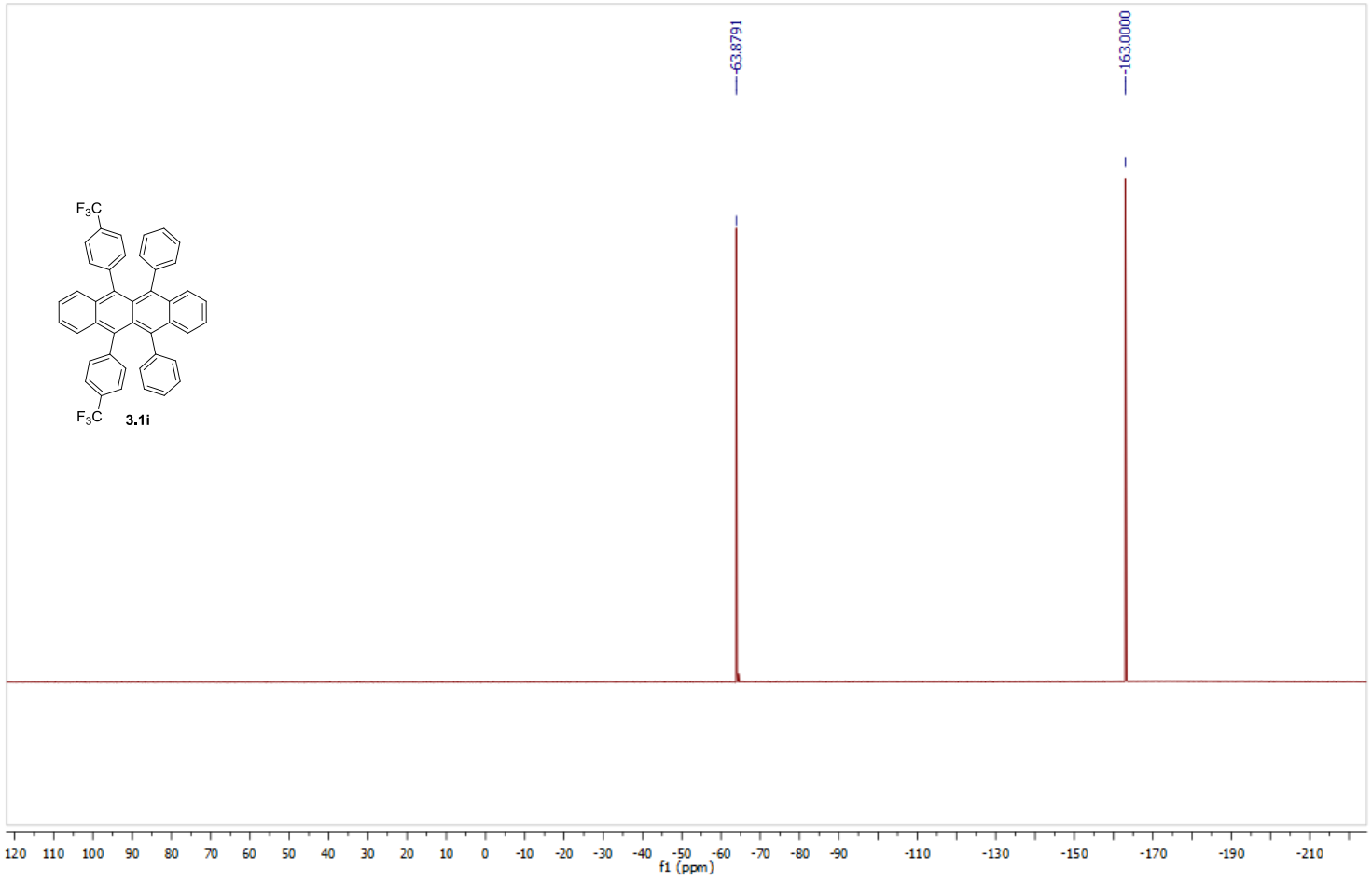

Parameter	Value
1 Data File Name	C:/ Users/ Katie/ Dropbox/ ChemResearch/ NMR data/ MRSEC/ tetra-p-CF3/ KAMii-287-ps/ 1/ fid
2 Solvent	CDCl3
3 Acquisition Date	2013-07-02T01:04:58
4 Spectrometer Frequency	500.13
5 Nucleus	1H

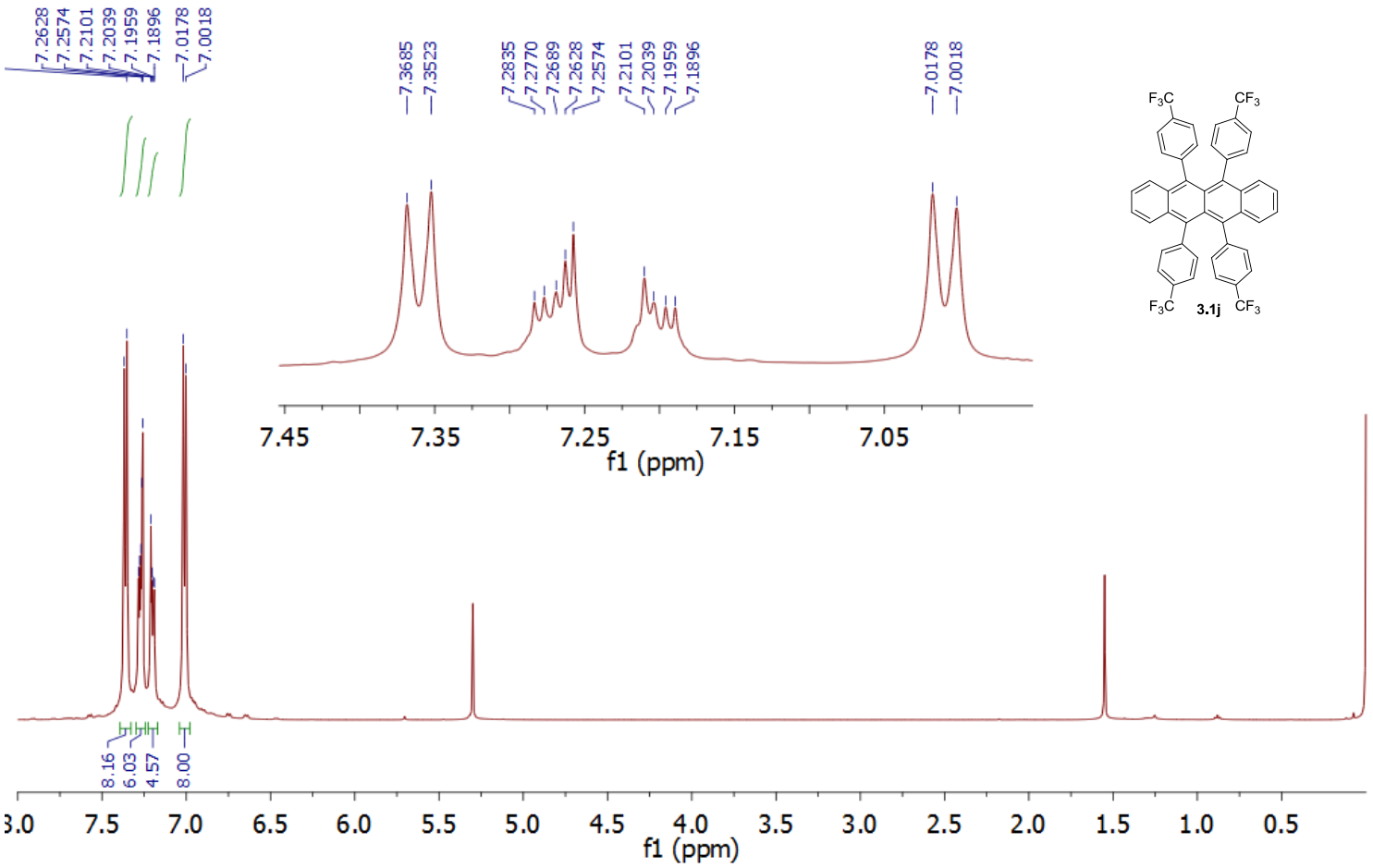

3.1j

Parameter	Value
1 Data File Name	C:/ Users/ Katie/ Dropbox/ ChemResearch/ NMR data/ MRSEC/ tetra-p-CF3/ KAMii-287-ps/ 2/ fid
2 Owner	cdokam
3 Acquisition Date	2013-07-02T01:08:08
4 Spectrometer Frequency	125.76
5 Nucleus	13C

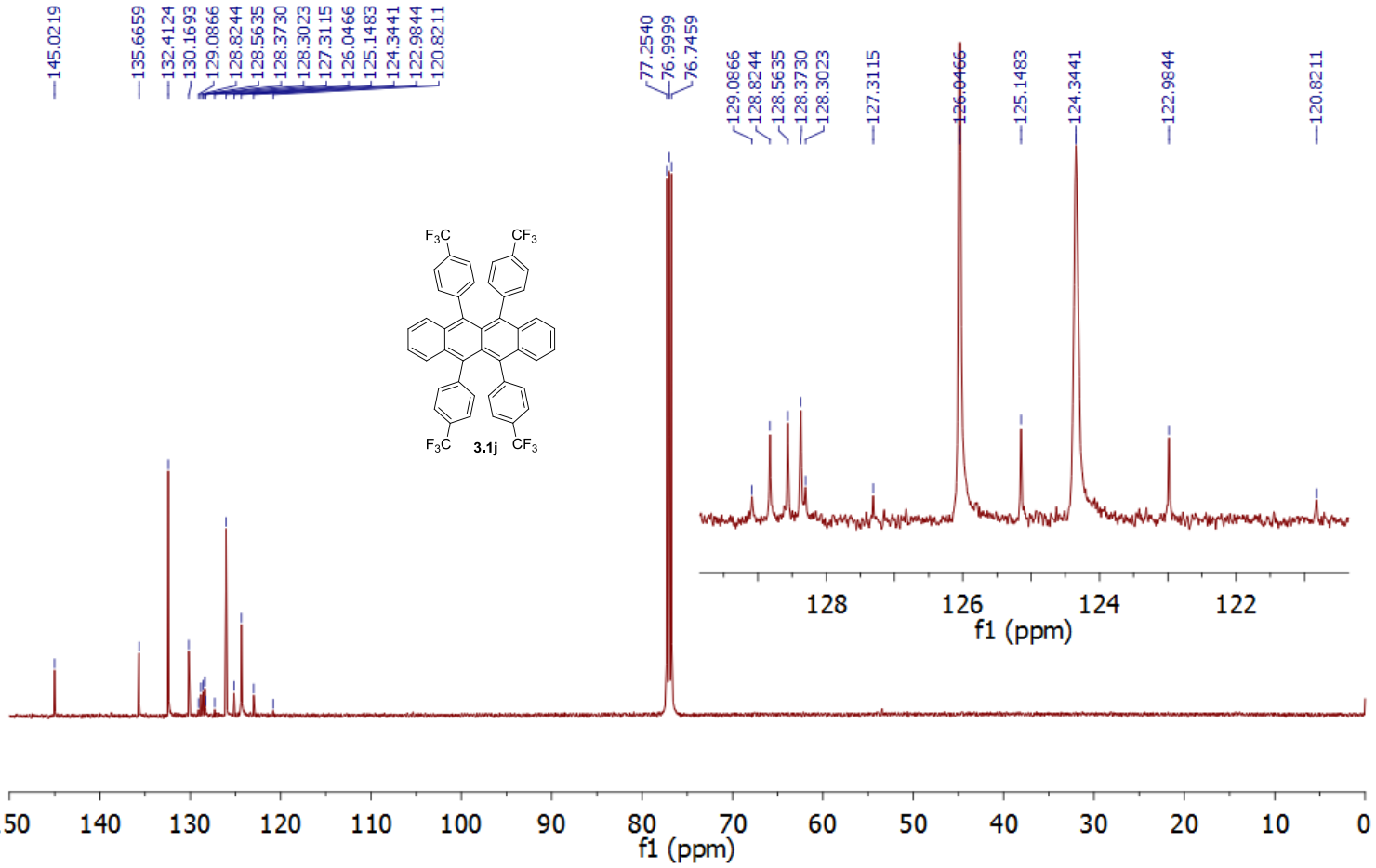

Parameter	Value
1 Data File Name	C:/ Users/ Katie/ Dropbox/ ChemResearch/ NMR data/ MRSEC/ tetra-p-CF3/ KAMii-287-ps-F19.fid/ fid
2 Solvent	cdcl3
3 Acquisition Date	2013-07-02T03:15:57
4 Spectrometer Frequency	282.43
5 Nucleus	19F

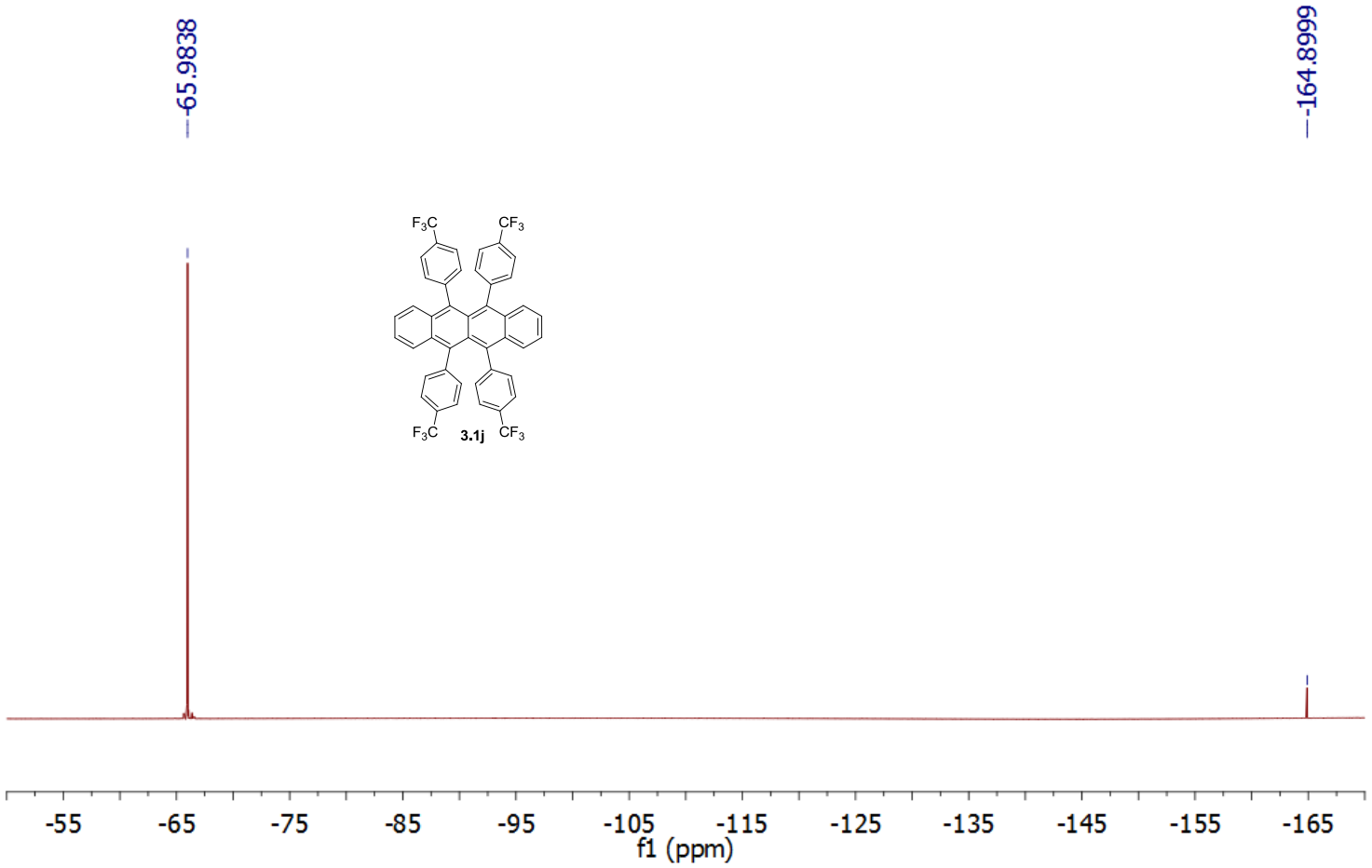

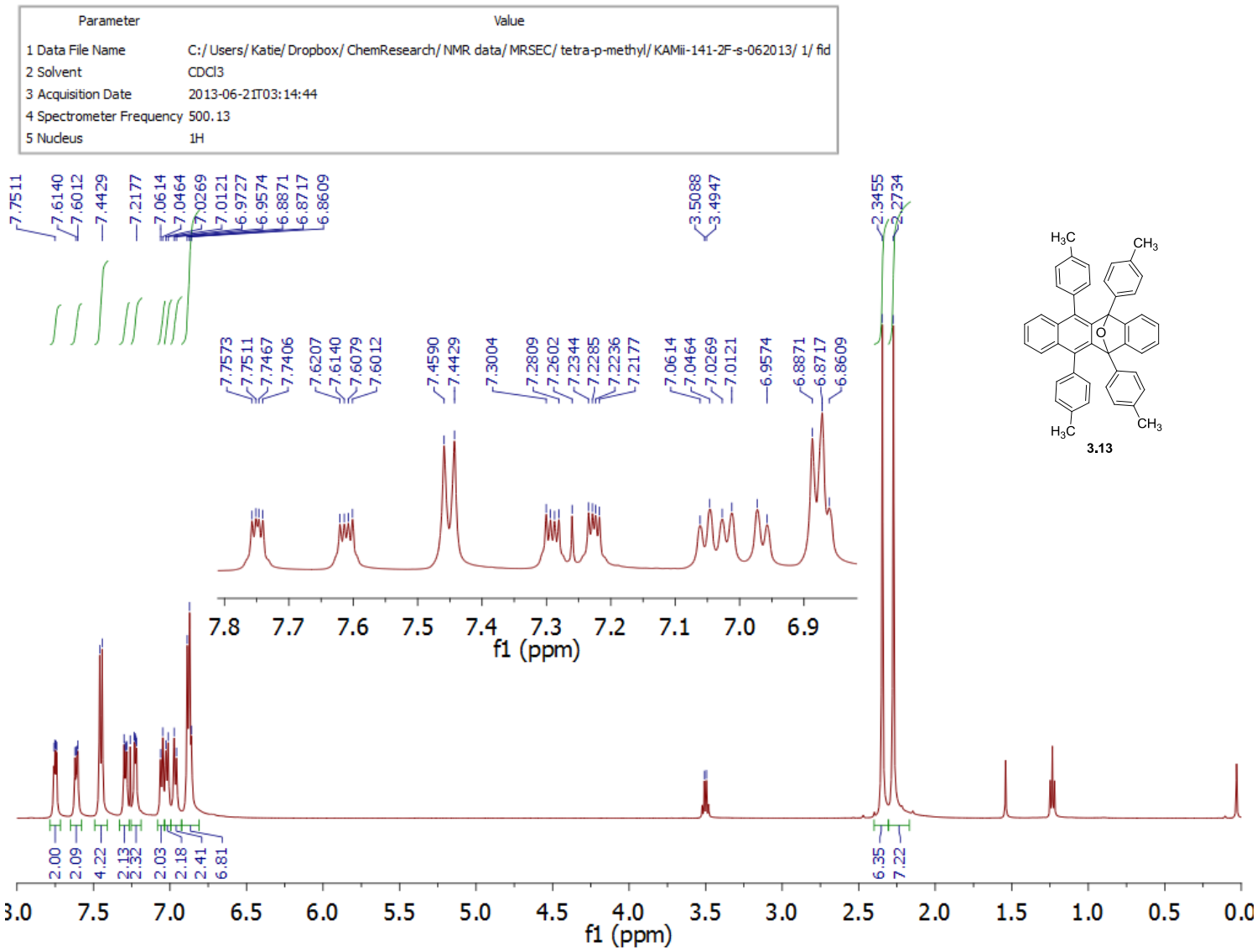
Parameter
Value
1 Data File Name
C:/ Users/ Katie/ Dropbox/ ChemResearch/ NMR data/ MRSEC/ tetra-p-methyl/ KAMii-141-2F-s-062013/ 1/ fid
2 Solvent
CDCl3
3 Acquisition Date
2013-06-21T03:14:44
4 Spectrometer Frequency
500.13
5 Nucleus
1H
7.7511
7.6140
7.6012
7.4429
7.2177
7.0614
7.0464
7.0269
7.0121
6.9727
6.9574
6.8871
6.8717
6.8609
3.5088
3.4947
2.3455
2.2734
7.7573
7.7511
7.7467
7.7406
7.6207
7.6140
7.6079
7.6012
7.4590
7.4429
7.3004
7.2809
7.2602
7.2344
7.2285
7.2236
7.2177
7.0614
7.0464
7.0269
7.0121
6.9574
6.8871
6.8717
6.8609
7.8 7.7 7.6 7.5 7.4 7.3 7.2 7.1 7.0 6.9
f1 (ppm)
2.00
2.09
4.22
2.13
2.32
2.03
2.18
2.41
6.81
6.35
7.22
3.0 7.5 7.0 6.5 6.0 5.5 5.0 4.5 4.0 3.5 3.0 2.5 2.0 1.5 1.0 0.5 0.0
f1 (ppm)
H3C
CH3
O
CH3
H3C
3.13

Parameter	Value
1 Data File Name	C:/ Users/ Katie/ Dropbox/ ChemResearch/ NMR data/ MRSEC/ tetra-p-methyl/ KAMii-141-2F-s-062013/ 2/ fid
2 Solvent	CDCl3
3 Acquisition Date	2013-06-21T03:17:44
4 Spectrometer Frequency	125.76
5 Nucleus	13C

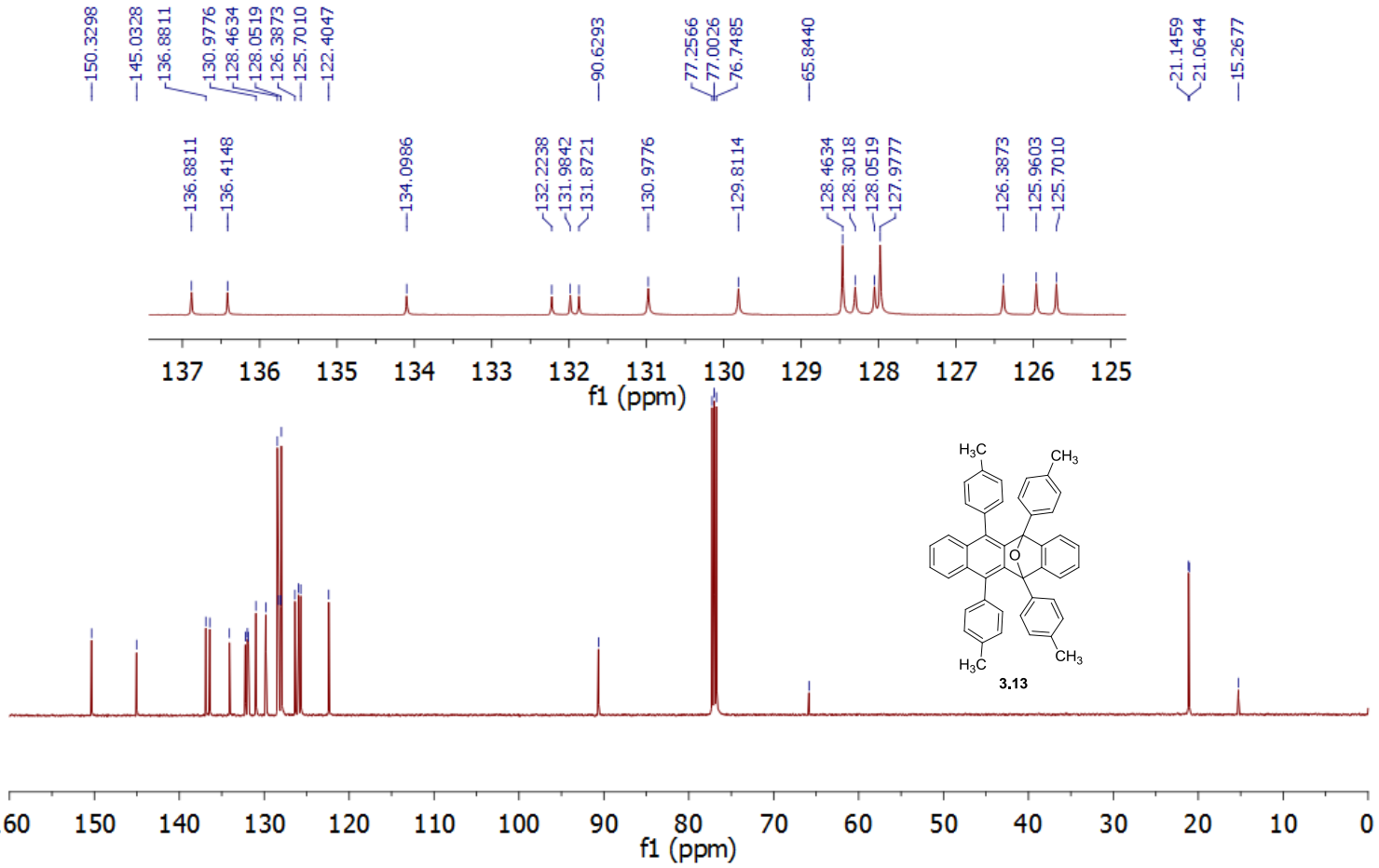

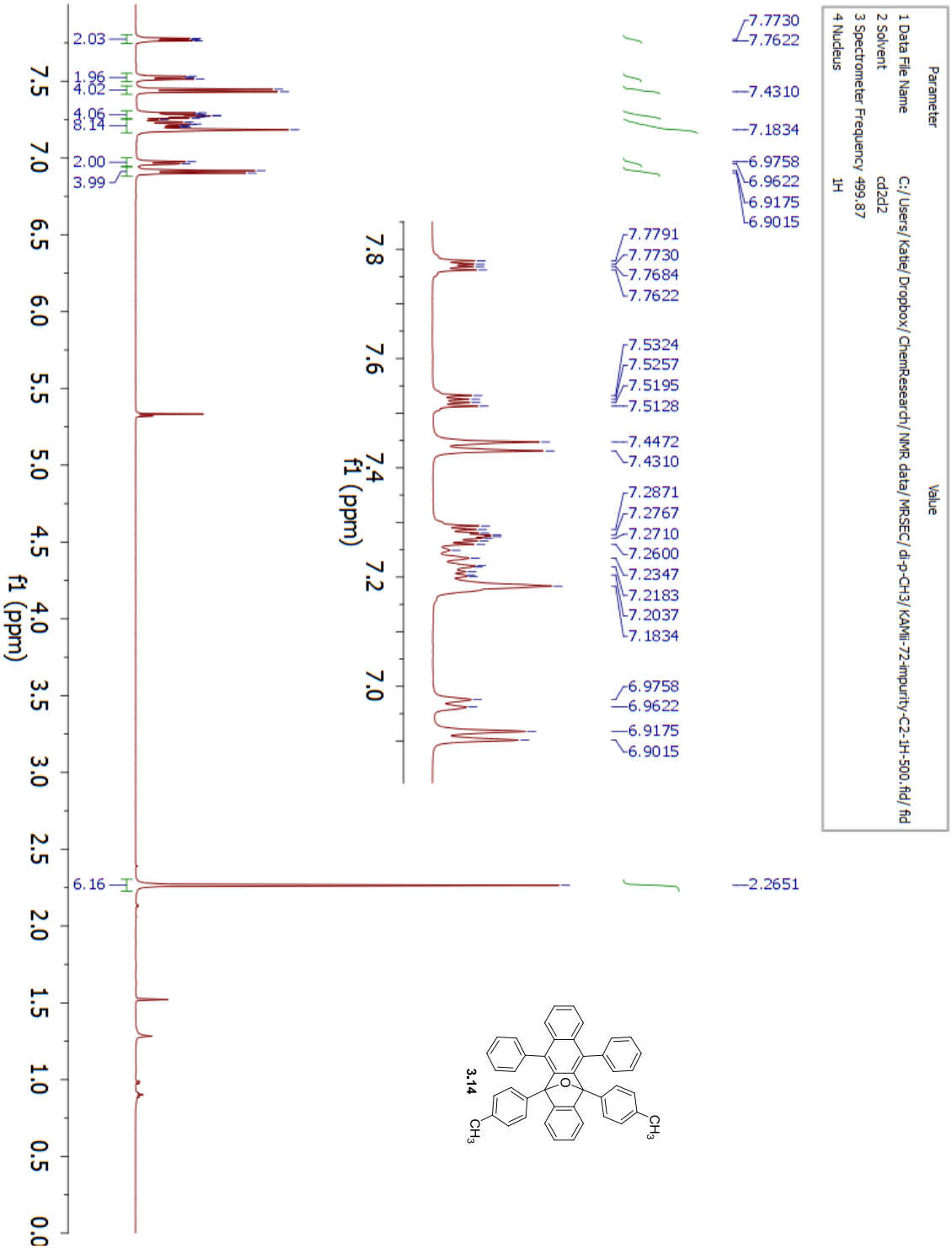
Parameter
Value
1 Data File Name
C:/Users/Katie/Dropbox/ChemResearch/NMR data/MRSEC/di-p-CH3/KAMii-72-impurity-C2-1H-500.fid/fid
2 Solvent
cd2cl2
3 Spectrometer Frequency
499.87
4 Nucleus
1H
7.7730
7.7622
7.4310
7.1834
6.9758
6.9622
6.9175
6.9015
2.2651
2.03
1.96
4.02
4.06
8.14
2.00
3.99
6.16
f1 (ppm)
7.7791
7.7730
7.7684
7.7622
7.5324
7.5257
7.5195
7.5128
7.4472
7.4310
7.2871
7.2767
7.2710
7.2600
7.2347
7.2183
7.2037
7.1834
6.9758
6.9622
6.9175
6.9015
3.14
CH3
CH3

Parameter	Value
1 Data File Name	C:/ Users/ Katie/ Dropbox/ ChemResearch/ NMR data/ MRSEC/ di-p-CH3/ KAMii-72-impurity-C13.fid/ fid
2 Solvent	cdcl3
3 Acquisition Date	2011-11-21T18:20:38
4 Spectrometer Frequency	75.49
5 Nucleus	13C

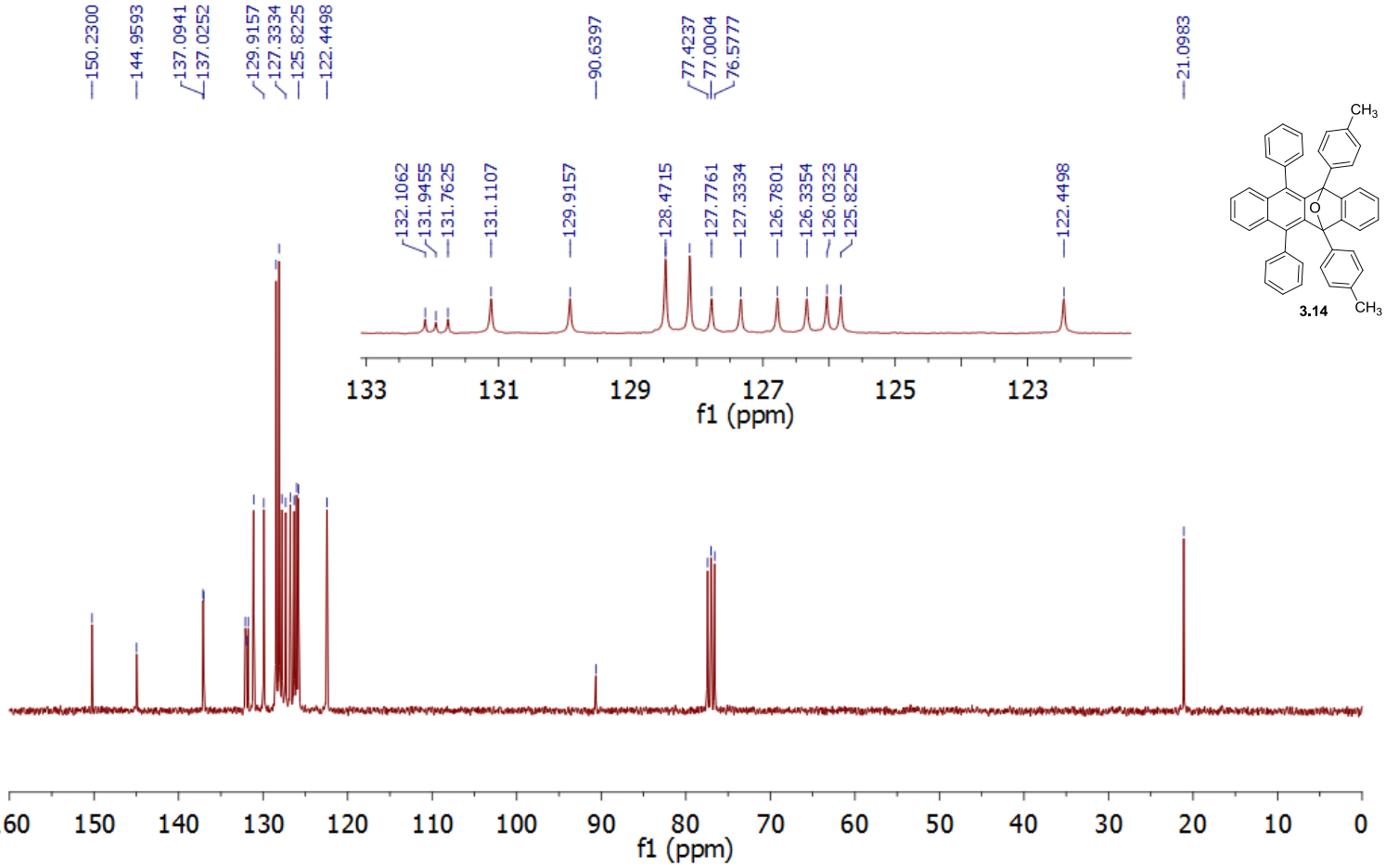

A2.3. CHAPTER 4 SPECTRA

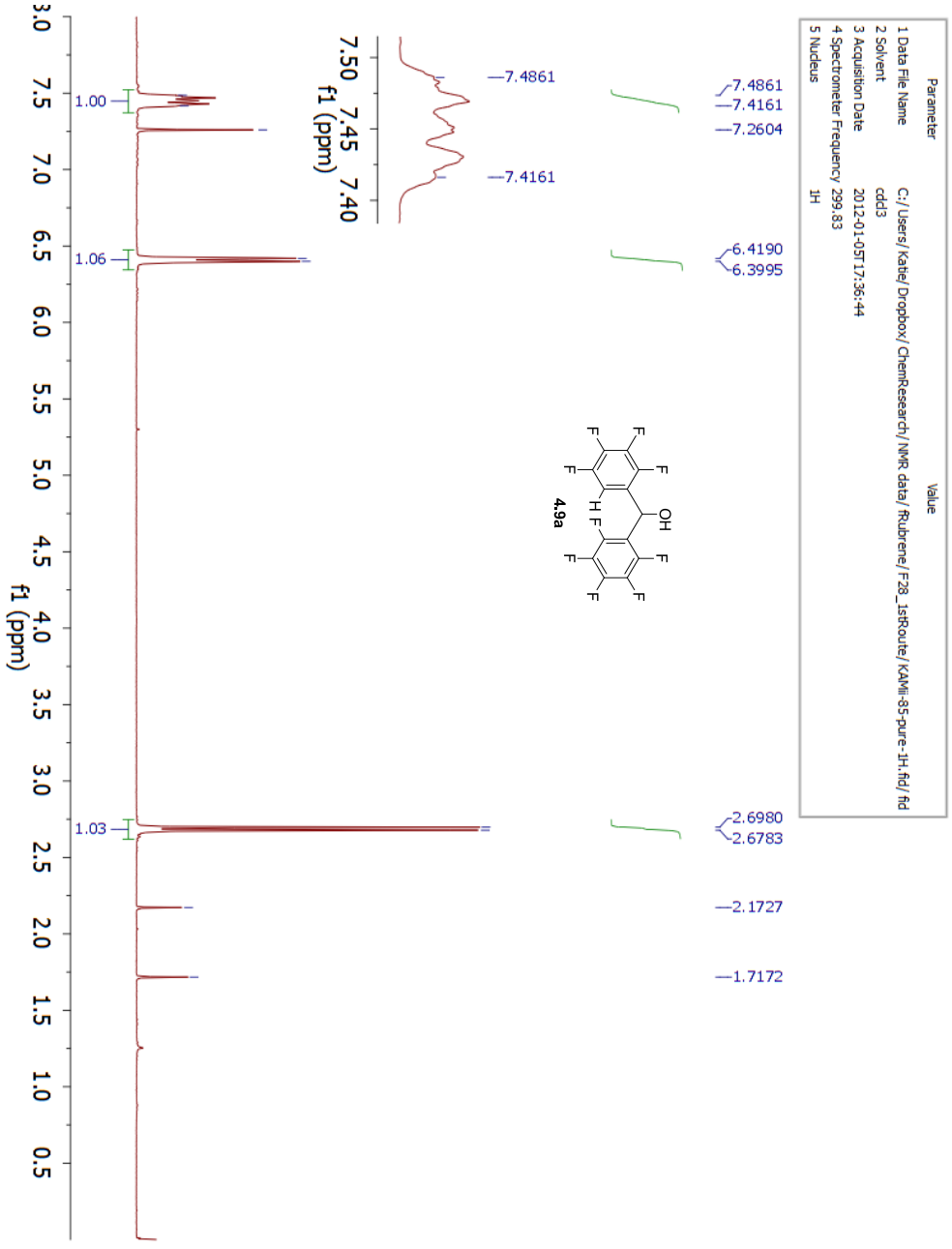

Parameter	Value
1 Data File Name	C:/ Users/ Katie/ Dropbox/ ChemResearch/ NMR data/ fRubrene/ F28_1stRoute/ KAMii-240-1-F19.fid/ fid
2 Solvent	cdcl3
3 Acquisition Date	2013-03-23T20:21:48
4 Spectrometer Frequency	282.43
5 Nucleus	19F

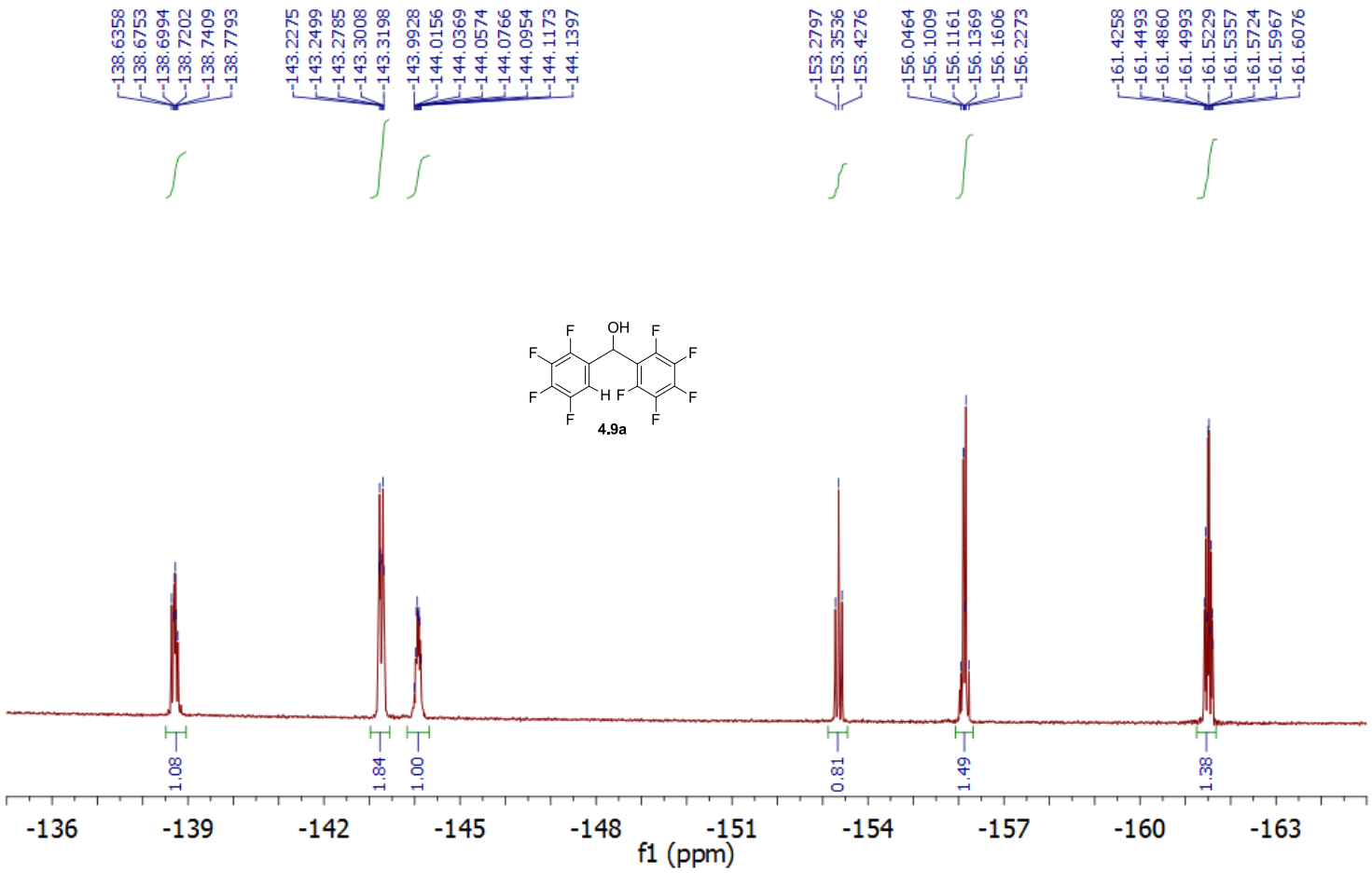

Parameter	Value
1 Data File Name	C:/ Users/ Katie/ Dropbox/ ChemResearch/ NMR data/ fRubrene/ F28_1stRoute/ KAMii-242-F2-F2-1H.fid/ fid
2 Solvent	cdcl3
3 Acquisition Date	2013-03-08T01:04:28
4 Spectrometer Frequency	300.17
5 Nucleus	1H

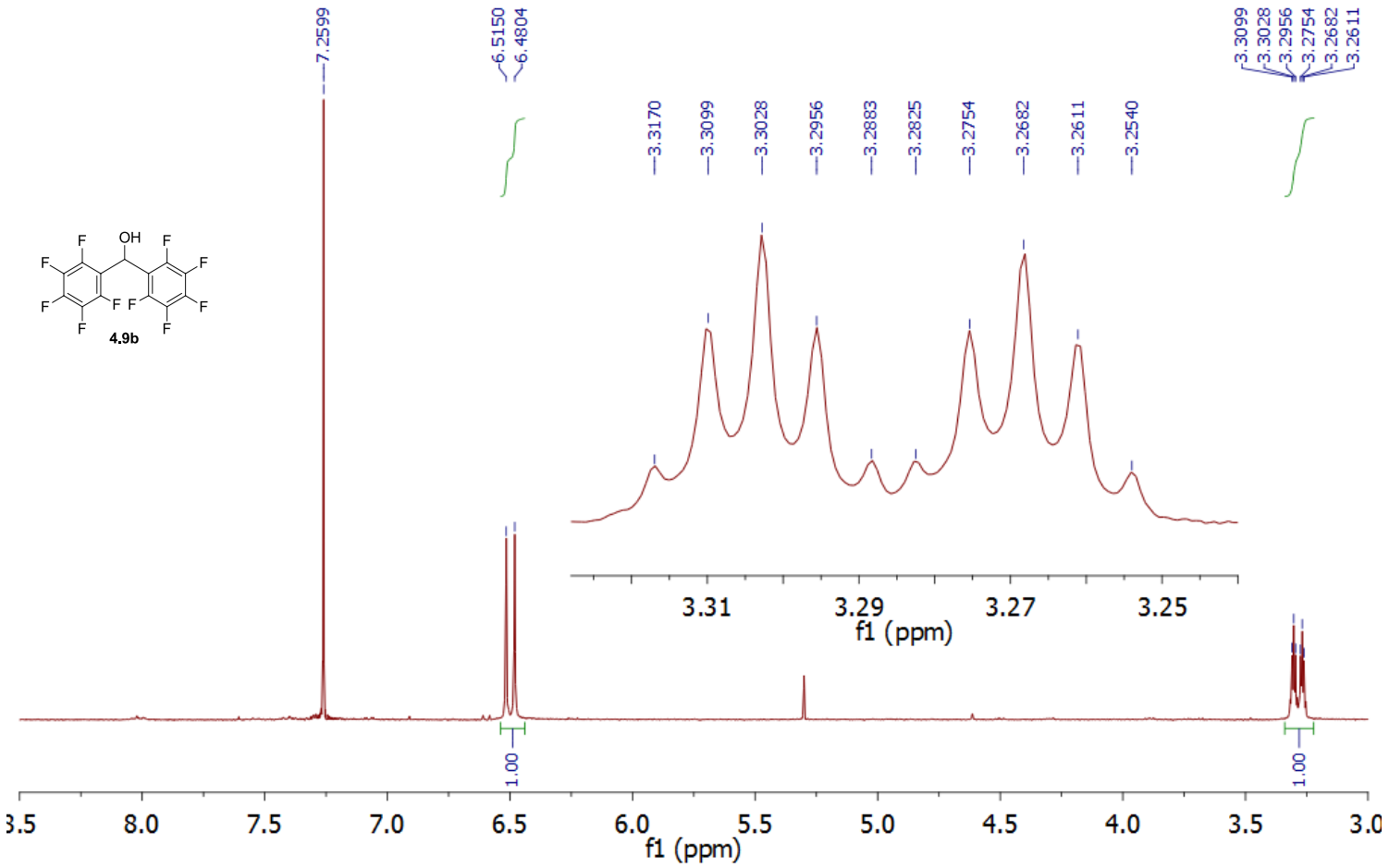

Parameter	Value
1 Data File Name	C:/ Users/ Katie/ Dropbox/ ChemResearch/ NMR data/ fRubrene/ F28_1stRoute/ KAMii-242-F2-F2-F19.fid/ fid
2 Solvent	cdcl3
3 Acquisition Date	2013-03-08T01:06:20
4 Spectrometer Frequency	282.43
5 Nucleus	19F

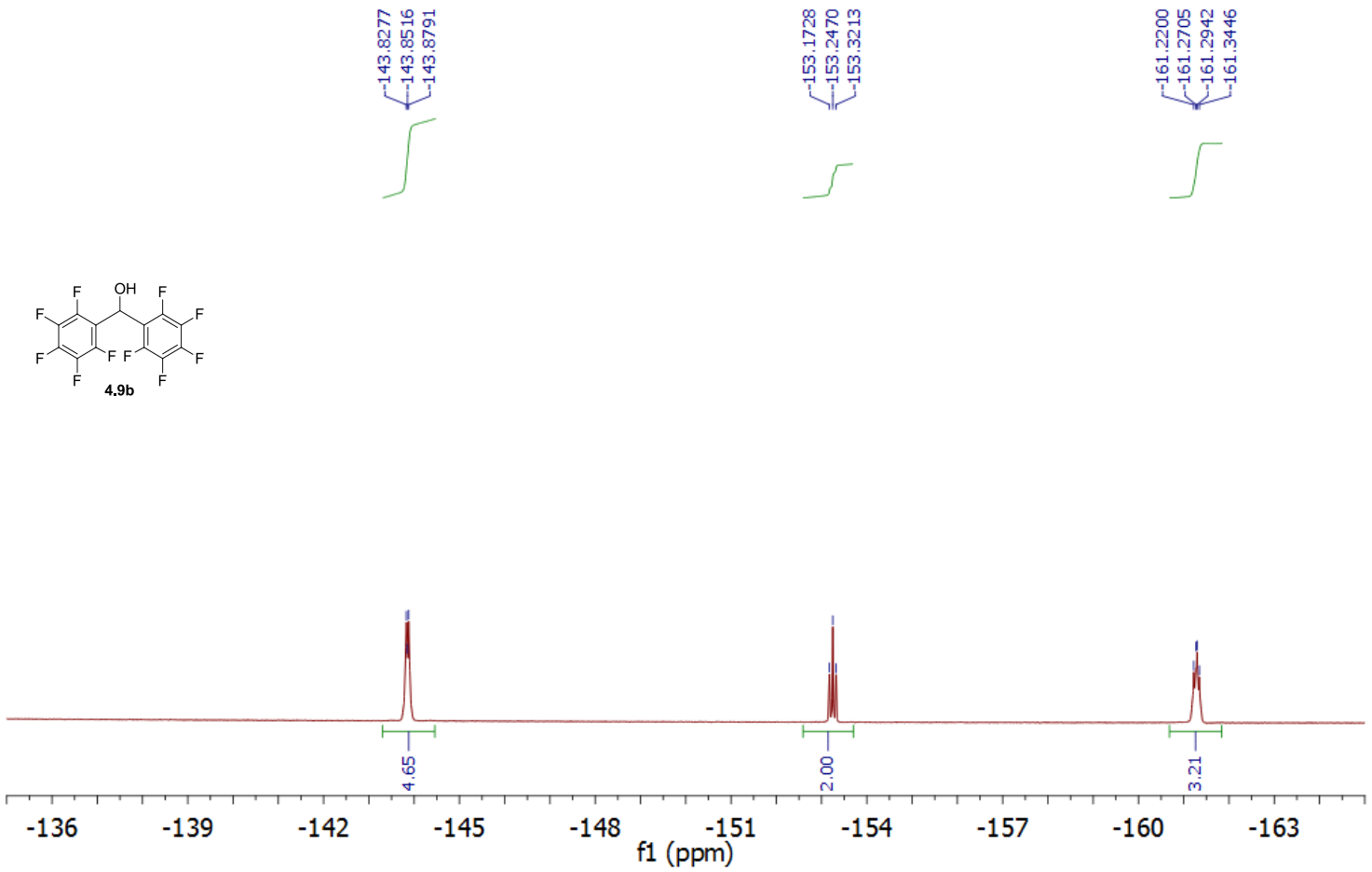

Parameter	Value
1 Data File Name	C:/ Users/ Katie/ Dropbox/ ChemResearch/ NMR data/ fRubrene/ F28_1stRoute/ KAMii-88-pure-1H.fid/ fid
2 Solvent	cdcl3
3 Acquisition Date	2012-01-06T19:13:15
4 Spectrometer Frequency	299.83
5 Nucleus	1H

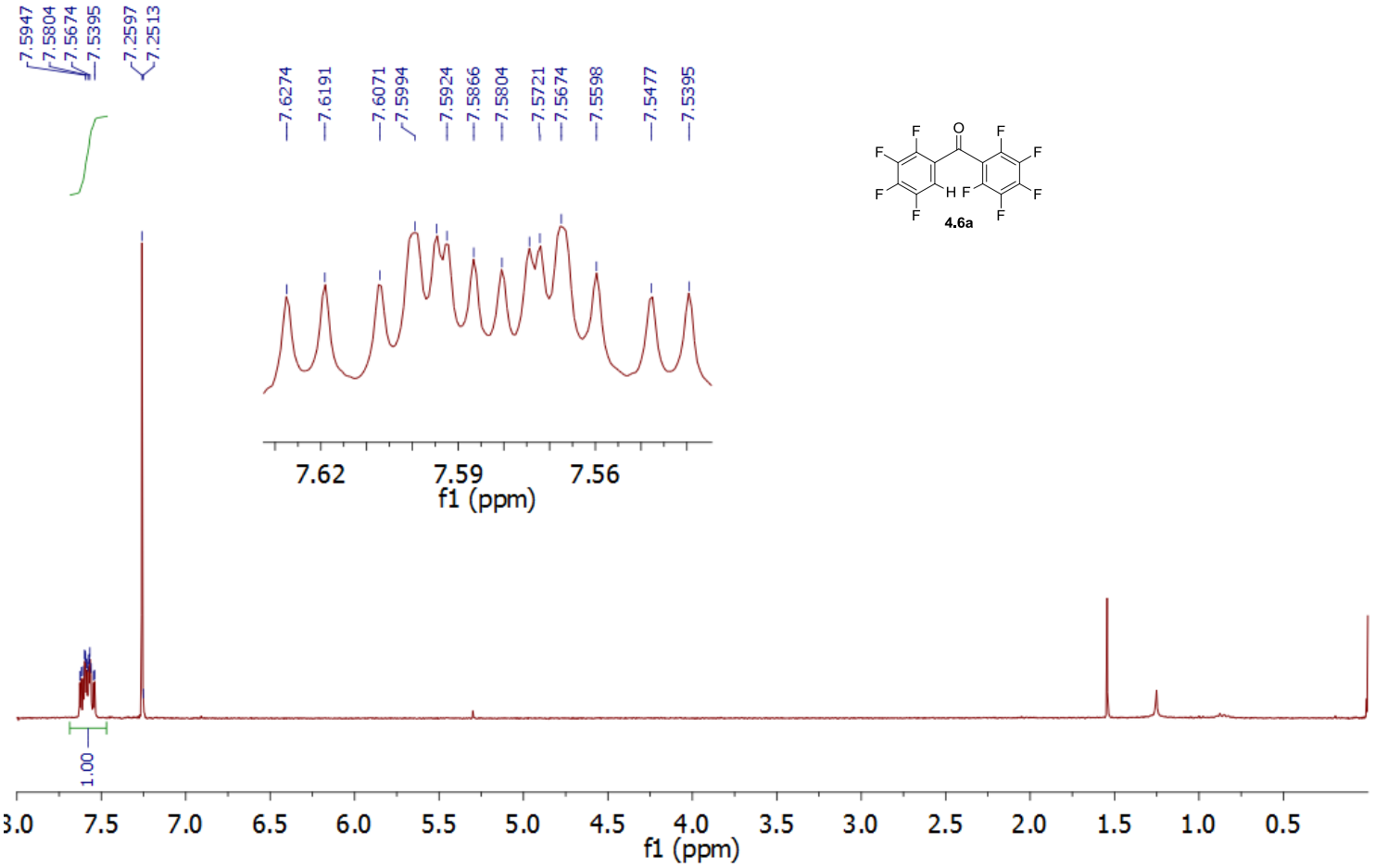

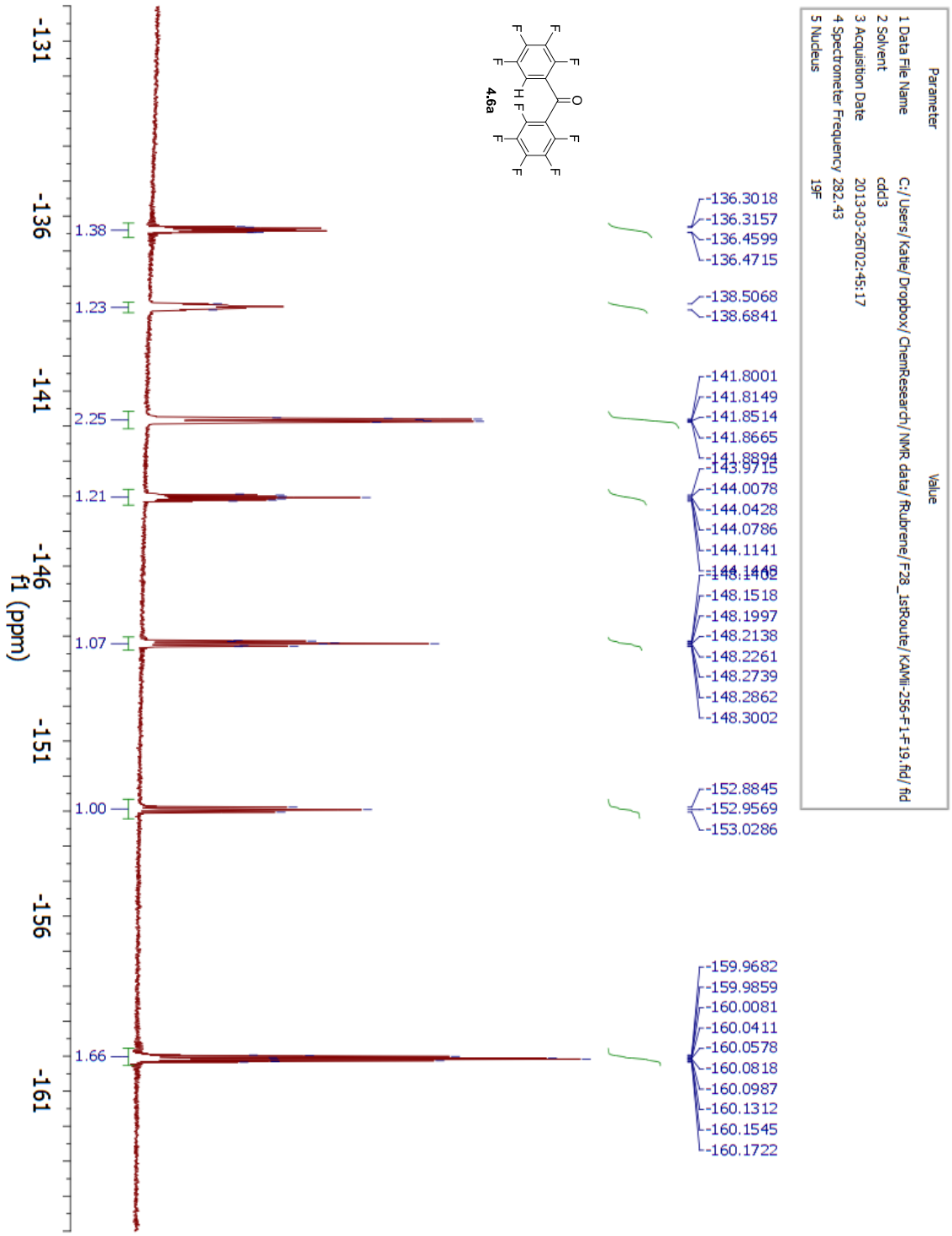
Parameter
Value
1 Data File Name
C:/Users/Katie/Dropbox/ChemResearch/NMR data/Rubrene/F28_1stRoute/KAMii-256-F1-F19.fid/fid
2 Solvent
cdcl3
3 Acquisition Date
2013-03-26T02:45:17
4 Spectrometer Frequency
282.43
5 Nucleus
19F
4.6a
-136.3018
-136.3157
-136.4599
-136.4715
-138.5068
-138.6841
-141.8001
-141.8149
-141.8514
-141.8665
-143.9715
-144.0078
-144.0428
-144.0786
-144.1141
-148.1402
-148.1518
-148.1997
-148.2138
-148.2261
-148.2739
-148.2862
-148.3002
-152.8845
-152.9569
-153.0286
-159.9682
-159.9859
-160.0081
-160.0411
-160.0578
-160.0818
-160.0987
-160.1312
-160.1545
-160.1722
1.38
1.23
2.25
1.21
1.07
1.00
1.66
-131
-136
-141
-146
-151
-156
-161
f1 (ppm)

Parameter	Value
1 Data File Name	C:/ Users/ Katie/ Dropbox/ ChemResearch/ NMR data/ fRubrene/ F28_1stRoute/ KAMii-242-1-F19.fid/ fid
2 Solvent	cdcl3
3 Acquisition Date	2013-03-06T18:32:20
4 Spectrometer Frequency	282.43
5 Nucleus	19F

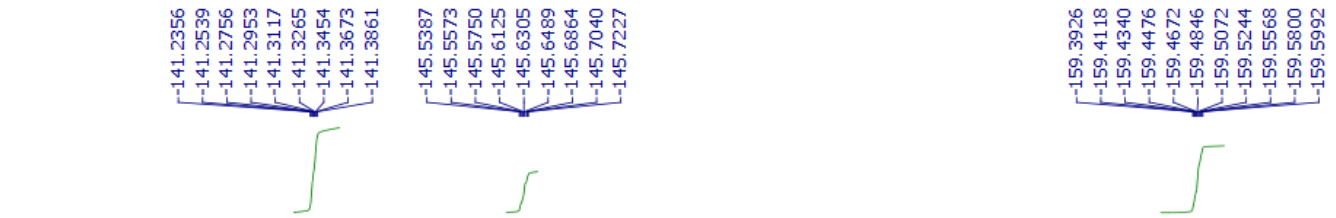

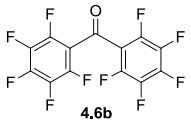

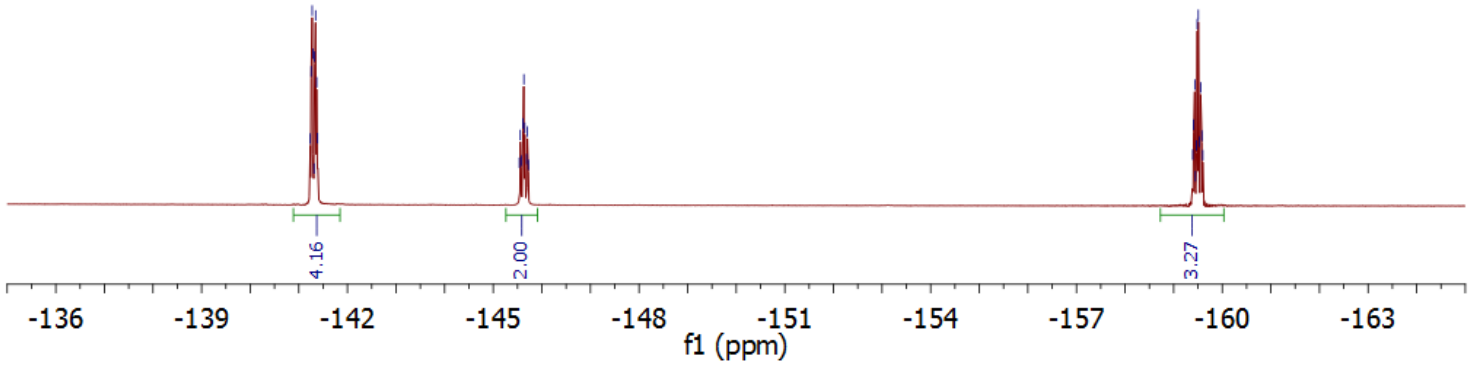

Parameter	Value
1 Data File Name	C:/ Users/ Katie/ Dropbox/ ChemResearch/ NMR data/ fRubrene/ F28_1stRoute/ KAMii-186-crude/ 1/ fid
2 Solvent	CDCl3
3 Acquisition Date	2012-09-27T21:20:22
4 Spectrometer Frequency	500.13
5 Nucleus	1H

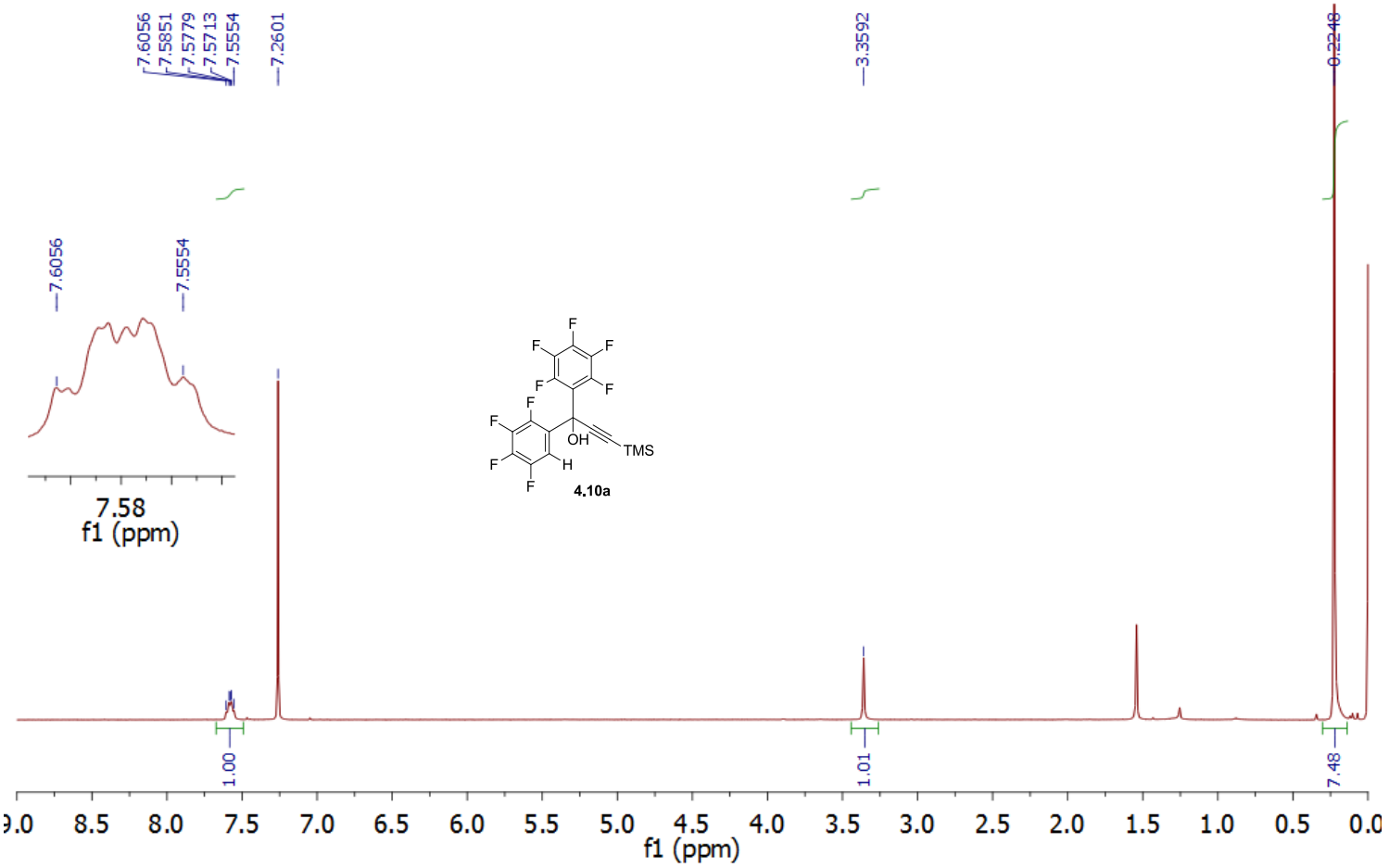

Parameter	Value
1 Data File Name	C:/ Users/ Katie/ Dropbox/ ChemResearch/ NMR data/ fRubrene/ F28_1stRoute/ KAMii-264-F19.fid/ fid
2 Solvent	cdcl3
3 Acquisition Date	2013-04-23T01:24:31
4 Spectrometer Frequency	282.43
5 Nucleus	19F

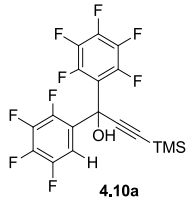

4.10a

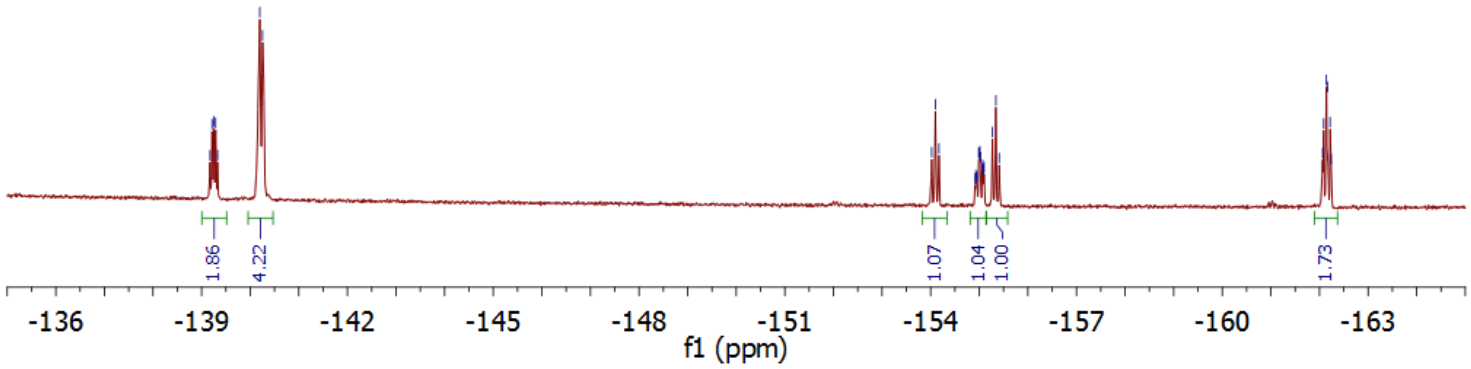

Parameter	Value
1 Data File Name	C:/ Users/ Katie/ Dropbox/ ChemResearch/ NMR data/ fRubrene/ F28_1stRoute/ KAMii-245-crude-1H.fid/ fid
2 Solvent	cdcl3
3 Acquisition Date	2013-03-13T22:33:41
4 Spectrometer Frequency	300.17
5 Nucleus	1H

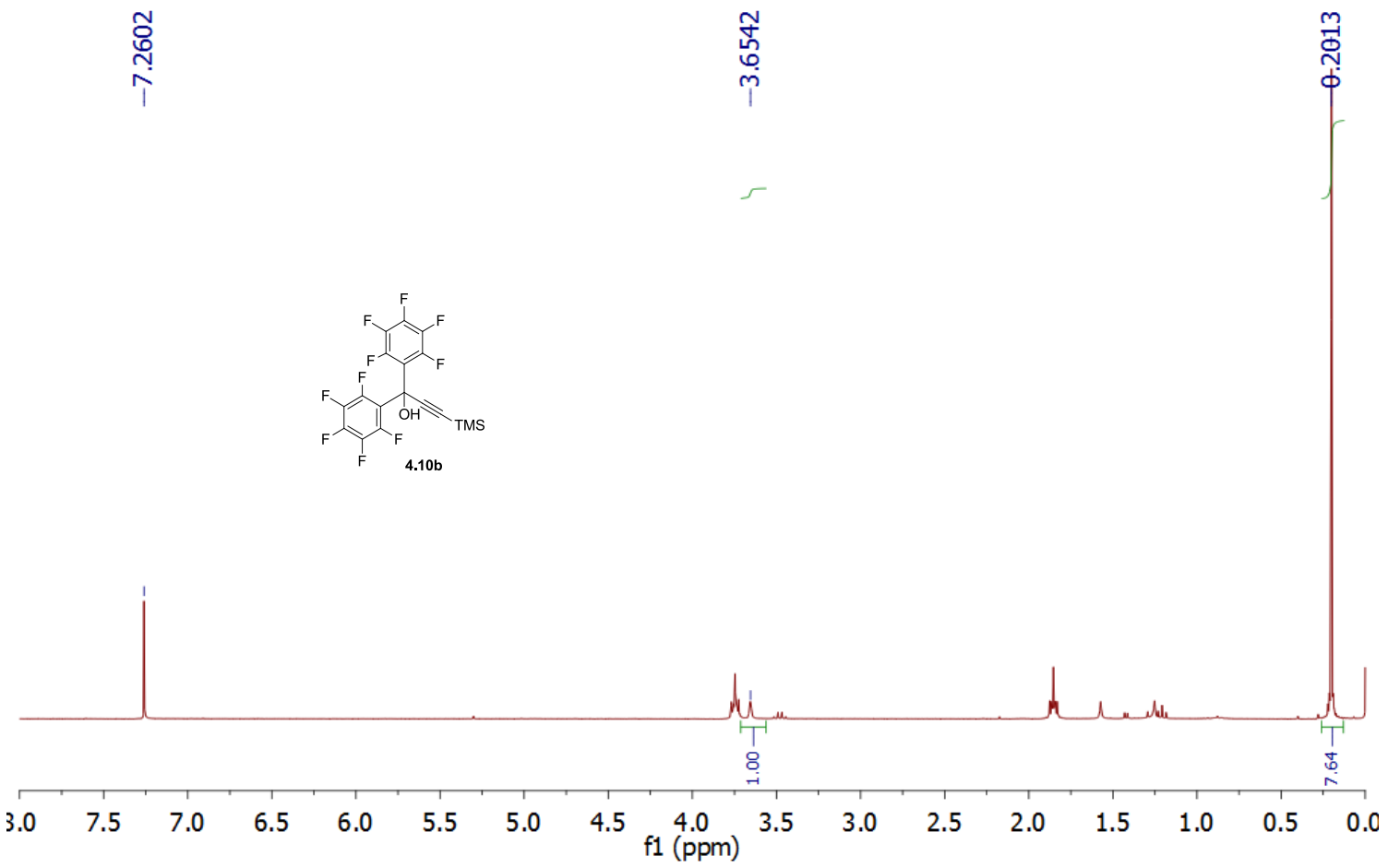

Parameter	Value
1 Data File Name	C:/ Users/ Katie/ Dropbox/ ChemResearch/ NMR data/ fRubrene/ F28_1stRoute/ KAMii-245-crude-F19.fid/ fid
2 Solvent	cdcl3
3 Acquisition Date	2013-03-13T22:35:49
4 Spectrometer Frequency	282.43
5 Nucleus	19F

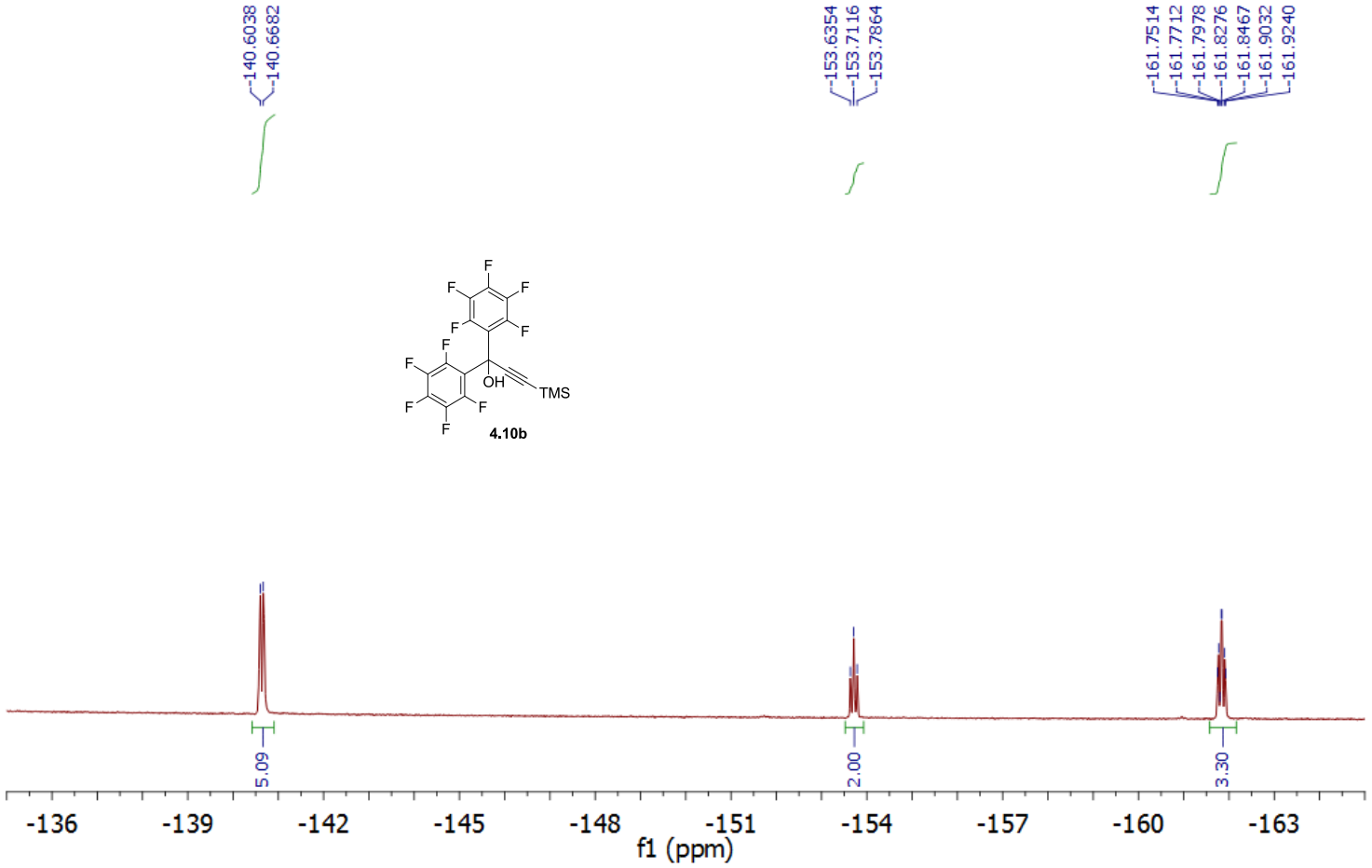

Parameter	Value
1 Data File Name	C:/ Users/ Katie/ Dropbox/ ChemResearch/ NMR data/ fRubrene/ F28_1stRoute/ KAMii-188-crude/ 1/ fid
2 Solvent	CDCl3
3 Acquisition Date	2012-09-28T23:20:09
4 Spectrometer Frequency	500.13
5 Nucleus	1H

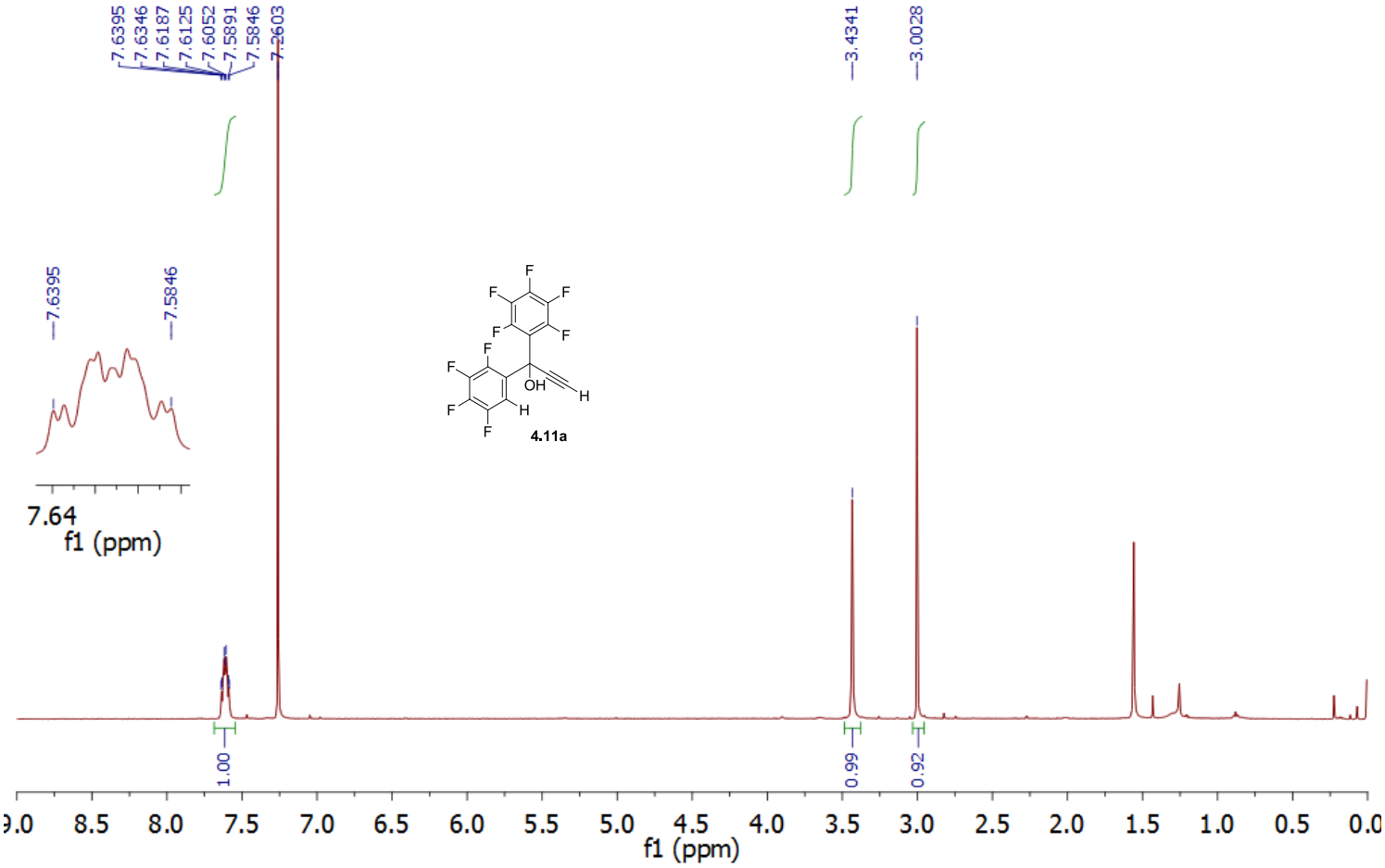

Parameter	Value
1 Data File Name	C:/ Users/ Katie/ Dropbox/ ChemResearch/ NMR data/ fRubrene/ F28_1stRoute/ KAMii-238-F19.fid/ fid
2 Solvent	cdcl3
3 Acquisition Date	2013-03-04T18:36:53
4 Spectrometer Frequency	282.43
5 Nucleus	19F

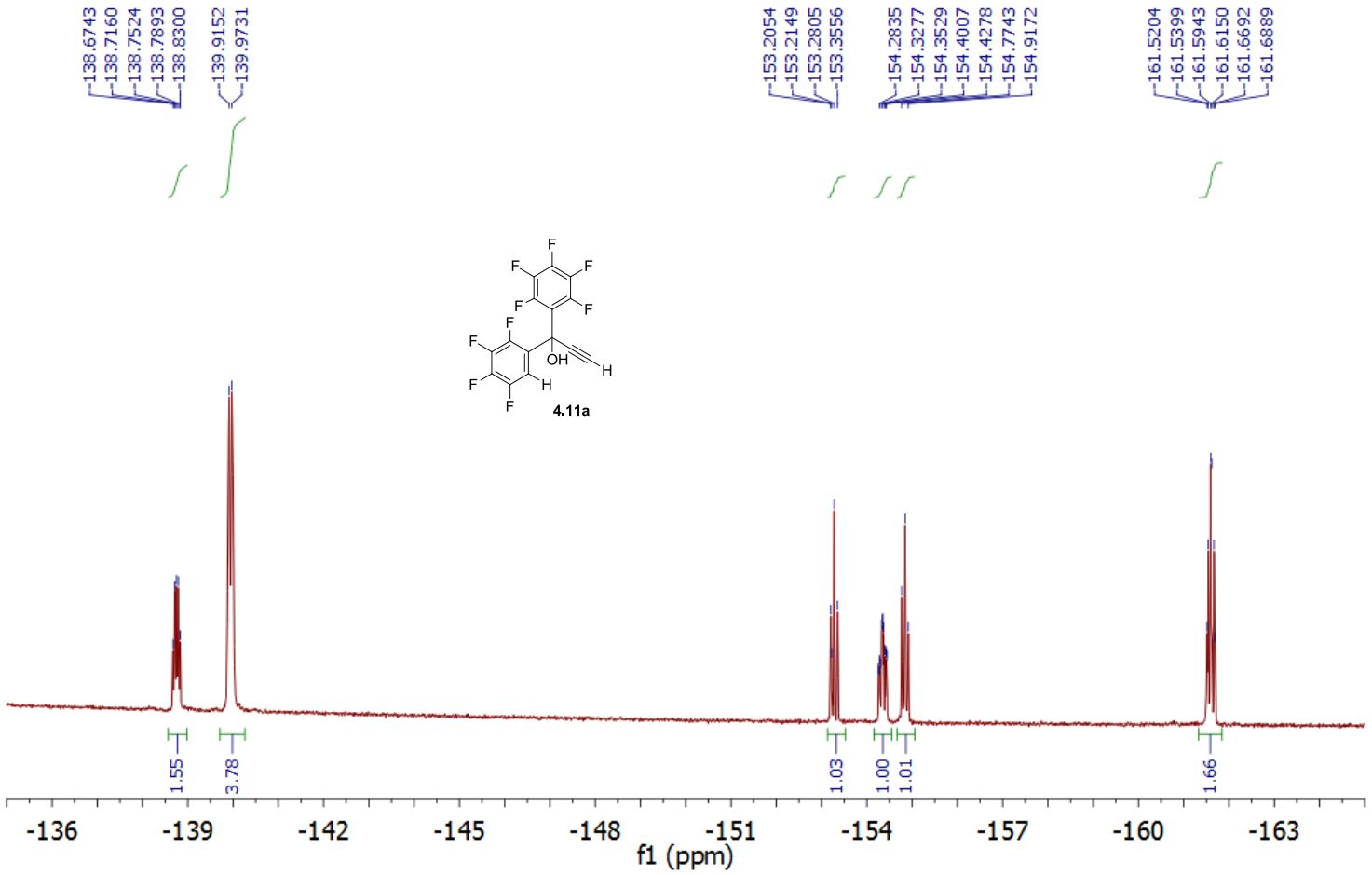

Parameter	Value
1 Data File Name	C:/ Users/ Katie/ Dropbox/ ChemResearch/ NMR data/ fRubrene/ F28_1stRoute/ KAMii-252-032013-1H.fid/ fid
2 Solvent	cdcl3
3 Acquisition Date	2013-03-21T20:01:39
4 Spectrometer Frequency	300.17
5 Nucleus	1H

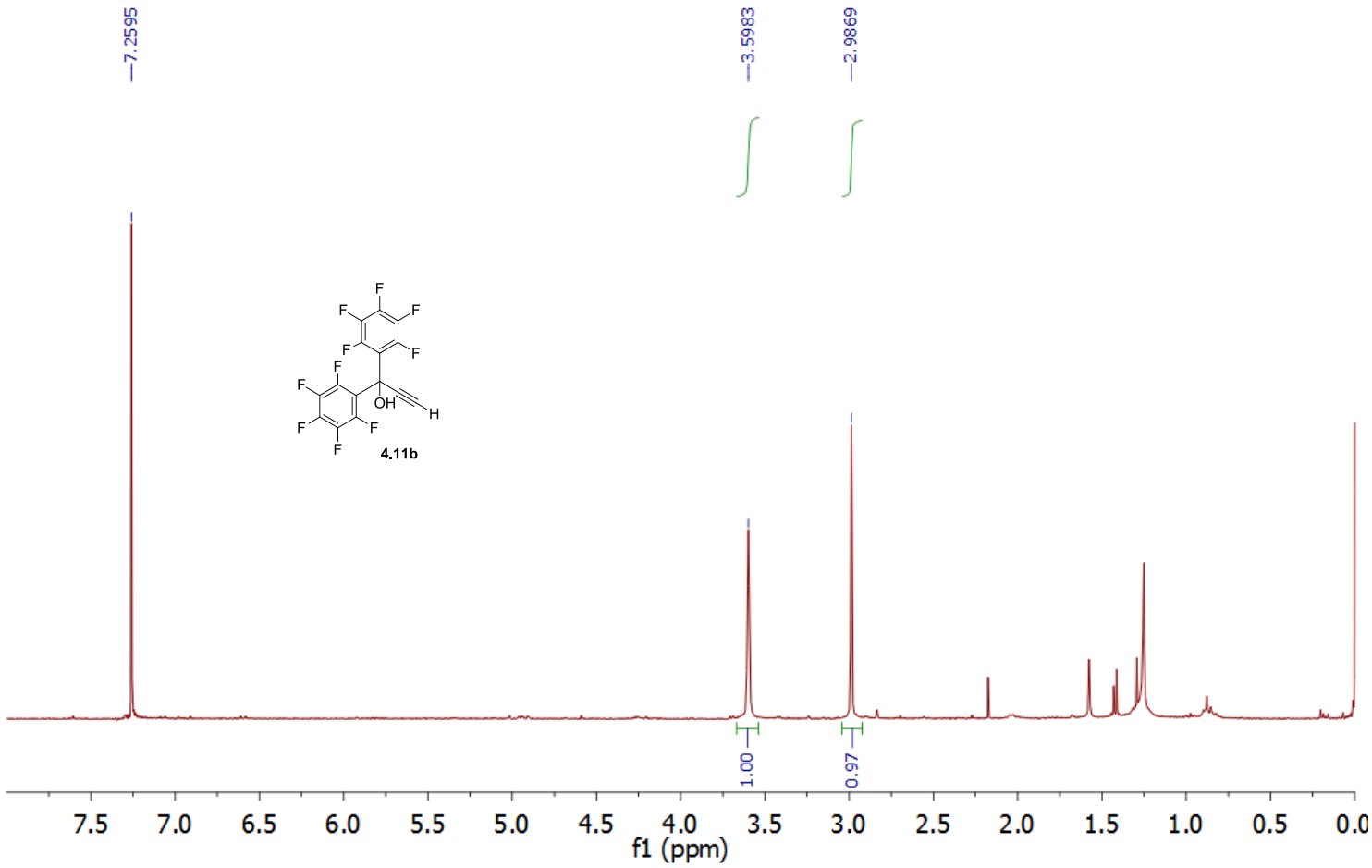

Parameter	Value
1 Data File Name	C:/ Users/ Katie/ Dropbox/ ChemResearch/ NMR data/ fRubrene/ F28_1stRoute/ KAMii-252-032113-F19.fid/ fid
2 Solvent	cdcl3
3 Acquisition Date	2013-03-21T20:02:44
4 Spectrometer Frequency	282.43
5 Nucleus	19F

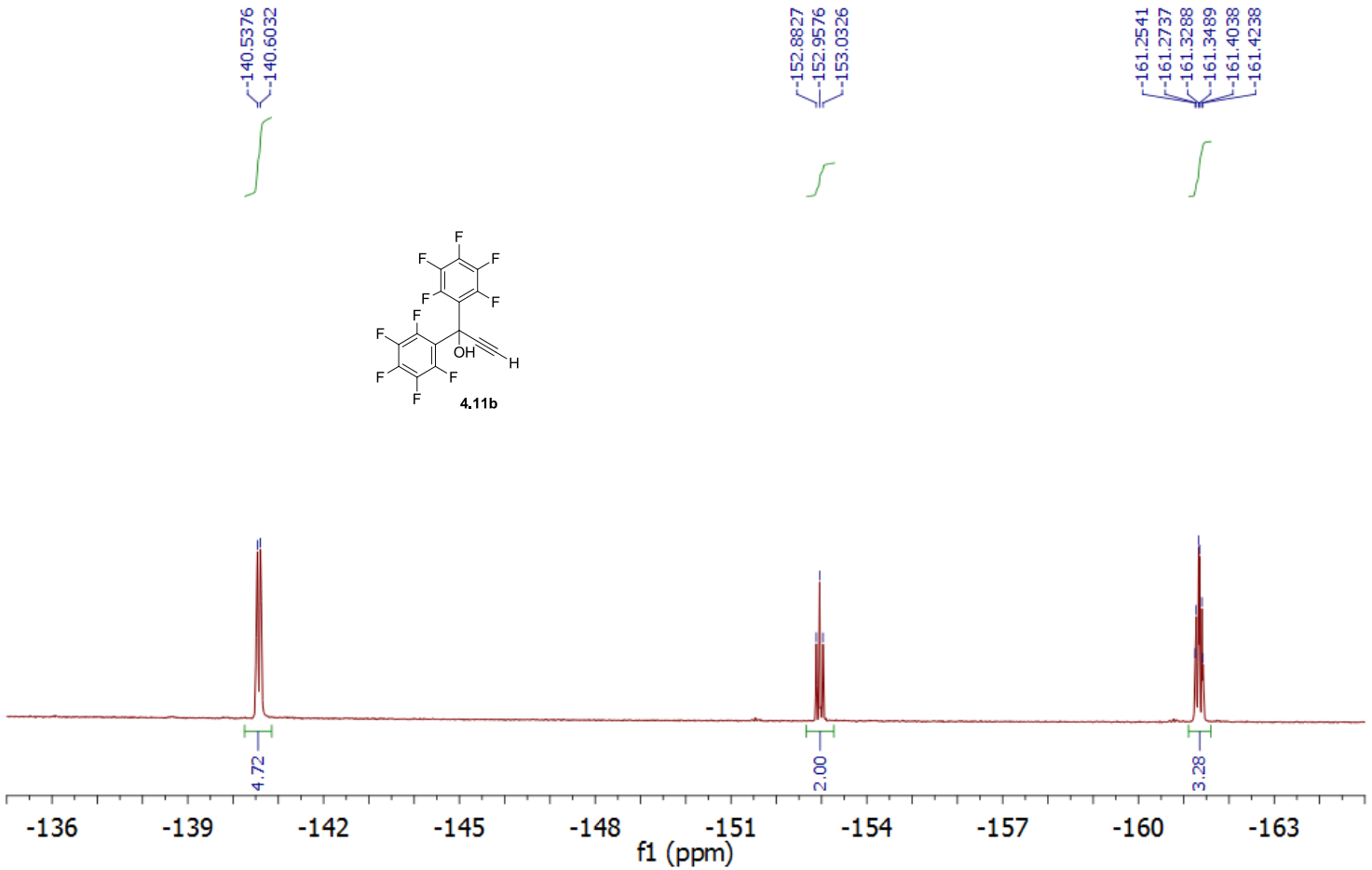

Parameter	Value
1 Data File Name	C:/ Users/ Katie/ Dropbox/ ChemResearch/ NMR data/ fRubrene/ F28_1stRoute/ KAMii-119-F1-F1/ 1/ fid
2 Solvent	CDCl3
3 Acquisition Date	2012-03-03T21:57:14
4 Spectrometer Frequency	500.13
5 Nucleus	1H

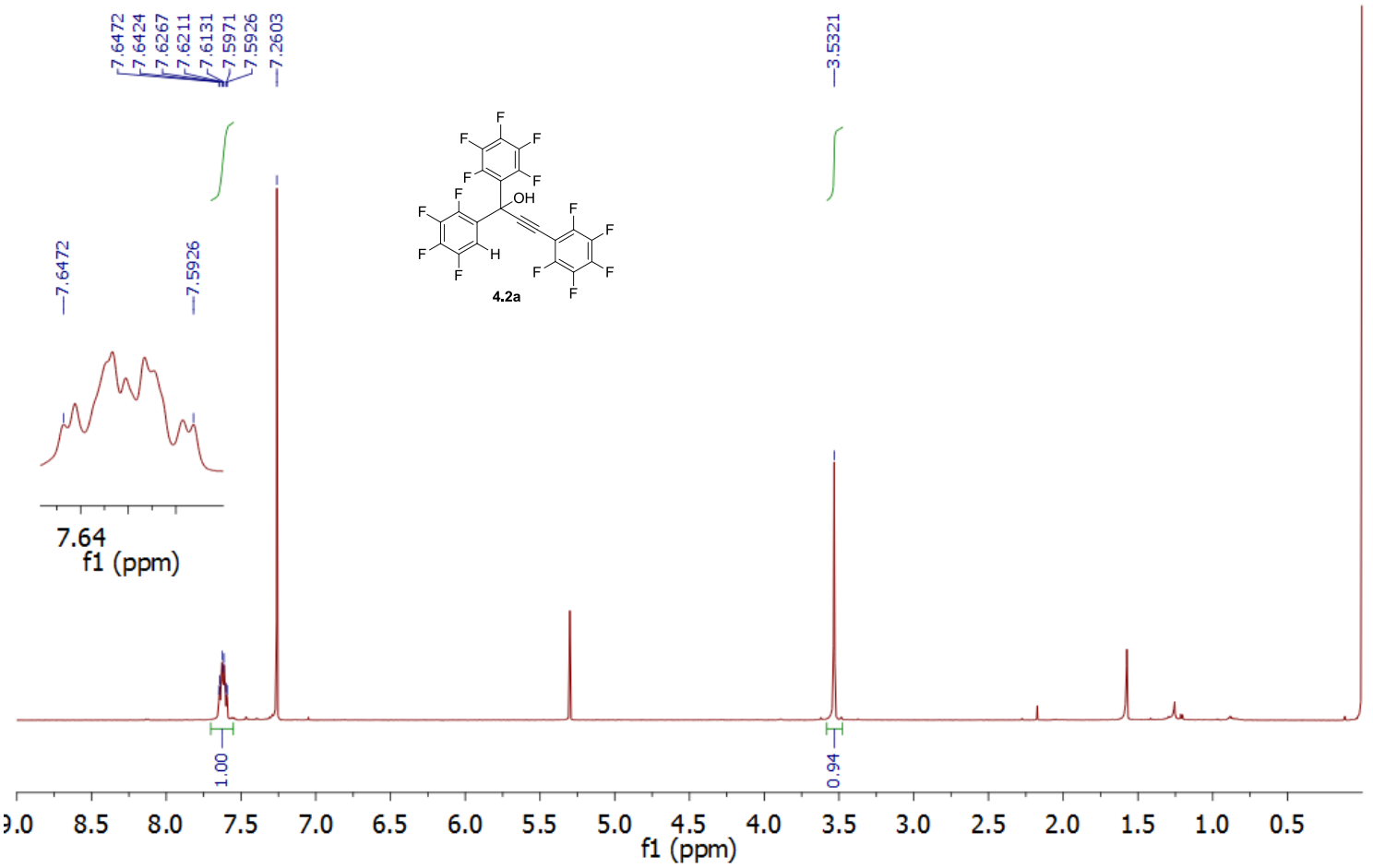

Parameter	Value
1 Data File Name	C:/ Users/ Katie/ Dropbox/ ChemResearch/ NMR data/ fRubrene/ cdokam-130804-10/ 20/ fid
2 Solvent	CDCl3
3 Acquisition Date	2013-08-05T03:31:08
4 Spectrometer Frequency	125.77
5 Nucleus	13C

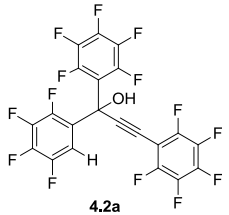

4.2a

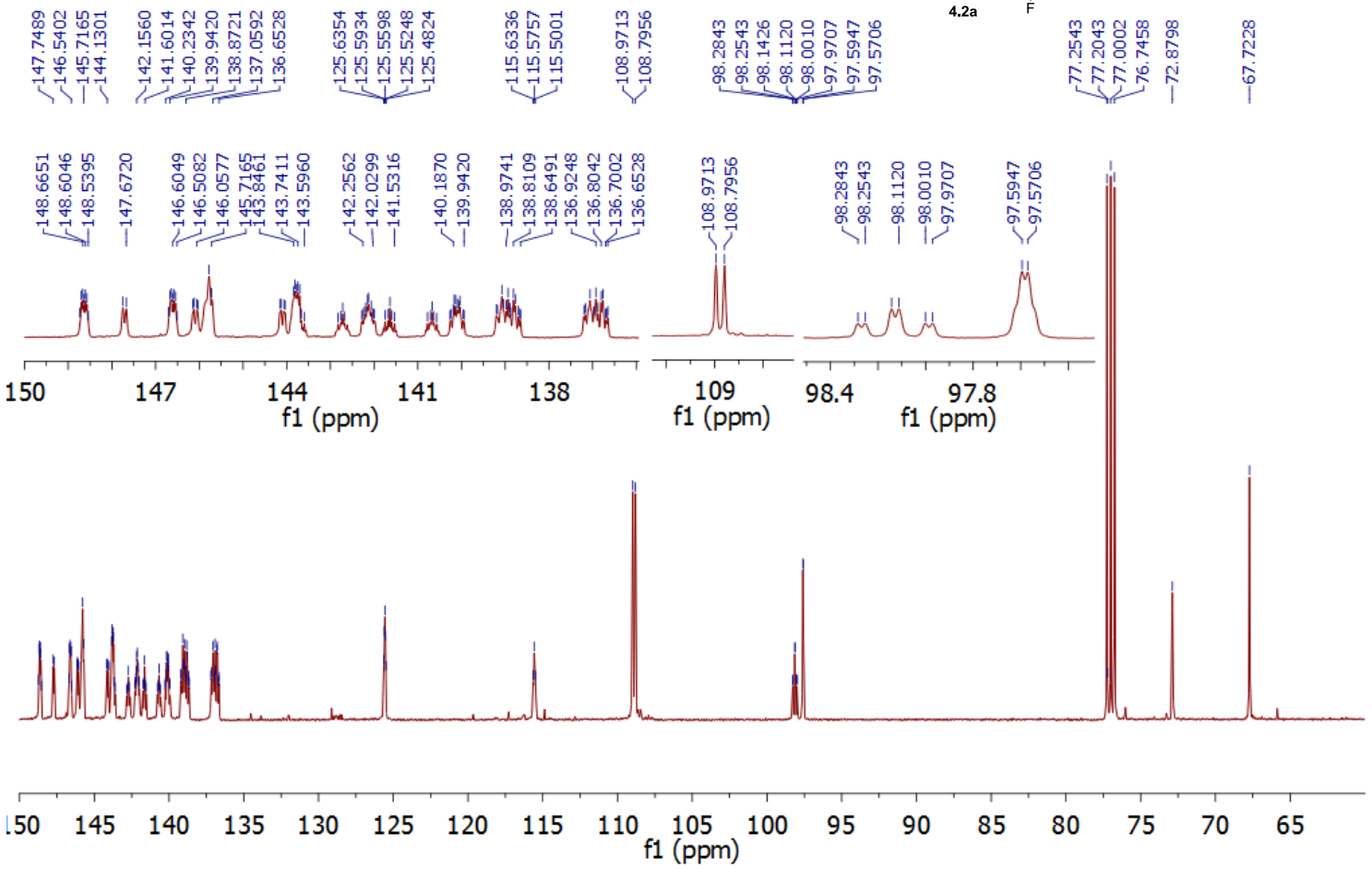

Parameter	Value
1 Data File Name	C:/ Users/ Katie/ Dropbox/ ChemResearch/ NMR data/ fRubrene/ F28_1stRoute/ KAMii-119-F1-F1-041112-F19.fid/ fid
2 Solvent	cdcl3
3 Acquisition Date	2012-04-11T22:34:29
4 Spectrometer Frequency	282.11
5 Nucleus	19F

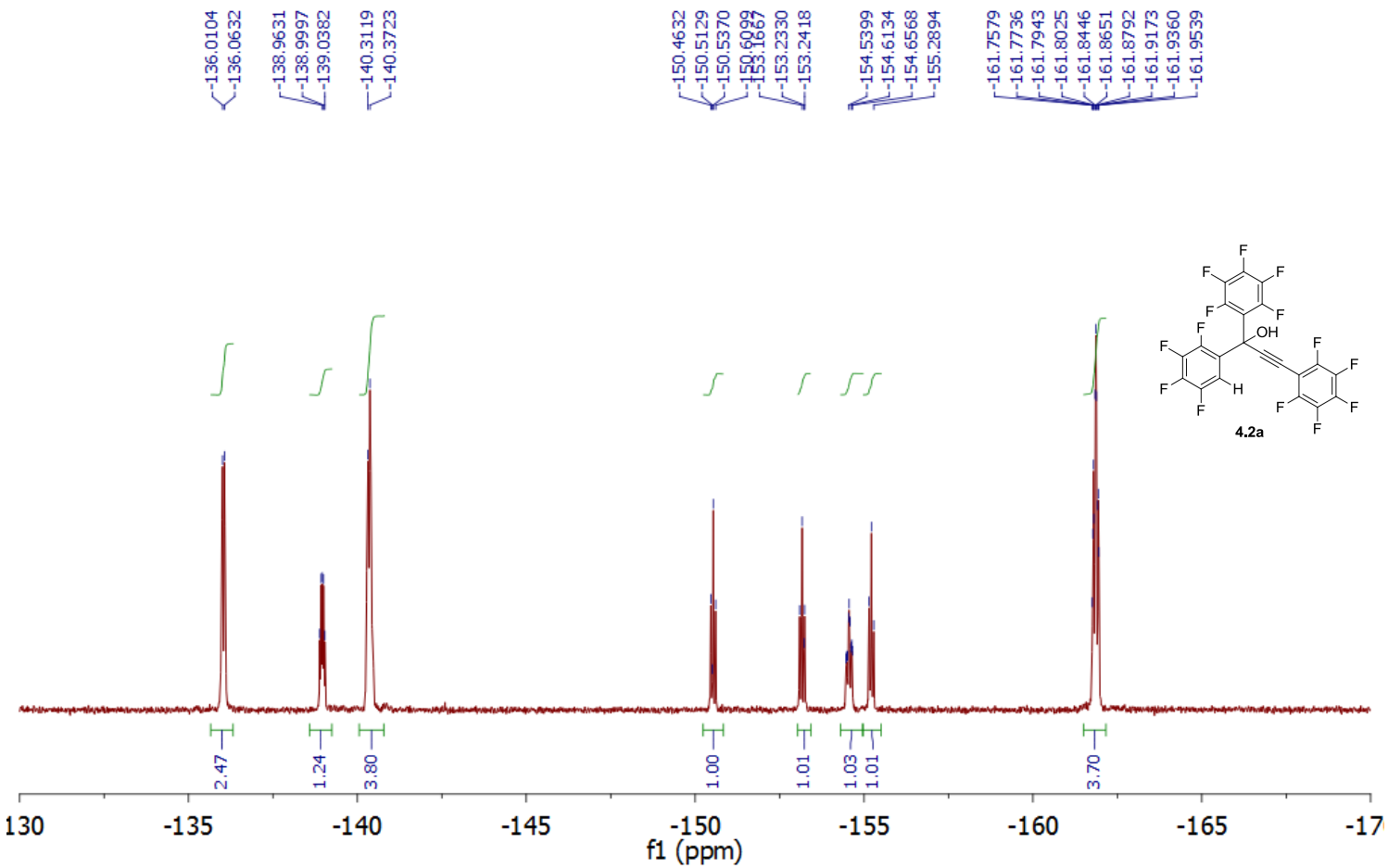

Parameter	Value
1 Data File Name	C:/ Users/ Katie/ Dropbox/ ChemResearch/ NMR data/ fRubrene/ F28_1stRoute/ KAMii-253-pure-1H.fid/ fid
2 Solvent	cdcl3
3 Acquisition Date	2013-03-22T15:44:49
4 Spectrometer Frequency	300.17
5 Nucleus	1H

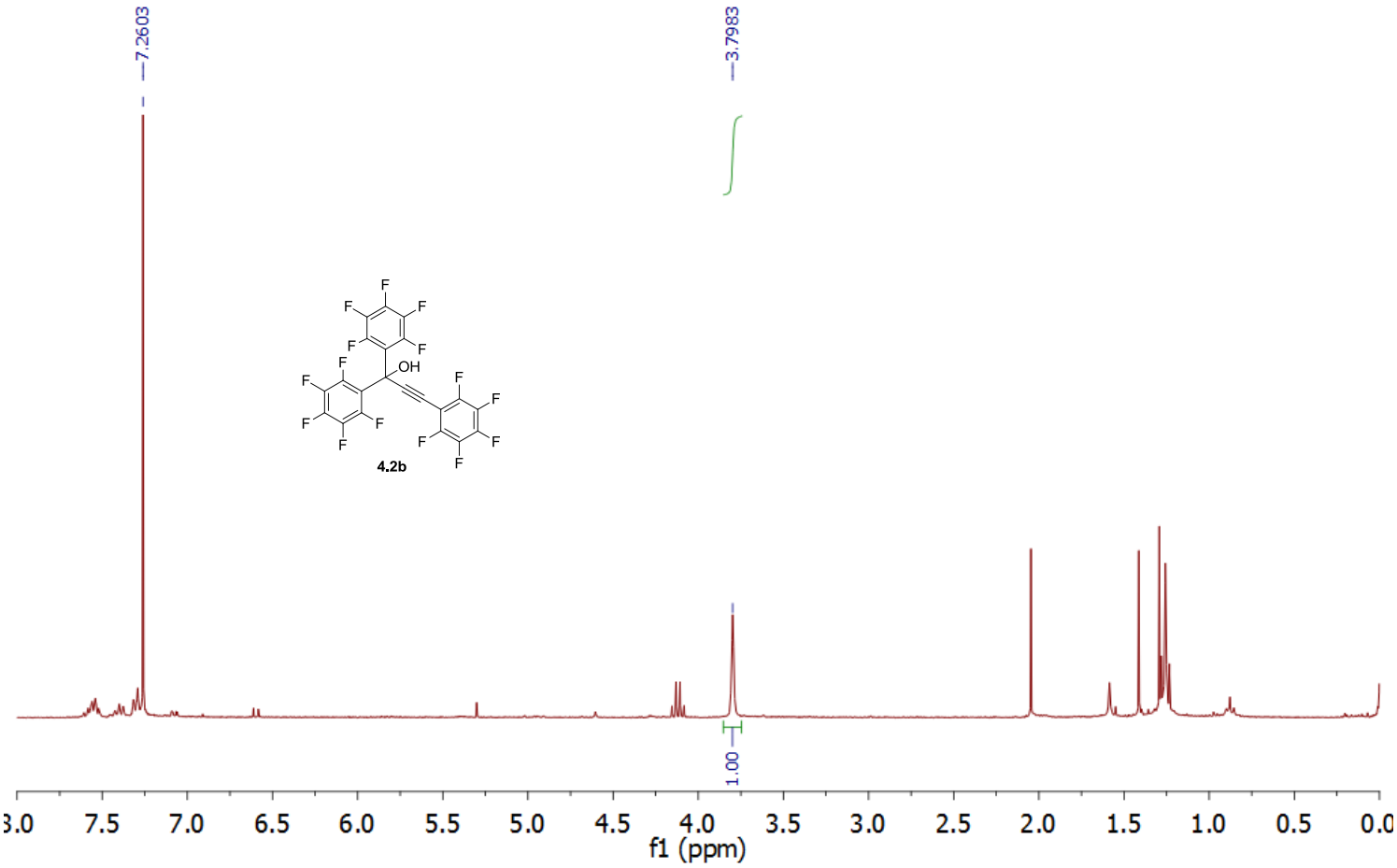

Parameter	Value
1 Data File Name	C:/ Users/ Katie/ Dropbox/ ChemResearch/ NMR data/ fRubrene/ F28_1stRoute/ KAMii-253-pure-F19.fid/ fid
2 Solvent	cdcl3
3 Acquisition Date	2013-03-22T15:46:30
4 Spectrometer Frequency	282.43
5 Nucleus	19F

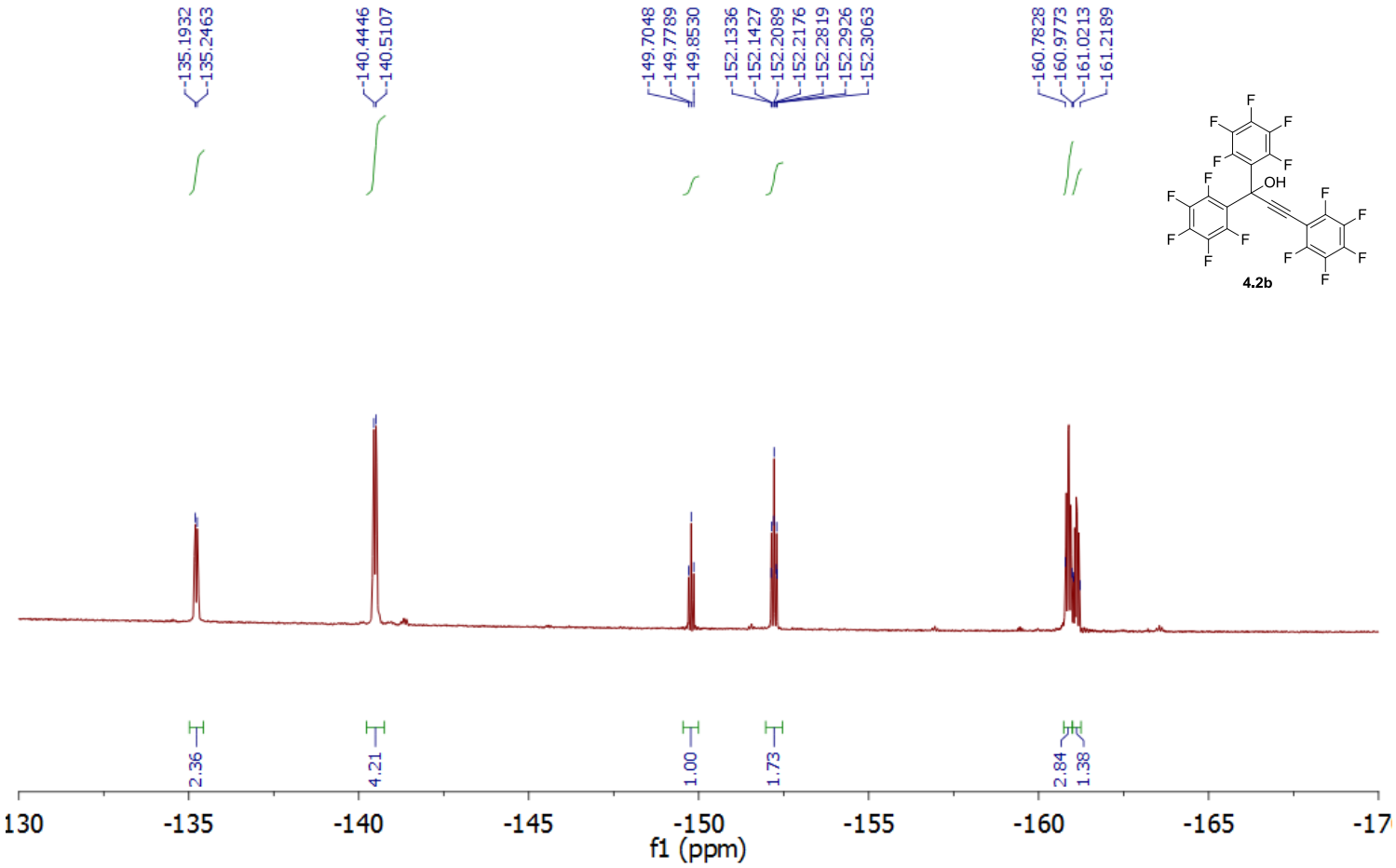

Parameter	Value
1 Data File Name	C:/ Users/ Katie/ Dropbox/ ChemResearch/ NMR data/ fRubrene/ F28_1stRoute/ KAMii-222f3-222f4-mix-1H-021313.fid/ fid
2 Solvent	cdcl3
3 Acquisition Date	2013-02-13T21:51:30
4 Spectrometer Frequency	300.17
5 Nucleus	1H

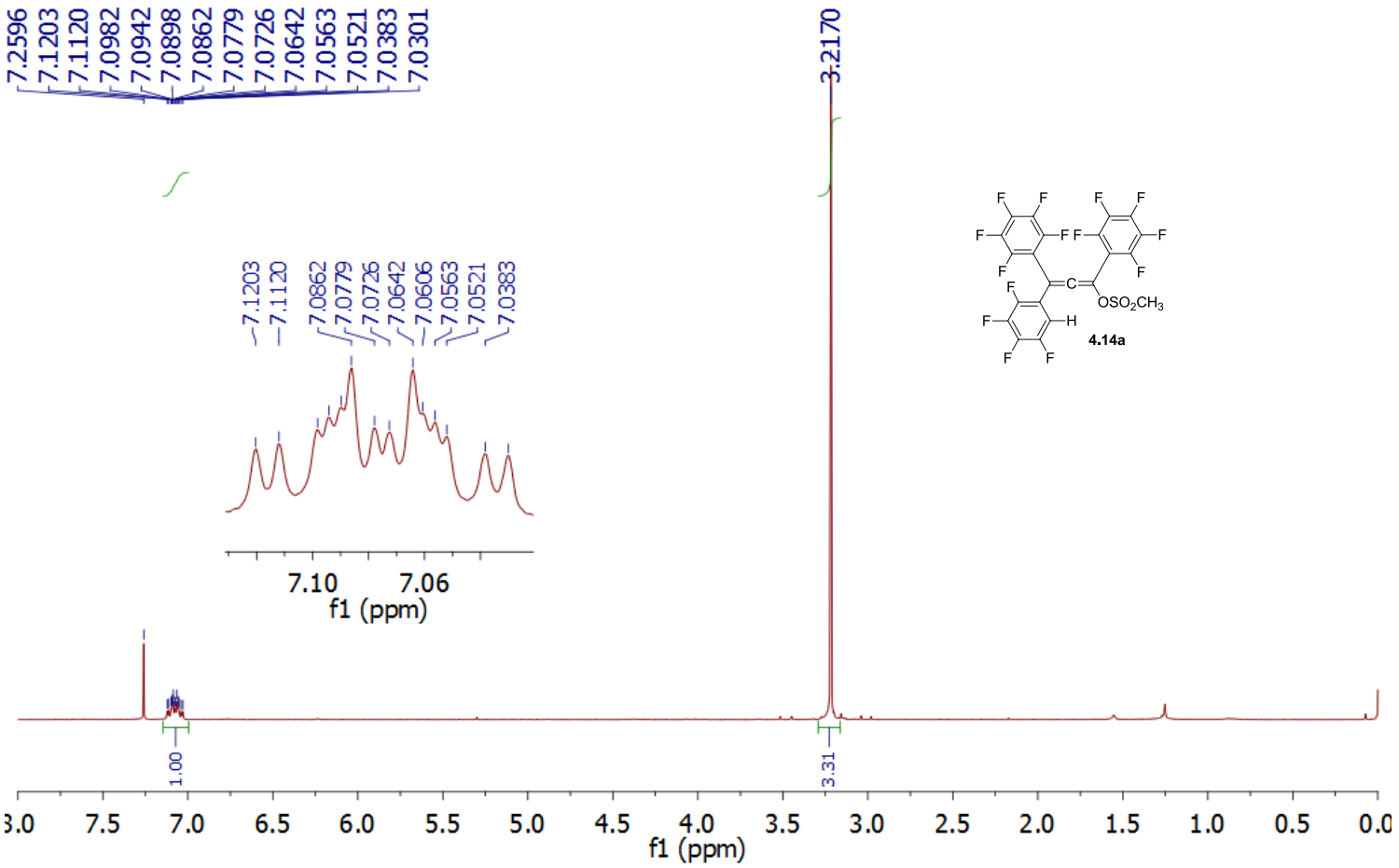

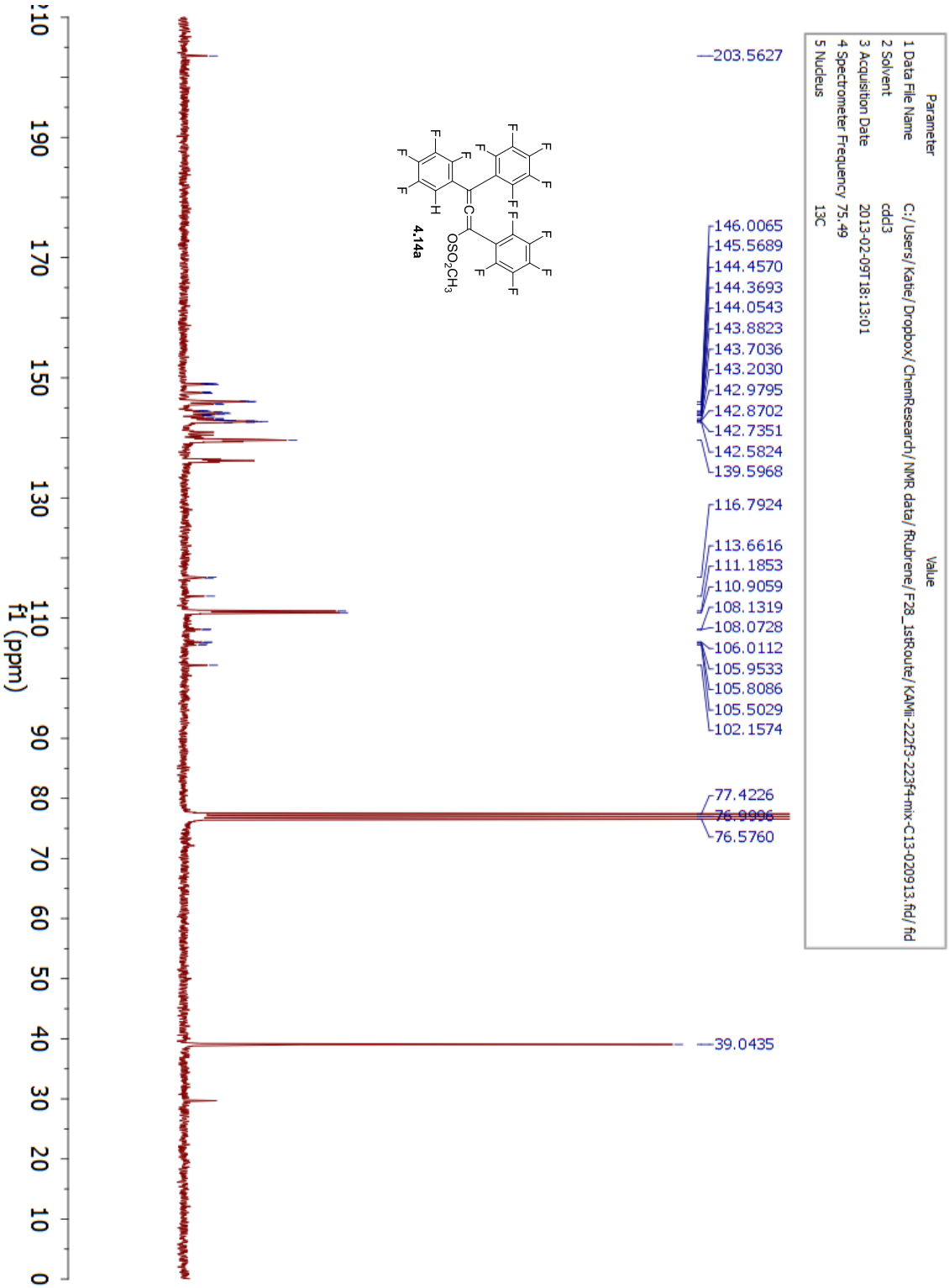
Parameter
Value
1 Data File Name
C:/Users/Katie/Dropbox/ChemResearch/NMR data/fRubrene/F28_1stRoute/KAMii-222f3-223f4-mix-C13-020913.fid/fid
2 Solvent
cdcl3
3 Acquisition Date
2013-02-09T18:13:01
4 Spectrometer Frequency 75.49
5 Nucleus
13C
4.14a
203.5627
146.0065
145.5689
144.4570
144.3693
144.0543
143.8823
143.7036
143.2030
142.9795
142.8702
142.7351
142.5824
139.5968
116.7924
113.6616
111.1853
110.9059
108.1319
108.0728
106.0112
105.9533
105.8086
105.5029
102.1574
77.4226
76.9996
76.5760
39.0435
f1 (ppm)

Parameter	Value
1 Data File Name	C:/ Users/ Katie/ Dropbox/ ChemResearch/ NMR data/ fRubrene/ F28_1stRoute/ KAMii-222f3-223f4-mix-F19-021313.fid/ fid
2 Solvent	cdcl3
3 Acquisition Date	2013-02-13T22:22:43
4 Spectrometer Frequency	282.43
5 Nucleus	19F

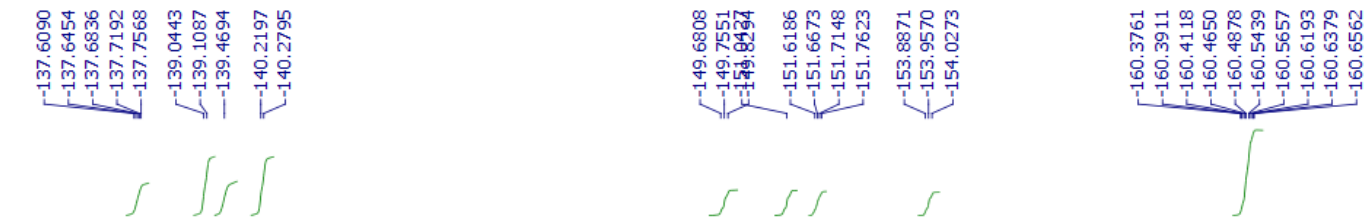

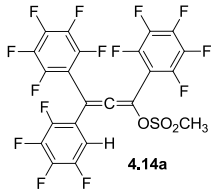

4.14a

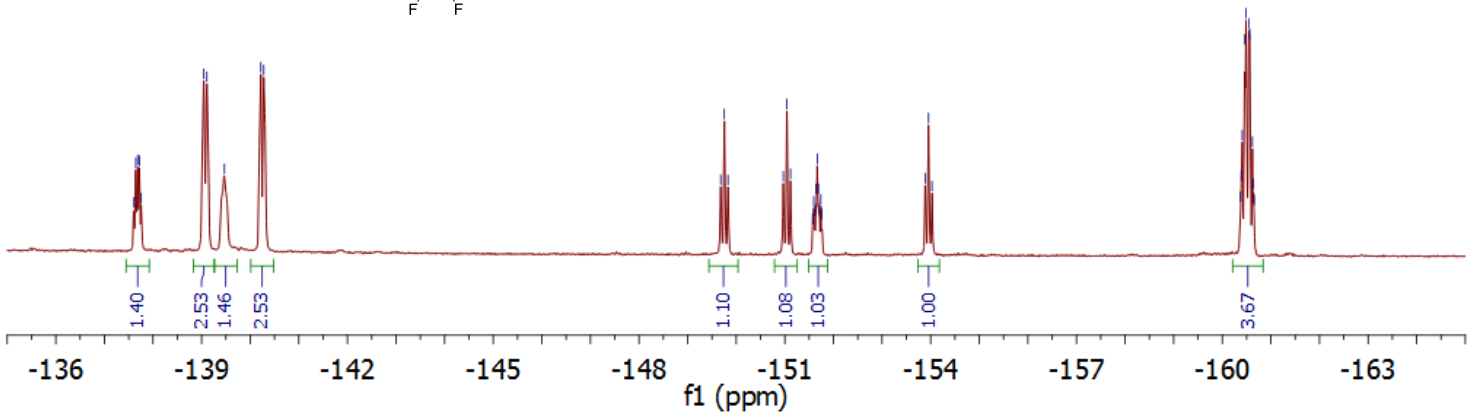

Parameter	Value
1 Data File Name	C:/ Users/ Katie/ Dropbox/ ChemResearch/ NMR data/ fRubrene/ F28_1stRoute/ KAMii-292-F2-1H.fid/ fid
2 Owner	cdokam
3 Acquisition Date	2013-07-22T22:53:41
4 Spectrometer Frequency	300.17
5 Nucleus	1H

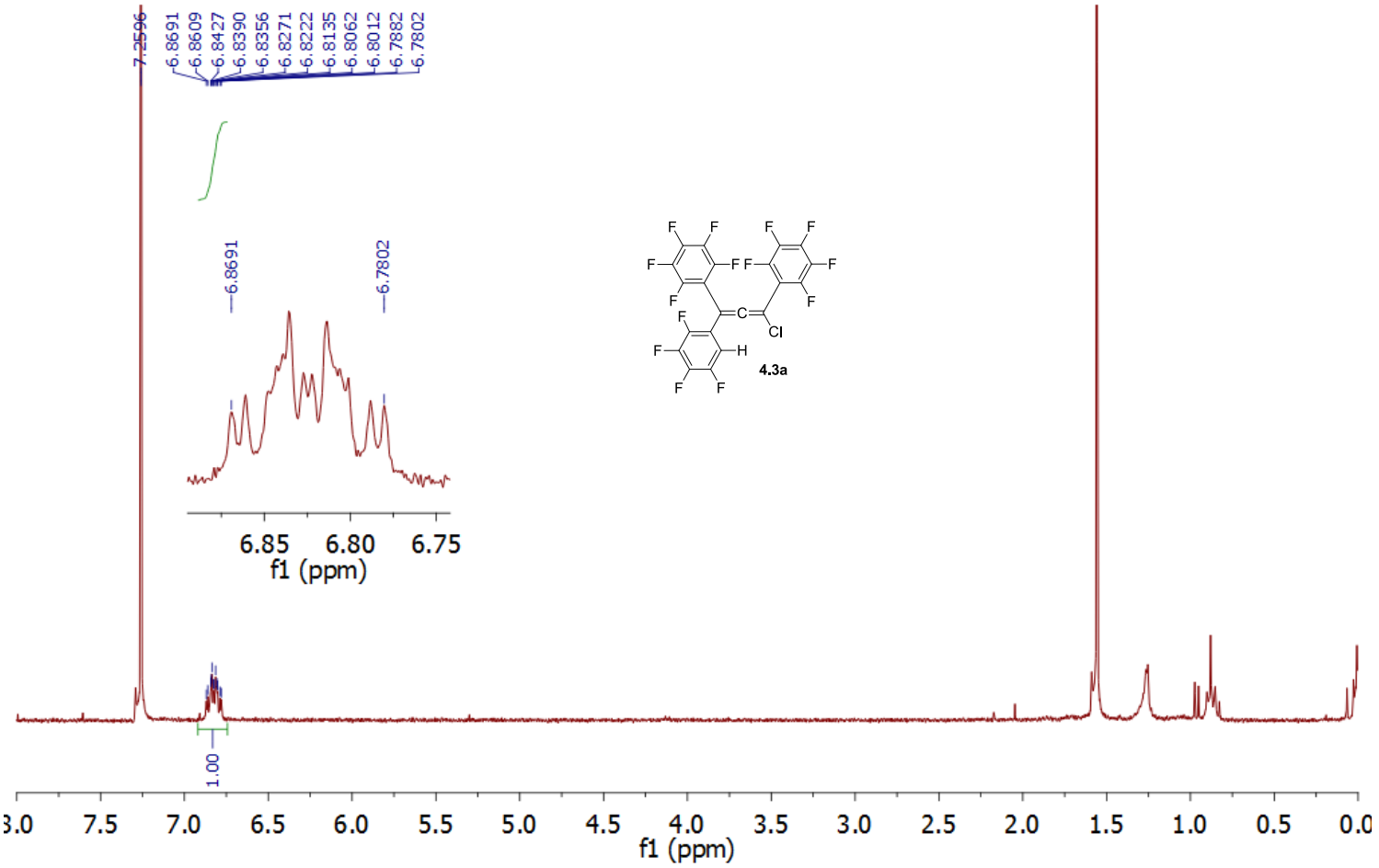

4.3a

Parameter	Value
1 Data File Name	C:/ Users/ Katie/ Dropbox/ ChemResearch/ NMR data/ fRubrene/ cdokam-130804-59/ 20/ fid
2 Solvent	CDCl3
3 Acquisition Date	2013-08-05T01:28:05
4 Spectrometer Frequency	125.77
5 Nucleus	13C

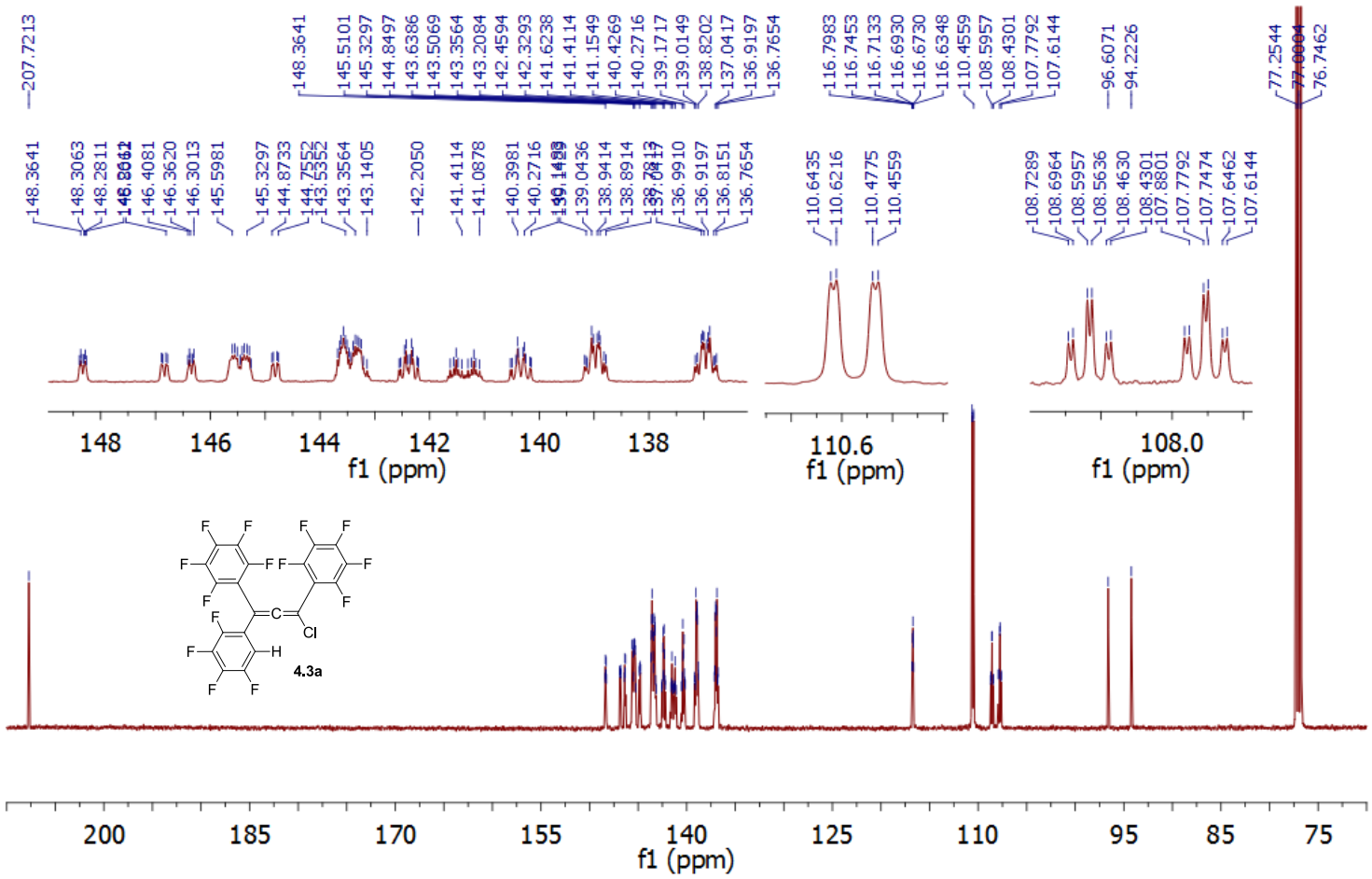

Parameter	Value
1 Data File Name	C:/ Users/ Katie/ Dropbox/ ChemResearch/ NMR data/ fRubrene/ F28_1stRoute/ KAMii-288-3-F1-F19good.fid/ fid
2 Solvent	cdcl3
3 Acquisition Date	2013-07-17T17:28:13
4 Spectrometer Frequency	282.41
5 Nucleus	19F

-137.8555 -137.8906 -137.9307 -137.9636 -137.9986 -139.0314 -139.6359 -139.6916 -150.5330 -150.6069 -150.6811 -150.9293 -151.0032 -151.0775 -152.0775 -152.1731 -153.6029 -153.6731 -153.7424 -160.2333 -160.2491 -160.2705 -160.3221 -160.3441 -160.3957 -160.4165 -160.4332 -160.4741 -160.4924 -160.5124 -160.5646 -160.5856 -160.6001 -160.6380 -160.6572 -160.6759

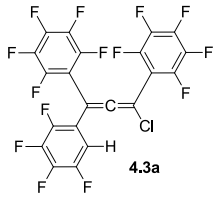

4.3a

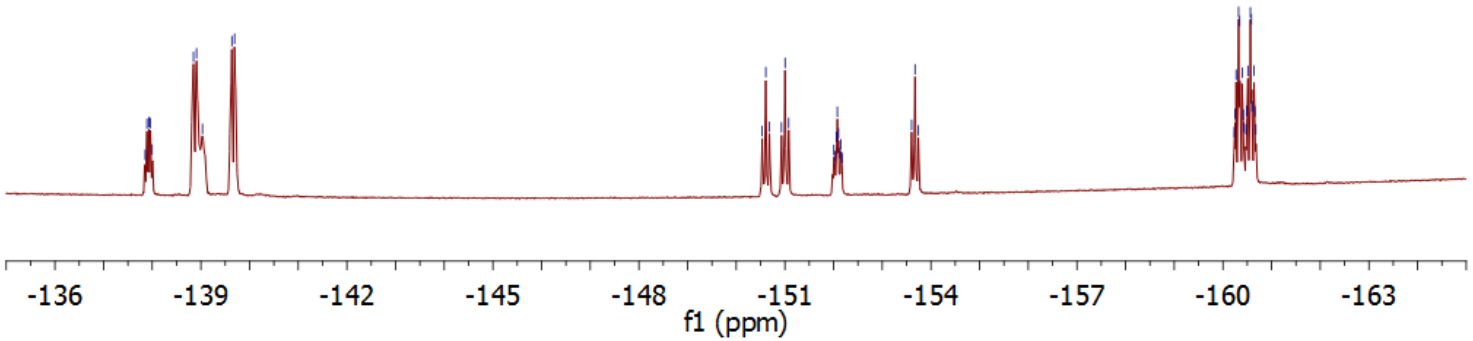

Parameter	Value
1 Data File Name	C:/ Users/ Katie/ Dropbox/ ChemResearch/ NMR data/ fRubrene/ F28_1stRoute/ KAMii-104-F1-F1/ 1/ fid
2 Solvent	CDCl3
3 Acquisition Date	2012-02-07T00:58:00
4 Spectrometer Frequency	500.13
5 Nucleus	1H

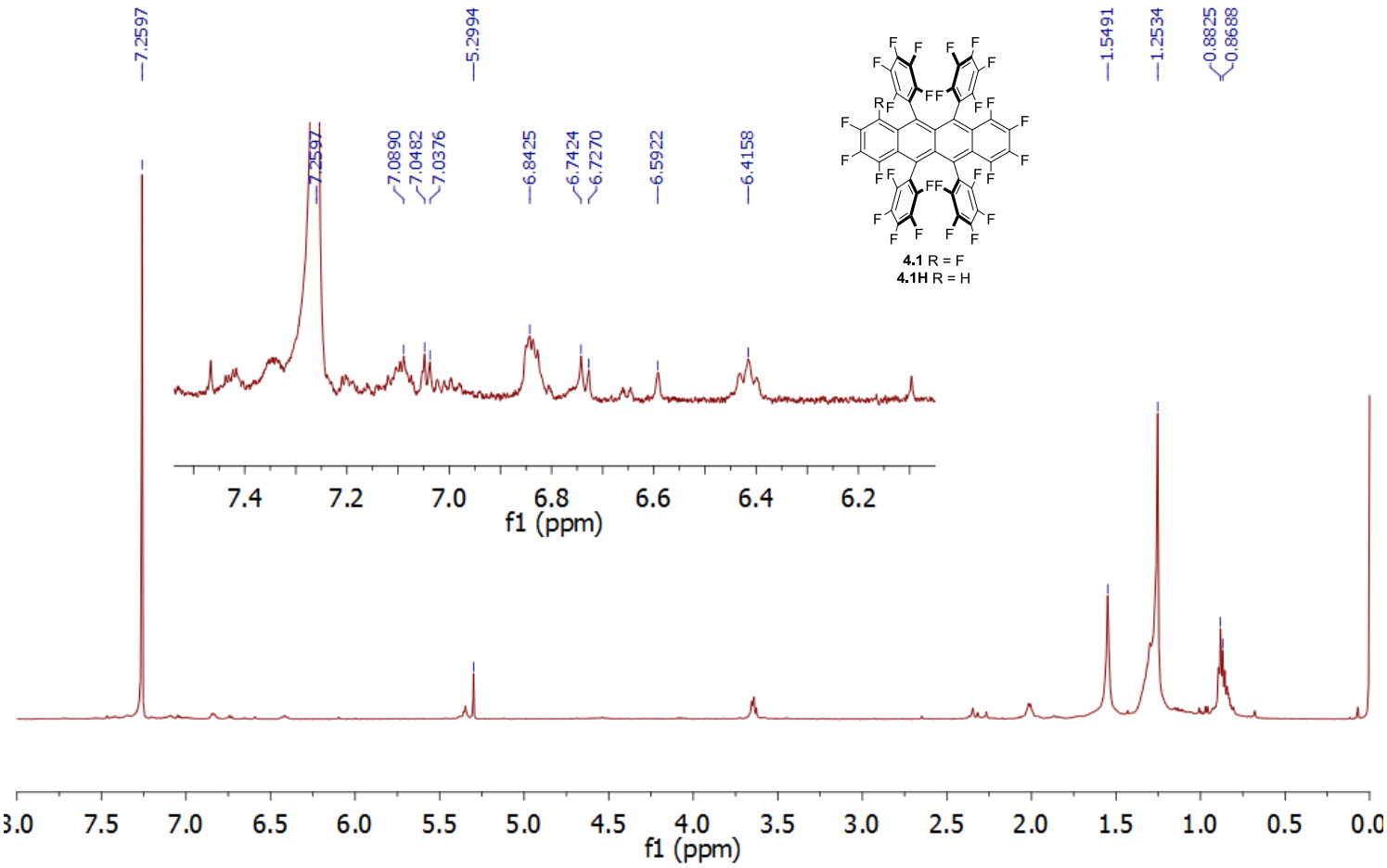

4.1 R = F
4.1H R = H

Parameter	Value
1 Data File Name	C:/ Users/ Katie/ Dropbox/ ChemResearch/ NMR data/ fRubrene/ F28_1stRoute/ KAMii-104-F1-F1/ 2/ fid
2 Solvent	CDCl3
3 Acquisition Date	2012-02-07T01:00:58
4 Spectrometer Frequency	470.59
5 Nucleus	19F

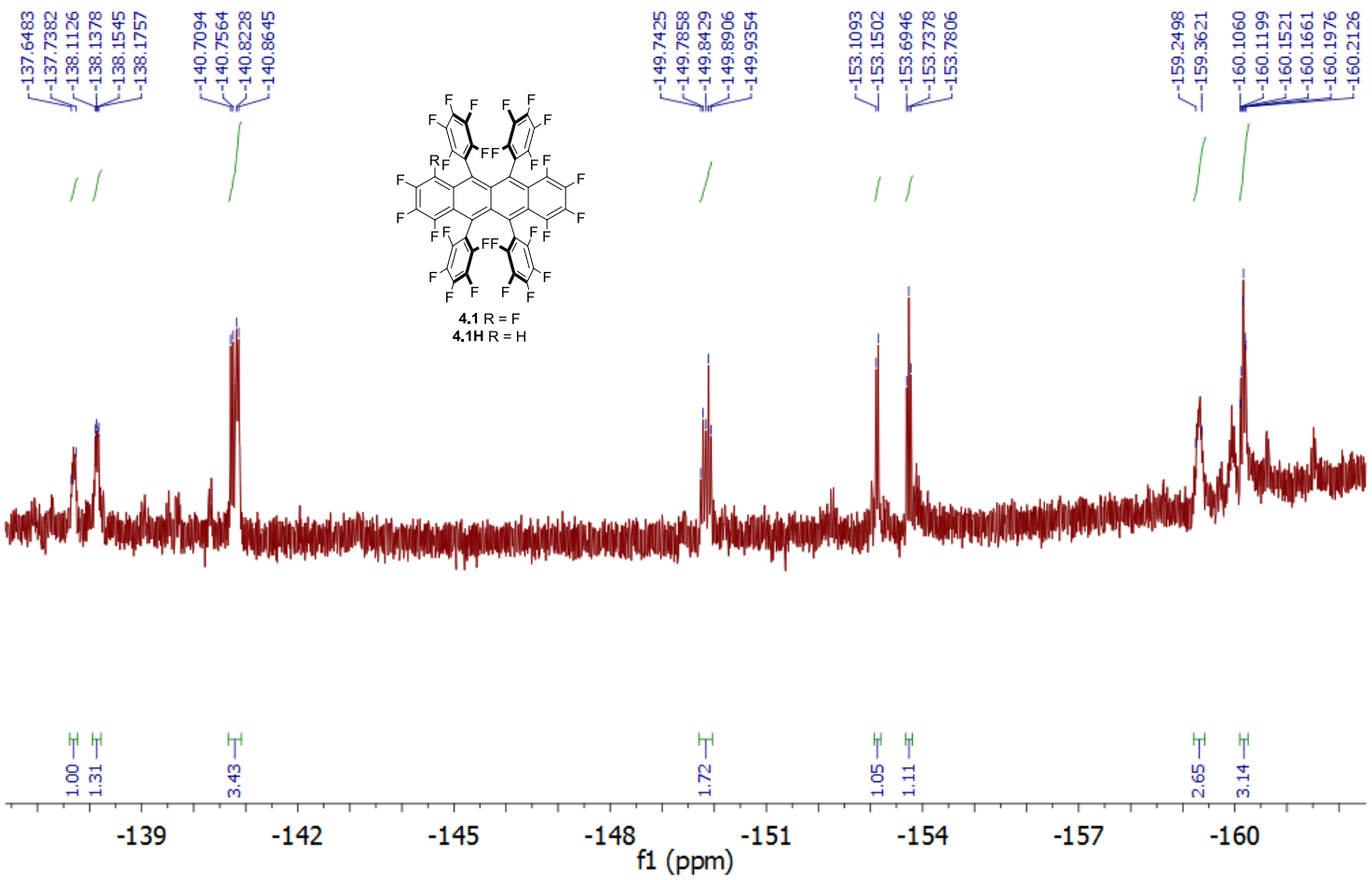

4.1 R = F
4.1H R = H

Parameter	Value
1 Data File Name	C:/ Users/ Katie/ Dropbox/ ChemResearch/ NMR data/ fRubrene/ F28_1stRoute/ KAMii-104-F1-F2/ 1/ fid
2 Solvent	CDCl3
3 Acquisition Date	2012-02-07T01:04:17
4 Spectrometer Frequency	500.13
5 Nucleus	1H

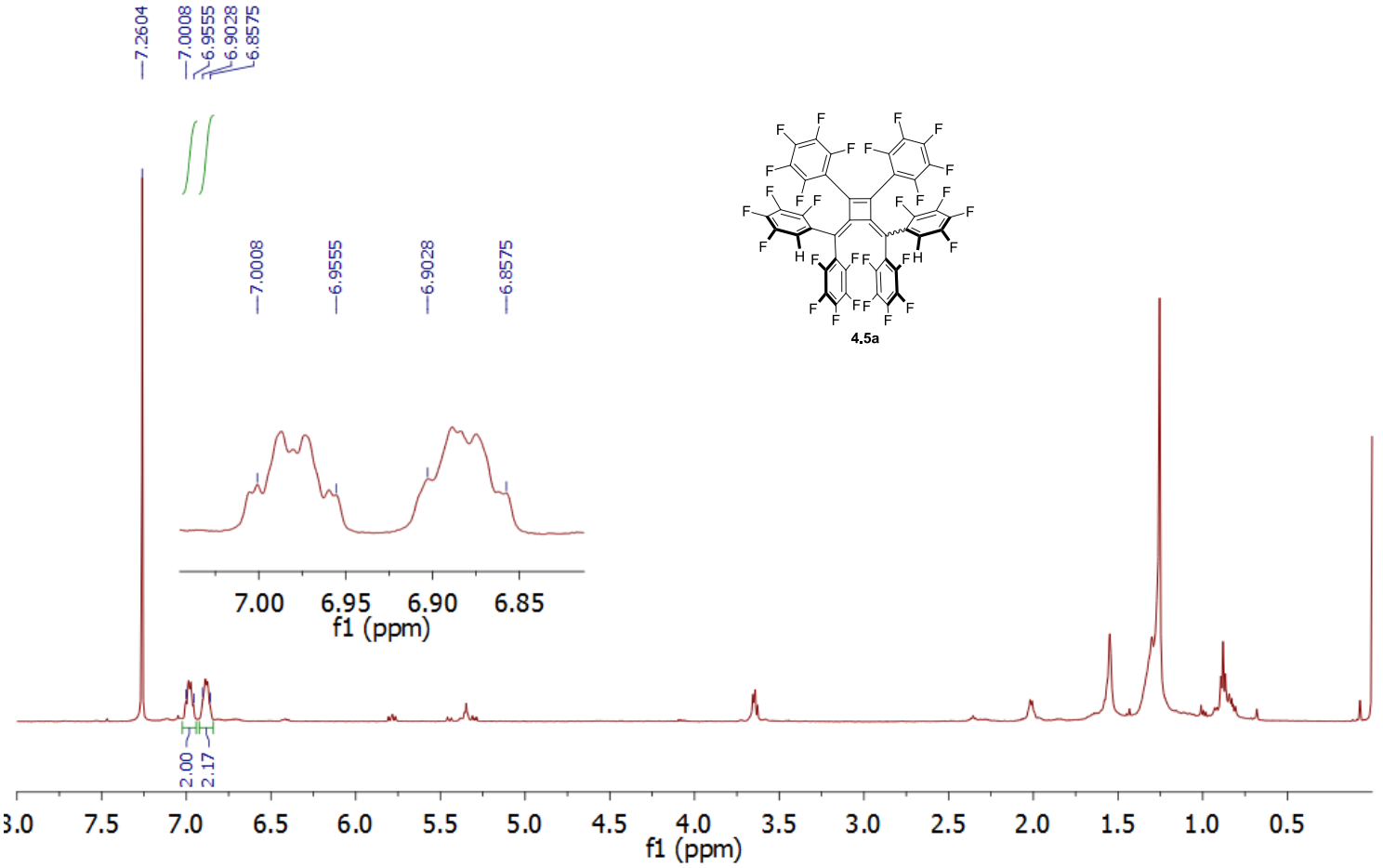

4.5a

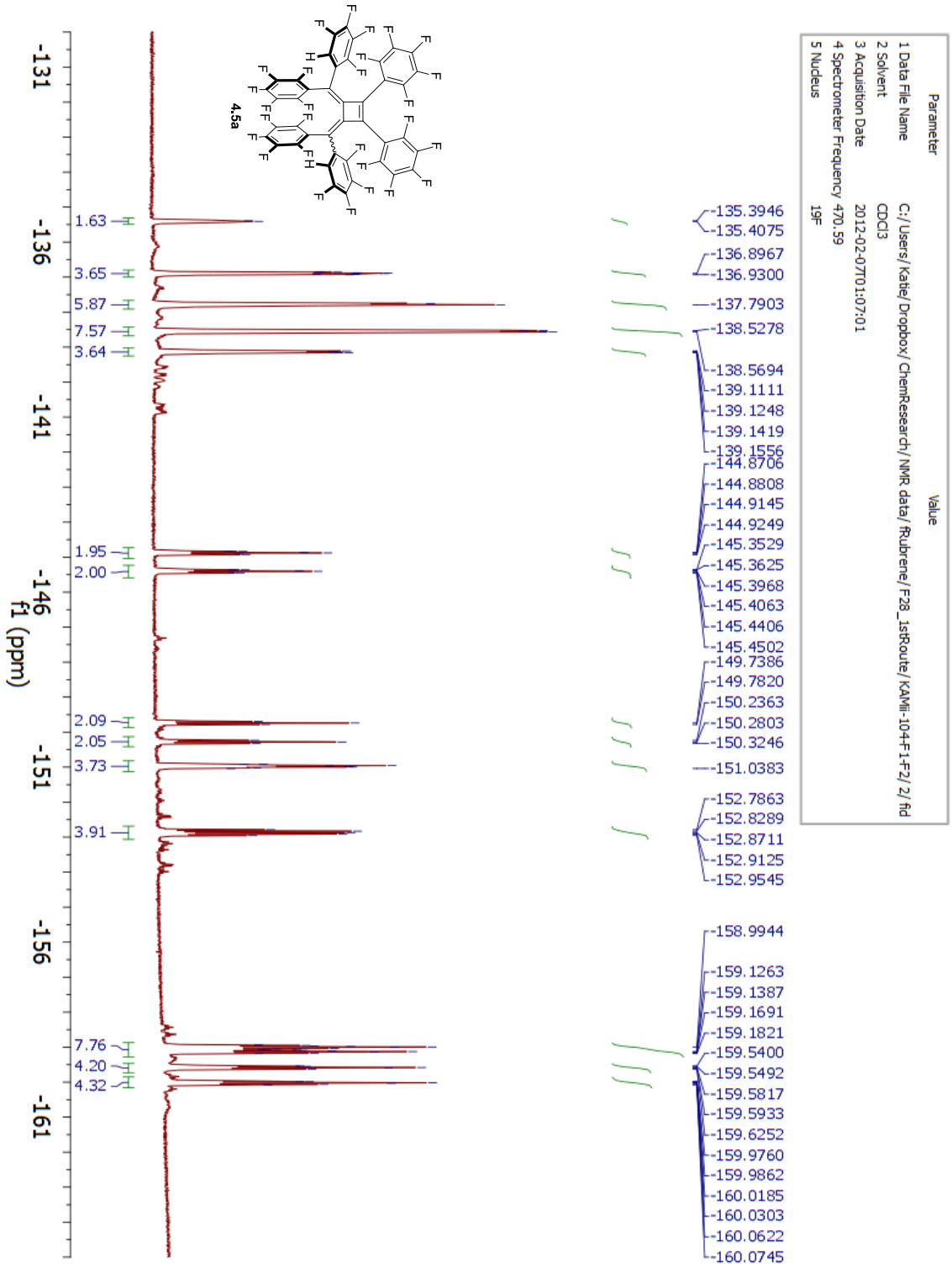
Parameter
Value
1 Data File Name
C:/Users/Katie/Dropbox/ChemResearch/NMR data/Rubrene/F28_1stRoute/KAMii-104-F1-F2/2/fid
2 Solvent
CDCl3
3 Acquisition Date
2012-02-07T01:07:01
4 Spectrometer Frequency 470.59
5 Nucleus
19F
4.5a
f1 (ppm)
-131
-136
-141
-146
-151
-156
-161
1.63
3.65
5.87
7.57
3.64
1.95
2.00
2.09
2.05
3.73
3.91
7.76
4.20
4.32
-135.3946
-135.4075
-136.8967
-136.9300
-137.7903
-138.5278
-138.5694
-139.1111
-139.1248
-139.1419
-139.1556
-144.8706
-144.8808
-144.9145
-144.9249
-145.3529
-145.3625
-145.3968
-145.4063
-145.4406
-145.4502
-149.7386
-149.7820
-150.2363
-150.2803
-150.3246
-151.0383
-152.7863
-152.8289
-152.8711
-152.9125
-152.9545
-158.9944
-159.1263
-159.1387
-159.1691
-159.1821
-159.5400
-159.5492
-159.5817
-159.5933
-159.6252
-159.9760
-159.9862
-160.0185
-160.0303
-160.0622
-160.0745

Parameter	Value
1 Data File Name	C:/ Users/ Katie/ Dropbox/ ChemResearch/ NMR data/ fRubrene/ F28_1stRoute/ KAMii-120-F2/ 1/ fid
2 Solvent	CDCl3
3 Spectrometer Frequency	500.13
4 Nucleus	1H

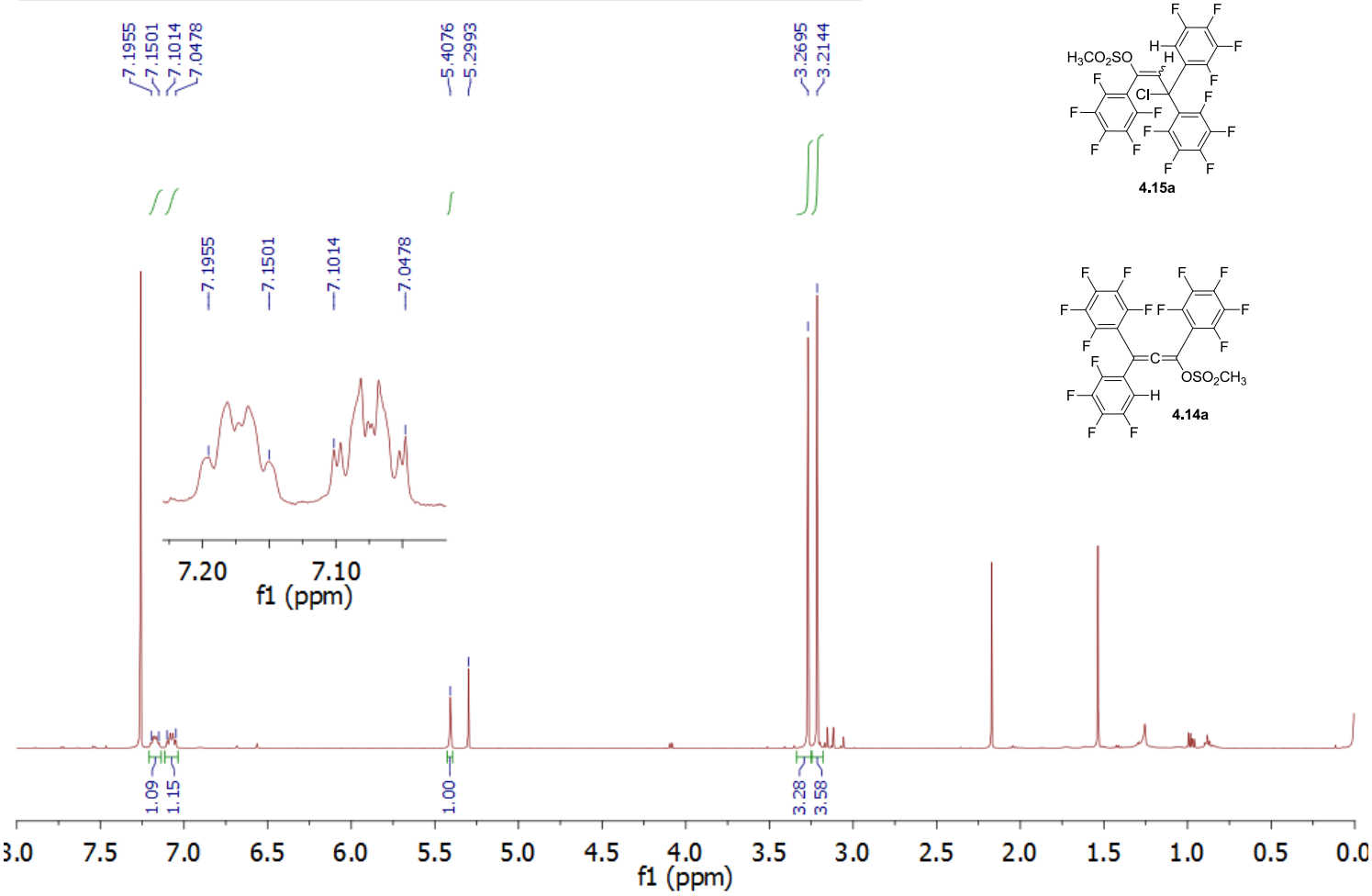

Parameter	Value
1 Data File Name	C:/ Users/ Katie/ Dropbox/ ChemResearch/ NMR data/ fRubrene/ F28_1stRoute/ KAMii-120-F2/ 2/ fid
2 Solvent	CDCl3
3 Acquisition Date	2012-03-06T16:07:50
4 Spectrometer Frequency	470.59
5 Nucleus	19F

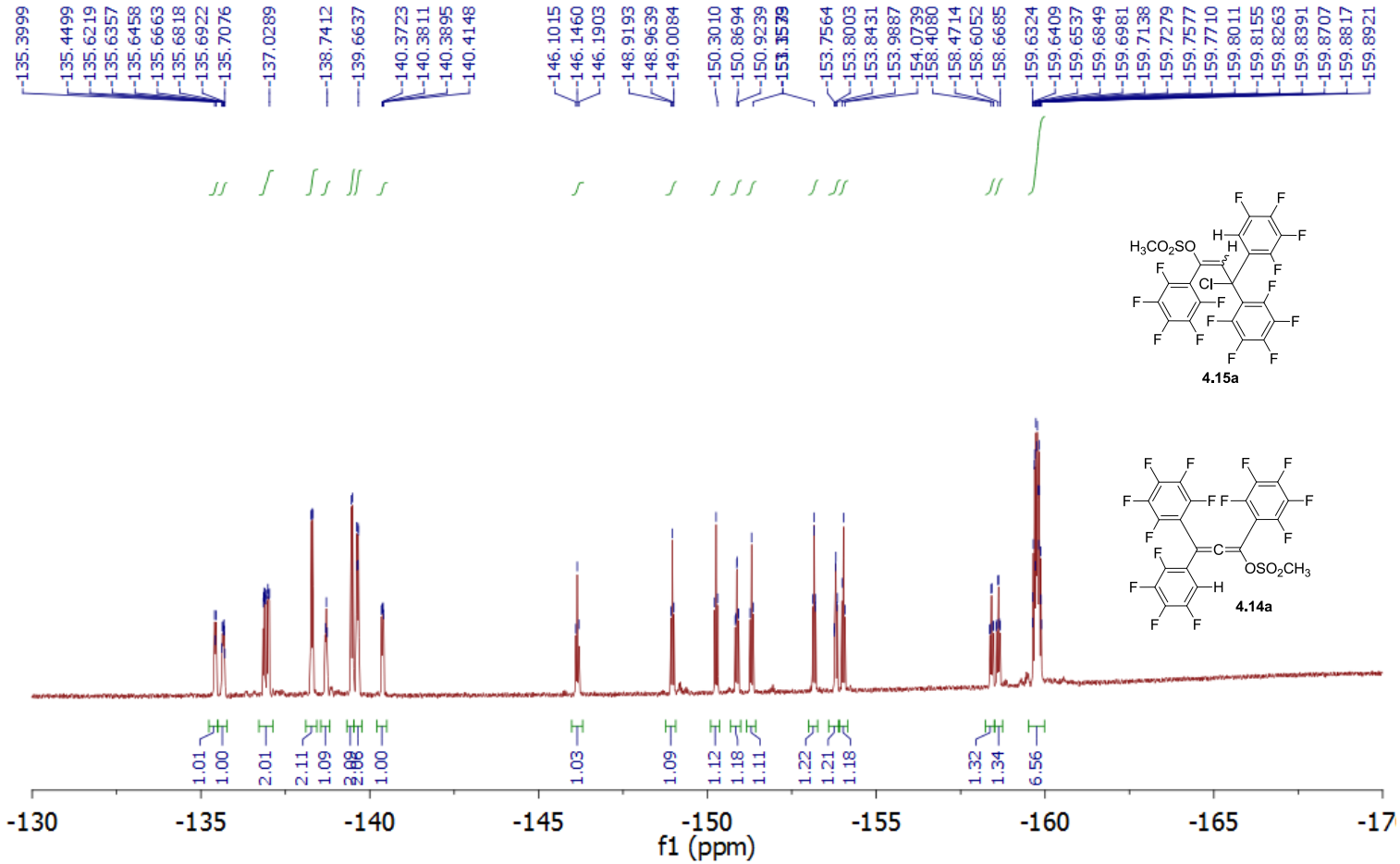

4.15a

4.14a

Parameter	Value
1 Data File Name	C:/ Users/ Katie/ Dropbox/ ChemResearch/ NMR data/ fRubrene/ F28_1stRoute/ KAMii-255-4-1H.fid/ fid
2 Solvent	cdcl3
3 Acquisition Date	2013-03-23T20:58:42
4 Spectrometer Frequency	300.17
5 Nucleus	1H

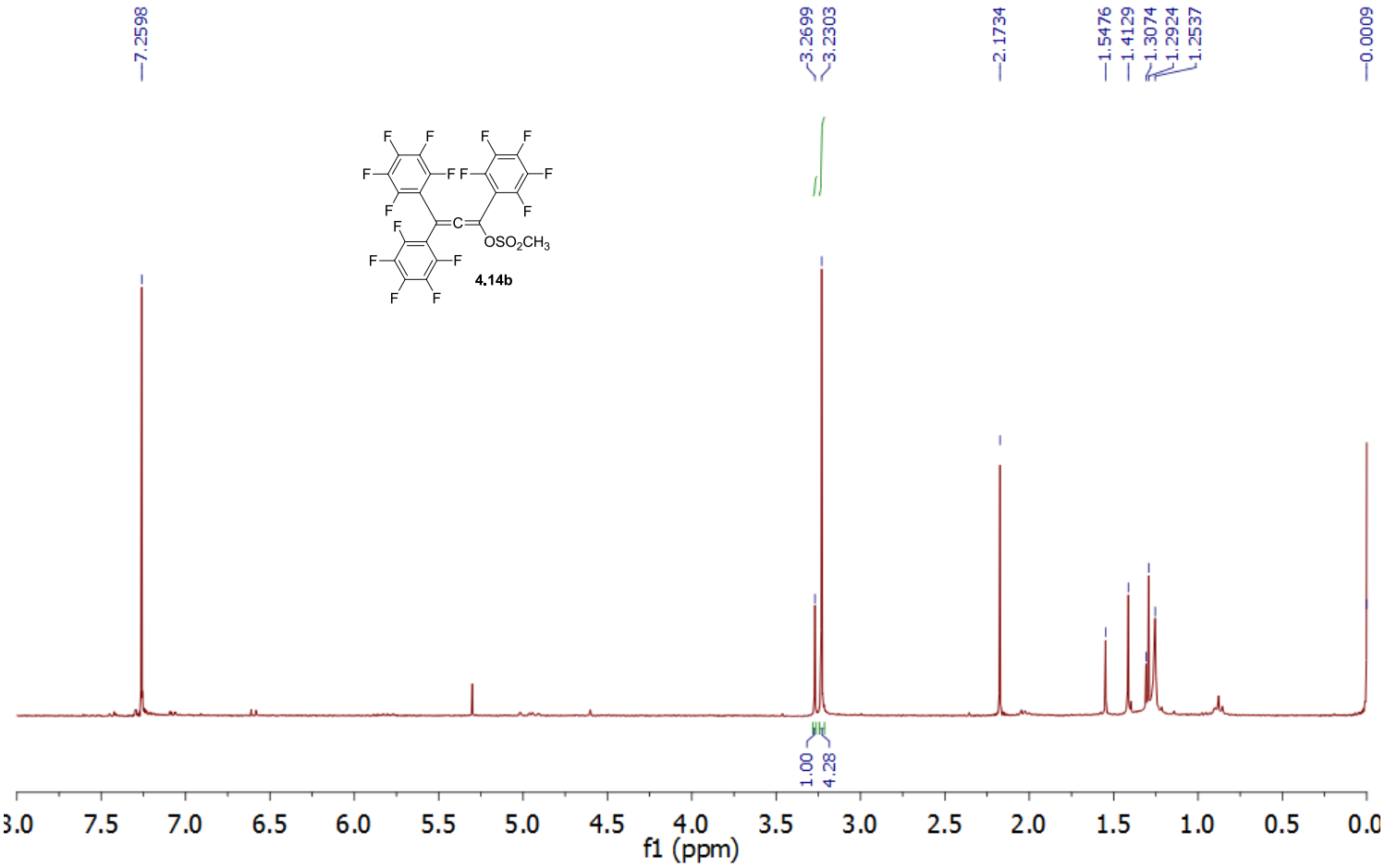

Parameter	Value
1 Data File Name	C:/ Users/ Katie/ Dropbox/ ChemResearch/ NMR data/ fRubrene/ F28_1stRoute/ KAMii-255-4-F19.fid/ fid
2 Solvent	cdcl3
3 Acquisition Date	2013-03-23T21:00:09
4 Spectrometer Frequency	282.43
5 Nucleus	19F

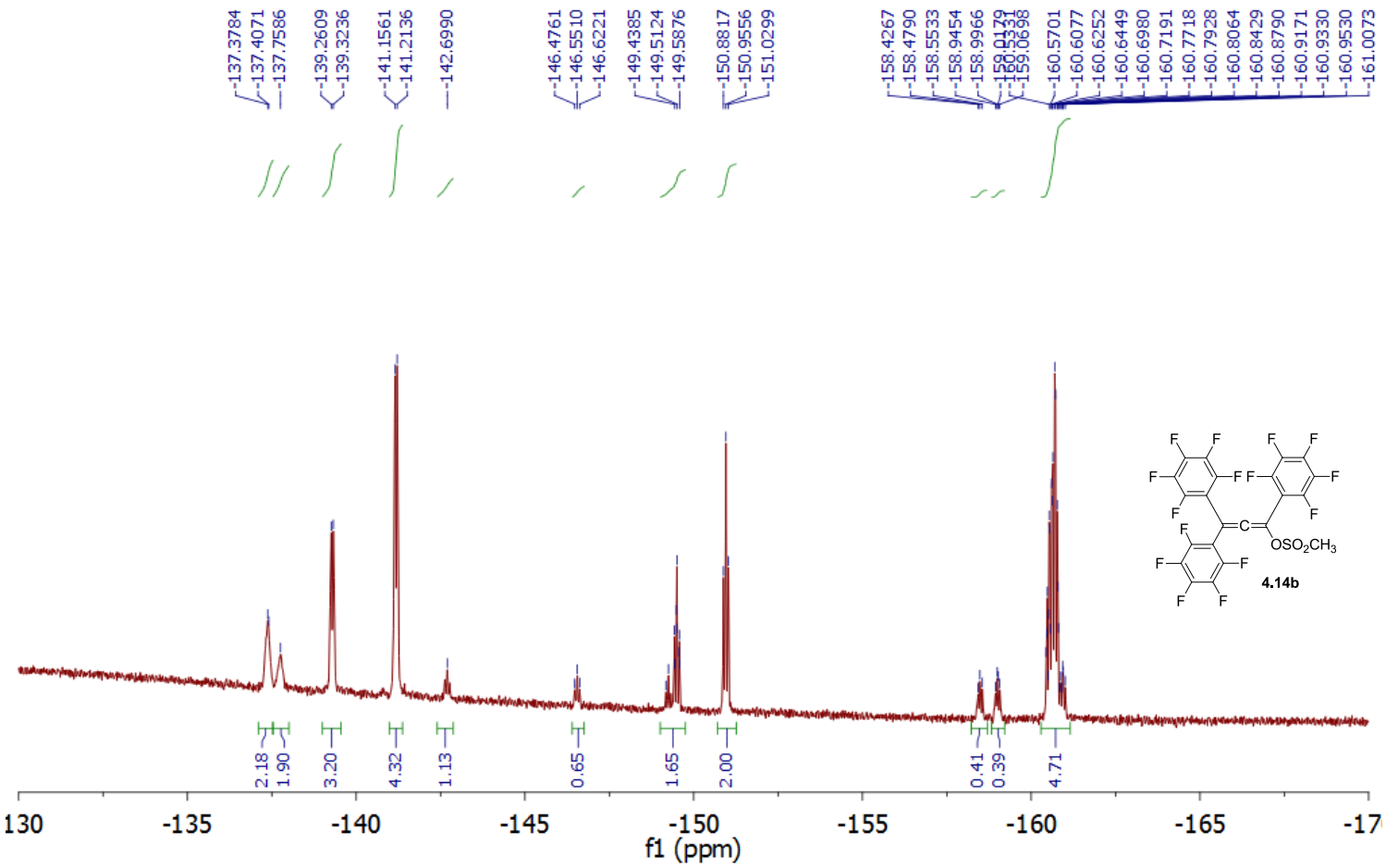

Parameter	Value
1 Data File Name	C:/ Users/ Katie/ Dropbox/ ChemResearch/ NMR data/ fRubrene/ F28_1stRoute/ KAMii-255-1-F19.fid/ fid
2 Solvent	cdcl3
3 Acquisition Date	2013-03-23T20:33:15
4 Spectrometer Frequency	282.43
5 Nucleus	19F

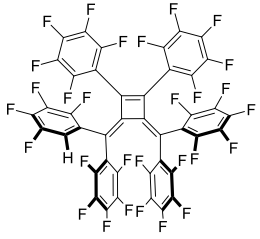

4.5b